frontiers | Research Topics

Total marrow irradiation

Edited by
Susanta Kumar Hui, Guy Storme, Jeffrey Wong, Cynthia Aristei,
Monzr M. Al Malki and Bulent Aydogan

Published in
Frontiers in Oncology

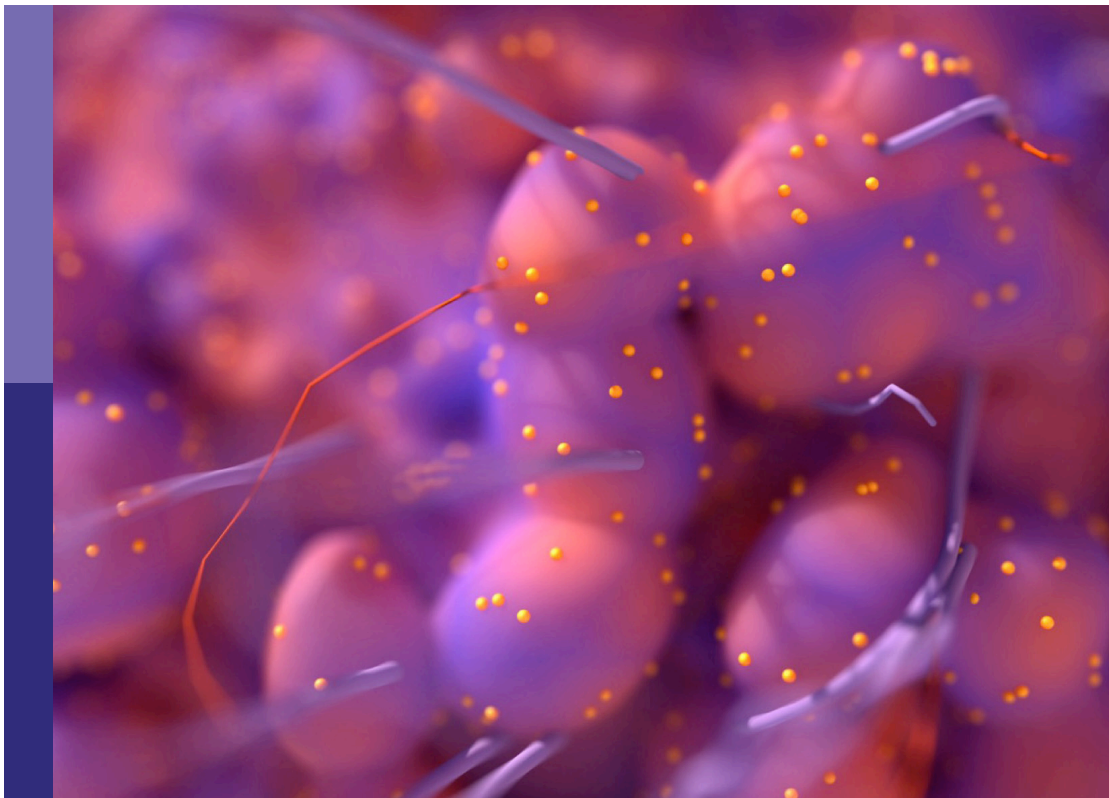

ISSN 1664-8714
ISBN 978-2-8325-2418-3
DOI 10.3389/978-2-8325-2418-3

About Frontiers

Frontiers is more than just an open access publisher of scholarly articles: it is a pioneering approach to the world of academia, radically improving the way scholarly research is managed. The grand vision of Frontiers is a world where all people have an equal opportunity to seek, share and generate knowledge. Frontiers provides immediate and permanent online open access to all its publications, but this alone is not enough to realize our grand goals.

Frontiers journal series

The Frontiers journal series is a multi-tier and interdisciplinary set of open-access, online journals, promising a paradigm shift from the current review, selection and dissemination processes in academic publishing. All Frontiers journals are driven by researchers for researchers; therefore, they constitute a service to the scholarly community. At the same time, the *Frontiers journal series* operates on a revolutionary invention, the tiered publishing system, initially addressing specific communities of scholars, and gradually climbing up to broader public understanding, thus serving the interests of the lay society, too.

Dedication to quality

Each Frontiers article is a landmark of the highest quality, thanks to genuinely collaborative interactions between authors and review editors, who include some of the world's best academicians. Research must be certified by peers before entering a stream of knowledge that may eventually reach the public - and shape society; therefore, Frontiers only applies the most rigorous and unbiased reviews. Frontiers revolutionizes research publishing by freely delivering the most outstanding research, evaluated with no bias from both the academic and social point of view. By applying the most advanced information technologies, Frontiers is catapulting scholarly publishing into a new generation.

What are Frontiers Research Topics?

Frontiers Research Topics are very popular trademarks of the *Frontiers journals series*: they are collections of at least ten articles, all centered on a particular subject. With their unique mix of varied contributions from Original Research to Review Articles, Frontiers Research Topics unify the most influential researchers, the latest key findings and historical advances in a hot research area.

Find out more on how to host your own Frontiers Research Topic or contribute to one as an author by contacting the Frontiers editorial office: frontiersin.org/about/contact

Total marrow irradiation

Topic editors

Susanta Kumar Hui — City of Hope National Medical Center, United States
Guy Storme — Vrije University Brussels, Belgium
Jeffrey Wong — City of Hope National Medical Center, United States
Cynthia Aristei — University of Perugia, Italy
Monzr M. Al Malki — Department of Hematology and Hematopoietic Cell Transplantation, City of Hope, United States
Bulent Aydogan — The University of Chicago, United States

Citation

Hui, S. K., Storme, G., Wong, J., Aristei, C., Al Malki, M. M., Aydogan, B., eds. (2023). *Total marrow irradiation*. Lausanne: Frontiers Media SA.
doi: 10.3389/978-2-8325-2418-3

Table of contents

frontiers | Frontiers in Oncology

TYPE Editorial
PUBLISHED 19 July 2023
DOI 10.3389/fonc.2023.1240530

OPEN ACCESS

EDITED AND REVIEWED BY
Timothy James Kinsella,
Brown University, United States

*CORRESPONDENCE
Susanta Kumar Hui
shui@coh.org

RECEIVED 15 June 2023
ACCEPTED 21 June 2023
PUBLISHED 19 July 2023

CITATION
Hui SK, Storme G, Wong J, Aristei C, Al Malki MM and Aydogan B (2023) Editorial: Total marrow irradiation. *Front. Oncol.* 13:1240530. doi: 10.3389/fonc.2023.1240530

Editorial: Total marrow irradiation

Susanta Kumar Hui[1]*, Guy Storme[2], Jeffrey Wong[3], Cynthia Aristei[4], Monzr M. Al Malki[5] and Bulent Aydogan[6]

[1]Department of Radiation Oncology, Beckman Research Center, City of Hope National Medical Center, Duarte, CA, United States, [2]Department of Radiation Oncology, Vrije University Brussels, Brussels, Belgium, [3]Department of Radiation Oncology, City of Hope National Medical Center, Duarte, CA, United States, [4]Department of Radiation Oncology, University of Perugia, Perugia, Perugia, Umbria, Italy, [5]Department of Hematology and Hematopoietic Cell Transplantation, City of Hope National Medical Center, Duarte, CA, United States, [6]Department of Radiation and Cellular Oncology, University of Chicago, Pritzker School of Medicine, Chicago, IL, United States

KEYWORDS

TMI, TBI, TMLI, conformal TBI, IMRT TBI

Editorial on the Research Topic
Total marrow irradiation

Although total body irradiation (TBI) is commonly used in conditioning regimens for allogeneic hematopoietic cell transplantation (HCT) in hematological diseases. major drawbacks are treatment-related toxicities and relapse. Despite advances in precision radiation for solid tumors, TBI for HCT has remained practically unchanged for over half a century due to a lack of i) advances in treatment delivery, 3D treatment planning, and organ-specific dosimetry, ii) limited understanding of the biological impact of systemic and targeted radiation, iii) appropriate clinical studies addressing innovative issues in hematological diseases and iv) integration across multidisciplinary fields to solve clinical uncertainties. The field of TBI has begun shifting from conventional TBI strategies towards 3D image-guided organ-specific treatment delivery i.e. “total marrow irradiation (TMI)”, “total marrow and lymphoid radiation (TMLI)”, “conformal whole-body irradiation” or intensity-modulated TMI (IMTMI). Despite subtle differences, all these treatments are referred to as TMI. Acceptance of TMI regimens is accelerating worldwide as TMI equipment is available from diverse manufacturers.

Since a full report about progress in this multidisciplinary field is acknowledged to be an unmet need, despite several individual studies, the present special issue was designed to cover recent advances in TMI technology, physics, biology, imaging, and clinical benefits. The series also reports on TMI standardization across manufacturers through a data-collecting consortium. Additionally, future advances through a multidisciplinary approach, including molecular imaging and automatization, will be achieved by bringing together international experts in different disciplines. Therefore, this project aims to be transformational, as it will cover advances in all aspects of this new field, inform about scientific progress, and guide clinical practice.

This Research Topic contains 15 articles covering a wide range of topics that were written by 238 contributors. They mainly fall into 4 categories:

1) Clinical studies

○ Vogel et al. reviewed the most common adverse effect of TBI i.e. pulmonary toxicity including the idiopathic pneumonia syndrome (IPS), emphasizing that definitions of IPS as well as demographic and treatment-related risk factors remain poorly characterized. Indeed, few data correlated dose distribution with toxicity. In the future, CT-guided intensity modulated TBI is expected to provide extremely precise calculations of 3D lung dose distributions in order to correlate dose volume histograms with toxicity. The authors suggested assessing risk factors for IPS in cohorts of pediatric and adult patients and adopting the diagnostic workup and definition as proposed by the American Thoracic Society.

○ Wong et al. analyzed data from over 500 patients who received, as part of conditioning regimens to various HCT, TMLI delivered by Tomotherapy or Linac-based VMAT. In a Phase II study, TMLI dose escalation to 20 Gy, combined with etoposide and cyclophosphamide, improved outcomes (2-year OS and PFS 48% and 33%) with 1-year non-relapse mortality (NRM) of 6%). Another innovation was the breakthrough development of chemotherapy-free conditioning based on 20 Gy TMLI followed by PTCy. It was designed to reduce the risk of GVHD while maintaining a high antileukemic effect in patients with AML in CR1/CR2 undergoing matched donor allogeneic HCT. Promising 2 year results were reported: OS =86.7%, relapse-free survival = 83.3%, GVHD-/relapse-free survival (GRFS) = 59.3% and no NRM. In conclusion, TMI/TMLI allowed dose escalation, was suitable for elderly patients, and was associated with good outcomes.

2) Clinical trials

○ Kobyzeva et al. treated a large cohort of children with leukemia with conformal TBI (12 Gy delivered in 6 or 4 fractions) The dose to the bone marrow was increased up to 15 Gy in a small cohort. All patients received standard chemotherapy followed by TCR-alpha/beta-depleted donor marrow to minimize the risk of GVHD and 88% received a haploidentical transplant. At a median follow-up of over 2 years, OS was 63%, and TRM 10.7%. Disease status heterogeneity could potentially have impacted outcomes. In patients with active disease increasing the BM-targeted radiation dose reduced disease recurrences and improved survival (47% vs 29%), suggesting higher BM-targeted radiation doses are needed to control enhanced disease burden in the bone marrow.

○ Ladbury et al. retrospectively evaluated the effects of RT on outcomes in 254 patients with refractory or relapsed AML or ALL who suffered extramedullary (EM) relapse after TMLI. RT was delivered with curative intent to 11 patients in whom significantly better OS and PFS were observed. The authors concluded RT effectively treated EM relapse, particularly if limited.

○ Kong et al. analyzed the feasibility and effectiveness of 12 Gy TMLI in the conditioning regimen for allogeneic HSCT in a small series of 1 patient with AML and 16 with ALL (median age 17 years; range 8-35). Although this pilot study showed TMLI was safe, a longer follow-up is needed to assess outcomes.

○ Saldi et al. retrospectively analyzed the main dosimetric parameters to determine the impact of RT doses to the intestine on the incidence of acute GvHD (aGvHD) in transplant recipients. No dosimetric parameter was associated with aGvHD, not even when the intestine was divided into sub-areas. The limitations of this study were a large dose variation in the intestine and a small cohort of patients. Furthermore, transplants and patient ages were mixed (HLA matched and HLA haploidentical transplants; young adults and older patients). As all patients received adoptive immunotherapy with Tcons and Tregs, untangling the role of RT was complex. Thus, a preclinical model was needed to elucidate the role of TMI in aGvHD occurrence. Indeed, lowering the radiation dose (~4 Gy) to the GI attenuated tissue damage, with less donor T-cell traffic to the GI system, resulting in reduced aGvHD [Sargur Madabushi et al. (2022), 140 (Supplement 1):4467-4469].

3) Physics and dosimetry

○ Using phantom and simulated motion, Kavak et al. studied the impact of respiratory motion on the lung dose, finding that it may impact small lung regions, but has a negligible effect on dose uncertainty.

○ Loginova et al. provided treatment planning details for TBI, comparing results in children treated with Tomotherapy (157) or VMAT (52); image-guided RT was used in all cases. Compared with VMAT, Tomotherapy displayed less variation between planned and delivered doses, was less time-consuming, and was easier to implement. Since both techniques were feasible, safe, and associated with acceptable toxicity rates, treatment can be performed with either.

○ Ladbury et al. reported treatment planning and dosimetry with VMAT, showing they were similar to previous observations with Tomotherapy and confirming VMAT is suitable for TMI treatment, even at doses up to 20Gy.

○ Han et al. evaluated dosimetric coverage for targets and organs at risk when TMLI was delivered with the standard 12 Gy or 20 Gy. Mean and median doses for most normal

organs at the escalated prescription dose of 20 Gy were increased less than the prescription dose scaling.

- Since TMI/TMLI requires extensive contouring of target volumes and organs of the entire body. As the contouring procedure is time-consuming and prone to errors, it constitutes a major barrier to clinical implementation, Watkins et al. developed a model of Artificial-Intelligence segmentation which offered a powerful solution for enhanced efficacy in TMLI treatment planning.
- Zuro et al. compared the dosimetric results of TMI treatment planning with intensity-modulated spot-scanning proton therapy (IMPT) and VMAT using photon beams. Except for the esophagus and thyroid, OAR doses were lower with IMPT, and higher for the skull surface and ribs. Nowadays, since IMPT is used for craniospinal irradiation (CSI) in hematological malignancies, a shift to TMI may be feasible in the near future, particularly for pediatric patients.

In summary, TMI treatment is delivered by means of machines from leading manufacturers, thus facilitating clinical studies worldwide.

4) Scientific advances

- Conformal radiation delivery in a preclinical model is extremely challenging as some vital organs are very close to the skeleton. Moreover, treatment delivery is long and complex. Abdelhamid et al. showed a novel Sparse Orthogonal Collimator (SOC) based intensity modulation for TMI treatment planning and delivery optimization which could enhance dosimetric conformality, reduce radiation exposures to all critical organs, automatize and shorten treatment delivery time.
- While the benefits of TMI are beginning to emerge in young adults and children, its role in treating older patients remains unknown. Myeloablative radiation has not been used in the elderly due to concerns that increased radiation may adversely affect bone marrow hematopoiesis and that its toxicity profile is unknown. Using preclinical TMI-based dose escalation in aging mice models, Lim et al. observed normal donor engraftment, significantly reduced tissue damage and preserved repair capacity.
- HCT offers a curative option for Sickle Cell Disease (SCD), a serious global health problem. Myeloablative TBI-based HCT is, however, associated with high mortality/morbidity rates. Conversely, RIC is associated with fewer organ toxicities, but a higher risk of graft rejection. Although it provides mixed chimerism, the donor component gradually reduces over time, leading to SCD relapse. Using a preclinical TMI-based SCD mice model, Madabushi et al. observed that increased BM-targeted radiation enhanced chimerism and stable engraftment, rescued red blood cells from sickle abnormalities, and significantly reduced organ toxicity.

In summary, preclinical models justify initiating new clinical trials for older patients (>55) with leukemia (NCT03494569) and patients with severe sickle cell disease (NCT05384756), such as those currently underway at the City of Hope.

Author contributions

All authors listed have made a substantial, direct, and intellectual contribution to the work and approved it for publication.

Funding

NIH 2RO1CA154491 and ONCOTEST (Ghent, Belgium).

Conflict of interest

The authors declare that the research was conducted in the absence of any commercial or financial relationships that could be construed as a potential conflict of interest.

Publisher's note

Reference

Sargur Madabushi, S., Ghimire, H., Lim, J. E., Vishwasrao, P., Abdelhamid, A. M., Storme, G., et al. (2022). Novel tissue-specific targeted radiation delivery reduces GI injury and T cell trafficking attenuating allogeneic immune attack to reduce GvHD in a murine BMT model. *Blood* 140 (Supplement 1), 4467–9.

frontiers in Oncology

REVIEW
published: 26 August 2021
doi: 10.3389/fonc.2021.708906

Pulmonary Toxicity After Total Body Irradiation – Critical Review of the Literature and Recommendations for Toxicity Reporting

Jennifer Vogel[1], *Susanta Hui*[2*], *Chia-Ho Hua*[3], *Kathryn Dusenbery*[4], *Premavarthy Rassiah*[5], *John Kalapurakal*[6], *Louis Constine*[7] *and Natia Esiashvili*[8*]

[1] Department of Radiation Oncology, Bon Secours Merch Health St. Francis Cancer Center, Greenville, SC, United States, [2] Department of Radiation Oncology, City of Hope National Medical Center, Duarte, CA, United States, [3] Department of Radiation Oncology, St Jude Children's Research Hospital, Memphis, TN, United States, [4] Department of Radiation Oncology, University of Minnesota, Minneapolis, MN, United States, [5] Department of Radiation Oncology, University of Utah Huntsman Cancer Hospital, Salt Lake City, UT, United States, [6] Department of Radiation Oncology, Northwestern University School of Medicine, Chicago, IL, United States, [7] Department of Radiation Oncology, University of Rochester Medical Center, Rochester, NY, United States, [8] Department of Radiation Oncology, Emory School of Medicine, Atlanta, GA, United States

OPEN ACCESS

Edited by:
Valdir Carlos Colussi, University Hospitals Cleveland Medical Center, United States

Reviewed by:
Raquel Bar-Deroma, Rambam Health Care Campus, Israel
Fiori Alite, Geisinger Commonwealth School of Medicine, United States

***Correspondence:**
Natia Esiashvili
nesiash@emory.edu
Susanta Hui
shui@coh.org

Specialty section:
This article was submitted to Radiation Oncology, a section of the journal Frontiers in Oncology

Received: *12 May 2021*
Accepted: *28 July 2021*
Published: *26 August 2021*

Citation:
Vogel J, Hui S, Hua C-H, Dusenbery K, Rassiah P, Kalapurakal J, Constine L and Esiashvili N (2021) Pulmonary Toxicity After Total Body Irradiation – Critical Review of the Literature and Recommendations for Toxicity Reporting. Front. Oncol. 11:708906. doi: 10.3389/fonc.2021.708906

Introduction: Total body irradiation is an effective conditioning regimen for allogeneic stem cell transplantation in pediatric and adult patients with high risk or relapsed/refractory leukemia. The most common adverse effect is pulmonary toxicity including idiopathic pneumonia syndrome (IPS). As centers adopt more advanced treatment planning techniques for TBI, total marrow irradiation (TMI), or total marrow and lymphoid irradiation (TMLI) there is a greater need to understand treatment-related risks for IPS for patients treated with conventional TBI. However, definitions of IPS as well as risk factors for IPS remain poorly characterized. In this study, we perform a critical review to further evaluate the literature describing pulmonary outcomes after TBI.

Materials and Methods: A search of publications from 1960-2020 was undertaken in PubMed, Embase, and Cochrane Library. Search terms included "total body irradiation", "whole body radiation", "radiation pneumonias", "interstitial pneumonia", and "bone marrow transplantation". Demographic and treatment-related data was abstracted and evidence quality supporting risk factors for pulmonary toxicity was evaluated.

Results: Of an initial 119,686 publications, 118 met inclusion criteria. Forty-six (39%) studies included a definition for pulmonary toxicity. A grading scale was provided in 20 studies (17%). In 42% of studies the lungs were shielded to a set mean dose of 800cGy. Fourteen (12%) reported toxicity outcomes by patient age. Reported pulmonary toxicity ranged from 0-71% of patients treated with TBI, and IPS ranged from 1-60%. The most common risk factors for IPS were receipt of a TBI containing regimen, increasing dose rate, and lack of pulmonary shielding. Four studies found an increasing risk of pulmonary toxicity with increasing age.

Conclusions: Definitions of IPS as well as demographic and treatment-related risk factors remain poorly characterized in the literature. We recommend routine adoption of

the diagnostic workup and the definition of IPS proposed by the American Thoracic Society. Additional study is required to determine differences in clinical and treatment-related risk between pediatric and adult patients. Further study using 3D treatment planning is warranted to enhance dosimetric precision and correlation of dose volume histograms with toxicities.

Keywords: radiation pneumonitis, pulmonary toxicity, allogeneic stem cell transplantation, total body irradiation, total body irradiation complications

INTRODUCTION

Acute leukemia is the most common cancer in children and adolescents, and exhibits a bimodal distribution with an initial peak among infants and exponential rise in adulthood (1, 2). Between 2001-2007, 29,682 individuals were diagnosed with acute leukemia, with an incidence ratio of 57.2 per 100,000 person years (2). Overall, acute myeloid leukemia (AML) accounted for 65.7% of cases, acute lymphoblastic leukemia or lymphoma (ALL/L) 31.0% of cases, and acute leukemia of ambiguous lineage 3.4% of cases (2).

Allogeneic stem cell transplant is used in a subset of patients with high risk or relapsed/refractory disease. In pediatric patients with ALL, myeloablative regimens containing total body irradiation (TBI) have demonstrated improvement in event free survival from 29-35% without TBI as compared to 50-58% with and remain the standard of care (3–5). In the adult setting, myeloablative regimens have demonstrated improvements in recurrence free survival at the cost of increased transplant related mortality compared to reduced intensity conditioning regimens (6, 7). The use of reduced-intensity conditioning regimens has therefore increased over the last decade, particularly in patients 50 years of age and older (8).

Transplant-related morbidity and mortality following a myeloablative transplant is significant. In particular, pulmonary toxicity and mortality has been reported in up to 60% of patients (9). Historically, approximately half of all pneumonias following stem cell transplant were secondary to infection, but use of prophylaxis has resulted in a relatively greater risk from noninfectious etiologies (10). In 1993 the National Institutes of Health (NIH) defined idiopathic pneumonia syndrome (IPS) as widespread alveolar injury without evidence of active lower tract infection or cardiogenic cause after transplant (11). Updated definitions now include newly described pathogens as determined on bronchoalveolar lavage (BAL) or lung biopsy (**Table 1**) (10).

As centers adopt more advanced treatment planning techniques for TBI or total marrow irradiation (TMI), there is a greater need to understand the patient and treatment-related risks for IPS. In addition, standardized evaluation and reporting of IPS is crucial to compare outcomes between treatment techniques. Therefore, in this report, we critically evaluate the literature with the goal of characterizing the workup and definitions of pulmonary toxicity as well as levels of evidence in support of risk factors for IPS following TBI-based myeloablative stem cell transplant.

MATERIALS AND METHODS

A search was undertaken in PubMed, Embase, and Cochrane Library. Articles from 1960-2020 were searched using terms including "total body irradiation", or "whole body radiation" and "radiation pneumonias" or "interstitial pneumonia" and "bone marrow transplantation" (**Supplemental Table 1**). Only English language reports of myeloablative transplant regimens were included. Studies in which the dose of TBI was not reported or intensity modulated techniques were used were omitted. Studies in which the incidence or risk factors for pneumonitis from TBI based regimens were not separately reported from those using chemotherapy alone were omitted.

Abstracted data included patient clinical characteristics such as age and disease; treatment-related characteristics including conditioning regimen, donor source, and graft *versus* host disease (GVHD) prophylaxis; TBI parameters including dose, dose rate, lung shielding, and beam arrangement; and outcomes including rates of acute GVHD.

We evaluated definitions of pulmonary complications in each publication. Any pulmonary complication was classified as pulmonary toxicity (PT). Pulmonary complications specifically reported as idiopathic were classified as IPS. Evidence reported to support these diagnoses including radiographic criteria, infectious workup, and change in pulmonary function tests was documented. Distinctions between acute and late toxicity, grading scales, and rates and mortality from acute PT and IPS were abstracted.

Evidence quality supporting risk factors for PT and IPS were categorized as: level Ia (evidence from meta-analyses of multiple randomized controlled trials), level Ib (evidence from ≥1 randomized controlled trial), level IIA (evidence from ≥1 controlled study without randomization), level IIb (evidence from ≥ other quasi experimental study), level III (evidence from non-experimental descriptive studies such as comparative studies, correlation studies, and case-control studies), and level IV (evidence from expert committee reports or opinions and/or clinical experience of respected authorities).

RESULTS

Clinical Characteristics

Of an initial 119,686 publications, 118 met inclusion criteria and were included for review (9, 12–127) (**Figure 1**). Studies were published between 1961-2020 and included patients from less

TABLE 1 | Definitions of pulmonary toxicity.

National Institutes of Health, 1993 (1)	I. Evidence of widespread alveolar injury. Criteria include: a. Multilobar infiltrates on routine chest radiographics or CT scans. b. Symptoms and signs of pneumonia, e.g., cough, dyspnea, rales. c. Evidence of abnormal pulmonary physiology. i. Increased alveolar to arterial oxygen gradient ii. New or increased restrictive pulmonary function test abnormality II. Absence of active lower respiratory tract infection. Appropriate evaluation includes: a. BAL negative for significant bacterial pathogens and/or lack of improvement with broad-spectrum antibiotics. b. BAL negative for pathogenic nonbacterial microorganisms. i. Routine bacterial viral and fungal cultures. ii. Shell-vial CMV culture iii. Cytology for CMV inclusions, fungi, and PCP iv. Detection methods for RSV, para-influenza virus, and other organisms (e.g., fluorescent antibiotics or culture) c. Transbronchial biopsy if condition of the patient permits. d. Ideally, a second confirmatory negative test for infection is done. This is usually performed 2 to 14 days after the initial negative BAL and may consist of a second BAL or open lung biopsy.
American Thoracic Society (2)	I. Evidence of widespread alveolar injury. a. Multilobar infiltrates on routine chest radiographics or CT scans. b. Symptoms and signs of pneumonia, e.g., cough, dyspnea, rales. c. Evidence of abnormal pulmonary physiology. i. Increased alveolar to arterial oxygen difference ii. New or increased restrictive pulmonary function test abnormality II. Absence of active lower respiratory tract infection. Appropriate evaluation includes: a. BAL negative for significant bacterial pathogens including acid-fast bacilli, *Nocardia*, and *Legionella* species b. BAL negative for pathogenic nonbacterial microorganisms. i. Routine bacterial viral and fungal cultures. ii. Shell-vial for CMV and respiratory RSV iii. Cytology for CMV inclusions, fungi, and PCP iv. Direct fluorescence staining with antibodies against CMV, RSV, HSV, VZV, influenza virus, parainfluenza virus, adenovirus, and other organisms c. Other organisms/tests to also consider: i. Polymerase chain reaction for human metapneumovirus, rhinovirus, coronavirus, and HHV6 ii. Polymerase chain reaction for *Chlamydia*, *Mycoplasma*, and *Aspergillus* species iii. Serum galactomannan ELISA for *Aspergillus* d. Transbronchial biopsy if condition of the patient permits. III. Absence of cardiac dysfunction, acute renal failure, or iatrogenic fluid overload as etiology for pulmonary dysfunction

than one year of age to 68 years of age (**Table 2**). Ten studies (8%) included patients with benign hematologic conditions and 17 included patients who received autologous stem cell transplants (16%). Most conditioning regimens were cyclophosphamide-based (88%) and most studies used methotrexate (MTX) for GVHD prophylaxis (57%). Rates of grade II-IV acute GVHD, when reported as such, ranged from 6-65%.

Definitions

Separate definitions for PT and IPS were reported in 59 studies (50%). The most common definition for pulmonary toxicity was "interstitial pneumonitis" (45%) and for IPS was "idiopathic interstitial pneumonitis" (21%) (**Table 2**).

Forty-six (39%) of studies included or referenced a definition including radiographic criteria and 40 (34%) described an infectious workup including blood, sputum, BAL, or biopsy. Ten studies (8%) reported changes in pulmonary function tests.

A minority of studies differentiated between acute and late pulmonary toxicities (9%). Of these, 38% used a cutoff of 90 days, 31% a cutoff of 100 days, and 31% a cutoff greater than 6 months.

A grading scale for PT was provided in 20 studies (17%). Of these, 37% used Common Terminology for Adverse Events (CTCAE), 16% used Radiation Therapy Oncology Group (RTOG), and 47% used an individualized definition proposed by the study.

Radiation Treatment Parameters

Of the studies evaluated, 59% reported the TBI source, 35% reported the beam arrangement, and 72% reported the dose rate. Of those that reported the source, 53% utilized Co-60 and of those that reported the beam arrangement 50% utilized anterior-posterior posterio-anterior (AP-PA) fields. Dose rate ranged from 1.2-30.0cGy/min.

Treatment fractionation was not described in 15% (**Table 3**). In 40% of studies patients were treated with a single fraction, most commonly to a total dose of 1000cGy (range 400-1754cGy). In 13% patients were treated with single daily fractions, most commonly to a total dose of 1200cGy (range 800-1575cGy). In 49% of studies patients were treated with twice daily fractions, most commonly to a total dose of 1200cGy (range 1020-1530cGy). In 4% of studies patients were treated three times per day, to a range of 1200-1610cGy.

Lung Shielding

Lung shielding techniques were not reported in 23% of studies evaluated (**Table 4**). In 26%, authors explicitly stated that no pulmonary shielding was used. In 42% of studies the lungs were shielded to a set mean dose, most commonly 800cGy (range 400cGy – prescription dose). Other studies reported pulmonary shielding by technique rather than dose limit, including use of 5-7 HVL blocks for a single treatment (3%), use of the patient's arms (3%), or use of bolus, compensators, attenuators, or other unspecified custom blocks (8%).

Pulmonary Toxicity

In studies where this was reported, PT occurred in 0-71% of patients treated with TBI, and IPS in 1-60%. Late PT occurred in 3-48% of patients treated with TBI and late IPS in 14-16%. Mortality from PT ranged from 0-61% and mortality from IPS ranged from 0-50%.

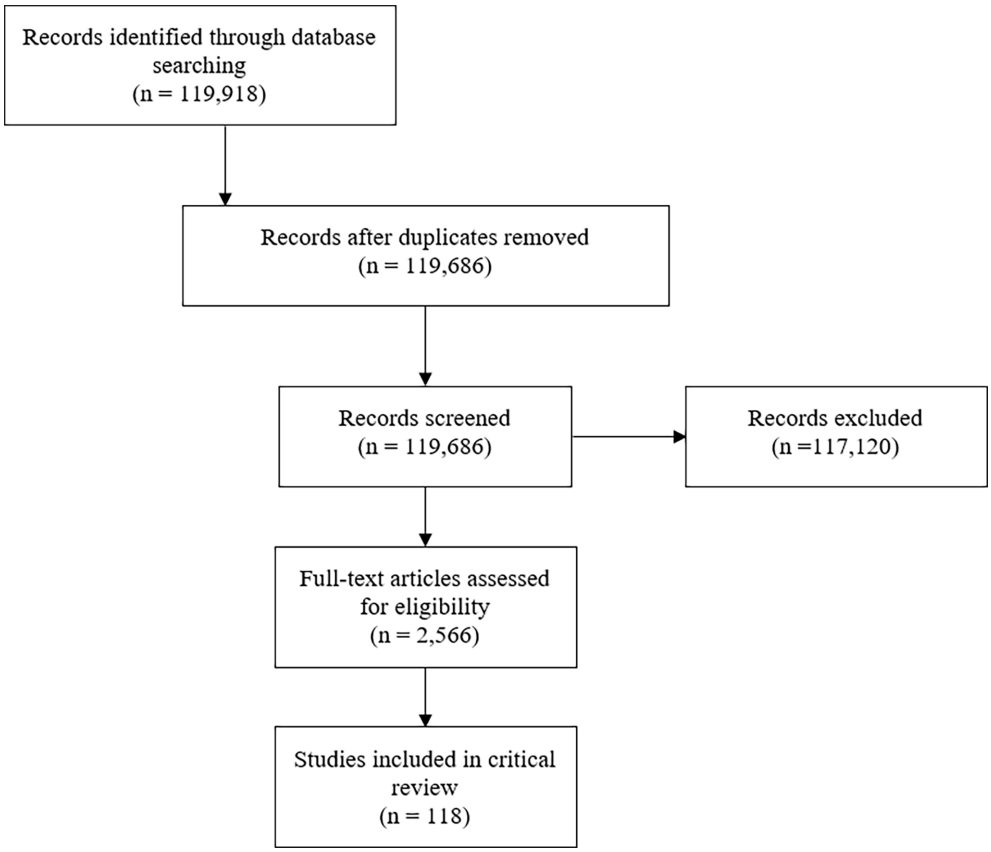

FIGURE 1 | PRISMA diagram.

Risk Factors for Pulmonary Toxicity

Fifty-three studies reported risk factors for PT (45%). Of these, the most frequently reported were GVHD (26%), older age (20%), increasing dose rate (13%), cytomegalovirus (8%), single fraction TBI (7%), and impaired pre-transplant pulmonary function tests (6%) (**Table 5**).

Risk Factors for IPS

Twenty-one studies reported risk factors for IPS. The most common risk factors were increased lung dose, increasing dose rate, receipt of a TBI containing regimen, and diagnosis (**Table 3**). Increased lung dose was associated with increased risk of toxicity in two studies (evidence level III). Increasing dose rate was associated with increased risk of pulmonary toxicity in two studies (evidence level III). Receipt of a TBI-containing regimen was associated with an increased risk of toxicity in two studies (evidence level III). Diagnosis was associated with increased risk of toxicity in two studies (evidence level III).

Age Specific Considerations

Of the studies evaluated, 14 (12%) reported toxicity outcomes by patient age or stratified between adult and pediatric patients. Four of these studies found an increasing risk of PT with increasing age, one of which determined a cutoff of >20 years old (19, 20, 37, 43). Eighteen studies evaluated pediatric patients only, one of which demonstrated an increasing risk of IPS with dose rate >15cGy/min and one of which found an increased risk associated with chronic GVHD (69, 75).

DISCUSSION

In this study, we perform a critical review of existing literature defining and reporting the incidence of PT in patients who receive hematopoietic stem cell transplant with a myeloablative, TBI-based regimen. In our review, we find that rates of IPS may be as high as 60% with mortality as high as 50%. However, there are significant limitations in the existing literature defining and providing high-level evidence of risk factors for IPS.

Defining IPS

Idiopathic pulmonary toxicity following TBI-based myeloablative transplant is thought to be due to direct injury to type II alveolar epithelial and endothelial cells from cells of lymphoid and myeloid origin as well as by inflammatory stimulators including TNF-α, lipo-polysaccharide, and reactive

TABLE 2 | Study characteristics.

Year (range)		1961-2020
Age (range, years)		<1-68
Conditions Included		
	Benign	10 (10%)
	Malignant	102 (99%)
Transplant Type		
	Autologous	17 (16%)
	Allogeneic	98 (95%)
Chemotherapeutic Backbone		
	Cyclophosphamide	91 (88%)
	Other/NR	12 (12%)
GVHD Prophylaxis		
	MTX	62 (60%)
	Other	14 (13%)
	NR	19 (18%)
	NA	5 (5%)
Rate of Acute Gr II-IV GVHD		7-65%
Definition of Pulmonary Toxicity		
	Interstitial pneumonitis	47 (45%)
Definition of Idiopathic Pulmonary Toxicity		
	Idiopathic interstitial pneumonitis	24 (23%)
Radiographic Criteria		
	Yes	46 (44%)
	No	57 (55%)
Infectious Workup		
	Yes	40 (38%)
	No	63 (61%)
Defined Acute *versus* Late		
	Yes	9 (9%)
	No	94 (91%)
Toxicity Grading Scale		
	None	84 (81%)
	CTCAE	7 (7%)
	RTOG	2 (2%)
	Individualized	10 (10%)

GVHD, graft versus host disease; MTX, methotrexate; NR, not reported; NA, not applicable; Gr, grade.

oxygen species (128–131). In mouse models of IPS, pulmonary toxicity due to host monocytes and donor T cells in the lungs occurs within the first 2 weeks of transplant (128). Increased cytotoxic T lymphocytes result in parenchymal damage and reduced compliance, total lung capacity, and increased wet and dry lung weights. In its advanced stages, IPS is characterized by cellular proliferation and matrix accumulation (132).

A standard clinical definition of IPS has been proposed (133). Criteria include evidence of widespread alveolar injury as evidenced by chest x-ray (CXR) or computed tomography (CT) scan, signs and symptoms of pneumonia, or abnormal pulmonary physiology, absence of active lower respiratory tract infection as diagnosed by BAL, transbronchial biopsy if feasible, and ideally a second confirmatory test to rule out infection. In this report, authors recommended against histopathologic definitions including "interstitial pneumonitis" citing concerns for accuracy. An expanded definition was proposed by the American Thoracic Society in which additional viral, fungal, and bacterial studies as well as evaluation of extra-pulmonary etiologies were recommended (10).

TABLE 3 | Dose and fractionation.

Fractionation	Dose (cGy)	N (%)
Fractionation not reported		19 (15)
	700-1440	1 (1)
	≥800	1 (1)
	≥900	1 (1)
	990-1600	1 (1)
	1000	1 (1)
	1000-1200	1 (1)
	1000-1440	1 (1)
	1000-1500	1 (1)
	1100-1400	1 (1)
	1125-1400	1 (1)
	1200	3 (3)
	1200-1500	1 (1)
	1200-1575	2 (2)
	1300-1375	1 (1)
Single treatment		47 (40)
	400-1505	1 (1)
	550	1 (1)
	550-900	1 (1)
	600	1 (1)
	700-850	1 (1)
	750	1 (1)
	750-900	1 (1)
	800	2 (2)
	800-1000	1 (1)
	950-1300	1 (1)
	900	1 (1)
	920	2 (2)
	1000	33 (28)
	1228-1754	1 (1)
Daily		15 (13)
	800	2 (2)
	900	1 (1)
	990	1 (1)
	1200	11 (9)
	1200-1500	1 (1)
	1400	1 (1)
	1575	3 (3)
Twice daily		58 (49)
	600-1200	1 (1)
	700-1100	1 (1)
	800-1200	1 (1)
	900-1200	1 (1)
	1000-1200	1 (1)
	1000-1320	1 (1)
	1000-1350	1 (1)
	1050-1400	1 (1)
	1100	2 (2)
	1100-1350	1 (1)
	1100-1320	1 (1)
	1200	34 (29)
	1200-1320	2 (2)
	1200-1360	2 (2)
	1200-1400	1 (1)
	1200-1700	1 (1)
	1320	7 (6)
	1320-1440	1 (1)
	1350	4 (3)
	1360	2 (2)
	1400	1 (1)
	1440	5 (4)
	1485	1 (1)
	1530	1 (1)

(Continued)

TABLE 3 | Continued

Fractionation	Dose (cGy)	N (%)
Three times daily		5 (4)
	1200-1610	1 (1)
	1320-1440	1 (1)
	1320	2 (2)
	1440	2 (2)

TABLE 4 | Lung shielding.

Technique or Dose	N (%)
Shielding not reported	27 (23)
No shielding	31 (26)
400cGy mean	1 (1)
500cGy mean	1 (1)
600cGy mean	2 (2)
730cGy mean	1 (1)
750cGy mean	2 (2)
800cGy mean	11 (9)
820cGy mean	1 (1)
850cGy mean	1 (1)
900cGy mean	8 (7)
1000cGy mean	10 (8)
1050cGy mean	4 (3)
1100cGy mean	2 (2)
1200cGy mean	4 (3)
Limit to prescription dose	2 (2)
10% shielding	1 (1)
40% shielding	1 (1)
50% shielding	1 (1)
Bolus/compensators/attenuators/custom blocks	10 (8)
5 HVL single treatment	1 (1)
6 HVL single treatment	2 (2)
7 HVL single treatment	1 (1)
Arms	3 (2)

TABLE 5 | Risk factors for pulmonary toxicity and IPS.

Risk Factors for Pulmonary Toxicity	N (%)
GVHD	14 (26)
Increasing age	9 (20)
Dose rate	7 (13)
CMV	4 (8)
Single fraction TBI	4 (8)
Impaired pre-transplant PFTs	3 (6)
Receipt of TBI	3 (6)
MTX	2 (4)
Performance status	2 (4)
Donor type	2 (4)
Lung dose/Lack of Shielding	2 (4)
Prior chemotherapy	1 (2)
>6 months from diagnosis to transplant	1 (2)
Prior radiation	1 (2)
T lymphocyte depletion	1 (2)
Infection	1 (2)
Non-CR at transplant	1 (2)
Co-60 based TBI	1 (2)
Diagnosis	1 (2)
Cyclosporine	1 (2)
Granulocyte infusion	1 (2)
Number of prior regimens	1 (2)
Graft failure	1 (2)
Year of BMT	1 (2)
AP-PA fields	1 (2)
Body weight	1 (2)
Prone position	1 (2)
Risk Factors for IPS	
Lung dose/Lack of Shielding	2 (10)
Dose rate	2 (10)
Receipt of TBI	2 (10)
Diagnosis	2 (10)
Myeloablative conditioning	1 (5)
CY dose	1 (5)
Anemia	1 (5)
CMV	1 (5)
Impaired pre-transplant PFTs	1 (5)
Parotitis	1 (5)
Single fraction TBI	1 (5)

GVHD, graft versus host disease; TBI, total body irradiation; MTX, methotrexate; CR, complete response; BMT, bone marrow transplant; AP-PA, anterio-posterior posterior-anterior; IPS, idiopathic pulmonary syndrome; CY, cyclophosphamide; CMV, cytomegalovirus.

The studies evaluated for this critical review utilize multiple definitions of PT and IPS. The majority did not distinguish between idiopathic and non-idiopathic pulmonary complications. Of those that did, many relied on a definition of "interstitial pneumonitis" and less than half documented radiographic or other criteria supporting the diagnosis. Given that many studies had limited diagnostic workup, the true incidence of IPS secondary to an inflammatory-mediated process may not be accurately reported. In addition, varying definitions of IPS limit comparisons of the incidence between treatment regimens and evaluation of risk factors for IPS specifically as compared to other infectious pulmonary toxicity.

The working group publications do not make recommendations regarding definitions of acute and late toxicity, which is also reflected in the limited reporting and lack of consensus seen in the studies evaluated. In general, idiopathic pulmonary toxicity is thought to occur early after transplant, historically reported between six to seven weeks, although more recently as early as 19 days (133–135). In their studies, Kim et al. and Gao et al. restricted pulmonary events to those occurring within 90-100 days of transplant based on previous data demonstrating a maximal risk for IPS within the first 100 days of transplantation (77, 110). However, Nagasawa et al. evaluated pulmonary toxicities occurring 3 months or more after HSCT (hematopoietic stem cell transplant) (75). They found a 16% (4/25) incidence of late non-infectious pulmonary toxicities for patients receiving a TBI-based myeloablative regimen, suggesting that late pulmonary complications may occur frequently.

In newer studies using intensity modulated techniques, pulmonary toxicity has been preliminarily evaluated. However, definitions in these publications are also variable. In their study, Shinde et al. rigorously defined radiation pneumonitis as greater than or equal to grade 3 pneumonitis not attributable to infection, graft *versus* host disease, or disease progression as assessed by standard institutional post-HCT protocols including bronchoscopy (136). Others have reported only rates of any pulmonary toxicity without specifying workup or etiology (137, 138).

Recommendations for Definition

We recommend routine adoption of the diagnostic workup and definition of IPS proposed by the American Thoracic Society.

Based on the available literature and previously used definitions we suggest a cutoff of early toxicity within 90 days of transplant and encourage continued patient follow-up for late treatment-related toxicity.

Grading IPS

Toxicity grading scales were not commented on in the working group publications and infrequently utilized in the papers studied for this review. Seven studies relied on CTCAE definitions and two utilized Radiation Therapy Oncology Group (RTOG) definitions (47, 55, 73, 81–83). Five defined toxicity with an individualized scale, one of which utilized the extent of imaging changes on CXR (41, 44, 52, 97). In studies without a grading scale, pulmonary toxicity is most often reported as present and resolved or a cause of mortality. Notably, no patient reported outcomes (PRO) were utilized in these studies, although PRO surveillance using the PRO-CTCAE has been shown to be feasible in the transplant setting (139). Studies using 3D treatment planning have relied on multiple grading scales including CTCAE and Bearman Toxicity Scale for bone marrow transplantation (136–138, 140).

Recommendations for Grading

There is little data to suggest benefit to one grading scale over another. However, given the availability of both provider and patient-reported outcomes, authors encourage consideration of the CTCAE for future toxicity reporting.

Risk Factors for IPS

The studies reporting risk factors for IPS were, in general, lower levels of evidence. Limitations of these publications included heterogeneous diagnoses for which patients may have received previous chemotherapy and/or radiation, wide age ranges, multiple conditioning regimens, approaches to GVHD prophylaxis, and a variety of donor sources which all impact the risk of complications and could not be controlled for in evaluation of risk factors for PT or IPS.

The details of TBI and cytotoxic chemotherapy were not uniformly reported and limit the ability to evaluate safety and efficacy between varying chemotherapy regimens, doses, dose rates, beam arrangements, and shielding techniques. Cytotoxic chemotherapy may result in pneumonitis without the addition of radiation, and few studies provided the regimen and doses of chemotherapy delivered in conjunction with TBI (141). In addition, all studies are limited by the accuracy of true lung dose assessment. The majority of TBI patients are treated with either right and left lateral or AP-PA fields without 3D treatment planning. Details of the techniques have been previously described (51, 142). It is difficult to assess the limiting lung dose, due particularly to inaccuracies in the largely inhomogeneous dose distribution within the lung resulting from the single-point dose calculation model generally used (143, 144). The CT based treatment planning simulation showed a highly inhomogeneous dose distribution from TBI delivery to different organs. The greatest variation in radiation dose in the lung was as much as 32% above that prescribed (145). Therefore, the exact correlation of the single point dose and lung pneumonitis from the reported studies will have to be carefully considered.

In spite of these limitations, some risk features were seen in multiple studies which may inform radiation planning parameters. Dose rate was found to be significantly associated with development of IPS in several non-randomized studies (**Table 6**). Abugideiri et al. evaluated 129 pediatric patients who underwent TBI-based myeloablative conditioning at dose rates from 2.6cGy/min to 20.9cGy/min and found a statistically significant association of dose rate with IPS on multivariate analysis (p=0.002) (69). Gao et al. evaluated 202 patients with acute leukemia at a dose rate from 8.7cGy/min to 19.2cGy/min. Patients treated with high dose rates, defined as >15cGy/min, had a 29% incidence of IPS as compared to 10% in those patients treated with lower dose rates (p<0.01). In a retrospective study of 92 patients with hematolymphoid malignancies treated with 900-1200cGy fractionated TBI, a trend towards decreased toxicity was seen in those treated at a lower dose rate, defined as <6cGy/min (p=0.07) (110). In their analysis, Barrett et al. found that dose rate had an effect on PT only at total lung doses of >900cGy without an effect at lower total doses (80).

Higher lung dose has also been found to be associated with IPS at a range of dose rates (**Table 7**). Weshler et al. evaluated 44 patients with malignant disorders treated with TBI containing myeloablative transplants (30). Their first 23 patients were treated to 1200cGy with fractionated TBI without lung shielding at a dose rate of 15-18cGy/min and found a 26% risk of IPS. The remainder were treated with a 50% transmission lung block at a dose rate of 15cGy/min with no IPS. Petersen et al. performed a phase I dose escalation trial utilizing TBI given at a rate of 8cGy/min in 200cGy fractions twice daily from 1200-1700cGy without lung shielding. They found 50% risk of PT at a dose of 1700cGy as compared to 15% after 1600cGy (87). Sampath et al. similarly evaluated 20 articles to develop a multivariate logistic regression to determine dosimetric and chemotherapeutic factors influencing the incidence of IPS (91). In their analysis, a conditioning regimen of 1200cGy fractionated TBI resulted in an incidence of IPS of 11% as compared to 2.3% with 50% lung shielding (p<0.05) without any effect from dose rate.

New advancements using CT guided intensity modulated TBI or TMI or TMLI allow 3D lung dose distribution to be calculated with high precision (146, 147). Reported rates of pneumonitis are low in spite of dose rates up to 200cGy/min (136, 148). Clinically, a mean lung dose of 800cGy or less has still been associated with decreased risk, suggesting need for further study using 3D planning to understand the relationship between dose rate, mean lung dose, and IPS (136).

There are limited data regarding differences in pulmonary risk and modifications to treatment planning that should be made based on patient age. In many of the studies evaluated, increasing age was found to be a risk factor for pulmonary toxicity. This may be due to worse pre-transplant pulmonary function, which has been found to be a risk factor for IPS (79). However, pediatric patients remain at risk of pulmonary toxicity.

TABLE 6 | Summary of key literature reports on the effect of dose rate and lung dose.

First author, publication year	*N*	Prescribed dose (Gy)/fx	Lung dose (Gy)	Dose rate (cGy/min)	Findings
Barrett, 1982 (80)	402*	7.5-10.5/1	1-12	2.5-46	Dose rate associated with incidence of PT only for lung dose ≥9 Gy.
Bortin, 1982 (95)	176*	≥8	NR	2.3-30	Dose rate ≤5.7 cGy/min associated with lower risk of PT 30% *vs*. 6%)
Weiner, 1986 (19)	932^	10/1 or 12/5-6	5.6-12.8	2-108	Dose rate significantly correlated with risk of PT only in those receiving MTX after transplantation.
Ozsahin, 1996 (43)	186^	10/1 or 12/6 BID	8 or 9	2.6-16.9	PT incidence was significantly higher in the high dose rate patients – 56% (> 9cGy/min) *vs*. 20% (≤4.8 cGy/min).
Corvo, 1999 (89)	93^	12/6 BID	10.8 or 12	2.5-15	PT incidence was correlated with higher dose rate – 33% (>6 cGy/min) *vs*. 12% (<6 cGy/min).
Carruthers, 2004 (53)	84^	12/6	NR	7.5 and 15	A higher dose rate associated with a higher risk of PT - 43% (15 cGy/min) *vs*. 13% (7.5 cGy/min).
Abugideiri, 2016 (69)	129±	10.5-14 (1.5-2 Gy/fx)	≤ 10	5.6-20.9	TBI dose rate ≥15 cGy/min significantly increased incidence of PT [HR 4.85] and IPS [HR 4.94].
Kim, 2018 (17)	92^	9-12/3-4 daily	5-10% attenuation	4.2-17.3	Reducing the dose rate decreased the risk of PT - 74.1% (≥6 cGy/min) *vs*. 43.5% (<6 cGy/min).
Gao, 2019 (77)	202^	13.2/8 BID	None	8.6-19.2	IPS in 29% (>15cGy/min) *vs* 10% (≤15cGy/min).
Petersen, 1992 (87)	36^	12 or 16/6 BID, 17/7 BID	Prescription	8	PT or IPS in 50% of patients receiving 17Gy as compared to 15% after 16Gy.
Sampath, 2005 (91)	1090*	Up to 15.6	Up to 15.6	3-41	Lung dose was associated with PT in patients receiving 1 fx/day – 2.3% if ≤6 Gy to lungs.
Soule, 2007 (57)	181≠	12 or 13.6 (1.5-1.7 Gy/fx bid)	6 to >13.6	12	Lung dose reduction should be employed primarily to decrease mortality from PT in high-risk patients.
Weschler, 1990 (30)	43^	6/4 BID (TLI) or 12/6 BID (TBI)	6 or 12	15-18	IPS occurred in 26% without lung shielding as compared to 0% with partial lung shielding.

*bid, twice a day; fx, fraction; HR, hazard ratio; IP, interstitial pneumonitis; IPS, idiopathic pneumonia syndrome; MTX, methotrexate; NR, not reported; PT, pulmonary toxicity; TBI, total body irradiation; TLI, total lymphoid irradiation; *ages not specified; ^adults and children; ±children; ≠adults and adolescents.*

TABLE 7 | Summary of key literature reports on the effect of lung dose.

First author, publication year	*N*	Prescribed dose (Gy)/fx	Lung dose (Gy)	Dose rate (cGy/min)	Dose rate finding
Petersen, 1992 (87)	36^	12 or 16/6 BID, 17/7 BID	Prescription	8	PT or IPS in 50% of patients receiving 17Gy as compared to 15% after 16Gy.
Sampath, 2005 (91)	1090*	Up to 15.6	Up to 15.6	3-41	Lung dose was associated with PT in patients receiving 1 fx/day – 2.3% if ≤6 Gy to lungs.
Soule, 2007 (57)	181≠	12 or 13.6 (1.5-1.7 Gy/fx bid)	6 to >13.6	12	Lung dose reduction should be employed primarily to decrease mortality from PT in high-risk patients.
Weschler, 1990 (30)	43^	6/4 BID (TLI) or 12/6 BID (TBI)	6 or 12	15-18	IPS occurred in 26% without lung shielding as compared to 0% with partial lung shielding.

*bid, twice a day; fx, fraction; IP, interstitial pneumonitis; IPS, idiopathic pneumonia syndrome; NR, not reported; PT, pulmonary toxicity; TLI: total lymphoid irradiation; *ages not specified; ^ adults and children ≠adults and adolescents.*

In a study of only pediatric patients, increasing dose rate was found to be a risk factor for IPS (69). Similarly, increasing mean lung dose, while not correlated with risk of IPS in any study of only pediatric patients, was correlated with reduced survival (100). TBI using intensity modulated techniques has been reported in children and young adults without any early evidence of increased risks of toxicity (149). However, longer follow up, larger patient numbers, and more comprehensive dosimetric evaluation is needed in order to obtain pediatric-specific planning parameters.

Recommendations for Dose Rate and Shielding

Risk factors for true IPS remain poorly defined given limitations in definitions, workup, and reporting of TBI parameters. A dose rate of ≤15cGy/min and a mean lung dose ≤600cGy using traditional planning techniques is supported by the literature.

Future Directions

As more centers adopt 3D image guided intensity modulated treatment planning for TBI to reduce the lung dose, quantitative knowledge of how dose distribution and lung volume coverage may be correlated with IPS should emerge. Consequently, standard methods of evaluating and reporting pulmonary toxicity will become even more critical. Efforts to adopt the definition and workup for IPS proposed by the NIH and American Thoracic Society are needed in addition to further studies of differences in risk factors and clinical outcomes between pediatric and adult patients and a greater understanding of the contribution of specific chemotherapy regimens to the overall risk. More comprehensive and reliable reporting of TBI dosimetric parameters will provide greater understanding of the range of treatment and planning techniques and their relationship to IPS.

AUTHOR CONTRIBUTIONS

JV, SH, and NE contributed to study design, data analysis, manuscript writing, and manuscript review. C-HH contributed to manuscript review and data presentation. KD, PR, JK, and LC contributed to manuscript review. All authors contributed to the article and approved the submitted version.

FUNDING

The work was partially supported by the National Institutes of Health under R01CA154491 (SH).

SUPPLEMENTARY MATERIAL

The Supplementary Material for this article can be found online at: https://www.frontiersin.org/articles/10.3389/fonc.2021.708906/full#supplementary-material

REFERENCES

1. Barrington-Trimis JL, Cockburn M, Metayer C, Gauderman JW, Wiemels J, McKean-Cowdin R. Trends in Childhood Leukemia Incidence Over Two Decades From 1992 to 2013. *Int J Cancer* (2017) 140:1000–08. doi: 10.1002/ijc.30487
2. Dores GM, Devesa SS, Curtis RE, Linet MS, Morton LM. Acute Leukemia Incidence and Patient Survival Among Children and Adults in the United States, 2001-2007. *Blood* (2012) 119:34–43. doi: 10.1182/blood-2011-04-347872
3. Bunin N, Aplenc R, Kamani N, Shaw K, Cnaan A, Simms S. Randomized Trial of Busulfan *vs* Total Body Irradiation Containing Conditioning Regimens for Children With Acute Lymphoblastic Leukemia: A Pediatric Blood and Marrow Transplant Consortium Study. *Bone Marrow Transplant* (2003) 32:543–48. doi: 10.1038/sj.bmt.1704198
4. Davies SM, Ramsay NK, Klein JP, Weisdorf DJ, Bolwell B, Cahn JY, et al. Comparison of Preparative Regimens in Transplants for Children With Acute Lymphoblastic Leukemia. *J Clin Oncol* (2000) 18:340–47. doi: 10.1200/JCO.2000.18.2.340
5. Eapen M, Raetz E, Zhang MJ, Muehlenbein C, Devidas M, Abshire T, et al. Outcomes After HLA-Matched Sibling Transplantation or Chemotherapy in Children With B-Precursor Acute Lymphoblastic Leukemia in a Second Remission: A Collaborative Study of the Children's Oncology Group and the Center for International Blood and Marrow Tr. *Blood* (2006) 107:4961–97. doi: 10.1182/blood-2005-12-4942
6. Scott BL, Pasquini MC, Logan BR, Wu J, Devine SM, Porter DL, et al. Myeloablative *Versus* Reduced-Intensity Hematopoietic Cell Transplantation for Acute Myeloid Leukemia and Myelodysplastic Syndromes. *J Clin Oncol* (2017) 35:1154–61. doi: 10.1200/JCO.2016.70.7091
7. Mohty M, Labopin M, Volin L, Gratwohl A, Soci G. Reduced-Intensity *Versus* Conventional Myeloablative Conditioning Allogeneic Stem Cell Transplantation for Patients With Acute Lymphoblastic Leukemia: A Retrospective Study From the European Group for Blood and Marrow Transplantation. *Blood* (2010) 116:4439–43. doi: 10.1182/blood-2010-02-266551
8. D'Souza A, Lee S, Zhu X, Pasquini M. Current Use and Trends in Hematopoietic Cell Transplantation in the United States. *Biol Blood Marrow Transplant* (2017) 23:1417–21. doi: 10.1016/j.bbmt.2017.05.035
9. Lichter AS, Tutschka PJ, Wharam MD, Elfenbein GJ, Sensenbrenner LL, Saral R, et al. The Use of Fractionated Radiotherapy as Preparation for Allogeneic Bone Marrow Transplantation. *Transplant Proc* (1979) 11:1492–94.
10. Panoskaltsis-Mortari A, Griese M, Madtes D, Belperio JA, Haddad IY, Folz RJ, et al. An Official American Thoracic Society Research Statement: Noninfectious Lung Injury After Hematopoietic Stem Cell Transplantation: Idiopathic Pneumonia Syndrome. *Am J Respir Crit Care Med* (2011) 183:1262–79. doi: 10.1164/rccm.2007-413ST
11. Shankar G, Cohen DA. Idiopathic Pneumonia Syndrome After Bone Marrow Transplantation: The Role of Pre-Transplant Radiation Conditioning and Local Cytokine Dysregulation in Promoting Lung Inflammation and Fibrosis. *Int J Exp Pathol* (2001) 82:101–13. doi: 10.1111/j.1365-2613.2001.iep182.x
12. Thomas ED, Clift RA, Hersman J, Sanders JE, Stewart P, Buckner CD, et al. Marrow Transplantation for Acute Nonlymphoblastic Leukemia in First Remission Using Fractionated or Single-Dose Irradiation. *IJROBP* (1982) 8:817–21. doi: 10.1016/0360-3016(82)90083-9
13. Thomas ED, Buckner CD, Clift RA, Fefer A, Johnson FL, Neiman PE, et al. Marrow Transplantation for Acute Nonlymphoblastic Leukemia in First Remission. *N Engl J Med* (1979) 301:597–99. doi: 10.1056/NEJM197909133011109
14. Torres JL, Bross DS, Chef LW, Wharam MD, Santos GW, Order SE, et al. Risk Factors in Interstitial Pneumonitis Following Allogenic Bone Marrow Transplantation. *IJROBP* (1982) 8:1031–37. doi: 10.1016/0360-3016(82)90579-X

15. Shank B, Chu FC, Dinsmore R, Kapoor N, Kirkpatrick D, Teitelbaum H, et al. Hyperfractionated Total Body Irradiation for Bone Marrow Transplantation Results in Seventy Leukemia Patients With Allogeneic Transplants. *IJROBP* (1983) 9:1607–11. doi: 10.1016/0360-3016(83)90412-1
16. Parkman R, Rappeport JM, Hellman S, Lipton J, Smith B, Geha R, et al. Busulfan and Total Body Irradiation as Antihematopoietic Stem Cell Agents in the Preparation of Patients With Congenital Bone Marrow Disorders for Allogenic Bone Marrow Transplantation. *Blood* (1984) 64:852–7. doi: 10.1182/blood.V64.4.852.bloodjournal644852
17. Kim TH, Rybka WB, Lehnert S, Podgorsak EB, Freeman CR. Interstitial Pneumonitis Following Total Body Irradiation for Bone Marrow Transplantation Using Two Different Dose Rates. *Int J Radiat Oncol Biol Phys* (1985) 11:1285–91. doi: 10.1016/0360-3016(85)90243-3
18. Sullivan KM, Meyers JD, Flournoy N, Rainer S, Thomas ED. Early and Late Interstitial Pneumonia Following Human Bone Marrow Transplantation. *Int J Cell Cloning* (1986) S:107–21. doi: 10.1002/stem.5530040712
19. Weiner RS, Bortin MM, Gale RP, Gluckman E, Kay HE, Kolb HJ, et al. Interstitial Pneumonitis After Bone Marrow Transplantation. *Ann Internal Med* (1986) 104:168–75. doi: 10.7326/0003-4819-104-2-168
20. Pecego R, Hill R, Appelbaum FR, Bruckner AD, Fefer A, Thomas ED. Interstitial Pneumonitis Following Autologous Bone Marrow Transplantation. *Transplantation* (1986) 42:515–17. doi: 10.1097/00007890-198611000-00015
21. Deeg HJ, Sullivan KM, Buckner CD, Storb R, Appelbaum FR, Clift RA, et al. Marrow Transplantation for Acute Nonlymphoblastic Leukemia in First Remission: Toxicity and Long-Term Follow-Up of Patients Conditioned With Single Dose or Fractionated Total Body Irradiation. *Bone Marrow Transplant* (1986) 1:151–7.
22. Cordonnier C, Bernaudin JF, Bierling P, Huet Y, Vernant JP. Pulmonary Complications Occurring After Allogeneic Bone Marrow Transplantation. A Study of 130 Consecutive Transplanted Patients. *Cancer* (1986) 58:1047–54. doi: 10.1002/1097-0142(19860901)58:5<1047::AID-CNCR2820580512>3.0.CO;2-Y
23. Dinsmore R, Kirkpatrick D, Flomenberg N, Gulati S, Kapoor N, Brochstein J, et al. Allogeneic Bone Marrow Transplantation for Patients With Acute Nonlymphocytic Leukemia. *Blood* (1984) 63:649–56. doi: 10.1182/blood.V63.3.649.649
24. Dinsmore R, Kirkpatrick D, Flomenberg N, Gulati S, Kapoor N, Shank B, et al. Allogeneic Bone Marrow Transplantation for Patients With Acute Lymphoblastic Leukemia. *Blood* (1983) 62:381–8. doi: 10.1182/blood.V62.2.381.381
25. Barrett A, Depledge MH, Powles RL. Interstitial Pneumonitis Following Bone Marrow Transplantation After Low Dose Rate Total Body Irradiation. *IJROBP* (1983) 9:1029–33. doi: 10.1016/0360-3016(83)90393-0
26. Sutedja TG, Apperley JF, Hughes JM, Aber VR, Kennedy HG, Nunn P, et al. Pulmonary Function After Bone Marrow Transplantation for Chronic Myeloid Leukaemia. *Thorax* (1988) 43:163–9. doi: 10.1136/thx.43.3.163
27. Thomas ED, Buckner CD, Banaji M, Clift RA, Fefer A, Flournoy N, et al. One Hundred Patients With Acute Leukemia Treated by Chemotherapy, Total Body Irradiation, and Allogeneic Marrow Transplantation. *Blood* (1977) 49:511–33. doi: 10.1182/blood.V49.4.511.511
28. Wingard JR, Mellits ED, Sostrin MB, Chen DY, Burns WH, Santos GW, et al. Interstitial Pneumonitis After Allogeneic Bone Marrow Transplantation. *Med (United States)* (1988) 67:175–86. doi: 10.1097/00005792-198805000-00004
29. Kim TH, McGlave PB, Ramsay N, Woods W, Bostrom B, Vercellotti G, et al. Comparison of Two Total Body Irradiation Regimens in Allogeneic Bone Marrow Transplantation for Acute Non-Lymphoblastic Leukemia in First Remission. *IJORBP* (1990) 19:889–97. doi: 10.1016/0360-3016(90)90009-9
30. Weshler Z, Breuer R, Or R, Naparstek E, Pfeffer MR, Lowental E, et al. Interstitial Pneumonitis After Total Body Irradiation: Effect of Partial Lung Shielding. *BJHaem* (1990) 74:61–4. doi: 10.1111/j.1365-2141.1990.tb02538.x
31. Socie G, Devergie A, Girinisky T, Reiffers J, Vernant JP, Le Bourgeois JP, et al. Influence of the Fractionation of Total Body Irradiation on Complications and Relapse Rate for Chronic Myelogenous Leukemia. The Group d'Etude Des Greffes De Moelle Osseus (GEGBM). *IJORBP* (1991) 20:397–404. doi: 10.1016/0360-3016(91)90048-9
32. Blaise D, Maraninchi D, Archimbaud E, Reiffers J, Devergie A, Jouet JP, et al. Allogeneic Bone Marrow Transplantation for Acute Myeloid Leukemia in First Remission: A Randomized Trial of a Busulfan-Cytoxan *Versus* Cytoxan-Total Body Irradiation as Preparative Regimen: A Report From the Groupe d'Etudes De La Greffe De Moelle Osseuse. *Blood* (1992) 79:2578–82. doi: 10.1182/blood.V79.10.2578.2578
33. Gonga NK, Morgan G, Downs K, Atkinson K, Biggs J. Lung Dose Rate and Interstitial Pneumonitis in Total Body Irradiation for Bone Marrow Transplantation. *Australas Radiol* (1992) 36:317–20. doi: 10.1111/j.1440-1673.1992.tb03208.x
34. Labar B, Bogdanic V, Nemet D, Mrsic M, Vrtar M, Grgic-Markulin L, et al. Total Body Irradiation With or Without Lung Shielding for Allogeneic Bone Marrow Transplantation. *Bone Marrow Transplant* (1992) 9:343–7.
35. Ozsahin M, Pne F, Touboul E, et al. Total-Body Irradiation Before Bone Marrow Transplantation. Results of Two Randomized Instantaneous Dose Rates in 157 Patients. *Cancer* (1992) 69:2853–65. doi: 10.1002/1097-0142(19920601)69:11<2853::AID-CNCR2820691135>3.0.CO;2-2
36. Appelbaum FR, Meyers JD, Fefer A, et al. Nonbacterial Nonfungal Pneumonia Following Marrow Transplantation in 100 Identical Twins. *Transplantation* (1982) 33:265–8. doi: 10.1097/00007890-198203000-00011
37. Granena A, Carreras E, Rozman C, Salgado C, Sierra J, Algara M, et al. Interstitial Pneumonitis After BMT: 15 Years Experience in a Single Institution. *Bone Marrow Transplant* (1993) 11:453–8.
38. Sutton L, Kuentz M, Cordonnier C, Blaise D, Devergie A, Guyotat D, et al. Allogeneic Bone Marrow Transplantation for Adult Acute Lymphoblastic Leukemia in First Complete Remission: Factors Predictive of Transplant-Related Mortality and Influence of Total Body Irradiation Modalities. *Bone Marrow Transplant* (1993) 12:583–9.
39. Valls A, Algara M, Marrugat J, Carreras E, Sierra J, Graena A. Risk Factors for Early Mortality in Allogeneic Bone Marrow Transplantation. A Multivariate Analysis on 174 Leukaemia Patients. *Eur J Cancer* (1993) 29:1523–8. doi: 10.1016/0959-8049(93)90287-P
40. Clift RA, Buckner CD, Thomas ED, Bryant E, Anasetti C, Bensinger WI, et al. Marrow Transplantation for Chronic Myeloid Leukemia: A Randomized Study Comparing Cyclophosphamide and Total Body Irradiation With Busulfan and Cyclophosphamide. *Blood* (1994) 84:2036–43. doi: 10.1182/blood.V84.6.2036.bloodjournal8462036
41. Demirer T, Petersen FB, Appelbaum FR, Barnett TA, Sanders J, Deeg HJ, et al. Allogeneic Marrow Transplantation Following Cyclophosphamide and Escalating Doses of Hyperfractionated Total Body Irradiation in Patients With Advanced Lymphoid Malignancies: A Phase I II Trial. *Int J Radiat Oncol Biol Phys* (1995) 32:1103–9. doi: 10.1016/0360-3016(95)00115-F
42. Morgan TL, Falk PM, Kogut N, Shah KH, Tome M, Kagan AR. A Comparison of Single-Dose and Fractionated Total-Body Irradiation on the Development of Pneumonitis Following Bone Marrow Transplantation. *IJROBP* (1996) 36:61–6. doi: 10.1016/S0360-3016(96)00246-5
43. Ozsahin M, Belkacmi Y, Pène F, Laporte J, Rio B, Leblond V, et al. Interstitial Pneumonitis Following Autologous Bone-Marrow Transplantation Conditioned With Cyclophosphamide and Total-Body Irradiation. *IJROBP* (1996) 34:71–7. doi: 10.1016/0360-3016(95)02063-2
44. Kantrow SP, Hackman RC, Boeckh M, Myerson D, Crawford SW. Idiopathic Pneumonia Syndrome: Changing Spectrum of Lung Injury After Marrow Transplantation. *Transplantation* (1997) 63:1079–86. doi: 10.1097/00007890-199704270-00006
45. Abraham R, Chen C, Tsang R, Simpson D, Murray C, Davidson M, et al. Intensification of the Stem Cell Transplant Induction Regimen Results in Increased Treatment-Related Mortality Without Improved Outcome in Multiple Myeloma. *Bone Marrow Transplant* (1999) 24:1291–7. doi: 10.1038/sj.bmt.1702060
46. Girinsky T, Benhamou E, Bourhis JH, Dhermain F, Guillot-Valls D, Ganansia V, et al. Prospective Randomized Comparison of Single-Dose *Versus* Hyperfractionated Total-Body Irradiation in Patients With Hematologic Malignancies. *J Clin Oncol* (2000) 18:981–6. doi: 10.1200/JCO.2000.18.5.981
47. Sobecks RM, Daugherty CK, Hallahan DE, Laport GF, Wagner ND, Larson RA. A Dose Escalation Study of Total Body Irradiation Followed by High-Dose Etoposide and Allogeneic Blood Stem Cell Transplantation for the Treatment of Advanced Hematologic Malignancies. *Bone Marrow Transplant* (2000) 25:807–13. doi: 10.1038/sj.bmt.1702230

48. Bieri S, Helg C, Chapuis B, Miralbell R. Total Body Irradiation Before Allogeneic Bone Marrow Transplantation: Is More Dose Better? *Int J Radiat Oncol Biol Phys* (2001) 49:1071–7. doi: 10.1016/S0360-3016(00)01491-7
49. Chen CI, Abraham R, Tsang R, Crump M, Keating A, Stewart AK. Radiation-Associated Pneumonitis Following Autologous Stem Cell Transplantation: Predictive Factors, Disease Characteristics and Treatment Outcomes. *Bone Marrow Transplant* (2001) 27:177–82. doi: 10.1038/sj.bmt.1702771
50. Gopal R, Ha CS, Tucker SL, Khouri IF, Giralt SA, Gajewski JL, et al. Comparison of Two Total Body Irradiation Fractionation Regimens With Respect to Acute and Late Pulmonary Toxicity. *Cancer* (2001) 92:1949–58. doi: 10.1002/1097-0142(20011001)92:7<1949::AID-CNCR1714>3.0.CO;2-1
51. Thomas O, Mahé MA. Long-Term Complications of Total Body Irradiation in Adults. *Int J Radiat Oncol Biol Phys* (2001) 49:125–31. doi: 10.1016/S0360-3016(00)01373-0
52. Lohr F, Wenz F, Schraube P, Flentje M, Haas R, Zierhut D, et al. Lethal Pulmonary Toxicity After Autologous Bone Marrow Transplantation/Peripheral Blood Stem Cell Transplantation for Hematological Malignancies. *Radiotherapy Oncol* (1998) 48:45–1. doi: 10.1016/S0167-8140(98)00045-0
53. Carruthers SA, Wallington MM. Total Body Irradiation and Pneumonitis Risk: A Review of Outcomes. (2004) 90:2080–4. doi: 10.1038/sj.bjc.6601751
54. Savani BN, Srinivasan R. Chronic GVHD and Pretransplantation Abnormalities in Pulmonary Function Are the Main Determinants Predicting Worsening Pulmonary Function in Long-Term Survivors After Stem Cell Transplantation. *Biol Blood Marrow Transplant* (2006) 12:1261–9. doi: 10.1016/j.bbmt.2006.07.016
55. Kornguth DG, Mahajan A, Woo S, Chan KW, Antolak J, Ha CS. Fludarabine Allows Dose Reduction for Total Body Irradiation in Pediatric Hematopoietic Stem Cell Transplantation. *Int J Radiat Oncol Biol Phys* (2007) 68:1140–4. doi: 10.1016/j.ijrobp.2007.01.003
56. Soejima T, Hirota S, Tsujino K, Yoden E, Fujii O, Ichimiya Y, et al. Total Body Irradiation Followed by Bone Marrow Transplantation: Comparison of Once-Daily and Twice-Daily Fractionation Regimens. *Radiat Med - Med Imaging Radiat Oncol* (2007) 25:402–6. doi: 10.1007/s11604-007-0157-z
57. Soule BP, Simone NL, Savani BN, Ning H, Albert PS, Barrett AJ, et al. Pulmonary Function Following Total Body Irradiation (With or Without Lung Shielding) and Allogeneic Peripheral Blood Stem Cell Transplant. *Bone Marrow Transplant* (2007) 40:573–8. doi: 10.1038/sj.bmt.1705771
58. Kennedy-Nasser AA, Bollard CM, Myers GD, Leung KS, Gottschalk S, Zhang Y, et al. Comparable Outcome of Alternative Donor and Matched Sibling Donor Hematopoietic Stem Cell Transplant for Children With Acute Lymphoblastic Leukemia in First or Second Remission Using Alemtuzumab in a Myeloablative Conditioning Regimen. *Biol Blood Marrow Transplant* (2008) 14:1245–52. doi: 10.1016/j.bbmt.2008.08.010
59. Neiman PE, Thomas ED, Reeves WC, Ray CG, Sale G, Lerner KG, et al. Opportunistic Infection and Interstitial Pneumonia Following Marrow Transplantation for Aplastic Anemia and Hematologic Malignancy. *Transplant Proc* (1976) 8:663–7.
60. Fujimaki K, Tanaka M, Takasaki H, Hyo R, Kawano T, Sakai R, et al. Thiotepa/Cyclophosphamide/TBI as a Conditioning Regimen for Allogeneic Hematopoietic Stem Cell Transplantation in Patients Aged 50 Years and Over. *Internal Med* (2008) 47:379–83. doi: 10.2169/internalmedicine.47.0598
61. Buckner CD, Clift RA, Thomas D, Sanders JE, Stewart PS, Storb R, et al. Allogeneic Marrow Transplantation for Acute Non-Lymphoblastic Leukemia in Relapse Using Fractionated Total Body Irradiation. *Leukemia Res* (1982) 6:389–94. doi: 10.1016/0145-2126(82)90102-3
62. Wang HX, Yan HM, Wang ZD, Xue M, Liu J, Guo ZK. Haploidentical Hematopoietic Stem Cell Transplantation in Hematologic Malignancies With G-CSF Mobilized Bone Marrow Plus Peripheral Blood Stem Cells Grafts Without T Cell Depletion: A Single Center Report of 29 Cases. *Leukemia Lymphoma* (2012) 53:654–9. doi: 10.3109/10428194.2011.624225
63. Li DZ, Kong PY, Sun JG, Wang XX, Li GH, Zhou YB, et al. Comparison of Total Body Irradiation Before and After Chemotherapy in Pretreatment for Hematopoietic Stem Cell Transplantation. *Cancer Biother Radiopharm* (2012) 27:119–23. doi: 10.1089/cbr.2011.1041
64. Bhatnagar B, Rapoport AP, Fang HB, Ilyas C, Marangoz D, Akbulut V, et al. Single Center Experience With Total Body Irradiation and Melphalan (TBI-MEL) Myeloablative Conditioning Regimen for Allogeneic Stem Cell Transplantation (SCT) in Patients With Refractory Hematologic Malignancies. *Ann Hematol* (2014) 93:653–60. doi: 10.1007/s00277-013-1908-9
65. Park J, Choi EK, Kim JH, Lee SW, Song SY, Yoon SM, et al. Effects of Total Body Irradiation-Based Conditioning on Allogeneic Stem Cell Transplantation for Pediatric Acute Leukemia: A Single-Institution Study. *Br J Cancer* (2014) 32:198–207. doi: 10.3857/roj.2014.32.3.198
66. Motohashi K, Fujisawa S, Onizuka M, Kako S, Sakaida E, Shono K, et al. Effects of the Order of Administration of Total Body Irradiation and Cyclophosphamide on the Outcome of Allogeneic Hematopoietic Cell Transplantation. *Blood* (2014) 124:3900. doi: 10.1182/blood.V124.21.3900.3900
67. Peters C, Matthes-Martin S, Poetschger U, Schrappe M, Schrauder A. Stem-Cell Transplantation in Children With Acute Lymphoblastic Leukemia:a Prospective International Multicenter Trial Comparing Sibling Donors With Matched Unrelated Donors-the ALL-SCT-BFM-2003 Trial. *J Clin Oncol* (2015) 33:1265–74. doi: 10.1200/JCO.2014.58.9747
68. Madden LM, Ngwube AI, Shenoy S, Druley TE, Hayashi RJ. Late Toxicity of a Novel Allogeneic Stem Cell Transplant Using Single Fraction Total Body Irradiation for Hematologic Malignancies in Children. *J Pediatr Hematol/Oncol* (2015) 37:e94–101. doi: 10.1097/MPH.0000000000000272
69. Abugideiri M, Nanda RH, Butker C, Zhang C, Kim S, Chiang KY, et al. Factors Influencing Pulmonary Toxicity in Children Undergoing Allogeneic Hematopoietic Stem Cell Transplantation in the Setting of Total Body Irradiation-Based Myeloablative Conditioning. *IJROBP* (2016) 94:349–59. doi: 10.1016/j.ijrobp.2015.10.054
70. Chiang Y, Tsai CH, Kuo SH, Liu CY, Yao M, Li CC, et al. Reduced Incidence of Interstitial Pneumonitis After Allogeneic Hematopoietic Stem Cell Transplantation Using a Modified Technique of Total Body Irradiation. *Sci Rep* (2016) 6:36730.
71. Ishibashi N, Maebayashi T, Sakaguchi M, Aizawa T, Saito T, Tanaka Y. Prospective Study of Total Body Irradiation as Pretreatment for Hematopoietic Stem Cell Transplantation. *Int J Radiat Oncol Biol Phys* (2014) 90:S682–83. doi: 10.1016/j.ijrobp.2014.05.2006
72. Ujaimi RK, Isfahanian N, Russa DJ, Samant R, Bredeson C, Genest P. Pulmonary Toxicity Following Total Body Irradiation for Acute Lymphoblastic Leukaemia: The Ottawa Hospital Cancer Centre (TOHCC) Experience. *J Radiother Pract* (2016) 15:54–60. doi: 10.1017/S1460396915000497
73. Stephens SJ, Thomas S, Rizzieri DA, Horwitz ME, Chao NJ, Engemann AM, et al. Myeloablative Conditioning With Total Body Irradiation for AML: Balancing Survival and Pulmonary Toxicity. *Adv Radiat Oncol* (2016) 1:272–80. doi: 10.1016/j.adro.2016.07.001
74. Byun HK, Yoon HI, Cho JH, Kim HJ, Cho Y, Suh CO. Factors Associated With Pulmonary Toxicity After Myeloablative Conditioning Using Total Body Irradiation. *Int J Radiat Oncol Biol Phys* (2017) 99:E179. doi: 10.1016/j.ijrobp.2017.06.1625
75. Nagasawa N, Mitsuiki N, Aoki Y, Ono T, Isoda T, Imai K, et al. Effect of Reduced-Intensity Conditioning and the Risk of Late-Onset Non-Infectious Pulmonary Complications in Pediatric Patients. *Eur J Haematol* (2017) 99:525–31. doi: 10.1111/ejh.12967
76. Gooptu M, Kim HT, Ho VT, Alyea EP, Koreth J, Armand P, et al. A Comparison of the Myeloablative Conditioning Regimen Fludarabine/Busulfan With Cyclophosphamide/Total Body Irradiation, for Allogeneic Stem Cell Transplantation in the Modern Era: A Cohort Analysis. *Biol Blood Marrow Transplant* (2018) 24:1733–40. doi: 10.1016/j.bbmt.2018.03.011
77. Gao RW, Weisdorf DJ, DeFor TE, Ehler E, Dusenbery KE. Influence of Total Body Irradiation Dose Rate on Idiopathic Pneumonia Syndrome in Acute Leukemia Patients Undergoing Allogeneic Hematopoietic Cell Transplantation. *Int J Radiat Oncol Biol Phys* (2019) 103:180–9. doi: 10.1016/j.ijrobp.2018.09.002
78. Sabloff M, Chhabra S, Wang T, Fretham C, Kekre N, Abraham A, et al. Comparison of High Doses of Total Body Irradiation in Myeloablative Conditioning Before Hematopoietic Cell Transplantation. *Biol Blood Marrow Transplant* (2019) 25:2398–407.

79. Wenger DS, Triplette M, Crothers K, Cheng GS, Hill JA, Milano F, et al. Incidence, Risk Factors, and Outcomes of Idiopathic Pneumonia Syndrome After Allogeneic Hematopoietic Cell Transplantation. *Biol Blood Marrow Transplant* (2020) 26:413–20. doi: 10.1016/j.bbmt.2019.09.034
80. Barrett A. Total Body Irradiation (TBI) Before Bone Marrow Transplantation in Leukaemia: A Co-Operative Study From the European Group for Bone Marrow Transplantation. *Br J Radiol* (1982) 55:562–7. doi: 10.1259/0007-1285-55-656-562
81. Oya N, Sasai K, Tachiiri S, Sakamoto T, Nagata Y, Okada T, et al. Influence of Radiation Dose Rate and Lung Dose on Interstitial Pneumonitis After Fractionated Total Body Irradiation: Acute Parotitis may Predict Interstitial Pneumonitis. *Int J Hematol* (2006) 83:86–91. doi: 10.1532/IJH97.05046
82. Kelsey CR, Horwitz ME, Chino JP, Craciunescu O, Steffey B, Folz RJ, et al. Severe Pulmonary Toxicity After Myeloablative Conditioning Using Total Body Irradiation: An Assessment of Risk Factors. *Int J Radiat Oncol Biol Phys* (2011) 81:812–8. doi: 10.1016/j.ijrobp.2010.06.058
83. De Felice F, Grapulin L, Musio D, Pomponi J, DI Felice C, Iori AP, et al. Treatment Complications and Long-Term Outcomes of Total Body Irradiation in Patients With Acute Lymphoblastic Leukemia: A Single Institute Experience. *Anticancer Res* (2016) 36:4859–64. doi: 10.21873/anticanres.11049
84. Brochstein JA, Kernan NA, Groshen S, Cirrincione C, Shank B, Emanuel D, et al. Allogeneic Bone Marrow Transplantation After Hyperfractionated Total-Body Irradiation and Cyclophosphamide in Children With Acute Leukemia. *N Engl J Med* (1987) 37:1618–24. doi: 10.1056/NEJM198712243172602
85. Clift RA. Allogeneic Marrow Transplantation Using Fractionated Total Body Irradiation in Patients With Acute Lymphoblastic Leukemia in Relapse. *Leukemia Res* (1982) 6:401–7. doi: 10.1016/0145-2126(82)90104-7
86. Resbeut M, Cowen D, Blaise D, Gluckman E, Cosset JM, Rio B, et al. Fractionated or Single-Dose Total Body Irradiation in 171 Acute Myeloblastic Leukemias in First Complete Remission: Is There a Best Choice? *Int J Radiat Oncol Biol Phys* (1995) 3:509–17. doi: 10.1016/0360-3016(94)00446-R
87. Petersen FB, Deeg HJ, Buckner CD, Appelbaum FR, Storb R, Clift RA, et al. Marrow Transplantation Following Escalating Doses of Fractionated Total Body Irradiation and Cyclophosphamide-a Phase I Trial. *Int J Radiat Oncol Biol Phys* (1992) 23:1027–32. doi: 10.1016/0360-3016(92)90909-2
88. Ringdn O, Ruutu T, Remberger M, Nikoskelainen J, Volin L, Vindelov L, et al. A Randomized Trial Comparing Busulfan With Total Body Irradiation as Conditioning in Allogeneic Marrow Transplant Recipients With Leukemia: A Report From the Nordic Bone Marrow Transplantation Group. *Blood* (1994) 83:2723–30. doi: 10.1182/blood.V83.9.2723.bloodjournal8392723
89. Corvo R, Paoli G, Barra S. Total Body Irradiation Correlates With Chronic Graft *Versus* Host Disease and Affects Prognosis of Patients With Acute Lymphoblastic Leukemia Receiving an HLA Identical Allogeneic Bone Marrow Transplant. *Int J Radiat Oncol Biol Phys* (1999) 43:497–503. doi: 10.1016/S0360-3016(98)00441-6
90. Huisman C, van der Straaten HM. Pulmonary Complications After T-Cell-Depleted Allogeneic Stem Cell Transplantation: Low Incidence and Strong Association With Acute Graft-*Versus*-Host Disease. *Bone Marrow Transplant* (2006) 38:561–6. doi: 10.1038/sj.bmt.1705484
91. Sampath S, Schultheiss TE, Wong J. Dose Response and Factors Related to Interstitial Pneumonitis After Bone Marrow Transplant. *Int J Radiat Oncol Biol Phys* (2005) 63:876–84. doi: 10.1016/j.ijrobp.2005.02.032
92. Thomas ED, Herman EC, Greenough WB, Hager EB, Cannon JH, Sahler OD, et al. Irradiation and Marrow Infusion in Leukemia. *Arch Internal Med* (1961) 107:95–111. doi: 10.1001/archinte.1961.03620060029006
93. Blume KG, Beutler E, Bross KJ, Chillar RK, Ellington OB, Fahey JL, et al. Bone-Marrow Ablation and Allogeneic Marrow Transplantation in Acute Leukemia. *N Engl J Med* (1980) 302:1041–6. doi: 10.1056/NEJM198005083021901
94. Winston DJ, Gale RP, Meyer DV, Young LS. Infectious Complications of Human Bone Marrow Transplantation. *Medicine* (1979) 58:1–31. doi: 10.1097/00005792-197901000-00001
95. Bortin MN, Kay HEM, Gale RP, Rimm AA. Factors Associated With Interstitial Pneumonitis After Bone Marrow Transplantation for Acute Leukaemia. *Lancet* (1982) 20:437–9. doi: 10.1016/S0140-6736(82)91633-6
96. Cosset JM, Baume D, Pico JL, Shank B, Girinski T, Benhamou E, et al. Single Dose *Versus* Hyperfractionated Total Body Irradiation Before Allogeneic Bone Marrow Transplantation: A Non-Randomized Comparative Study of 54 Patients at the Institut Gustave-Roussy. *Radiother Oncol* (1989) 174:92–104. doi: 10.1016/0167-8140(89)90129-1
97. Bearman SI, Appelbaum FR, Buckner CD, Petersen FB, Fisher LD, Clift RA, et al. Regimen-Related Toxicity in Patients Undergoing Bone Marrow Transplantation. *J Clin Oncol* (1988) 6:1562–8. doi: 10.1200/JCO.1988.6.10.1562
98. Volpe AD, Ferreri AJM, Annaloro C, Mangili P, Rosso A, Calandrino R, et al. Lethal Pulmonary Complications Significantly Correlate With Individually Assessed Mean Lung Dose in Patients With Hematologic Malignancies Treated With Total Body Irradiation. *Int J Radiat Oncol Biol Phys* (2002) 52:483–8. doi: 10.1016/S0360-3016(01)02589-5
99. Gore EM, Lawton CA, Ash RC, Lipchik RJ. Pulmonary Function Changes in Long-Term Survivors of Bone Marrow Transplantation. *Int J Radiat Oncol Biol Phys* (1996) 36:67–75. doi: 10.1016/S0360-3016(96)00123-X
100. Esiashvili N, Lu X, Ulin K, Laurie F, Kessel S, Kalapurakal JA, et al. Higher Reported Lung Dose Received During Total Body Irradiation for Allogeneic Hematopoietic Stem Cell Transplantation in Children With Acute Lymphoblastic Leukemia Is Associated With Inferior Survival: A Report From the Children's Oncology Group. *Int J Radiat Oncol Biol Phys* (2019) 104:513–21. doi: 10.1016/j.ijrobp.2019.02.034
101. Neiman P, Wasserman PB, Wentworth BB, Kao GF, Lerner KG, Storb R, et al. Interstitial Pneumonia and Cytomegalovirus Infection as Complications of Human Marrow Transplantation. *Transplantation* (1973) 15:478–85. doi: 10.1097/00007890-197305000-00011
102. Clift RA, Buckner CD, Appelbaum FR, Bryant E, Bearman SI, Petersen FB, et al. Allogeneic Marrow Transplantation in Patients With Chronic Myeloid Leukemia in the Chronic Phase: A Randomized Trial of Two Irradiation Regimens. *Blood* (1991) 77:1660–5. doi: 10.1182/blood.V77.8.1660.bloodjournal7781660
103. Le Bourgeois J, Vernant J, Thiellet A. Unusual Incidence of Localized Pneumonitis After Total Body Irradiation for Bone Marrow Transplantation. *Exp Hematol* (1984) S:12–23.
104. Ozsahin M, Schwartz LH, Pene F, Touboul E, Schlienger M, Laugier A. Is Body Weight a Risk Factor of Interstitial Pneumonitis After Bone Marrow Transplantation? *Bone Marrow Transplant* (1992) 10:97.
105. Gluckman E, Devergie A, Dutreix A, Dutreix J, Boiron M, Bernard J. Total Body Irradiation in Bone Marrow Transplantation. Hopital Saint-Louis Results. *Pathologie Biologie* (1979) 27:349–52.
106. Speck B, Cornu P, Nissen C, Gratwohl A, Sartorius J. The Basel Experience With Total Body Irradiation for Conditioning Patients With Acute Leukemia for Allogeneic Bone Marrow Transplantation. *Pathologie Biologie* (1979) 27:353–5.
107. Brunvand MW, Bensinger WI, Soll E, Weaver CH, Rowley SD, Appelbaum FR, et al. High-Dose Fractionated Total-Body Irradiation, Etoposide and Cyclophosphamide for Treatment of Malignant Lymphoma: Comparison of Autologous Bone Marrow and Peripheral Blood Stem Cells. *Bone Marrow Transplant* (1996) 18:131–41.
108. Neiman PE, Reeves W, Ray G, Flournoy N, Lerner KG, Sale GE, et al. A Prospective Analysis of Interstitial Pneumonia and Opportunistic Viral Infection Among Recipients of Allogeneic Bone Marrow Grafts. *J Infect Dis* (1977) 136:754–67. doi: 10.1093/infdis/136.6.754
109. Singh AK, Karimpour SE, Savani BN, Guion P, Hope AJ, Mansueti JR, et al. Pretransplant Pulmonary Function Tests Predict Risk of Mortality Following Fractionated Total Body Irradiation and Allogeneic Peripheral Blood Stem Cell Transplant. *Int J Radiat Oncol Biol Phys* (2006) 66:520–7. doi: 10.1016/j.ijrobp.2006.05.023
110. Kim DY, Kim IH, Yoon SS, Kang HJ, Shin HY, Kang HC. Effect of Dose Rate on Pulmonary Toxicity in Patients With Hematolymphoid Malignancies Undergoing Total Body Irradiation. *Radiat Oncol* (2018) 13:180. doi: 10.1186/s13014-018-1116-9
111. Faraci M, Barra S, Cohen A, Lanino E, Grisolia F, Miano M, et al. Very Late Nonfatal Consequences of Fractionated TBI in Children Undergoing Bone Marrow Transplant. *Int J Radiat Oncol Biol Phys* (2005) 63:1568–75. doi: 10.1016/j.ijrobp.2005.04.031
112. Bredeson C, Le-Rademacher J, Zhu X, Burkart J, Kato K, Armstrong E, et al. Improved Survival With Intravenous Busulfan (IV BU) Compared to Total

Body Irradiation (TBI)-Based Myeloablative Conditioning Regimens: A Cibmtr Prospective Study. *Biol Blood Marrow Transplant* (2013) 19:S110–1. doi: 10.1016/j.bbmt.2012.11.030

113. Lucchini G, Labopin M, Beohou E, Dalissier A, Dalle JH, Cornish J, et al. Impact of Conditioning Regimen on Outcomes for Children With Acute Myeloid Leukemia Undergoing Transplantation in First Complete Remission. An Analysis on Behalf of the Pediatric Disease Working Party of the European Group for Blood and Marrow Transplant. *Biol Blood Marrow Transplant* (2017) 23:467–74. doi: 10.1016/j.bbmt.2016.11.022
114. Holter-Chakrabarty JL, Pierson N, Zhang MJ, Zhu X, Akpek G, Aljurf MD, et al. The Sequence of Cyclophosphamide and Myeloablative Total Body Irradiation in Hematopoietic Cell Transplantation for Patients With Acute Leukemia. *Biol Blood Marrow Transplant* (2015) 21:1251–7. doi: 10.1016/j.bbmt.2015.03.017
115. Kebriaei P, Anasetti C, Zhang MJ, Wang HL, Aldoss I, de Lima M, et al. Intravenous Busulfan Compared With Total Body Irradiation Pretransplant Conditioning for Adults With Acute Lymphoblastic Leukemia. *Biol Blood marrow Transplant* (2018) 24:726–33. doi: 10.1016/j.bbmt.2017.11.025
116. Arai Y, Aoki K, Takeda J, Kondo T, Eto T, Ota S, et al. Clinical Significance of High-Dose Cytarabine Added to Cyclophosphamide/Total-Body Irradiation in Bone Marrow or Peripheral Blood Stem Cell Transplantation for Myeloid Malignancy. *J Hematol Oncol* (2015) 8:102. doi: 10.1186/s13045-015-0201-x
117. Linsenmeier C, Thoennessen D, Negretti L, Bourquin JP, Streller T, Lütolf UM, et al. Total Body Irradiation (TBI) in Pediatric Patients: A Single-Center Experience After 30 Years of Low-Dose Rate Irradiation. *Strahlentherapie und Onkologie* (2010) 186:614–20. doi: 10.1007/s00066-010-2089-2
118. Freycon F, Casagranda L, Trombert-Paviot B. The Impact of Severe Late-Effects After 12 Gy Fractionated Total Body Irradiation and Allogeneic Stem Cell Transplantation for Childhood Leukemia (1988-2010). *Pediatr Hematol Oncol* (2019) 36:86–102. doi: 10.1080/08880018.2019.1591549
119. Harden SV, Routsis DS, Geater AR, Thomas SJ, Coles C, Taylor PJ, et al. Total Body Irradiation Using a Modified Standing Technique: A Single Institution 7 Year Experience. *Br J Radiol* (2001) 74:1041–7. doi: 10.1259/bjr.74.887.741041
120. Veys P, Wynn RF, Ahn KW, Samarasinghe S, He W, Bonney D, et al. Impact of Immune Modulation With *in Vivo* T-Cell Depletion and Myleoablative Total Body Irradiation Conditioning on Outcomes After Unrelated Donor Transplantation for Childhood Acute Lymphoblastic Leukemia. *Blood* (2012) 119:6155–61.
121. Sakellari I, Gavriilaki E, Chatziioannou K, Papathanasiou M, Mallouri D, Batsis I, et al. Long-Term Outcomes of Total Body Irradiation Plus Cyclophosphamide *Versus* Busulfan Plus Cyclophosphamide as Conditioning Regimen for Acute Lymphoblastic Leukemia: A Comparative Study. *Ann Hematol* (2018) 97:1987–94. doi: 10.1007/s00277-018-3383-9
122. Tseng YD, Stevenson PA, Cassaday RD, Cowan A, Till BG, Shadman M, et al. Total Body Irradiation Is Safe and Similarly Effective as Chemotherapy-Only Conditioning in Autologous Stem Cell Transplantation for Mantle Cell Lymphoma. *Biol Blood Marrow Transplant* (2018) 24:282–7. doi: 10.1016/j.bbmt.2017.10.029
123. Yoshimi A, Nannya Y, Sakata-Yanagimoto M, Oshima K, Takahashi T, Kanda Y, et al. A Myeloablative Conditioning Regimen for Patients With Impaired Cardiac Function Undergoing Allogeneic Stem Cell Transplantation: Reduced Cyclophosphamide Combined With Etoposide and Total Body Irradiation. *Am J Hematol* (2008) 83:635–9. doi: 10.1002/ajh.21208
124. Küenkele A, Engelhard M, Hauffa BP, Mellies U, Müntjes C, Hüer C, et al. Long-Term Follow-Up of Pediatric Patients Receiving Total Body Irradiation Before Bone Marrow Transplantation. *Pediatr Blood Cancer* (2013) 60:1792–7. doi: 10.1002/pbc.24702
125. Saglio F, Zecca M, Pagliara D, Giorgiani G, Balduzzi A, Calore E, et al. Occurrence of Long-Term Effects After Hematopoietic Stem Cell Transplantation in Children Affected by Acute Leukemia Receiving Either Busulfan or Total Body Irradiation: Results of an AIEOP (Associazione Italiana Ematologia Oncologia Pediatrica) Retrospe. *Bone Marrow Transplant* (2020) 55:1918–27. doi: 10.1038/s41409-020-0806-8
126. Belkacemi Y, Labopin M, Giebel S, Miszyk L, Loganadane G, Michallet M, et al. Fractionated-TBI Schedules Prior to Allograft: Study From the Acute Leukemia Working Party (EBMT). *Radiother Oncol* (2017) 123:S17–8. doi: 10.1016/S0167-8140(17)30486-3
127. Litzow MR, Prez WS, Klein JP, Bolwell BJ, Camitta B, Copelan EA, et al. Comparison of Outcome Following Allogeneic Bone Marrow Transplantation With Cyclophosphamide-Total Body Irradiation *Versus* Busulphan-Cyclophosphamide Conditioning Regimens for Acute Myelogenous Leukaemia in First Remission. *Br J Haematol* (2002) 119:1115–24. doi: 10.1046/j.1365-2141.2002.03973.x
128. Panoskaltsis-Mortari A, Taylor PA, Yaeger TM. The Criticla Early Proinflammatory Events Associated With Idiopathic Pneumonia Syndrome in Irradiated Murine Allogeneic Recipients Are Due to Donor T Cell Infusion and Potentiated by Cyclophosphamide. *J Clin Investigations* (1997) 100:1015–27. doi: 10.1172/JCI119612
129. Cooke KR, Kobzik L, Martin TR, Brewer J, Delmonte J Jr, Crawford JM, et al. An Experimental Model of Idiopathic Pneumonia Syndrome After Bone Marrow Transplantation: 1. The Roles of Minor H Antigens and Endotoxin. *Blood* (1996) 88:3230–39. doi: 10.1182/blood.V88.8.3230.bloodjournal8883230
130. Janin A, Deschaumes C, Daneshpouy M, Estaquier J, Micic-Polianski J, Rajagopalan-Levasseur P, et al. CD95 Engagement Induces Disseminated Endothelial Cell Apoptosis *in Vivo*: Immunopathologic Implications. *Blood* (2002) 99:2940–7. doi: 10.1182/blood.V99.8.2940
131. Panoskaltsis-Mortari A, Hermanson JR, Haddad IY, Wangensteen OD, Blazar BR. Intercellular Adhesion Molecule-I (ICAM-I, CD54) Deficiency Segregates the Unique Pathophysiological Requirements for Generating Idiopathic Pneumonia Syndrome (IPS) *Versus* Graft-*Versus*-Host Disease Following Allogeneic Murine Bone Marrow Transplantation. *Biol Blood Marrow Transplant* (2001) 7:368–77. doi: 10.1053/bbmt.2001.v7.pm11529486
132. Goldstein RH. Control of Type I Collagen Formation in the Lung. *Am J Physiol* (1991) 261:L29–40. doi: 10.1152/ajplung.1991.261.2.L29
133. Clark JG, Hansen JA, Hertz MI, Parkman R, Jensen L, Peavy HH. Idiopathic Pneumonia Syndrome After Bone Marrow Transplantation. *Am Rev Respir Dis* (1993) 147:1601–06. doi: 10.1164/ajrccm/147.6_Pt_1.1601
134. Fukuda T, Hackman RC, Guthrie KA, Sandmaier BM, Boeckh M, Maris MB, et al. Risks and Outcomes of Idiopathic Pneumonia Syndrome After Nonmyeloablative and Conventional Conditioning Regimens for Allogeneic Hematopoietic Stem Cell Transplantation. *Blood* (2003) 102:2777–85. doi: 10.1182/blood-2003-05-1597
135. Keates-Baleeiro J, Moore P, Koyama T, Manes B, Calder C, Frangoul H. Incidence and Outcome of Idiopathic Pneumonia Syndrome in Pediatric Stem Cell Transplant Recipients. *Bone Marrow Transplant* (2006) 38:285–9. doi: 10.1038/sj.bmt.1705436
136. Shinde A, Yang D, Frankel P, Liu A, Han C, Del Vecchio B, et al. Radiation-Related Toxicities Using Organ Sparing Total Marrow Irradiation Transplant Conditioning Regimens. *Int J Radiat Oncol Biol Phys* (2019) 105:1025–33. doi: 10.1016/j.ijrobp.2019.08.010
137. Stein A, Palmer J, Tasi NC, Malki MM, Aldoss I, Ali H, et al. Phase I Trial of Total Marrow and Lymphoid Irradiation Transplantation Conditioning in Patients Wtih Relapsed/Refractory Acute Leukemia. *Biol Blood Marrow Transplant* (2017) 23:618–24. doi: 10.1016/j.bbmt.2017.01.067
138. Wong J, Forman S, Somlo G, Rosenthal J, Liu A, Schultheiss T, et al. Dose Escalation of Total Marrow Irradiation With Concurrent Chemotherapy in Patients With Advanced Acute Leukemia Undergoing Allogeneic Hematopoietic Cell Transplantation. *Int J Radiat Oncol Biol Phys* (2013) 84:148–56. doi: 10.1016/j.ijrobp.2012.03.033
139. Wood WA, Deal AM, Abernethy A, Basch E, Battaglini C, Kim YH, et al. Feasibility of Frequent Patient-Reported Outcome Surveillance in Patients Undergoing Hematopoietic Cell Transplantation. *Blood Marrow Transplant* (2013) 19:450–59. doi: 10.1016/j.bbmt.2012.11.014
140. Rosenthal J, Wong J, Stein A, Qian D, Hitt D, Naeem H, et al. Phase 1/2 Trial of Total Marrow and Lymph Node Irradiation to Augment Reduced-Intensity Transplantation for Advanced Hematologic Malignancies. *Blood* (2010) 117:309–15. doi: 10.1182/blood-2010-06-288357
141. Wong R, Rondon G, Saliiba RM, Shannon VR, Giralt SA, Champlin RE, et al. Idiopathic Pneumonia Syndrome After High-Dose Chemotherapy and Autologous Hematopoietic Stem Cell Transplantation for High-Risk Breast Cancer. *Bone Marrow Transplant* (2003) 31:1157–63. doi: 10.1038/sj.bmt.1704141
142. Dusenbery KE, Gerbi BJ. Total Body Irradiation Conditioning Regimens in Stem Cell Transplantation. In: Levitt SH, Purdy JA, editors. *Technical Basis of Radiation Therapy. Medical Radiology (Radiation Oncology)*. Berlin, Heidelberg: Springer (2006).

143. Briot E, Dutreix A, Bridier A. Dosimetry for Total Body Irradiation. *Radiother Oncol* (1990) 18:16–29. doi: 10.1016/0167-8140(90)90175-V
144. Planskoy B, Bedford AM, Davis FM, Tapper PD, Loverock LT. Physical Aspects of Total-Body Irradiation at the Middlesex Hospital (UCL Group of Hospitals), London 1988-1993: I. Phantom Measurements and Planning Methods. *Phys Med Biol* (1996) 41:2307–26. doi: 10.1088/0031-9155/41/11/005
145. Hui SK, Das RK, Thomadsen B, Henderson D. CT-Based Analysis of Dose Homogeneity in Total Body Irradiation Using Lateral Beam. *J Appl Clin Med Phys* (2004) 5:71–9. doi: 10.1120/jacmp.2022.25311
146. Hui SK, Kapatoes J, Fowler J, Henderson D, Olivera G, Manon RR, et al. Feasibility Study of Helical Tomotherapy for Total Body or Total Marrow Irradiation. *Med Phys* (2005) 32:3214–24. doi: 10.1118/1.2044428
147. Dandapani SV, Wong JYC. Modern Total Body Irradiation (Tbi): Intensity-Modulated Radiation Treatment (IMRT). In: Wong J, Hui S, editors. *Total Marrow Irradiation*. Cham: Springer (2020).
148. Sarradin V, Simon L, Huynh A, Gilhods J, Filleron T, Izar F. Total Body Irradiation Using Helical Tomotherapy: Treatment Technique, Dosimetric Results, and Initial Clinical Experience. *Cancer Radiother* (2018) 22:17–24. doi: 10.1016/j.canrad.2017.06.014
149. Gruen A, Ebell W, Wlodarczyk W, Neumann O, Kuehl JS, Stromberger C, et al. Total Body Irradiation Using Helical Tomotherapy in Children and Young Adults Undergoing Stem Cell Transplantation. *Radiat Oncol* (2013) 8:92. doi: 10.1186/1748-717X-8-92

Conflict of Interest: The authors declare that the research was conducted in the absence of any commercial or financial relationships that could be construed as a potential conflict of interest.

Publisher's Note: All claims expressed in this article are solely those of the authors and do not necessarily represent those of their affiliated organizations, or those of the publisher, the editors and the reviewers. Any product that may be evaluated in this article, or claim that may be made by its manufacturer, is not guaranteed or endorsed by the publisher.

frontiers in Oncology

ORIGINAL RESEARCH
published: 16 December 2021
doi: 10.3389/fonc.2021.785916

Optimized Conformal Total Body Irradiation Among Recipients of TCRαβ/CD19-Depleted Grafts in Pediatric Patients With Hematologic Malignancies: Single-Center Experience

Daria Kobyzeva[1†], Larisa Shelikhova[2†], Anna Loginova[1†], Francheska Kanestri[1†], Diana Tovmasyan[1†], Michael Maschan[2†], Rimma Khismatullina[2], Mariya Ilushina[2], Dina Baidildina[3], Natalya Myakova[4] and Alexey Nechesnyuk[1†]*

[1] Department of Radiation Oncology, Dmitry Rogachev National Research Center of Pediatric Hematology, Oncology and Immunology, Moscow, Russia, [2] Department of Hematopoietic Cell Transplantation, Dmitry Rogachev National Research Center of Pediatric Hematology, Oncology and Immunology, Moscow, Russia, [3] Department of Pediatric Hematology and Oncology, Dmitry Rogachev National Research Center of Pediatric Hematology, Oncology and Immunology, Moscow, Russia, [4] Department of Onco-hematology, Dmitry Rogachev National Research Center of Pediatric Hematology, Oncology and Immunology, Moscow, Russia

OPEN ACCESS

Edited by:
Jeffrey Wong,
City of Hope National Medical Center,
United States

Reviewed by:
Chunhui Han,
City of Hope National Medical Center,
United States
Savita Dandapani,
City of Hope National Medical Center,
United States

***Correspondence:**
Daria Kobyzeva
daria.kobyzeva@gmail.com

[†]These authors have contributed equally to this work

Specialty section:
This article was submitted to Radiation Oncology, a section of the journal Frontiers in Oncology

Received: 29 September 2021
Accepted: 15 November 2021
Published: 16 December 2021

Citation:
Kobyzeva D, Shelikhova L, Loginova A, Kanestri F, Tovmasyan D, Maschan M, Khismatullina R, Ilushina M, Baidildina D, Myakova N and Nechesnyuk A (2021) Optimized Conformal Total Body Irradiation Among Recipients of TCRαβ/CD19-Depleted Grafts in Pediatric Patients With Hematologic Malignancies: Single-Center Experience. Front. Oncol. 11:785916. doi: 10.3389/fonc.2021.785916

Total body irradiation (TBI) in combination with chemotherapy is widely used as a conditioning regimen in pediatric and adult hematopoietic stem cell transplantation (HSCT). The combination of TBI with chemotherapy has demonstrated superior survival outcomes in patients with acute lymphoblastic and myeloid leukemia when compared with conditioning regimens based only on chemotherapy. The clinical application of intensity-modulated radiation therapy (IMRT)-based methods (volumetric modulated arc therapy (VMAT) and TomoTherapy) seems to be promising and has been actively used worldwide. The optimized conformal total body irradiation (OC-TBI) method described in this study provides selected dose reduction for organs at risk with respect to the most significant toxicity (lungs, kidneys, lenses). This study included 220 pediatric patients who received OC-TBI with subsequent chemotherapy and allogenic HSCT with TCRαβ/CD19 depletion. A group of 151 patients received OC-TBI using TomoTherapy, and 40 patients received OC-TBI using the Elekta Synergy™ linac with an Agility-MLC (Elekta, Crawley, UK) using volumetric modulated arc therapy (VMAT). Twenty-nine patients received OC-TBI with supplemental simultaneous boost to bone marrow—(SIB to BM) up to 15 Gy: 28 patients (pts)—TomoTherapy; one patient—VMAT. The follow-up duration ranged from 0.3 to 6.4 years (median follow-up, 2.8 years). Overall survival (OS) for all the patients was

63% (95% CI: 56–70), and event-free survival (EFS) was 58% (95% CI: 51–65). The cumulative incidence of transplant-related mortality (TRM) was 10.7% (95% CI: 2.2–16) for all patients. The incidence of early TRM (<100 days) was 5.0% (95% CI: 1.5–8.9), and that of late TRM (>100 days) was 5.7 (95% CI: 1.7–10.2). The main causes of death for all the patients were relapse and infection. The concept of OC-TBI using IMRT VMAT and helical treatment delivery on a TomoTherapy treatment unit provides maximum control of the dose distribution in extended targets with simultaneous dose reduction for organs at risk. This method demonstrated a low incidence of severe side effects after radiation therapy and predictable treatment effectiveness. Our initial experience demonstrates that OC-TBI appears to be a promising technique for the treatment of pediatric patients.

Keywords: TBI, IMRT, total body irradiation, Total marrow and lymphoid irradiation, acute leukemia, pediatric patients, boost to bone marrow, TomoTherapy

INTRODUCTION

Total body irradiation (TBI) in combination with chemotherapy is widely used worldwide as a conditioning regimen prior to transplanting hematopoietic stem cells in patients with malignant hematological diseases.

The main benefits of TBI include tumor cell elimination and general immunosuppressive effects. The combination of TBI with chemotherapy has demonstrated superior survival results in patients with acute lymphoblastic and myeloid leukemia when compared with conditioning regimens, including chemotherapy alone (1–7). However, TBI-based regimens show significant disadvantages for intermediate and long-term toxicity, especially pulmonary toxicity (up to 33% incidence of grade 3+) (8, 9). The incidence of pneumonitis after TBI-conditioning regimens varies, covering a range of 10.3%–45%, and it depends on many factors, such as patient characteristics and treatment technique (10–12). For many years, conventional techniques using low-dose rates (5–15 cGy/min) and lung shielding have historically been a method of choice for TBI treatment (13–16). The irradiation of healthy organs and tissues with high radiosensitivity, such as the lungs and kidneys, may occasionally bring about lethal side effects (8, 11, 17). The disadvantage of the conventional TBI treatment technique is the lack of sparing organs at risk (OARs), with the exception of the lungs. In addition, there is no capability to measure the dose in a small voxel volume and to create dose/volume histograms (DVHs) for the planning target volume (PTV) and OARs to correlate toxicities with received radiation doses.

The clinical application of modern radiotherapy methods, such as intensity-modulated radiation therapy (IMRT), as well as the feasibility of irradiation of extended targets with helical TomoTherapy, have been investigated for TBI and total bone marrow and lymphoid irradiation (TMLI) in adult patients (18–21). However, the number of reports on the application of these methods for the treatment of pediatric patients remains limited (22–25).

In our center, pediatric patients with hematologic malignancies receive TCR-alpha/beta-depleted grafts to minimize the incidence of GVHD and to achieve fast immune reconstitution after HSCT (26–28).

Our goal was to develop and implement the optimized conformal total body irradiation (OC-TBI) method in pediatric practice as a part of the patient conditioning protocol prior to allogeneic bone marrow transplantation (29, 30). The OC-TBI method described in this study provides reproducible dose reduction for OARs that are prone to significant radiotoxicity (lungs, kidneys, lenses).

The main objective of OC-TBI is to irradiate the PTV with maximum homogeneity with simultaneous dose reduction to the critical organs with planning and treatment optimization based on the age of pediatric patients.

We present initial experience and results of implementing the new TomoTherapy- and VMAT-based OC-TBI method in pediatric practice and the toxicity and survival rates in TCRαβ/CD19-depleted graft recipients.

The IMRT-based OC-TBI method provides the opportunity to deliver additional doses to sanctuary sites (i.e., bone marrow, extramedullary sites) to improve radiation treatment effectiveness for advanced patients (30, 31).

We also report outcomes for patients with refractory leukemia who received local dose escalation (boost) to bone marrow.

MATERIALS AND METHODS

Patient Characteristics

Two hundred and twenty (220) patients underwent optimized conformal IMRT-based total body irradiation (OC-TBI) in a myeloablative conditioning regimen at the Radiotherapy Department of the Dmitriy Rogachev National Medical Research Center of Pediatric Hematology, Oncology and Immunology in Moscow, Russia between July 2012 and September 2020. Radiation therapy was followed by chemotherapy and allogenic HSCT with TCRαβ/CD19 depletion. The majority of the patients had ALL (n = 165). All patients were included in the respective high-risk groups. Detailed patient characteristics are presented in **Table 1**. All the data were retrieved from the patients' medical records.

Immediately after OC-TBI treatment, the patients received chemotherapy according to the different schedules. Conditioning

regimens, donor type, and graft composition details are provided in **Table 1**.

Twenty-nine patients (13%) (19 with active disease prior to HSCT) received radiation treatment with simultaneous integrated boost to bone marrow (SIB to BM) with doses up to 15 Gy followed by chemotherapy in accordance with an individual schedule based on unfavorable performance status and/or the etiology of the main disease.

The study was approved by the local ethics committee of the Dmitriy Rogachev National Medical Research Center for Pediatric Hematology, Oncology and Immunology, in accordance with the Helsinki Declaration, and patients and/or their legal guardians provided informed consent to participate in the study.

Radiation Therapy Preparation

CT Simulation

Our Radiation Therapy Department is equipped with one TomoTherapy™, Accuray Inc. (Sunnyvale, CA, USA) and two Elekta Synergy™ treatment units with an Agility-MLC (Elekta) and one CT scanner—GE LightSpeed RT16.

Approximately 1 week prior to the treatment, all the patients underwent CT simulation using individualized fixation. The patients were immobilized in the supine position, laid in vacuum bags for body and extremity fixation, and used thermoplastic masks for head and neck fixation, as shown in **Figure 1**.

Following patient fixation, planning CT images were acquired using slice thicknesses of 5 mm. Patients taller than 115 cm were scanned twice. The first scan included the upper part of the body down to the knee joints, and the second scan included legs from the toes up to the upper third of the thigh. A fiducial marker was placed in the middle of the thigh to assist in determining the juncture between the two images.

Thirty-two patients (15%) of younger ages underwent both CT simulation and radiotherapy treatment under general anesthesia.

TABLE 1 | Patient and treatment characteristics.

Patients	(*n* = 220)
Sex	
Male	151 (69%)
Female	69 (31%)
Median (range) age at TBI (year)	10.2 (3.0–21.0)
Disease	
ALL	165 (75%)
T-cell ALL	*63 (38% of ALL)*
B-cell ALL	*102 (62% of ALL)*
AML	25 (11%)
Other (NHL, biphenotypic/bilineal leukemia, JMML)	30 (14%)
Disease status at transplantation	
ALL	
CR 1	44 (27%)
CR 2	86 (52%)
≥CR 3	23 (14%)
Active disease	12 (7%)
AML	
CR 2/3	5 (20%)
Active disease	20 (80%)
Others	
CR 1	9 (30%)
CR 2/3	14 (47%)
Active disease	7 (23%)
Conditioning regimens	
OC-TBI 12 Gy	220 (100%)
SIB to BM up to 15 Gy	*29 (13%)*
Fludarabine	220 (100%)
Thiotepa	164 (74%)
VP-16	49 (22%)
Donor characteristics	
Type of donor	
Haplo-	192 (88%)
MSD	14 (6%)
MUD	14 (6%)
Cell dose infused, median (range)	
$CD34^+$ cells × 106/kg	9.21 (0.9–15.64)
$\alpha\beta^+$ T cells × 103/kg	35.6 (4.3–377.2)

ALL, acute lymphoblastic leukemia; AML, acute myeloid leukemia; NHL, non-Hodgkin lymphoma; JMML, juvenile myelomonocytic leukemia; CR, complete remission; OC-TBI, Optimized Conformal Total Body Irradiation; SIB to BM, simultaneous integrated boost to bone marrow; VP-16, etoposide; MSD, matched sibling donor; MUD, matched unrelated donor.

Dose Prescription

Monaco 5.11 (Elekta Inc.) MIM Maestro™ software was used to contour the target and OAR volumes.

The lungs, kidneys, and lenses were selected as critical organs based on reported literature data (4, 6, 8–11, 32–35).

The PTV included the patient's whole body minus critical structures (OARs). The following structures were created: external body contour, PTV (consisting of body without skin with 3 mm inner margin), eyes, lenses, lungs, and kidneys.

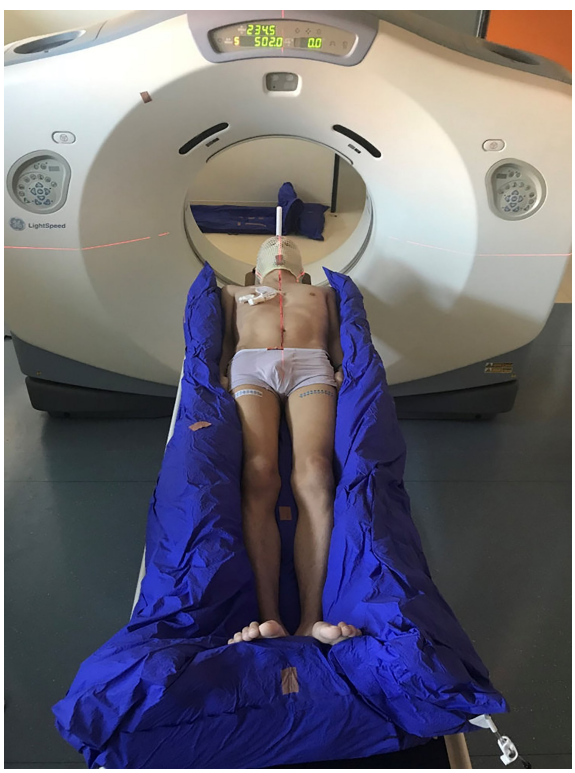

FIGURE 1 | CT simulation using a vacuum bag for body and extremity fixation and a thermoplastic mask for head and neck fixation.

In cases when the patient's body height exceeded 115 cm, the total body volume was divided into two planning target volumes —PTV_Body and PTV_Legs.

Additional contours were defined in support of treatment planning tasks. For dose control between eyes (small children have part of the brain located in this area), we additionally created the contour named the "forehead area" (**Figure 2**).

Ribs were contoured as an additional target volume within the PTV and with a set-prescribed Dmin for better control of steeply decreasing dose gradient in the area between lungs and PTV.

For the TomoTherapy patients, a virtual volume of 1 cm thickness was added to the PTV as an additional target (PTV+1 cm) and was used to account for the patient's motion and breathing while providing the required dose to the skin (**Figure 2**). For the Elekta patients, we used the Monaco 5.11 (Elekta inc., UK, Crawley) Auto-Flash option with a 1-cm margin.

For the patients who received SIB to BM, the contoured addition structure PTV_1500 included all skeletal bones. Treatment volume for skeletal bones in the case of SIB was created without additional margin.

The prescribed total dose for the PTV was 12 Gy delivered in single fractions of 2.0 Gy or 3.0 Gy. The prescribed total doses for OAR are given in **Table 2**.

We established targeted and acceptable values for all the structures with the objective of optimizing treatment planning and plan optimization procedures (**Table 2**).

TREATMENT PLANNING AND RESULTS

TomoTherapy 4.5 (Accuray Inc., Sunnyvale, CA, USA) and Monaco 5.11 (Elekta Inc.) planning systems were used for treatment planning. The received results with standard deviations after calculation of the treatment plans are presented in **Table 3**.

The separate treatment plan was created for PTV_Legs in feet-first rotate position with the 5-cm "juncture area" between "body" and "legs" treatment volumes for helical TomoTherapy patients.

Average dose volume histograms (DVHs) calculated for the 151 patients treated using TomoTherapy and 40 patients treated using VMAT are shown in **Figure 3**.

All VMAT-based plans were created using multi-isocenters technique. The treatment isocenters are set up on separate parts of the PTV_Body (head, chest, abdomen, pelvis). The isocenter number was from 4 to 9 and correlated with patient's height. For PTV_Legs in Elekta patients, we used two different strategies: for small patients (105–145 cm), we used VMAT technique with two treatment isocenters, and for bigger patients (from 145 cm), we used several IMRT beams with static gantry position and couch rotation to 90°/270°.

Average DVHs for the patients who received SIB to BM (TomoTherapy: 28 patients; Elekta VMAT: one patient) are presented, and the treatment plan with dose distributions for PTV_1200 (TBI) and PTV_1500 (TMI) is shown in **Figure 4**.

DOSIMETRIC QA

Quality assurance included absolute dosimetry for each treatment plan using dose measurements with an ionization chamber (ExtraDIN IND Chambers, A1SL), 8-chanel electrometer (Tomo Elektrometer from Standart Imaging) and tissue equivalent phantom (Cheese Phantom). For the VMAT-based plans, individual checks included composite measurements of the two-dimensional dose distributions using an array of ionization chambers MatriXX (IBA Dosimetry).

RADIATION THERAPY TREATMENT CHARACTERISTICS

Fractionation

The treatment was carried out daily, with the fractions given twice a day with an interfraction interval of 5–6 h over 3 days (group 1). Since April 2020, we have revised the fractionation schedule and reduced the number of treatment sessions to minimize patient/staff contact due to COVID-19. The new treatment schedule included one treatment session per day

FIGURE 2 | Anatomical differences in "forehead area" in the example of **(A)** 5- and **(B)** 14-year-old patients.

TABLE 2 | Dose prescriptions with "target" and "acceptable" values.

Structure	Target value	Acceptable value
PTV	Mean dose (12 Gy) ± 2%	Mean dose (12 Gy) ± 5%
	D98% >11.4 Gy	D95% >11.4 Gy
	D2% <13 Gy	D5% <13 Gy
Forehead	D98% >11.4 Gy	D95% >11.4 Gy
	D2% <13 Gy	D5% <13 Gy
Ribs	D95% >10 Gy	D90% >10 Gy
Lungs	D99% >6 Gy	D90% > 6Gy
	V8 <40%	V8 <40%
Kidneys	Dmean <8 Gy	Dmean < 8Gy
Lenses	As low as achievable	

TABLE 3 | Treatment plan calculation results.

Structure	TomoTherapy (*n* = 151) Dose ± SD or %	VMAT Elekta (*n* = 40) Dose ± SD or %
PTV (Dmean)	12.05 ± 0.05	12.16 ± 0.12
Lung_L (Dmean)	7.88 ± 0.12	7.62 ± 0.14
Lung_R (Dmean)	7.84 ± 0.13	7.57 ± 0.14
Lung_L (V8)	37.55 ± 3.82	38.81 ± 2.79
Lung_R (V8)	36.52 ± 3.96	38.45 ± 2.66
Kidney_L (Dmean)	7.44 ± 0.42	7.31 ± 0.35
Kidney_R (Dmean)	7.49 ± 0.45	7.40 ± 0.29
Ribs (Dmean)	11.21 ± 0.12	11.62 ± 0.21
Lens_L	6.23 ± 0.55	6.13 ± 0.55
Lens_R	6.10 ± 0.75	6.30 ± 0.51
Forehead/Brain	12.01 ± 0.04	12.32 ± 0.09

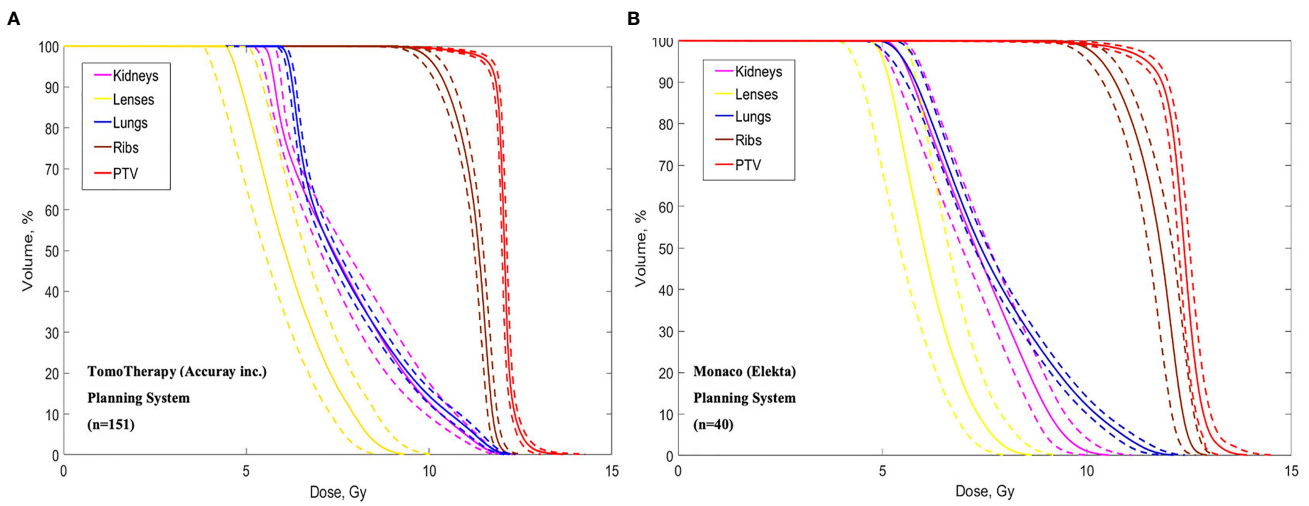

FIGURE 3 | Dose volume histograms calculated in the TomoTherapy **(A)** and Monaco **(B)** Planning systems. Dotted lines show standard deviations.

with a single dose of 3.0 Gy (group 2). Radiobiology modeling supposes that increased dose-per-fraction is associated with higher normal tissue toxicity (36). To determine the effect of this new fractionation schedule, we calculated DVHs using a linear quadratic model using different alpha/beta values with the help of MIM Maestro™ to assess the influence of increased single doses for organs at risk (lungs, kidneys). The increased single dose did not significantly affect the prescribed dose values for the lungs and kidneys (**Figure 5**).

Treatment Procedure

Positioning was verified prior to each treatment session using megavoltage (MV) CTs and cone-beam (CB)-CTs with subsequent corrections of the setup errors.

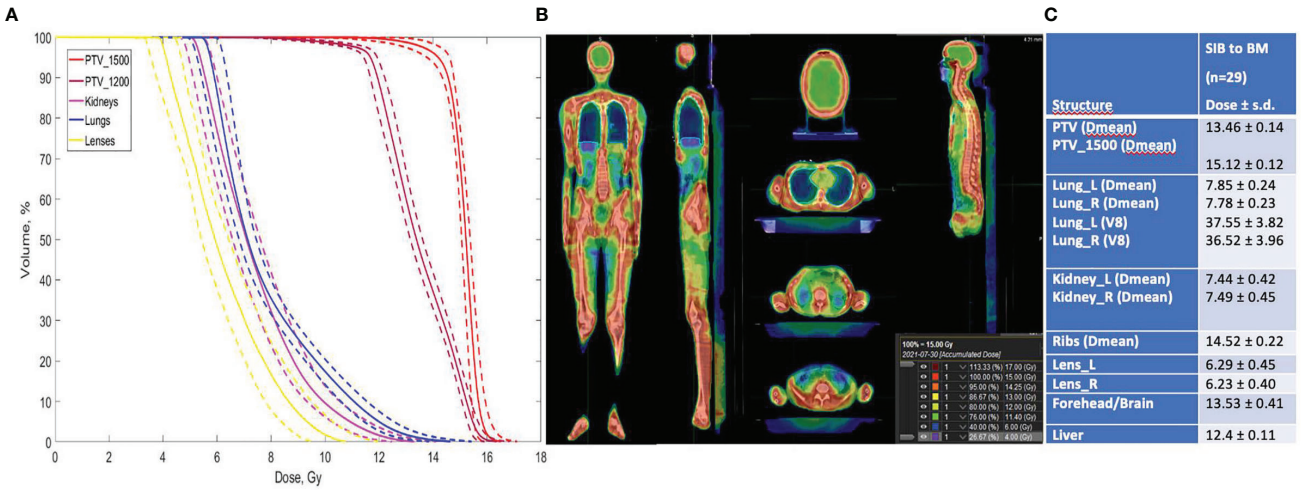

Structure	SIB to BM (n=29) Dose ± s.d.
PTV (Dmean)	13.46 ± 0.14
PTV_1500 (Dmean)	15.12 ± 0.12
Lung_L (Dmean)	7.85 ± 0.24
Lung_R (Dmean)	7.78 ± 0.23
Lung_L (V8)	37.55 ± 3.82
Lung_R (V8)	36.52 ± 3.96
Kidney_L (Dmean)	7.44 ± 0.42
Kidney_R (Dmean)	7.49 ± 0.45
Ribs (Dmean)	14.52 ± 0.22
Lens_L	6.29 ± 0.45
Lens_R	6.23 ± 0.40
Forehead/Brain	13.53 ± 0.41
Liver	12.4 ± 0.11

FIGURE 4 | **(A)** Dose volume histograms in the TomoTherapy and Monaco (Elekta) Planning System for pts with SIB to BM (n = 29). Dotted lines show standard deviations. **(B)** Treatment plan for TBI + SIB to BM, calculated in TPS TomoTherapy (Accuray Inc.) Planning System. **(C)** Treatment plan calculation results.

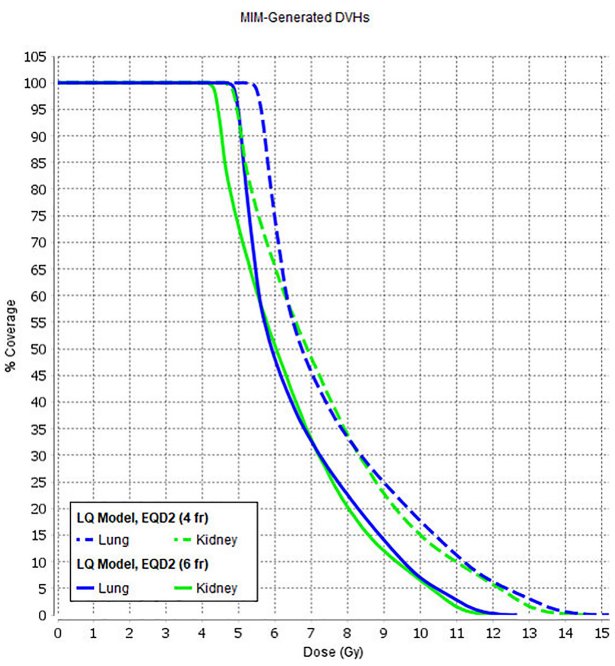

FIGURE 5 | Lung and kidney DVH variations with a linear quadratic model using different alpha/beta values.

The dose delivery time ranged from 16 to 50 min (average 30 min) and was dependent on the patient's height. Dose delivery times were approximately the same for both the TomoTherapy and VMAT approaches. Total treatment time, including imaging and patient setup, was significantly different for the two methods, with up to 60 min for TomoTherapy and up to 90 min for VMAT.

Radiation therapy treatment was held with a 24-h intravenous infusion (Sodium Chloride 0,9% + sodium bicarbonate—125 ml/h). All the patients received preventive antivomiting prescription (antagonist of the 5-HT3 receptors: 4–8 mg, dexamethasone: 4–6 mg) once per day.

STATISTICAL ANALYSIS

Statistical analysis was performed using XLSTAT (Addinsoft, 2021) software.

Two hundred and twenty patients who received OC-TBI and underwent allogenic HSCT with TCRαβ/CD-19 depletion were included in the final analysis. Overall survival (OS) and event-free survival (EFS) were calculated using the Kaplan-Meier method. OS was defined as the probability of survival, regardless of disease status, from the time of TBI to the time of death or of the last follow-up (surviving patients were censored at the last follow-up, whereas only death from any cause was considered an event). The following events were considered for EFS: death from any cause, relapse and progression of the main disease (patients with advanced disease). We calculated transplant-related mortality (TRM) and relapse according to the competing risk model, where these two events were considered to be mutually competitive.

RADIATION-INDUCED TOXICITY EVALUATION AND RESULTS

We followed up patients for acute toxicity (nausea/vomiting/diarrhea, headache, veno-occlusive disease (VOD))—during radiation therapy and 30 days after SCT, subacute toxicity (IP)

—up to the 100th day after SCT and late toxicity in the lungs and kidneys—for at least 100 days after SCT in accordance with the RTOG/EORTC scale (37).

Acute Toxicity: Results

Acute toxicity during radiation therapy was expressed in nausea and vomiting and headache, symptoms of parotitis and enteritis. We observed a correlation between the frequency of nausea/vomiting ($p = 0.02$) with the amount of a single radiation dose. We also noticed the larger number of patients with headache in 3 Gy\fr group, and it seemed to be correlated with the amount of a single dose, but was not statistically significant ($p > 0.05$) (**Table 4**).

All patients were able to complete the planned radiation treatment program and received HSCT.

Subacute Toxicity: Transplant-Related Toxicity and Death

Subacute toxicity among the patients who received OC-TBI ($n = 191$) was observed in 0.4% of the patients ($n = 1$) (interstitial pneumonia, 3–4 stage according to RTOG) at +81 days after TBI (**Table 5**). The patient died from respiratory failure. No radiation-induced kidney toxicity was observed among the patients.

Among the patients who received SIB to bone marrow up to 15 Gy (29 pts), we observed 3 (10%) cases of veno-occlusive disease (VOD), which appeared on days +14, + 21, and +26. One patient developed transitory hepatic failure symptoms (**Table 5**). All these patients died from the disease relapse.

The cumulative incidence of TRM for the entire patient cohort was 10.7 (95% CI: 2.2–16).

Most of the TRM cases were induced by infection and subsequent sepsis with multiorgan failure ($n = 20$). One patient died because of the COVID-19 infection. The full list of infections and its localization is displayed in **Table 6**.

The incidence of TRM for the patients who received 1st HSCT was 8.7% (95% CI: 5.5–15), and it had significantly higher values for the patients with 2nd HSCT—18.7% (95% CI: 9.5–37.5) ($p = 0.03$) (see **Figure 6**).

The cumulative incidence of early TRM (<100 days) was 5.0 (95% CI: 1.5–8.9), and that of late TRM (>100 days) was 5.7 (95% CI: 1.7–10.2).

The incidence of early TRM (<100 days) was significantly lower for the patients who were in complete remission (CR) before HSCT —3.9% (95% CI: 1.4–8.0) compared with active disease (AD) patients—9.0% (95% CI: 5.0–9.6) ($p < 0.0001$) (**Figure 6**).

Survival Analysis

We retrospectively analyzed a cohort of 220 patients who received OC-TBI with subsequent allogenic SCT with TCRαβ/CD-19 depletion in our clinic during a period of time from July 2014 to September 2020.

The follow-up period was from 0.3 to 6.4 years (the median follow-up for the surviving patients—2.8 years).

The OS for all patients was 63% (95% CI: 56–70), and the EFS was 58% (95% CI: 51–65).

The OS in the patients with acute leukemia was 63% (95% CI: 43–71) in the ALL group and 52% (95% CI: 32–72) in the AML group ($p = 0.09$). The EFS for the patients with ALL was 57% (95% CI: 49-65), and the EFS for the patients with AML was 52% (95% CI: 32–72) ($p = 0.3$) (**Table 7**).

The OS and EFS for patients with other diseases (NHL, biphenotypic/bilinear leukemia, JMML, etc.) were more related to patients with ALL and AML, with an OS of 71% (95% CI: 54–88) and EFS of 70% (95% CI: 53–86). These results are attributed to the different disease characteristics in this group and are not significant (**Table 7**).

The OS and EFS values in the patients with CR before HSCT ($n = 181$) were 68% (95% CI: 60–76) and 63% (95% CI: 56–70), respectively.

The OS and EFS values for the patients with AD prior to HSCT were significantly lower: OS 36% (95% CI: 20–52) and EFS 36% (95% CI: 20–52) compared with the CR ($n = 181$) patients ($p < 0.0001$) (**Figure 7**). The patients who received treatment in the CR relapsed from the following sites: 36 patients had bone marrow relapse, one patient with ALL had isolated CNS relapse, 12 patients had combined relapses from bone marrow and extramedullary sites (**Table 7**).

TABLE 4 | Radiation-induced acute toxicity.

Toxicity criteria (RTOG)	GROUP 1 2 Gy × 6 fractions/twice daily	GROUP 2 3 Gy × 4 fractions	*p*-value
Number of pts	201	19	
Nausea and vomit			
• Grades 0–1	124 (62%)	6 (32%)	0.020
• Grades 2–3	77 (38%)	13 (68%)	
Headache			
• Grades 0–1	114 (56%)	12 (63%)	>0.05 (0.751)
• Grades 2–3	87 (44%)	7 (39%)	
Parotitis			
• No clinical symptoms	109 (54%)	9 (47%)	>0.05 (0.755)
• Grade 1 clinical symptoms	92 (46%)	10 (53%)	
Enteritis			
• No clinical symptoms	122 (61%)	10 (53%)	>0.05 (0.733)
• Grade 1	64 (32%)	7 (36%)	
• Grade 2	15 (7%)	2 (11%)	

TABLE 5 | Radiation-induced subacute toxicity and causes of death.

Patient No.	Ds	TBI	Clinical manifestation	Time of manifestation	Number of HCST	Chemotherapy	Result
1	ALL	12 Gy	**IP***	+81 days after TBI	1st (MUD)	Fludarabine 150 mg/m^2 + thiotepa 10 mg/kg	*Death* Respiratory failure
2	ALL	12 Gy + SIB to BM 15 Gy	**VOD***	+21 days after TBI	2nd (Haplo)	Fludarabine 150 mg/m^2 + thiotepa 10 mg/kg	Hepatic failure symptoms *Death* Relapse
3	AML, M2	12 Gy + SIB to BM 15 Gy	**VOD***	+14 days after TBI	2nd (Haplo)	Fludarabine 150 mg/m^2 + thiotepa 300 mg/kg	*Death* Relapse
4	AML, M4	12 Gy + SIB to BM 15 Gy	**VOD***	+26 days after TBI	1st (Haplo)	Fludarabine 150 mg/m^2 + thiotepa 10 mg/kg + Velcade 1.3 mg/m^2	*Death* Relapse

**IP - interstitial pneumonia.*
**VOD - venoocclusive disease.*

TABLE 6 | TRM-related death characteristic (n = 22).

TRM-related death	Number of patients (% of all 220 patients)	Cumulative incidence (%)
All patients	**22 (10)**	**10.7 (95% CI, 2.2–16)**
1st HSCT (180 patients)	**15 (7)**	**8.7 (95% CI, 5.5–15)**
TRM <100 days	7	3.8 (95% CI, 1.8–8)
TRM >100 days	8	5.0 (95% CI, 2.5–10)
2nd HSCT (40 patients)	**7 (3)**	**18.7 (95% CI: 9.5–37.5)**
TRM <100 days	4	10.0 (95% CI, 4.0–25.3)
TRM >100 days	3	8.0 (95% CI: 2.6–24.0)
TRM <100 days	**11 (5)**	**5.0 (95% CI: 1.5–8.9)**
CR (181 patients)	7	3.9% (95% CI: 1.4–8.0)
AD patients (39 patients)	4	9.0% (95% CI: 5.0–9.6)
TRM >100 days	**11 (5)**	**5.7 (95% CI: 1.7–10.2)**
CR (181 patients)	9	5.8 (95% CI: 1.9–11.0)
AD (39 patients)	2	5.3 (95% CI: 1.4–20.0)
Cause of death		
Infection	20 (9)	
Sepsis		
- Bacterial (*Pseudomonas aeruginosa*, *Klebsiella pneumonia*)	9 (4)	
- Fungal and mixed infection (*Aspergillosis*, *Candidiasis*, CMV)	3 (1.3)	
Lung infection		
- Bacterial (*Klebsiella pneumonia*, CMV, ADV)	5 (2)	
- Mixed infection	2 (0.8)	
Gastrointestinal + skin infection		
- Zygomycosis	1 (0.4)	
Interstitial pneumonia (IP)	1 (0.4)	
Other		
COVID-19	1 (0.4)	

CMV, cytomegalovirus; ADV, adenovirus. The bold values defines patients groups sorted by difference criteria (i.e. number of transplantation, TRM time).

Active Disease Patients

A total of 39 patients had an active disease status prior to HSCT. Among those, 19 patients received conformal TBI with an additional dose escalation (SIB) to BM (Boost+), and 20 patients received 12 Gy conformal TBI (Boost−). We calculated and compared OS, EFS, and cumulative incidence of TRM and relapse in these two groups of patients.

We noticed the difference in the OS and the EFS among this group of patients: the OS and EFS for the Boost+ patients had the same value and was 47% (95% CI: 25–70), while among the Boost − patients OS, and EFS was 29% (95% CI: 8–49) and 27% (95% CI: 6–48) (p = 0.4) (**Figure 8**). The lower number of bone marrow recurrence/disease progression cases were registered in the Boost+ patients compared with the Boost− group—five (26%) versus nine (45%). The difference between bone marrow relapse rate in the described groups was not statistically significant (p-value = 0.342; Chi-square test). We did not observe CNS relapses in patients receiving SIB to BM. Meanwhile, the cumulative incidence of TRM between the Boost− and Boost+ groups was equal, with a value of 15.8% (95% CI: 8–45).

DISCUSSION

The main aim of this study was to develop an optimized approach toward TBI planning in pediatric patients using IMRT and TomoTherapy-based conformal avoidance

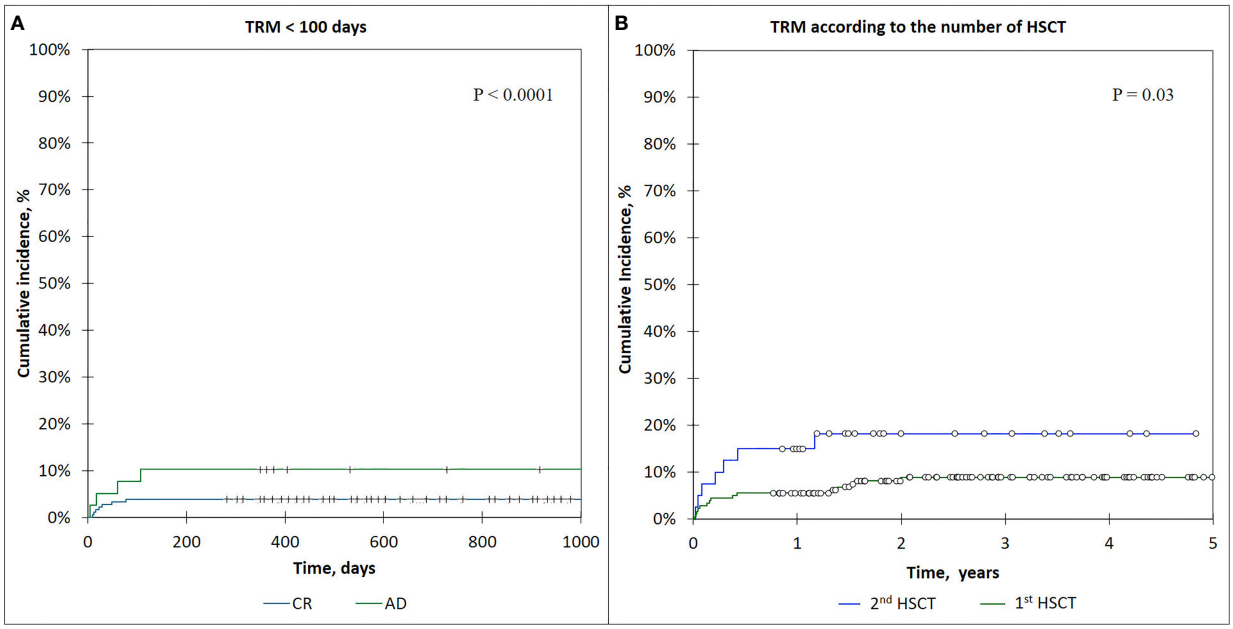

FIGURE 6 | **(A)** The cumulative incidence of TRM <100-day curves, comparison of CR and AD patients. **(B)** The incidence of TRM in patients according to the number of HSCTs.

TABLE 7 | The survival analysis results for the different patient groups.

Disease	OS % (95%CI)	EFS % (95%CI)	Relapse site (number of pts)
All patients	63 (56-70)	58 (51-65)	
ALL	63 (55-71)	57 (49-65)	BM – 38 BM + CNS – 6 BM + Testicles – 1 BM + uterus + ovaries - 1 BM + bones - 2 Isolated CNS - 1
AML	52 (32-71)	52 (32-72)	BM – 7 BM + Testicles + EM bones – 1 BM + CNS – 1 EM (bones) -1
Other (NHL, Biphenotypic/bilineal leukemia, JMML)	71 (54-88)	70 (53-86)	BM – 3 BM + EM sites - 3
Disease status at HSCT	**OS % (95%CI)**	**EFS % (95%CI)**	
CR 1/2/3 (182 pts)	68 (60–76)	63 (56-70)	BM – 36 BM + CNS – 6 BM + EM sites – 4 BM + Testicles - 1 BM + uterus + ovaries – 1 Isolated CNS - 1
AD (39 pts)	36 (20-52)	36 (20-52)	
AD SIB to BM + (19 pts)	47 (25-70)	47 (25-70)	BM – 4 BM + EM - 3
AD SIB to BM – (20 pts)	29 (8-49)	27 (6-48)	BM – 8 BM + CNS – 1 BM + EM - 2

BM, bone marrow; CNS, central nervous system; EM, extramedullary site.

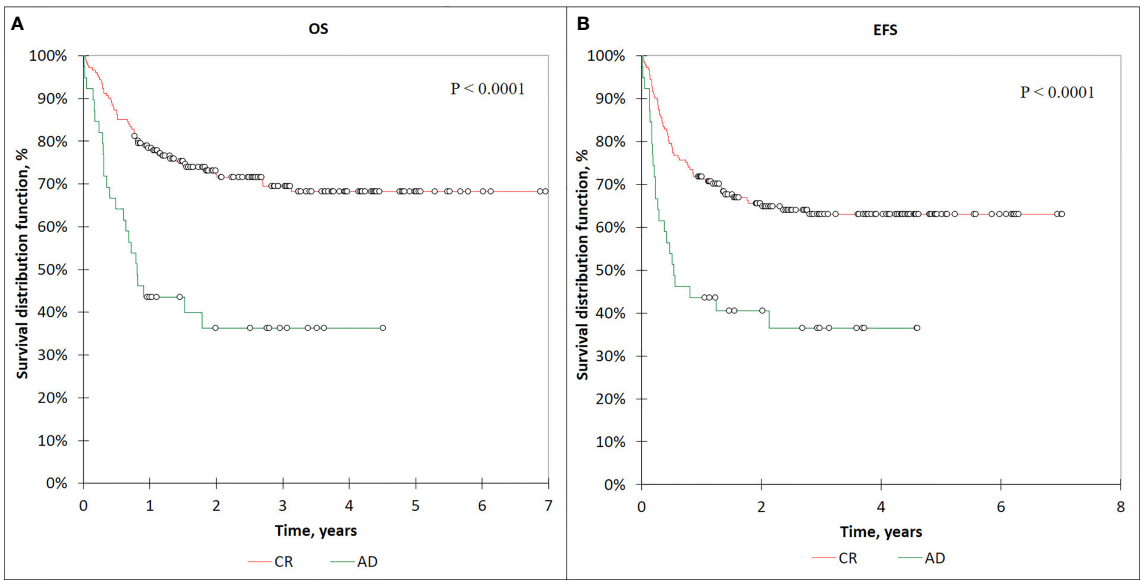

FIGURE 7 | The OS **(A)** and EFS **(B)** curves for the CR and AD patients.

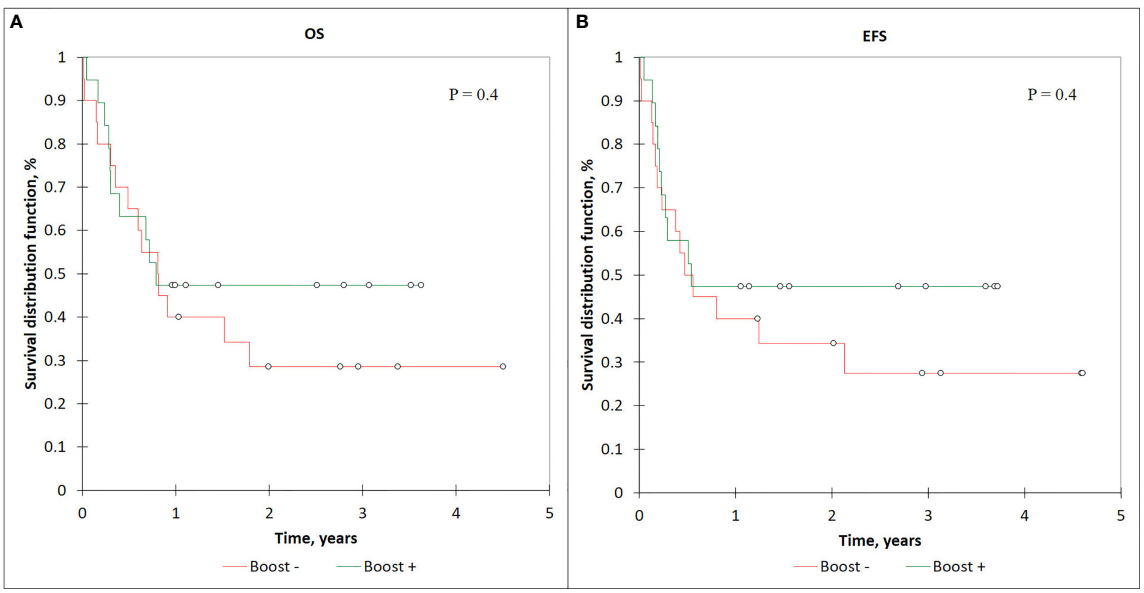

FIGURE 8 | OS **(A)** and EFS **(B)** curves for AD patients who received SIB to BM.

techniques and to evaluate the safety and potential efficacy of this treatment for patients with varying characteristics and disease features.

We did not observe any significant effect of OC-TBI with the described dose limits to the OAR organs at risk on transplant-related mortality. We observed that a single day of fractionation with a higher single dose increased acute radiation-induced toxicity (nausea/vomiting and headache). However, an additional investigation of other nonlethal toxicities for a larger number of patients and a longer follow-up period is required to elucidate disadvantages.

Considering the long-term survival period in a pediatric cohort with remission and a good response to received therapy, the development of radiation-induced late side effects (such as hormone dysfunction, hypogonadism, cognitive dysfunction, secondary malignancies) significantly influences

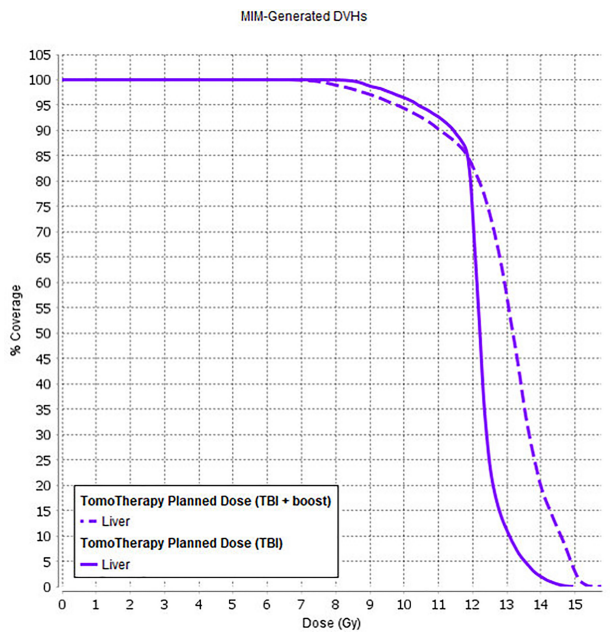

FIGURE 9 | Liver dose for patients who received OC-TBI (solid line) and for patients who received OC-TBI with SIB to BM (dashed line).

the patient's quality of life. In this manner, a preferred option for the TBI method would be to use it in combination with total bone marrow irradiation (TMI) and/or total lymphoid irradiation (TMLI). This approach would facilitate redistribution of the radiation dose within the patient's body, leading to dose reduction to the OAR (such as gonads, thyroid, liver, etc.) with a simultaneous increase in the total dose to the bone marrow. Local dose escalation to sanctuary sites (such as bone marrow) with higher doses (up to 18–20 Gy) would likely lead to an increase in the survival rates for active disease patients (**Figure 8**), but it can also be complex in terms of higher toxicity incidence. We explored the initial feasibility of using IMRT and TomoTherapy techniques for planning and delivery of simultaneous additional dose escalation (SIB) to the bone marrow (BM) up to 15 Gy in patients with refractory leukemia. During the early follow-up, we observed a higher incidence of VOD in this group of patients [n = 3 (10%)]. The EQD2-calculated liver dose for these patients and its comparison with OC-TBI are presented in **Figure 9**.

Taking into account the published data on the risk factors for VOD development (38–40), we assume that this issue can be resolved by further reducing the dose to the liver parenchyma. Even though TMLI provides a more conformally targeted radiotherapy for patients undergoing HCT, organ sparing could potentially increase the risk of extramedullary relapse and decrease the efficacy of radiation treatment.

We had early experience with seven patients who received a total marrow dose of 15 Gy plus a total lymphoid dose of 12 Gy irradiation using TMLI. At this point, it is too early to draw any conclusions regarding the effectiveness and survival rates for this treatment approach. Nevertheless, taking into account the VOD cases among the patients who received OC-TBI with SIB to bone marrow, we decided to replace this method with total marrow and lymphoid irradiation (with the additional dose reduction to the heart, liver, intestine, thyroid, ovaries, etc.). We saved a 12-Gy treatment dose to the most susceptible extramedullary sites for patients with pediatric leukemia (brain; forehead area for younger patients - **Figure 2**; testicles) and controlled the dose in these areas (D95 >11.4 Gy).

The concept of conformal total body irradiation (TBI) using IMRT VMAT and helical treatment delivery on a TomoTherapy accelerator provides the maximum control of the dose distribution in extended targets (PTV) with a simultaneous dose decrease in organs at risk. It leads to a reduced incidence of severe side effects after radiation therapy and high treatment effectiveness.

OC-TBI with precise dose prescription for organs at risk and image-guided treatment delivery allows us to estimate potential efficacy and radiation-induced toxicity in comparable groups of treated patients. The limited number of pediatric patients who receive OC-TBI requires multidisciplinary and multicenter collaboration and discussion to create new ideas and improve the approach for this complex radiation treatment procedure.

DATA AVAILABILITY STATEMENT

The original contributions presented in the study are included in the article/supplementary material. Further inquiries can be directed to the corresponding author.

ETHICS STATEMENT

The studies involving human participants were reviewed and approved by Local Ethics Committee of the Dmitriy Rogachev National Medical Research center of pediatric hematology, oncology and immunology. Written informed consent to participate in this study was provided by the participants' legal guardian/next of kin. Written informed consent was obtained from the individual(s) and minor(s)' legal guardian/next of kin for the publication of any potentially identifiable images or data included in this article.

AUTHOR CONTRIBUTIONS

DA collected and analyzed data and wrote the paper. AN, LS, and MM designed the study, analyzed data and reviewed the paper. FK, DT, and AL collected and analyzed data and wrote the paper. RK and MI collected and analyzed data and reviewed the paper. DB and NM contributed to study design and reviewed the paper. All authors contributed to the article and approved the submitted version.

REFERENCES

1. Davies SM, Ramsay NK, Klein JP, Weisdorf DJ, Bolwell B, Cahn JY, et al. Comparison of Preparative Regimens in Transplants for Children With Acute Lymphoblastic Leukemia. *J Clin Oncol* (2000) 18(2):340–7. doi: 10.1200/jco.2000.18.2.340
2. Blume KG, Forman SJ, Snyder DS, Nademanee AP, O'Donnell MR, Fahey JL, et al. Allogeneic Bone Marrow Transplantation for Acute Lymphoblastic Leukemia During First Complete Remission. *Transplantation* (1987) 43 (3):389–92. doi: 10.1097/00007890-198703000-00014
3. Glasgow GP, Wang S, Stanton J. A Total Body Irradiation Stand for Bone Marrow Transplant Patients. *Int J Radiat Oncol Biol Phys* (1989) 16(3):875–7. doi: 10.1016/0360-3016(89)90508-7
4. Mody R, Li S, Dover DC, Sallan S, Leisenring W, Oeffinger KC, et al. Twenty-Five–Year Follow-Up Among Survivors of Childhood Acute Lymphoblastic Leukemia: A Report From the Childhood Cancer Survivor Study. *Blood* (2008) 111(12):5515–23. doi: 10.1182/blood-2007-10-117150
5. Ozsahin M, Pène F, Touboul E, Gindrey-Vie B, Dominique C, Lefkopoulos D, et al. Total-Body Irradiation Before Bone Marrow Transplantation. Results of Two Randomized Instantaneous Dose Rates in 157 Patients. *Cancer* (1992) 69 (11):2853–65. doi: 10.1002/1097-0142(19920601)69:11<2853::AID-CNCR2820691135>3.0.CO;2-2
6. Locatelli F, Merli P, Pagliara D, Li Pira G, Falco M, Pende D, et al. Outcome of Children With Acute Leukemia Given HLA-Haploidentical HSCT After αβ T-Cell and B-Cell Depletion. *Blood* (2017) 130(5):677–85. doi: 10.1182/blood-2017-04-779769
7. Blaise D, Maraninchi D, Michallet M, Reiffers J, Jouet JP, Milpied N, et al. Long-Term Follow-Up of a Randomized Trial Comparing the Combination of Cyclophosphamide With Total Body Irradiation or Busulfan as Conditioning Regimen for Patients Receiving HLA-Identical Marrow Grafts for Acute Myeloblastic Leukemia in First Complete Remission. *Blood* (2001) 97(11):3669–71. doi: 10.1182/blood.V97.11.3669
8. Kelsey CR, Horwitz ME, Chino JP, Craciunescu O, Steffey B, Folz RJ, et al. Severe Pulmonary Toxicity After Myeloablative Conditioning Using Total Body Irradiation: An Assessment of Risk Factors. *Int J Radiat Oncol Biol Phys* (2011) 81(3):812–8. doi: 10.1016/j.ijrobp.2010.06.058
9. Abugideiri M, Nanda RH, Butker C, Zhang C, Kim S, Chiang KY, et al. Factors Influencing Pulmonary Toxicity in Children Undergoing Allogeneic Hematopoietic Stem Cell Transplantation in the Setting of Total Body Irradiation-Based Myeloablative Conditioning. *Int J Radiat Oncol Biol Phys* (2016) 94(2):349–59. doi: 10.1016/j.ijrobp.2015.10.054
10. Hanania AN, Mainwaring W, Ghebre YT, Hanania NA, Ludwig M. Radiation-Induced Lung Injury: Assessment and Management. *Chest* (2019) 156(1):150–62. doi: 10.1016/j.chest.2019.03.033
11. Carruthers SA, Wallington MM. Total Body Irradiation and Pneumonitis Risk: A Review of Outcomes. *Brit J Cancer* (2004) 90(11):2080–84. doi: 10.1038/sj.bjc.6601751
12. Chiang Y, Tsai CH, Kuo SH, Liu CY, Yao M, Li CC, et al. Reduced Incidence of Interstitial Pneumonitis After Allogeneic Hematopoietic Stem Cell Transplantation Using a Modified Technique of Total Body Irradiation. *Sci Rep-UK* (2016) 6(1):1–11. doi: 10.1038/srep36730
13. Cosset JM, Baume D, Pico JL, Shank B, Girinski T, Benhamou E, et al. Single Dose Versus Hyperfractionated Total Body Irradiation Before Allogeneic Bone Marrow Transplantation: A non-Randomized Comparative Study of 54 Patients at the Institut Gustave-Roussy. *Radiother Oncol* (1989) 15(2):151–60. doi: 10.1016/0167-8140(89)90129-1
14. Travis EL, Peters LJ, McNeill J, Thames HD Jr, Karolis C. Effect of Dose-Rate on Total Body Irradiation: Lethality and Pathologic Findings. *Radiother Oncol* (1985) 4(4):341–51. doi: 10.1016/S0167-8140(85)80122-5
15. Esiashvili N, Lu X, Ulin K, Laurie F, Kessel S, Kalapurakal JA, et al. Higher Reported Lung Dose Received During Total Body Irradiation for Allogeneic Hematopoietic Stem Cell Transplantation in Children With Acute Lymphoblastic Leukemia is Associated With Inferior Survival: A Report From the Children's Oncology Group. *Int J Radiat Oncol Biol Phys* (2019) 104(3):513–21. doi: 10.1016/j.ijrobp.2019.02.034
16. Sampath S, Schultheiss T, Wong J. Dose Response and Factors Related to Interstitial Pneumonitis After Bone Marrow Transplant. *Int J Radiat Oncol Biol Phys* (2005) 63(3):876–84. doi: 10.1016/j.ijrobp.2005.02.032
17. Barrett A, Nicholls J, Gibson B. Late Effects of Total Body Irradiation. *Radiother Oncol* (1987) 9(2):131–5. doi: 10.1016/S0167-8140(87)80200-1
18. Hui SK, Kapatoes J, Fowler J, Henderson D, Olivera G, Manon RR, et al. Feasibility Study of Helical Tomotherapy for Total Body or Total Marrow Irradiation. *Med Phys* (2005) 32(10):3214–24. doi: 10.1118/1.2044428
19. Wong JY, Liu A, Schultheiss T, Popplewell L, Stein A, Rosenthal J, et al. Targeted Total Marrow Irradiation Using Three-Dimensional Image-Guided Tomographic Intensity-Modulated Radiation Therapy: An Alternative to Standard Total Body Irradiation. *Biol Blood Marrow Tr* (2006) 12(3):306–15. doi: 10.1016/j.bbmt.2005.10.026
20. Schultheiss TE, Wong J, Liu A, Olivera G, Somlo G. Image-Guided Total Marrow and Total Lymphatic Irradiation Using Helical Tomotherapy. *Int J Radiat Oncol Biol Phys* (2007) 67(4):1259–67. doi: 10.1016/j.ijrobp.2006.10.047
21. Wong JY, Rosenthal J, Liu A, Schultheiss T, Forman S, Somlo G. Image-Guided Total-Marrow Irradiation Using Helical Tomotherapy in Patients With Multiple Myeloma and Acute Leukemia Undergoing Hematopoietic Cell Transplantation. *Int J Radiat Oncol Biol Phys* (2009) 73:273–9. doi: 10.1016/j.ijrobp.2008.04.071
22. Peñagarícano JA, Chao M, Van Rhee F, Moros EG, Corry PM, Ratanatharathorn V. Clinical Feasibility of TBI With Helical Tomotherapy. *Bone Marrow Transpl* (2011) 46:929–35. doi: 10.1038/bmt.2010.237
23. Gruen A, Ebell W, Wlodarczyk W, Neumann O, Kuehl JS, Stromberger C, et al. Total Body Irradiation (TBI) Using Helical Tomotherapy in Children and Young Adults Undergoing Stem Cell Transplantation. *Radiat Oncol* (2013) 8(1):1–8. doi: 10.1186/1748-717X-8-92
24. Konishi T, Ogawa H, Najima Y, Hashimoto S, Wada A, Adachi H, et al. Safety of Total Body Irradiation Using Intensity-Modulated Radiation Therapy by Helical Tomotherapy in Allogeneic Hematopoietic Stem Cell Transplantation: A Prospective Pilot Study. *J Radiat Res* (2020) 61(6):969–76. doi: 10.1093/jrr/rraa078
25. Shueng PW, Lin SC, Chong NS, Lee HY, Tien HJ, Wu LJ, et al. Total Marrow Irradiation With Helical Tomotherapy for Bone Marrow Transplantation of Multiple Myeloma: First Experience in Asia. *Tech Canc Res Treat* (2009) 8 (1):29–37. doi: 10.1177/153303460900800105
26. Maschan M, Shelikhova L, Shekhovtsova Z, Balashov D, Kurnikova E, Muzalevsky Y, et al. TCR Alpha/Beta and CD19 Depletion in Transplantation From Matched Unrelated and Haploidentical Donors in Pediatric Leukemia Patients: Comparison of Two Gvhd Prophylaxis Regimens. *Biol Blood Marrow Transplant* (2016) 22(3):385–5. doi: 10.1016/j.bbmt.2015.11.901
27. Maschan M, Shelikhova L, Ilushina M, Kurnikova E, Boyakova E, Balashov D, et al. TCR-Alpha/Beta and CD19 Depletion and Treosulfan-Based Conditioning Regimen in Unrelated and Haploidentical Transplantation in Children With Acute Myeloid Leukemia. *Bone Marrow Transpl* (2016) 51 (5):668–74. doi: 10.1038/bmt.2015.343
28. Shelikhova L, Shekhovtsova Z, Balashov D, Boyakova E, Muzalevskyi I, Gutovskaya E, et al. Tcrαβ+/CD19+-Depletion in Hematopoietic Stem Cells Transplantation From Matched Unrelated and Haploidentical Donors Following Treosulfan or TBI-Based Conditioning in Pediatric Acute Lymphoblastic Leukemia Patients. *Blood* (2016) 128(22):4672. doi: 10.1182/blood.V128.22.4672.4672
29. Loginova AA, Kobyzeva DA, Tovmasyan DA, Chernyaev AP, Lisovskaya AO, Maschan MA, et al. Comparison of Total Body Irradiation Using TomoTherapy and Volume-Modulated Rotational Radiation Therapy Elekta. A Single Center Experience on Pediatric Patients. *Pediatr Hemat/Oncol Immunopath* (2019) 18 (4):49–57. doi: 10.24287/1726-1708-2019-18-4-49-57
30. Jiang Z, Jia J, Yue C, Pang Y, Liu Z, Ouyang L, et al. Haploidentical Hematopoietic SCT Using Helical Tomotherapy for Total-Body Irradiation and Targeted Dose Boost in Patients With High-Risk/Refractory Acute Lymphoblastic Leukemia. *Bone Marrow Transpl* (2018) 53(4):438–48. doi: 10.1038/s41409-017-0049-5
31. Corvò R, Zeverino M, Vagge S, Agostinelli S, Barra S, Taccini G, et al. Helical Tomotherapy Targeting Total Bone Marrow After Total Body Irradiation for Patients With Relapsed Acute Leukemia Undergoing an Allogeneic Stem Cell Transplant. *Radiat Oncol* (2011) 98(3):382–6. doi: 10.1016/j.radonc.2011.01.016
32. Borg M, Hughes T, Horvath N, Rice M, Thomas AC. Renal Toxicity After Total Body Irradiation. *Int J Radiat Oncol Biol Phys* (2002) 54(4):1165–73. doi: 10.1016/S0360-3016(02)03039-0

33. Esiashvili N, Chiang KY, Hasselle MD, Bryant C, Riffenburgh RH, Paulino AC. Renal Toxicity in Children Undergoing Total Body Irradiation for Bone Marrow Transplant. *Radiat Oncol* (2009) 90(2):242–6. doi: 10.1016/j.radonc.2008.09.017
34. Cheng JC, Schultheiss TE, Wong JY. Impact of Drug Therapy, Radiation Dose, and Dose Rate on Renal Toxicity Following Bone Marrow Transplantation. *Int J Radiat Oncol Biol Phys* (2008) 71(5):1436–43. doi: 10.1016/j.ijrobp.2007.12.009
35. Chou RH, Wong GB, Kramer JH, Wara DW, Matthay KK, Crittenden MR, et al. Toxicities of Total-Body Irradiation for Pediatric Bone Marrow Transplantation. *Int J Radiat Oncol Biol Phys* (1996) 34(4):843–51. doi: 10.1016/0360-3016(95)02178-7
36. Wheldon TE. The Radiobiological Basis of Total Body Irradiation. *Brit J Radiol* (1997) 70(840):1204–7. doi: 10.1259/bjr.70.840.9505837
37. Cox JD, Stetz J, Pajak TF. Toxicity Criteria of the Radiation Therapy Oncology Group (RTOG) and the European Organization for Research and Treatment of Cancer (EORTC). *Int J Radiat Oncol Biol Phys* (1995) 31(5):1341–46. doi: 10.1016/0360-3016(95)00060-C
38. Mohty M, Malard F, Abecassis M, Aerts E, Alaskar AS, Aljurf M, et al. Sinusoidal Obstruction Syndrome/Veno-Occlusive Disease: Current Situation and Perspectives—A Position Statement From the European Society for Blood and Marrow Transplantation (EBMT). *Bone Marrow Transpl* (2015) 50 (6):781–9. doi: 10.1038/bmt.2015.52
39. Mcdonald GB, Sharma P, Matthews DE, Shulman HM, Thomas ED. Venocclusive Disease of the Liver After Bone Marrow Transplantation: Diagnosis, Incidence, and Predisposing Factors. *Hepatology* (1984) 4 (1):116–22. doi: 10.1002/hep.1840040121
40. Coppell JA, Richardson PG, Soiffer R, Martin PL, Kernan NA, Chen A, et al. Hepatic Veno-Occlusive Disease Following Stem Cell Transplantation: Incidence, Clinical Course, and Outcome. *Biol Blood Marrow Transplant* (2010) 16(2):157–68. doi: 10.1016/j.bbmt.2009.08.024

Conflict of Interest: The authors declare that the research was conducted in the absence of any commercial or financial relationships that could be construed as a potential conflict of interest.

Publisher's Note: All claims expressed in this article are solely those of the authors and do not necessarily represent those of their affiliated organizations, or those of the publisher, the editors and the reviewers. Any product that may be evaluated in this article, or claim that may be made by its manufacturer, is not guaranteed or endorsed by the publisher.

frontiers in Oncology

ORIGINAL RESEARCH
published: 10 March 2022
doi: 10.3389/fonc.2022.785917

Optimized Conformal Total Body Irradiation methods with Helical TomoTherapy and Elekta VMAT: Implementation, Imaging, Planning and Dose Delivery for Pediatric Patients

Anna Anzorovna Loginova[1*], *Diana Anatolievna Tovmasian*[1,2], *Anastasiya Olegovna Lisovskaya*[1], *Daria Alexeevna Kobyzeva*[1], *Michael Alexandrovich Maschan*[1], *Alexander Petrovich Chernyaev*[2], *Oleg Borisovich Egorov*[3] and *Alexey Vladimirovich Nechesnyuk*[1]

[1] Dmitry Rogachev National Research Center of Pediatric Hematology, Oncology and Immunology, Moscow, Russia, [2] Faculty of Physics, Federal State Budget Educational Institution of Higher Education, M.V. Lomonosov Moscow State University, Moscow, Russia, [3] Research and Development Department, E&H Scientific, West Richland, WA, United States

OPEN ACCESS

Edited by:
Bulent Aydogan,
University of Chicago, United States

Reviewed by:
André Haraldsson,
Skåne University Hospital, Sweden
Chunhui Han,
City of Hope National Medical Center, United States

***Correspondence:**
Anna Anzorovna Loginova
aloginovaa@gmail.com

Specialty section:
This article was submitted to Radiation Oncology, a section of the journal Frontiers in Oncology

Received: 29 September 2021
Accepted: 10 February 2022
Published: 10 March 2022

Citation:
Loginova AA, Tovmasian DA, Lisovskaya AO, Kobyzeva DA, Maschan MA, Chernyaev AP, Egorov OB and Nechesnyuk AV (2022) Optimized Conformal Total Body Irradiation methods with Helical TomoTherapy and Elekta VMAT: Implementation, Imaging, Planning and Dose Delivery for Pediatric Patients. Front. Oncol. 12:785917. doi: 10.3389/fonc.2022.785917

Optimized conformal total body irradiation (OC-TBI) is a highly conformal image guided method for irradiating the whole human body while sparing the selected organs at risk (OARs) (lungs, kidneys, lens). This study investigated the safety and feasibility of pediatric OC-TBI with the helical TomoTherapy (TomoTherapy) and volumetric modulated arc (VMAT) modalities and their implementation in routine clinical practice. This is the first study comparing the TomoTherapy and VMAT modalities in terms of treatment planning, dose delivery accuracy, and toxicity for OC-TBI in a single-center setting. The OC-TBI method with standardized dosimetric criteria was developed and implemented with TomoTherapy. The same OC-TBI approach was applied for VMAT. Standardized treatment steps, namely, positioning and immobilization, contouring, treatment planning strategy, plan evaluation, quality assurance, visualization and treatment delivery procedure were implemented for 157 patients treated with TomoTherapy and 52 patients treated with VMAT. Both modalities showed acceptable quality of the planned target volume dose coverage with simultaneous OARs sparing. The homogeneity of target irradiation was superior for TomoTherapy. Overall assessment of the OC-TBI dose delivery was performed for 30 patients treated with VMAT and 30 patients treated with TomoTherapy. The planned and delivered (sum of doses for all fractions) doses were compared for the two modalities in groups of patients with different heights. The near maximum dose values of the lungs and kidneys showed the most significant variation between the planned and delivered doses for both modalities. Differences in the patient size did not result in statistically significant differences for most of the investigated parameters in either the TomoTherapy or VMAT modality. TomoTherapy-based OC-TBI

showed lower variations between planned and delivered doses, was less time-consuming and was easier to implement in routine practice than VMAT. We did not observe significant differences in acute and subacute toxicity between TomoTherapy and VMAT groups. The late toxicity from kidneys and lungs was not found during the 2.3 years follow up period. The study demonstrates that both modalities are feasible, safe and show acceptable toxicity. The standardized approaches allowed us to implement pediatric OC-TBI in routine clinical practice.

Keywords: pediatric, TBI, TMLI, VMAT, TomoTherapy, dose delivery, robustness, standardization

INTRODUCTION

Total body irradiation (TBI) is used in the treatment of hematological malignancies as part of conditioning regimens before hematopoietic stem cell transplantation (HSCT). Conventional TBI at extended source-surface distances has been established and demonstrated to be a reliable method, but its use is limited by its high toxicity (1–3).

There are methods of optimized TBI with a relatively short source-to-surface distance and intensity modulation (4, 5). They make it possible to use more homogeneous targeted irradiation than conventional TBI by reducing the dose to the organs at risk (OARs), but such methods are still not considered conformal.

The first optimized conformal TBI and total marrow irradiation (TMI) methods were tested using helical TomoTherapy (6–8) and later with a standard linac (9, 10). A benefit with regard to dose distribution and selective OAR dose sparing was demonstrated by other authors in an adult cohort (11–13) and by Gruen et al. in a pediatric cohort (14).

Currently, much attention is given to total marrow irradiation (TMI) and total marrow and lymphoid irradiation (TMLI) (15). TMI and TMLI show promise with respect to the toxicity profile because targeted irradiation enables reduction of the dose to the OARs and the feasibility of possible dose escalation to improve disease control in refractory and relapsed patients (15–17).

Potentially, TMI and TMLI could increase the relapse rate caused by underdosages to nontargeted regions. Kim et al. investigated extramedullary relapse in adult patients treated with TMLI and did not find an association of its incidence with lower dose regions (18). However, the application of TMI and TMLI as standard treatment approaches for pediatric patients with leukemia requires additional research to ensure safety, quality, clinical outcomes, toxicity, and feasibility.

Pediatric TBI approaches are quite different among clinics and depend on technical capacities and individual establishment (19, 20). There are no common practical recommendations for OC-TBI treatment planning and preparation. The main task for our department was to develop an optimized conformal total body irradiation (OC-TBI) method with sparing of the selected organs at risk (OARs) (lungs, kidneys, and lenses) and implement it in clinical practice. The development and implementation of the TomoTherapy-based OC-TBI method was carried out by our Center between 2014 and 2017. The rationale was to provide OC-TBI as close as possible to conventional TBI, which is used as standard treatment of care and assumes impartial lung shielding with better outcomes at lung doses <8 Gy (19–21). To achieve this we prescribed a minimum dose of 6 Gy to lungs. There is no direct clinical evidence of the minimum dose requirement for TBI treatment, but studies have shown that fractionated conventional TBI <9–10 Gy results in increased nonengraftment and disease relapse (22, 23). Prescription of a minimum dose up to 9–10 Gy would negatively affect lung and kidney sparing in treatment plan optimization.

Furthermore, the same approach has been applied for VMAT (since 2017). One of the important tasks was to provide the possibility to perform similar OC-TBI treatment for our patients using both modalities. This is the first study comparing the TomoTherapy and VMAT modalities in terms of treatment planning, dose delivery accuracy, and safety for OC-TBI in a single-center setting. The results of this study can be useful for clinics considering the possibility of implementing OC-TBI on an ongoing basis, given the different equipment used for this purpose and a detailed description of the methods.

MATERIALS AND METHODS

Patient Characteristics

Between July 2014 and July 2021, OC-TBI was implemented for a total of 341 pediatric patients who received HSCT, 279 of whom underwent helical TomoTherapy Hi-Art system (Accuray Inc., Sunnyvale, CA, USA) and 62 of whom underwent Elekta VMAT. Standardized treatment steps, namely, positioning and immobilization, contouring, treatment planning strategy, plan evaluation, quality assurance, visualization and treatment delivery procedure, were implemented for 157 patients treated with TomoTherapy and 52 patients treated with VMAT from June 2017 to May 2021. Patient age in the standardized group varied from 3 to 21 years (median—10.4 years old). Twenty patients were treated under general anesthesia. Anesthesia was delivered according to age. We also used general anesthesia in some cases with unsatisfactory patient psychological and performance status. The median age of patients receiving TBI under general anesthesia was 4.8 years.

We followed up patients for acute toxicity (nausea/vomiting/diarrhea, headache) during radiation therapy, subacute toxicity (IP) up to the 100th day after HSCT and late toxicity in the lungs and kidneys for at least 100 days after HSCT in accordance with the RTOG/EORTC scale (24).

Standardized Immobilization and CT Simulation

Standard CT imaging preceded whole body immobilization in the supine position using a vacuum mattress with rigid attachments to the couch with head fixation using pillows and thermoplastic masks (Elekta, UK, Crawley). The hands and arms of the patient were placed as close as possible to the body to minimize the lateral distance and improve the target dose homogeneity for the TomoTherapy plan with helical delivery and to maximize the body volume within the field of view of the Megavoltage Computed Tomography (MVCT) or Cone Beam Computed Tomography (CBCT) imaging. The body of the patient was set up tightly into the mattress, and the feet rested firmly on the mattress as described by Haraldsson et al. (25). Longitudinal laser lines were marked along the entire body to facilitate reproducibility of the patient setup.

CT images were obtained using a LightSpeed RT16 Computer Tomography (General Electric, Boston, USA) scanner. Images were acquired in free breathing with a slice thickness of 5 mm using 120 kV X-ray tube voltage and the largest available field of view (FOV) of 65 cm.

Images for patients with heights greater than 115 cm were obtained using two scans carried out in opposite directions to overcome the limitations of the treatment length for both the TomoTherapy and Elekta treatment units. The first scan included the upper body up to the knees in the head-first supine position of the patients. The second scan started from the tips of the feet to the pelvis in a feet-first supine position using a vacuum mattress rotated by 180°. Scan overlap was needed to perform image registration and manage junction dose. The fiducial junction markers were placed on the midsection of the patient to enable control of the junction area.

Dose Prescription

A dose of 12 Gy was given twice daily in 6 fractions or once daily in 4 fractions as part of the HSCT conditioning regimens. The planned target volume (PTV) included the whole body with a 3-mm inside margin and excluded the lungs, kidneys, and lenses.

The dose to the lung was prescribed at V8 <40% (that is, the volume of each lung receiving 8 Gy was not to exceed 40% of the whole lung volume) with a minimum dose of at least 6 Gy. The mean kidney dose was prescribed at <8 Gy.

Dose constraints to the eye lens were not prescribed, but effort was made to reduce the dose to these organs while maintaining the coverage of 95% of the prescribed dose in the adjacent PTV. For this aim, the PTV area near the eye was additionally contoured and used as a separate target when optimizing the plan.

Treatment Plan Calculation Strategy

TomoTherapy Optimized Conformal Total Body Irradiation Calculation Strategy

General OC-TBI Treatment Planning Strategy for TomoTherapy

OC-TBI plans for TomoTherapy were created using the non-Volo TomoTherapy 4.5 (Accuray Inc., Sunnyvale, CA, USA) treatment planning system (TPS) and treatment planning software using Helical dose delivery without the TomoEdge option. In the OC-TBI method, the OARs underwent dose reduction and minimum dose prescription simultaneously. Even though the lungs and kidneys were not included in the PTV, they were nonetheless used as part of the target during the dose optimization process.

Patient Size-Dependent OC-TBI Treatment Planning Strategy for TomoTherapy

Helical TomoTherapy delivery is associated with peripheral dose heterogeneity, which depends on plan modulation (26, 27). To reduce this effect, we chose TomoTherapy plan parameters depending on the size of the patient. For patients with height <115 cm, we used a field width of 2.5 cm, pitch of 0.43 and modulation factor of 1.9. For patients with height >115 cm and with right to left PTV size <17 cm, we used a field width of 5 cm, pitch of 0.43, and modulation factor of 1.9. For patients with height >115 cm and right to left PTV size >17 cm, we used a field width of 5 cm, pitch = 0.287 and modulation factor = 2.6.

Junction Between Upper and Lower Body Management for TomoTherapy-Based OC-TBI Treatment Planning

For patients with height >115 cm separate series of images were acquired for the upper and lower bodies, dose calculations were carried out independently for the two series (**Figure 1A**).

Our version of the TomoTherapy TPS does not allow image fusion and dose optimization of the lower body based on the upper body dose distribution. There is no possibility to compensate for possible deviations of the upper-body junction from the prescribed gradient while optimizing the lower body dose. The optimization of the junction area therefore would require ensuring a precisely prescribed dose gradient. For this reason, we use a nonoptimized method with an offset between the PTVs (28, 29).

In the case of TomoTherapy, the dose decrease at the edge of the field in the longitudinal direction was found to be quite smooth due to helical dose delivery (**Figure 1 A**).

During plan optimization, a contour offset was maintained between the upper and lower PTVs, while the dose distribution in the junction area was set to satisfy a uniform 90–120% of the prescribed dose. The dimension of the offset depends on the field width, pitch, modulation factor, optimization of the selected plan and CT slice thickness; our typical value is 5.5 cm. The external software MIM Maestro™ (MIM Software Inc., Cleveland, OH, USA) with the image fusion option was used to ensure that the dose in the junction area was maintained within the prescribed dose.

Additional Property Providing TomoTherapy Plan Robustness to Possible Patient Positioning Errors

The concept of a virtual bolus was used to ensure that the treatment plan was less sensitive to patient positioning errors. To accomplish this, we created an additional structure, PTV + 1 cm, and optimized it as the target. Since the PTV was created using a negative 3 mm margin from the skin surface, the virtual bolus involved in the optimization was a shell around the PTV, consisting of a 3 mm thick skin layer and a 7 mm thick air layer. Fifty percent of the structure volume of PTV + 1 cm was

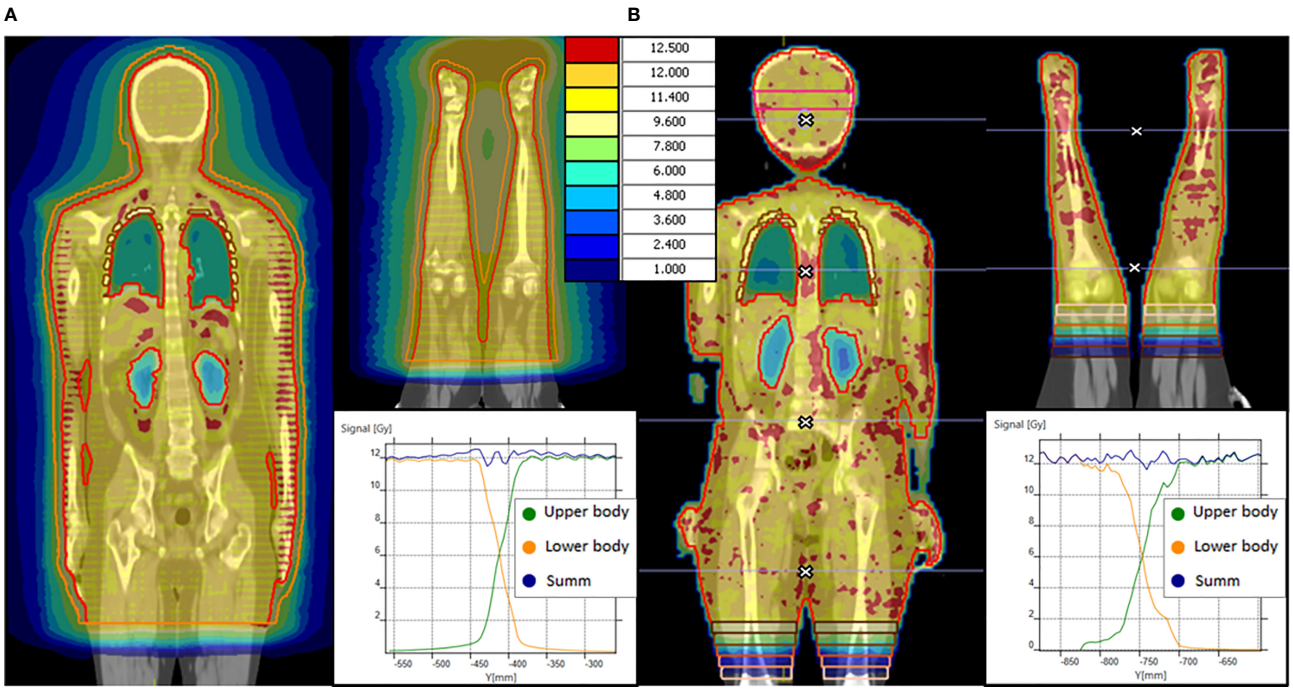

FIGURE 1 | OC-TBI dose distribution and dose profile in junction area between upper and lower body for **(A)** TomoTherapy and **(B)** VMAT.

prescribed a dose of 6 Gy. The prescription of a half dose to the virtual bolus allowed the optimizer to not create an excess fluence but one closer to that generated the PTV.

VMAT OC-TBI Calculation Strategy

General Treatment Planning Strategy for VMAT-Based OC-TBI

All VMAT-based plans were created using the multi-isocenter technique (30–34). Treatment plan optimization was performed using Monaco 5.11 treatment planning software (Elekta Inc., UK, Crawley) and the Monte Carlo algorithm with a statistical uncertainty of 3% per plan. A voxel size of 5 mm was chosen for the optimization stage. The final dose was recalculated with a 3 mm voxel size and statistical uncertainty of 1%.

Simultaneous optimization of all beams was carried out only for smaller patients, as presented in **Table 1**. In cases of taller patients, the PTV was split into several subsections and calculated one by one using the bias dose option.

We used coplanar 360° VMAT dose delivery on an Elekta Synergy treatment unit equipped with an Agility collimator (Elekta Inc., UK, Crawley). The gantry was moved clockwise and counterclockwise, with positions of the isocenters differing from each other only in the longitudinal coordinate. The energy of the photon beams was set to 6 and 10 MeV. The collimator position was set to 90°, as described by Nalichowski et al. (35). The collimator jaws were selected in accordance with the individual anatomy of the patient to ensure coverage of the subregions of the corresponding patient, consisting of the areas of the head and neck, lungs, abdomen, and pelvis as described by Mancosu et al. (36). When irradiating the lower extremities, we used a static position for the gantry and several beams with intensity modulation and 90° rotation of the treatment couch.

Treatment Planning Strategy in Relation to Patient Size for VMAT-Based OC-TBI

To obtain a desired dose distribution, we developed three different treatment planning strategies depending on patient height. We used anteroposterior–posteroanterior IMRT beams for the pelvis and lower extremities for large patients, which significantly helped reduce the MU/fraction ratio and decrease the fraction time. The VMAT-based OC-TBI treatment planning strategies are presented in **Table 1**.

Management of Junction Between Upper and Lower Body for VMAT-Based OC-TBI

For the VMAT plan, we use gradient junction optimization described previously (37). In the junction area of the upper body, the PTV was divided into 5 sequential volumes (thickness 2 cm) with dose value prescriptions of 11, 9, 6, 3, and 1 Gy in the crania-caudal direction. Following rigid image registration, identical structures were created for the lower-body image series. Next, the bias dose option was used to prescribe dose values of 1, 3, 6, 9, and 11 Gy and obtain a total dose of 12 Gy for each sequential volume (**Figure 1B**).

Additional Properties Providing VMAT Plan Robustness to Possible Patient Positioning Errors

The treatment beams were positioned to cover the whole PTV with overlap along the longitudinal axis from 2 to 4 cm at the

TABLE 1 | Patient size-dependent treatment planning strategies for VMAT-based OC-TBI.

Height of the patient, cm	Head	Chest	Abdomen	Pelvis	Upper legs	Lower legs	Number of isocenters
<105				One plan for whole body			4
	VMAT	VMAT		VMAT	VMAT		
105–145		upper body Plan			lower body Plan		6
	VMAT	VMAT	VMAT	VMAT	VMAT	VMAT	
>145		upper body Plan			lower-body plan		9
	VMAT	VMAT	VMAT	2 IMRT fields (10 and 170 Gantry angles) with couch rotated to 90°	2 AP-PA fields IMRT	2 AP-PA fields IMRT	

isocenter level, thereby providing the ability to automatically optimize the dose to the PTV, namely, the overlapped areas. Those areas were selected in a manner to eliminate or minimize intersection with the organs at risk.

To increase the plan robustness in relation to patient positioning, we used the Monaco 5.11 (Elekta Inc., UK, Crawley) Auto-Flash option with a 1 cm margin. After applying the Auto-Flash Option, an extension of the dose outside the body surface is created, so even under inhalation motion, irradiation of the superficial tissues can still be guaranteed (38).

Standard Criteria for the Treatment Plan Evaluation and Comparison of OC-TBI Using TomoTherapy and VMAT

For the PTV and OARs, we established target dose values that we attempted to meet during the plan optimization step with the TomoTherapy treatment planning station (see **Table 2**). However, the plans were considered acceptable in terms of the deviation from the target values, which were defined as acceptable values for balancing planning time and plan complexity (**Table 2**).

The majority of patients were treated using TomoTherapy. To ensure consistent results, the same plan acceptance criteria (**Table 2**) were applied for the VMAT plans.

Standardized treatment entailing standardized positioning/immobilization, contouring, treatment planning strategies, plan evaluation, quality assurance, visualization and treatment delivery procedures was implemented for 157 patients treated with TomoTherapy and 52 patients treated with VMAT. The comparison of planned doses for the above two groups of patients was performed using the metrics presented in **Table 2** as the mean ± s.d.

The two modalities were compared using the mean dose (D mean) to the OARs, the near maximum dose D_{2max} and near minimum D_{98min} dose to the whole body PTV and Ribs volumes and the homogeneity index (HI), which describes the degree of uniformity of the target irradiation:

$HI = \frac{D_{2\,max} - D_{98\,min}}{D_{50\,\%}} \cdot 100\,\%$, where $D_{50\%}$ is the median of the absorbed dose.

Individual Quality Assurance Procedures for OC-TBI Treatment Plans

The individual quality assurance procedures included dosimetry checks for each treatment plan.

For the OC-TBI treatment plans, absolute dose measurements were performed using ionization chambers (ExtraDIN Chambers, A1SL), an 8-channel electrometer (TomoElectrometer) and a tissue-equivalent phantom (Cheese Phantom) provided by Accuray Inc. (Sunnyvale, CA, USA). Measurements were carried out by placing the ionization chambers at four selected locations: two corresponding to the OARs, and the other two to the target area. The maximum permissible deviation of the measured dose from the calculated dose was less than 3%. In-house software was used for additional quality assurance. Exit detector data from the onboard MVCT imaging system were obtained during the Static Couch quality assurance procedure, a procedure in which irradiation is performed in the absence of a phantom and movement of the couch while maintaining the movement of the gantry and collimator. The received signal is recorded by onboard detectors. Obtained data was compared with a sinogram from the TPS (39). The 2D-gamma index was used for data comparison of the selected treatment plan (40).

For the VMAT-based plans, individual quality assurance procedures included composite measurements (41) of the two-dimensional dose distributions using an array of MatriXX Evolution ionization chambers (IBA Dosimetry, Belgium) with applied angular correction (42).

The 3%/3 mm Gamma criterion was assessed with a 95% passing rate for both modalities.

TABLE 2 | Acceptance criteria of OC-TBI plans for TomoTherapy.

Structure	Target value	Acceptable value
PTV	Mean dose (12 Gy) ± 2%	Mean dose (12 Gy) ± 5%
	$D_{98\%}$ >11.4 Gy	$D_{95\%}$ >11.4 Gy
	$D_{2\%}$ <13 Gy	$D_{5\%}$ <13 Gy
Ribs	$D_{95\%}$ >10 Gy	$D_{90\%}$ >10 Gy
Lung R,	V6 >99%	V6 >90%
Lung L	V8 <40%	V8 <40%
Kidney R, Kidney L	Dmean < 8 Gy	

Pretreatment Visualization With MVCT and CBCT

Imaging procedures based on MVCT or CBCT were performed before each treatment session to verify the position of the patient. A single long MVCT scan included a large volume from the head up to the pelvic bones. For the lower body, an additional two scans were performed for the knees and foot regions. Only the first registration of the knee was applied, and averaging was not performed. If necessary, the position of the patient was corrected, and the scanning process was repeated.

In the case of a VMAT modality, CBCT registration was performed in the first treatment isocenter (head area) with translational shift applied to the current position of the patient. Next, several scans corresponding to the planned isocenters were carried out one after the other without application of registration results. The distance between isocenters was strictly controlled; the movement from one isocenter to another was carried out exclusively by moving the treatment couch in the longitudinal direction. Treatment began only after visualization of all planned positions was finished. If the results of image registration were unsatisfactory with respect to PTV or OAR positioning, the patient setup was manually adjusted, and all scans were repeated.

Overall Assessment of Treatment Delivery Accuracy

For the VMAT treatment, several CBCTs corresponding to the planned isocenter positions were available. The translational shifts obtained during pretreatment visualization were applied to all CBCTs. Hounsfield unit to electron density (HU to ED) conversions were applied to the CBCT images in accordance with the predefined HU to ED calibration curves for each CBCT scanning protocol and the size of the patient. As a result, the impact of scatter contamination during CBCT image acquisition to HU was normalized, and original CBCTs were transformed into ED series (electron density series). Head, chest, abdomen, pelvis, and legs ED series were used to construct a single combined CBCT series of the full body. The combined CBCT series were masked with the planning CT to assure full image coverage at the FOV and generate the full CBCT if needed.

For TomoTherapy treatment, it is possible to select a scanning area with the required length from head to pelvis. However, the TomoTherapy MVCT scanner has an FOV of 40 cm, so the area outside the MVCT imaging diameter was masked with the planning CT to obtain full MVCT.

One third of the patients were scanned outside the FOV of the arms. Full MVCTs and CBCTs were used as primary series during deformable image registration (DIR), while the planning CTs were the secondary series. In this manner, the planning CTs were deformed to match the geometry of daily images, and synthetic CTs were obtained.

The procedures for processing, contouring, registering and deforming images were carried out using automated workflows of the MIM Maestro software. An overview of the data preprocessing is presented in **Figure 2**.

Synthetic CTs and original DICOM RT plan files were used to recalculate daily fractional dose. Dose calculations were performed using Monaco 5.11 for the VMAT plans and the MIM SureCalc® MonteCarlo Plan verification module for the TomoTherapy plans. The Monte Carlo algorithm with an uncertainty of 1% was used in both cases.

The delivered doses (the sum of doses for all fractions) were compared to the planned dose by analyzing the dose-volume histograms (DVH) in terms of mean dose, near minimum (D_{98min}) and near maximum (D_{2max}) doses, 90% ($D_{90\%}$) and 95% ($D_{95\%}$) doses of an OAR structure, and the volumes of structures covered by 6 Gy (V6), 8 Gy (V8) and 10 Gy (V10). To assess dose delivery, the PTV was divided into several subvolumes. Both skeletal and regional PTV (head, chest, neck and shoulders, abdomen) dose variations were considered.

Overall assessment of the OC-TBI delivery accuracy was performed for each individual treatment fraction for 60 patients, 30 of whom were treated with VMAT and 30 with TomoTherapy, and for patients of different heights [≤130 cm (small) versus >130 cm (large)].

Statistical Analysis

Statistical analysis was performed using IBM SPSS Statistics (USA) software. Two hundred and nine patients who received OC-TBI and underwent allogenic HSCT were included in the final analysis. Toxicity difference between 157 patients treated with TomoTherapy and 52 patients treated with VMAT was assessed with a chi-square test for independence. Comparison of planned doses for above patients groups and also the statistical analysis of delivered dose for 30 VMAT and 30 TomoTherapy patients was performed using unpaired two-sample t-tests at the 5% significance level. The normality of quantitative data was analyzed using Shapiro–Wilk test. To test the hypothesis of equality of variances we used F-test of equality of variances. The graphs of percentage difference between delivered (sum of all fractions) and planned doses were presented as a Box plot.

RESULTS

Comparison of the OC-TBI Treatment Planning Results for Two Groups of Patients Treated by TomoTherapy and VMAT

A comparison of the DVH data for the OC-TBI treatment plans of the two patient groups (TomoTherapy and VMAT) who received standardized treatment is presented in **Tables 3** and **4**.

A comparison of the averaged dose-volume histograms between the two groups of patients who received standardized OC-TBI with TomoTherapy (n = 157) and VMAT (n = 52) is shown in **Figure 3**.

Individual Quality Assurance Procedures for OC-TBI Treatment Plans

For the VMAT treatment plans, the results of composite dose verification with applied angular sensitivity correction, the percentages of the points meeting the 2%/2 mm and 3%/3 mm Gamma criteria, were 92.1 ± 1.7% (s.d.) and 99.2 ± 1.6% (s.d.), respectively.

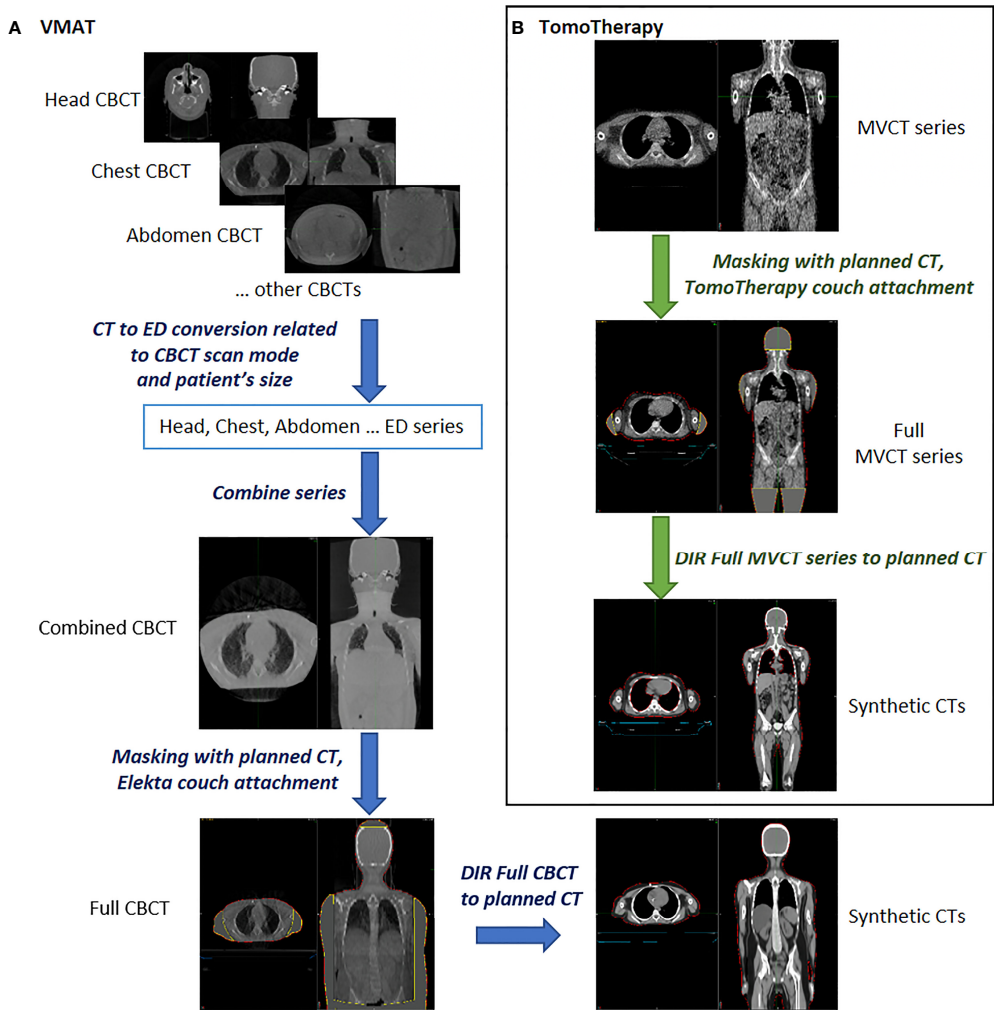

FIGURE 2 | Overview of the data preprocessing for synthetic CT creation using predeveloped workflows in MIM Maestro™ software. **(A)** for VMAT **(B)** for TomoTherapy.

The TomoTherapy-based plans showed satisfactory results in dosimetry assessment. In 96% of the cases, the measured dose was within 3% of the calculated value from the TPS. Comparison of the exit detector data with a sinogram from the TPS indicated that the percentage of points meeting the 3%/3 mm Gamma criterion were 95.3 ± 1.9% (s.d.).

Overall Assessment of Treatment Delivery Accuracy for VMAT- and TomoTherapy-Based OC-TBI

The percentage dose difference between the delivered (sum of all fractions) and planned 95% dose (D95%) for the following six subregions of the PTV is shown in **Figure 4**: a) skeleton (Bones),

TABLE 3 | OC-TBI treatment plan comparison for the two groups of patients who received standardized treatment.

Structure	Modality	D_{2max}	$D_{90\%}$	$D_{95\%}$	$D_{98\ min}$	Dmean	HI
PTV	VMAT	13.31 ± 0.23	11.77 ± 0.14	11.39 ± 0.21	10.71 ± 0.33	12.29 ± 0.09	0.21 ± 0.05
	Tomo	12.86 ± 0.40	11.83 ± 0.10	11.65 ± 0.15	11.13 ± 0.33	12.09 ± 0.15	0.14 ± 0.04
	p	<0.01	<0.05	<0.01	<0.01	<0.01	<0.01
Ribs	VMAT	12.63 ± 0.22	10.68 ± 0.25	10.34 ± 0.26	9.98 ± 0.28	11.64 ± 0.20	0.42 ± 0.05
	Tomo	12.06 ± 0.52	10.62 ± 0.40	10.33 ± 0.40	10.02 ± 0.39	11.33 ± 0.44	0.36 ± 0.04
	p	<0.01	0.27	0.92	0.44	<0.01	<0.01

TomoTherapy group, n = 157 and VMAT group, n = 52. The following metrics are presented for the OC-TBI plans for target structures PTV and Ribs: D_{2max}, $D_{90\%}$, $D_{95\%}$, $D_{98\ min}$, Dmean, V10 values and HI (the homogeneity index).

TABLE 4 | OC-TBI treatment plan comparison for the two groups of patients who received standardized treatment.

Structure	Modality	Dmean	D_{2max}	$D_{98\ min}$	V6	V8	V10
Kidney_L	VMAT	7.40 ± 0.28	9.80 ± 0.32	5.41 ± 0.35	83.84 ± 7.76	34.60 ± 7.01	1.78 ± 1.50
	Tomo	7.64 ± 0.34	11.12 ± 0.71	5.85 ± 0.57	83.78 ± 11.05	36.11 ± 7.70	10.22 ± 5.50
	p	<0.01	<0.01	<0.01	0.97	0.26	<0.01
Kidney_R	VMAT	7.48 ± 0.25	9.86 ± 0.31	5.54 ± 0.34	86.43 ± 7.11	36.43 ± 6.52	1.99 ± 1.61
	Tomo	7.64 ± 0.34	11.12 ± 0.69	5.84 ± 0.56	84.03 ± 10.96	35.95 ± 7.83	10.25 ± 5.30
	p	<0.01	<0.01	<0.01	0.08	0.79	<0.01
Lung_L	VMAT	7.72 ± 0.12	11.28 ± 0.29	5.32 ± 0.23	86.04 ± 4.17	38.81 ± 2.79	11.88 ± 1.98
	Tomo	7.85 ± 0.15	11.58 ± 0.39	6.12 ± 0.18	98.73 ± 2.35	37.55 ± 3.82	13.43 ± 3.62
	p	<0.01	<0.01	<0.01	<0.01	<0.05	<0.01
Lung_R	VMAT	7.67 ± 0.12	11.30 ± 0.26	5.19 ± 0.27	83.28 ± 4.86	38.45 ± 2.66	12.26 ± 2.04
	Tomo	7.80 ± 0.15	11.55 ± 0.34	6.11 ± 0.22	98.45 ± 2.91	36.52 ± 3.96	12.84 ± 3.23
	p	<0.01	<0.01	<0.01	<0.01	<0.01	0.17
Lens_L	VMAT	6.15 ± 0.43					
	Tomo	6.05 ± 0.74					
	p	1.34					
Lens_R	VMAT	6.33 ± 0.53					
	Tomo	5.99 ± 0.76					
	p	0.74					

TomoTherapy group, n = 157 and VMAT group, n = 52. For the OC-TBI plans, the metrics Dmean, D_{2max}, $D_{98\ min}$, V6, V8, V10 values are presented for the organ at risk structures Lung_L Lung_R, Kidney_L and Kidney_R and the mean doses for the Lens_L and Lens_R structures.

b)PTV head, c) PTV_Neck&Shoulders, d) PTV_Chest, e) PTV_Abdomen, and f) Ribs. A comparison of the TomoTherapy and VMAT OC-TBI plans for patients with height ≤130 cm (small, n = 30) and height >130 cm (large, n = 30) is also presented.

A full data comparison between the delivered doses and planned dose to PTV subregions in terms of near maximum D_{2max}, 90% ($D_{90\%}$), 95% ($D_{95\%}$), near minimum $D_{98\ min}$ of a structure, and mean dose for the TomoTherapy and VMAT OC-TBI modalities and for different patient heights [≤130 cm (small) and >130 cm (large)] are presented in **Supplementary Table 1**.

The VMAT and TomoTherapy percentage dose differences for the OARs between the delivered (sum of all fractions) and planned dose are displayed in **Figure 5**.

A full data comparison between the delivered doses (sum of doses for all fractions) and planned doses to the OARs in terms of mean, near maximum D_{2max}, and near minimum $D_{98\ min}$ dose of a structure and 90% volumes of structures covered by 6 Gy (V6), 8 Gy (V8), and 10 Gy (V10) for the TomoTherapy and VMAT OC-TBI modalities and for different patient heights [≤130 cm (small) and >130 cm (large)] are presented in **Supplementary Table 2**.

The averaged planned and delivered DVHs for the lung and ribs for both TomoTherapy and VMAT OC-TBI are displayed in **Figure 6**. The blue line represents the resulting delivered lung dose, the dark blue line represents the original lung planned dose, the orange line represents the resulting delivered rib dose and the

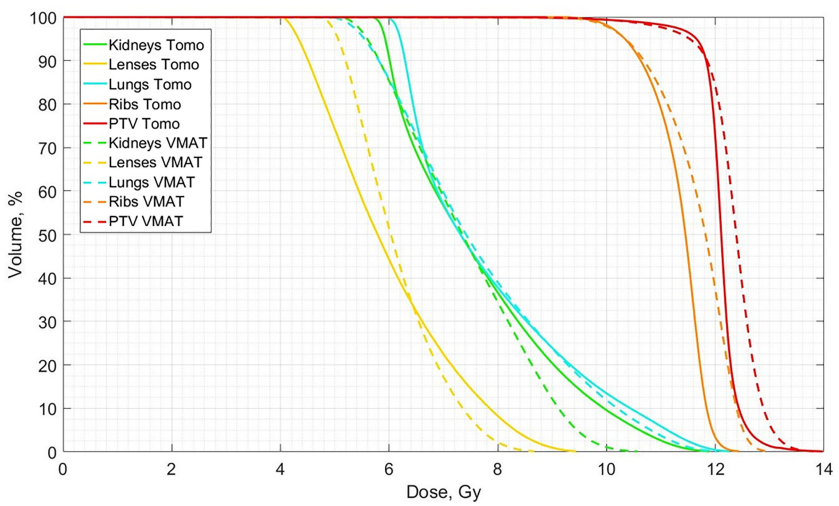

FIGURE 3 | Comparison of averaged dose-volume histograms between the standardized OC-TBI for TomoTherapy (n = 157, Tomo, solid lines) and VMAT (n = 52, VMAT, dotted lines) plans.

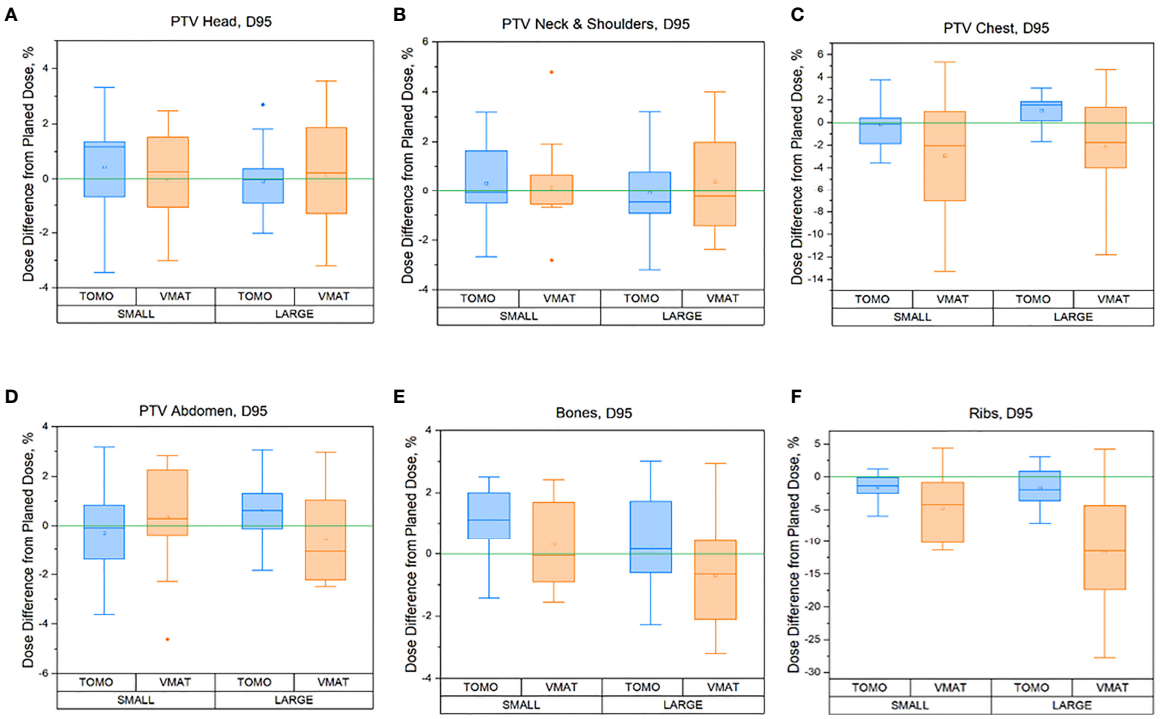

FIGURE 4 | Regional percentage dose differences between delivered (sum of all fraction) and planned 95% (D95%) doses for the TomoTherapy and VMAT OC-TBI plans for the following six PTV subregions for small (height ≤130 cm, n = 30) and large patients (height >130 cm) patients: **(A)** skeleton (Bones), **(B)** PTV head, **(C)** PTV_Neck&Shoulders, **(D)** PTV_Chest, **(E)** PTV_Abdomen, and **(F)** Ribs.

dark red line represents the original planned rib dose; the dotted lines represent the standard deviations.

Toxicity Assessment

The results of acute toxicity during radiation therapy are presented in **Table 5**.

Subacute toxicity (IP) up to the 100th day after HSCT was not observed. The median follow up period was 2.3 years. The late toxicity from kidneys and lungs was not found during the follow up period.

DISCUSSION

OC-TBI Clinical Implementation

The introduction of a standardized OC-TBI treatment significantly reduces the treatment preparation time and results in an overall more straightforward implementation of OC-TBI procedures in routine practice. This has enabled us to perform OC-TBI for three patients per week in a busy radiotherapy department setting, ensuring continuity of the radiation treatment course for patients, despite possible equipment technical malfunctions. A prerequisite for the successful implementation of OC-TBI is good communication and collaboration within the team of radiation therapists, hematologists, and medical physicists.

During pretreatment imaging, the user has access to various settings for the scanning protocols. In this case, the quality of the resulting image trades off with the speed of the scanning process and the imaging dose applied to the patient. We used fast scan protocols with bone registration for both CBCT and MVCT. The CBCT image feature has better soft tissue contrast and image resolution than MVCT, but separate scans are required for each isocenter position. MVCT does not have limitations related to the maximum length of the scan area. Zuro et al. (16) showed the advantage of whole-body imaging over partial body imaging in reducing overall patient positioning error.

Due to its technical features, the Elekta treatment unit used in VMAT treatment is less capable of irradiation of long targets than TomoTherapy. The development of the OC-TBI technique using VMAT required additional effort in treatment planning and also the physical and technical provision of quality assurance procedures. In our department, we use OC-TBI with VMAT as a backup modality to irradiate patients without potential interruption from technical issues. No patients are specifically selected for VMAT.

VMAT-based OC-TBI plans have a high number of Monitor Units. On average, one VMAT field accounts for 838 [670; 1,058] Monitor Units for the head or pelvis region and 1,760 [1,296; 2,276] MU for the chest or abdomen, which is caused by a high degree of plan modulation due to sparing of the organs at risk. Despite this fact, the results of a composite dose verification of

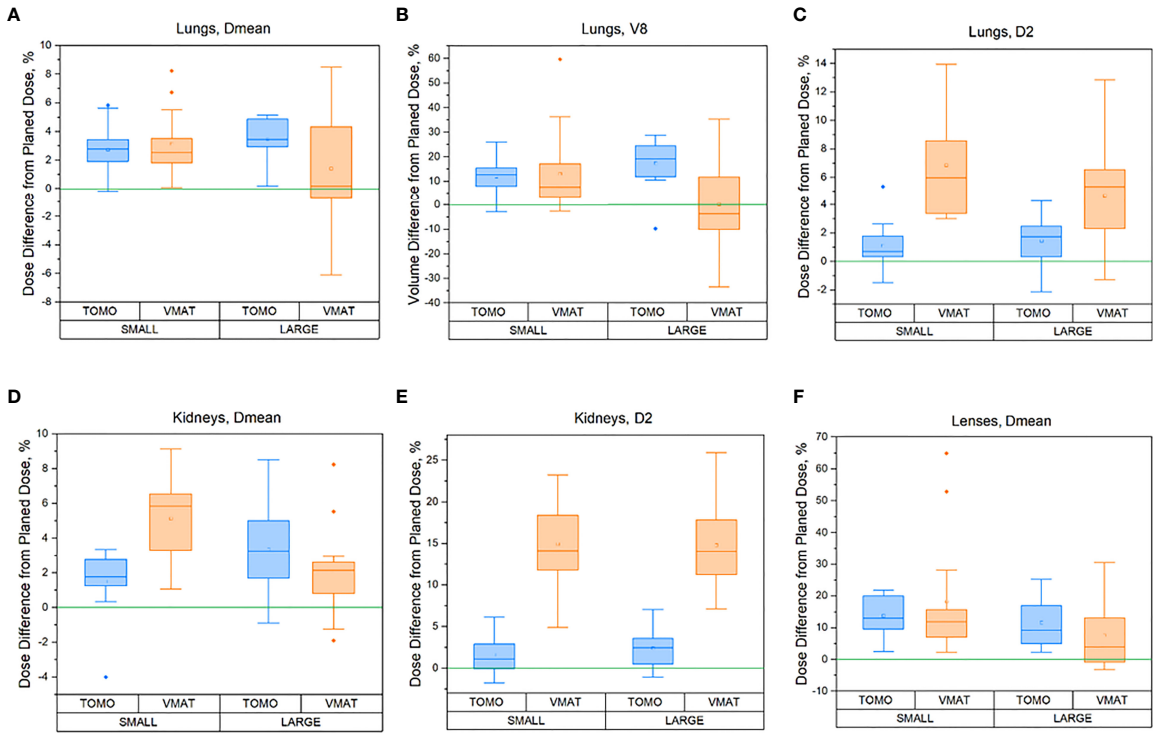

FIGURE 5 | Percentage difference between delivered (sum of all fractions) and planned doses for the OARs for different patient heights [≤130 cm (small) and >130 cm (large)]: **(A)** Lungs in terms of Dmean, **(B)** Lungs in terms of V8, **(C)** Lungs in terms of D2max, **(D)** Kidneys in terms of Dmean, **(E)** Kidneys in terms of D2max, **(F)** Lens in terms of Dmean for TomoTherapy and VMAT OC-TBI plans.

the VMAT treatment plans appeared to be satisfactory. The requirement to use multiple overlapping fields in VMAT-based OC-TBI plans can lead to additional uncertainties regarding the actual delivered dose in the area of beam overlap. The feasibility and safety of the VMAT method had been previously demonstrated (24, 30, 31).

In the case of OC-TBI or TMLI, whole-body structures must be contoured. Automation of the contouring procedures is highly advantageous and ensures a reduction in the duration of the procedure. For VMAT, a significant number of additional structures is required for dose control in the area of beam overlap and junctions. Initially, we spent at least 1 h contouring structures for

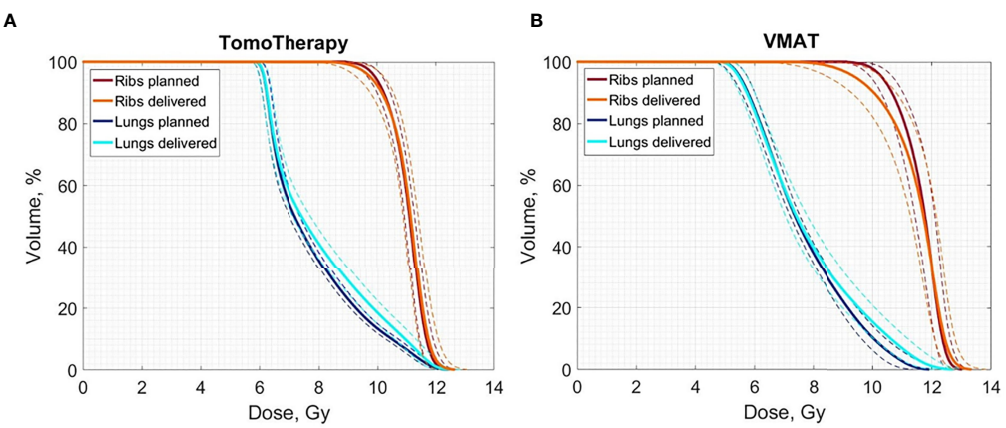

FIGURE 6 | Averaged delivered (sum of all fractions) and planned Lungs and Ribs DVH for the 30 **(A)** TomoTherapy and **(B)** 30 VMAT OC-TBI plans. Blue line represents the resulting delivered lung dose, dark blue represents the original lung planned dose, and orange line represents the resulting delivered rib dose and dark red represents the original planned rib dose; dotted lines represent standard deviations.

TABLE 5 | The results of acute toxicity during radiation therapy in TomoTherapy and VMAT patients.

Toxicity criteria (RTOG)	TomoTherapy	Vmat	P-value
Number of pts	157	52	
Nausea and vomit			
Grade 0–1	104 (66%)	33 (63%)	0.71
Grade 2–3	54 (34%)	19 (37%)	
Headache			
Grade 0–1	103 (65%)	36 (69%)	0.63
Grade 2–3	54 (35%)	16 (31%)	
Parotitis			
No clinical symptoms	63 (51%)	27 (52%)	0.14
1 Grade clinical symptoms	94 (59%)	25 (49%)	
Enteritis			
No clinical symptoms	97 (62%)	30 (57%)	0.87
Grade 1	47 (30%)	17 (33%)	
Grade 2	13 (8%)	5 (10%)	

TomoTherapy (25 structures) and 2 h for VMAT (38 structures). After introducing semiautomated contouring methods, namely, preconfigured workflows, using MIM Maestro™ software (MIM Software Inc., Clevland, OH, USA), the duration of the contouring process was reduced up to 10–15 min for both modalities.

The time required for full calculation of the treatment plan using TomoTherapy 4.5 Non-VoLO™ Systems ranges from 2 to 5 h per patient, depending on the size of the patient. We used 200–250 iterations in the background without staff involvement. Together with the initial beamlet calculation, this took up to 4.5 h and then up to approximately 50 iterations with the participation of the planner. Template-based planning speeds up the process and reduces the dose calculation time involving staff up to 40 min.

The treatment planning speed depends not only on the size of the patient but also on the hardware configuration of the TPS. Using our HP 840 workstation with 256 GB of RAM required up to 4 h to calculate the full dose of VMAT-based OC-TBI. Using plan templates reduced the required time involving staff to approximately 2 h per plan.

The dose delivery time depends on patient height and is approximately the same for both modalities—on average 30 min (from 16 to 50 min)—but the total treatment time is different, approximately up to 60 min for TomoTherapy versus up to 90 min for VMAT. Applying surface scanning systems and recent advances in imaging equipment may reduce the total fraction time, making it practical for routine application (25).

Comparison of the OC-TBI Treatment Planning Results Between TomoTherapy and VMAT

When applying the OC-TBI approach initially developed for TomoTherapy to the VMAT modality, we experienced challenges in meeting certain dose constraint criteria.

Meeting the acceptance criteria of V8 <40% for the lungs was only possible if another plan acceptance criterion related to the 6 Gy lung coverage was violated. Thus, the near minimum dose to the lungs is approximately 6 Gy for TomoTherapy and 5 Gy for the VMAT plans. The lung volume receiving a dose of 8 Gy did not exceed 40% for either case, but its mean dose differed slightly. The average dose to the kidneys was similar for TomoTherapy and the VMAT, while the volume of kidneys that received the near maximum dose was 13.1% lower for the VMAT plans due to the smoother achieved dose gradient.

Both methods showed acceptable quality in the PTV dose coverage while maintaining OAR sparing, but the mean PTV dose was 1.6% higher in the VMAT plans. The uniformity of PTV irradiation was superior for TomoTherapy, as evidenced by the lower HI values for TomoTherapy relative to VMAT.

Overall Assessment of Treatment Delivery Accuracy for VMAT- and TomoTherapy-Based OC-TBI

Pretreatment visualizations (MVCT or CBCT) were used to correct patient position prior to treatment. However, the anatomical changes of the patient between fractions and positioning errors affect dose delivery during the treatment course. Accurate knowledge of the delivered dose to the OARs and to the target could prove advantageous in the future analysis of treatment outcomes.

Pediatric patients have a significant range in body size. We evaluated whether our OC-TBI methods provide sufficient plan robustness when applied to patients of varying sizes. Differences in the patient size did not result in significant differences for most parameters in either TomoTherapy- or VMAT-based OC-TBI.

However, differences between TomoTherapy and VMAT delivery were observed. In general, TomoTherapy-based OC-TBI treatment plans were more robust and less affected by variations in daily patient positioning (**Figure 6**, **Supplementary Table 2**). The percentage difference between planned and delivered doses (sum of all fractions) in the D_{2max} value for both the lungs and kidneys showed higher values for VMAT than for TomoTherapy. Thus, the D_{2max} percentage difference between the delivered (sum of all fractions) and planned dose in the right kidneys (large height group) was 2.4 [1.1; 3.7] % for TomoTherapy versus 15.1 [12.4; 17.8] % for VMAT plans. This might have been caused by the features of VMAT OC-TBI treatment plans, which had higher mean PTV doses and contained hotspots in the abdomen/pelvic junction area (**Figure 1**). Given that the planned D_{2max} dose in the

kidneys was lower for VMAT than for TomoTherapy (9.8 versus 11.1 Gy), the absolute values of the delivered dose looked acceptable (11.3 vs. 11.4 Gy).

The parts of the lungs receiving doses in excess of 8 Gy included a high dose gradient and were susceptible to dose delivery variations (**Figure 6**). These areas were characterized by an approximately 10% excess of the delivered dose relative to the planned dose for both TomoTherapy and VMAT. At the same time, the near minimum lung doses were less subject to changes. These results are consistent with the report of Zuro (16). Nevertheless, the mean delivered dose to the lungs increased by an average of less than 5.4% relative to the planned dose.

In relation to the mean dose to the PTV and its subregions, both modalities showed consistent results. The average percentage difference between delivered and planned mean doses to the PTV subregions was within 1% (**Supplementary Table 1**). The variation between planned and delivered values of $D_{95\%}$ coverage for the Head, Neck and Shoulders, Abdomen and Bones PTV subregions remained within 5% for both the TomoTherapy and VMAT modalities (**Figure 4**), which indicates the reliability of dose delivery to these regions.

Figure 6 shows that TomoTherapy plans were more robust with respect to $D_{95\%}$ for rib dose coverage. We observed higher percentage variations in the Ribs $D_{95\%}$ for the VMAT plans [−11.5 (−15.7, −7.3) %] than for TomoTherapy [−1.7 (−3.3, −0.1) %] in the large height patient group. This could be caused by the steeper dose gradient in the chest area for the TomoTherapy planning dose distribution relative to VMAT.

Our method of estimating the delivered dose has limitations. We do not receive images during or after the treatment. If the patient changes his position during the treatment, we cannot consider this. An important advantage of OC-TBI is the ability to treat pediatric patients in the supine position, which is the most comfortable for the patient and provides good reproducibility of the patient setup and high accuracy of the dose delivery

Conclusions and Future Direction

The study demonstrates that both the TomoTherapy and VMAT modalities are feasible, safe and provide acceptable toxicity in pediatric OC-TBI.

Our previous results also demonstrated that OC-TBI appears to be a promising technique for the treatment of pediatric patients (43, 44). Applying a standardization approach allowed us to homogeneously implement pediatric OC-TBI in routine clinical practice. OC-TBI is a technically complex, resource-intensive treatment modality, and its implementation requires automation and standardization at all stages of pretreatment preparation.

Despite of the detected planned and delivered dose difference between TomoTherapy and VMAT there were no significant differences in acute and subacute toxicity. The developed standardized OC-TBI with accurate dose delivery assessment may give the possibility to investigate the correlation between the delivered dose and the clinical outcomes. Automation of the pretreatment processes and application of fast semiautomatic planning or knowledge-based planning optimization solutions will help increase the availability of TBI/TMLI treatment techniques for more patients.

The accumulation of new clinical data and potential advantages of OAR sparing combined with possible target dose escalation could open new possibilities for the transition from OC-TBI to new, more targeted approaches for certain cohorts of pediatric patients.

DATA AVAILABILITY STATEMENT

The original contributions presented in the study are included in the article/**Supplementary Material**. Further inquiries can be directed to the corresponding author.

ETHICS STATEMENT

The studies involving human participants were reviewed and approved by the Local Ethics Committee of the Dmitry Rogachev National Medical Research Center of Pediatric Hematology, Oncology and Immunology. Written informed consent to participate in this study was provided by the participants' legal guardian/next of kin.

AUTHOR CONTRIBUTIONS

AAL, DT, DK, AOL, and AN contributed equally to this work. AAL, DT and AN designed the study, collected and analyzed data, and wrote the paper. AOL collected and analyzed data. DK collected, analyzed data and wrote the paper. MM and AC contributed to study design and reviewed the paper. OE contributed to data analysis and reviewed the paper. All authors listed have made a substantial, direct, and intellectual contribution to the work and approved it for publication.

SUPPLEMENTARY MATERIAL

The Supplementary Material for this article can be found online at: https://www.frontiersin.org/articles/10.3389/fonc.2022.785917/full#supplementary-material

REFERENCES

1. Carruthers SA, Wallington MM. Total Body Irradiation and Pneumonitis Risk: A Review of Outcomes. *Brit J Cancer* (2004) 90(11):2080–4. doi: 10.1038/sj.bjc.6601751
2. Kelsey CR, Horwitz ME, Chino JP, Craciunescu O, Steffey B, Folz RJ, et al. Severe Pulmonary Toxicity After Myeloablative Conditioning Using Total Body Irradiation: An Assessment of Risk Factors. *Int J Radiat Oncol Biol Phys* (2011) 81(3):812–8. doi: 10.1016/j.ijrobp.2010.06.058
3. Abugideiri M, Nanda RH, Butker C, Zhang C, Kim S, Chiang KY, et al. Factors Influencing Pulmonary Toxicity in Children Undergoing Allogeneic Hematopoietic Stem Cell Transplantation in the Setting of Total Body Irradiation-Based Myeloablative Conditioning. *Int J Radiat Oncol Biol Phys* (2016) 94(2):349–59. doi: 10.1016/j.ijrobp.2015.10.054

4. Keane JT, Fontenla DP, Chui CS. Applications of IMAT to Total Body Radiation (TBI). *Int J Radiat Oncol Biol Phys* (2000) 48(3S1):239–9. doi: 10.1016/S0360-3016(00)80274-6
5. Hussain A, Villarreal-Barajas JE, Dunscombe P, Brown DW. Aperture Modulated, Translating Bed Total Body Irradiation. *Med Phys* (2011) 38 (2):932–41. doi: 10.1118/1.3534196
6. Hui SK, Kapatoes J, Fowler J, Henderson D, Olivera G, Manon RR, et al. Feasibility Study of Helical Tomotherapy for Total Body or Total Marrow Irradiation. *Med Phys* (2005) 32(10):3214–24. doi: 10.1118/1.2044428
7. Wong JY, Liu A, Schultheiss T, Popplewell L, Stein A, Rosenthal J, et al. Targeted Total Marrow Irradiation Using Three-Dimensional Image-Guided Tomographic Intensity-Modulated Radiation Therapy: An Alternative to Standard Total Body Irradiation. *Biol Blood Marrow Transplant* (2006) 12 (3):306–15. doi: 10.1016/j.bbmt.2005.10.026
8. Hui SK, Verneris MR, Froelich J, Dusenbery K, Welsh JS. Multimodality Image Guided Total Marrow Irradiation and Verification of the Dose Delivered to the Lung, PTV, and Thoracic Bone in a Patient: A Case Study. *Technol Cancer Res Treat* (2009) 8(1):23–8. doi: 10.1177/153303460900800104
9. Aydogan B, Mundt AJ, Roeske JC. Linac-Based Intensity Modulated Total Marrow Irradiation (IM-TMI). *Technol Cancer Res Treat* (2006) 5(5):513–9. doi: 10.1177/153303460600500508
10. Wilkie JR, Tiryaki H, Smith BD, Roeske JC, Radosevich JA, Aydogan B. Feasibility Study for Linac-Based Intensity Modulated Total Marrow Irradiation. *Med Phys* (2008) 35(12):5609–18. doi: 10.1118/1.2990779
11. Ouyang L, Folkerts M, Zhang Y, Hrycushko B, Lamphier R, Lee P, et al. Volumetric Modulated Arc Therapy Based Total Body Irradiation: Workflow and Clinical Experience With an Indexed Rotational Immobilization System. *Phys Imaging Radiat Oncol* (2017) 4:22–5. doi: 10.1016/j.phro.2017.11.002
12. Tas B, Durmus IF, Okumus A, Uzel OE, Gokce M, Goksoy HS, et al. Total-Body Irradiation Using Linac-Based Volumetric Modulated Arc Therapy: Its Clinical Accuracy, Feasibility and Reliability. *Radiother Oncol* (2018) 129 (3):527–33. doi: 10.1016/j.radonc.2018.08.005
13. Springer A, Hammer J, Winkler E, Track C, Huppert R, Bohm A, et al. Total Body Irradiation With Volumetric Modulated Arc Therapy: Dosimetric Data and First Clinical Experience. *Radiat Oncol* (2016) 11:46. doi: 10.1186/s13014-016-0625-7
14. Gruen A, Ebell W, Wlodarczyk W, Neumann O, Kuehl JS, Stromberger C, et al. Total Body Irradiation (TBI) Using Helical Tomotherapy in Children and Young Adults Undergoing Stem Cell Transplantation. *Radiat Oncol* (2013) 8:92. doi: 10.1186/1748-717X-8-92
15. Wong JY, Filippi AR, Scorsetti M, Hui S, Muren LP, Mancosu P. Total Marrow and Total Lymphoid Irradiation in Bone Marrow Transplantation for Acute Leukaemia. *Lancet Oncol* (2020) 21(10):e477–87. doi: 10.1016/S1470-2045(20)30342-9
16. Zuro D, Vagge S, Broggi S, Agostinelli S, Takahashi Y, Brooks J. Multi-Institutional Evaluation of MVCT Guided Patient Registration and Dosimetric Precision in Total Marrow Irradiation: A Global Health Initiative by the International Consortium of Total Marrow Irradiation. *Radiother Oncol* (2019) 141:275–82. doi: 10.1016/j.radonc.2019.07.010
17. Stein A, Palmer J, Tsai NC, Al Malki MM, Aldoss I, Ali H, et al. Phase I Trial of Total Marrow and Lymphoid Irradiation Transplantation Conditioning in Patients With Relapsed/Refractory Acute Leukemia. *Biol Blood Marrow Transplant* (2017) 23(4):618–24. doi: 10.1016/j.bbmt.2017.01.067
18. Kim JH, Stein A, Tsai N, Schultheiss TE, Palmer J, Liu A, et al. Extramedullary Relapse Following Total Marrow and Lymphoid Irradiation in Patients Undergoing Allogeneic Hematopoietic Cell Transplantation. *Int J Radiat Oncol Biol Phys* (2014) 89(1):75–81. doi: 10.1016/j.ijrobp.2014.01.036
19. Hoeben BAW, Pazos M, Albert MH, Seravalli E, Bosman ME, Losert C, et al. Towards Homogenization of Total Body Irradiation Practices in Pediatric Patients Across SIOPE Affiliated Centers. A Survey by the SIOPE Radiation Oncology Working Group. *Radiother Oncol* (2021) 155:113–9. doi: 10.1016/j.radonc.2020.10.032
20. Rassiah P, Esiashvili N, Olch AJ, Hua CH, Ulin K, Molineu A, et al. Practice Patterns of Pediatric Total Body Irradiation Techniques: A Children's Oncology Group Survey. *Int J Radiat Oncol Biol Phys* (2021) 111(5):1155–64. doi: 10.1016/j.ijrobp.2021.07.1715
21. Esiashvili N, Lu X, Ulin K, Laurie F, Kessel S, Kalapurakal JA, et al. Higher Reported Lung Dose Received During Total Body Irradiation for Allogeneic Hematopoietic Stem Cell Transplantation in Children With Acute Lymphoblastic Leukemia Is Associated With Inferior Survival: A Report From the Children's Oncology Group. *Int J Radiat Oncol Biol Phys* (2019) 104(3):513–21. doi: 10.1016/j.ijrobp.2019.02.034
22. Frassoni F, Scarpati D, Bacigalupo A, Vitale V, Corvo R, Miceli S, et al. The Effect of Total Body Irradiation Dose and Chronic Graft-Versus-Host Disease on Leukaemic Relapse After Allogeneic Bone Marrow Transplantation. *Br J Haematol* (1989) 73(2):211–6. doi: 10.1111/j.1365-2141.1989.tb00254.x
23. Scarpati D, Frassoni F, Vitale V, Corvo R, Franzone P, Barra S, et al. Total Body Irradiation in Acute Myeloid Leukemia and Chronic Myelogenous Leukemia: Influence of Dose and Dose-Rate on Leukemia Relapse. *Int J Radiat Oncol Biol Phys* (1989) 17(3):547–52. doi: 10.1016/0360-3016(89)90105-3
24. Cox JD, Stetz J, Pajak TF. Toxicity Criteria of the Radiation Therapy Oncology Group (RTOG) and the European Organization for Research and Treatment of Cancer (EORTC). *Int J Radiat Oncol Biol Phys* (1995) 31(5):1341–46. doi: 10.1016/0360-3016(95)00060-C
25. Haraldsson A, Engellau J, Lenhoff S, Engelholm S, Bäck S, Engström PE. Implementing Safe and Robust Total Marrow Irradiation Using Helical Tomotherapy - A Practical Guide. *Phys Med* (2019) 60:162–7. doi: 10.1016/j.ejmp.2019.03.032
26. Takahashi Y, Verneris MR, Dusenbery KE, Wilke CT, Storme G, Weisdorf DJ, et al. Peripheral Dose Heterogeneity Due to the Thread Effect in Total Marrow Irradiation With Helical Tomotherapy. *Int J Radiat Oncol Biol Phys* (2013) 87 (4):832–9. doi: 10.1016/j.ijrobp.2013.07.017
27. Chen M, Chen Y, Chen Q, Lu W. Theoretical Analysis of the Thread Effect in Helical TomoTherapy. *Med Phys* (2011) 38(11):5945–60. doi: 10.1118/1.3644842
28. Usui K, Isobe A, Hara N, Shikama N, Sasai K, Ogawa K. Appropriate Treatment Planning Method for Field Joint Dose in Total Body Irradiation Using Helical Tomotherapy. *Med Dosim* (2019) 44(4):344–53. doi: 10.1016/j.meddos.2018.12.003
29. Loginova AA, Tovmasyan DA, Chernyaev AP, Varzar' SM, Kobyzeva DA, Nechesnyuk AV. Field Junction Technique for Helical Tomotherapy-Based Total Body Irradiation. *Med Radiol Radiat Saf* (2018) 63(2):55–61. doi: 10.12737/article_5ac622371650f7.48983677
30. Aydogan B, Yeginer M, Kavak GO, Fan J, Radosevich JA, Gwe-Ya K. Total Marrow Irradiation With RapidArc Volumetric Arc Therapy. *Int J Radiat Oncol Biol Phys* (2011) 81(2):592–9. doi: 10.1016/j.ijrobp.2010.11.035
31. Mancosu P, Navarria P, Reggiori G, Cozzi L, Fogliata A, Gaudino A, et al. *In-Vivo* Dosimetry With Gafchromic Films for Multi-Isocentric VMAT Irradiation of Total Marrow Lymph-Nodes: A Feasibility Study. *Radiother Oncol* (2015) 10:86. doi: 10.1186/s13014-015-0391-y
32. Fogliata A, Cozzi L, Clivio A, Ibatici A, Mancosu P, Navarria P, et al. Preclinical Assessment of Volumetric Modulated Arc Therapy for Total Marrow Irradiation. *Int J Radiat Oncol Biol Phys* (2011) 80(2):626–36. doi: 10.1016/j.ijrobp.2010.11.028
33. Han C, Schultheisss TE, Wong JY. Dosimetric Study of Volumetric Modulated Arc Therapy Fields for Total Marrow Irradiation. *Radiother Oncol* (2012) 102 (2):315–20. doi: 10.1016/j.radonc.2011.06.005
34. Symons K, Morrison C, Parry J, Woodings S, Zissiadis Y. Volumetric Modulated Arc Therapy for Total Body Irradiation: A Feasibility Study Using Pinnacle3 Treatment Planning System and Elekta Agility™ Linac. *J Appl Clin Med Phys* (2018) 19(2):103–10. doi: 10.1002/acm2.12257
35. Nalichowski A, Eagle DG, Burmeister J. Dosimetric Evaluation of Total Marrow Irradiation Using 2 Different Planning Systems. *Med Dosim* (2016) 41(3):230–35. doi: 10.1016/j.meddos.2016.06.001
36. Mancosu P, Navarria P, Castagna L, Roggio A, Pellegrini C, Reggiori G, et al. Anatomy Driven Optimization Strategy for Total Marrow Irradiation With a Volumetric Modulated Arc Therapy Technique. *J Appl Clin Med Phys* (2012) 13(1):138–47. doi: 10.1120/jacmp.v13i1.3653
37. Mancosu P, Navarria P, Castagna L, Reggiori G, Stravato A, Gaudino A, et al. Plan Robustness in Field Junction Region From Arcs With Different Patient Orientation in Total Marrow Irradiation With VMAT. *Phys Med* (2015) 31 (7):677–82. doi: 10.1016/j.ejmp.2015.05.012
38. WangL, QiuG, YuJ, ZhangQ, ManL, ChenL, et al. Effect of Auto Flash Margin on Superficial Dose in Breast Conserving Radiotherapy for Breast Cancer. *J Appl Clin Med Phys* (2021) 22(6):60–70. doi: 10.1002/acm2.13287

39. Tovmasian DA, Loginova AA, Chernyaev AP, Nechesnyuk AV. Non-Standard Use of TomoTherapy Exit Imaging Detectors for Quality Assurance Procedures. *Moscow Univ Phys Bull*+ (2021) 76(6):470–76. doi: 10.3103/S0027134921060096
40. Low DA, Harms WB, Mutic S, Purdy JA. A Technique for the Quantitative Evaluation of Dose Distributions. *Med Phys* (1998) 25(5):656–61. doi: 10.1118/1.598248
41. Miften M, Olch A, Mihailidis D, Moran J, Pawlicki T, Molineu A, et al. Tolerance Limits and Methodologies for IMRT Measurement-Based Verification QA: Recommendations of AAPM Task Group No. 218. *Med Phys* (2018) 45(4):e53–83. doi: 10.1002/mp.12810
42. Loginova AA, Tovmasian DA, Kokoncev DA, Varzar SM, Chernyaev AP. Angular Dependence Investigation of the MatriXX Detector Array for Dosimetric Verification of Treatment Plans With Intensity Modulation. *Moscow Univ Phys Bull*+ (2021) 76(5):384–91. doi: 10.3103/S0027134921050118
43. Kobyzeva D, Shelikhova L, Shekhovtsova Z, Khismatullina R, Ilushina M, Loginova A, et al. Total Body Irradiation Among Recipients of Tcrαβ/CD19-Depleted Grafts in a Cohort of Children With Hematologic Malignances: Single Center Experience. *Blood* (2020) 136:2–2. doi: 10.1182/blood-2020-139282
44. Dunaikina M, Zhekhovtsova Z, Shelikhova L, Glushkova S, Nikolaev R, Blagov S, et al. Safety and Efficacy of the Low-Dose Memory (CD45RA-Depleted) Donor Lymphocyte Infusion in Recipients of αβ T Cell-Depleted Haploidentical Grafts: Results of a Prospective Randomized Trial in High-Risk Childhood Leukemia. *Bone Marrow Transpl* (2021) 56(7):1614–24. doi: 10.1038/s41409-021-01232-x

Conflict of Interest: The authors declare that the research was conducted in the absence of any commercial or financial relationships that could be construed as a potential conflict of interest.

Publisher's Note: All claims expressed in this article are solely those of the authors and do not necessarily represent those of their affiliated organizations, or those of the publisher, the editors and the reviewers. Any product that may be evaluated in this article, or claim that may be made by its manufacturer, is not guaranteed or endorsed by the publisher.

frontiers | Frontiers in Oncology

METHODS
published: 18 July 2022
doi: 10.3389/fonc.2022.941814

Feasibility of a Novel Sparse Orthogonal Collimator–Based Preclinical Total Marrow Irradiation for Enhanced Dosimetric Conformality

*Amr M. H. Abdelhamid[1,2,3], Lu Jiang[4], Darren Zuro[5], An Liu[1], Srideshikan Sargur Madabushi[1], Hemendra Ghimire[1], Jeffrey Y. C. Wong[1], Simonetta Saldi[2], Christian Fulcheri[2], Claudio Zucchetti[2], Antonio Pierini[2], Ke Sheng[4], Cynthia Aristei[2] and Susanta K. Hui[1]**

[1] Department of Radiation Oncology, City of Hope Medical Center, Duarte, CA, United States, [2] Radiation Oncology Section, Department of Medicine and Surgery, Perugia University and General Hospital, Perugia, Italy, [3] Department of Clinical Oncology and Nuclear Medicine, Faculty of Medicine, Ain Shams University, Cairo, Egypt, [4] Department of Radiation Oncology, University of California Los Angeles, Los Angeles, CA, United States, [5] Department of Radiation Oncology, University of Oklahoma, Norman, OK, United States

OPEN ACCESS

Edited by:
James Chow,
University of Toronto, Canada

Reviewed by:
Evgeniia Sukhikh,
Tomsk Polytechnic University, Russia
Ruijie Yang,
Peking University Third Hospital, China

***Correspondence:**
Susanta K. Hui
shui@coh.org

Specialty section:
This article was submitted to Radiation Oncology, a section of the journal Frontiers in Oncology

Received: 11 May 2022
Accepted: 23 June 2022
Published: 18 July 2022

Citation:
Abdelhamid AMH, Jiang L, Zuro D, Liu A, Madabushi SS, Ghimire H, Wong JYC, Saldi S, Fulcheri C, Zucchetti C, Pierini A, Sheng K, Aristei C and Hui SK (2022) Feasibility of a Novel Sparse Orthogonal Collimator–Based Preclinical Total Marrow Irradiation for Enhanced Dosimetric Conformality. Front. Oncol. 12:941814. doi: 10.3389/fonc.2022.941814

Total marrow irradiation (TMI) has significantly improved radiation conditioning for hematopoietic cell transplantation in hematologic diseases by reducing conditioning-induced toxicities and improving survival outcomes in relapsed/refractory patients. Recently, preclinical three-dimensional image–guided TMI has been developed to enhance mechanistic understanding of the role of TMI and to support the development of experimental therapeutics. However, a dosimetric comparison between preclinical and clinical TMI reveals that the preclinical TMI treatment lacks the ability to reduce the dose to some of the vital organs that are very close to the skeletal system and thus limits the ability to evaluate radiobiological relevance. To overcome this limit, we introduce a novel Sparse Orthogonal Collimator (SOC)–based TMI and evaluate its ability to enhance dosimetric conformality. The SOC-TMI–based dose modulation technique significantly improves TMI treatment planning by reducing radiation exposures to critical organs that are close to the skeletal system that leads to reducing the gap between clinical and preclinical TMI.

Keywords: TBI, TMI, SOC, HCT, RAO, CBCT (cone beam computed tomography)

INTRODUCTION

Radiotherapy is an important component of bone marrow transplantation condition regimens for hematological diseases (1). For more than 50 years, total body irradiation (TBI) has been a standard of care as a conditioning regimen for the host immune suppression and for the reduction of disease burden to allow donor engraftment (2, 3). Several randomized trials have demonstrated superior outcomes using TBI compared to non-TBI–containing regimens (4, 5). Although TBI-based dose

escalation reduces relapse in high-risk patients with leukemia, no benefit in overall survival was observed due to organ toxicity (6). This further emphasized the unmet clinical need for advanced technology.

Hui et al., for the first in the field, have developed a more targeted conformal form of TBI delivery [total marrow irradiation (TMI)] (7). TMI approach is to spare the organs at risk (OARs) and the remaining healthy tissues in the body, maintaining the coverage of target hematopoietic or lymphoid tissues with respect to the standard TBI. The feasibility and early clinical data of TMI were reported both by helical tomotherapy (HT)–based approaches (7–10), conventional Linac using intensity-modulated radiation therapy (IMRT) (11, 12), and volumetric modulated arc therapy (VMAT) using rapid arc approach (Varian Medical Systems, Palo Alto, CA) (13, 14).

Although new clinical technology supported clinical advancement, the relapse rate remains high. For a mechanistic understanding of the role of TMI on engraftment, antileukemic effect, etc., and to envelope future experimental therapeutics, a preclinical mouse model is essential. A film-based two-dimensional (2D) image guidance method identifying organ position and copper compensator was used to develop the first-generation preclinical TMI (15). However, it lacks three-dimensional (3D) imaging to detect targets and organs, generating organ dosimetry such as dose-volume histograms (DVHs), the inclusion of tissue heterogeneity, and the ability to vary dose exposures. Therefore, we developed the second-generation CT image–guided 3D-TMI (16), which, however, showed limited ability to reduce dose to organs that are close to the skeletal system (e.g., lungs and kidney). In this study, we introduce a new concept Sparse Orthogonal Collimator (SOC)–based TMI (SOC-TMI). Comparative analysis of SOC-TMI planning and dosimetry from recently reported 3D-TMI and several clinical TMI plans shows substantial improvements in dosimetric control while accompanying SOC in preclinical TMI platforms.

MATERIAL AND METHODS

Clinical TMI Studies

We reviewed published articles, in which patients with leukemia were treated with TMI techniques using either HT (Tomotherapy, Madison, WI) or Linac-based volumetric arc therapy. From the available literature, we selected four papers that were conducted to evaluate whether TMI obtained optimal dosimetric coverage of the PTV and sparing of various organs such as the heart, gut, lungs, kidneys, and liver (8, 9, 13, 14). Furthermore, data from two unpublished clinical TMI studies from the Radiation Oncology Department of the Perugia University and City of Hope Radiation Oncology Center were analyzed. Because target prescription dose varies across centers, we calculated the percentage dose exposure to organs with respect to the prescribed dose. This relative dose exposure is then compared with the relative dose exposure obtained from 3D-TMI and SOC-TMI preclinical models.

TMI Preclinical Models

The preclinical TMI treatments were performed using the x-ray irradiator (Precision X-Ray, North Branford, CT) in compliance with the current guidelines (17). It has a maximum tube potential of 225 kV. Photons were filtered through a beryllium window with an additional 2.0-mm aluminum filter for imaging and 0.32-mm copper filter for treatment (18). We have used five-mice cases for both TMI preclinical models. The animal was placed in a custom-designed animal holder under isoflurane anesthesia to ensure its immobilization and reproducible positioning. Cone Beam Computed Tomography (CBCT) scans of reference animals in the prone position were acquired using 40-kVp and 3-mA beam settings with a 0.2-mm voxel size. Using velocity, soft tissue organs were identified and contoured for use in treatment planning. Moreover, we contoured the entire body minus the skeletal bones and the spleen to calculate the integral dose to the body. After contouring, images were exported to the planning systems to generate TMI plans.

3D-TMI Preclinical

The 3D-TMI preclinical model was developed as a second-generation TMI preclinical model (16). Mice 3D-TMI preclinical radiation treatment plans are generated by following steps: The whole-body mouse CBCT scan was performed. Next, whole-body CT scans separated into seven regions: head, cervical spine, dorsal spine and spleen, lumber spine, femurs, tibias, and shoulders. Visualization of a projected radiation beam on a 3D CT image allowed for adjustment of beam size and isocenter to cover the target and reduce exposure to adjacent critical organs. Each region has its beam size, isocenter location, and normalization point, and parallel-opposed beams with varied beam size were used to create a homogenized dose. Field matching is achieved by imposing different beam sizes [40 mm × 40 mm (standard), 20 mm × 20 mm (standard), 10 mm × 10 mm (standard), 10 mm × 10 mm (cylinder), and 5 mm × 5 mm (cylinder)], both parallelism and coincidence between the side planes of adjacent fields (**Figures 1A–C**). However, the spleen, femurs, and tibias beams are matched with dorsal and lumber beams. Matched beams in those regions have some hot spots because of the intersection between lateral parallelized beams and perpendicular beams (**Figures 1D–F**). Mice TMI is a 3D treatment planning with kilovoltage (kV) radiation beams on whole-body CBCT image, and dose distribution and absorbed dose are significantly affected by HU CBCT pixel values, as bone areas absorbed more than 250% of the prescribed dose due to kV-radiation beams (19, 20) (**Figures 3A, B**). The CT-guided Monte Carlo dose calculations accounted for tissue heterogeneity, enhancing accuracy of organ dose evaluation. Detail validation of Monte Carlo–based treatment planning system (TPS) including calculation of dose to medium was previously published (17, 18).

GAFChromic EBT3 film- and dosimeter-based dosimetry was used for the dosimetric validation. Briefly, the film was calibrated for treatment settings at the isocenter up to 5 Gy. After calibration, the film was placed under the mouse, and a tissue prescription dose of 2 Gy was delivered. Afterward, different regions of interest were outlined in the film identifying the exit

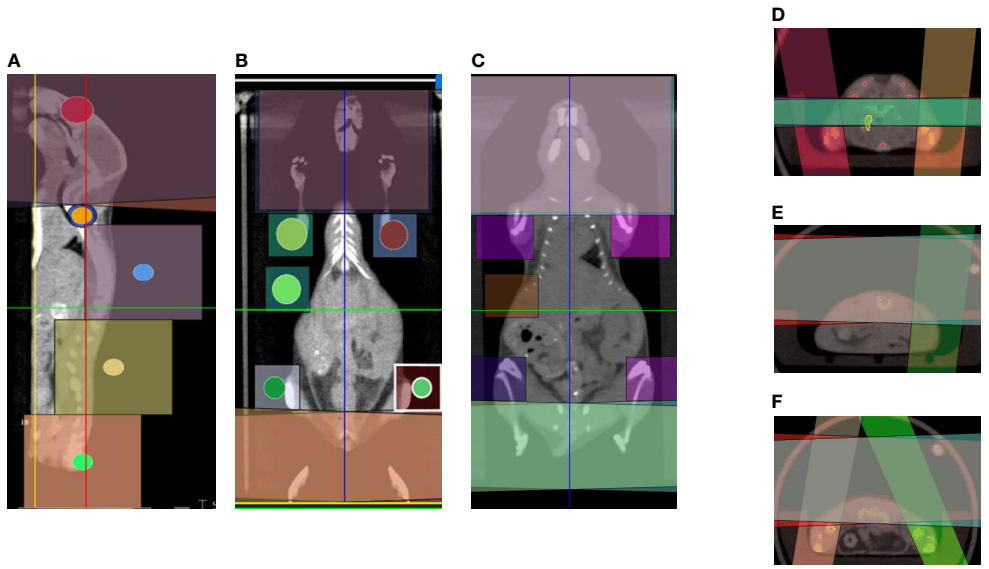

FIGURE 1 | Common beam arrangements of 3D-TMI treatment. Beam arrangement for parallel opposed beams in **(A)** sagittal view. **(B, C)** Coronal views demonstrating different body levels. **(D–F)** Axial view in the thoracic, abdominal, and pelvic level showing beams overlapping.

dose through the spine, lungs, and gut to accommodate density variation in the path of the x-ray. The mean dose measurement was compared with the TPS at the film location to establish an agreement. We used 2 Gy for film validation so that the dose response was in the linear region of the EBT3 film. The overall time of 3D-TMI preclinical planning is approximately 75 min: 15 min for beam placement; 45 min for planning, optimization, and dose calculation; and 25 min for the estimated delivery time.

SOC-TMI Preclinical

Mouse position, immobilization, and CBCT imaging are the same as in the 3D-TMI preclinical model. The SOC system is designed and fabricated with four orthogonal, double-focused tungsten leaf pairs, which is programmed and controlled by the Rectangular Aperture Optimization (RAO) algorithm (21, 22), which solves an inverse optimization problem for IMRT planning. The SOC can be installed on the small animal irradiator (Precision X-Ray, North Branford, CT) with a 3D printed adapter. The plan is uploaded to the SOC control module, which drives tungsten leaf pairs to form rectangular apertures and delivers the dose to mouse bones and spleen while sparing adjacent organs at risk. The SOC plans are utilizing seven equally distributed coplanar fields. In each coplanar field, there are several rectangular components made by tungsten collimators to deliver the dose. **Figure 2A** shows the four orthogonal, double-focused tungsten leaf pairs closed before planning optimization. **Figure 2B** shows how tungsten collimators move to form rectangular components at the coronal angle, and color yellow means the area that beams can go through to the PTV. Overall, each IMRT SOC-TMI preclinical plan uses 61 to 93 rectangles per field to intensity modulate the x-ray fluence. The number of rectangles depends on the size and complexity of the target as a result of RAO inverse optimization. **Figures 2C, D** show SOC-TMI and 3D-TMI schematic beam arrangement according to the X-RAD SmART small animal image-guided irradiation system, respectively. SOC-TMI preclinical model uses convolution/superposition code with a 225-kV x-ray poly-energetic kernel in a distributed multiple GPU framework, as described (21–23) for the beamlet dose calculation; its accuracy in profile dose is below 2% on average from Monte Carlo simulation, but it is faster and more flexible to meet performance requirements for most users. A fast-iterative shrinkage-thresholding algorithm is used to optimize the treatment plan. The beam commissioning data were acquired on the small animal irradiator (Precision X-Ray, North Branford, CT) (21). The beamlet resolution at the isocenter was 1 mm × 1 mm. The dose array resolution was 0.25 mm × 0.25 mm × 0.25 mm. The source-to-isocenter distance (SID) was 30.54 cm. For SOC-TMI plans, the field size is extended to 120 mm × 120 mm. The dose calculation and optimization were performed on a Xeon 40-core CPU server operating at 3.10-GHz clock with MATLAB. The overall time of SOC planning is approximately 45 min: 25 min for planning, optimization, and dose calculation and 20 min for the estimated delivery time.

RESULTS

For each of the five mice, median dose percent, average, and standard deviation for organs at risk in both 3D-TMI preclinical model and SOC-TMI preclinical model are listed in **Table 1**. The median dose of TMI clinical and preclinical studies with treatment protocol, treatment technique, and prescription dose

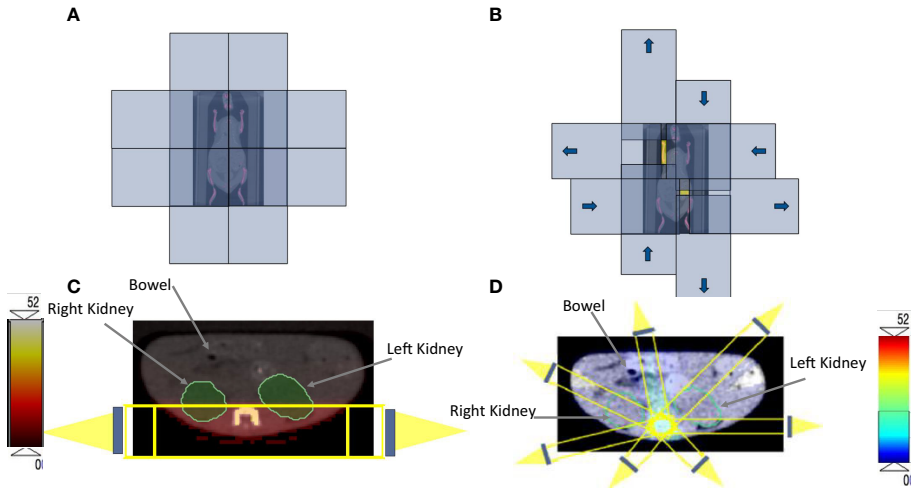

FIGURE 2 | **(A)** The four orthogonal, double-focused tungsten leaf pairs before the optimization. **(B)** The four orthogonal, double-focused tungsten leaf pairs after applying the rectangular components to cover the target volume; the yellow color represents the area that beams can go through to the PTV. Identical axial CBCT image at the abdomen level that is showing the kidneys and bowel for both **(C)** 3D-TMI preclinical model beam arrangements. **(D)** SOC-TMI schematic beams arrangement according to the X-RAD SmART small animal image-guided irradiation system.

and a few fractionation schemes with number of enrolled patients are listed in **Table 2**. A total of eight studies (six clinical TMI studies, average of five mice 3D-preclinical TMI plans, and average of five mice SOC-preclinical plans) were enrolled in this dosimetric analysis, aiming to compare the clinical and preclinical models and to highlight the advantages of the SOC-preclinical model. For the preclinical models, the bar chart of median dose with the standard variation for organs at

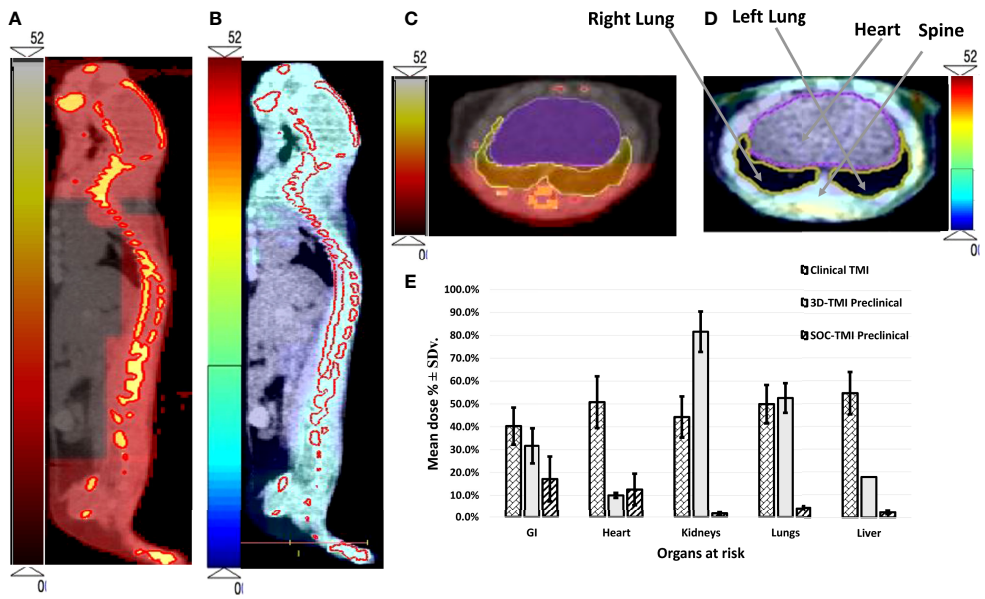

FIGURE 3 | The dose distribution of both **(A)** 3D-TMI preclinical model and **(B)** SOC-TMI preclinical model. **(C, D)** Identical axial CBCT image obtained at the level of the lungs of mouse shows conformal dose distribution for spine, ribs, and sternum for both SOC-preclinical and 3D-preclinical model, respectively. **(E)** Bar chart shown for critical organs—GI, heart, kidneys, lungs, and liver. Three bars in each group represent the mean dose for average of six clinical TMI studies, 3D-TMI preclinical, and SOC-TMI preclinical.

TABLE 1 | The median dose with standard deviation of the organs at risks for the 3D-TMI preclinical model versus the SOC-TMI preclinical model.

OARs' median dose percent in both 3D-TMI and SOC-TMI										
OARs	**Bowel %**		**Heart %**		**Kidneys %**		**Lungs %**		**Liver %**	
Plan	**SOC**	**3D**	**SOC**	**3D**	**SOC**	**3D**	**SOC**	**3D**	**SOC**	**3D**
m1	28.3	37.5	6.5	6.511.1	0.9	91.3	4.8	58.3	2.5	22.5
m2	27.4	38.0	5	9.3	1.4	70.0	4.6	43.8	1.6	13.8
m3	8.6	24.2	20.3	11.3	2.3	89.0	4.7	48.3	1.4	9.8
m4	11.9	22.5	18.7	9.2	1.6	76.3	4.1	53.8	3.1	18.8
m5	9.7	36.3	12.4	9.1	1.6	81.3	2.9	58.8	2.8	23.8
Average	17.2	31.7	12.6	10	1.6	81.6	4.2	52.6	2.3	17.7
SD	9.8	7.7	6.9	1.1	0.5	8.8	0.8	6.5	0.7	5.9

risk for the average of five mice in both 3D-TMI and SOC-TMI is presented **Figure 3E**. The median dose difference is represented as a percentage of the prescription dose. OARs are the heart, kidneys, liver, lungs, and gastrointestinal (GI). For the six clinical TMI studies, the average median doses of the OARs were approximately 30%–65% of the prescribed PTV dose. Otherwise, the 3D-TMI preclinical model reduced heart, liver, and GI doses compared to clinical studies. Whereas the lungs and kidneys doses were very high due to their proximity to the spine, the median dose was about 52.6% and 81.6% of the prescribed dose, respectively. SOC-TMI preclinical model has more organ dose sparing capability, especially the kidneys and lungs. Dose to the lungs was reduced by 95.8% ± 0.8%, to the kidneys by 98.4 ± 0.5%, and to the liver by 97.7± 0.7% of the prescription dose. GI and heart doses have been reduced by 82.8 ± 9.8% and 87.4 ± 11.3% of the prescription dose, respectively.

SOC-TMI average integral dose was 53.1% of the prescribed dose, whereas 3D-TMI dose was 70.7% of the prescribed dose. SOC-TMI has shown a significant median dose reduction to the lungs by 48.4% ($p = 0.014$) and to the kidneys by 80.6% ($p = 0.013$), but non-significant reductions were observed in the liver and GI by 15.4% and 14.5%, respectively. The heart received a slightly greater median dose by 2.6%.

The dose coverage to the whole-body is shown in a color wash presentation in **Figures 3A, B** for 3D-preclinical TMI and SOC-preclinical TMI, respectively. The color map is the dose level between 0 Gy as minimum to 52 Gy as the maximum dose range in preclinical TMI models. We used a different color scale between the two preclinical models to discriminate and show the dose distributions differences. Highly conformal dose coverage of the bone marrow sites was achieved in SOC-TMI preclinical model, as shown in **Figure 3B**. The dose distribution to the target and OARs (lungs and liver) in the transverse image at the level of the mediastinum in both SOC-preclinical and 3D-preclinical models is shown in **Figures 3C, D**. Moreover, SOC-TMI compared with 3D-TMI has further reduced the body integral dose by an average of 17.6% ± 6.2%.

Figure 4 shows dose volume histograms for PTV and various organs from six clinical TMI studies, 3D-preclinical TMI, and SOC-preclinical TMI treatments (**Figures 4A–E**). DVH indicated the successful sparing of the major normal organs of the SOC-preclinical TMI. The SOC-preclinical TMI (dark red dashed lines) showed a significant reduction in dose exposures for various OARs compared to 3D-preclinical TMI and clinical studies' dose levels. PTV is covered by 85%–95% of the prescribed dose in all six different clinical studies. Preclinical PTV covered by 85% of the prescribed dose in both 3D-TMI and SOC-TMI models.

DISCUSSION

The TMI treatment technique is increasingly becoming an alternative to TBI for conditioning regimens for hematopoietic cell transplantation because it reduces radiation exposure to all organs. Dose-escalated TMI has been successfully implemented with improved survival (24). Subsequently, TMI preclinical models (2D and 3D) were developed to enhance our understanding of the role of TMI in hematological malignancies

TABLE 2 | Dosimetric results of median dose in percent of the dose prescription of organs at risks for different clinical and preclinical TMI models.

Study	Clinical 1	Clinical 2	Clinical 3	Clinical 4 (A)	Clinical 4 (B)	Clinical 5	Clinical 6	3D-Preclinical	SOC-Preclinical
Treatment technique	IMRT-Linac	HT	VMAT-Linac	HT	VMAT-Linac	HT	HT	3D-Preclinical TMI	SOC-Preclinical TMI
Prescription dose (Gy)	12	6	12	12	12	13.5	20	12	12
Number of planned patients	3	1	6	4	4	12	8	5	5
OAR metric					**Median Dose (%)**				
Heart	52	70	46	53	48	35.5	31	10	12.6
Kidneys	47	40	45	60	40	33.7	29.7	81.6	1.6
Liver	50	70	49	60	54	44	NA	17.7	2.3
Lungs	36	57	60	48	50	48.5	32.7	52.6	4.2
Bowel	29	NA	49	40	47	36.4	38.9	31.7	17.2

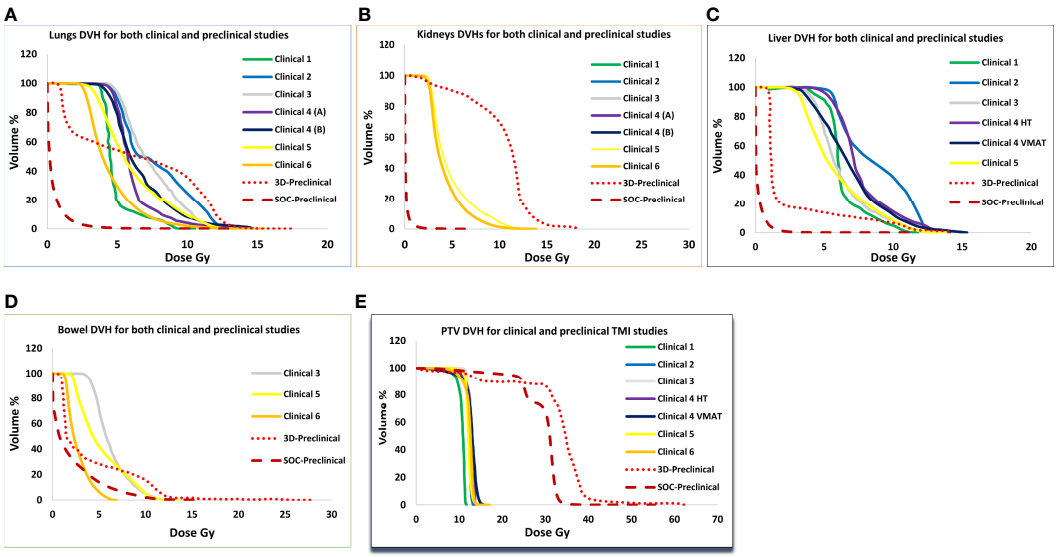

FIGURE 4 | Comparison of average dose volume histograms (DVH) for the **(A)** lungs, **(B)** kidneys, **(C)** liver, **(D)** bowel, and **(E)** PTV between six clinical TMI plans, 3D-preclinical model (red dotted lines), and the SOC-preclinical TMI model (dark red dashed lines).

(15, 16). Through a detailed comparative evaluation of dosimetric coverage, we observed that lungs and kidney proximal to the skeletal target received relatively higher doses in preclinical TMI than in clinical TMI. One of the most important late effects of higher doses to the OAR is lung pneumonitis (25–30). Lung pneumonitis is known to be the major dose-limiting factor and has been reported to correlate with the mean lung dose (25–28). Thus, sparing normal tissues while maintaining dose conformality to the target might further reduce the normal tissue complications, and thus, there is a need for evaluating detail of OAR dosimetry and adaptation of technology to reduce/vary dose to organs/tissues. IMRT is widely used for conformal dose delivery in the clinic and is being adopted for TMI. However, performing IMRT for small animal experiments to closely mimic human clinical scenarios faced insurmountable engineering challenges. To mitigate the discrepancy and make the preclinical model more translatable, we evaluated the next-generation preclinical TMI using SOC for enhanced dosimetric conformality. SOC system is designed and fabricated to be the first general-purpose small animal IMRT platform.

To this end, we compared the dosimetric results of clinical TMI studies, 3D-TMI preclinical model, and SOC-TMI preclinical model. PTV of both clinical and preclinical TMI studies showed good coverage. DVH of PTV in preclinical TMI models showed a relatively high dose to bone medium due to the photoelectric absorption of low energy x-ray (effective energy of 78.8 keV) (17). The 3D-TMI showed larger dose heterogeneity in comparison to SOC-TMI. This is because there is limited available collimator to accurately cover the irregular shaped geometry that causes overlap in some regions, leading to some hot spots and less coverage in some regions, leading to the cold spot. On the other hand, SOC-TMI uses automated and varied rectangular apertures to cover the target, and reducing the heterogeneity.

Clinical TMI studies showed a large dose variation in organs between centers. This is potentially due to the difference in dose constraints, treatment machine, treatment techniques, patient positioning, etc. Although the 3D-TMI preclinical model was shown to be equivalent to the clinical TMI (16), the dose to the lungs and kidneys was relatively higher due to their proximity to the spine and lower 3D plan dose conformity. The SOC-TMI method is based on RAO planning (31) and SOC dose modulator (22, 32) for IMRT planning. Compared with the MLC-based IMRT, SOC uses substantially fewer leaves while maintaining the modulation resolution. Therefore, SOC is more conducive to miniaturization. The performance of SOC for preclinical small-field radiation has been physically demonstrated. Moreover, SOC-TMI preclinical model showed a low integral dose to the body compared with the 3D-TMI preclinical model. Whether SOC-TMI delivery can improve integral dose may also be an important question, particularly in association with secondary cancer (33). As reported by D'Souza (34) in solid tumors, beam margin size and beam energy are the most relevant parameters, with smaller margins and higher energy consistently reducing the integral dose to the body regardless of the number of beams. In the two preclinical models, given the same beam energy of 225 keV (effective energy of 78.8-keV x-ray), one would expect that the smaller margin used in SOC-TMI model because of the shaped rectangular collimators leads to a reduction of the integral dose. The 3D-TMI model dose delivery scheme increases the (normalized) average dose to the body, thus increasing the integral dose as well. According to the two TMI model planning, number of beams, beam direction, and relative beam weight have little effect on the integral dose. The superior SOC-TMI dosimetry is evident in this study.

Compared with the 3D-TMI technique utilizing parallel-opposed beams with manually created conformal fields, SOC-TMI presents several major technological advances. The SOC-TMI model will help to automatize treatment planning and delivery and to achieve a more conformal and homogeneous target dose. The SOC-TMI will also allow varying radiation doses for each organ at risk for a larger range than the current clinical and preclinical system. It will help us to enhance scientific knowledge, namely, i) obtaining a radiobiological correlation of dose versus tissue damage and their impact on the tissue repair process and ii) understanding how varying radiation exposure to organs could impact engraftment. Our recent study suggests that a very low body dose may adversely impact engraftment (16). However, little is known on how dose variation stimulates factors (inflammatory cytokines, growth factors, etc.) that support engraftment. This knowledge is essential to developing an optimal radiation conditioning to achieve stable engraftment as well as reduced toxicity. iii) There is clinical concern that reduced doses to organs may reduce treatment efficacy because of the systemic nature of the hematological disease. Therefore, our initial clinical TMI development was to maintain a certain low level of organ dose (to prevent increased toxicity) while increasing BM-specific radiation to enhance the antileukemic effect. Therefore, clinical question of preferred dose to specific organs is not settled. This will require further investigation using preclinical TMI in BMT and disease models. Such knowledge radiation and biology will strengthen developing a rationale for translation in future clinical trials which may require further improvement in conformal radiation delivery by available clinical machines.

The data presented in this study demonstrate the versatility of SOC technology in providing exceptional target coverage and OAR sparing capabilities for difficult techniques like TMI. SOC-TMI preclinical model allowed a high-precision dose optimization for targets such as bone, bone marrow, and spleen and non-target vital organs. SOC-TMI preclinical has statistically improved the TMI plan quality. In addition, the SOC-TMI plans could deliver TMI treatment in an efficient manner in terms of treatment time. The overall SOC-TMI treatment planning time was approximately 45 min, which is 40% lower than the treatment time of the 3D-TMI model (~75 min). This offers a flexibility to tailor the treatment delivery within a reasonable amount of time. This novel RAO for SOC preclinical planning will substantially advance the preclinical radiation research and reduces the gap in treatment plan quality between clinical and preclinical radiotherapy, potentially increasing the translatability of small animal studies.

Despite the advantages of SOC-TMI, the current SOC-TMI has several limitations. i) Tissue heterogeneity is not incorporated in the model. Corrections were made for bone and lungs based on their density table. ii) Availability of SOC hardware is limited, preventing wide adoption and actual testing of SOC-TMI. However, this simulation shows dosimetric advantages for installing and commissioning of SOC-TMI in the future.

CONCLUSION

The preliminary results of SOC-TMI preclinical model are promising. SOC-TMI dosimetry result shows that this technique offers many attractive advantages. SOC-TMI preclinical model could be used as a new method for delivering TMI with high accuracy. SOC-TMI preclinical model demonstrates excellent target dose conformity and the ability to avoid unnecessary doses to critical structures adjacent to the target volumes. In addition to the lungs and kidneys, substantial radiation dose reductions to all sensitive structures are possible with this new technique of a SOC for small animal intensity-modulated TMI therapy.

DATA AVAILABILITY STATEMENT

The original contributions presented in the study are included in the article/supplementary material. Further inquiries can be directed to the corresponding author.

AUTHOR CONTRIBUTIONS

AA designed the study, collected, analyzed data, and wrote the paper. LJ and KS calculated dose for SOC-TMI and wrote the manuscript. DZ, AL, SM, HG, JW, SS, CF, CZ, and AP collected data and aided in the results. CA edited the manuscript. SH designed, wrote the manuscript, provided guidance. All authors contributed to the article and approved the submitted version.

FUNDING

Research reported in this publication is supported by the National Institutes of Health (2R01CA154491-01 to SH and R01CA259008 to KS).

REFERENCES

1. Thomas ED, Lochte HL, Cannon JH, Sahler OD, Ferrebee JW. Supralethal Whole Body Irradiation and Isologous Marrow Transplantation in Man. *J Clin Invest* (1959) 38(10):1709–16. doi: 10.1172/JCI103949
2. Ferrebee JW, Thomas ED. Factors Affecting the Survival of Transplanted Tissues. *Am J Med Sci* (1958) 235(4):369–86. doi: 10.1097/00000441-195804000-00001
3. Copelan EA. Hematopoietic Stem-Cell Transplantation. *N Engl J Med* (2006) 354(17):1813–26. doi: 10.1056/NEJMra052638
4. Ringdén O, Ruutu T, Remberger M, Nikoskelainen J, Volin L, Vindeløv L, et al. A Randomized Trial Comparing Busulfan With Total Body Irradiation as Conditioning in Allogeneic Marrow Transplant Recipients With Leukemia: A Report From the Nordic Bone Marrow Transplantation Group. *Blood* (1994) 83(9):2723–30. doi: 10.1182/blood.V83.9.2723.2723

5. Bunin N, Aplenc R, Kamani N, Shaw K, Cnaan A, Simms S. Randomized Trial of Busulfan vs Total Body Irradiation Containing Conditioning Regimens for Children With Acute Lymphoblastic Leukemia: A Pediatric Blood and Marrow Transplant Consortium Study. *Bone Marrow Transplant* (2003) 32 (6):543–8. doi: 10.1038/sj.bmt.1704198
6. Clift RA, Buckner CD, Appelbaum FR, Sullivan KM, Storb R, Thomas ED. Long-Term Follow-Up of a Randomized Trial of Two Irradiation Regimens for Patients Receiving Allogeneic Marrow Transplants During First Remission of Acute Myeloid Leukemia. *Blood* (1998) 92(4):1455–6. doi: 10.1182/blood.V92.4.1455
7. Hui SK, Kapatoes J, Fowler J, Henderson D, Olivera G, Manon RR, et al. Feasibility Study of Helical Tomotherapy for Total Body or Total Marrow Irradiationa). *Med Phys* (2005) 32(10):3214–24. doi: 10.1118/1.2044428
8. Hui SK, Verneris MR, Higgins P, Gerbi B, Weigel B, Baker SK, et al. Helical Tomotherapy Targeting Total Bone Marrow - First Clinical Experience at the University of Minnesota. *Acta Oncol Stockh Swed* (2007) 46(2):250–5. doi: 10.1080/02841860601042449
9. Wong JYC, Liu A, Schultheiss T, Popplewell L, Stein A, Rosenthal J, et al. Targeted Total Marrow Irradiation Using Three-Dimensional Image-Guided Tomographic Intensity-Modulated Radiation Therapy: An Alternative to Standard Total Body Irradiation. *Biol Blood Marrow Transplant* (2006) 12 (3):306–15. doi: 10.1016/j.bbmt.2005.10.026
10. Wong JYC, Rosenthal J, Liu A, Schultheiss T, Forman S, Somlo G. Image Guided Total Marrow Irradiation (TMI) Using Helical TomoTherapy in Patients With Multiple Myeloma and Acute Leukemia Undergoing Hematopoietic Cell Transplantation (HCT). *Int J Radiat Oncol Biol Phys* (2009) 73(1):273–9. doi: 10.1016/j.ijrobp.2008.04.071
11. Aydogan B, Mundt AJ, Roeske JC. Linac-Based Intensity Modulated Total Marrow Irradiation (IM-TMI). *Technol Cancer Res Treat* (2006) 5(5):513–9. doi: 10.1177/153303460600500508
12. Wilkie JR, Tiryaki H, Smith BD, Roeske JC, Radosevich JA, Aydogan B. Feasibility Study for Linac-Based Intensity Modulated Total Marrow Irradiation. *Med Phys* (2008) 35(12):5609–18. doi: 10.1118/1.2990779
13. Aydogan B, Yeginer M, Kavak GO, Fan J, Radosevich JA, Gwe-Ya K. Total Marrow Irradiation With RapidArc Volumetric Arc Therapy. *Int J Radiat Oncol Biol Phys* (2011) 81(2):592–9. doi: 10.1016/j.ijrobp.2010.11.035
14. Han C, Schultheisss TE, Wong JYC. Dosimetric Study of Volumetric Modulated Arc Therapy Fields for Total Marrow Irradiation. *Radiother Oncol* (2012) 102(2):315–20. doi: 10.1016/j.radonc.2011.06.005
15. Hui S, Takahashi Y, Holtan SG, Azimi R, Seelig D, Yagi M, et al. Early Assessment of Dosimetric and Biological Differences of Total Marrow Irradiation Versus Total Body Irradiation in Rodents. *Radiother Oncol* (2017) 124(3):468–74. doi: 10.1016/j.radonc.2017.07.018
16. Zuro D, Madabushi SS, Brooks J, Chen BT, Goud J, Salhotra A, et al. First Multimodal, Three-Dimensional, Image-Guided Total Marrow Irradiation Model for Preclinical Bone Marrow Transplantation Studies. *Int J Radiat Oncol Biol Phys* (2021) 111(3):671–83. doi: 10.1016/j.ijrobp.2021.06.001
17. Verhaegen F, van Hoof S, Granton PV, Trani D. A Review of Treatment Planning for Precision Image-Guided Photon Beam Pre-Clinical Animal Radiation Studies. *Z Med Phys* (2014) 24(4):323–34. doi: 10.1016/j.zemedi.2014.02.004
18. van Hoof SJ, Granton PV, Verhaegen F. Development and Validation of a Treatment Planning System for Small Animal Radiotherapy: SmART-Plan. *Radiother Oncol* (2013) 109(3):361–6. doi: 10.1016/j.radonc.2013.10.003
19. Chow J, Owrangi A. SU-E-T-142: Effect of the Bone Heterogeneity On the Unflattened and Flattened Photon Beam Dosimetry: A Monte Carlo Comparison. *Med Phys* (2014) 41(6Part13):255–5. doi: 10.1118/1.4888472
20. Bazalova M, Carrier JF, Beaulieu L, Verhaegen F. Dual-Energy CT-Based Material Extraction for Tissue Segmentation in Monte Carlo Dose Calculations. *Phys Med Biol* (2008) 53(9):2439–56. doi: 10.1088/0031-9155/53/9/015
21. Woods K, Nguyen D, Neph R, Ruan D, O'Connor D, Sheng K. A Sparse Orthogonal Collimator for Small Animal Intensity-Modulated Radiation Therapy Part I: Planning System Development and Commissioning. *Med Phys* (2019) 46(12):5703–13. doi: 10.1002/mp.13872
22. Woods K, Neph R, Nguyen D, Sheng K. A Sparse Orthogonal Collimator for Small Animal Intensity-Modulated Radiation Therapy. Part II: Hardware Development and Commissioning. *Med Phys* (2019) 46(12):5733–47. doi: 10.1002/mp.13870
23. Neph R, Ouyang C, Neylon J, Yang Y, Sheng K. Parallel Beamlet Dose Calculation *via* Beamlet Contexts in a Distributed Multi-GPU Framework. *Med Phys* (2019) 46(8):3719–33. doi: 10.1002/mp.13651
24. Stein AS, Al Malki MM, Yang D, Palmer J, Tsai NC, Aldoss I, et al. Total Marrow and Lymphoid Irradiation (TMLI) at a Dose of 2000cgy in Combination With Post-Transplant Cyclophosphamide (PTCy)-Based Graft Versus Host Disease (GvHD) Prophylaxis Is Safe and Associated With Favorable GvHD-Free/Relapse-Free Survival at 1 Year in Patients With Acute Myeloid Leukemia (AML). *Blood* (2020) 136:41–2. doi: 10.1182/blood-2020-141469
25. Leiper AD. Late Effects of Total Body Irradiation. *Arch Dis Child* (1995) 72 (5):382–5. doi: 10.1136/adc.72.5.382
26. Blaise D, Maraninchi D, Archimbaud E, Reiffers J, Devergie A, Jouet JP, et al. Allogeneic Bone Marrow Transplantation for Acute Myeloid Leukemia in First Remission: A Randomized Trial of a Busulfan-Cytoxan Versus Cytoxan-Total Body Irradiation as Preparative Regimen: A Report From the Group D'Etudes De La Greffe De Moelle Osseuse. *Blood* (1992) 79(10):2578–82. doi: 10.1182/blood.V79.10.2578.bloodjournal79102578
27. Ringdén O, Remberger M, Ruutu T, Nikoskelainen J, Volin L, Vindeløv L, et al. Increased Risk of Chronic Graft-Versus-Host Disease, Obstructive Bronchiolitis, and Alopecia With Busulfan Versus Total Body Irradiation: Long-Term Results of a Randomized Trial in Allogeneic Marrow Recipients With Leukemia. Nordic Bone Marrow Transplantation Group. *Blood* (1999) 93(7):2196–201. doi: 10.1182/blood.V93.7.2196
28. Socié G, Clift RA, Blaise D, Devergie A, Ringden O, Martin PJ, et al. Busulfan Plus Cyclophosphamide Compared With Total-Body Irradiation Plus Cyclophosphamide Before Marrow Transplantation for Myeloid Leukemia: Long-Term Follow-Up of 4 Randomized Studies. *Blood* (2001) 98(13):3569–74. doi: 10.1182/blood.V98.13.3569
29. Della Volpe A, Ferreri AJM, Annaloro C, Mangili P, Rosso A, Calandrino R, et al. Lethal Pulmonary Complications Significantly Correlate With Individually Assessed Mean Lung Dose in Patients With Hematologic Malignancies Treated With Total Body Irradiation. *Int J Radiat Oncol Biol Phys* (2002) 52(2):483–8. doi: 10.1016/S0360-3016(01)02589-5
30. Van Dyk J, Keane TJ, Kan S, Rider WD, Fryer CJ. Radiation Pneumonitis Following Large Single Dose Irradiation: A Re-Evaluation Based on Absolute Dose to Lung. *Int J Radiat Oncol Biol Phys* (1981) 7(4):461–7. doi: 10.1016/0360-3016(81)90131-0
31. Nguyen D, Ruan D, O'Connor D, Woods K, Low DA, Boucher S, et al. A Novel Software and Conceptual Design of the Hardware Platform for Intensity Modulated Radiation Therapy. *Med Phys* (2016) 43(2):917–29. doi: 10.1118/1.4940353
32. Le Beau MM. Chromosomal Fragile Sites and Cancer-Specific Breakpoints–a Moderating Viewpoint. *Cancer Genet Cytogenet* (1988) 31(1):55–61. doi: 10.1016/0165-4608(88)90011-8
33. Han C, Liu A, Wong JYC. Estimation of Radiation-Induced, Organ-Specific, Secondary Solid-Tumor Occurrence Rates With Total Body Irradiation and Total Marrow Irradiation Treatments. *Pract Radiat Oncol* (2020) 10(5):e406–14. doi: 10.1016/j.prro.2020.03.006
34. D'Souza WD, Rosen II. Nontumor Integral Dose Variation in Conventional Radiotherapy Treatment Planning. *Med Phys* (2003) 30(8):2065–71. doi: 10.1118/1.1591991

Conflict of Interest: The authors declare that the research was conducted in the absence of any commercial or financial relationships that could be construed as a potential conflict of interest.

frontiers | Frontiers in Oncology

ORIGINAL RESEARCH
published: 26 July 2022
doi: 10.3389/fonc.2022.946725

Target Coverage and Normal Organ Sparing in Dose-Escalated Total Marrow and Lymphatic Irradiation: A Single-Institution Experience

Chunhui Han, An Liu and Jeffrey Y.C. Wong*

City of Hope Comprehensive Cancer Center, Duarte, CA, United States

Purpose/Objectives: The aim of this study is to report historical treatment planning experience at our institution for patients receiving total marrow and lymphatic irradiation (TMLI) as part of the conditioning regimen prior to hematopoietic stem cell transplant.

Materials/Methods: Based on a review of all historical clinical TMLI treatments plans, we retrieved a 12-Gy cohort of 108 patients with a prescription dose of 12 Gy to the skeletal bones, lymph nodes, spleen, and spinal canal, and retrieved a 20-Gy cohort of 120 patients with an escalated prescription dose of 20 Gy to the skeletal bones, lymph nodes, spleen, and spinal cord, and 12 Gy to the brain and liver. Representative dosimetric parameters including mean and median dose, D80, and D10 (dose covering 80% and 10% of the structure volume, respectively) for targets and normal organs were extracted and compared between the two groups of patients.

Results: For the 12-Gy cohort, the average mean dose for normal organs ranged from 18.3% to 78.3% of 12 Gy, and the average median dose ranged from 18.3% to 77.5% of 12 Gy. For the 20-Gy cohort, the average mean dose for normal organs ranged from 13.0% to 76.0% of 20 Gy, and the average median dose ranged from 12.5% to 75.0% of 20 Gy. Compared to the mean dose to normal organs in the 12-Gy cohort, the average mean dose to normal organs increased from 0.0% to 73.1%, with only four normal organs showing a >50% increase. Normal organ dose in TMLI plans using volumetric modulated arc therapy fields fell within the dose range in historical TMLI plans.

Conclusion: Dosimetric data in historical TMLI plans at our institution are summarized at prescription dose levels of 12 Gy and 20 Gy, respectively. Compared to the normal organ dose with a prescription dose of 12 Gy, the mean and median dose to most normal organs at an escalated prescription dose of 20 Gy had an increase less than prescription dose scaling. Dosimetric results from this study can be used as reference data to facilitate clinical implementation of TMLI at other institutions.

Keywords: helical tomotherapy, VMAT, acute lymphoid leukemia, hematopoietic stem cell transplant, total marrow and lymphatic irradiation

OPEN ACCESS

Edited by:
Humberto Rocha, University of Coimbra, Portugal

Reviewed by:
Daria Kobyzeva, Dmitry Rogachev National Research Center of Pediatric Hematology, Oncology and Immunology, Russia
Conghua Xie, Zhongnan Hospital of Wuhan University, China

****Correspondence:***
Chunhui Han
chan@coh.org

Specialty section:
This article was submitted to Radiation Oncology, a section of the journal Frontiers in Oncology

Received: *17 May 2022*
Accepted: *22 June 2022*
Published: *26 July 2022*

Citation:
Han C, Liu A and Wong JYC (2022) Target Coverage and Normal Organ Sparing in Dose-Escalated Total Marrow and Lymphatic Irradiation: A Single-Institution Experience. Front. Oncol. 12:946725. doi: 10.3389/fonc.2022.946725

INTRODUCTION

Total body irradiation (TBI) is typically used as part of the conditioning regimen for patients undergoing hematopoietic stem cell transplant (1). Traditionally, TBI is delivered using open photon fields at an extended distance from the patient (2). When TBI is given at myeloablative dose levels, shielding of the lungs is necessary to reduce the risk of interstitial pneumonitis. On the other hand, most other body organs receive full dose with conventional TBI treatments. Conventional TBI is associated with numerous acute and long-term complications, among which interstitial pneumonitis is the most common toxicity and contributes to treatment-related mortalities (2). Although previous randomized trials showed that TBI dose escalation reduced post-transplant relapse rate for patients with acute and chronic myeloid leukemia, the therapeutic gain was negated by excessive radiation toxicity with dose escalation (3–6).

To minimize treatment-related toxicities in TBI treatments and to allow for dose escalation, intensity modulated radiotherapy (IMRT) techniques were proposed to deliver radiation dose to targeted sites. Helical tomothearpy was first used to deliver total marrow irradiation (TMI) and total marrow and lymphatic irradiation (TMLI) (7–9). Later, TMI and TMLI were implemented with IMRT fields on conventional medical linear accelerators (linacs) (10–12). Dose escalation clinical trials were carried out at some institutions to evaluate the potential benefits of improvement in therapeutic outcomes with reduced toxicities. Preliminary results from some clinical trials show that TMLI can be safely delivered at an escalated dose of up to 20 Gy without increased rate of extramedullary relapse compared with data using conventional TBI (13–16).

There is growing interest in the radiation oncology community in using the IMRT technique to deliver TMI/TMLI for patients undergoing hematopoietic stem cell transplant. However, TMI/TMLI treatments are currently performed in a small number of institutions and many clinicians lack experience in TMI/TMLI treatment planning. Our group has treated over 400 TMLI patients in the past 17 years under different dose escalation clinical trials and has accumulated many clinical TMLI treatment plans at different dose escalation levels. The purpose of this study is to summarize and present our dosimetric planning experience in TMLI treatment planning to facilitate clinical adoption of this modality by other institutions.

MATERIALS AND METHODS

Our institution started TMLI treatments since 2005. Over the years, patient simulation and setup techniques underwent several changes to increase patient comfort and to improve immobilization quality. Current patient setup techniques are presented here.

During CT simulation, the patient is first set up on the CT simulator couch in a head-in supine position. A whole-body vacuum bag extending from the shoulders to the feet is used to immobilize the patient. Both arms are kept straight and close to the body with hands forming loose fists. A thermoplastic head-to-shoulder mask is used to immobilize the head, neck, and shoulder regions, while another thermoplastic mask covers both feet of the patient for immobilization of the lower extremities. Three radiopaque triangulation markers were placed in the abdominal area in the same axial plane to mark the origin of the coordinates used in the CT images. Another set of two radiopaque markers were placed in an axial plane at the upper thigh level to assist with setup of treatment fields for the upper body and lower extremities. A CT simulation is then performed to scan the patient from the top of skull to mid-thigh with an axial slice thickness of 7.5 mm and a field of view that is sufficient to include the patient's lateral dimension. The patient is asked to maintain normal breathing during the CT simulation. To further evaluate the respiratory motion of internal organs, two additional CT simulations are subsequently taken in the thoracic region with the patient holding breath at the end of normal inspiration and expiration, respectively.

After the upper body CT simulations, the patient is then set up on the couch in a feet-in supine position with the same immobilization devices. A set of three radiopaque triangulation markers are placed at the mid-shin level to mark the origin for the lower-extremity CT simulation. A CT simulation is performed from the lower pelvis to the feet with an axial slice thickness of 7.5 mm and a field of view that is sufficient to include the patient's lateral dimension.

The upper-body and lower-extremity CT images were sent to a treatment planning system (TPS) (Eclipse, Varian Medical Systems, Palo Alto, California) where the two sets of images were registered based on bony anatomy in the overlapping lower pelvis and upper thigh regions. The CT images taken at the end of inspiration and expiration phases were registered to the CT images with normal breathing based on the same DICOM coordinates. Over 20 normal organ volumes were delineated on the upper body CT simulation images including eyes, lenses, parotids, oral cavity, optic nerves and chiasm, larynx, thyroid, esophagus, lungs (left and right), heart, upper GI, lower GI, kidneys (left and right), bladder, and rectum. For female patients, breasts, ovaries, and uterus are also delineated. For male patients, testes are delineated and, depending on the disease type and treatment protocol, may be treated as one target volume. The upper GI volume includes the stomach and duodenum, while the lower GI volume includes the small and large intestines. Based on CT images at different breathing phases, respiratory motion is included in the contours for certain organs including the esophagus, kidneys, spleen, and liver. Depending on the specific treatment protocol, some or all of the following volumes will be treated: the skeletal bones (excluding the ribs and skull), ribs, skull, spinal canal, lymph nodes, spleen, brain, liver, and testes. To better control dose to some part of the skeletal bone volume, the skull and the ribs are delineated as separate target volumes. The mandible is excluded from the skeletal bone target to better spare adjacent normal organs. To create the planning target volume (PTV) for the skeletal bones, 5- to 10-mm margins are added from the cortical bone surface with larger margins used to the arms, lower extremities, and shoulders. The skeletal bone PTV is then modified to be inside

the skin and away from the kidneys and esophagus by at least 5 mm. In addition, no margin is added anteriorly from the vertebrae or into the pelvic cavity to facilitate normal organ sparing. Only outer margins are used for the skull and the rib targets to avoid overlapping with the brain or the lungs.

Historically, TMLI treatments were predominantly given on helical tomotherapy machines at our institution. A jaw size of 5 cm is used for the upper body TMLI treatment plan. The lower extremities are typically treated with three-dimensional conformal radiotherapy (3D-CRT) treatment plans on helical tomotherapy using anterior–posterior (AP) and posterior–anterior (PA) beams.

More recently, TMLI treatments are given with volumetric modulated arc therapy (VMAT) fields on a conventional linac (TrueBeam, Varian Medical Systems, Palo Alto, CA) at our institution. Four to five isocenters are used for the upper body TMLI treatment plan for an adult patient, with two arc fields typically placed for each isocenter. The isocenters are positioned along a longitudinal axis of the patient with no shift in the lateral of anterior–posterior direction. A 120-leaf multi-leaf collimator (MLC) is used to modulate the VMAT fields with a leaf width of 5 mm for the central 40 leaf pairs and a leaf width of 1 cm for the peripheral 20 leaf pairs. The collimator angle is at 90° so that the MLC leaves move along the longitudinal direction of the patient. Asymmetric jaws are used along the patient's longitudinal direction so that two arc fields at each isocenter cover different patient body lengths. A 6-MV photon beam is used for all the VMAT fields. The lower extremities are treated with static AP/PA photon fields. The upper body VMAT TMLI plan is summed with the lower extremity plans for verification of adequate dose in the junction region at the upper thigh.

Volumetric imaging is used for daily patient setup. On helical tomotherapy, a megavoltage CT (MVCT) or kilovoltage CT (kVCT) scan is performed from the skull to iliac crest. On the conventional linac, two cone-beam CT (CBCT) scans are performed, one in the head and neck region and the other in the abdominal and pelvic region. The average shifts from image registrations of the two CBCT scans with the simulation CT images are used to correct the couch position. After VMAT fields at one isocenter are delivered, the couch is shifted longitudinally to the next isocenter. Orthogonal kV images are taken at the new isocenter for position verification before delivering VMAT fields at the new isocenter.

We started clinical TMLI treatments in 2005. As of now, more than 400 patients received TMLI treatments at different prescription dose levels as dose was escalated in clinical trials, with the prescription dose escalated up to 20 Gy. When prescription dose was escalated to a higher level, treatment plans for the first several patients were optimized to achieve optimal organ sparing. Treatment plans for subsequent patients at this dose level were generated by using normal organ dosimetric results from the first several treatment plans as a reference to evaluate plan quality. In recent years, the dosimetric constraints to the lung volume were updated in our institutional TMLI treatment planning guidelines by requiring the mean lung dose to be less than 8 Gy, based on lung toxicity studies (16, 17).

In this study, treatment plans for the following patient cohorts were retrieved and analyzed:

1. 12-Gy cohort: A dose of 12 Gy was prescribed to the skeletal bones (excluding the ribs and skull), ribs, skull, lymph nodes, spinal canal, and spleen. The brain and liver were normal organs and the dose to them were kept low in plan optimization. The treatment was given in 8 equal fractions with two fractions delivered each day.

2. 20-Gy cohort: A dose of 20 Gy was prescribed to the skeletal bones (excluding the ribs and skull), ribs, skull, lymph nodes, spinal canal, and spleen, while a dose of 12 Gy was prescribed to the liver and brain. The treatment was given in 10 equal fractions with two fractions delivered each day.

A total of 108 patients were found for the 12-Gy cohort while 120 patients were found for the 20-Gy cohort. **Table 1** lists patient characteristics for each cohort. In the 12-Gy cohort, one patient was treated with a VMAT treatment plan on a conventional linac, while other patients were treated with helical tomotherapy. In the 20-Gy cohort, four patients were treated with VMAT treatment plans on a conventional linac, while other patients were treated with helical tomotherapy. Treatments plans using the updated MLD constraint in the 20-Gy cohort were analyzed separately to evaluate the dosimetric impact to the lung and the rib target volume.

To facilitate TMLI plan evaluation in our clinical treatment planning workflow, reference dosimetric tables are used. A reference dosimetric table lists representative dosimetric parameters from several previous TMLI plans with the same prescription dose. Such dosimetric parameters include D80 (dose covering 80% of a structure volume), D50 (median dose), and D10 (dose covering 10% of a structure volume) for both targets and normal organs. These parameters were used in our reference dosimetric tables because they are select points on the dose volume histogram (DVH) curves and are representative of the DVH curve shape. To provide reference dosimetric data for institutions that lack clinical TMLI treatment planning experience, we extracted and analyzed dosimetric parameters including D80, D50, mean dose, and D10 from all the historical TMLI treatment plans. The TMLI treatment plan for each patient was retrieved and the treatment plan data containing dose and structure contours were exported as DICOM files. In-house software applications were developed to extract and analyze dosimetric parameters for the targets and normal organs from the DICOM data files. To illustrate the spread of values for each dosimetric parameter, we calculated and presented the 1st quartiles and 3rd quartiles, in addition to the average values,

TABLE 1 | Patient characteristics.

Patient cohort	12-Gy cohort	20-Gy cohort
Number of patients	108	120
Sex (Male/Female)	56/52	64/56
Age/years-old	54 ± 13	40 ± 12
(Range)	(10–71)	(17–64)
Prescription dose (Gy)	12	20
Number of fractions	8	10
Dose per fraction (Gy)	1.5	2.0

for each dosimetric parameter in each cohort, where the 1st quartile is defined as the middle value between the minimum value and the median value, and the 3rd quartile is defined as the middle value between the maximum value and the median value for a given parameter. Unpaired *t*-tests were used to compare data between different groups of patients, where the result is regarded as statistically significant when the two-tailed *p*-value is less than 0.05. Statistical analysis in this study was performed with a data analysis software system (Excel version 2102, Microsoft Corp., Redmond, WA).

RESULTS

Table 2 lists mean dose and median dose statistics (average, standard deviation, and 1st and 3rd quartiles) for each structure with the 12-Gy cohort. On average, the mean dose for the target volumes ranged from 12.1 Gy to 12.5 Gy and the median dose for the target volumes ranged from 12.3 Gy to 12.6 Gy. Relative to the prescription dose of 12 Gy, the average mean dose for normal organ volumes ranged from 18.3% to 78.3% and the average median dose for normal organ volumes ranged from 18.3% to 77.5%. Among the normal organ structures, the lenses showed the lowest average mean and median dose values while the female breasts showed the highest average mean and median dose values. Of note, the mean lung dose had an average of 6.2 ± 0.6 Gy at this prescription dose level. **Figure 1** shows the average DVH for each structure in the 12-Gy cohort. **Table 3** lists statistics of D80 and D10 for targets and normal organs with the 12-Gy cohort.

Table 4 lists mean dose and median dose statistics (average, standard deviation, and 1st and 3rd quartiles) for each structure with the 20-Gy cohort. Of note, the brain and liver were prescribed 12 Gy while the other target volumes were prescribed 20 Gy. All the target volumes had a mean dose greater than the prescribed dose except the ribs, which had an average mean dose of 19.6 Gy, while all the target volumes had a median dose greater than the prescribed dose. Relative to the prescription dose of 20 Gy, the average mean dose for the normal organ volumes ranged from 13.0% to 76.0%, and the average median dose for the normal organs ranged from 12.5% to 75.0%. Among the normal organ structures, the lenses showed the lowest average mean and median dose values while the female breasts showed the highest average mean and median dose values. The mean lung dose had an average of 8.5 ± 0.8 Gy for the 20-Gy cohort. **Figure 2** shows the average DVH for each structure in the 20-Gy cohort. **Table 5** lists statistics of D80 and D10 for targets and normal organs with the 20-Gy cohort.

Table 4 also lists dose statistics for the total lung and the ribs target volume when only the cases after clinical implementation of the updated mean lung dose constraint in 2018 were included. The mean lung dose had an average of 7.8 ± 0.4 Gy while the rib target volume had an average of 19.3 ± 0.8 Gy. Unpaired *t*-tests were performed on the mean lung dose and mean rib target dose between the treatment plans in this 20-Gy cohort before 2018 and those after 2018, and the results showed a statistically significant difference (two-tailed *p*-value < 0.01 for both structures). To illustrate the difference in the lung dose distributions, **Figure 3**

TABLE 2 | Statistics of mean dose and median dose (D50) for each structure with the 12-Gy cohort.

Structure	Mean dose (Gy)			Median dose (Gy)		
	Avg ± StdDev	1st quartile	3rd quartile	Avg ± StdDev	1st quartile	3rd quartile
Skeletal bones	**12.4 ± 0.2**	**12.3**	**12.6**	**12.6 ± 0.3**	**12.4**	**12.8**
Lymph nodes	**12.4 ± 0.3**	**12.2**	**12.5**	**12.6 ± 0.3**	**12.4**	**12.8**
Spinal canal	**12.4 ± 0.4**	**12.1**	**12.6**	**12.4 ± 0.4**	**12.2**	**12.6**
Spleen	**12.5 ± 0.4**	**12.2**	**12.7**	**12.6 ± 0.4**	**12.4**	**12.8**
Skull	**12.3 ± 0.3**	**12.1**	**12.4**	**12.3 ± 0.3**	**12.2**	**12.5**
Ribs	**12.1 ± 0.4**	**11.9**	**12.3**	**12.4 ± 0.4**	**12.2**	**12.6**
Brain	6.7 ± 0.9	6.0	7.2	6.4 ± 1.1	5.6	7.2
Liver	7.2 ± 0.9	6.6	7.9	6.6 ± 1.1	6.1	7.4
Bladder	7.6 ± 1.5	6.4	8.7	7.2 ± 1.8	5.9	8.6
Female breasts	9.4 ± 1.0	8.8	10.0	9.3 ± 1.1	8.6	10.0
Esophagus	4.9 ± 0.9	4.1	5.5	4.5 ± 0.9	3.7	5.1
Eyes	4.0 ± 1.6	2.5	5.4	3.9 ± 1.7	2.1	5.4
Heart	6.1 ± 1.0	5.5	6.8	5.7 ± 1.1	5.0	6.4
Lower GI	5.9 ± 0.9	5.3	6.3	5.3 ± 1.0	4.7	5.7
Upper GI	5.2 ± 0.8	4.7	5.6	4.7 ± 0.9	4.1	5.0
Kidneys (total)	5.9 ± 1.4	4.8	7.1	5.3 ± 1.4	4.1	6.5
Larynx	5.0 ± 1.4	4.0	5.9	4.4 ± 1.5	3.4	5.3
Lenses (total)	2.2 ± 0.9	1.5	2.7	2.2 ± 1.0	1.4	2.6
Lungs (total)	6.2 ± 0.6	6.0	6.6	5.7 ± 0.4	5.4	6.0
Optic nerves and chiasm	6.0 ± 1.4	4.9	6.9	5.8 ± 1.4	4.7	6.8
Oral cavity	3.2 ± 0.6	2.8	3.5	3.2 ± 0.6	2.8	3.5
Uterus and ovaries	6.4 ± 1.7	5.4	7.3	5.9 ± 1.9	4.4	7.0
Parotids (total)	5.4 ± 1.1	4.6	5.9	4.9 ± 1.3	3.9	5.5
Rectum	4.9 ± 1.0	4.1	5.4	4.3 ± 1.0	3.7	4.8
Thyroid	6.0 ± 1.7	4.8	6.9	5.7 ± 1.8	4.5	6.8

The target volumes are denoted with bold font. The structure of skeletal bones does not include the ribs or skull.

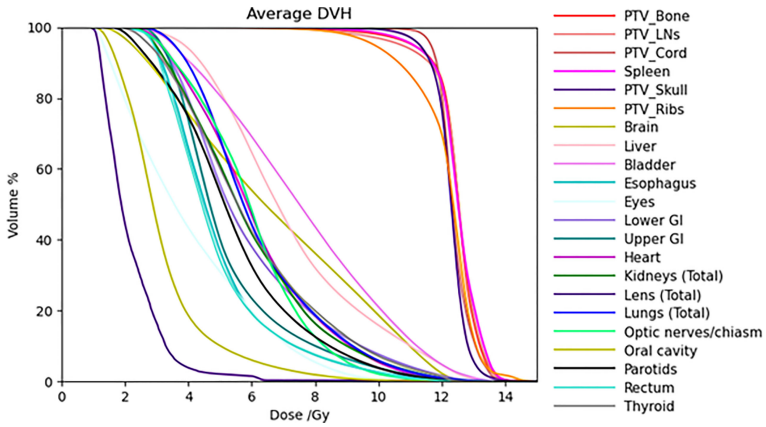

FIGURE 1 | Average DVHs of all the treatment plans for target volumes and most normal organs in the 12-Gy cohort.

TABLE 3 | Statistics of D80 and D10 for each structure with the 12-Gy cohort.

Structure	D80 (Gy)			D10 (Gy)		
	Avg ± StdDev	1st quartile	3rd quartile	Avg ± StdDev	1st quartile	3rd quartile
Skeltal bones	**12.2 ± 0.1**	**12.1**	**12.3**	**13.0 ± 0.4**	**12.7**	**13.3**
Lymph nodes	**12.2 ± 0.3**	**12.0**	**12.4**	**13.0 ± 0.4**	**12.7**	**13.3**
Spinal canal	**12.1 ± 0.5**	**11.9**	**12.3**	**12.7 ± 0.4**	**12.4**	**13.0**
Spleen	**12.2 ± 0.4**	**12.0**	**12.4**	**13.0 ± 0.4**	**12.6**	**13.3**
Skull	**12.0 ± 0.3**	**11.9**	**12.2**	**12.7 ± 0.4**	**12.5**	**12.8**
Ribs	**11.5 ± 0.7**	**11.3**	**11.8**	**13.0 ± 0.4**	**12.7**	**13.1**
Brain	3.7 ± 1.0	3.0	4.4	10.8 ± 0.7	10.3	11.4
Liver	5.4 ± 0.9	4.8	6.0	10.8 ± 1.2	10.3	11.5
Bladder	5.6 ± 1.4	4.2	7.0	10.6 ± 1.5	9.9	11.6
Female breasts	7.7 ± 1.2	6.9	8.5	11.8 ± 0.8	11.3	12.4
Esophagus	3.9 ± 0.7	3.3	4.4	6.9 ± 1.7	5.6	7.8
Eyes	2.8 ± 1.3	1.7	3.7	5.9 ± 2.2	3.7	7.9
Heart	4.6 ± 1.0	3.9	5.4	8.8 ± 1.2	8.2	9.5
Lower GI	4.2 ± 0.9	3.6	4.6	9.1 ± 1.2	8.1	10.0
Upper GI	4.0 ± 0.7	3.4	4.4	7.4 ± 1.6	6.1	8.8
Kidneys (total)	4.7 ± 1.3	3.6	5.6	8.5 ± 1.8	7.2	10.0
Larynx	3.4 ± 1.2	2.6	3.8	7.8 ± 1.9	6.3	9.3
Lens (total)	1.9 ± 0.7	1.3	2.3	2.6 ± 1.4	1.7	3.2
Lungs (total)	4.6 ± 0.7	4.0	5.1	9.0 ± 0.9	8.4	9.6
Optic nerves and chiasm	5.0 ± 1.3	3.9	5.9	7.4 ± 1.8	6.1	8.6
Oral cavity	2.3 ± 0.6	1.9	2.7	5.0 ± 1.2	4.3	5.8
Uterus and ovaries	4.8 ± 1.6	3.6	5.5	9.1 ± 2.3	7.8	10.6
Parotids (total)	4.0 ± 1.2	2.8	4.7	8.0 ± 1.3	7.2	8.7
Rectum	3.9 ± 0.8	3.2	4.4	6.8 ± 1.9	5.4	8.1
Thyroid	4.6 ± 1.7	3.4	5.3	8.2 ± 1.9	6.9	9.7

The target volumes are denoted with bold font. The structure of skeletal bones does not include the ribs or skull.

shows the DVHs of the total lung for patients in the 12-Gy cohort, patients in the 20-Gy cohort before the updated mean lung dose constraint was used in treatment planning, and patients in the 20-Gy cohort after the updated mean lung dose constraint was used, respectively. Average lung DVH curves are also shown in **Figure 3D** for each of the three groups of patients.

Figure 4 compares average mean dose to each normal organ volumes between the 12-Gy cohort and the 20-Gy cohort. Compared to the average mean dose in the 12-Gy cohort plans, the average mean dose in the 20-Gy cohort plans had an increase ranging from 0.0% to 73.1%, while the prescription dose increased by 66.7% from 12 Gy to 20 Gy. Compared to the average median dose in the 12-Gy cohort plans, the average median dose for the normal organ volumes had an increase/decrease ranging from –7.7% to 77.6%. Four normal organ volumes showed more than 50% increase in both the average mean dose and median dose (female breasts, lower GI, upper GI, and optic nerves and chiasm), and three normal organ volumes (lower GI, upper GI, and optic

TABLE 4 | Statistics of mean dose and median dose (D50) for each structure with the 20-Gy cohort.

Structure	Mean dose (Gy)			Median dose (Gy)		
	Avg ± StdDev	1st quartile	3rd quartile	Avg ± StdDev	1st quartile	3rd quartile
Skeletal bones	**20.8 ± 0.4**	**20.6**	**21.0**	**21.1 ± 0.4**	**20.8**	**21.3**
Lymph nodes	**20.4 ± 0.4**	**20.1**	**20.6**	**21.0 ± 0.5**	**20.7**	**21.2**
Spinal canal	**20.5 ± 0.4**	**20.3**	**20.7**	**20.6 ± 0.4**	**20.4**	**20.8**
Spleen	**20.6 ± 0.4**	**20.4**	**20.9**	**20.9 ± 0.5**	**20.7**	**21.2**
Skull	**20.6 ± 0.4**	**20.4**	**20.8**	**20.9 ± 0.4**	**20.6**	**21.0**
Ribs	**19.6 ± 0.8**	**19.3**	**20.0**	**20.4 ± 0.8**	**20.1**	**20.9**
	19.3 ± 0.8*	**18.8***	**19.8***	**20.2 ± 0.9***	**19.9***	**20.8***
Brain	**13.6 ± 0.7**	**13.0**	**14.2**	**13.0 ± 0.6**	**12.6**	**13.4**
Liver	12.9 ± 0.6	12.5	13.2	13.0 ± 0.6	12.6	13.3
Bladder	9.7 ± 1.5	8.7	10.6	8.6 ± 1.8	7.5	9.7
Female breasts	15.2 ± 1.6	14.3	16.1	15.0 ± 1.9	13.9	16.0
Esophagus	6.5 ± 0.9	6.1	6.9	5.7 ± 0.7	5.4	6.0
Eyes	4.0 ± 0.8	3.4	4.3	3.6 ± 0.8	3.1	3.9
Heart	7.4 ± 0.6	7.0	7.8	6.5 ± 0.6	6.1	6.9
Lower GI	10.2 ± 1.1	9.5	10.8	9.0 ± 1.3	8.2	9.6
Upper GI	9.0 ± 1.4	8.1	9.9	8.0 ± 1.5	6.9	8.9
Kidneys (total)	7.3 ± 0.7	6.8	7.8	6.0 ± 0.7	5.5	6.4
Larynx	7.5 ± 2.2	6.1	8.7	6.6 ± 2.4	4.9	8.2
Lenses (total)	2.6 ± 0.4	2.3	2.7	2.5 ± 0.4	2.2	2.6
Lungs (total)	8.5 ± 0.8	7.9	9.1	7.4 ± 0.6	6.8	7.9
	7.8 ± 0.4*	7.7*	7.9*	6.7 ± 0.4*	6.4*	7.0*
Optic nerves and chiasm	10.2 ± 1.9	8.8	11.3	10.3 ± 2.5	8.4	12.5
Oral cavity	4.4 ± 1.0	3.7	4.9	3.6 ± 0.8	3.0	4.0
Uterus and ovaries	8.6 ± 2.1	7.6	9.8	7.6 ± 2.1	6.1	8.5
Parotids (total)	8.1 ± 1.3	7.2	8.8	7.0 ± 1.5	5.9	7.8
Rectum	6.5 ± 0.9	5.9	6.9	5.5 ± 0.8	5.0	6.0
Thyroid	8.0 ± 2.1	6.8	8.6	7.4 ± 2.3	6.2	8.0

The target volumes are denoted with bold font. The structure of skeletal bones does not include the ribs or skull.
**Dosimetric data after the updated mean lung dose criteria was used in treatment planning.*

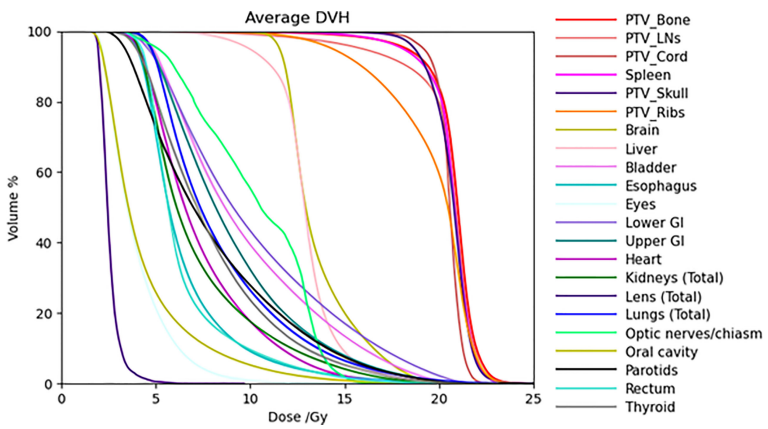

FIGURE 2 | Average DVHs of all the treatment plans for target volumes and some normal organs in the 20-Gy cohort.

nerves and chiasm) showed higher average mean dose in the 20-Gy cohort than the average mean dose 12-Gy cohort scaled by the prescription dose ratio of 20/12.

Figure 5 shows distributions of mean dose for target volumes and major normal organ volumes in historical TMLI treatment plans for the 20-Gy cohort. The minimum, maximum, and first, second, and third quartiles of the mean dose are shown in the box plot for each target and each normal organ. For comparison, the mean dose data to targets and normal organ volumes in the four VMAT TMLI treatment plans in the 20-Gy cohort are also included in **Figure 5.**

DISCUSSION

This study presents a comprehensive summary of dosimetric plan data in clinical TMLI treatment plans at two prescription

TABLE 5 | Statistics of D80 and D10 for each structure with the 20-Gy cohort.

Structure	D80 (Gy)			D10 (Gy)		
	Avg ± StdDev	1st quartile	3rd quartile	Avg ± StdDev	1st quartile	3rd quartile
Skeletal bones	20.3 ± 0.3	20.3	20.5	21.7 ± 0.5	21.4	22.0
Lymph nodes	20.0 ± 0.6	19.8	20.4	21.6 ± 0.5	21.3	21.9
Spinal canal	20.2 ± 0.4	20.1	20.4	21.0 ± 0.5	20.7	21.3
Spleen	20.2 ± 0.5	20.0	20.5	21.6 ± 0.6	21.2	21.9
Skull	19.9 ± 0.5	19.7	20.2	21.6 ± 0.6	21.3	21.8
Ribs	17.9 ± 1.3	17.4	18.8	21.6 ± 0.6	21.3	21.8
Brain	12.2 ± 0.4	12.0	12.4	16.2 ± 1.5	14.7	17.6
Liver	12.1 ± 0.4	11.9	12.3	14.7 ± 1.3	13.7	15.4
Bladder	6.4 ± 1.3	5.4	7.0	15.4 ± 2.1	14.2	16.8
Female breasts	12.2 ± 1.9	11.0	13.1	19.8 ± 1.4	19.3	20.8
Esophagus	4.8 ± 0.6	4.4	5.1	9.6 ± 2.0	8.4	10.7
Eyes	2.7 ± 0.5	2.4	2.9	6.0 ± 1.6	4.9	6.6
Heart	5.0 ± 0.6	4.7	5.4	11.5 ± 1.1	10.8	12.2
Lower GI	6.3 ± 1.2	5.5	7.0	16.7 ± 1.5	15.8	17.6
Upper GI	6.3 ± 1.4	5.3	7.2	13.8 ± 1.9	12.7	15.1
Kidneys (total)	4.9 ± 0.6	4.5	5.3	12.0 ± 1.6	11.0	12.9
Larynx	4.7 ± 1.7	3.6	5.2	12.2 ± 3.1	10.2	14.2
Lens (total)	2.3 ± 0.3	2.1	2.4	2.9 ± 0.6	2.5	3.2
Lungs (total)	5.6 ± 0.6	5.3	6.0	13.3 ± 1.6	12.1	14.5
Optic nerves and chiasm	8.3 ± 2.5	6.7	9.9	13.0 ± 1.6	12.5	14.0
Oral cavity	2.8 ± 0.6	2.4	3.2	7.8 ± 2.4	5.8	9.1
Uterus and ovaries	5.8 ± 1.3	4.9	6.4	13.7 ± 3.8	11.3	16.2
Parotids (total)	4.7 ± 1.1	4.0	5.2	13.8 ± 2.0	12.3	15.0
Rectum	5.0 ± 0.7	4.6	5.5	9.5 ± 2.2	7.9	11.0
Thyroid	5.7 ± 1.9	4.5	5.8	11.9 ± 2.7	10.0	13.4

The target volumes are denoted with bold font. The structure of skeletal bones does not include the ribs or skull.

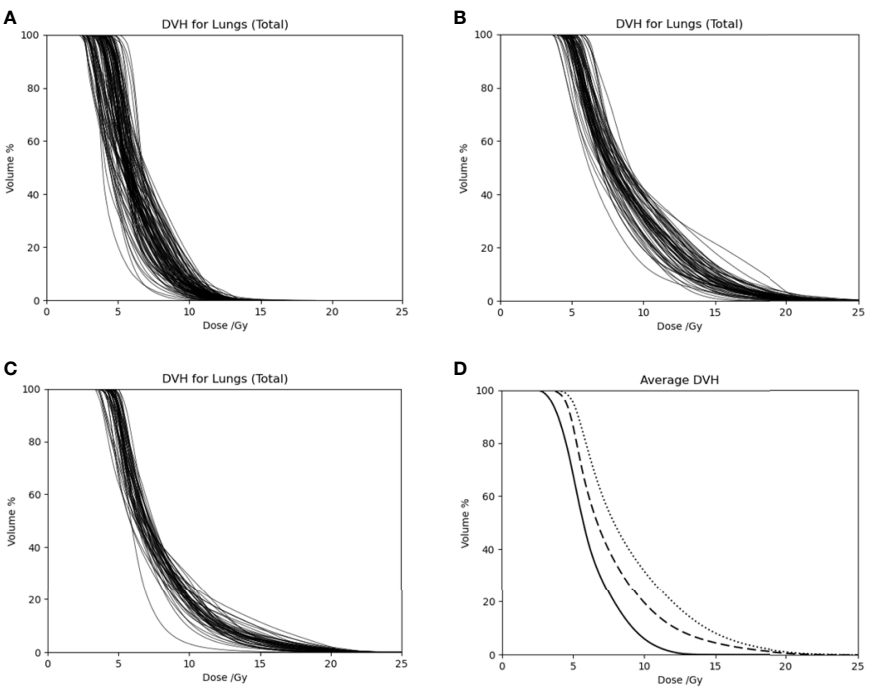

FIGURE 3 | Dose volume histograms of the total lung for **(A)** patients in the 12-Gy cohort, **(B)** patients in the 20-Gy cohort before the updated mean lung dose constraint was used, and **(C)** patients in the 20-Gy cohort after the updated mean lung dose constraint was used. **(D)** Average DVH curves for patients in the 12-Gy cohort (solid curve), patients in the 20-Gy cohort before the updated mean lung dose constraint was used (dotted curve), and patients in the 20-Gy cohort after the mean lung dose constraint was used (dashed curve).

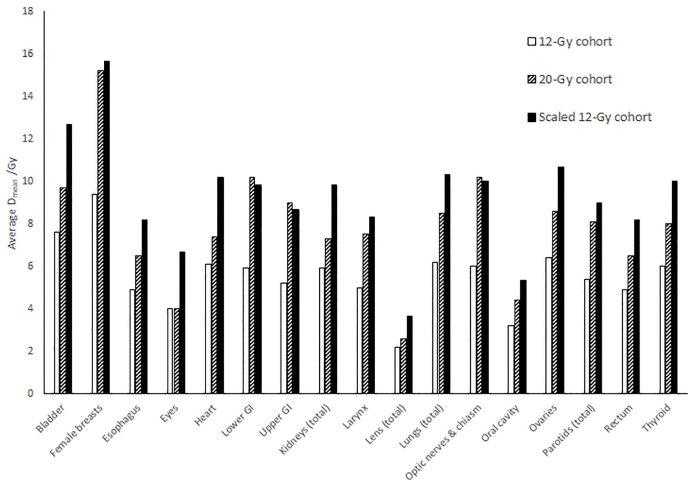

FIGURE 4 | Comparison of average mean dose (D_{mean}) to each normal organ between the 12-Gy cohort and the 20-Gy cohort. The "Scaled 12-Gy cohort" data series shows average D_{mean} for the 12-Gy cohort scaled by the prescription dose ratio (20/12).

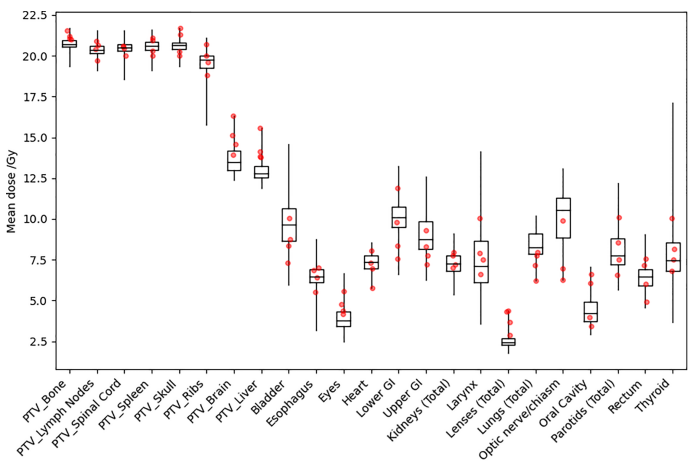

FIGURE 5 | Distribution of mean dose (Dmean) for target volumes and major normal organs in the 20-Gy cohort. The median value of Dmean for each structure is shown at the horizontal bar in the middle of each rectangle. The 1st and 3rd quartiles are shown as the lower and upper horizontal sides of each rectangle. The minimum and maximum range of Dmean is shown as the vertical lines extending from each rectangle. The red dots are Dmean data in the four VMAT TMLI treatment plans in the 20-Gy cohort.

dose levels, one at the standard myeloablative dose level of 12 Gy and the other at the dose escalation level of 20 Gy. This study includes the largest TMLI patient cohorts to date. Representative dosimetric data in the historical TMLI treatment plans are provided, which can be used as reference data to facilitate clinical implementation of TMLI at other institutions.

Wong et al. evaluated dosimetric feasibility of dose escalation with TMI or TMLI up to 20 Gy in an early study (8). However, in that study, only the bone marrow volume was escalated to 20 Gy while 12 Gy was prescribed to the lymphatic volume, skull, and ribs. This current study showed practically achievable normal organ sparing in clinical TMLI treatment plans at the 20-Gy prescription dose level given to the lymphatic volume, skull, and ribs. **Table 5** shows that most of the normal organs had less than 50% increase in mean and median dose in the 20-Gy cohort treatment plans compared to the 12-Gy cohort treatment plans, despite an increase of 66.7% from 12 Gy to 20 Gy for most target volumes and inclusion of the brain and liver as target volumes. Only four organ volumes showed more than 50% increase in mean and median dose. Of note, inclusion of the brain and liver as target volumes in the 20-Gy dose escalation protocols negatively affected sparing of some normal organs. The optic nerves and chiasm had more than 50% increase because it is partially surrounded by the brain and skull, while the upper GI

and lower GI had more than 50% increase partly because of the proximity to the liver. The female breasts also showed more than 50% increase in median and mean dose due to proximity to the ribs.

Tables 2–**5** show that dose to the ribs was lower compared to other target volumes as dose to the ribs was negatively affected by sparing of the lungs, as we prioritized lung sparing rather than dose coverage to the ribs. In addition, **Table 4** shows that dose to the ribs was lower in those plans with the updated MLD criteria. Of note, even with the updated MLD criteria in treatment planning, the ribs still received escalated dose with an average median dose of 19.3 Gy and an average mean dose of 20.2 Gy. Dosimetric consistency of the ribs was also affected by sparing of the lungs. **Table 4** shows that dose to the ribs had greater variation compared to other target volumes. Based on our clinical planning experience, the rib volume is the most challenging target volumes to achieve dosimetric consistency in TMLI treatment planning. Further improvement in treatment planning techniques is needed to deliver consistent dose to the ribs.

Clinical TMLI treatments using VMAT fields started in 2021 at our institution. We have delivered TMLI treatments using VMAT fields on conventional linacs for more than ten patients with prescription dose ranging from 12 Gy to 20 Gy. In this study, the dosimetry data for those VMAT TMLI plans with a prescription dose of 20 Gy were presented. **Figure 5** shows that dose in the VMAT TMLI plans fell within the range in historical TMLI plans for most normal organs. Treatment planning and delivery using VMAT fields present unique challenges. Due to field size limits, multiple isocenters are needed and adjacent fields need to overlap to ensure adequate target dose coverage. In an image-guided patient setup, multiple image acquisitions are needed at different isocenters due to limitations in CBCT image size in the longitudinal direction. On the other hand, since conventional linacs are more widely available, this technique provides access for more patients receiving TMLI treatments. Therefore, we are actively making improvement in treatment planning and delivery efficiency in VMAT-based TMLI and plan to present our treatment planning and delivery experience in a separate report.

CONCLUSIONS

Dosimetric data in historical TMLI plans at our institution are summarized at prescription dose levels of 12 Gy and 20 Gy, respectively. Compared to the normal organ dose with a prescription dose of 12 Gy, the mean and median dose to most normal organs at an escalated prescription dose of 20 Gy had an increase less than prescription dose scaling. The VMAT TMLI plans achieved normal organ dose sparing within the range of historical TMLI plans. Dosimetric results from this study can be used as reference data to facilitate clinical implementation of TMLI at other institutions.

DATA AVAILABILITY STATEMENT

The original contributions presented in the study are included in the article/supplementary material. Further inquiries can be directed to the corresponding author.

AUTHOR CONTRIBUTIONS

CH performed data collection, data analysis, and manuscript preparation. AL participated in the design of this study and performed critical review of the manuscript. JW participated in the design of this study, creation of methods for this study, and data analysis, and performed critical review of the manuscript. All authors contributed to the article and approved the submitted version.

FUNDING

This research was partially supported by funding provided by Accuray, Inc and Varian Medical Systems, Inc. The funder Varian Medical Systems, Inc. was not involved in the study design, collection, analysis, interpretation of data, the writing of this article or the decision to submit it for publication.

REFERENCES

1. Aristeri C, Latini P, Terenzi A, Felicini R, Aversa F. Total Body Irradiation-Based Regimen in the Conditioning of Patients Submitted to Haploidentical Stem Cell Transplantation. *Radiother Oncol* (2001) 58:247–9. doi: 10.1016/S0167-8140(00)00333-9
2. Wong JYC, Filippi AR, Dabaja BS, Yahalom J, Specht L. Total Body Irradiation: Guidelines From the International Lymphoma Radiation Oncology Group (ILROG). *Int J Radiat Oncol Biol Phys* (2018) 101:521–9. doi: 10.1016/j.ijrobp.2018.04.071
3. Marks DI, Forman SJ, Blume KG, Perez WS, Weisdorf DJ, Keating A, et al. A Comparison of Cyclophosphamide and Total Body Irradiation With Etoposide and Total Body Irradiation as Conditioning Regimens for Patients Undergoing Sibling Allografting for Acute Lymphoblastic Leukemia in First or Second Complete Remission. *Biol Blood Marrow Transplant* (2006) 12:438–53. doi: 10.1016/j.bbmt.2005.12.029
4. Clift RA, Buckner CD, Appelbaum FR, Bearman SI, Petersen FB, Fisher LD, et al. Allogeneic Marrow Transplantation in Patients With Acute Myeloid Leukemia in First Remission: A Randomized Trial of Two Irradiation Regimens. *Blood* (1990) 76:1867–71. doi: 10.1182/blood.V76.9.1867.1867
5. Clift RA, Buckner CD, Appelbaum FR, Bryant E, Bearman SI, Petersen FB, et al. Allogeneic Marrow Transplantation in Patients With Chronic Myeloid Leukemia in the Chronic Phase: A Randomized Trial of Two Irradiation Regimens. *Blood* (1991) 77:1660–5. doi: 10.1182/blood.V77.8.1660.1660
6. Clift RA, Buckner CD, Appelbaum FR, Sullivan KM, Storb R, Thomas ED. Long-Term Follow-Up of a Randomized Trial of Two Irradiation Regimens for Patients Receiving Allogeneic Marrow Transplants During First Remission of Acute Myeloid Leukemia. *Blood* (1998) 92:1455–6. doi: 10.1182/blood.V92.4.1455
7. Hui S, Kapatoes J, Fowler J, Henderson D, Olivera G, Manon RR, et al. Feasibility Study of Helical Tomotherapy for Total Body or Total Marrow Irradiation. *Med Phys* (2005) 32:3214–24. doi: 10.1118/1.2044428

8. Wong JYC, Liu A, Schultheiss TE, Popplewell L, Stein A, Rosenthal J, et al. Targeted Total Marrow Irradiation Using Three-Dimensional Image-Guided Tomographic Intensity-Modulated Radiation Therapy: An Alternative to Standard Total Body Irradiation. *Biol Blood Marrow Transplant* (2006) 12:306–15. doi: 10.1016/j.bbmt.2005.10.026
9. Schultheiss TE, Wong J, Liu A, Olivera G, Somlo G. Image-Guided Total Marrow and Total Lymphatic Irradiation Using Helical Tomotherapy. *Int J Radiat Oncol Biol Phy* (2007) 67:1259–67. doi: 10.1016/j.ijrobp.2006.10.047
10. Aydogan B, Mundt AJ, Roeske JC. Linac-Based Intensity Modulated Total Marrow Irradiation (IM-TMI). *Technol Canc Res Treat* (2006) 5:513–9. doi: 10.1177/153303460600500508
11. Han C, Schultheiss TE, Wong JYC. Dosimetric Study of Volumetric Modulated Arc Therapy Fields for Total Marrow Irradiation. *Radiother Oncol* (2012) 102:315–20. doi: 10.1016/j.radonc.2011.06.005
12. Fogliata A, Cozzi L, Clivio A, Ibatici A, Mancosu P, Navarria P, et al. Preclinical Assessment of Volumetric Modulated Arc Therapy for Total Marrow Irradiation. *Int J Radiat Oncol BiolPhys* (2011) 80:628–36. doi: 10.1016/j.ijrobp.2010.11.028
13. Wong JYC, Forman S, Somlo G, Rosenthal J, Liu A, Schultheiss T, et al. Dose Escalation of Total Marrow Irradiation With Concurrent Chemotherapy in Patients With Advanced Acute Leukemia Undergoing Allogeneic Hematopoietic Cell Transplantation. *Int J Radiat Biol Phy* (2013) 85:148–56. doi: 10.1016/j.ijrobp.2012.03.033
14. Stein A, Palmer J, Tsai NC, Al Malki MM, Aldoss I, Ali H, et al. Phase I Trial of Total Marrow and Lymphoid Irradiation Transplantation Conditioning in Patients With Relapsed/Refractory Acute Leukemia. *Biol Blood Marrow Transplant* (2017) 23:618–24. doi: 10.1016/j.bbmt.2017.01.067
15. Hui S, Brunstein C, Takahashi Y, DeFor T, Holtan SG, Bachanova V, et al. Dose Escalation of Total Marrow Irradiation in High-Risk Patients Undergoing Allogeneic Hematopoietic Stem Cell Transplantation. *Biol Blood Marrow Transplant* (2017) 23:1110–6. doi: 10.1016/j.bbmt.2017.04.002
16. Shinde S, Yang D, Frankel P, Liu A, Han C, Vecchio B, et al. Radiation-Related Toxicities Using Organ Sparing Total Marrow Irradiation Transplant Conditioning Regimens. *Int J Radiat Oncol Biol Phys* (2019) 105:1025–33. doi: 10.1016/j.ijrobp.2019.08.010
17. Esiashvili N, Lu X, Ulin K, Laurie F, Kessel S, Kalapurakal JA, et al. Higher Reported Lung Dose Received During Total Body Irradiation for Allogeneic Hematopoietic Stem Cell Transplantation in Children With Acute Lymphoblastic Leukemia is Associated With Inferior Survival: A Report From the Children's Oncology Group. *Int J Radiat Oncol Biol Phys* (2019) 104:513–21. doi: 10.1016/j.ijrobp.2019.02.034

Conflict of Interest: This study received funding from Accuray, Inc. The funder had the following involvement with the study: Part of the fund was used to support establishment of a total marrow irradiation patient registry at our institution. All authors declare no other competing interests.

frontiers | Frontiers in Oncology

TYPE Original Research
PUBLISHED 28 July 2022
DOI 10.3389/fonc.2022.955004

OPEN ACCESS

EDITED BY
Tsair-Fwu Lee,
National Kaohsiung University of Science and Technology, Taiwan

REVIEWED BY
James Chow,
University of Toronto, Canada
Jeffrey Tuan,
National Cancer Centre Singapore, Singapore

*CORRESPONDENCE
Darren M. Zuro
imad-ali@ouhsc.edu

SPECIALTY SECTION
This article was submitted to Radiation Oncology, a section of the journal Frontiers in Oncology

RECEIVED 27 May 2022
ACCEPTED 05 July 2022
PUBLISHED 28 July 2022

CITATION
Zuro DM, Vidal G, Cantrell JN, Chen Y, Han C, Henson C, Ahmad S, Hui S and Ali I (2022) Treatment planning of total marrow irradiation with intensity-modulated spot-scanning proton therapy.
Front. Oncol. 12:955004.
doi: 10.3389/fonc.2022.955004

Treatment planning of total marrow irradiation with intensity-modulated spot-scanning proton therapy

Darren M. Zuro[1]*, Gabriel Vidal[1], James Nathan Cantrell[1], Yong Chen[1], Chunhui Han[2], Christina Henson[1], Salahuddin Ahmad[1], Susanta Hui[2] and Imad Ali[1]

[1]Department of Radiation Oncology, University of Oklahoma Health Science Center (HSC), Oklahoma City, OK, United States, [2]Department of Radiation Oncology, City of Hope, Durate, CA, United States

Purpose: The goal of this study is to investigate treatment planning of total marrow irradiation (TMI) using intensity-modulated spot-scanning proton therapy (IMPT). The dosimetric parameters of the intensity-modulated proton plans were evaluated and compared with the corresponding TMI plans generated with volumetric modulated arc therapy (VMAT) using photon beams.

Methods: Intensity-modulated proton plans for TMI were created using the Monte Carlo dose-calculation algorithm in the Raystation 11A treatment planning system with spot-scanning proton beams from the MEVION S250i Hyperscan system. Treatment plans were generated with four isocenters placed along the longitudinal direction, each with a set of five beams for a total of 20 beams. VMAT-TMI plans were generated with the Eclipse-V15 analytical anisotropic algorithm (AAA) using a Varian Trilogy machine. Three planning target volumes (PTVs) for the bones, ribs, and spleen were covered by 12 Gy. The dose conformity index, D80, D50, and D10, for PTVs and organs at risk (OARs) for the IMPT plans were quantified and compared with the corresponding VMAT plans.

Results: The mean dose for most of the OARs was reduced substantially (5% and more) in the IMPT plans for TMI in comparison with VMAT plans except for the esophagus and thyroid, which experienced an increase in dose. This dose reduction is due to the fast dose falloff of the distal Bragg peak in the proton plans. The conformity index was found to be similar (0.78 vs 0.75) for the photon and proton plans. IMPT plans provided superior superficial dose coverage for the skull and ribs in comparison with VMAT because of increased entrance dose deposition by the proton beams.

Conclusion: Treatment plans for TMI generated with IMPT were superior to VMAT plans mainly due to a large reduction in the OAR dose. Although the current IMPT-TMI technique is not clinically practical due to the long overall treatment time, this study presents an enticing alternative to conventional TMI with photons by providing superior dose coverage of the targets, increased

sparing of the OARs, and enhanced radiobiological effects associated with proton therapy.

KEYWORDS

total marrow irradiation (TMI), volumetric arc radiotherapy, proton radiation therapy, dosimetric analyses, radiation therapy

Introduction

Total body irradiation (TBI) is widely used as a conditioning treatment regimen for hematopoietic stem cell transplantation (HCT) (1). Conventional TBI cannot deliver higher radiation dose safely without increasing toxicity to surrounding normal tissues from excess dose especially the lungs, negating any potential advantage to overall survival (2–8). Additionally, the conventional TBI technique is associated with non-uniform dose distributions, high doses to organs at risk (OARs), and hot spots in normal tissues (9). To overcome this obstacle, total marrow irradiation (TMI) with helical tomography was developed, allowing for dose reduction to normal tissues while providing conformal dose coverage to the planning target volumes (PTVs) (9–16). With initial clinical trials demonstrating TMI to be successful for patient treatment (17), the expansion of TMI into advanced clinical modalities could potentially impact the efficiency, quality, and outcomes of patient treatment.

In recent years, volumetric modulated arc therapy (VMAT) for TMI has been used to provide highly conformal dose distributions to the TMI targets and lower doses to OARs, which is superior to conventional radiation treatment techniques (18, 19). Advancement in dose delivery techniques and radiation therapy modalities particularly proton therapy provides an appealing avenue for TMI treatment. Proton therapy provides conformal dose distributions with fast dose falloff and no exit doses due to the Bragg peak, and it is associated with higher radiobiological effective doses compared with photon therapy (20). Currently, no attempts have been made to adapt TMI to a proton therapy because of the clinical and technical limitations. The goal of this study is to investigate treatment planning of TMI using intensity-modulated spot-scanning proton therapy (IMPT). The dosimetric parameters of the intensity-modulated proton plans were evaluated and compared with the corresponding TMI plans generated with VMAT using photon beams.

Methods

Patient selection and organ contouring

The computed tomography (CT) images with 512 × 512 pixels with 6-mm slice thickness for five patients who were previously treated with craniospinal irradiation (CSI) were used for TMI treatment planning in this study. Table 1 lists the demographics of the patients used in this study. Patients were positioned headfirst supine for simulation, with the CT images for these patients consisting of nearly whole-body scans covering from the top of the skull past the pelvis. The clinical target volume (CTV) was defined as all the bones and lymph nodes from the vertex to the mid femur except for the humeri, ulnae, radii, and hands. Standard CSI patient setup required setting the arms away from the body to avoid any extra irradiation to the extremities; thus, the extremities (arms) were excluded from dosimetric calculation and assessment in this study. The bones outlined for CSI were modified such that a custom-made 5-mm margin to the bones with a 1-mm cropping away from OARs except for cranial bones where a 2-mm margin was applied for the PTV. This bone PTV matched with previously reported dosimetric margins used in TMI treatment planning (21). Mandible and maxillary structures were excluded from the

TABLE 1 Patient demographics used for treatment planning.

TMI study designation	Sex	Age (years)	Length of upper-body PTV (cm)	Weight (kg)	Volume of PTV (cm^3)
TMI_001	M	9	69	34.3	4,027.6
TMI_002	F	9	72.76	24.8	3,168.9
TMI_003	M	13	84.76	37.6	6,460.7
TMI_004	M	4	59.03	16	2,451.2
TMI_005	F	18	88.13	50	7,534.5

TMI, total marrow irradiation; PTV, planning target volume.

bone PTV following the methodology of Wong et al. (11). The same CT images with the outlined TMI targets and OARs were used for both IMPT and VMAT planning in the proton and photon treatment planning systems, respectively.

Intensity-modulated spot-scanning total marrow irradiation planning technique

Intensity-modulated proton plans for TMI were created using the Monte Carlo dose-calculation algorithm in the Raystation 11A treatment planning system with spot-scanning proton beams from the MEVION S250i Hyperscan proton therapy system (MEVION Medical Systems, Littleton, MA, USA). The proton plans were generated with four to five isocenters placed midline along the cranial–caudal direction of the patient where each isocenter included a set of five beams with a total of 20–25 beams to cover the whole body. Four proton beams were placed at gantry angles of 45° and 125° with table rotations of 0° and 180°, and a fifth beam was directed along the patient posteriorly at a gantry angle of 180°. The field size was set to the maximum of 20 × 20 cm with a 2-cm overlap for each field in the cranial–caudal direction as seen in Figures 1A, B. Several different beam configurations were tested, the results of which can be found in the Supplementary Material. The dose calculation grid was set to a 2-mm resolution to consider the variations in high-dose gradient regions. Multi-field optimization (MFO) technique was used with the tolerance set to 1E−5 and a maximum number of iterations of 200 to achieve a conformal dose coverage of the different targets. Raystation reports dose in units of cGy-RBE, which includes the enhanced relative biological effectiveness (RBE) with proton beams, allowing for direct comparisons between VMAT-TMI and IMPT-TMI. The parameters of the spot filtering setting used for dose optimization and calculation are given in Table 2 for the IMPT plans.

Volumetric modulated arc therapy–total marrow irradiation planning technique

The VMAT-TMI treatment plans were generated with the Eclipse-V15 treatment planning system with the analytical anisotropic dose-calculation algorithm (AAA) using a Varian Trilogy machine and a Millennium MLC system (Varian Medical Systems, Palo Alto, CA, USA). Photon optimization settings were done using extended convergence mode with a 2-mm dose grid resolution for all the VMAT plans. The beam design with arcs and isocenters for VMAT-TMI is shown in Figure 1C. Three to four isocenters were used for treatment

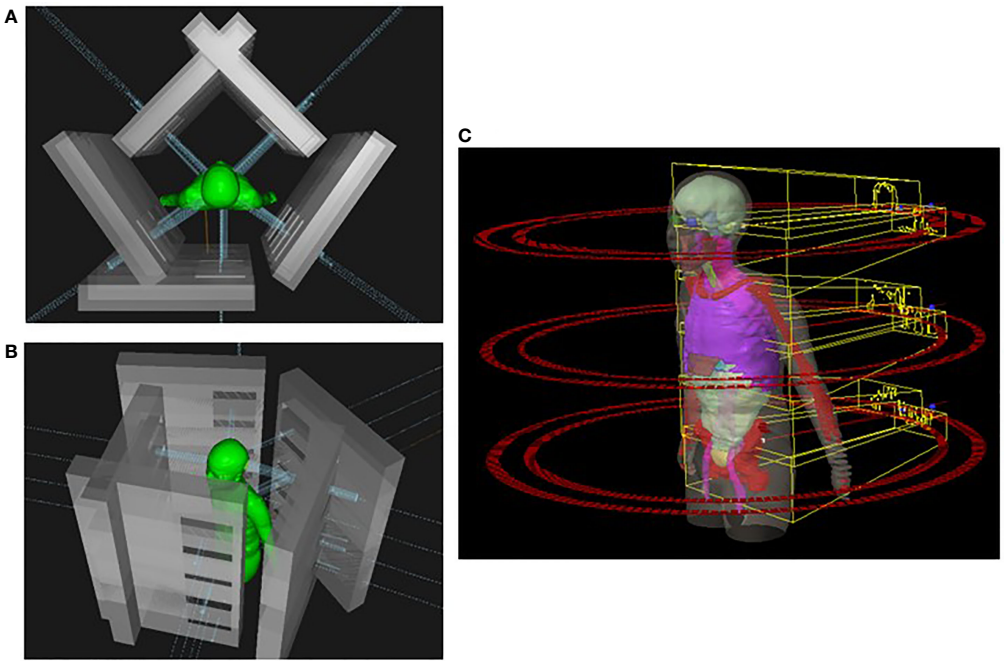

FIGURE 1
(A) Head-to-toe view of IMPT plan taken from Raystation planning system. Five beams were used for each isocenter in this example. **(B)** Side view of IMPT plan. **(C)** Representation of a VMAT-TMI plan with arcs and isocenters from Eclipse planning system. IMPT, intensity-modulated spot-scanning proton therapy; VMAT, volumetric modulated arc therapy; TMI, total marrow irradiation.

TABLE 2 Settings of dose parameters used for proton optimization and planning.

Spot filtering settings		
Iterations before spit filtering		40
Min spot meterset (MU/fx)		0.135
Max spot meterset (MU/fx)		42
Meterset limit margin (%)		5
	Proton plan optimization	
ROI	Description	Weight
PTV_TMI	Min dose 1,100 cGy (RBE)	250
PTV_TMI	Max dose 1,440 cGy (RBE)	1,000
Airway	Max dose 650 cGy (RBE)	100
Bladder	Max dose 650 cGy (RBE)	100
Bowel	Max dose 650 cGy (RBE)	100
Brain	Max dose 650 cGy (RBE)	100
Esophagus	Max dose 650 cGy (RBE)	100
Heart	Max dose 400 cGy (RBE)	100
LT optic nerve	Max dose 650 cGy (RBE)	100
LT orbit	Max dose 650 cGy (RBE)	100
Parotids	Max dose 650 cGy (RBE)	100
RT optic nerve	Max dose 650 cGy (RBE)	100
RT orbit	Max dose 650 cGy (RBE)	100
Spleen	Min dose 1,200 cGy (RBE)	100
Stomach	Max dose 650 cGy (RBE)	100
Thyroid	Max dose 650 cGy (RBE)	100
Total lung	Max dose 650 cGy (RBE)	250
Total kidneys	Max dose 750 cGy (RBE)	100

ROI, region of interest; PTV, planning target volume; TMI, total marrow irradiation; RBE, relative biological effectiveness.

planning, which were separated by 24 cm in the cranial–caudal direction. The collimators were rotated by 90° to enable the use of asymmetric jaws, allowing for full-range travel of the MLC for intensity modulation following the previously reported methodology (15, 18, 19, 22). Photon treatment fields use full arc rotations starting from 181° in the clockwise direction and 179° in the counterclockwise direction, with large fields of 30 × 40 cm^2. A 2-cm overlap in the cranial–caudal direction between adjacent arcs for the different isocenters was planned to ensure appropriate dose deposition in the junction regions.

Plan comparison and analysis

The different PTVs for the TMI treatment planning consisted of the structures spine, ribs, skull, lymph nodes, and spleen, which were covered with a total dose of 12 Gy, and the OARs included the bladder, esophagus, eyes, heart, kidneys, lungs, optic nerves, parotids, small intestine, stomach, and thyroid, which were constrained to achieve dose sparing within tolerance doses as reported from Aydogan et al. (19). The contours were outlined initially by a medical physicist using intensity-level thresholding and manual contouring tools in the Eclipse treatment planning system and then reviewed and approved by a radiation oncologist. The dose conformity index, D80, D50, and D10, for PTVs and OARs for the IMPT plans were quantified and used for dose evaluation and comparison with the corresponding VMAT plans.

Statistical analysis was performed using GraphPad Prism v 7.04 (GraphPad Software Inc., La Jolla, CA, USA). The outliers were identified using a robust non-linear regression method, ROUT (Q = 1%, 'Q' is the maximum desired false discovery rate), which were assessed for the different targets and OARs used in the TMI treatment planning. Multiple group comparisons were performed with a one-way ANOVA test, correcting for multiple comparisons. Group comparisons were performed with an unpaired two-tailed Student's test. A p-value of ≤.05 was considered statistically significant.

Results

The VMAT-TMI dose distributions and the corresponding IMPT dose distributions with the dose difference between the two plans for patient 1 are shown in Figure 2. Figures 2A, B show the axial dose distributions for the thoracic cavity and pelvis regions, which demonstrated

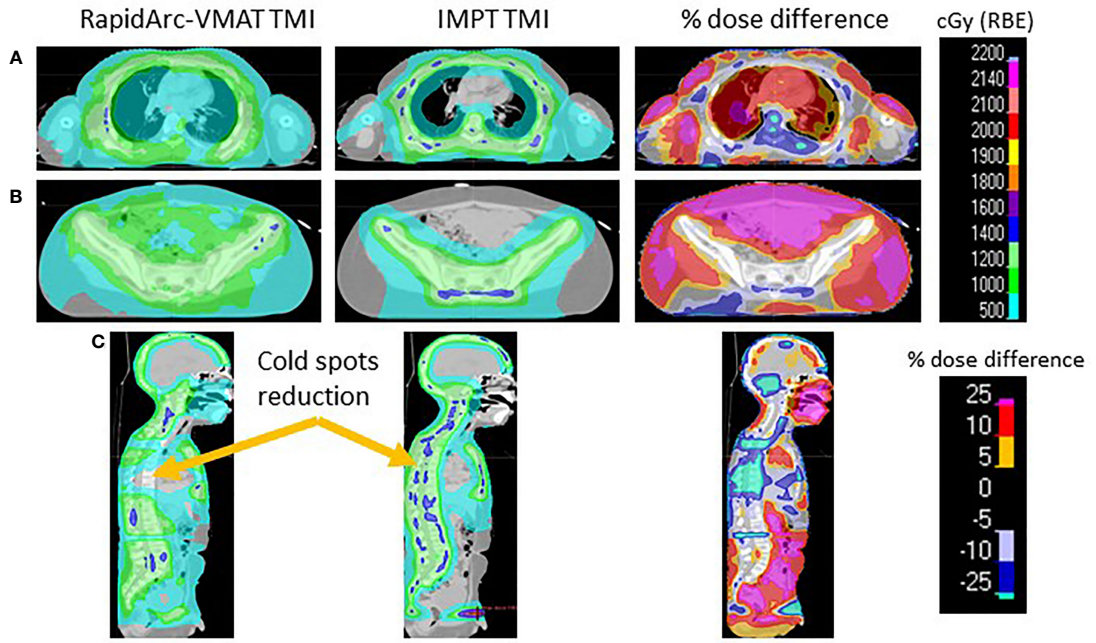

FIGURE 2
(A) Comparing the VMAT, IMPT, and percentage dose difference of the thoracic cavity. **(B)** Pelvis region comparing TMI plans. **(C)** Sagittal view demonstrating the cold spots present in VMAT-TMI. VMAT, volumetric modulated arc therapy; IMPT, intensity-modulated spot-scanning proton therapy; TMI, total marrow irradiation.

dose reductions in the lung and bowel regions caused by the falloff after the distal Bragg peak of the proton plans in comparison with the corresponding photon plans. Another advantage of the proton plans was the reduction of cold dose spots in the T-spine and L-spine regions by 33% ± 14% from the VMAT plan as seen in Figure 2C. This was achieved by heavily weighting the lung OAR during the proton plan optimization.

Figure 3 lists the D80, D50, and D10 dosimetric results of both VMAT and IMPT plans for each patient for the PTVs: skull, ribs, spine, spleen, and lymph nodes. Figure 4 shows the D80, D50, and D10 in bar graph format for each PTV. The D80 coverage for the skull, ribs, and spleen was lower by 7.4%, 7.3%, and 8.7%, respectively, for IMPT plans compared to VMAT. Despite the lower D80 dose in IMPT plans, it was not significantly different when compared to VMAT plans (p >.08). The D10 for the skull was 6.3% higher in the IMPT plans compared to VMAT (p = .02). The maximum dose was higher in IMPT plans by 16.8% compared to VMAT-TMI (p <.05). The dose coverage uncertainty was 5% higher in the D80 compared to D10 for IMPT plans. All the other dose metrics for PTV dose coverages were within ±5% for the proton and photon modalities.

Table 3 lists the mean dose for each OAR structure. The OARs that experienced the largest reductions in the mean doses in the IMPT plans were the bladder (50.4%) and intestine (50.4%). The fast dose falloff in proton plans and reduced scatter radiation led to less secondary radiation in these structures as compared to VMAT plans. The mean doses were higher in the esophagus and thyroid by 43.4% and 33.8%, respectively, in the IMPT plans (p <.01). Figure 5 displays the average dose–volume histograms (DVHs) for the OARs, which show the dose sparing for organs such as the stomach, parotids, bladder, and intestine.

Discussion

This is one of the first simulation studies demonstrating the potential of intensity-modulated spot-scanning proton therapy as an alternative technique for total marrow irradiation treatment. The IMPT plans achieved similar dosimetric coverage as compared to VMAT while reducing the dose to OARs such as the lungs and kidneys. In certain PTVs such as the T-spine, the bone PTV experienced a loss in dose coverage due to normal tissue sparing in VMAT; however, IMPT has the advantage of not having such cold spots. This study demonstrated several dosimetric advantages of IMPT over VMAT for TMI, which can provide potential avenues for further TMI treatment planning development and possible clinical implementation.

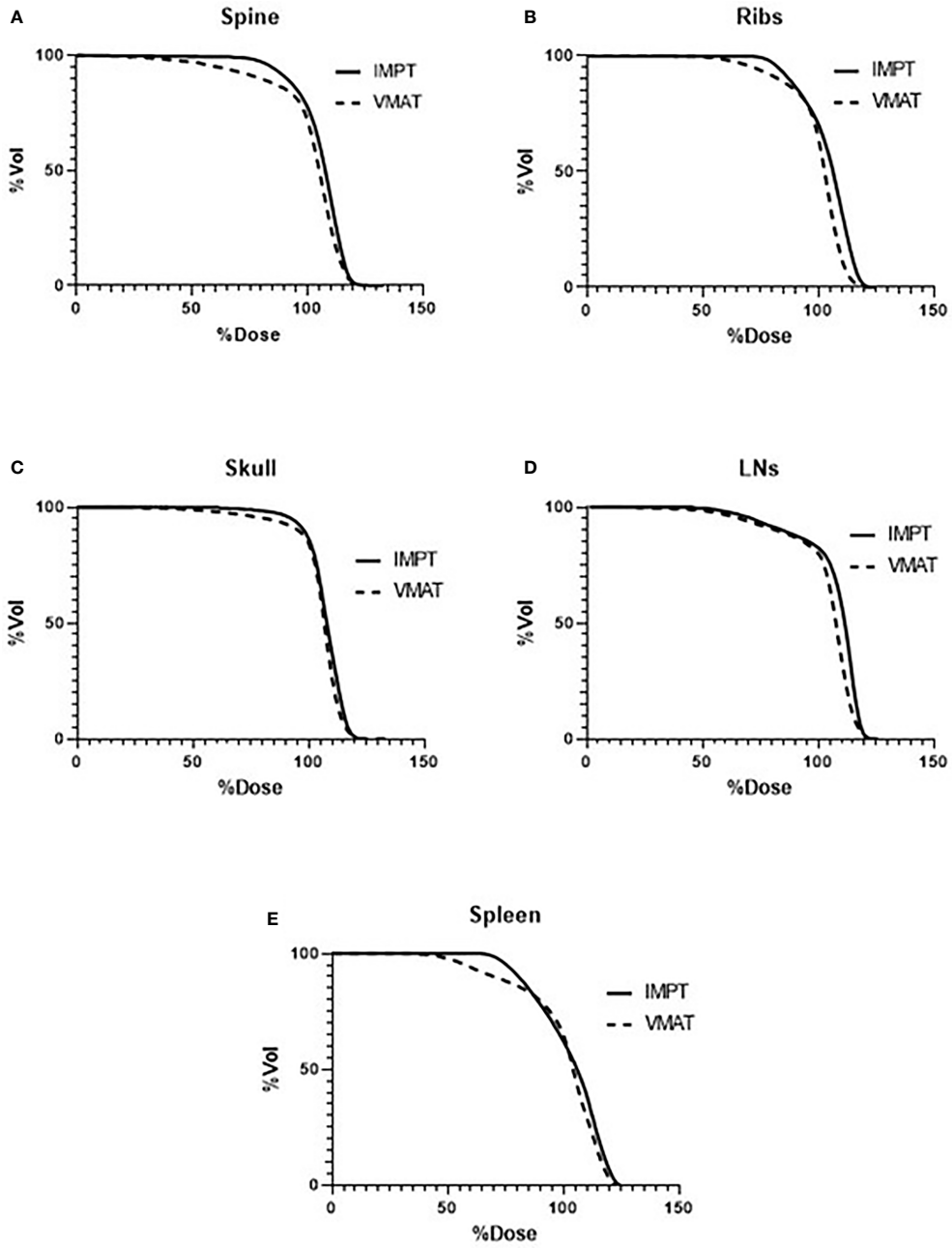

FIGURE 3
Average DVHs comparing VMAT to IMPT plans of the targets: **(A)** spine, **(B)** ribs, **(C)** skull, **(D)** lymph nodes, and **(E)** spleen. DVHs, dose–volume histograms; VMAT, volumetric modulated arc therapy; IMPT, intensity-modulated spot-scanning proton therapy.

Clinical advantages of proton treatments versus photon radiation treatment planning for bone marrow environment

One of the main advantages of protons over photons is reduced dose deposition in normal tissue and the enhanced deposition of radiation dose in the target region set by the spread-out Bragg peak of charged particles. This physical characteristic of the protons is reflected in current dosimetric planning in which the IMPT plans achieved similar target coverage compared to VMAT planning while providing a reduction in the dose deposition to OARs. This dose reduction to OARs in IMPT plans can be used to justify dose-escalation studies, which may provide better disease

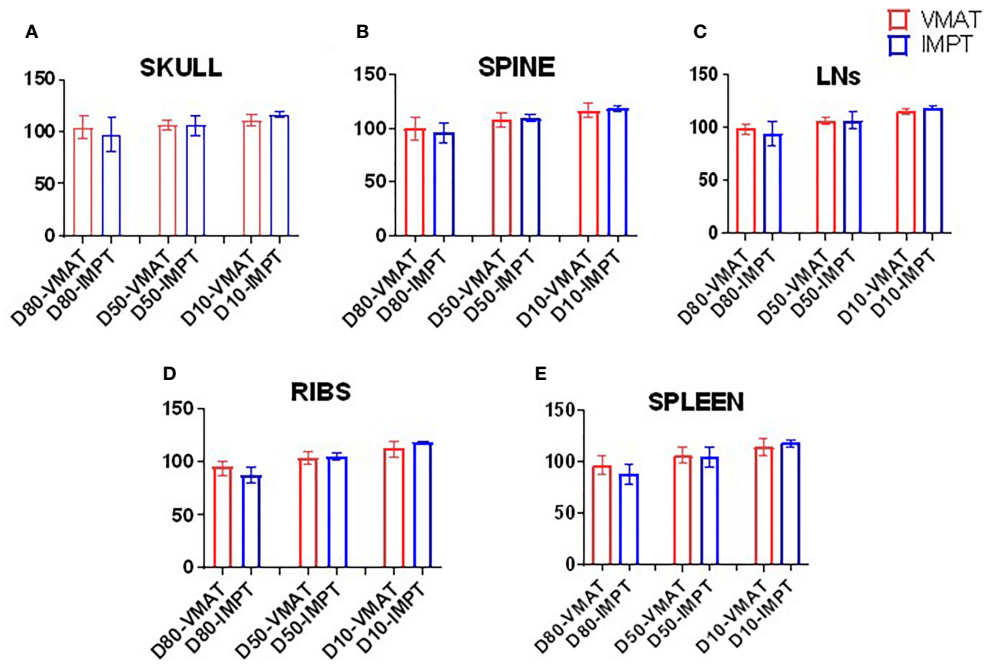

FIGURE 4
Bar graphs of the D80, D50, and D10 of targets. **(A)** Skull, **(B)** spine, **(C)** lymph nodes, **(D)** ribs, and **(E)** spleen.

control as suggested by previous work (23). Based on several *in vitro* studies, the RBE of the protons is considered 1.1, which is superior to that of photons (24). Furthermore, there may be increased RBE due to enhanced linear energy transfer when protons are close to the Bragg peak (25). A recent study by Zuro et al. (26) suggests that a certain level of radiation dose to the body may be essential for sustained donor marrow engraftment, indicating that a complex biological mechanism controls donor cell homing and expansion. Therefore, beyond toxicity reduction, the mechanism of how proton TMI will support successful donor cell engraftment requires further investigation. Furthermore, a better understanding of the RBE of protons in the context of leukemia cell killing and the effects of proton therapy on the bone marrow microenvironment in the *in vivo* system will strengthen the clinical translation of this technique.

TABLE 3 Mean OAR doses and percentage differences between the VMAT and IMPT plans.

Average OAR doses (cGy) for n = 5 patients				
OAR	**VMAT-TMI**	**IMPT**	**%diff**	**p-Value**
Brain	612.8	609.0	0.6	0.96
Bladder	772.6	383.0	50.4	<0.01
Esophagus	401.0	575.0	−43.4	<0.01
Eyes	293.6	287.8	2.0	0.81
Heart	483.8	418.2	13.6	0.37
Intestine	809.0	401.0	50.4	<0.01
Kidneys	709.4	542.8	23.5	0.01
Lungs	732.6	632.8	13.6	0.02
Parotids	468.4	437.0	6.7	0.57
Stomach	491.8	460.8	6.3	0.72
Thyroid	415.8	556.2	−33.8	<0.01
Liver	630.4	634.8	−0.7	0.92

OAR, organ at risk; VMAT, volumetric modulated arc therapy; TMI, total marrow irradiation; IMPT, intensity-modulated spot-scanning proton therapy.

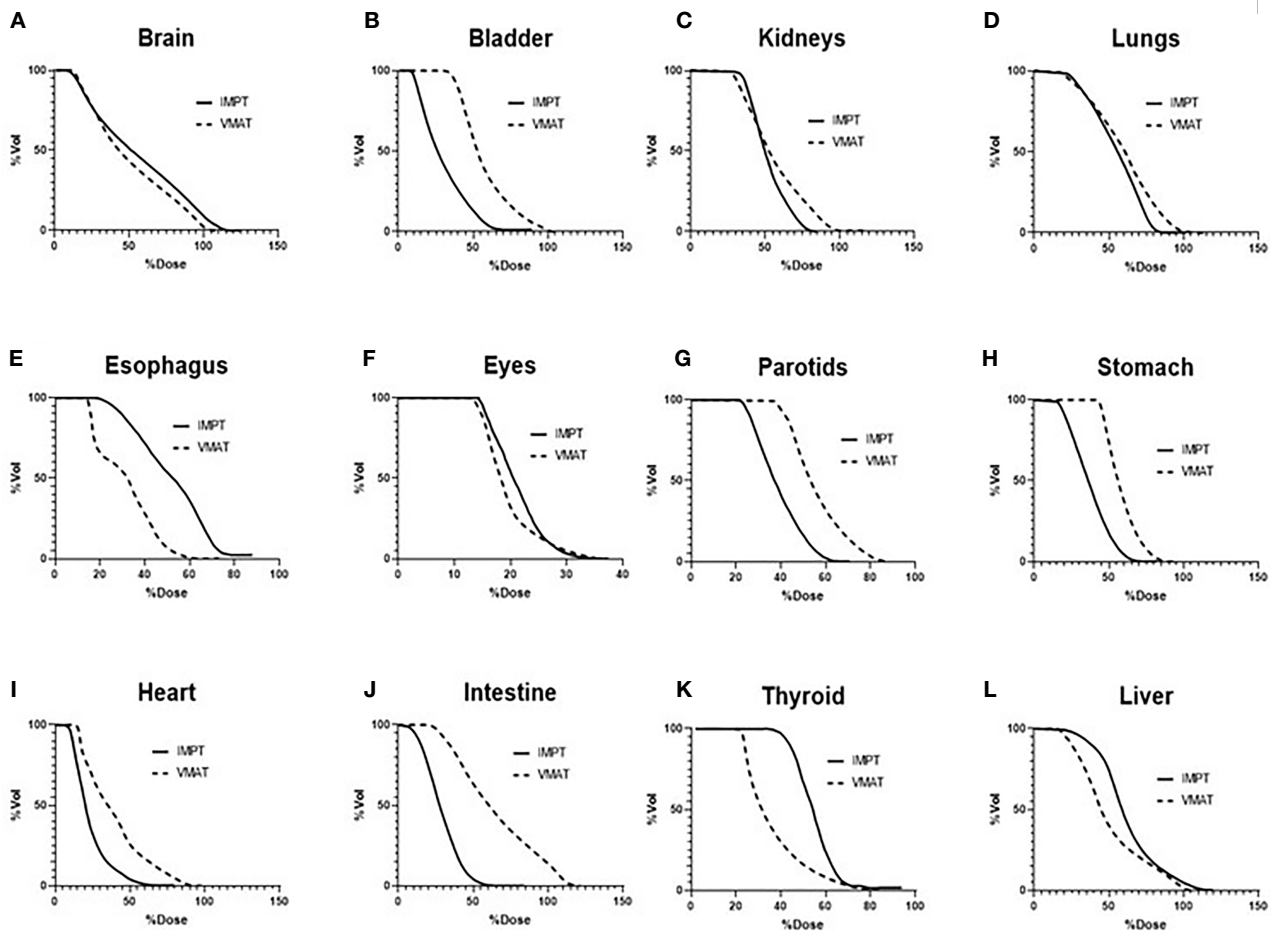

FIGURE 5
Average DVHs of the OARs comparing VMAT to IMPT plans: **(A)** brain, **(B)** bladder, **(C)** kidneys, **(D)** lungs, **(E)** esophagus, **(F)** eyes, **(G)** parotids, **(H)** stomach, **(I)** heart, **(J)** intestine, **(K)** thyroid, and **(L)** liver. DVHs, dose–volume histograms; OARs, organs at risk; VMAT, volumetric modulated arc therapy; IMPT, intensity-modulated spot-scanning proton therapy.

Potential impact of proton arc therapy on total marrow irradiation

Photon TMI was originally conceived with arc therapy using the TomoTherapy system and later the RapidArc system from Varian. Several works have demonstrated the benefits of VMAT versus conventional photon treatment planning for a variety of different sites (27–29). Typically, VMAT offers superior dose coverage and reduction of OAR dose as compared to step-and-shoot intensity-modulated radiation therapy (IMRT) at the cost of increased planning time. Currently, proton arc therapy does not exist for clinical use; however, recent technological advancements have demonstrated potential clinical feasibility (30, 31). Several proton arc studies have even shown superior dose coverage of the tumor and OAR sparing, which could prove to be potentially superior dosimetrically to VMAT-TMI (32). Another potential benefit of proton arc therapy is a reduction in clinical treatment times (32). Currently, the Raystation system allows for fast optimization, usually with 20–30 min of total planning time for proton plans compared to Eclipse arc planning, which can be 3–6 h for photon plans. However, the proton dose delivery time for regular proton fields directed from several discrete angles is estimated to be more than 2 h due to the nature of spot-scanning proton therapy, as in this simulation study. Proton arc beams can greatly reduce the total treatment time required for dose delivery.

Conclusion

This simulation study demonstrates several dosimetric advantages of proton therapy versus photon therapy for TMI. IMPT plans displayed better dose conformity, reduction in cold dose spots inside the PTVs, and reduced OAR doses as compared to VMAT-TMI except for the esophagus and thyroid. Technical

advancement in the treatment planning and dose delivery of proton therapy such as the development of arc-based proton therapy might enable the feasibility and clinical implementation of proton therapy for TMI. In addition to these dosimetric advantages, proton therapy may have superior radiobiological effects for the TMI treatment, which requires further investigation.

Data availability statement

The original contributions presented in the study are included in the article/supplementary material. Further inquiries can be directed to the corresponding author.

Author contributions

DZ: First and Corresponding author; GV: first author; JC: first author; YC: second author; CHa: second author; CHe: second author; SA: second author; SH: senior author; IA: senior author. All authors contributed to the article and approved the submitted version.

Conflict of interest

The authors declare that the research was conducted in the absence of any commercial or financial relationships that could be construed as a potential conflict of interest.

Publisher's note

Supplementary material

The Supplementary Material for this article can be found online at: https://www.frontiersin.org/articles/10.3389/fonc.2022.955004/full#supplementary-material

References

1. Thomas ED. A history of haemopoietic cell transplantation. *Br J Haematol* (1999) 105(2):330–9. doi: 10.1111/j.1365-2141.1999.01337.x

2. Clift RA, Buckner CD. Marrow transplantation for acute myeloid leukemia. *Cancer Invest* (1998) 16(1):53–61. doi: 10.3109/07357909809039755

3. Clift RA, Buckner CD, Appelbaum FR, Bearman SI, Petersen FB, Fisher LD, et al. Allogeneic marrow transplantation in patients with acute myeloid leukemia in first remission: a randomized trial of two irradiation regimens. *Blood* (1990) 76 (9):1867–71. doi: 10.1182/blood.V76.9.1867.1867

4. Clift RA, Buckner CD, Appelbaum FR, Bryant E, Bearman SI, Petersen FB, et al. Allogeneic marrow transplantation in patients with chronic myeloid leukemia in the chronic phase: a randomized trial of two irradiation regimens. *Blood* (1991) 77(8):1660–5. doi: 10.1182/blood.V77.8.1660.1660

5. Clift RA, Buckner CD, Appelbaum FR, Sullivan KM, Storb R, Thomas ED. Long-term follow-up of a randomized trial of two irradiation regimens for patients receiving allogeneic marrow transplants during first remission of acute myeloid leukemia. *Blood* (1998) 92(4):1455–6. doi: 10.1182/blood.V92.4.1455

6. Clift RA, Thomas EDSeattle Marrow Transplant T. Follow-up 26 years after treatment for acute myelogenous leukemia. *N Engl J Med* (2004) 351(23):2456–7. doi: 10.1056/NEJM200412023512326

7. Bieri S, Helg C, Chapuis B, Miralbell R. Total body irradiation before allogeneic bone marrow transplantation: is more dose better? *Int J Radiat Oncol Biol Phys* (2001) 49(4):1071–7. doi: 10.1016/S0360-3016(00)01491-7

8. Esiashvili N, Lu X, Ulin K, Laurie F, Kessel S, Kalapurakal JA, et al. Higher reported lung dose received during total body irradiation for allogeneic hematopoietic stem cell transplantation in children with acute lymphoblastic leukemia is associated with inferior survival: A report from the children's oncology group. *Int J Radiat Oncol Biol Phys* (2019) 104(3):513–21. doi: 10.1016/j.ijrobp.2019.02.034

9. Hui SK, Verneris MR, Froelich J, Dusenbery K, Welsh JS. Multimodality image guided total marrow irradiation and verification of the dose delivered to the lung, PTV, and thoracic bone in a patient: a case study. *Technol Cancer Res Treat* (2009) 8(1):23–8. doi: 10.1177/153303460900800104

10. Wong JY, Liu A, Schultheiss T, Popplewell L, Stein A, Rosenthal J, et al. Targeted total marrow irradiation using three-dimensional image-guided tomographic intensity-modulated radiation therapy: an alternative to standard total body irradiation. *Biol Blood Marrow Transplant* (2006) 12(3):306–15. doi: 10.1016/j.bbmt.2005.10.026

11. Wong JY, Rosenthal J, Liu A, Schultheiss T, Forman S, Somlo G. Image-guided total-marrow irradiation using helical tomotherapy in patients with multiple myeloma and acute leukemia undergoing hematopoietic cell transplantation. *Int J Radiat Oncol Biol Phys* (2009) 73(1):273–9. doi: 10.1016/j.ijrobp.2008.04.071

12. Schultheiss TE, Wong J, Liu A, Olivera G, Somlo G. Image-guided total marrow and total lymphatic irradiation using helical tomotherapy. *Int J Radiat Oncol Biol Phys* (2007) 67(4):1259–67. doi: 10.1016/j.ijrobp.2006.10.047

13. Hui SK, Kapatoes J, Fowler J, Henderson D, Olivera G, Manon RR, et al. Feasibility study of helical tomotherapy for total body or total marrow irradiation. *Med Phys* (2005) 32(10):3214–24. doi: 10.1118/1.2044428

14. Hui SK, Lusczek E, DeFor T, Dusenbery K, Levitt S. Three-dimensional patient setup errors at different treatment sites measured by the tomotherapy megavoltage CT. *Strahlenther Onkol* (2012) 188(4):346–52. doi: 10.1007/s00066-011-0066-z

15. Han C, Schultheisss TE, Wong JY. Dosimetric study of volumetric modulated arc therapy fields for total marrow irradiation. *Radiother Oncol* (2012) 102(2):315–20. doi: 10.1016/j.radonc.2011.06.005

16. Corvo R, Zeverino M, Vagge S, Agostinelli S, Barra S, Taccini G, et al. Helical tomotherapy targeting total bone marrow after total body irradiation for patients with relapsed acute leukemia undergoing an allogeneic stem cell transplant. *Radiother Oncol* (2011) 98(3):382–6. doi: 10.1016/j.radonc.2011.01.016

17. Stein A, Palmer J, Tsai NC, Al Malki MM, Aldoss I, Ali H, et al. Phase I trial of total marrow and lymphoid irradiation transplantation conditioning in patients with Relapsed/Refractory acute leukemia. *Biol Blood Marrow Transplant* (2017) 23 (4):618–24. doi: 10.1016/j.bbmt.2017.01.067

18. Mancosu P, Cozzi L, Muren LP. Total marrow irradiation for hematopoietic malignancies using volumetric modulated arc therapy: A review of treatment planning studies. *Phys Imaging Radiat Oncol* (2019) 11:47–53. doi: 10.1016/j.phro.2019.08.001

19. Aydogan B, Yeginer M, Kavak GO, Fan J, Radosevich JA, Gwe-Ya K. Total marrow irradiation with RapidArc volumetric arc therapy. *Int J Radiat Oncol Biol Phys* (2011) 81(2):592–9. doi: 10.1016/j.ijrobp.2010.11.035

20. Newhauser WD, Zhang R. The physics of proton therapy. *Phys Med Biol* (2015) 60(8):R155–209. doi: 10.1088/0031-9155/60/8/R155

21. Zuro D, Vagge S, Broggi S, Agostinelli S, Takahashi Y, Brooks J, et al. Multi-institutional evaluation of MVCT guided patient registration and dosimetric precision in total marrow irradiation: A global health initiative by the international consortium of total marrow irradiation. *Radiother Oncol* (2019) 141:275–82. doi: 10.1016/j.radonc.2019.07.010

22. Li C, Muller-Runkel R, Vijayakumar S, Myrianthopoulos LC, Kuchnir FT. Craniospinal axis irradiation: an improved electron technique for irradiation of the spinal axis. *Br J Radiol* (1994) 67(794):186–93. doi: 10.1259/0007-1285-67-794-186

23. Hui S, Brunstein C, Takahashi Y, DeFor T, Holtan SG, Bachanova V, et al. Dose escalation of total marrow irradiation in high-risk patients undergoing allogeneic hematopoietic stem cell transplantation. *Biol Blood Marrow Transplant* (2017) 23 (7):1110–6. doi: 10.1016/j.bbmt.2017.04.002

24. Paganetti H, Blakely E, Carabe-Fernandez A, Carlson DJ, Das IJ, Dong L, et al. Report of the AAPM TG-256 on the relative biological effectiveness of proton beams in radiation therapy. *Med Phys* (2019) 46(3):e53–78. doi: 10.1002/mp.13390

25. Paganetti H. Relative biological effectiveness (RBE) values for proton beam therapy. variations as a function of biological endpoint, dose, and linear energy transfer. *Phys Med Biol* (2014) 59(22):R419–72. doi: 10.1088/0031-9155/59/22/R419

26. Zuro D, Madabushi SS, Brooks J, Chen BT, Goud J, Salhotra A, et al. First multimodal, three-dimensional, image-guided total marrow irradiation model for preclinical bone marrow transplantation studies. *Int J Radiat Oncol Biol Phys* (2021) 111(3):671–83. doi: 10.1016/j.ijrobp.2021.06.001

27. Studenski MT, Bar-Ad V, Siglin J, Cognetti D, Curry J, Tuluc M, et al. Clinical experience transitioning from IMRT to VMAT for head and neck cancer. *Med Dosim* (2013) 38(2):171–5. doi: 10.1016/j.meddos.2012.10.009

28. Lee YK, Bedford JL, McNair HA, Hawkins MA. Comparison of deliverable IMRT and VMAT for spine metastases using a simultaneous integrated boost. *Br J Radiol* (2013) 86(1022):20120466. doi: 10.1259/bjr.20120466

29. Deng Z, Shen L, Zheng X, Zhou Y, Yi J, Han C, et al. Dosimetric advantage of volumetric modulated arc therapy in the treatment of intraocular cancer. *Radiat Oncol* (2017) 12(1):83. doi: 10.1186/s13014-017-0819-7

30. Li X, Liu G, Janssens G, De Wilde O, Bossier V, Lerot X, et al. The first prototype of spot-scanning proton arc treatment delivery. *Radiother Oncol* (2019) 137:130–6. doi: 10.1016/j.radonc.2019.04.032

31. Ding X, Li X, Zhang JM, Kabolizadeh P, Stevens C, Yan D. Spot-scanning proton arc (SPArc) therapy: The first robust and delivery-efficient spot-scanning proton arc therapy. *Int J Radiat Oncol Biol Phys* (2016) 96(5):1107–16. doi: 10.1016/j.ijrobp.2016.08.049

32. Ferguson S, Ahmad S, Ali I. Simulation study of proton arc therapy with the compact single-room MEVION-S250 proton therapy system. *J Radiotherapy practice* (2020) 19(4):347–54. doi: 10.1017/S1460396919000888

frontiers | Frontiers in Oncology

TYPE Methods
PUBLISHED 11 August 2022
DOI 10.3389/fonc.2022.936985

OPEN ACCESS

EDITED BY
Jeffrey Wong,
City of Hope National Medical Center,
United States

REVIEWED BY
Chunhui Han,
City of Hope National Medical Center,
United States
Joseph Rosenthal,
City of Hope National Medical Center,
United States
Savita Dandapani,
City of Hope National Medical Center,
United States

*CORRESPONDENCE
Yuexin Guo
guoyx0371@126.com

SPECIALTY SECTION
This article was submitted to Radiation Oncology, a section of the journal Frontiers in Oncology

RECEIVED 05 May 2022
ACCEPTED 18 July 2022
PUBLISHED 11 August 2022

CITATION
Kong F, Liu S, Liu L, Pi Y, Pei Y, Xu D, Jia F, Han B and Guo Y (2022) Clinical study of total bone marrow combined with total lymphatic irradiation pretreatment based on tomotherapy in hematopoietic stem cell transplantation of acute leukemia. *Front. Oncol.* 12:936985. doi: 10.3389/fonc.2022.936985

Clinical study of total bone marrow combined with total lymphatic irradiation pretreatment based on tomotherapy in hematopoietic stem cell transplantation of acute leukemia

Fanyang Kong, Shuaipeng Liu, Lele Liu, Yifei Pi, Yuntong Pei, Dandan Xu, Fei Jia, Bin Han and Yuexin Guo*

Department of Radiation Therapy, First Affiliated Hospital of Zhengzhou University, Zhengzhou, China

Objective: Allogeneic hematopoietic stem cell transplantation (allo-HSCT) is an effective method for the treatment of refractory and relapsed acute leukemia, and the preconditioning methods before transplantationis one of the important factors affecting the survival of patients. Radiotherapy combined with chemotherapy is the most commonly used preconditioning method before transplantation. This study evaluated the safety and efficacy of total bone marrow combined with total lymphatic irradiation as a preconditioning method before hematopoietic stem cell transplantation.

Methods: Seventeen patients with acute leukemia who were admitted to our center from 2016 to 2020 were selected. The median age was 17 years (8-35). The target area for TMLI includes the total bone marrow and total lymphatic space, and the organs at risk include the lens, lungs, kidneys, intestine, heart, and liver. The patients received a total bone marrow and lymphatic irradiation preconditioning regimen, the related acute adverse reactions were graded, and the prognosis of the patients after transplantation was observed.

Results: During patient preconditioning, only grade 1-2 toxicity was observed, and grade 3-4 toxicity did not occur. Except for one patient whose platelets were not engrafted, all the other patients were successfully transplanted. The median time of neutrophil implantation was 14 d (9-15 d), and the median time of platelet implantation was 14 d (13-21 d). With a median follow-up of 9 months (2-48), 4 relapses occurred, 3 died, and 10 leukemia patients survived and were disease-free. One-year overall survival was 69.8%, cumulative recurrence was 19.5%, disease-free-survival was 54.2%.

Conclusion: The Allo-HSCT pretreatment regimen of total bone marrow combined with total lymphatic irradiation is safe and effective in the treatment of malignant hematological diseases. Total bone marrow combined with total lymphatic irradiation may completely replace total body irradiation, and the clinically observed incidence of acute toxicity is not high.

KEYWORDS

acute leukemia, total bone marrow and lymphatic irradiation, tomotherapy, acute toxicity, GvHD

Hematopoietic stem cell transplantation (HSCT) is one of the main treatments for leukemia, and pretreatment regimen before transplantation is an important factor affecting the survival of patients after transplantation. Total body irradiation (TBI) is usually combined with chemotherapy as a pretreatment regimen for bone marrow transplant patients. TBI can act on certain organs that cannot be reached by chemotherapy drugs to eliminate leukemia cells, and can also suppress the patient's immune function so that the donor's hematopoietic stem cells can be successfully engrafted (1, 2).

However, due to the lack of accuracy and organ targeting of TBI, high radiation doses will involve normal tissues or organs (lung, heart, liver and kidney), leading to radiation-related toxicity and increased transplant-related mortality (TRM). There are many potential complications of TBI, acute and subacute side effects include nausea, dry mouth, oral mucositis, and interstitial pneumonia (IP); long-term side effects may include venous occlusive disease, neurocognitive impairment, heart disease, cataracts, and secondary tumors (3, 4).

If the prescribed dose of a single treatment is lower than 6 Gy, the risk of transplant failure and post-transplant recurrence is greatly increased, and the incidence of interstitial pneumonia increases significantly when the single dose is increased to more than 10 Gy (5). Fractional irradiation patterns of 12 to 15 Gy had no higher side effects than a single 10 Gy treatment, and treatment mortality was reduced (6). The more common pattern of fractional TBI was 12Gy/6F (7).

Due to concerns about late toxicity, the use of TBI is gradually decreasing as part of the preconditioning methods before transplantation for patients with acute leukemia. Total marrow irradiation (TMI) and total bone marrow combined with total lymphatic irradiation (TMLI) as part of tomotherapy is a more targeted approach to radiation therapy, which can prioritize the delivery of doses to areas with a high tumor burden while reducing toxicity and increasing the dose that is projected to the bone marrow (8–10).

In the pretreatment of leukemia patients, the optimal irradiation dose of TMLI and combination chemotherapy are still under exploration. Because TMI/TMLI is in the exploratory stage of development, it has not yet been used as a standard pre-transplant component. This study mainly evaluated the safety and efficacy of total bone marrow combined with total lymphatic irradiation as a preconditioning method before allogeneic peripheral blood stem cell transplantation.

Materials and methods

Patients in the group

The functions of the heart, liver and kidney were basically normal, and the KPS score was ≥ 80. The clinical diagnosis is clear and indicates bone marrow transplantation. As shown in Table 1, a total of 17 patients with TMLI were selected from January 2016 to March 2020, including 15 males and 2 females, aged 8 to 35 years (median 17 years). There were 9 patients with acute B lymphoblastic leukemia, 7 patients with acute T lymphoblastic leukemia and 1 patient with acute myeloid leukemia.

Equipment and CT positioning

Tomo HD integrates the X-ray beam of 6 MeV and the CT image guidance function of 3.5 MeV in a single device and can modulate tumors with lengths of 135 cm and widths of 60 cm. Before the CT scan, the patient was fixed in a vacuum pad that covered the whole body, and a thermoplastic mold of the head, neck and shoulder mold was used in combination with the body vacuum pad in the supine position. A 1-cm tissue compensation membrane was placed in the patient's hands, feet and ribs to ensure that the built-up area was formed. The knee was bent slightly to minimize bending of the lumbar spine. Patients whose height is less than 135 cm underwent CT that scanned, in an advanced manner, all areas from the top of the head to the toes. For patients who are taller than 135 cm, metal marks are placed in the middle of the patient's thighs, and CT scans are performed

TABLE 1 Patient introduction.

Patient No.	Gender	Age	Diagnosis
1	Male	16	B-ALL
2	Male	12	T-ALL
3	Male	18	B-ALL
4	Male	14	B-ALL
5	Male	10	B-ALL
6	Male	17	B-ALL
7	Male	8	B-ALL
8	Female	10	B-ALL
9	Male	12	T-ALL
10	Male	11	T-ALL
11	Male	35	AML
12	Male	22	T-ALL
13	Male	12	T-ALL
14	Female	16	B-ALL
15	Male	9	B-ALL
16	Male	10	T-ALL
17	Male	25	T-ALL

in two segments. The first segment is from the top to the lower thigh, the head is advanced, and the layer thickness is 5 mm. The other part removes the thermoplastic mold of the head, neck and shoulder. From the toe to the upper thigh, the foot is advanced, the layer thickness is 5 mm, and the two segments overlap approximately 20 cm. Multiple cross-sectional lines were drawn on all the limbs, and the corresponding position was drawn on the vacuum pad so that the position was more accurate during treatment.

Target delineation

After CT scanning, the data were transmitted to the Varian TPS planning system for target and organ delineation. TBI target definition: subtract all human tissues from the lens and bilateral lungs. The target area of TMLI is defined as total bone marrow and all lymph nodes, including the spleen, brain and testes. Total bone marrow includes skull, mandible, humerus, scapula, clavicle, sternum, vertebra, rib, hip, femur, limb bone, etc. Lymph nodes include cervical lymph nodes, mediastinal lymph nodes, supraclavicular lymph nodes, and inguinal lymph nodes, etc. Organs at risk include the lens, lung, heart, kidney, intestine, liver, etc. The target area for TMLI is delineated, as shown in Figure 1. A CTV uniformly expanded by 5 mm is defined as the PTV.

Plan design

TBI and TMLI plans based on Tomo TPS were designed for the patients in the group. The Field Width is 5.054 cm, the Pitch is 0.287, and the modulation factor is 3. The Dose Calc Grid is Fine mode 1.95 mm. For lower limb MF=2.0, the other parameters are consistent. The PTV prescription was 12 Gy/6 F, and TBI and TMLI plans were normalized to 95% of the prescription dose volume. Each patient plans to iterate 300 times, and it takes approximately 15 hours for each plan to optimize the modulation time. However, the patients actually adhered to the TMLI plan, as shown in Table 4. The treatment was administered twice a day with an interval of 8 hours.

Efficacy evaluation indicators after transplantation

Hematopoietic reconstruction indicators, that is, the time of granulocyte and platelet engraftment (the first day of neutrophil implantation is defined as neutrophil implantation time when neutrophils $\geq 0.5\times10^9$/L for 3 consecutive days, and platelet implantation time is defined as platelet implantation time when neutrophils are counted for 7 consecutive days $\geq 20\times10^9$/L without blood transfusion); all patients were graded for preconditioning-related acute adverse reactions; the occurrence of GVHD after transplantation and the prognosis after transplantation were observed.

SPSS 26.0 was used for statistical analysis

R software was used to plot Kaplan-Meier survival curve and one-year OS, CIR, DFS estimates, and log-rank test was used to

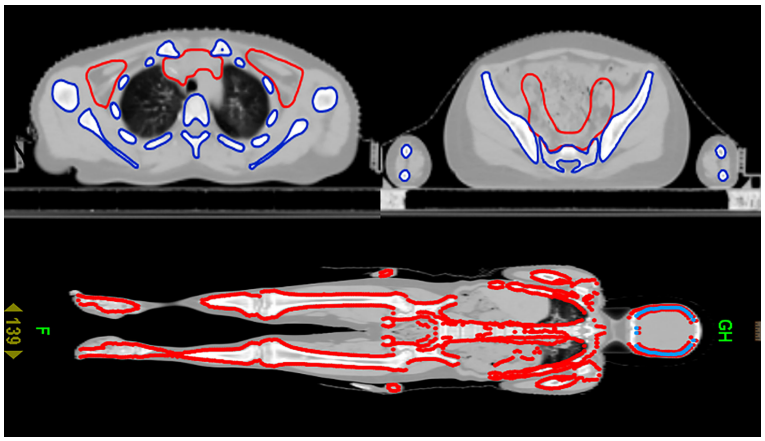

FIGURE 1
Cross-sectional and coronal display of the TMLI target.

compare whether there were statistical differences between different survival curves. The test level is $\alpha = 0.05$, and the difference is considered to be statistically significant when the $P<0.05$ is performed.

Results

As shown in Table 2, compared with the TBI regimen, the DVHs of the TMLI regimen with the same dose showed that almost all the important organs at risk had varying degrees of risk reduction. The TMLI regimen reduced the average dose administered to organs by 15.0% to 57.6%. The average doses administered to the lungs, liver, heart, intestine and stomach decreased by 17%, 45.1%, 52.9%, 40.7% and 55.3%, respectively. The average treatment time of TBI was 32.4 min. The average treatment time of TMLI was 29.9 min. The cross-sectional dose distribution and coronal dose distribution of TMLI based on HT (12 Gy) were shown in Figure 2.

Every patient received two MVCT images with which to perform image-guided treatment, and the corresponding MVCT scan areas were the head-to-chest area and the pelvic area. Each image was registered with a corresponding kilovoltage CT (kVCT) image. If the pitch, yaw or roll were more than 2° or the offset of X, Y or Z was more than 5 mm, the positioning was redone. MVCT was acquired again to ensure that the pitch, yaw and roll were less than 2°, and the offsets of X, Y and Z were less than 5 mm. The average value of the offset of the two positions was taken as the final registration result. Once accepted, the examination table was moved to the registration position to begin the treatment.

TABLE 2 Comparison of the average dose of TBI and TMLI endangered organs (12 Gy).

Organs at risk (OARs)	TBI Dose (Gy) Mean	TMLI Dose (Gy) Mean	Average Dose Reduction (%)
Left Lens	3.94	3.18	19.3%
Right Lens	3.72	3.15	15.3%
Left Eye	8.61	5.47	36.5%
Right Eye	8.56	5.46	36.2%
Left Parotid	12.78	5.93	53.6%
Right Parotid	12.75	5.72	55.1%
Heart	12.00	5.65	52.9%
Left Lung	7.36	6.11	17.0%
Right Lung	7.32	6.08	16.9%
Left Kidney	12.69	5.40	57.5%
Right Kidney	12.71	5.39	57.6%
Stomach	12.44	5.56	55.3%
Liver	12.44	6.83	45.1%
Intestine	12.47	7.40	40.7%
Body	12.24	10.4	15.0%

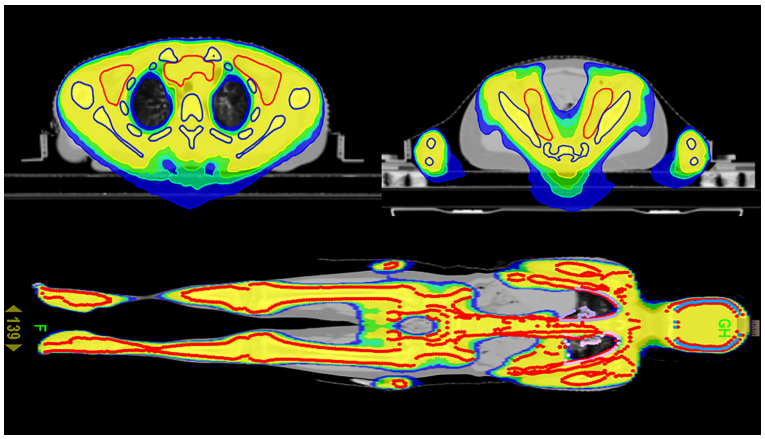

FIGURE 2
Cross-sectional dose distribution and coronal dose distribution of TMLI based on HT (12 Gy).

As shown in Figure 3, if the patient is taller than 135cm, the treatment was carried out in two stages, including the upper section head advanced mode and the lower foot advanced mode.

As shown in Table 3, 17 patients were classified into regimen-related toxicity according to organ system (11). Toxicity was most common in the Mucosa and Gut. Only grade I-II toxicity was observed, and grade III-IV toxicity did not appear. After symptomatic treatment with antiemetic drugs, antidiarrheal drugs, rehydration drugs, etc., all patients tolerated it. Mild toxic reactions occurred during pretreatment, and no radiation pneumonia and hepatic radiation-induced veno-occlusive occurred.

All patients were successfully transplanted except one patient whose platelets were not implanted. The median time of neutrophil implantation was 14 d (9~15 d), and the median time of platelet implantation was 14 d (13~21 d).

In Table 4, all patients were set to a prescribed dose of 12Gy/6F.Four patients were given only 10Gy/5F due to reasons such as diarrhea and other machine failures. Follow-up observation was conducted after transplantation, as shown in Table 4, and the follow-up was performed September 1st, 2021. The median follow-up period was 9 months (2-48 months). Among all patients, 1 patient developed acute graft-versus-host disease, and 2 patients developed chronic graft-versus-host disease. 4 patients experienced recurrence, 3 patients died, and 10 patients with leukemia survived and were disease-free. Except for 1 case of extramyelial recurrence, the others were hematologic recurrence.

As shown in Figure 4, one-year overall survival (OS) was 69.8%, cumulative incidence recurrence (CIR) was 19.5%, disease-free-survival (DFS) was 54.2%. Patients who received Haploidentical versus HLA-matched transplantation had no statistically significant difference in OS,DFS and CIR, as shown in Figure 5.

FIGURE 3
The upper section head advanced mode and the lower foot advanced mode.

TABLE 3 Regimen-related toxicity according to organ system.

	Grade 0		Grades I or II		Grades III or IV	
	n	%	n	%	n	%
Heart	17	100	0	0	0	0
Bladder	17	100	0	0	0	0
Kidneys	17	100	0	0	0	0
Lungs	17	100	0	0	0	0
Liver	17	100	0	0	0	0
CNS	17	100	0	0	0	0
Mucosa	15	88.2	2	11.8	0	0
Gut	11	64.7	6	35.3	0	0

Discussion

In the TBI regimen, the main dose limiting factor is pulmonary toxicity. Gruen et al. (7) found that when the average lung dose of the HT-based FTBI 12 Gy/6 F/3 D regimen was 9.14 Gy, no grade 3-4 side effects were observed during 15 months of follow-up. Shinde et al. (12) evaluated hematopoietic cell transplantation in 142 patients with primary multiple myeloma or acute leukemia, and the probability of radiation pneumonia was 0.7% when the average lung dose was kept within 8 Gy. The median dose of left and right lungs in this protocol is 6.1 Gy. Gerstein et al. (13) found that the tolerance dose of the kidney to a fractionated dose of TBI was 14 Gy in adults and 12 Gy in children. The median dose of kidney in this protocol is 5.4 Gy. Hepatic radiation-induced veno-occlusive disease is a complication involving whole liver irradiation. Radiation-induced veno-occlusive disease is almost eliminated by significantly reducing the dose of large volume liver (14). In this protocol, the median dose of liver was reduced by 45.1%, and no hepatic radiation-induced veno-occlusive occurred.

Compared with traditional TBI techniques, Haraldsson et al. (8) studied the helical tomography-based total bone marrow irradiation technique in 23 patients with no increase in GVHD toxicity, recurrence or severity. Whole-body irradiation using helical tomography is feasible and can deliver higher doses to sites at high risk of recurrence while sparing major normal organs such as the lungs, liver, and kidneys, therefore reducing the severity and frequency of late complications (15, 16).

Studies have shown that comparing patients with TMLI and TBI, the rate of extramedullary recurrence after hematopoietic stem cell transplantation is comparable, although TMLI provides patients with more conservative targeted radiation

TABLE 4 Disease condition of patients before and after transplantation and survival time after transplantation.

Patient No.	Pretransplant state	Transplantation type	Dose (Gy)	Survival time (months)	Survival state
1	CR	Haploidentical	10	20	disease-free
2	CR	Haploidentical	12	21	disease-free
3	NR	Haploidentical	10	3	died
4	CR	Haploidentical	12	10	recurred
5	CR	HLA-matched	10	8	recurred
6	CR	HLA-matched	12	18	disease-free
7	CR	Haploidentical	12	6	disease-free
8	CR	Haploidentical	12	28	recurred
9	CR	Haploidentical	12	5	died
10	CR	Haploidentical	12	6	disease-free
11	CR	HLA-matched	10	6	recurred
12	CR	HLA-matched	12	13	disease-free
13	CR	HLA-matched	12	5	disease-free
14	CR	Haploidentical	12	9	disease-free
15	CR	Haploidentical	12	2	died
16	CR	Haploidentical	12	48	disease-free
17	CR	HLA-matched	12	13	disease-free

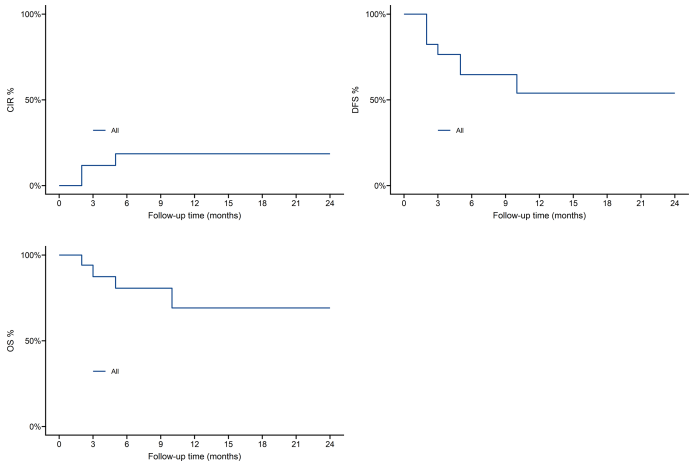

FIGURE 4
Survival outcomes in 17 patients.

therapy, which does not increase the incidence of extramedullary recurrence risk. Except for 1 case of extramyelial recurrence, the others were hematologic recurrence. Kim et al. (17) studied 101 patients and found that the extramedullary recurrence rate after TMLI was equivalent to the results of the TBI regimen, and there was no increase in the risk of extramedullary recurrence. Wong et al. (18) reported the long-term toxicity of 142 patients who received the TMLI regimen from 2005 to 2016. They believed that the higher dose rate of HT would not cause organ dysfunction. The effect of the dose rate is alleviated by reducing the dose to the organs at risk and changing the fractional exposure pattern.

Hui et al. (19) explained the molecular level changes in mice treated with TBI/TMI and found that the content of stromal cell-derived factor (SDF-1) in the organs or bone marrow of mice treated with TBI increased. The content of SDF-1 in the organs or bone marrow of the latter mice did not increase, which indicated that the donor cells could successfully aggregate into the bone marrow to achieve the goal of successful engraftment. As a chemokine, SDF-1 can cause donor cells to accumulate from the blood to the organ rather than the bone marrow, thus resulting in reduced transplantation efficiency.

Rosenthal et al. (20) proved through experiments that when chemotherapy is combined with TMLI, the intensity of

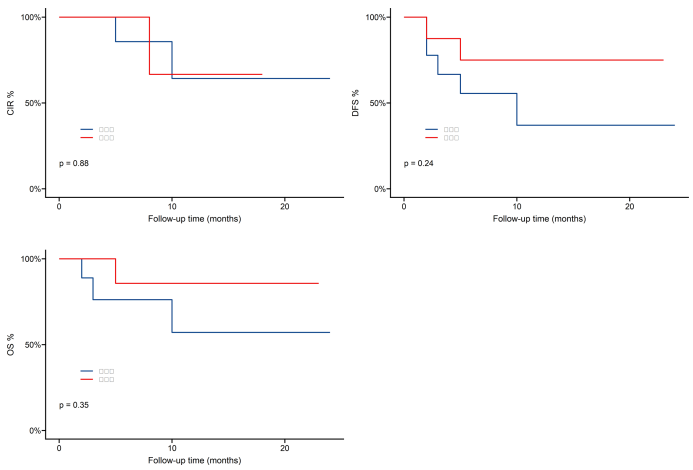

FIGURE 5
Survival outcomes of Haploidentical versus HLA-matched transplantation.

chemotherapy can be appropriately reduced so that patients can obtain transplantation with low toxicity, while the recurrence rate of transplantation does not increase, and the success rate of transplantation is higher. In TMLI, irradiation of the total body skeleton and major lymph nodes can provide an adequate immunosuppressive response to the graft. Existing clinical studies have confirmed that TMLI can reduce the occurrence of graft-versus-host disease (21). In addition, the graft-versus-tumor effect can be preserved (22).

DVH plays an important role in predicting the radiation toxicity of organs (23). Acute complications of absolute logarithmic therapy are caused by the response of these organs, and data from these targeted TMLI schemes can predict a reduction in incidence. In the preliminary design of the TMLI scheme study, only grade 1-2 toxicity was observed, and grade 3-4 toxicity did not appear. There was 1 patient with acute graft-versus-host disease and 2 patients with chronic graft-versus-host disease, of which 4 patients experienced recurrence, 3 patients died and 10 patients with leukemia survived and were disease-free. one-year overall survival was 69.8%, cumulative incidence recurrence was 19.5%, disease-free-survival was 54.2%. As a preconditioning radiotherapy for patients with acute leukemia, TMLI is safe and effective.

For patients with relapsed and refractory leukemia, compared with TBI, the dose of TMI should be increased while ensuring an effective reduction in the recurrence rate without causing a corresponding degree of severe radiotherapy-related toxicity (24, 25). Hui et al. (26) studied that TMI dose escalation to 15 Gy is feasible with acceptable toxicity in pediatric and adult patients with high-risk leukemia undergoing umbilical cord blood and sibling donor transplantation. In the pretreatment of leukemia patients, the optimal irradiation dose of TMI and combination chemotherapy are still under exploration. After accumulating more TMLIs experience, dose escalation is the next step of our radiotherapy center.

Conclusion

The results of this study suggest that helical tomographic intensity-modulated radiation therapy is clinically feasible for TMLI, TMLI can replace TBI as preconditioning before bone marrow transplantation, and TMI-based conditioning regimens can reduce preconditioning complications compared with TBI. No grade 3-4 toxicity occurred in 12 patients in this study, and no case of interstitial pneumonia or hepatic veno-occlusive disease occurred in the later follow-up. Allogeneic blood stem cell transplantation based on TMLI is a safe and effective method for the treatment of malignant hematological diseases with a wider range of indications and treatment. Due to the limited development time of this treatment plan and the small number of cases, its long-term efficacy is still uncertain, and a large-sample randomized controlled study is needed to further confirm its advantages and make its application prospects more promising.

Data availability statement

The original contributions presented in the study are included in the article/supplementary material. Further inquiries can be directed to the corresponding author.

Ethics statement

This study was reviewed and approved by The first affiliated hospital of Zhengzhou University. Written informed consent to participate in this study was provided by the participants' legal guardian/next of kin.

Author contributions

FK was in charge of data analysis and thesis writing. SL, LL, YFP, YTP and DX collected literature. FJ and BH were responsible for data verification and analysis. YG directed the writing and revision of the thesis. All authors contributed to the article and approved the submitted version.

Conflict of interest

The authors declare that the research was conducted in the absence of any commercial or financial relationships that could be construed as a potential conflict of interest.

Publisher's note

References

1. Lussana F, Rambaldi A. Allogeneic hematopoietic stem cell transplantation in patients with polycythemia vera or essential thrombocythemia transformed to myelofibrosis or acute myeloid leukemia: a report from the MPN subcommittee of the chronic malignancies working party of the e. *Haematologica* (2014) 99(5):916–21. doi: 10.3324/haematol.2013.094284

2. Lmamura M, Shigematsu A. Perspectives on the use of a medium-dose etoposide, cyclophosphamide, and total body irradiation conditioning regimen in allogeneic hematopoietic stem cell transplantation: The Japanese experience from 1993 to present. *J Clin Med* (2019) 8(5):569. doi: 10.3390/jcm8050569

3. Ricardi U, Filippi AR, Biasin E, Ciammella P, Botticella A, Francoet P, et al. Late toxicity in children undergoing hematopoietic stem cell transplantation with TBI-containing conditioning regimens for hematological malignancies. *Strahlenther Onkol Organ Deutschen Rontgengesellschaft* (2009) 185 Suppl 2 (2):17. doi: 10.1007/s00066-009-1008-x

4. Buchali A, Fe Yer P, Groll J, Massenkeil G, Arnold R, Budach V. Immediate toxicity during fractionated total body irradiation as conditioning for bone marrow transplantation. *Radiother Oncol J Eur Soc Ther Radiol Oncol* (2000) 54(2):157–62. doi: 10.1016/S0167-8140(99)00178-4

5. Inoue T, Ikeda H, Yamazaki H, Tang J, Masaoka T. Role of total body irradiation as based on the comparison of preparation regimens for allogeneic bone marrow transplantation for acute leukemia in first complete remission. *Strahlenther Onkol* (1993) 169(4):250–5.

6. Tomblyn MB, Defor TE, Tomblyn MR, Macmillan ML, Weisdorf DJ, Higgins PD, et al. Impact of total body irradiation technique on interstitial pneumonitis and clinical outcomes of 623 patients undergoing hematopoietic cell transplantation for ALL: 25 years at the university of Minnesota. *Int J Radiat Oncol Biol Phys* (2007) 69 (3):S575–5. doi: 10.1016/j.ijrobp.2007.07.1854

7. Gruen A, Ebell W, Wlodarczyk W, Neumann O, Sven Kuehl J, Stromberger C, et al. Total body irradiation (TBI) using helical tomotherapy in children and young adults undergoing stem cell transplantation. *Radiat Oncol* (2013) 8(1):92. doi: 10.1186/1748-717X-8-92

8. Haraldsson A, Engellau J, Lenhoff S, Engelholm S, Engstrm PE. Implementing safe and robust total marrow irradiation using helical tomotherapy– a practical guide. *PhysicaMedica* (2019) 60:162–7. doi: 10.1016/j.ejmp.2019.03.032

9. Pjycw A, Parf B, Pmsc D, Psh A, Plpm E, Pm D. Total marrow and total lymphoid irradiation in bone marrow transplantation for acute leukaemia. *Lancet Oncol* (2020) 21(10):e477–87.

10. Wong JYC, Liu A, Schultheiss T, Popplewell L, Stein A, Rosenthal J, et al. Targeted total marrow irradiation using three-dimensional image-guided tomographic intensity-modulated radiation therapy: an alternative to standard total body irradiation. *Biol Blood Marrow Transplant* (2006) 12(3):306–15. doi: 10.1016/j.bbmt.2005.10.026

11. Bearman SI, Appelbaum FR, Buckner CD, Petersen FB, Thomas ED. Regimen-related toxicity in patients undergoing bone marrow transplantation. *J Clin Oncol* (1988) 6(10):1562–8. doi: 10.1200/JCO.1988.6.10.1562

12. Shinde A, Yang D, Frankel P, Liu A, Wong JYC. Radiation related toxicities using organ sparing total marrow irradiation transplant conditioning regimens. *Int J Radiat Oncol Biol Phys* (2019) 105(5):1025–33. doi: 10.1016/j.ijrobp.2019.08.010

13. Gerstein J, Meyer A, Sykora KW, Frühauf J, Bremer M. Long-term renal toxicity in children following fractionated total-body irradiation (TBI) before allogeneic stem cell transplantation (SCT). *Strahlenther Onkol* (2009) 185 (11):751–5. doi: 10.1007/s00066-009-2022-8

14. Schultheiss TE, Wong J, Liu A, Olivera G, Somlo G. Image-guided total marrow and total lymphatic irradiation using helical tomotherapy. *Int J Radiat Oncol Biol Phys* (2007) 67(4):1259–67. doi: 10.1016/j.ijrobp.2006.10.047

15. Sarradin V, Simon L, Huynh A, Gilhodes J, Filleron T, Izar F. Total body irradiation using helical tomotherapy®: Treatment technique, dosimetric results and initial clinical experience. *Cancer Radiother* (2018) 22(1):17–24. doi: 10.1016/j.canrad.2017.06.014

16. Wong J, Rosenthal J, Liu A, Schultheiss T, Forman S, Somlo G. Image-guided total-marrow irradiation using helical tomotherapy in patients with multiple myeloma and acute leukemia undergoing hematopoietic cell transplantation. *Int J Radiat Oncol Biol Phys* (2009) 73(1):273–9. doi: 10.1016/j.ijrobp.2008.04.071

17. Kim JiH, Stein A, Tsai N, chultheiss TE, Palmer J, Liu A, et al. Extramedullary relapse following total marrow and lymphoid irradiation in patients undergoing allogeneic hematopoietic cell transplantation. *Int J Radiat Oncol Biol Phys* (2014) 89(1):75–81. doi: 10.1016/j.ijrobp.2014.01.036

18. Wong JYC, Forman S, Somlo G, Rosenthal J, Liu A, Schultheiss T, et al. Dose escalation of total marrow irradiation with concurrent chemotherapy in patients with advanced acute leukemia undergoing allogeneic hematopoietic cell transplantation. *Int J Radiat Oncol Biol Phys* (2013) 85(1):148–56. doi: 10.1016/j.ijrobp.2012.03.033

19. Hui S, Takahashi Y, Holtan SG, Rezvan A, Davis S, Masashi Y, et al. Early assessment of dosimetric and biological differences of total marrow irradiation versus total body irradiation in rodents. *Radiother Oncol* (2017) 124(3):468–74. doi: 10.1016/j.radonc.2017.07.018

20. Rosenthal J, Wong J, Stein A, Qian D, Hitt D, Naeem HG, et al. Phase 1/2 trial of total marrow and lymph node irradiation to augment reduced-intensity transplantation for advanced hematologic malignancies. *Blood* (2010). doi: 10.1182/blood-2010-06-288357

21. Lan F, Zeng D, Higuchi M, Higgins JP, Strober S. Host conditioning with total lymphoid irradiation and antithymocyte globulin prevents graft-versus-host disease: the role of CD1-reactive natural killer T cells. *Biol Blood Marrow Transplant* (2003) 9(6):355–63. doi: 10.1016/S1083-8791(03)00108-3

22. Ram R, Yeshurun M, Vidal L, Shpilberg O, Gafter-Gvili A. Mycophenolate mofetil vs. methotrexate for the prevention of graft-versus-host-disease - systematic review and meta-analysis. *Leuk Res -Oxf-* (2014) 38(3):352–60. doi: 10.1016/j.leukres.2013.12.012

23. Fita JV, Anton JLM, Torres MC, Tortosa S. EP-1633: Analysis of dose-volume histogram parameters on prediction esophageal toxicity in radiotherapy for lung tumors. *Radiother Oncol* (2015) 115(December):S894–5. doi: 10.1016/S0167-8140(15)41625-1

24. Chilukuri S, Sundar S, Thiyagarajan R, Easow J, Sawant M, Krishanan G, et al. Total marrow and lymphoid irradiation with helical tomotherapy: A practical implementation report. *Radiat Oncol J* (2020) 38(3):207–16. doi: 10.3857/roj.2020.00528

25. Paix A, Antoni D, Waissi W, Ledoux MP, Bilger K, Fornecker L, et al. Total body irradiation in allogeneic bone marrow transplantation conditioning regimens: A review. *Crit Rev Oncol Hematol* (2018) 123:138–48. doi: 10.1016/j.critrevonc.2018.01.011

26. Hui S, Brunstein C, Takahashi Y, Defor T, Holtan SG, Bachanova V, et al. Dose escalation of total marrow irradiation in high-risk patients undergoing allogeneic hematopoietic stem cell transplantation. *Biol Blood Marrow Transplant* (2017) 23(7):1110–16. doi: 10.1016/j.bbmt.2017.04.002

frontiers | Frontiers in Oncology

TYPE Original Research
PUBLISHED 30 August 2022
DOI 10.3389/fonc.2022.970425

OPEN ACCESS

EDITED BY
Xiaodong Wu,
The University of Iowa, United States

REVIEWED BY
Manthala Padannayil Noufal,
Apollo Proton Cancer Centre, India
Yinglin Peng,
Sun Yat-sen University Cancer Center (SYSUCC), China

*CORRESPONDENCE
William Tyler Watkins
watkins.medical.physics@gmail.com

SPECIALTY SECTION
This article was submitted to Radiation Oncology, a section of the journal Frontiers in Oncology

RECEIVED 15 June 2022
ACCEPTED 21 July 2022
PUBLISHED 30 August 2022

CITATION
Watkins WT, Qing K, Han C, Hui S and Liu A (2022) Auto-segmentation for total marrow irradiation. *Front. Oncol.* 12:970425. doi: 10.3389/fonc.2022.970425

Auto-segmentation for total marrow irradiation

William Tyler Watkins*, Kun Qing, Chunhui Han, Susanta Hui and An Liu

Department of Radiation Oncology, City of Hope National Medical Center, Duarte, CA, United States

Purpose: To evaluate the accuracy and efficiency of Artificial-Intelligence (AI) segmentation in Total Marrow Irradiation (TMI) including contours throughout the head and neck (H&N), thorax, abdomen, and pelvis.

Methods: An AI segmentation software was clinically introduced for total body contouring in TMI including 27 organs at risk (OARs) and 4 planning target volumes (PTVs). This work compares the clinically utilized contours to the AI-TMI contours for 21 patients. Structure and image dicom data was used to generate comparisons including volumetric, spatial, and dosimetric variations between the AI- and human-edited contour sets. Conventional volume and surface measures including the Sørensen–Dice coefficient (Dice) and the 95th% Hausdorff Distance (HD95) were used, and novel efficiency metrics were introduced. The clinical efficiency gains were estimated by the percentage of the AI-contour-surface within 1mm of the clinical contour surface. An unedited AI-contour has an efficiency gain=100%, an AI-contour with 70% of its surface<1mm from a clinical contour has an efficiency gain of 70%. The dosimetric deviations were estimated from the clinical dose distribution to compute the dose volume histogram (DVH) for all structures.

Results: A total of 467 contours were compared in the 21 patients. In PTVs, contour surfaces deviated by >1mm in 38.6% $\pm$ 23.1% of structures, an average efficiency gain of 61.4%. Deviations >5mm were detected in 12.0% $\pm$ 21.3% of the PTV contours. In OARs, deviations >1mm were detected in 24.4% $\pm$ 27.1% of the structure surfaces and >5mm in 7.2% $\pm$ 18.0%; an average clinical efficiency gain of 75.6%. In H&N OARs, efficiency gains ranged from 42% in optic chiasm to 100% in eyes (unedited in all cases). In thorax, average efficiency gains were >80% in spinal cord, heart, and both lungs. Efficiency gains ranged from 60-70% in spleen, stomach, rectum, and bowel and 75-84% in liver, kidney, and bladder. DVH differences exceeded 0.05 in 109/467 curves at any dose level. The most common 5%-DVH variations were in esophagus (86%), rectum (48%), and PTVs (22%).

Conclusions: AI auto-segmentation software offers a powerful solution for enhanced efficiency in TMI treatment planning. Whole body segmentation including PTVs and normal organs was successful based on spatial and dosimetric comparison.

KEYWORDS

auto-segmentation, auto-contouring, artificial intelligence, total marrow irradiation, total marrow lymphoid irradiation

1 Introduction

Segmentation of human anatomy on medical images is a critical component of targeted radiation therapy (RT). Delineations are used to design radiation therapy treatment plans including conformal avoidance in 3D-conformal RT (3DCRT) and as input to optimization algorithms for intensity modulated radiation therapy (IMRT). These delineations are typically performed by clinicians utilizing manual contouring software, which allows for drawing structures on medical images and tools including smoothing, interpolation, and intensity-based thresholding. The accuracy of the delineation is perceived as a critical element of modern IMRT and currently serves as a safety mechanism for monitoring dose to organs at risk (OARs). The 3D-dose distribution is evaluated using a 2-dimensional dose volume histogram (DVH) of proximal OARs and targets, and the results of many studies reports "safe" DVH levels for OARs based on clinical trials and clinical experience to guide future treatments. The process of manual segmentation, DVH evaluation, and multiple layers of human review (dosimetrists, physicians, and physicists) has allowed for the successful introduction of high-precision IMRT, including total marrow irradiation (TMI) and total marrow and lymphoid irradiation (TMLI) (1–3). TMI and TMLI treatment planning requires extensive contouring but allows enhancement the antileukemic effect by delivering higher doses to the region of leukemia niche, the bone marrow and lymph nodes, while reducing organ dose exposure compared to conventional total body irradiation (TBI). TMLI significantly improved overall survival in patient with relapse/refractory leukemia when compared to TBI (4). Dose escalation using conventional TBI did not improve survival because of radiation-induced toxicities (5). While evidence of the clinical advantages of TMI is growing, clinical implementation will rely on the technological capabilities of adopting institutions. The significant manual effort required in contouring the entire body including OARs, and TMLI target volumes is a major barrier to clinical implementation.

The potential to replace human delineation with computerized methods has been a focus of image science for decades. The continued interest in Artificial Intelligence (AI) for this manual task is predicated on the accuracy, consistency, and human trust in the software. However, there are not universally accepted methods to determine whether segmentation is accurate, precise, or reliable in human- or algorithm- defined delineations. Despite significant efforts in computer vision and shape modeling including atlas-based methods (6, 7), deformable-image registration (DIR) (8–10), probabilistic modeling (11), and AI, fully automated segmentation remains infeasible. None of these advancements have broken through to consistently replace manual delineation in RT (12, 13) despite retrospective evidence that auto-contouring may be more consistent in estimating DVH dose associated risk (14). In order to validate auto-segmentation for clinical use, tools include human scoring (12, 15) and computational indices including the Sørensen-Dice coefficient (Dice) and the Hausdorff Distance (HD) have consistently been deployed, but they provide limited value in measuring clinical efficiency gains.

The perceived critical importance of contour accuracy has led to considerable time and effort in manual review and manual edits of automated contours produced by these algorithms, and limited efficiency gains. More recently, AI- deep and transfer learning methods are being used for auto-segmentation with significant promise for clinical adoption due to their accuracy and consistency despite the lack of widely accepted criteria for defining accuracy and consistency. Several recent studies report on head-and-neck (H&N) and pelvis auto-segmentation have been evaluated using Dice, HD and other metrics (16). Dice and HD were also used to evaluate the H&N Auto-Segmentation Challenge 2015 (17). The common approach of the reviewed studies is three-fold, (1) select sets of comparison metrics, (2) generate auto-segmentations, and (3) compare auto-segmentations with clinical/database contours. This approach has been published in anatomic sub-sites including H&N (16, 18), thorax (19, 20), abdomen (21, 22), pelvis (23–25), and whole body (26). Unlike these studies, our institution has clinically introduced an AI- auto-segmentation software, Medical Mind, Inc. (27) for all RT patients. All patient images are auto segmented prior to dosimetrist and physician interaction in the treatment planning system. The Medical Mind software has been clinically deployed for all normal contours in external beam treatment planning including brain, H&N, thorax, abdomen, and pelvic RT. Using this approach, this work demonstrates prospective congruence between AI- and clinical segmentations.

As an experienced innovator in TMI/TMLI treatment, a TMI/TMLI AI-contouring model was developed based on clinical data from patients treated at our institution. By providing approximately 100 prior clinical cases of total body contouring from TMI/TMLI treatments including planning target volumes (PTVs), a TMI/TMLI AI-contouring model was optimized using the Medical Mind software. The TMI/TMLI model includes 27 individual OARs and 4 PTVs to assist with the laborious task of total body contouring and to create consistency in the clinical treatment planning workflow. The TMI/TMLI PTVs are based on normal anatomy (not tumors) and therefore can potentially be reliably, automatically identified. The OAR set includes important regions of brain, H&N, thorax, abdomen, pelvis, and extremities in a single set of contours. In the current workflow, clinicians including dosimetrists, physicians, and physicists are presented with the auto-segmentations prior to human delineation. In this method, the clinician must make a clinical judgement about whether an AI- contour edit is important and necessary to clinical treatment plans. This work describes the initial experience and success of the TMI/TMLI contouring model in a prospective approach.

2 Methods

The Medical Mind AI-software was trained on 100 prior clinical TMLI clinical patients including OARs and PTVs. The 100 TMI patients were treated consecutively at our institution. The datasets and contours include multiple dosimetrist, physicist, and physician contributions and standard planning guidelines were used to ensure consistency. The model was implemented using Python 3.6 (28) and PyTorch 1.0 (29). The dataset was split into a training set, a validation set, and the testing set. The training set contained 70 patients, the validation set contained 15 patients and the testing set also contained 15 patients. The Medical Mind software uses a Convolutional Neural Network (CNN) following the U-Net architecture. It contains an encoder and a decoder, and the convolutional layers are replaced by context aggregation blocks. Both the encoder and decoder consist of five context aggregation blocks. The feature maps in the encoder part are concatenated to the corresponding feature map in the decoder part. The Adam optimization algorithm (30) was used with a 0.001 learning rate. The model was trained over 50 epochs and the best model was selected, which is the one that had the lowest validation loss score. The convolutional layers were initialized using Xavier Uniform Initialization (31). All these convolution layers were followed by a batch normalization layer and a Rectified Linear Unit (ReLU) layer. The model was trained and tested using a GTX 1660-S GPU.

The model was deployed clinically, and this work details our initial (6-month) experience with the TMI/TMLI patients using the system. This work compares the final, clinically approved and the original AI- contours through volume, surface, and composite comparison metrics. The edited and original AI contour dosimetry evaluated on the planning dose are also compared and correlated to the various comparison metrics. Efficiency gains are estimated based on the relative number of manual edits performed on the AI-contours.

Computed Tomography (CT) simulation for TMI/TMLI treatment planning is acquired in a head-first supine (HFS) position spanning head-to-toes. The HFS images are sent from CT-simulation to the Medical Mind software, auto-segmentation is performed by selecting the TMI/TMLI model, delineating, and sending for import into treatment planning software. The process of opening the Medical Mind software *via* a secure interface to an on-network PC, identifying the patient, auto-segmentation of the patient, sending to clinical treatment planning software, and importing the AI-contours is typically<7 min. For each patient, at least one dosimetrist and at least one radiation oncologist review the AI-segmentations and edit PTVs and OARs prior to clinical treatment planning. The HFS CT is split at mid-thigh and flipped to FFS for treatment delivery from head to mid-thigh in HFS, and from the toes to mid-thigh in FFS, with composite dosimetry in the junction evaluated at the time of treatment planning. Contours and dosimetry were evaluated only on the HFS scan. In the FFS scan, only PTV-bone is included and delivery is often simple parallel-opposed beams.

The Medical Mind TMI-model generates 21 unique OARs (plus 6-additional Left/Right pairs) and 4 PTVs. The OARs are detailed in Table 1. The four PTVs are the PTV-Bone, the PTV-lymph nodes (PTV-LNs), PTV-ribs, and PTV-skull. The PTVs are 1-10 mm expansions of anatomic structures visible on CT and were trained on clinically utilized PTVs from the 100 prior TMI patients. The PTV-Bone is approximately an 8 mm expansion of all bone excluding skull and rib. The PTV-skull is an approximate 1-mm expansion of the skull. PTV-LNs includes approximately 5 mm margins about cervical, axillary, mediastinal, paraaortic, and pelvic lymph nodes. The PTV-ribs includes the chest wall, all ribs, and abuts the spinal canal. Figure 1 shows an example PTV set generated from the Medical Mind TMI/TMLI model.

Since introducing the auto-segmentation TMLI-model and compilation of data, 21 patients were treated with this workflow. All CT scans were performed with 7.5 mm slice spacing (range of 134-262 slices per patient), and in-plan voxel resolution ranged from 0.98-1.56 mm. Treatment Delivery was designed to deliver dose to bone, bone marrow, blood, and lymphoid tissue. Treatment planning has been previously examined in detail including early development on Tomotherapy (Accuray, Inc) for helical delivery (1) and on Eclipse for multi-iso volumetric modulated arc therapy (VMAT) (32). Eighteen of the patients were treated with helical Tomotherapy, three were treated with multi-isocenter VMAT on the Varian Truebeam (Varian Medical Systems, Palo Alto, CA) linear accelerator.

TABLE 1 Organ at Risk (OAR) contours included in the TMI/TMLI auto-segmentation model.

H&N		Thorax	Abdomen	Pelvis
Brain	Mandible	Esophagus	Spleen	Bowel Bag
Eyes (L+R)	Oral Cavity	Heart	Stomach	Bladder
Lens (L+R)	Larynx	Lungs (L+R)	Liver	Rectum
Optic Nerve (L+R)	Thyroid	Spinal Cord	Kidneys (L+R)	
Optic Chiasm	Parotids (L+R)			

2.1 Region of interest comparison metrics

Common metrics to compare AI- and edited segmentations include volume and surface overlap measures. Volume overlap methods include the Sørensen-Dice coefficient (Dice). Dice presents the relative overlap of two segmentations, where a value of 0 is no overlap and a value of 1 is 100% overlapped. However, Dice can be very misleading in terms of segmentation quality. For example, structures with large volumes can have a high-volume overlap (Dice > 90%) with possibly 100% of the surface deviating by a large distance. For 2-spheres of radius r1 and r2, dice is >0.90 for all r1/r2 within 3%, which is >3mm for all r1, r2>10cm. Dice is an important measure of contour quality and overlap, but perhaps not a sufficient measure of contour quality or efficiency.

Surface metrics to measure contour accuracy include the Hausdorff Distance (HD) (33). Measured at each point of the surface, the HD creates a distribution of Euclidean distances to nearest points. HD is typically expressed as a percentile; the 95th percentile (HD95) presents the maximum distance from surface-to-surface for 95% of the reference to test contour surface. An HD95 = 5 mm demonstrates 95% of the surface points are less than 5 mm. However, presenting HD at a percentile does not provide adequate information to assess clinical contour quality or efficiency gains. For example, an HD95 = 3.1mm could imply 100% of the contour deviates by >3mm or could imply 94.9% has HD<1mm and 5.1% deviates by >3mm. Like Dice, HD95 offers value but is not an adequate assessment of contour quality or efficiency gains.

Due to the limitations in classical volume overlap including Dice and HD percentiles (for example HD95) for estimating

FIGURE 1
TMI/TMLI target volumes include total bone with margin (PTV-Bone), lymph nodes extending from the head and neck to the pelvis with margin (PTV-Lymph Nodes), the chestwall containing ribs and the mediastinum (PTV-ribs), and the skull (PTV-skull).

contour quality and efficiency gains, we aim to measure the congruence of the AI- and human- contour by the relative surface which deviates by less than a fixed distance δ. This can be presented as the fraction or the percent of the surface which deviates by less than this distance. For segmentations defined by the set of 3D-points X and Y with elements xi and yi, the HD can be written

$$HD(X,Y) = \max\left\{\sup_{xi\in X} inf\ \ (xi,\ \ Y), \sup_{yi\in Y}\ \ inf(X,yi)\right\}$$

Where sup is the least upper bound or supremum, inf is the greatest upper bound or the infimum. We define the efficiency gain (*Eff*) at a spatial tolerance δ by the ratio of the cardinality (card) of the sets HD(X,Y)<δ and HD(X,Y):

$$Eff(\delta) = \frac{card(HD < \delta)}{card(HD)}$$

Where it is assumed, all elements are unique since each represents a unique spatial position on the surface. We propose the efficiency measure evaluated at distance δ =1mm, and efficiency is the relative contour surface with HD<1mm. The 1mm distance is approximately equal to the axial intra-voxel spacing of the image and therefore can be considered the relative amount of the AI-contour which was edited by the clinician, and an unedited contour is related to enhanced efficiency. The clinical efficiency gain was estimated by the percentage of the AI-contour-surface within 1mm of the clinical contour surface. Examples of efficiency gains include unedited AI-contours will have HD<1mm = 100% and an efficiency gain of 100%, an AI-contour with HD<1mm = 70% has an efficiency gain of 70%.

Computation of Dice and HD was performed in MATLAB using binary images defined on the CT-coordinates. Sub-voxel vertices were not considered. Dice is a built-in function of MATLAB (34) and was computed on AI and human edited AI contours for all OARs and PTVs. HD was computed as the Euclidean distance arrays between voxels of the binary images *via* the distance transform function in MATLAB (35). In this analysis, Dice, HD<1mm, and HD95 each provide unique information about overall contour quality (Dice volume overlap), the potential efficiency gains (HD<1mm), and the magnitude of the surface deviations (HD95). Section 3.1 details contour similarity metrics in the patient dataset.

2.2 Dose volume histogram comparison

All treatments were delivered twice-daily (BID) at PTV dose levels including 12 Gy in 8 fractions, 14 Gy in 8 fractions, 18 Gy in 9 fractions, and 20 Gy in 10 fractions. Doses varied based on protocol and patient, but dosimetry goals in the PTVs consistently included the volume which receives 100% of prescription dose was > 85% (V100%>85%). DVH planning objectives for OARs followed institutional protocols (36) including dose to 10% volume (D10), dose to 50% volume (D50), and dose to 80% volume (D80) with levels specified from population statistics of various initial testing and patient cases. Lung mean dose was limited to 8 Gy in all cases, kidney dose was not limited consistently. The clinical dose distribution of the upper body plans includes H&N, thorax, abdomen, and pelvic regions. This clinical dose distribution was used to computed cumulative DVH based on sampling both clinical and AI- contours. Plans were not re-optimized on each contour set. The DVHs were compared in order to estimate the potential dosimetric significance of contour error.

The cumulative DVH was computed for all AS- and clinical-contours utilizing the dicompyler python module (37). DVH calculations were performed at the axial voxel resolutions (0.98-1.56 mm) and three dose and ROI slices per 7.5 mm CT-slice resulted in a longitudinal resolution of 2.5 mm. DVH was computed for each ROI, and DVH-differences were estimated at all dose levels for all structures in 1 cGy dosimetric bins. Using a relative volume difference of 0.05 at any dose level to flag a potentially clinically significant DVH difference, then DVH was compared along neighboring dose levels using a dose tolerance threshold of 20 cGy. All DVH differences which exceed 0.05 relative volume difference at dose levels ≥20cGy were flagged as "failing" criteria.

To compare the distributions of Dice, HD95, and HD<1mm between "passing" and "failing" structure DVH sets, the two-sample Kolmogorov-Smirnov (KS) test was used as implemented in MATLAB. The 2-sample KS-test assumes continuous distributions, and significance testing was performed at a 5% significance level. In order to determine which contour metric (Dice, HD95, and HD<1mm) best predicts DVH variations, the KS test statistic was used to measure distance between the distributions. Section 3.2 summarizes the observed dosimetric differences and correlations them with Dice, HD95, and HD<1mm.

3 Results

3.1 Region of interest comparisons

A total of 467 contours were compared in the 21 patients. In estimates from clinical staff, contouring time for complete contouring of TMI/TMLI cases was reduced from 4-8 hours for full manual contouring to 1-3 hours by editing the AI-contours, or roughly a 75% efficiency gain. These efficiency gains were directly reflected in high rates of unedited contours estimated from HD<1mm. In all OARs, deviations >1mm were detected in 24.4% ± 27.1% of the structure surfaces; an average clinical efficiency gain of 75.6%. Deviations > 5mm were detected in 7.2% ± 18.0% of all OAR contours. The efficiency metric was not well correlated to DICE (r = 0.76) or negatively

correlated to HD95 (r=-0.52) indicating the efficiency gains from AI-contouring is not trivially related to these traditional overlap or surface metrics.

Figure 2 shows dice and HD<1mm for all OAR structures (right/left pairs are grouped). Of the 21 structures, 18/21 have Dice>0.8, with esophagus, optic nerves, and optic chiasm with significantly lower Dice coefficients. As shown in Figure 2, average Dice > 0.9 was observed in relatively large structures including stomach, oral cavity, rectum, and bowel but average HD<1mm was<0.7 in these cases.

In H&N OARs, efficiency gains ranged from a low of 42% in optic chiasm to 100% in eyes (unedited in all cases), with mean and standard deviation 77.3% ± 18.9%. HD95 was >1mm in only oral cavity (1.02mm). The optic nerves and chiasm were edited significantly for all patients, but this may be a function of large slice spacing used in TMI/TMLI CT-simulation, in general the clinical contours were larger than the AI-contours. The HD95 was not well correlated to HD<1mm (r=-0.34) in the H&N area.

In thorax OARs, average efficiency gains were >80% in spinal cord, heart, and both lungs, with average esophagus HD<1mm just 21%. HD95 was ≤1 mm in lungs and spinal cord, heart, and spinal cord. Differences in lung and heart were visually evident in structures with Dice< 0.9 and in at least one case, were due human error due to window/leveling variations in borders. Differences in spinal cord were evident but minimal. The esophagus consistently scored low dice, low efficiency, and relatively high HD95. The AI-segmented esophagus did not extend superiorly into the cricoid cartilage border, instead including just a portion of the esophagus in the T-spine region, leading to significant human edits.

In abdomen and pelvis OARs, efficiency gains ranged from 60-70% in spleen, stomach, rectum, and bowel and 75-84% in liver, kidney, and bladder. These results were associated with relatively high values of HD95 indicating clinically significant edits in spleen (2.1 ± 4.0 mm), rectum (2.7 ± 3.2 mm), and bowel (2.5 ± 2.8 mm). Bowel was dependent on edits to include the entire bowel bag, or individual bowel loops. Similar to esophagus, the kidneys consistently showed human edits to correct the superior border of the AI-contours. Average HD<1mm was 75.8%, and HD95 was 1.4 ± 1.6 mm. However, in the (approximately) 25% of the non-overlapping, superior region of kidney was HD95 was 8.7 mm. In this case, manually adding slices to the superior kidney contour can still represent a significant clinical efficiency gain even though metrics indicate edits could be significant.

Results in PTVs were generally worse than in OARs but still show significant efficiency gains in 4 PTVs. All PTV data is shown in Table 2. Average Dice across all patients and PTVs was 86% ± 15%, HD<1mm was 61% ± 23%, and HD95 was 11.0 ± 22.2 mm.

There was a weak correlation between Dice and HD<1mm (r=0.79). Dice values >0.8 did not imply high values of HD<1mm, demonstrating that structures can have significant overlap with potentially meaningful surface disagreement. Figure 3 shows HD<1mm as a function of Dice. In general, only a very high Dice value (>0.98) ensures and HD<1mm is >0.7. Correlations between HD<1mm and HD95 were not strong (r=-0.65). This weak correlation is expected, HD95 describes the largest discrepancy, HD<1mm is a very stringent metric demonstrating overlapping surfaces. An example patient image including manual and AI contours is shown in Figure 4.

3.2 Dose volume histogram comparisons

DVH differences exceeded 5% relative volume difference in 109/467 of all curves at any dose level. The most common 5%-DVH variations were in esophagus (86%), rectum (48%), and PTVS (22%).

Dice, HD95, and HD<1mm were statistically different between the pass and fail groups ($p<10^{-7}$ in all comparisons). The KS-statistic measures distance between the distributions and indicates the Dice KS-statistic (0.65) was more predictive than

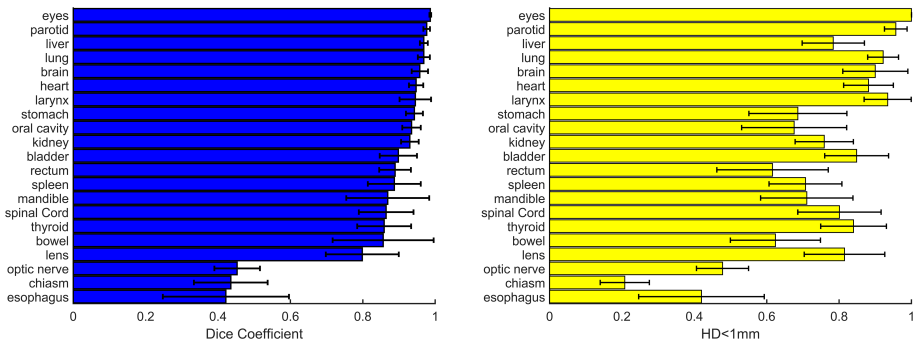

FIGURE 2
Dice (left) and relative contour surface with HD<1mm (right) for all structures. Standard deviations for the patient population for each structure are shown. In 18/21 contours average Dice is >0.8. Efficiency gains estimated from HD<1mm are >0.60 in 18/21 structures.

TABLE 2 PTV statistics are summarized including Dice, relative surface with Hausdorff Distance<1mm (HD<1mm), and the 95th percentile of HD.

PTV	PTV-Bone	PTV-Lymph nodes	PTV-Ribs	PTV-Skull
Dice	85.1% ± 21.9%	83.0% ± 16.6%	94.6% ± 4.4%	81.4% ± 9.9%
HD<1mm	40.6% ± 22.1%	53.4% ± 12.8%	80.1% ± 11.7%	72.4% ± 20.0%
HD95	30.5 mm ± 38.0mm	7.5mm ± 3.6mm	3.0mm ± 2.6mm	2.8mm ± 2.2mm

HD95 (0.37) or HD<1mm (0.48) in predicating DVH differences. The average Dice in passing vs. failing DVH was 0.91 ± 0.16 vs. 0.71 ± 0.24. Average HD95 was 2.2 ± 4.6 mm vs. 11.9 ± 22.6 mm and HD<1mm was 80% ± 22% vs. 51% ± 27%. All values show a clear distinction between passing and failing DVH-criteria groups, and the distributions are shown in Figure 5. This result is intuitive since Dice and DVH are volume-based metrics whereas HD is a surface metric.

The obvious result that DVH metrics will fail with low DICE is not thought-provoking. In 15 cases where low Dice score passed the DVH criteria of 0.05 relative volume/20cGy tolerance level, 6 were in optic chiasm and 5 were in optic nerves. This demonstrates limitations cumulative DVH, as significant dose-volume differences can be hidden by normalizing to relative volume even in high-gradient areas. Another source of false-positive DVH match is uniform dose; any 2 structures will have equal cumulative DVH in a uniform dose area. In lens, 6/21 cases failed DVH criteria, with 2/21 cases showing major differences in maximum dose between clinical contours (Dmax<3.5 Gy) and AI-contours (>5 Gy). In optic structures including chiasm and nerves, 6/63 cases failed the DVH criteria with Dmax differences >2 Gy in 3 cases.

There is possibly a lower limit on usable structures in dose and DVH calculation from AI-contours (where Dice<0.6), but there also exists a grey area in Dice correlation where the pass/fail distributions significantly overlap in the range 0.7-0.98. Structures which failed DVH-criteria with Dice in the range of 0.7-0.98 include 13 PTVs and 56 OARs. PTVs which failed DVH-criteria with Dice>0.7 show the AI-DVH is lower than the human contour DVH, indicating AI-contours outside of the clinically used volumes. Over-contouring of PTVs, if used in planning, would result in high dose to normal, untargeted tissues. Despite relatively high DICE scores (>0.93) in six cases, DVH differences exceeded 0.30 relative volume at all doses in many cases. These results demonstrate the critical importance of PTV contouring in highly conformal radiation such as TMI/TMLI.

There were 56 OARs which failed DVH-criteria with Dice>0.7 including 6 brain contours, 5 thyroid contours, 6 kidney contours, and 9 rectum contours. Consistent DVH differences were observed for the same OARs across many patients. In the case of Rectum, 8/9 AI-DVHs were > human-DVHs due to humans adding regions of sigmoid bowel to the rectum contour. In the case of Kidney, missing regions of superior kidney resulted in AI-DVHs< human DVHs in all cases. Figure 6 shows DVH computed on AI and human contours for (top) 3 rectum cases. Dice ranges from 0.71 (left) to 0.91 (right), but the DVH differences are not significantly reduced as Dice increases. Similar results were observed in Kidney (middle) and Thyroid (bottom) with Dice ranging from 0.77 to 0.93. There was not a significant reduction in DVH differences as Dice is increased from 0.7-0.9 in these structures.

4 Discussion

The TMI model was trained on >100 patients and validated in the current study on 21 patients. This modest sample size showed excellent results in most structures in all patients, but it is possible additional patients may reveal additional problems with the AI-segmentations. AI-models from trained from limited data are known to be susceptible to overfitting, including in auto-

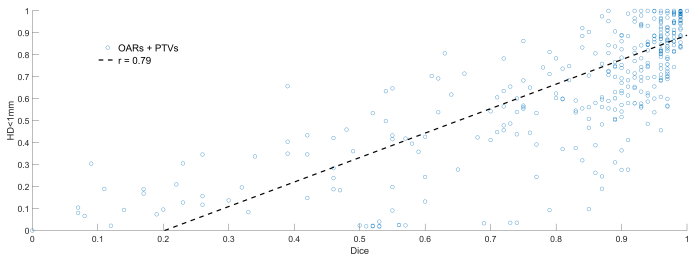

FIGURE 3
Dice (x-axis) vs. relative surface area with Hausdorff Distance<1mm (HD<1mm). Low Dice values (<0.5) equated to low HD<1mm in almost all cases, but the converse was not true. High Dice (>0.8) could still result in significant human editing, with HD<1mm ranging from 0.1-0.9 in this region.

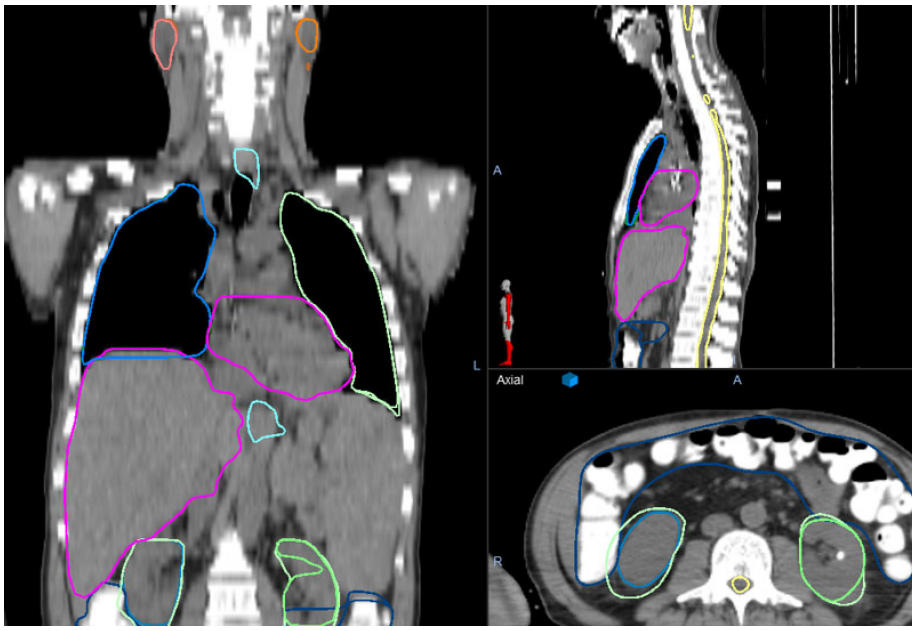

FIGURE 4
An example patient image is shown including manual and AI contours in parotids, larynx, lung, heart, liver, and kidneys. The human and TMI contours are indistinguishable in most organs, however the kidneys demonstrate some variation In the axial image (borrom right) the human drawn kidneys are significantly larger than the AI-kidneys due to clinician preference.

segmentation (38). In this sample, we have shown the Medical Mind TMI/TMLI model is consistent and reliable for contouring a vast majority of structures. We show significant DVH differences in high gradient areas (PTVs and optic structures) which reinforces our current workflow of AI-contouring followed by manual review. However, for many OARs, even low Dice overlap may not result in significant errors in DVH estimates and may be reliable to use clinically without edits.

The clinical validity of AI-defined OARs evaluated by Dice and HD95 has been assumed in prostate (39) including in physician-edited contours in a prospective study (40). The current study has demonstrated limited value in Dice and HD95, and therefore introduces a more stringent comparison metric, HD<1mm. HD<1mm is the relative proportion of contour surface within 1mm of the clinical contour. In prospective studies where AI-contours are used as a starting point for clinical contours, we strongly recommend using this or a similar, more challenging metric in describing the accuracy of the segmentation.

In DVH calculation, we found Dice is the strongest predictor of DVH congruence. However, a high Dice value did not ensure DVH differences<0.05, and DVH for structures with Dice >0.9 was not significantly different than structures with dice in the range of 0.7-0.8.

The TMI/TMLI dataset is unique for its use of relatively large slice spacing (7.5 mm). However, from a clinical perspective this is equivalent to defining contours on every other 2.5mm slice and utilizing interpolation. DVH calculation was performed on a 2.5mm grid, so that large axial contour

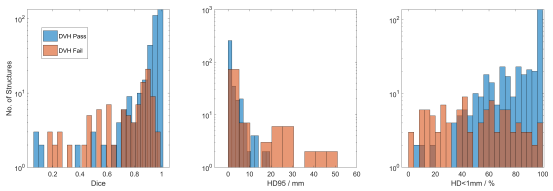

FIGURE 5
Dice, HD95, and HD<1mm cases which pass (blue) and fail (red) the applied DVH criteria. Low Dice and low HD<1mm still showed similar DVH in structures which received low, or no dose. HD95>20mm showed no passing DVH.

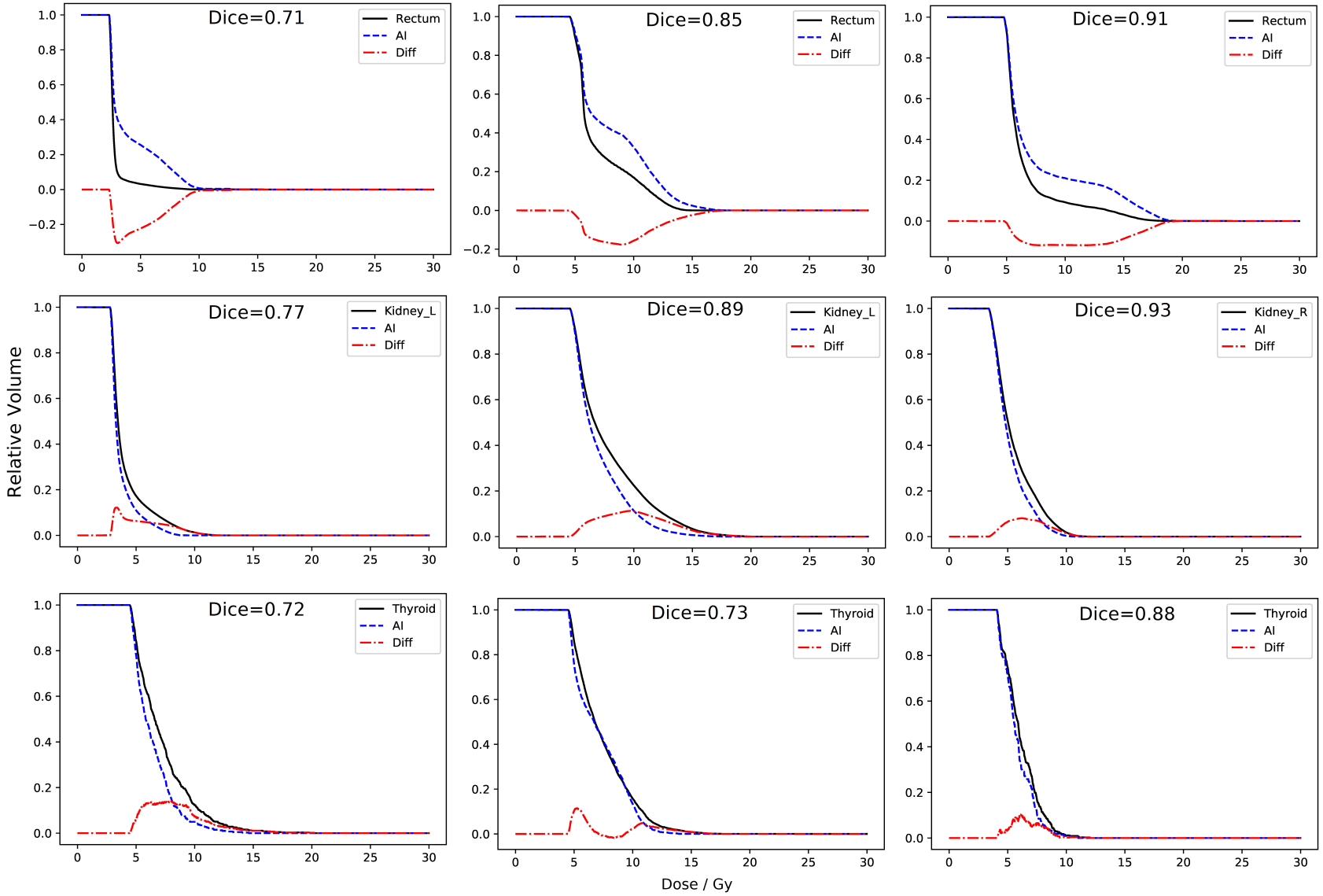

FIGURE 6
DVHs computed from Human (solid) and AI- (dashed) contours, with difference. (top) AI-rectum contours were > human DVH in 8/9 cases. (middle) Kidney AI-contours of kidney resulted in DVHs consistently lower than the human contours. Thyroid showed minor differences independent of relatively low Dice values.

10.3389/fonc.2022.970425

variations would not heavily influence dose evaluation. Medical physics datasets including H&N MRI (18) and thoracic cancers (19, 20), rectal cancers (41), and cervical cancers (25, 42) have been made available to validate and inter-compare auto-segmentation algorithms. The TMI/TMLI experience at our institution can contribute to this meaningful inter-institution comparison of AI algorithms for total body contouring. This is the first study demonstrating AI-segmentation in the whole body simultaneously. Chen et al. (26) introduced an AI-algorithm called "WBNet" and achieved average Dice in the range of 0.81-0.84 in a large number of datasets including H&N, thorax, abdomen, and pelvis sites individually. In our comparisons, only esophagus, lens, optic nerves, and optic chiasm showed average Dice<0.85. These impressive results were realized in terms of clinical efficiency gains as well, with team members routinely reporting 50-90% efficiency gains in contouring these complex cases.

In small structures such as lens and optic nerves and chiasm, a low Dice score does not imply a poor contour. Due to their limited size, a very small deviation can lead to a very low Dice score. A known limitation of multi-layer deep learning in image recognition and segmentation is limited number of features (43–45) which may explain why optic nerves, and chiasm are among the worst scoring structures in Dice in the current study. However, average Dice 0.42-0.45 in the optic structures are not significantly lower than those reported in other studies, 0.37-0.65 (46) and 0.45-0.69 (47). In these small structures, a single 7.5-mm slice difference in the TMI/TMLI contour set can lead to large deviations. From a clinical efficiency perspective, these relatively small structures (<1cc volume) are defined on as few as 1 TMLI slice and do not add significant workload to manual contouring when compared to larger structures like brain, lung, and liver which require contouring on dozens of CT-slices. In esophagus, boundary errors led to low DSC and high HD95. Esophagus needs closer scrutiny; it's known to potentially include large inter-slice positional variations and low CT-contrast. In optic structures, esophagus, and similar structures which can vary significantly over small regions of cranio-caudal anatomy, training AI on large slice spacing images may lead to significant errors if applied to finer resolution images.

It may be possible to link AI algorithms with contour quality assurance using, for example a multi-parametric approach (15, 48) or machine learning approach (48) including sensitivity in Tumor Control Probability (TCP) and Normal Tissue Complication Probability (NTCP) (49). A recent review article agrees multiple endpoints are needed in assessing contour quality, and clinical validation of meaningful TCP/NTCP endpoints will guide meaningful contour deviations (50). In dose escalated TMI/TMLI maximum dose may not be a critical evaluation datapoint. Instead, volume-based metrics such as V10, V50, and V80 may be more useful to identify quality treatment plans. Our results demonstrate that DVH-based metrics are not closely related to Dice, HD-95, or HD<1mm in OARs, but in general HD<1mm > 60% and Dice>90% led to consistent DVHs. In PTVs, the scenario is much different, and we consistently observed PTV-DVH differences >0.30 across all dose levels even with very high Dice scores. Sufficient target delineation is an essential requirement of conformal radiation to ensure disease control and reduce the possibility of underdosing the target (51). Over-contouring PTV results in a larger treatment volume in normal tissue, which is very familiar to conventional TBI regimens but may not be appropriate for TMI and TMLI.

5 Conclusions

Utilization of auto-segmentation for TMI and TMLI treatment planning presents a breakthrough for clinical efficiency in implementation of TMI/TMLI treatments. Efficiency gains of 80-90% are possible in >20 structures including PTVs and OARs.

Data availability statement

The data supporting the conclusions of this article will be made available by the corresponding author upon request with permission from City of Hope National Medical Center and Medical Mind, Inc. where applicable.

Author contributions

WW collected data, wrote scientific code, performed analysis, and designed the study. AL developed the TMI model and co-developed the scientific design of the study. KQ, CH, and SH provided expertise in the area of TMI/TMLI and contributed to the article text. All authors contributed to the article and approved the submitted version.

Conflict of interest

AL, KQ, CH, and TW have a research collaboration with Medical Mind, Inc.

The remaining author declares that the research was conducted in the absence of any commercial or financial relationships that could be construed as a potential conflict of interest.

Publisher's note

References

1. Hui SK, Kapatoes J, Fowler J, Henderson D, Olivera G, Manon RR, et al. Feasibility study of helical tomotherapy for total body or total marrow irradiation. *Med Phys* (2005) 32:3214–24. doi: 10.1118/1.2044428

2. Wong JYC, Liu A, Schultheiss T, Popplewell L, Stein A, Rosenthal J, et al. Targeted total marrow irradiation using three-dimensional image-guided tomographic intensity-modulated radiation therapy: an alternative to standard total body irradiation. *Biol Blood Marrow Transplant* (2006) 12:306–15. doi: 10.1016/j.bbmt.2005.10.026

3. Wong JYC, Filippi AR, Scorsetti M, Hui S, Muren LP, Mancosu P. Total marrow and total lymphoid irradiation in bone marrow transplantation for acute leukaemia. *Lancet Oncol* (2020) 21:e477–87. doi: 10.1016/S1470-2045(20)30342-9

4. Stein A. Dose escalation of total marrow and lymphoid irradiation in advanced acute leukemia. In: JYC Wong and SK Hui, editors. *Total marrow irradiation: A comprehensive review*. Springer International Publishing; New York (2020). p. 69–75. doi: 10.1007/978-3-030-38692-4_4

5. Clift RA, Buckner CD, Appelbaum FR, Bearman SI, Petersen FB, Fisher LD, et al. Allogeneic marrow transplantation in patients with acute myeloid leukemia in first remission: a randomized trial of two irradiation regimens. *Blood* (1990) 76:1867–71. doi: 10.1182/blood.V76.9.1867.1867

6. Langerak TR, Berendsen FF, van der Heide UA, Kotte ANTJ, Pluim JPW. Multiatlas-based segmentation with preregistration atlas selection. *Med Phys* (2013) 40:091701. doi: 10.1118/1.4816654

7. Fritscher KD, Peroni M, Zaffino P, Spadea MF, Schubert R, Sharp G, et al. Automatic segmentation of head and neck CT images for radiotherapy treatment planning using multiple atlases, statistical appearance models, and geodesic active contours. *Med Phys* (2014) 41:051910. doi: 10.1118/1.4871623

8. Sharp G, Fritscher KD, Pekar V, Peroni M, Shusharina N, Veeraraghavan H, et al. Vision 20/20: perspectives on automated image segmentation for radiotherapy. *Med Phys* (2014) 41:050902. doi: 10.1118/1.4871620

9. Brock KK, Mutic S, McNutt TR, Li H, Kessler ML. Use of image registration and fusion algorithms and techniques in radiotherapy: Report of the AAPM radiation therapy committee task group no. *132 Med Phys* (2017) 44:e43–76. doi: 10.1002/mp.12256

10. Rigaud B, Simon A, Castelli J, Lafond C, Acosta O, Haigron P, et al. Deformable image registration for radiation therapy: principle, methods, applications and evaluation. *Acta Oncol* (2019) 58:1225–37. doi: 10.1080/0284186X.2019.1620331

11. Qazi AA, Pekar V, Kim J, Xie J, Breen SL, Jaffray DA. Auto-segmentation of normal and target structures in head and neck CT images: A feature-driven model-based approach. *Med Phys* (2011) 38:6160–70. doi: 10.1118/1.3654160

12. Wong J, Huang V, Wells D, Giambattista J, Giambattista J, Kolbeck C, et al. Implementation of deep learning-based auto-segmentation for radiotherapy planning structures: a workflow study at two cancer centers. *Radiat Oncol* (2021) 16:101. doi: 10.1186/s13014-021-01831-4

13. Harrison K, Pullen H, Welsh C, Oktay O, Alvarez-Valle J, Jena R, et al. Machine learning for auto-segmentation in radiotherapy planning. *Clin Oncol (R Coll Radiol)* (2022) 34:74–88. doi: 10.1016/j.clon.2021.12.003

14. Thor M, Apte A, Haq R, Iyer A, LoCastro E, Deasy JO, et al. Using auto-segmentation to reduce contouring and dose inconsistency in clinical trials: the simulated impact on rtog 0617. *Int J Radiat Oncol Biol Phys* (2021) 109:1619–26. doi: 10.1016/j.ijrobp.2020.11.011

15. Hui CB, Nourzadeh H, Watkins WT, Trifiletti DM, Alonso CE, Dutta SW, et al. Quality assurance tool for organ at risk delineation in radiation therapy using a parametric statistical approach. *Med Phys* (2018) 45:2089–96. doi: 10.1002/mp.12835

16. Liu Y, Lei Y, Fu Y, Wang T, Zhou J, Jiang X, et al. Head and neck multi-organ auto-segmentation on CT images aided by synthetic MRI. *Med Phys* (2020) 47:4294–302. doi: 10.1002/mp.14378

17. Raudaschl PF, Zaffino P, Sharp GC, Spadea MF, Chen A, Dawant BM, et al. Evaluation of segmentation methods on head and neck CT: Auto-segmentation challenge 2015. *Med Phys* (2017) 44:2020–36. doi: 10.1002/mp.12197

18. Cardenas CE, Mohamed ASR, Yang J, Gooding M, Veeraraghavan H, Kalpathy-Cramer J, et al. Head and neck cancer patient images for determining auto-segmentation accuracy in T2-weighted magnetic resonance imaging through expert manual segmentations. *Med Phys* (2020) 47:2317–22. doi: 10.1002/mp.13942

19. Feng X, Qing K, Tustison NJ, Meyer CH, Chen Q. Deep convolutional neural network for segmentation of thoracic organs-at-risk using cropped 3D images. *Med Phys* (2019) 46:2169–80. doi: 10.1002/mp.13466

20. Yang J, Veeraraghavan H, van Elmpt W, Dekker A, Gooding M, Sharp G, et al. CT images with expert manual contours of thoracic cancer for benchmarking auto-segmentation accuracy. *Med Phys* (2020) 47(12):3250–3255. doi: 10.1002/mp.14107

21. Kim H, Jung J, Kim J, Cho B, Kwak J, Jang JY, et al. Abdominal multi-organ auto-segmentation using 3D-patch-based deep convolutional neural network. *Sci Rep* (2020) 10:6204. doi: 10.1038/s41598-020-63285-0

22. Tong N, Gou S, Niu T, Yang S, Sheng K. Self-paced DenseNet with boundary constraint for automated multi-organ segmentation on abdominal CT images. *Phys Med Biol* (2020) 65:135011. doi: 10.1088/1361-6560/ab9b57

23. Dong X, Lei Y, Tian S, Wang T, Patel P, Curran WJ, et al. Synthetic MRI-aided multi-organ segmentation on male pelvic CT using cycle consistent deep attention network. *Radiother Oncol* (2019) 141:192–9. doi: 10.1016/j.radonc.2019.09.028

24. Kalantar R, Lin G, Winfield JM, Messiou C, Lalondrelle S, Blackledge MD, et al. Automatic segmentation of pelvic cancers using deep learning: State-of-the-Art approaches and challenges. *Diagnostics (Basel)* (2021) 11:1964. doi: 10.3390/diagnostics11111964

25. Ma C-Y, Zhou JY, Xu XT, Guo J, Han MF, Gao YZ, et al. Deep learning-based auto-segmentation of clinical target volumes for radiotherapy treatment of cervical cancer. *J Appl Clin Med Phys* (2022) 23:e13470. doi: 10.1002/acm2.13470

26. Chen X, Sun S, Bai N, Han K, Liu Q, Yao S, et al. A deep learning-based auto-segmentation system for organs-at-risk on whole-body computed tomography images for radiation therapy. *Radiother Oncol* (2021) 160:175–84. doi: 10.1016/j.radonc.2021.04.019

27. Medical Mind. *Medical mind* . Available at: https://medmind.ai/.

28. *Python Release Python 3.6.8. python.org* . Available at: https://www.python.org/downloads/release/python-368/.

29. *PyTorch* . Available at: https://www.pytorch.org.

30. Kingma DP, Ba J. Adam: A method for stochastic optimization. (2017). Available from: http://arxiv.org/abs/1412.6980 DOI: 10.48550/arXiv.1412.6980.

31. Glorot X, Bengio Y. Understanding the difficulty of training deep feedforward neural networks. *AISTATS* (2010) 8:249–256. doi: 10.4236/jsip.2015.62006.

32. Han C, Schultheisss TE, Wong JYC. Dosimetric study of volumetric modulated arc therapy fields for total marrow irradiation. *Radiother Oncol* (2012) 102:315–20. doi: 10.1016/j.radonc.2011.06.005

33. Cooper JS, Pajak TF, Rubin P, Tupchong L, Brady LW, Leibel SA, et al. Second malignancies in patients who have head and neck cancer: incidence, effect on survival and implications based on the RTOG experience. *Int J Radiat Oncol Biol Phys* (1989) 17:449–56. doi: 10.1016/0360-3016(89)90094-1

34. *Sørensen-dice similarity coefficient for image segmentation - MATLAB dice* . Available at: https://www.mathworks.com/help/images/ref/dice.html.

35. *Distance transform of binary image - MATLAB bwdist* . Available at: https://www.mathworks.com/help/images/ref/bwdist.html?s_tid=doc_ta.

36. Wong JYC, Forman S, Somlo G, Rosenthal J, Liu A, Schultheiss T, et al. Dose escalation of total marrow irradiation with concurrent chemotherapy in patients with advanced acute leukemia undergoing allogeneic hematopoietic cell transplantation. *Int J Radiat Oncol Biol Phys* (2013) 85:148–56. doi: 10.1016/j.ijrobp.2012.03.033

37. *Dicompyler-core • PyPI* . Available at: https://pypi.org/project/dicompyler-core/.

38. Zhao Y, Rhee DJ, Cardenas C, Court LE, Yang J. Training deep-learning segmentation models from severely limited data. *Med Phys* (2021) 48:1697–706. doi: 10.1002/mp.14728

39. Duan J, Bernard M, Downes L, Willows B, Feng X, Mourad WF, et al. Evaluating the clinical acceptability of deep learning contours of prostate and organs-at-risk in an automated prostate treatment planning process. *Med Phys* (2022) 49:2570–81. doi: 10.1002/mp.15525

40. Casati M, Piffer S, Calusi S, Marrazzo L, Simontacchi G, Di Cataldo V, et al. Clinical validation of an automatic atlas-based segmentation tool for male pelvis CT images. *J Appl Clin Med Phys* (2022) 23:e13507. doi: 10.1002/acm2.13507

41. Men K, Dai J, Li Y. Automatic segmentation of the clinical target volume and organs at risk in the planning CT for rectal cancer using deep dilated convolutional neural networks. *Med Phys* (2017) 44:6377–89. doi: 10.1002/mp.12602

42. Wang Z, Chang Y, Peng Z, Lv Y, Shi W, Wang F, et al. Evaluation of deep learning-based auto-segmentation algorithms for delineating clinical target volume and organs at risk involving data for 125 cervical cancer patients. *J Appl Clin Med Phys* (2020) 21:272–9. doi: 10.1002/acm2.13097

43. Hesamian MH, Jia W, He X, Kennedy P. Deep learning techniques for medical image segmentation: achievements and challenges. *J Digit Imaging* (2019) 32:582–96. doi: 10.1007/s10278-019-00227-x

44. Zhou X, Takayama R, Wang S, Hara T, Fujita H. Deep learning of the sectional appearances of 3D CT images for anatomical structure segmentation based on an FCN voting method. *Med Phys* (2017) 44:5221–33. doi: 10.1002/mp.12480

45. Wang R, Lei T, Cui R, Zhang B, Meng H, Nandi AK, et al. Medical image segmentation using deep learning: a survey. *IET Image Process* (2022) 16:1243–67. doi: 10.1049/ipr2.12419

46. Ibragimov B, Xing L. Segmentation of organs-at-risks in head and neck CT images using convolutional neural networks. *Med Phys* (2017) 44:547–57. doi: 10.1002/mp.12045

47. Zhu W, Huang Y, Zeng L, Chen X, Liu Y, Qian Z, et al. AnatomyNet: Deep learning for fast and fully automated whole-volume segmentation of head and neck anatomy. *Med Phys* (2019) 46:576–89. doi: 10.1002/mp.13300

48. Nourzadeh H, Hui C, Ahmad M, Sadeghzadehyazdi N, Watkins WT, Dutta SW, et al. Knowledge-based quality control of organ delineations in radiation therapy. *Med Phys* (2022) 49:1368–81. doi: 10.1002/mp.15458

49. Nourzadeh H, Watkins WT, Ahmed M, Hui C, Schlesinger D, Siebers JV, et al. Clinical adequacy assessment of autocontours for prostate IMRT with meaningful endpoints. *Med Phys* (2017) 44:1525–37. doi: 10.1002/mp.12158

50. Sherer MV, Lin D, Elguindi S, Duke S, Tan LT, Cacicedo J, et al. Metrics to evaluate the performance of auto-segmentation for radiation treatment planning: A critical review. *Radiother Oncol* (2021) 160:185–91. doi: 10.1016/j.radonc.2021.05.003

51. Tomé WA, Fowler JF. On cold spots in tumor subvolumes. *Med Phys* (2002) 29:1590–8. doi: 10.1118/1.1485060

frontiers | Frontiers in Oncology

TYPE Original Research
PUBLISHED 06 September 2022
DOI 10.3389/fonc.2022.969429

OPEN ACCESS

EDITED BY
Hakan Özdoğu,
Başkent University, Turkey

REVIEWED BY
Can Boga,
Başkent University, Turkey
Ozan Cem Guler,
Başkent University, Turkey
Ali Bülent Antmen,
Acıbadem Adana Hospital, Turkey

*CORRESPONDENCE
Susanta K. Hui
shui@coh.org

†These authors have contributed equally to this work

SPECIALTY SECTION
This article was submitted to Radiation Oncology, a section of the journal Frontiers in Oncology

RECEIVED 15 June 2022
ACCEPTED 05 August 2022
PUBLISHED 06 September 2022

CITATION
Sargur Madabushi S, Fouda R, Ghimire H, Abdelhamid AMH, Lim JE, Vishwasrao P, Kiven S, Brooks J, Zuro D, Rosenthal J, Guha C, Gupta K and Hui SK (2022) Development and characterization of a preclinical total marrow irradiation conditioning-based bone marrow transplant model for sickle cell disease.
Front. Oncol. 12:969429.
doi: 10.3389/fonc.2022.969429

Development and characterization of a preclinical total marrow irradiation conditioning-based bone marrow transplant model for sickle cell disease

Srideshikan Sargur Madabushi[1†], Raghda Fouda[2†], Hemendra Ghimire[1], Amr M. H. Abdelhamid[1,3,4], Ji Eun Lim[1], Paresh Vishwasrao[1], Stacy Kiven[2], Jamison Brooks[1,5], Darren Zuro[1,6], Joseph Rosenthal[7], Chandan Guha[8], Kalpna Gupta[2,9,10] and Susanta K. Hui[1*]

[1]Department of Radiation Oncology, City of Hope National Medical Center, Duarte, CA, United States, [2]Department of Medicine, Division of Hematology/Oncology, University of California, Irvine, CA, United States, [3]Radiation Oncology Section, Department of Medicine and Surgery, Perugia University and General Hospital, Perugia, Italy, [4]Department of Clinical Oncology and Nuclear Medicine, Faculty of Medicine, Ain Shams University, Cairo, Egypt, [5]Department of Radiation Oncology, Mayo Clinic, Rochester, MN, United States, [6]Department of Radiation Oncology, University of Oklahoma Health Sciences Center (HSC), Oklahoma City, OK, United States, [7]Department of Pediatrics, City of Hope National Medical Center, Duarte, CA, United States, [8]Department of Radiation Oncology, Albert Einstein College of Medicine, Montefiore Medical Center, Bronx, NY, United States, [9]Department of Medicine, Division of Hematology, Oncology and Transplantation, University of Minnesota, Minneapolis, MN, United States, [10]Southern California Institute for Research and Education, Veterans Affairs (VA) Medical Center, Long Beach, CA, United States

Sickle cell disease (SCD) is a serious global health problem, and currently, the only curative option is hematopoietic stem cell transplant (HCT). However, myeloablative total body irradiation (TBI)-based HCT is associated with high mortality/morbidity in SCD patients. Therefore, reduced-intensity (2–4 Gy) total body radiation (TBI) is currently used as a conditioning regimen resulting in mixed chimerism with the rescue of the SCD disease characteristic features. However, donor chimerism gradually reduces in a few years, resulting in a relapse of the SCD features, and organ toxicities remained the primary concern for long-term survivors. Targeted marrow irradiation (TMI) is a novel technique developed to deliver radiation to the desired target while sparing vital organs and is successfully used for HCT in refractory/relapsed patients with leukemia. However, it is unknown if TMI will be an effective treatment for a hematological disorder like SCD without adverse effects seen on TBI. Therefore, we examined preclinical feasibility to determine the tolerated dose escalation, its impact on donor engraftment, and reduction in organ damage using our recently developed TMI in the humanized homozygous Berkley SCD mouse model (SS). We show that dose-escalated TMI (8:2) (8 Gy to the bone marrow and 2 Gy

to the rest of the body) is tolerated with reduced organ pathology compared with TBI (4:4)-treated mice. Furthermore, with increased SCD control (AA) mice (25 million) donor BM cells, TMI (8:2)-treated mice show successful long-term engraftment while engraftment failed in TBI (2:2)-treated mice. We further evaluated the benefit of dose-escalated TMI and donor cell engraftment in alleviating SCD features. The donor engraftment in SCD mice completely rescues SCD disease features including recovery in RBCs, hematocrit, platelets, and reduced reticulocytes. Moreover, two-photon microscopy imaging of skull BM of transplanted SCD mice shows reduced vessel density and leakiness compared to untreated control SCD mice, indicating vascular recovery post-BMT.

KEYWORDS

total marrow irradiation, bone marrow transplantation, sickle cell disease, engraftment, chimerism, mast cells, two-photon microscopy, histopathology

Introduction

Sickle cell disease (SCD) is a global inherited red blood cell disorder that affects over 100 million people in the US and several million worldwide (1). The only curative treatment option currently available for this disorder is allogenic hematopoietic stem cell transplant (HCT) after myeloablative conditioning. Almost all of the currently available treatments are palliative, leaving SCD patients with poor quality of life due to extreme pain episodes, end-organ damage, and reduced life expectancy (2–4). Although the myeloablative-HCT regimen results in complete donor cell engraftment alleviating the disease features, long-term damage to organs is a major concern in patients with chronic state of SCD from palliative treatment. Therefore, an alternative standard of care is reduced-intensity conditioning and HCT, which results in reduced organ damage yielding transient intermittent/mixed chimerism, alleviating the disease features during that stage; however, it eventually results in graft failure and relapse (5, 6). Although partial chimerism leads to clinical improvement of SCD, pathological and hematological abnormalities, such as hemolysis, anemia, and vaso-occlusive crisis, are not recovered completely at low RBC chimerism (7). TBI-based dose escalation from 2 Gy to 4 Gy increased chimerism and reduced graft rejection in SCD patients (8). However, TBI-based increased dose also increases organ damage and the technique cannot be used to further improve chimerism and long-term engraftment.

Similarly, the myeloablative TBI regimen is commonly used for HCT in hematological malignancy for over five decades (9–13). However, there has been little or no long-term improvement in outcomes for patients with treatment-refractory acute leukemia. Previous efforts to further increase radiation using TBI could reduce the leukemia burden (14). However, toxicities related to TBI encountered during dose escalation offset any gains in overall survival (11). Therefore, there is an unmet need to develop targeted delivery of radiation and reduce radiation exposure to the organs to preserve organ function and improve the quality of life. To overcome this technological gap, Hui et al. first developed total marrow irradiation (TMI) using helical tomotherapy (15). We have successfully adopted the TMI technique escalating radiation dose to 20 Gy to the bone marrow (BM)-containing skeletal system while reducing the dose to other vital organs like liver, lung, and GI to enhance the anti-leukemic effect in young adults (≤55 years of age) and refractory/relapsed patients with leukemia; a Phase II (NCT02094794) trial shows a 2-year overall survival (OS) rate of 41% (16), in contrast to the <10% survival rate reported for similar patients (17).

Although the clinical development of TMI technology has led to many clinical trials worldwide, a lack of advanced preclinical technology has limited the scope of further scientific advancement. The conventional mouse TBI treatment lacks imaging to identify organs and a three-dimensional (3D) dosimetric model to calculate detailed organ dosimetry, and it ignores the dosimetric effect of tissue heterogeneity. We recently developed a novel multimodal image-guided preclinical TMI model for bone marrow transplant (BMT) using immunocompetent (C57BL/6) mice, which maintained long-term engraftment with reconstitution potential and reduced organ damage. However, the SS mouse model is highly radiosensitive, and previous studies have shown the myeloablative dose around 6 Gy, compared to 10–11 Gy, which is the standard in B6 mice. Furthermore, the pathology of SS mice organs is similar to human SCD with evidence of intravascular hemolysis, cardiomegaly, nephropathy, liver infarcts, vascular congestion, apoptotic Purkinje cells,

pulmonary hemorrhages, and siderosis (excess iron deposit in heart, lungs, kidney, etc.) (18), which perhaps makes them more sensitive to radiation doses. Therefore, standard TMI doses used on B6 mice may still be toxic to SS mice. Hence, a feasibility study to test the tolerance of dose-escalated TMI in SS mice is essential.

We therefore successfully implemented our recently developed novel preclinical high-precision TMI to deliver a higher radiation dose to the BM while sparing vital organs (15, 19) in the Berkeley SS-BMT mouse model. Additionally, we have also recently successfully used TMI as an HCT conditioning regimen in three patients with SCD. However, post-HCT, it is unclear how TMI affects BM engraftment, hematological recovery, and organ toxicity. A recent study using our developed 3D image-guided TMI mouse BMT model suggests that for a successful engraftment with reduced organ damage, we need an optimal balance of radiation exposure to the BM and other vital organs (20). Therefore, in the current proof-of-concept study, we first evaluated the feasibility of dose escalation using TMI in SCD mice. After determining the tolerated TMI dose, next, we evaluated the effect of dose escalation on donor cell chimerism and recovery of SCD features in donor-engrafted SS mice. Dose escalation using TMI was tolerated by SS mice with reduced organ damage. For complete engraftment, dose escalation and increased donor cell number were essential, and furthermore, only long-term engrafted mice showed recovery of SCD phenotypes, suggesting a reversal of sickling features by healthy HbA RBCs post-TMI-BMT.

Materials and methods

Animals

All studies were performed in accordance with the Institutional Animal Care and Use Committee at City of Hope, National Medical Center, Duarte, CA. The C57B/L6 mice (stock #000664) were purchased from Jackson Laboratory, Maine, USA. The Berkeley SS mice (*Hbatm1 (HBA)Tow Hbbtm2(HBG1,HBB*)Tow* [homozygous SS]) (Stock # # 003342) were purchased from Jackson Laboratory, Maine, USA and housed at the COH facility during the study. The donor Berkeley AA mice (*Hbatm1(HBA)Tow Hbbtm3 (HBG1,HBB)Tow* [homozygous AA]) expressing normal human HbA were bred and maintained as previously described (21).

Study design

The study aim is to determine whether dose-escalated TMI is feasible in an SCD mouse model. The primary end point is to assess the tolerated TMI dose in SCD mice and survival of mice at 30 days post-BMT. The SS mice will be treated with different doses of TMI and TBI and transplanted with donor AA mice BM cells, and survival will be assessed at day 30 post-BMT. The secondary end point of the study is to assess organ damage and measure subsequent short-term (7, 14, and 30 days post-BMT) and long-term donor cell chimerisms (3 months post-BMT). The respective organ toxicities (liver, kidney, spleen, femur, lung, and skin) at different time points will be assessed by histopathology. The details of the TMI treatment, BM transplantation, and histopathology analysis methods are given below in the respective methods and results section.

TMI treatment plan

The TMI treatment was performed using the Precision X-RAD SMART Plus/225cx (Precision X-Ray, North Branford, CT, USA). The SS mice were treated with a TMI treatment plan according to a previous study but with some modifications (20). As the SS mice are radiosensitive and have enhanced organ damage due to sickling, particularly lung and kidney, we modified our TMI plan to further reduce doses to these organs. The isocenter of the T spine beam above the lung was moved up to further reduce doses to the lungs. For the kidneys, we divided the abdomen region into an upper and a lower section, and the isocenter for the beams for the abdomen region that has the kidneys was moved up, to further reduce the dose to the kidney. In a pilot study, we realized that a higher dose to the oral cavity was lethal to SS mice probably due to mucositis, and we kept the dose to the skull and oral cavity to a maximum of 2 Gy in the TMI plan. The comparison of the standard TMI plan and SCD modified TMI plan is shown in Figure 1. The radiation doses used in the study were as follows: TMI (4:0), TMI (4:2), TMI (6:2), TMI (8:2), TBI (2:2), and TBI (4:4). TMI (4:2) indicates a 4-Gy dose to the BM and a 2-Gy dose to the rest of the body. To keep the nomenclature consistent, for TBI 4 Gy, we use TBI (4:4), i.e., 4 Gy to the BM and 4 Gy to the rest of the body.

Congenic bone marrow transplant study

For BMT studies, control HbAA-BERK (AA) mice were used as donors. AA mice are littermates of HbSS-BERK (SS) mice and hence have similar mixed genetic background. AA mice like SS mice do not have murine globin genes but exclusively express normal human hemoglobin A (human α and β globins). AA mice were bred as homozygous and the donor AA mice have CD45.1 immunophenotype. For the BMT study, host SS (CD45.2 or CD45.1/CD45.2 mixed immunophenotype) were treated with a single varying dose of TBI/TMI and 24 h later transplanted with different amounts of donor CD45.1 AA BM cells (5–25 million BM cells).

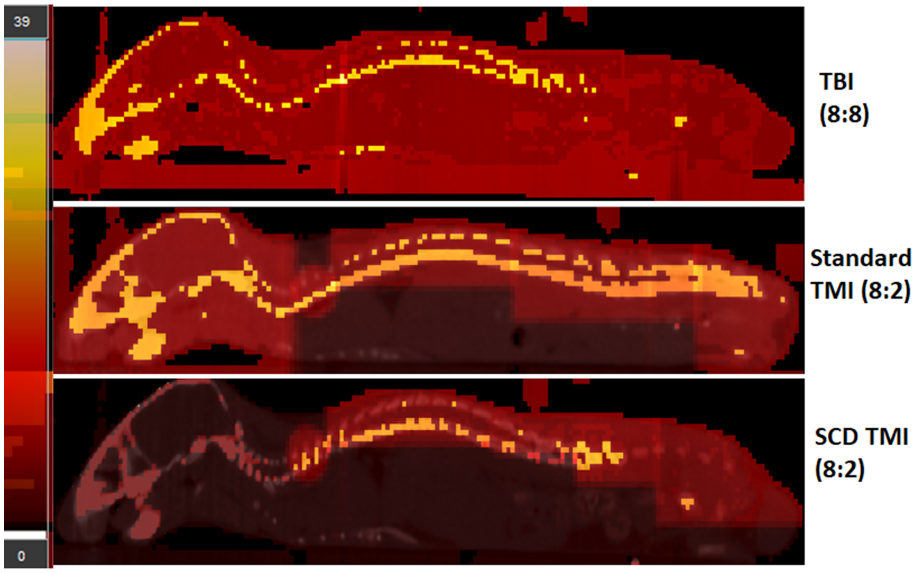

FIGURE 1
The modified TMI plan for SCD mouse. The TBI (8:8), standard TMI (8:2), and modified TMI (8:2) treatment plan for SCD are shown. The standard TMI (8:2) plan was modified by slightly adjusting the beam placements on the spine over the lung and kidney region. In addition, the dose to the skull was maintained at 2 Gy while the rest of the skeletal system received a prescription dose of 8 Gy. The dose painting clearly shows the difference in dose distribution in the new SCD TMI mice plan. The skull, face, and vital organs like liver, lung, and GI receive only ~2 Gy while the rest of the skeletal system is delivered with the prescribed dose. In addition, the TBI (8:8) mice dose painting clearly shows full prescription dose (~8Gy) to all the organs.

Donor chimerism study

The peripheral blood was collected from the tail vein at different time points (7, 14, 30, and 90 days post-BMT) and donor chimerism was analyzed by flow cytometry using anti CD45.1 and CD45.2 antibody. The antibody-stained cells were acquired using BD fortessa and data were analyzed using FlowJo V10.1 software.

Bone marrow cell harvest and stem cell staining

The BM cells were harvested and stained according to standard protocol (22). Briefly, the BM cells were collected by crushing the bones in PBS and filtered using a 30-micron MACS Smartstrainer (Cat # 130-098-458, Miltenyi Biotec, Auburn, CA). The RBCs were lysed from BM cells using ACK lysis buffer (Cat # A1049201 Gibco, Thermo Fisher Scientific, CA, USA) and single cells were stained with antibodies for CD45.1, CD45.2, lineage cells, cKit, Sca1, CD150, CD48, CD16/32, and CD34 (BioLegend, CA). The details about antibody are given in Supplementary Materials. The gating strategy for HSC was according to our previous published studies (22). The stained cells were acquired using a BD fortessa flow cytometer, and data were analyzed using FlowJo V 10.1.

Hemoglobin electrophoresis

Hemoglobin electrophoresis is performed using a cystamine hemoglobin (Hb) cellulose acetate electrophoresis procedure (Adams et al., 2001). Briefly, 6 µl of whole blood is mixed with 9.5 µl of a cystamine solution containing 112 mg of cystamine dihydrochloride (Sigma Aldrich, Saint Louis, MO, USA), 0.9 ml sterile water, 0.5 ml of 0.3% ammonium hydroxide, and 100 µl of DTT at 15.43 mg/ml in a 1:3 dilution with sterile water. The mixture is incubated at room temperature for 15 min before applying to Titan III cellulose acetate plates (Helena Laboratories, Beaumont, TX), pre-soaked in SupraHeme buffer (Helena Laboratories) for 20 min. The loaded plates are then electrophoresed for 45 min at 280 V in SupraHeme buffer (Helena Laboratories). Gels are poststained using Ponceau S (Sigma), and washed in 5% acetic acid, methanol,and a Clear-Aid de-stain solution containing 300 ml of glacial acetic acid, 700 ml of methanol, and 40 ml of Clear-Aid (Helena Laboratories) for hemoglobin visualization. Interpretation: Using validated standards for human sickle (HbS) and normal human Hb (HbA), we can see a single band of HbS for homozygous pups (SS), a single band of human HbA for control pups (AA), and two bands comprising of one HbS and one HbA band for hemizygous (AS) pups.

CBC and reticulocyte analysis

The peripheral blood was collected by cardiac puncture after euthanasia, in K3 EDTA tubes (BD biosciences). The CBC was analyzed using VetScan HM5 (Abaxis, Inc., Union City, CA, USA) (23). Reticulocytes were determined using BD Retic-Count (cat # 349204, BD Biosciences) according to the manufacturer's instructions. Briefly, for 5 µl of blood, 1 ml of BD retic reagent was added, mixed and incubated in the dark for 30 min, and flow analyzed within 2 h of after incubation. As control, 5 µl of blood in PBS was used to normalize reticulocyte number.

Multiphoton microscopy imaging

The MPM imaging using cranial window was carried out on SS mice according to a previous published study (24). Briefly, the day before microscopy imaging, a custom titanium head plate with an inner diameter of 8 mm was affixed directly on the frontal bone region of calvarium using Pearson PQ glass ionomer cement. To do headplate fixing, mice were first anesthetized using isoflurane, and surgery was performed to remove the skin and periosteum above the cranium. A stereotactic apparatus with a bite bar was utilized to keep the mouse stable during surgery. Herein, a headplate was used to stabilize the mouse head movement (even during breathing) while restraining the animal on the heated microscope stage. A 27-gauge catheter connected to an extension set is inserted into the mouse tail before loading mice on the microscope stage. The catheter allows the tail vein infusions of contrasts during imaging.

Equipment setup and imaging

A Prairie ultima multiphoton microscope (Bruker Corporation, Billica, MA) with Olympus XLUMPlanFL 20× objective (1.00 NA water objective) was used for image acquisition of all images. Imaging is performed on the frontal bone region of the calvarium. During imaging, four-channel acquisition was kept at far red, red, green, and blue. The channel gains, wavelength, and the laser power change for time lapse (TSeries) images, vascular blood pool (ZSeries) images, and blood flow measurements, but we keep these parameters uniform for all mouse types.

Image tiling

For tiling, images were acquired by collecting approximately a 2 × 3 grid series of overlapping z-stack images. The images were overlapping by 15% with a resolution of 512 by 512 pixels and a z-slice spacing of 15 µm. Tiled images were stitched together using ImageJ (Fiji) grid collection/stitching plug-in.

Image analysis

In this study, we have analyzed the irradiation and BMT-induced alteration in vessel morphology and their physiology. Vascular diameter and the number of vessel branches per area were quantified using ImageJ (Fiji).

Histopathology

After euthanasia, the tissues (liver, kidney, spleen, femur, lung, and skin) were harvested from respective mice and fixed in 10% Neutral Buffered Formalin (NBF) overnight and paraffin embedded according to SOP from the COH histology core. The formalin-fixed paraffin-embedded (FFPE) sections were stained with hematoxylin and eosin (H&E), Prussian Blue stain, and periodic acid Schiff–hematoxylin using standard protocols. Images were visualized using an Olympus microscope AX80 with a 10×, 20×, 40× eyepiece and an Olympus U-CMAD3 camera, with infinity analyze software from Lumenera Corporation. Morphologic findings of vascular congestion and iron deposits were analyzed according to the scoring system (18) that ranges from 0 for absent lesions up to a score of 6 for severe abundant lesions occupying 90%–100% of the field. For the kidney section, glomerular vascular congestion and renal tubular lesion were assessed as previously described (25). In H&E-stained kidney sections, a minimum of 30 glomeruli were evaluated/section under 400× magnification from 10 randomly selected fields of the renal cortex, glomerular vascular congestion was calculated as the percentage of total glomeruli with congestion present in at least 25% of the glomeruli, and results were averaged for each kidney. Tubular brush border thickness was assessed on periodic acid Schiff–hematoxylin-stained sections using a 0–4 grading scale: 0 for no changes; 1 for lesions involving <25% of the area; 2 for lesions involving 25%–50% of the area; 3 for lesions involving >50% of the area; and 4 for lesions involving nearly 100% of the area. Short-term damage assessment: TBI (4:4)-, TMI (8:2)-, and TMI (4:0)-treated mice 30 days post-BMT with age-matched untreated SS control (n = 3). Long-term damage assessment: TMI (8:2)-treated mice 90 days post-BMT (n = 3) and untreated age-matched SS control (n = 2) (25).

Mast cell analysis in skin sections

Skin sections were stained with toluidine blue for mast cell analysis (23). Toluidine blue stain was prepared by dissolving 0.25 g of toluidine blue (Sigma-Aldrich) in 35 ml of distilled water, 15 ml of ethanol 100%, and 1 ml of HCl. After deparaffinization, the skin sections were incubated in toluidine

blue for 1 min at room temperature, washed with distilled water, and air-dried. The stained specimens were observed under an Olympus microscope AX80 at (600× magnification) to count the MCs recognized by red-purple metachromatic staining color on a blue background. Mast cells were counted in 20 fields, 2 sections per slide, and expressed as total mast cell number, number of degranulated mast cells, and percentage of degranulated cells. Degranulated mast cells were defined as cells associated with ≥8 granules outside the cell membrane at 600× magnification as described previously (23).

Statistical analysis

Statistical analyses were calculated using GraphPad Prism software (GraphPad Software Inc., La Jolla, CA, USA). Statistics were performed using the two-tailed unpaired *t*-test, and one-way ANOVA test, and the data are presented as mean ± SEM. When *p*-values were <0.05, the difference was considered significant. Ns = not significant, $*p < 0.05$, $**p < 0.01$, $***p < 0.001$, $****p < 0.0001$.

Results

The SCD Berkeley SS mouse model was used in this study to evaluate the feasibility of dose-escalated TMI. In this study, we used our recently developed preclinical 3D-TMI model to develop a treatment plan for SS mice (Figure 1). However, the standard TMI plan was modified to further reduce the mean lung dose by ~18% and kidney dose by ~50% (Table 1). The SS mice due to the underlying pathophysiology of the disease are radiosensitive and therefore the dose to the skull and oral cavity was kept at 2 Gy for all TMI treatment.

First, we carried out a pilot study to evaluate the tolerated dose in the Berkeley SS mouse. The SS mouse was treated with TBI (4:4) and TBI (6:6) radiation and transplanted with 5 million donor whole BM cells from AA mouse to check the tolerated dose in SS mice. TBI 6 Gy was completely lethal while 4 Gy mice survived for 30 days post-BMT with no lethality (Figure 2A). We then evaluated the tolerated dose in the TMI model in SCD mice ($n \geq 3$). Due to the limited availability of SS mice, we tested TMI (4:0) (4 Gy to BM, 0 Gy to the rest of the body) TMI (4:2) (4 Gy to BM, 2 Gy to the rest of the body), and TMI (8:2) (8 Gy to BM, 2 Gy to the rest of the body), increased the dose by 100%, and transplanted with donor BM cells. Because of the previous experience from the TMI mouse model and engraftment failure in TMI 12:0, we also chose to treat mice with a 2-Gy body dose while varying the dose to the BM.The SS mice tolerated TMI (4:0), TMI (4:2), and TMI (8:2) dose escalation.

Next, we evaluated the donor chimerism at D7, D14, and D30 post-BMT in peripheral blood. The SS mice were treated with TBI (4:4), TMI (4:0), and TMI (8:2) and transplanted with 5 million donor HbA BM cells. TBI (4:4) and TMI (8:2) had similar donor chimerism at D7 and D14 but higher than TMI (4:0)-treated mice; however, the engraftment failed (less than 10% chimerism) in all groups by day 30 (Figure 2B), suggesting a short-term engraftment failure. The initial chimersim observed on D7 and 14, maybe due to the mature cells from transplanted donor BM cells and this also resulted in reduced reticulocytes in TMI (8:2) treated mice (Figure 2C).

Although the chimerism failed in these mice, we wanted to evaluate the organ damage by radiation post-BMT in SS mice. Therefore, we evaluated the organ damage from TBI (4:4)-, TMI (4:0)-, and TMI (8:2)-treated mice and age-matched untreated SS mice ($n = 3$/group). We carried out histopathology, at 30 days post-BMT, on femur, lung, liver, kidney, and spleen (Figures 3A, B). We observed a statistically significant reduction in splenic sinusoidal congestion in TMI (8:2)-treated mice (p-value = 0.048 vs. untreated SS mice and p-value = 0.0126 vs. TBI-treated mice). This was associated with a significant reduction in splenic iron deposits compared to untreated SS in both TMI doses TMI (4:0) (p-value = 0.0248) and in TMI (8:2) ($p = 0.0143$) as well as a significant reduction in comparison to TBI (4:4)-treated mice [TBI (4:4) vs. TMI (4:0), $p = 0.0328$; TBI (4:4) vs. TMI (8:2), $p = 0.0188$]. The liver of TBI (4:4)-treated mice showed more sinusoidal congestion [$p = 0.0283$ vs. untreated SS, $p = 0.0032$ vs. TMI (4:0), and $p = 0.0029$ vs. TMI (8:2)]. TMI (4:0) and TMI (8:2) showed significantly reduced liver iron deposits compared to untreated SS mice ($p = 0.0197$ and = 0.0009, respectively); this significant reduction was also observed compared to TBI (4:4)-treated mice ($p = 0.0136$ and $p = 0.0007$,

TABLE 1 Comparison between the SCD TMI, Standard TMI (8:2), and TBI (8:8) plan.

Organs	SCD TMI (8:2) Mean dose (Gy)	Standard TMI (8:2) Mean dose (Gy)	TBI (8:8) Mean dose (Gy)	SCD TMI (8:2) vs. Standard TMI (8:2) Difference %
Intestine	2.9	4.2	8.3	31
Liver	2.4	3.4	8	29.4
Lungs	4.5	5.5	9.3	18.2
Heart	2.2	2.9	8.3	24.1
Kidneys	3.7	7.4	8	50

The modified SCD plan reduces the mean doses on vital organs (liver: ~29%; lungs: ~18%; heart: ~24%; and kidney: ~50%) than the standard TMI (8:2) plan in B6 mice. TBI (8:8) delivers full prescription dose (~8 Gy) to all the organs.

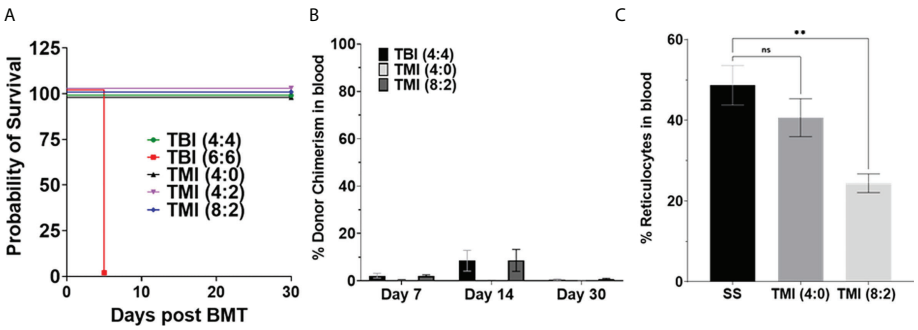

FIGURE 2
Sickle cell disease mice tolerated radiation dose and chimerism post-BMT. Berkeley SS mouse was treated with different dose of radiation and transplanted with 5 million donor AA bone marrow cells, and survival and chimerism were monitored over 30 days post-BMT. **(A)** Kaplan–Meier survival curve showing that TBI 6 Gy was lethal even after BMT, while TMI (8:2) was tolerated by SS mice ($n \geq 3$). **(B)** Donor chimerism was measured in blood at D7, D14, and D30+ post-BMT. The data are representative of one experiment ($n = 5$) and was not repeated due to the limited availability of mice. **(C)** Peripheral blood reticulocytes were analyzed using BD Retic-Count by flow cytometry. The TMI (8:2) showed lower reticulocytes than TMI (4:0), perhaps due to initial donor chimerism seen at D14, suggesting that donor RBCs transplanted could temporarily rescue this phenotype. Significance was determined using two-tailed Student's *t*-test and two-way ANOVA and was considered significant when *p*-value was <0.05. ns= non-significant, $^{**}p < 0.01$.

respectively). Lung tissue from TMI (8:2)-treated mice showed relatively 42% reduction in capillary congestion compared to TBI (4:4)-treated mice. TMI treated mice showed significant reduction in inflammatory infiltrate compared to untreated SS mice ($p = 0.0454$) and to TBI (4:4) ($p = 0.0307$), as well as significant reduction in lung iron store deposits in both TMI doses compared to TBI (4:4). Kidneys of TBI (4:4)-treated mice showed significantly congested glomerular capillaries compared to untreated ($p = 0.0120$) and TMI (4:0)-treated ($p = 0.0032$) mice. Both doses of TMI showed significantly less tubular brush border lesion as observed in the analysis of PAS-stained slides, in addition to reduced renal iron deposits in TMI (8:2)- compared to TBI (4:4)-treated ($p = 0.0425$) mice. Our observations from the morphological assessment of this pilot study support our hypothesis that TMI results in significantly less tissue damage compared to TBI. As TBI (4:4) caused more damage than TMI (8:2), which had ~2 Gy lower dose administered to these organs, for all further studies, we only considered treatment with 2 Gy or less body dose.

Although SS mice tolerated dose-escalated TMI (8:2), they could not sustain engraftment with 5 million donor BM cells. Therefore, we evaluated whether SS mice could tolerate a high dose of radiation conditioning regimen for BMT with modifying donor cells and how this might impact optimization of engraftment/chimerism. This was achieved by transplanting 10 million and 25 million donor AA BM cells into TMI (4:0)- and TMI (8:2)-treated mice. Although 25 million donor cells increase the donor chimerism in both groups at D7, TMI (8:2) had the highest chimerism at all time points and showed sustained donor chimerism while TMI (4:0) failed at D30 post-BMT (Figures 4A, B). However, the TMI (8:2)-treated mice transplanted with 25 million donor BM cells showed a sustained long-term engraftment even at 90 days post-BMT (Figure 4B), which will be described later.

Furthermore, as 25 million cells showed sustained engraftment, we evaluated if TMI (8:2) dose escalation was essential for this sustained engraftment, or if a higher cell number was enough. We treated SS mice with TBI (2:2), TMI (4:2), and TMI (8:2) and transplanted 25 million HbA donor BM cells. At day 7 post-BMT, chimerism was much better in all groups, but TMI (4:2) and TMI (8:2) were higher than TMI (4:0) and TBI (2:2). However, only TMI (8:2)-treated mice could retain higher donor chimerism (>60%) by day 30 (Figure 4C), suggesting that both dose escalation and increasing donor cells were necessary for successful short- and long-term engraftment. We also measured HbA and HbS levels in peripheral blood post-BMT using CAE. With increasing donor BM cells (from 5 to 25 million), we observed an increase in HbA:HbS ratio by D14 in TBI (4:4) and TMI (8:2), while TMI (4:0) showed no change. However, 25 million donor BM cells showed the highest improvement in HbA:HbS ratio in TMI (8:2)-treated mice while TMI (4:0) still showed minimum to no change (Figure 4D), correlating with the enhanced donor chimerism in TMI (8:2) and failed chimerism in TMI (4:0).

Since only TMI (8:2)-treated mice sustained donor chimerism long term, we compared the organ morphology of TMI (8:2)-treated mice with that of untreated SS mice to evaluate organ histopathology 90 days post-BMT. The respective organs' FFPE sections were stained with H&E, PAS (kidney), and Prussian blue (iron deposits), and organ morphology was analyzed for vascular congestion, inflammatory infiltrates, infarcts, and iron deposits as described before (18, 25). Histopathological findings support

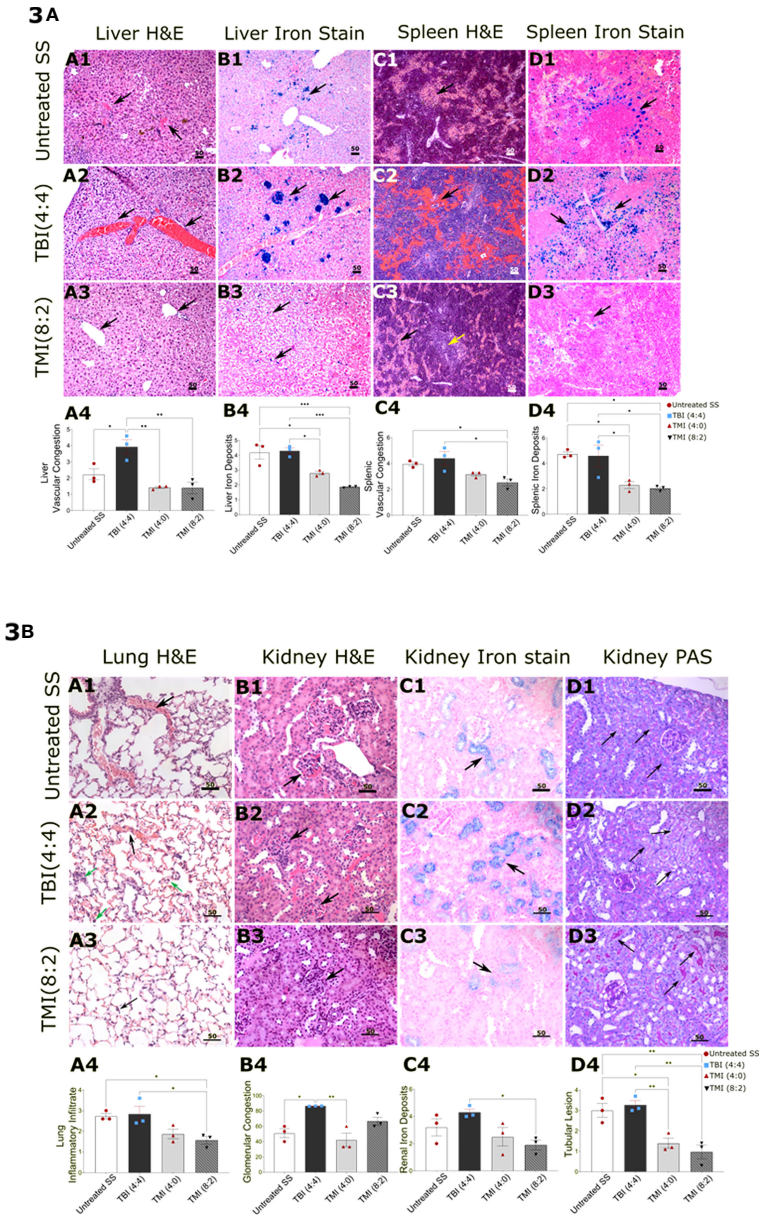

FIGURE 3
Comparison of histopathology in TBI, TMI, and untreated SS BMT control mice. Sections were stained with hematoxylin and eosin, Iron stain (Prussian Blue stain), and periodic acid Schiff–hematoxylin using standard protocols. Images were visualized using an Olympus microscope AX80 with a 10×, 20×, 40× eyepiece. Ten randomly selected fields, acquired from two sections per specimen from the liver, spleen, lungs, and kidneys, were scored for different parameters including vascular congestion, mononuclear inflammatory infiltrate, and iron deposits using Manci et al.'s scoring system (1). Glomerular vascular congestion was assessed on hematoxylin and eosin-stained sections and calculated as the percentage of total glomeruli with congestion present in at least 25% of the glomerulus as described (2). The microscopic findings in untreated SS are shown in figures **(A1–D1)**, TBI (4:4)-treated mice in **(A2–D2)**, and TMI (8:2)-treated mice in **(A3–D3)**, while **(A4–D4)** are showing the statistical analysis representative figures for the corresponding histopathological finding. **(A)** The histology sections demonstrate the hepatic findings showing more sinusoidal congestion in TBI (4:4) **(A2)**, black arrow) and siderosis [**(B2)**, black arrow] than TMI (8:2) **(A3, B3)**, black arrow). Spleen in TBI (4:4) showed more sinusoidal congestion **(C2)**, black arrow) and siderosis [**(D2)**, black arrow) than in TMI (8:2) [**(C3, D3)**, black arrow]. The yellow arrow in C3 represents preserved white pulp in TMI (8:2)-treated mice. **(B)** Pulmonary findings in the TBI (4:4) included more vascular congestion [**(A2)**, black arrow] and inflammatory infiltrate [**(A2)**, green arrow] than TMI (8:2) **(A3)**. Renal findings in TBI (4:4) included markedly congested glomerular (B2, black arrow) and denser iron deposits (**C2**, black arrow) than TMI (8:2) **(B3, C3)**. TBI (4:4) showed more renal tubular lesions marked by a significant loss in the tubular brush border lesion as observed in the analysis of PAS-stained slides [**(D2)**, black arrow]. Liver and spleen H&E and Iron stain original magnification, 100×. Lungs (H&E, Iron stain) and kidney (H&E, Iron stain, PAS) original magnification, 200×. Statistical analysis figures are generated by GraphPad software; ordinary one-way ANOVA, Tukey's multiple comparisons test. Data are shown as mean ± SEM. *$p < 0.05$; **$p < 0.01$; ***$p < 0.001$. H&E, hematoxylin and eosin; PAS, Periodic acid Schiff; TBI, total body radiation; TMI, targeted marrow irradiation.

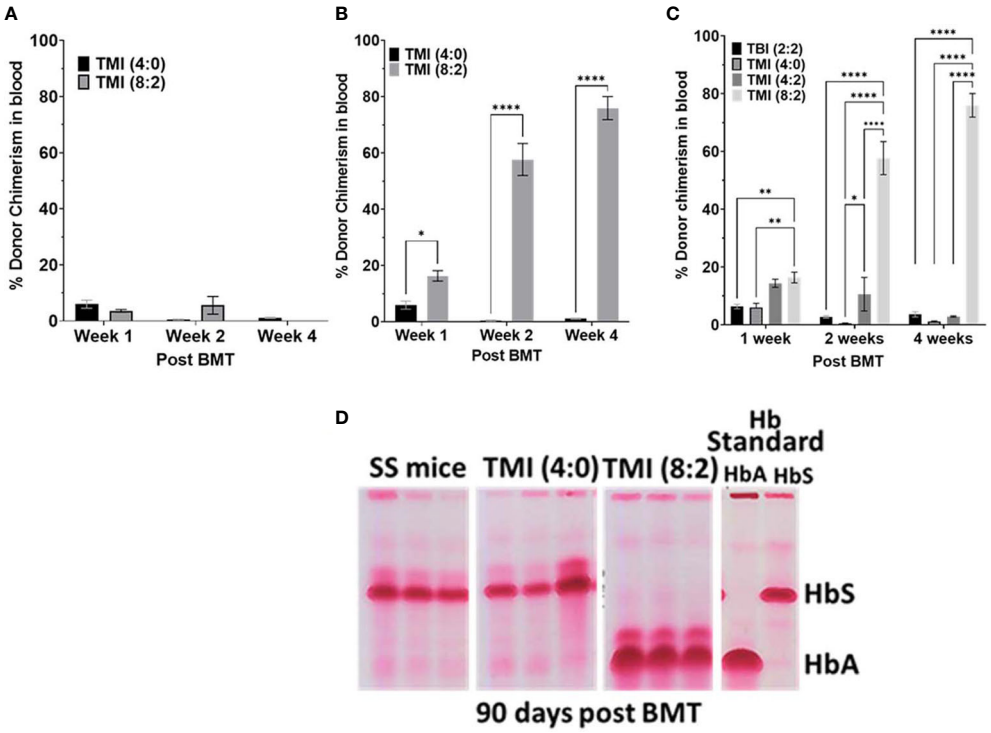

FIGURE 4
Effect of increasing donor cell number on chimerism and evaluation of blood hemoglobin for HbA and HbS. **(A, B)** The SS mice treated with TM (4:0) and TMI (8:2) transplanted with 10 million **(A)** and 25 million **(B)** AA donor BM cells and chimerism was measured in peripheral blood at D7, D14, and D30 post-BMT. **(C)** SS mice treated with different radiation doses were transplanted with 25 million AA donor BM cells and chimerism was checked at D7, D14, and D30 post-BMT in peripheral blood. Only TMI (8:2)-treated mice sustained chimerism at D30 post-BMT and was ~>65% ($n \geq 3$). **(D)** CAE electrophoresis analysis of HbA and HbS 90 days post-BMT in peripheral blood. SS mouse was treated with TMI (4:0) and TMI (8:2) (Day −1) and 24 h later (Day 0) transplanted with 25 million donor AA BM cells. CAE analysis of TMI (8:2)- and TMI (4:0)-treated mice transplanted with 25 million cells on D90 post-BMT. Hb standard: from homozygous AA (HbA) and SS (HbS), and hemizygous AS (AFSC) mouse RBCs. Significance was determined using 2 way ANOVA and was considered significant when p value was < 0.05. * p<0.05, ** p< 0.01, **** p<0.0001.

that TMI (8:2) results in less tissue damage (Figure 5A) as evidenced by a significant reduction in vascular congestion (lung $p = 0.0142$, liver $p = 0.0137$, and spleen = 0.0135), inflammatory infiltrate (lung $p = 0.0306$, liver $p = 0.0045$), liver infarcts ($p = 0.0034$), and iron deposits in the liver ($p = 0.0414$) and kidney ($p = 0.0205$). At the level of renal tubules, untreated mice showed a significant loss in the tubular brush border when compared to TMI (8:2)-treated mice ($p = 0.0082$). BM in TMI (8:2) (cellularity ~70%) showed improvement in cellular differentiation and topography in comparison to the untreated (cellularity ~90%) mice that were packed with minimal fat spaces, thin trabeculae, and marked erythroid hyperplasia.

The mast cell activation has been shown to be responsible for enhanced pain, a sickle cell pathophysiology (23). We then investigated the total number of mast cells in skin of untreated SS mice and TMI (8:2)-treated SS mice 90 days post-BMT. The skin sections were stained with toulidine blue and the total number of mast cells and degranulating mast cells (activated) was calculated as described in *Materials and Methods*. The relative number of mast cells in TMI (8:2)-treated SS mice was slightly lower but not significantly different than age- and sex-matched untreated SS mice. However, the number (~45 vs. ~15) and percentage of degranulating mast cells (~85% vs. 50%) were signifcanlty lower than untreated SS mice ($p < 0.05$) (Figure 5B), suggesting that TMI (8:2) treatment and successful engraftment of donor cells may also reduce pain phenotype in SS mice.

The CBC analysis of peripheral blood at 3 months post-BMT from TMI (8:2)-treated mice showed a significant improvement in RBC numbers, Hb content, and platelets compared to the age- and sex-matched untreated SS mice (Figure 6A). The reticulocyte number in peripheral blood was also drastically reduced to ~5% in TMI (8:2)-treated mice compared to HbS control mice (~50%) (Figure 6B). These data suggest the recovery of sickle cell phenotype due to the replacement of sickle HbS RBCs with healthy HbA RBCs produced from AA donor cells.

Next, we investigated the microvascular structure of SCD mice post-TMI-BMT using our recently developed intravital multi photon microscopy (MPM) imaging using a cranial

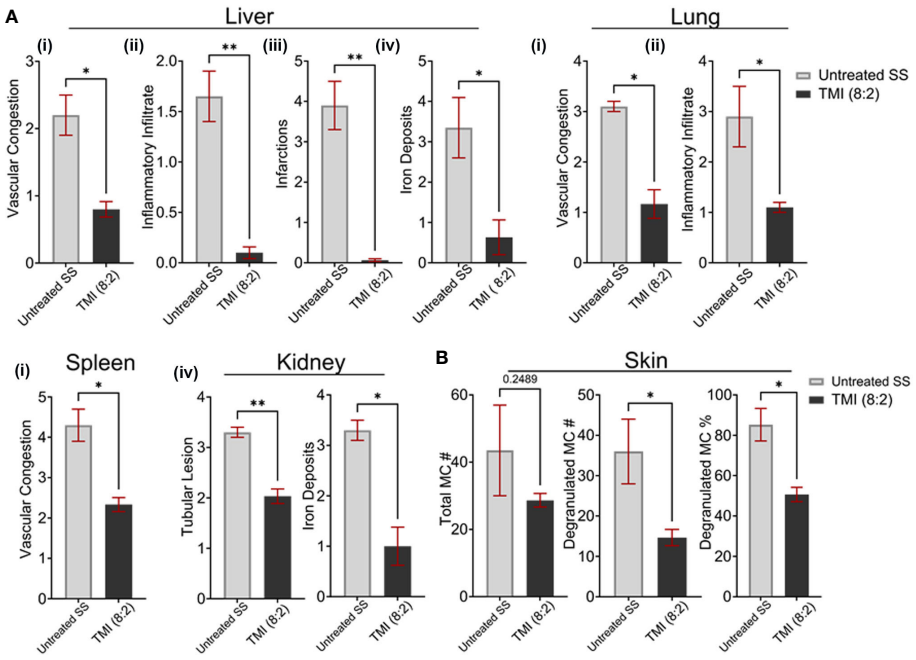

FIGURE 5
TMI (8:2)-treated mice long-term organ morphology assessment. We analyzed H&E- and PAS-stained sections of several organs for vascular congestion, inflammatory infiltrate infarcts, and iron deposits as described before (1). **(A)** Compared to untreated SS mice, the TMI (8:2)-treated mice showed significant reduction in (i) vascular congestion in lungs, liver, and spleen; (ii) inflammatory infiltrates in liver and lungs; (iii) infarction in liver infarction; and (iv) iron deposits in the liver and kidney. **(B)** Mast cell number, degranulated mast cell number, and percentage were determined from toluidine blue-stained skin sections from untreated SS mice and TMI (8:2)-treated mice 90 days post-BMT. The TMI-treated mice showed slightly lower but not significantly different mast cell numbers in the skin; however, the relative number and percentage of degranulated mast cells (activated) were significantly lower in TMI-treated mice than in untreated SS mice. Data are shown as mean ± SEM, analyzed with unpaired *t*-test, and two-tailed using GraphPad Prism *$p < 0.05$, *$p < 0.01$, **$p < 0.01$.

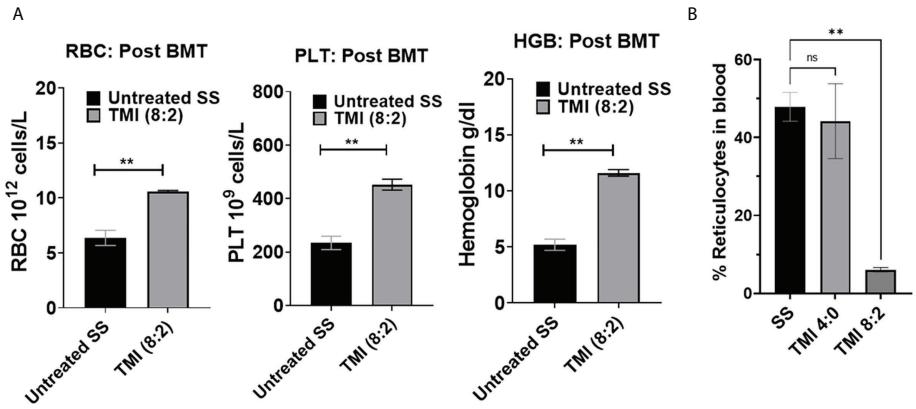

FIGURE 6
CBC analysis and peripheral blood reticulocytes from SS mice post-BMT. CBC was analyzed for TMI (8:2)-treated SS mice 90 days post-BMT. **(A)** RBC PLT and hemoglobin were significantly increased in BMT SS mice in comparison to untreated SS mice ($p = 0.0042$, 0.0067, and 0.0012, respectively), suggesting recovery of SCD phenotypes by BMT. **(B)** The reticulocytes were also significantly reduced in SS mice post-BMT ($p = 0.0015$) compared to untreated SS mice. Significance was determined using student's 't' test and 2 way ANOVA and was considered significant when p value was < 0.05. ns=non-significant, **p< 0.01.

window. Using dextran as a blood pool agent, we visualized vessels and measured the average number of vessels and vascular diameter within the imaging window. The SCD mice showed a significanly higher number of vessels while vascular diameter was much smaller than control C57BL/6 and AA mice (Figures 7A–F). Interestingly, the TMI (8:2)-treated SCD mice 90 days post-BMT showed a microvascular structure similar to that of control AA mice, suggesting the recovery of microvascular niche post-BMT.

The hematopoietic stem and progenitor cells were analyzed in untreated control and TMI (8:2)-treated SS mice 3 months post-BMT. The Lin- cKit+ Sca1+ (LSK) HSCs were not significantly different than control HbS mice; however, we observed a slightly lower but not significantly different frequency of Lin- cKit+ Sca1- (LK) committed progenitors, particularly CMP and GMP in BMT mice. Interestingly, MEP progenitor cells that are committed to make megakaryocyte and erythroid cells were significantly increased in TMI (8:2)-treated mice post-BMT (Supplementary Figure S1A). This increase in MEP correlates with CBC data showing increased RBC number in peripheral blood in TMI-treated mice 90 days post-BMT. However, this is a limited mouse study and therefore more mouse data are required to confirm this observation.

Discussion

This report is a first-in-field proof-of-concept study showing that the 3D image-guided TMI-based dose escalation is feasible for successful donor engraftment, rescue from SCD, and reduction of organ toxicity in an SCD mouse model. Due to the severity of the organ damage, TBI-based HCT is often avoided and palliative treatment is used until the disease becomes severe to accept. Reduced-intensity TBI was used as an alternative, which is less effective to cure SCD and toxicity remained high. Practically, there was no technological breakthrough to address this global health problem, and thus, curative option with good quality of life is severely limited for patients with SCD. Encouraged by our recent success of developing TMI delivering target-specific conformal radiation in HCT (15) and improving the clinical outcome of patients with high-risk leukemia (16), we conceptualized that TMI can be an effective treatment alternative for SCD patients. However, the lack of preclinical model limits our scientific understanding of the role of TMI in hematological disorder such as SCD and future clinical development.

SCD mice are radiosensitive, perhaps due to their underlying pathophysiology due to sickle RBCs. Like previous studies (26),

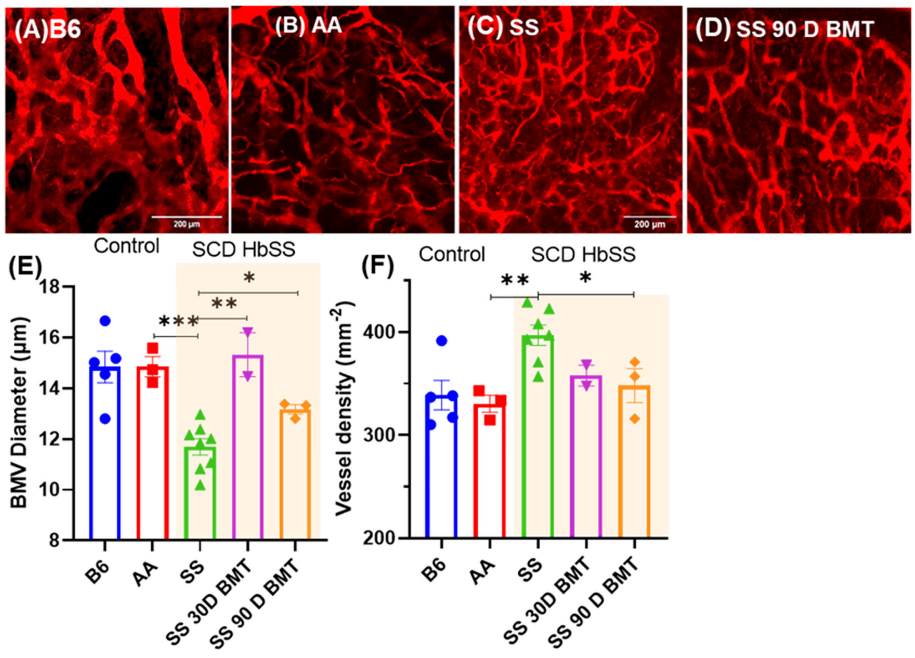

FIGURE 7
TPM imaging of microvasculature in SS mice and SS mice post-BMT. **(A–D)** TPM tiled images of SS mice and the controls, B6, AA, and 90 days post-BMT. The SCD mice have distinctly abnormal and disorganized BM vasculature **(C)** compared to that of control **(A, B)**; however, 90 days post-BMT in TMI (8:2)-treated mice, the microvasculature of the SS mice recovered and was like that of control mice **(D)**. **(E, F)** Vascular diameter and the number of vessel branches per area were quantified for the statistical measures. Statistically significant difference between average vessel diameter can be seen between SCD mouse and their controls **(E)** and the same is true for the vessel numbers/density **(F)**. Data shown as mean ± SEM for $n \geq 3$ mice in each group. Significance determined using two-tailed unpaired *t*-test and considered significant when $p < 0.05$, *p<0.05, **p< 0.01, ***p<0.001.

the 6-Gy TBI dose was found to be highly toxic in a pilot study we conducted. Using a limited number of mice ($n \geq 3$), we show that SCD mice could tolerate TMI (8:2) dose, that is, 8-Gy dose was delivered to the BM while 2 Gy was delivered to the rest of the body. Although no mice died in the pilot survival study, TMI (8:2) treatment sometimes resulted in death (~20%–40%, one to two out of five mice) in some studies. Death may be due to a combination of the pathophysiology of SCD mice and TMI treatment conditions, as the mice are anesthetized using isoflurane for over 30 min for TMI treatment. However, death of SS mice occurred around 4–6 days post-BMT, suggesting that cause of death is not due to hematopoietic failure, which usually occurs around 10–14 days post-BMT. Future studies are planned to understand the underlying cause of death by conducting necropsy of these mice.

After determining the tolerated TMI dose, we then evaluated the donor cell chimerism after dose escalation. The TBI (2:2)-, TMI (4:0)-, and TMI (4:2)-treated mice could not maintain chimerism by 30 days post-BMT even with increased 25 million donor cells, suggesting that these low-dose radiation was perhaps not sufficient to remove host HSC from their niche to create space for donor HSC to home and maintain a sustained long-term engraftment. Furthermore, in TMI (8:2) dose escalation, although no sustained engraftment was seen when 5 and 10 million donor cells were used, 25 million donor BM cells resulted in sustained engraftment, suggesting that increased dose could create space for donor HSC to home; however, sustained engraftment was possible only with higher donor BM cells. Similarly, in a previous study in SCD mice, increasing donor cell numbers from 10 to 50 million did not improve chimerism in nonmyeloablative Treosulfan conditioning; however, chimerism increased only when the conditioning dose of treosulfan was increased (27). Therefore, increased dose to the BM using TMI was also essential along with increased donor BM cells for sustained engraftment.

Although TBI (2:2) failed to engraft with 25 million donor cells, TBI (4:4) may have shown better chimerism and long-term engraftment with 25 million donor cells. However, organ damage in TBI (4:4)-treated mice and TMI (8:2)-treated mice clearly show that the 4-Gy dose to the organs damages more than 2 Gy used in TMI (8:2). Additionally, using TMI (8:4), we may be able to improve chimerism with lower donor cells, but the benefit of organ protection from TMI will be compromised. However, the use of TMI in combination with radiomitigators like thrombopoietin mimetics could be an alternative to protect organs by increasing the body dose to 4 Gy to reduce donor cell numbers. In addition, TPO is also known to stimulate HSC expansion post-BMT (28), perhaps improving donor chimerism by donor HSC expansion beyond radioprotection of organs. Therefore, further studies using such radiomitigators and reagents to expand HSC post-BMT should be tested in combination with TMI.

The stem cell analysis in long-term engrafted SCD mice showed an increased MEP progenitor population. These data could explain the recovery of RBC numbers and platelets in peripheral blood as MEP progenitors produce megakaryocytes (platelets) and erythroid cells (RBCs). The erythroid cell analysis using anti-CD71 and anti-Ter119 flow analysis from the spleen of TMI (8:2)-treated mice post-BMT also indicated normal erythropoiesis, unlike SCD mice that show accumulation of CD71 and Ter119 high immature cells (data not shown), consistent with increased percentage of reticulocytes in peripheral blood.

Long-term donor cell-engrafted mice also show recovery of reticulocyte percentage in peripheral blood, further suggesting recovery of erythropoiesis in SS mice post-BMT. The HbA:HbS ratio was also very high in long-term engrafted mice, further confirming the alleviation of HbS sickle cell phenotype. In addition, we also measured the activation of mast cells by determining the number and percentage of degranulated mast cells in the skin of SCD mice and post-BMT mice. The TMI (8:2) mice showed a reduced number and percentage of degranulated mast cells, suggesting the lower activation of mast cells. Mast cell activation has been shown to play an important role in pain perception in SCD (29, 30). Therefore, TMI (8:2) treatment not only improved chimerism but may have reduced pain in these mice. However, we need more studies to determine if donor engraftment or reduced skin dose in TMI (8:2) treatment or a combination of both was responsible for this phenotype.

The microvascular structure is altered significantly in SCD mice due to sickling of HbS RBC, which results in vaso-occlusion crisis. We have used cranial window and MPM to assess the BM vascular structure in the context of BMT in SS mice. The MPM imaging shows increased vascular density and reduced diameter in comparison to age- and sex-matched SS mice. Interestingly, the vessel density and diameter post-BMT was recovered to control AA mouse levels, indicating an association between recovery of microvascular structure and increased healthy HbA RBCs. Similarly, previous studies show that expression of HbF in SS mice resulted in normalization of microvascular and hemodynamic parameters by decreasing the sickling-induced transient vaso-occlusion events (31). However, in TMI (4:0) mice where chimerism completely failed, the vascular structure resembled untreated SS mice. This clearly suggests that donor engraftment and dose escalation enabled BM vasculature recovery. However, further studies are required to understand the mechanism of vascular niche remodeling in SCD mice post-BMT.

One of the limitations of the current study is that this is a congenic BMT study, resembling a matched donor-based allogeneic transplant in clinic. Matched donor is the first step to confirm the success of engraftment before moving towards mismatched or haploidentical donor settings. Haploidentical allogenic-HCT is often used for SCD patients due to the limited availability of HLA matched donors. We currently do not have AA mice in an allogenic mouse background. In the

future, we can backcross the AA mice on an HLA mismatch genetic background mice like BALB/c and used the mismatched AA BM cells as donor to create an allogenic BMT study using TMI in SS mice.

Extramedullary hematopoiesis (EMH), a compensatory phenomenon to chronic hemolytic anemias, favors certain sites, mainly the spleen, and other sites such as the liver and the paraspinal regions of the thorax (32, 33). Thus, we have further evaluated EMH using histopathology. In SS untreated mice, we observed significant findings of EMH in the form of congested splenic sinusoids with hematopoietic cells including myeloid elements with different grades of maturation, erythroid cells, and megakaryocytes. These findings showed a reduction in the TMI (8:2) in treated mice after 90 days post-BMT, denoting that successful engraftment could reduce the EMH, one of the pathological features in SCD (data not shown). In agreement with this finding, there was a reduction of splenic EMH after hematopoietic stem cell transplantation in patients with myeloproliferative neoplasm-associated myelofibrosis (MPN-MF), another hematological disorder manifesting with splenomegaly secondary to extramedullary hematopoiesis (34).

In the future, we will use the currently developed TMI-SCD model to investigate how to increase donor chimerism and stabilize engraftment, leading to the long-term reversal of SCD phenotype. Our pilot data (not shown) and previous reports found that radiation exposure can increase hepatic thrombopoietin (35). TPO also plays a role in *HSC* self-renewal, proliferation, and differentiation (28, 36, 37). It is anticipated that reduced body (including liver) dose in TMI could reduce TPO, thus limiting the availability to support HSC expansion. Therefore, we will test whether varying radiation dose to liver could change TPO level (and other inflammatory cytokines), which could influence HSC homing and engraftment using TPO knockout mice. Finding a target (such as TPO) may allow us to use it along with TMI to improve engraftment (without increasing donor cells) and maintain normal BM hematopoiesis. Also, increasing BM-targeted radiation could adversely affect bone marrow environment (BME); therefore, future studies will require a thorough investigation on how to preserve BME.

In conclusion, we have evaluated the feasibility of dose-escalated TMI in the SCD mouse model. We show that dose escalation of TMI (8:2) is tolerated by SCD mice, but increased donor BM cells were essential for sustained engraftment. Higher donor chimerism reduces SCD features by increasing RBC number, platelets, hemoglobin content, and HbA:HbS ratio in RBCs while reducing reticulocyte number in peripheral blood. Therefore, this study provides the basis to conduct further studies using preclinical TMI to further improve the methodology and understand the mechanism for improved chimerism and reduction of SCD phenotypes. This preliminary study provides an opportunity to develop a new TMI-based preconditioning regimen for SCD patients that could reduce organ damage while increasing chimerism, and could therefore be a potential curative alternative to myeloablative HCT.

Data availability statement

The original contributions presented in the study are included in the article/Supplementary Material. Further inquiries can be directed to the corresponding author.

Ethics statement

This study was reviewed and approved by institutional animal care and use committee (IACUC). Protocol number #16064.

Author contributions

SH and SSM: concept and experimental design, data analysis, interpretation of results, and manuscript writing and editing. JL and PV: BMT experimental design, data acquisition, and analysis. CG and JR: experimental design and manuscript editing. AMHA, DZ, and HG: experimental design and TMI treatment. HG and JB: MPM experimental design, data acquisition, analysis and interpretation of results, and manuscript editing. KG: experimental design, data analysis, and interpretation of histopathology and experiments with SCD and control mice and manuscript editing. RF: all histopathology analysis, interpretation, and co-wrote the manuscript. SK: phenotyping for sickle and normal human Hb, breeding and phenotyping control and sickle mice, and editing the manuscript. All authors contributed to the article and approved the submitted version.

Funding

This work has been supported by NIH grants 2R01CA154491 (SH), RO1 HL147562 (KG), and U18 EB029354 (KG), and a Diversity Supplement 3R01HL147562-03S (SK). The content is solely the responsibility of the authors and does not necessarily represent the official views of the National Institutes of Health.

Conflict of interest

KG: Honoraria: *Tautona Group*, *Novartis* and *CSL Behring*. Research Grants: *Cyclerion*, *1910 Genetics, Novartis*, Zilker LLC, *Grifols*, *UCI Foundation and SCIRE Foundation.* SH receives honoraria from and consults for Janssen Research and Development, LLC.

The remaining authors declare that the research was conducted in the absence of any commercial or financial relationships that could be construed as a potential conflict of interest.

Publisher's note

All claims expressed in this article are solely those of the authors and do not necessarily represent those of their affiliated organizations, or those of the publisher, the editors and the reviewers. Any product that may be evaluated in this article, or claim that may be made by its manufacturer, is not guaranteed or endorsed by the publisher.

Supplementary material

The Supplementary Material for this article can be found online at: https://www.frontiersin.org/articles/10.3389/fonc.2022.969429/full#supplementary-material

References

1. Yawn BP, Buchanan GR, Afenyi-Annan AN, Ballas SK, Hassell KL, James AH, et al. Management of sickle cell disease: summary of the 2014 evidence-based report by expert panel members. *Jama* (2014) 312(10):1033–48. doi: 10.1001/jama.2014.10517

2. Gladwin MT, Vichinsky E. Pulmonary complications of sickle cell disease. *New Engl J Med* (2008) 359(21):2254–65. doi: 10.1056/NEJMra0804411

3. Powars DR, Chan LS, Hiti A, Ramicone E, Johnson C. Outcome of sickle cell anemia: a 4-decade observational study of 1056 patients. *Medicine* (2005) 84 (6):363–76. doi: 10.1097/01.md.0000189089.45003.52

4. Ballas SK, Lieff S, Benjamin LJ, Dampier CD, Heeney MM, Hoppe C, et al. Definitions of the phenotypic manifestations of sickle cell disease. *Am J hematol* (2010) 85(1):6–13. doi: 10.1002/ajh.21550

5. Horan JT, Liesveld JL, Fenton P, Blumberg N, Walters MC. Hematopoietic stem cell transplantation for multiply transfused patients with sickle cell disease and thalassemia after low-dose total body irradiation, fludarabine, and rabbit anti-thymocyte globulin. *Bone Marrow Transplantation* (2005) 35(2):171–7. doi: 10.1038/sj.bmt.1704745

6. Iannone R, Casella JF, Fuchs EJ, Chen AR, Jones RJ, Woolfrey A, et al. Results of minimally toxic nonmyeloablative transplantation in patients with sickle cell anemia and β-thalassemia. *Biol Blood Marrow Transplantation* (2003) 9(8):519–28. doi: 10.1016/S1083-8791(03)00192-7

7. Iannone R, Luznik L, Engstrom LW, Tennessee SL, Askin FB, Casella JF, et al. Effects of mixed hematopoietic chimerism in a mouse model of bone marrow transplantation for sickle cell anemia. *Blood* (2001) 97(12):3960–5. doi: 10.1182/blood.v97.12.3960

8. Bolanos-Meade J, Cooke KR, Gamper CJ, Ali SA, Ambinder RF, Borrello IM, et al. Effect of increased dose of total body irradiation on graft failure associated with HLA-haploidentical transplantation in patients with severe haemoglobinopathies: a prospective clinical trial. *Lancet Haematol* (2019) 6(4): e183–e93. doi: 10.1016/s2352-3026(19)30031-6

9. Thomas ED, Clift RA, Hersman J, Sanders JE, Stewart P, Buckner CD, et al. Marrow transplantation for acute nonlymphoblastic leukemic in first remission using fractionated or single-dose irradiation. *Int J Radiat Oncol Biol Phys* (1982) 8 (5):817–21. doi: 10.1016/0360-3016(82)90083-9

10. Brochstein JA, Kernan NA, Groshen S, Cirrincione C, Shank B, Emanuel D, et al. Allogeneic bone marrow transplantation after hyperfractionated total-body irradiation and cyclophosphamide in children with acute leukemia. *New Engl J Med* (1987) 317(26):1618–24. doi: 10.1056/nejm198712243172602

11. Clift RA, Buckner CD, Appelbaum FR, Bearman SI, Petersen FB, Fisher LD, et al. Allogeneic marrow transplantation in patients with acute myeloid leukemia in first remission: a randomized trial of two irradiation regimens. *Blood* (1990) 76 (9):1867–71. doi: 10.1182/blood.V76.9.1867.1867

12. Petersen FB, Deeg HJ, Buckner CD, Appelbaum FR, Storb R, Clift RA, et al. Marrow transplantation following escalating doses of fractionated total body irradiation and cyclophosphamide–a phase I trial. *Int J Radiat Oncol Biol Phys* (1992) 23(5):1027–32. doi: 10.1016/0360-3016(92)90909-2

13. Demirer T, Petersen FB, Appelbaum FR, Barnett TA, Sanders J, Deeg HJ, et al. Allogeneic marrow transplantation following cyclophosphamide and escalating doses of hyperfractionated total body irradiation in patients with advanced lymphoid malignancies: a phase I/II trial. *Int J Radiat Oncol Biol Phys* (1995) 32(4):1103–9. doi: 10.1016/0360-3016(95)00115-f

14. Kal HB, Loes van Kempen-Harteveld M, Heijenbrok-Kal MH, Struikmans H. Biologically effective dose in total-body irradiation and hematopoietic stem cell transplantation. *Strahlenther Onkol* (2006) 182(11):672–9. doi: 10.1007/s00066-006-1528-6

15. Hui SK, Kapatoes J, Fowler J, Henderson D, Olivera G, Manon RR, et al. Feasibility study of helical tomotherapy for total body or total marrow irradiation. *Med physics* (2005) 32(10):3214–24. doi: 10.1118/1.2044428

16. Stein A. *Dose Escalation of Total Marrow and Lymphoid Irradiation in Advanced Acute Leukemia*. Total Marrow Irradiation Eds. J. Wong, S. Hui (2020). Springer, Cham. PP 69–75. doi: 10.1007/978-3-030-38692-4_4

17. Duval M, Klein J, He W, Cahn J, Cairo M, Camitta B, et al. Hematopoietic stem-cell transplantation for acute leukemia in relapse or primary induction failure. *J Clin Oncol* (2010) 28(23):3730. doi: 10.1200/JCO.2010.28.8852

18. Manci EA, Hillery CA, Bodian CA, Zhang ZG, Lutty GA, Coller BS. Pathology of Berkeley sickle cell mice: similarities and differences with human sickle cell disease. *Blood* (2006) 107(4):1651–8. doi: 10.1182/blood-2005-07-2839

19. Stein A, Palmer J, Tsai NC, Al Malki MM, Aldoss I, Ali H, et al. Phase I trial of total marrow and lymphoid irradiation transplantation conditioning in patients with Relapsed/Refractory acute leukemia. *Biol Blood marrow Transplant J Am Soc Blood Marrow Transplantation* (2017) 23(4):618–24. doi: 10.1016/j.bbmt.2017.01.067

20. Zuro D, Madabushi SS, Brooks J, Chen BT, Goud J, Salhotra A, et al. First multimodal, three-dimensional, image-guided total marrow irradiation model for preclinical bone marrow transplantation studies. *Int J Radiat OncolBiolPhys* (2021) 111(3):671–83. doi: 10.1016/j.ijrobp.2021.06.001

21. Sagi V, Song-Naba WL, Benson BA, Joshi SS, Gupta K. Mouse models of pain in sickle cell disease. *Curr Protoc Neurosci* (2018) 85(1):e54. doi: 10.1002/cpns.54

22. Kumar B, Madabushi SS. Identification and isolation of mice and human hematopoietic stem cells. In: *Singh SR, rameshwar p, editors. somatic stem cells: Methods and protocols*. New York, NY: Springer New York (2018). p. 55–68.

23. Vincent L, Vang D, Nguyen J, Gupta M, Luk K, Ericson ME, et al. Mast cell activation contributes to sickle cell pathobiology and pain in mice. *Blood* (2013) 122(11):1853–62. doi: 10.1182/blood-2013-04-498105

24. Brooks J, Zuro D, Song JY, Madabushi SS, Sanchez JF, Guha C, et al. Longitudinal preclinical imaging characterizes extracellular drug accumulation after radiation therapy in the healthy and leukemic bone marrow vascular microenvironment. *Int J Radiat Oncol Biol Phys* (2022) 112(4):951–63. doi: 10.1016/j.ijrobp.2021.10.146

25. Kasztan M, Fox BM, Speed JS, De Miguel C, Gohar EY, Townes TM, et al. Long-term endothelin-a receptor antagonism provides robust renal protection in humanized sickle cell disease mice. *J Am Soc Nephrol* (2017) 28(8):2443–58. doi: 10.1681/asn.2016070711

26. Pestina TI, Hargrove PW, Zhao H, Mead PE, Smeltzer MP, Weiss MJ, et al. Amelioration of murine sickle cell disease by nonablative conditioning and γ-globin gene-corrected bone marrow cells. *Mol Ther Methods Clin Dev* (2015) 2:15045. doi: 10.1038/mtm.2015.45

27. Devadasan D, Sun CW, Westin ER, Wu LC, Pawlik KM, Townes TM, et al. Bone marrow transplantation after nonmyeloablative treosulfan conditioning is curative in a murine model of sickle cell disease. *Biol Blood marrow Transplant J Am Soc Blood Marrow Transplantation* (2018) 24(8):1554–62. doi: 10.1016/j.bbmt.2018.04.011

28. Fox N, Priestley G, Papayannopoulou T, Kaushansky K. Thrombopoietin expands hematopoietic stem cells after transplantation. *J Clin Invest* (2002) 110 (3):389–94. doi: 10.1172/jci15430

29. Aich A, Jones MK, Gupta K. Pain and sickle cell disease. *Curr Opin Hematol* (2019) 26(3):131–8. doi: 10.1097/moh.0000000000000491

30. Gupta K, Jahagirdar O, Gupta K. Targeting pain at its source in sickle cell disease. *Am J Physiol Regul Integr Comp Physiol* (2018) 315(1):R104–r12. doi: 10.1152/ajpregu.00021.2018

31. Kaul DK, Liu XD, Chang HY, Nagel RL, Fabry ME. Effect of fetal hemoglobin on microvascular regulation in sickle transgenic-knockout mice. *J Clin Invest* (2004) 114(8):1136–45. doi: 10.1172/jci21633

32. Delicou S. Extramedullary Haemopoiesis in Hemoglobinopathies. *J Hematol Transfus* (2017) 5(2): 1066.

33. Blouin MJ, De Paepe ME, Trudel M. Altered hematopoiesis in murine sickle cell disease. *Blood* (1999) 94(4):1451–9. doi: 10.1182/blood.V94.4.1451

34. Pizzi M, Gergis U, Chaviano F, Orazi A. The effects of hematopoietic stem cell transplant on splenic extramedullary hematopoiesis in patients with myeloproliferative neoplasm-associated myelofibrosis. *Hematol Oncol Stem Cell Ther* (2016) 9(3):96–104. doi: 10.1016/j.hemonc.2016.07.002

35. Mouthon MA, Vandamme M, Gourmelon P, Vainchenker W, Wendling F. Preferential liver irradiation enhances hematopoiesis through a thrombopoietin-independent mechanism. *Radiat Res* (1999) 152(4):390–7. doi: 10.2307/3580223

36. Kobayashi M, Laver JH, Kato T, Miyazaki H, Ogawa M. Thrombopoietin supports proliferation of human primitive hematopoietic cells in synergy with steel factor and/or interleukin-3. *Blood* (1996) 88(2):429–36. doi: 10.1182/blood.V88.2.429.bloodjournal882429

37. Sitnicka E, Lin N, Priestley GV, Fox N, Broudy VC, Wolf NS, et al. The effect of thrombopoietin on the proliferation and differentiation of murine hematopoietic stem cells. *Blood* (1996) 87(12):4998–5005. doi: 10.1182/blood.V87.12.4998.bloodjournal87124998

frontiers | Frontiers in Oncology

TYPE Review
PUBLISHED 03 October 2022
DOI 10.3389/fonc.2022.1003908

OPEN ACCESS

EDITED BY
Wei Liu,
Mayo Clinic Arizona, United States

REVIEWED BY
Xin Wang,
University of Texas MD Anderson Cancer Center, United States
Ramzi Abboud,
Washington University in St. Louis, United States
Jacopo Mariotti,
Humanitas Research Hospital, Italy

*CORRESPONDENCE
Jeffrey Y.C. Wong
jwong@coh.org

SPECIALTY SECTION
This article was submitted to Radiation Oncology, a section of the journal Frontiers in Oncology

RECEIVED 26 July 2022
ACCEPTED 12 September 2022
PUBLISHED 03 October 2022

CITATION
Wong JYC, Liu A, Han C, Dandapani S, Schultheiss T, Palmer J, Yang D, Somlo G, Salhotra A, Hui S, Al Malki MM, Rosenthal J and Stein A (2022) Total marrow irradiation (TMI): addressing an unmet need in hematopoietic cell transplantation - a single institution experience review. *Front. Oncol.* 12:1003908. doi: 10.3389/fonc.2022.1003908

Total marrow irradiation (TMI): Addressing an unmet need in hematopoietic cell transplantation - a single institution experience review

Jeffrey Y.C. Wong[1*], An Liu[1], Chunhui Han[1], Savita Dandapani[1], Timothy Schultheiss[1], Joycelynne Palmer[2], Dongyun Yang[2], George Somlo[3], Amandeep Salhotra[3], Susanta Hui[1], Monzr M. Al Malki[3], Joseph Rosenthal[4] and Anthony Stein[3]

[1]Departments of Radiation Oncology, City of Hope, Duarte, CA, United States, [2]Department Computational and Quantitative Medicine, City of Hope, Duarte, CA, United States, [3]Department of Hematology and Hematopoietic Cell Transplantation, City of Hope, Duarte, CA, United States, [4]Department of Pediatrics, City of Hope, Duarte, CA, United States

Purpose: TMI utilizes IMRT to deliver organ sparing targeted radiotherapy in patients undergoing hematopoietic cell transplantation (HCT). TMI addresses an unmet need, specifically patients with refractory or relapsed (R/R) hematologic malignancies who have poor outcomes with standard HCT regimens and where attempts to improve outcomes by adding or dose escalating TBI are not possible due to increased toxicities. Over 500 patients have received TMI at this center. This review summarizes this experience including planning and delivery, clinical results, and future directions.

Methods: Patients were treated on prospective allogeneic HCT trials using helical tomographic or VMAT IMRT delivery. Target structures included the bone/marrow only (TMI), or the addition of lymph nodes, and spleen (total marrow and lymphoid irradiation, TMLI). Total dose ranged from 12 to 20 Gy at 1.5-2.0 Gy fractions twice daily.

Results: Trials demonstrate engraftment in all patients and a low incidence of radiation related toxicities and extramedullary relapses. In R/R acute leukemia TMLI 20 Gy, etoposide, and cyclophosphamide (Cy) results in a 1-year non-relapse mortality (NRM) rate of 6% and 2-year overall survival (OS) of 48%; TMLI 12 Gy added to fludarabine (flu) and melphalan (mel) in older patients (≥ 60 years old) results in a NRM rate of 33% comparable to flu/mel alone, and 5-year OS of 42%; and TMLI 20 Gy/flu/Cy and post-transplant Cy (PTCy) in haplo-identical HCT results in a 2-year NRM rate of 13% and 1-year OS of 83%. In AML in complete remission, TMLI 20 Gy and PTCy results in 2-year NRM, OS, and GVHD free/relapse-free survival (GRFS) rates of 0%, 86·7%, and 59.3%, respectively.

Conclusion: TMI/TMLI shows significant promise, low NRM rates, the ability to offer myeloablative radiation containing regimens to older patients, the ability to dose escalate, and response and survival rates that compare favorably to published results. Collaboration between radiation oncology and hematology is key to successful implementation. TMI/TMLI represents a paradigm shift from TBI towards novel strategies to integrate a safer and more effective target-specific radiation therapy into HCT conditioning beyond what is possible with TBI and will help expand and redefine the role of radiotherapy in HCT.

KEYWORDS

total marrow irradiation, total marrow and lymphoid irradiation, tomotherapy, VMAT, acute leukemia, hematopoietic stem cell transplant, bone marrow transplantation, total body irradiation

Background and rationale

Total marrow irradiation (TMI) and total marrow and lymphoid irradiation (TMLI) are methods to deliver organ sparing targeted radiotherapy using intensity modulated radiation therapy (IMRT). This approach offers radiation oncologists, hematologists and the bone marrow transplant team the ability to reduce dose to critical organs or any other anatomic region, while increasing dose to user-defined targets depending on the clinical situation. TMI and TMLI represent a departure from total body irradiation (TBI) and a paradigm shift in the use of radiotherapy as part of the conditioning regimen in hematopoietic cell transplantation (HCT).

The concept of TMI was first proposed in 2001. To implement this concept required close collaboration between radiation oncology and hematology, the development of treatment planning methods (2002) (1–3), the design of three initial pilot and phase 1 clinical trials (2003–2004), and culminated in treatment of the first patient in June, 2005 (4, 5) using a TomoTherapy HiArt System®. TMI and TMLI were originally developed by our group to address an unmet need in patients undergoing HCT, specifically patients with advanced, refractory or relapsed (R/R) hematologic malignancies who have poor outcomes with standard conditioning regimens, who could not tolerate standard total body irradiation (TBI), and where attempts to improve outcomes by adding or dose escalating conventional TBI was not possible due to associated toxicities. Clinical settings where TMI and TMLI were felt to have potential application included 1) patients older than 60 years of age who cannot tolerate standard TBI; 2) patients who have poor outcomes with reduced intensity conditioning (RIC) regimens and where the addition of TBI to RIC is not feasible (6); and 3) patients with R/R acute leukemia where dose escalation of TBI reduced relapse rates but also increased toxicities, negating any gains in survival (7). The emphasis was on redefining and expanding the use of radiation containing conditioning regimens to a new group of patients, in addition to reducing toxicities from conventional TBI for existing patients.

Since the first patient was treated with TMI in 2005, over 500 patients have been treated at this center. This review will summarize this clinical experience; the total doses, dose distributions, and fractionation schedules used; the approach to planning and delivery; the rationale and results of past and current trials; and perspectives on the future directions in this field.

Implementation of TMI

Initial treatment planning studies

The development of TMI at this center from initial concept to treatment of the first patient spanned 4 years and involved from the beginning collaboration between radiation oncologists, medical physicists and hematologists. We proposed the concept of TMI to TomoTherapy, Inc. in 2001, prior to FDA approval of the TomoTherapy Hi-Art system in 2002. Initially, the TomoTherapy Hi-Art system was not designed to plan and deliver TMI. Software and hardware modifications to the treatment planning system had to be made by the manufacturer since TMI planning required large complex data sets due to the need for whole body imaging and multiple organ contouring on a scale that had not been attempted before.

The first TMI treatment plan, where the target region was defined as the skeletal bone, was based on a whole-body CT data set of a 20-year-old woman with acute myelogenous leukemia (Figure 1). Treatment planning studies compared TMI to standard TBI using 50% transmission lung blocks with electron boost to the underlying chest wall. This demonstrated

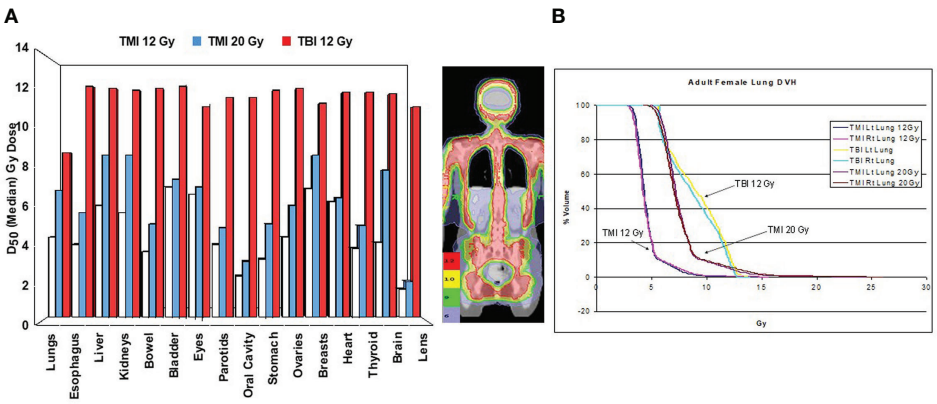

FIGURE 1
First TMI treatment plan comparison at City of Hope comparing in the same patient TBI 12 Gy, TMI 12 Gy and TLI 20 Gy (4). **(A)** Median organ doses. **(B)** Dose volume histogram curves for lung.

median organ doses with TMI that were 20-70% of the target dose, significantly less than TBI where most organs received 11.5-13.1 Gy and the shielded lungs 9.0-9.7 Gy. This predicted for a reduction of acute and late toxicities compared to TBI. At TMI doses up to 20 Gy, median doses to all organs were still below that of TBI to 12 Gy (Figure 1A). At 20 Gy TMI lung dose volume histogram (DVH) plots (Figure 1B) demonstrated the minimum dose to at least 80% of the lung volume (D_{80}) was comparable to 12 Gy TBI.

These initial plan comparisons determined radiation dose distributions and organ dose constraints for the initial clinical trials. These plan comparison studies also helped to communicate the concept and advantages of TMI and TMLI to our hematologists, leading to clinical trial development, acquisition of the first TomoTherapy system and the treatment of the first patient. The highest prescribed dose level on phase I trials was limited to 20 Gy since lung doses began to approach that of conventional TBI with lung shielding (4), predicting for comparable risks of pneumonitis (8). For all trials the mandible was not included as a target structure to reduce the likelihood of severe oral mucositis, which was a primary toxicity of the myeloablative TBI and etoposide regimens used at this center. TMLI preceded chemotherapy as with standard TBI regimens used at this center. Fraction size and schedule was 1.5 to 2.0 Gy twice a day with a minimum of 6 hours between fractions, a fractionation schedule widely used to deliver TBI.

Figure 2 displays radiation dose distribution patterns used at this center. The term TMI is used if the target structure is bone and was used in an initial tandem autologous HCT trial in patients with advanced multiple myeloma (Figure 2A) (9, 14). The term TMLI is used when the major lymph node chains and spleen are added as target regions to achieve the immunosuppression needed for allogeneic HCT and is used at this center primarily for patients 60 years of age or older (Figure 2B) (11, 15). In patients younger than age 60 undergoing allogeneic HCT, liver and brain are added as target regions to TMLI (Figure 2C) (16).

TMI and TMLI have been delivered on clinical trials at this institution so that data could be prospectively collected to address questions and concerns prior to treating the first patient. Was the delivery of TMI and TMLI feasible and safe? Would the higher dose rates compared to conventional TBI increase organ toxicities, graft versus host disease (GVHD), or engraftment failure? Would dose reduction to organs at risk (OARs) and the helical tomographic or volumetric modulated arc radiotherapy (VMAT) delivery of radiation therapy spare circulating leukemia cells and lead to increased relapse rates?

Simulation, planning, and treatment delivery

CT simulation is performed in the supine position. Immobilization is with a body vac-lok™ bag (CIVCO Medical Systems, Kalona, IA) from the base of neck to the feet, a type-S thermoplastic head frame (CIVCO, Kalona, Iowa, IA), and Accuform™ cushion to immobilize the head and shoulders. CT scans are obtained using 5-8mm slice thickness. A body CT scan is obtained with normal quiet breathing and is used of treatment planning. 4D CT scans of the chest and abdomen are utilized to account for any organ motion with respiration. Radiopaque markers are placed at mid-thigh to identify the junction for planning. If treatment will be on a Tomotherapy unit, the patient is positioned with the top of the head 5 cm from the end of the couch and the couch height is 10 cm below the isocenter of the gantry.

Contouring is done on an Eclipse workstation (Varian Medical Systems, Palo Alto, California). The following organs are contoured in all patients: lungs, heart, kidneys, liver, esophagus, oral cavity, parotid glands, thyroid gland, eyes,

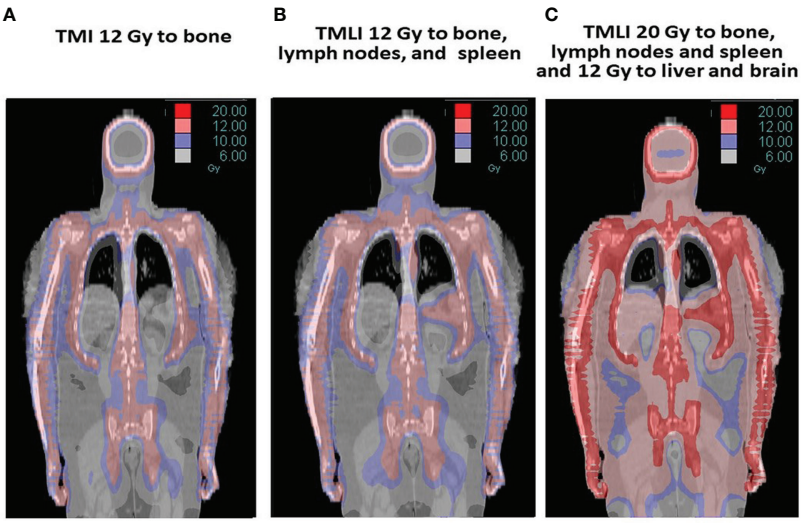

FIGURE 2
The term TMI is used if the target is bone **(A)** and was used in a tandem autologous HCT multiple myeloma trial (9, 10). TMLI adds the major lymph node chains and spleen as target regions and is used in allogeneic HCT regimens **(B)** (11). In some studies, TMLI also includes the liver and brain to 12 Gy while other target regions (bone, lymph nodes and spleen) are escalated to 20 Gy **(C)** (12, 13).

lens, optic chiasm and nerves, brain, stomach, small and large intestine, breasts, rectum, testes, ovary and bladder. Target structures are defined by the treatment team and clinical trial. The 4D CT datasets are used for contouring the ribs, kidneys, spleen and liver to account for any respiratory motion. Maxillary and mandibular bones are excluded as targets to reduce oral cavity dose. A 5-10 mm margin around the CTV is usually used to define the PTV. The use of whole-body auto-segmentation software has significantly reduced the time needed for contouring.

The majority of patients to date have been treated on a TomoTherapy system. With TomoTherapy planning system optimum results are achieved when organ dose reduction is performed first followed by target dose optimization. For most plans the target receives a minimum of 85% of the prescribed dose. Most patients are treated using a jaw setting of 5 cm, modulation factor of 2.5, and pitch of 0.287. Legs and feet are planned in Tomo-Direct mode or with conventional AP/PA fields. Volumetric imaging is used for daily patient setup. On TomoTherapy, a megavoltage CT (MVCT) or kilovoltage CT (kVCT) scan is performed from the skull to iliac crest.

TMLI has also been delivered at this center using a Varian TrueBeam linear accelerator (Varian Medical Systems, Palo Alto, California) with VMAT capability (17). Four to five isocenters are used for the upper body TMLI treatment plan, with two arc fields typically placed for each isocenter. A 120-leaf multi-leaf collimator is used. The leaf width is 5 mm for the central 40 leaf pairs and 1 cm for the peripheral 20 leaf pairs. The collimator angle is at 90°C so that the MLC leaves move along the longitudinal direction of the patient. Asymmetric jaws are used along the patient's longitudinal direction so that the two arc fields at each isocenter cover different patient body lengths. A 6-MV photon beam is used for all the VMAT fields. The lower extremities are planned and treated with junctioned AP-PA fields. For setup on the Varian TrueBeam linear accelerator, two cone-beam CT (CBCT) scans are performed, one in the head & neck region and the other in the abdominal and pelvic region.

A review of organ doses on over 200 patients treated at this center with TMLI has recently been published by Han et al. (18). Tables 1, 2 provide select mean organ doses for patients treated at 12 and 20 Gy TMLI. Average dose-rates are 130-180 cGy/minute to the target and 70-90 cGy/minute to the lung. TMI and conventional TBI planning and delivery at this center require similar time and resources (19). Details regarding simulation, immobilization, planning, and treatment delivery have previously been published by Liu et al. (19), Han et al. (18) and Schultheiss et al. (1, 2, 5).

Review of clinical results

Initial demonstration of feasibility, acceptable toxicities and dose escalation using TMI

Somlo et al. first reported the results of a Phase I/II trials using TMI in patients with multiple myeloma undergoing

TABLE 1 Summary of mean organ dose (Gy) for patients treated with 12 Gy TMLI (n = 108).

Organ at Risk	Mean Dose ± SD (Gy)12 Gy TMLI	Range (Gy)12 Gy TMLI
Bladder	7.60 ± 1.53	3.75 - 11.47
Brain	6.68 ± 0.88	5.09 - 8.99
Esophagus	4.95 ± 0.92	3.19 – 7.72
Heart	6.12 ± 1.01	3.80 – 8.39
GI - Lower	5.91 ± 0.87	4.61 – 9.00
GI - Upper	5.22 ± 0.84	3.78 - 7.82
Kidneys	5.68 ± 1.37	3.10 – 8.34
Lens	2.17 ± 0.94	1.00 – 6.93
Liver	7.22 ± 0.94	3.17 – 9.07
Lungs	6.20 ± 0.61	4.40 – 7.41
Oral Cavity	3.20 ± 0.61	1.78. – 5.05
Parotids	5.43 ± 1.12	3.41 – 9.61
Rectum	4.87 ± 1.00	2.36 – 7.54
Thyroid	5.98 ± 1.70	3.08 - 12.15

Target structures are bone, major lymph node chains and spleen (Figure 2B) (18).

autologous tandem HCT (9). High dose melphalan conditioning is often used (20, 21). Myeloablative TBI added to high dose melphalan was not feasible due to dose-limiting mucositis (22). Since this trial was the first-in-human use of TMI and given the concerns of increased toxicities due to higher dose-rate, TMI was delivered without concurrent chemotherapy and a fractionation schedule similar to standard TBI was used.

Patients with Salmon-Durie stage I-III multiple myeloma and with stable or responding disease after first line therapy were entered. Patients first received melphalan (200 mg/m^2) followed by autologous HCT. Six to ten weeks later they received TMI to bone (Figure 2A) followed by a second autologous HCT. TMI dose was escalated from 10 to 18 Gy. The fractionation was 2 Gy delivered twice a day with 6 hours between fractions. Median organ doses were 11% to 81% of the prescribed bone dose (9), A maximum tolerated dose (MTD) of 16 Gy was defined based on toxicities seen at 18 Gy (1 patient with reversible grade 3 pneumonitis and 1 patient with grade 3 hypotension attributed to engraftment syndrome). This was followed by an expansion of patients treated at 16 Gy TMI (10). Of the 54 patients on this study, 30 patients (55.6%) underwent TMI at the MTD of 16 Gy. Median follow-up of surviving patients was 12.3 years (9.2 - 15.5+). Overall survival (OS) at 10 years were 38.8% with a progression-free survival (PFS) plateau of 20.4%. The first patient with stage I disease remains in remission 18 years after TMI. TMI for multiple myeloma before autologous HCT warrants further study.

TABLE 2 Summary of mean organ dose (Gy) for patients treated with 20 Gy TMLI (n = 120).

Organ at Risk	Mean Dose ± SD (Gy)20 Gy TMLI	Range (Gy)20 Gy TMLI
Bladder	9.71 ± 1.49	5.96 – 14.56
Esophagus	6.50 ± 0.87	3.17 – 8.73
Heart	7.38 ± 0.56	5.78 – 8.55
GI - Lower	10.15 ± 1.11	6.60 – 13.23
GI - Upper	9.01 ± 1.34	6.24 – 12.59
Kidneys	7.28 ± 0.69	5.39 – 9.08
Lens	2.55 ± 0.41	1.78 – 4.36
Lungs	8.48 ± 0.83	6.22 – 10.19
Oral Cavity	4.43 ± 0.97	2.95 – 7.08
Parotids	8.05 ± 1.31	5.64 – 12.21
Rectum	6.46 ± 0.88	4.58 – 9.06
Thyroid	8.01 ± 2.13	3.67 – 17.12

Target structures are bone, major lymph node chains and spleen with liver and brain limited to 12 Gy (Figure 2C) (18).

Dose escalation of TMLI in younger patients (< 60 Years Old) with relapsed/ refractory acute leukemia

There is a dose response for acute leukemia. For chloromas local control rates are approximately 20% after doses < 10 Gy, 40% after 10-20 Gy and over 80% after doses > 20 Gy (23). A decrease in relapse rate with higher TBI doses has been observed (24–26). Randomized phase II single institution trials have compared 12 Gy versus 15.75 Gy TBI combined with cyclophosphamide (Cy) (7, 27). In patients with AML in first remission, TBI to 15.75 Gy resulted in a reduction in relapse rate (14% versus 39% p = 0.06), but an increase in NRM rate (38% versus 19%, p = 0.05), resulting in no difference in overall survival between the two arms (7). A higher incidence of grade 3-4 hepatotoxicity, grade 3-4 renal toxicity, grade 2 mucositis and GVHD was observed with the higher TBI dose (28, 29). These data suggest that a more targeted form of radiotherapy such as TMLI, which reduces dose to the liver, kidneys, lungs, oral cavity, esophagus and GI tract, is needed before clinically important dose escalation becomes feasible with acceptable toxicities. In addition, escalation of conditioning regimens by adding chemotherapy to myeloablative regimens in patients with active leukemia resulted in long term cure in up to 30-40% cases, indicating that escalation of conditioning intensity may induce cure in some patients with advanced leukemia (30).

Dose escalation trials at this center were initiated in patients with R/R AML and ALL. Long term OS and PFS rates in these patients are less than 20% after standard allogeneic HCT (31). TMLI, busulfan [days -12 to -8 (800 uM min)] and etoposide [day -3 (30 mg/kg)] conditioning was evaluated in a phase I trial (32). TMLI dose was 12 Gy (n=18) and 13.5 Gy (n=2) at 1.5 Gy twice daily. The target structures were bone and bone marrow, major lymph node regions and spleen. Liver and brain received 12 Gy. (Figure 2C). Twenty patients were treated, with 19 patients still with detectable blasts in marrow and 13 detectable circulating blasts prior to HCT. Grade 4 dose limiting toxicities of stomatitis and sinusoidal obstructive syndrome (SOS) were seen at 13.5 Gy. Hepatotoxicity was likely due the combination of busulfan and a liver dose of 12 Gy, each of which has been associated with a risk of SOS. TMLI dose escalation was not feasible with this regimen.

Stein et al. (16) reported results of a phase I trial using a conditioning regimen of escalating doses of TMLI [(range: 12-20 Gy, in 2 Gy increments) 1.2 - 2 Gy twice a day, from day -10 to day -6] with Cy (100 mg/kg day -3) and VP-16 (60 mg/kg day -5). in a phase I trial of 51 patients with R/R AML (n=33) and ALL (n=16) (NCT02446964). The target structures were bone and bone marrow, major lymph node regions and spleen. Liver and brain were kept at 12 Gy. (Figure 2C). Fifty patients had detectable blasts in marrow (median 52%, range 5-98% involvement) and 27 patients had circulating blasts in the week prior to HCT conditioning. Dose-limiting toxicity (DLT) (Bearman scale grade 3 mucositis) (28) was observed in 1 patient at the 15 Gy dose level. No further DLTs were observed up to 20 Gy. All patients engrafted without delays. Median follow-up was 24.6 months in surviving patients. The 1-year OS was 55.5% and PFS was 40.0%. NRM rates were 3.9% at day 100 and 8.1% at 1-year.

A subsequent phase II trial evaluating the same regimen is currently ongoing at this center (NCT 02094794). A recent analysis of the first 57 patients with AML (n=43) and ALL (n=14) treated with TMLI doses of 20 Gy reported a 1-year NRM rate of 6% and 2-year OS and PFS of 48% and 33%, respectively, which compare favorably to published results (12, 33). All patients engrafted. Mean organ doses were 20-51% of the target dose. Mean organ doses (Gy) were lung 9.1, kidneys 7.3, GI tract 10.3, esophagus 6.7, and oral cavity 4.3. In summary TMLI to 20 Gy can be safely delivered with etoposide and cyclophosphamide with low NRM rates of <10% and with encouraging PFS and OS in patients < 60 years old with R/R acute leukemia.

These trials are in patients with relapsed and refractory acute leukemia with detectable blasts in marrow and circulation just prior to TMLI. These patients have a dismal outcome after HCT with a long-term survival of 16% to 19% (31). Patients with acute leukemia who relapse after first remission are usually unable to achieve a second remission with salvage chemotherapy and have very few therapeutic options outside of clinical trials (34). Patients with relapsed and refractory acute leukemia are not transplanted at most center. Therefore, there are no consensus standard of care HCT regimens that the results of these trials can be compared to. Case examples that follow illustrate the type of patients entered on these studies.

Case example. A 29-year-old female with relapsed AML in marrow, CNS and lymph nodes. The patient initially achieved complete remission after 7 + 3 induction and 1 cycle consolidation with high dose cytarabine. She developed right orbital and CNS relapse. She received intrathecal chemotherapy followed by whole brain radiotherapy to 12 Gy. She then developed back and left leg pain from enlarged retroperitoneal and bilateral common iliac and internal iliac lymph nodes. Bone marrow and lymph node biopsies were positive for AML. She was started on mitoxantrone, etoposide and cytarabine chemotherapy. Prior to transplant CSF and marrow were negative for disease but FDG-PET scan demonstrated persistently positive lymph nodes. She received TMLI 20 Gy (12 Gy to liver and brain), etoposide, and cyclophosphamide followed by matched related donor stem cell infusion. She remains relapse free at 6 years and 1 month with mild oral and cutaneous chronic GVHD.

TMLI integrated with reduced intensity conditioning fludarabine and melphalan in older patients (> 60 years old) with R/R acute leukemia

In patients older than 60 years of age, myeloablative regimens can lead to unacceptably high NRM rates of ~20% at 100 days and 40% at 3 years (35). In these patients reduced intensity conditioning (RIC) regimens have been used (36) and are better tolerated, but can be less cytotoxic and rely more on the graft-versus-leukemia (GVL) effects to eradicate disease. As a result RIC regimens can result in a significant increase in relapse rates and decrease in OS and relapse-free survival (RFS) (37). Attempts to add standard 9 Gy TBI to a RIC regimen to reduce relapse rates resulted in unacceptable toxicities (6). Organ sparing targeted radiotherapy such as TMLI is needed (11, 15, 38, 39), specifically for older patients with limited HCT options, who present frequently with more aggressive and chemo-resistant disease, are unable to tolerate standard myeloablative regimens (40, 41), and where reduced intensity conditioning (RIC) regimens can be associated with increased relapse rates (37).

Rosenthal et al. in a pilot trial (NCT 00544466) evaluated TMLI 12 Gy (1.5 Gy twice a day, days -7 to -4) added to an established RIC regimen of fludarabine (flu) (25 mg/m^2/d Days -7 to -4) and melphalan (mel) (140 mg/m^2 Day -2) in patients with R/R acute leukemia in patients > 60 years old or those who could not tolerate TBI containing regimens due to co-morbidities (11, 15). Flu-mel is a frequently used conditioning regimen in high risk acute leukemia patients in complete first or second remission (CR1/CR2), which is the reason TMLI was added for R/R acute leukemia with higher tumor burden. The target structures included bone/marrow, major lymph node regions and spleen (Figure 2B). Brain and testes were included in patients with ALL. Sixty-one patients were treated with a median age of 55 years (9-70 years) (15). Acute leukemia comprised 72% of the study population (AML 57% and ALL 17%). The most common toxicity was mucositis. All patients engrafted without delays. Median follow-up was 7.4 years. Five-year OS, event free survival (EFS), cumulative incidence of relapse (CIR), and NRM were 42%, 41%, 26%, and 33%, respectively. Results confirmed that the addition of 12 Gy TMLI to Flu/Mel was feasible, with favorable long-term outcomes and with a NRM rate that was comparable to flu/mel alone (42–45).

Case example. A 65-year-old male with AML was entered on this trial with induction failure. He had failed to achieve remission after 7 + 3 induction chemotherapy, cladribine, cytarabine, idarubicin, decitabine, high dose cytarabine and NK cells, and anti-CD34 antibody-chemotherapy conjugate therapy. He was referred to City of Hope from another tertiary bone marrow transplant program for this trial. He received 12 Gy TMLI, fludarabine 25 mg/m^2 for 5 days, melphalan 140 mg/m^2 followed by matched related donor stem cell infusion. He remains relapse free at 5.5 years and has mild GVHD of the gut (mouth and stomach).

A successor phase I trial (NCT 03490569) is ongoing and is focused on dose escalation in this same population. To reduce toxicities and allow for dose escalation, the regimen was modified to evaluate TMLI 12-20 Gy (1.5-2.0 Gy twice a day, days -9 to -5) combined with reduced doses of fludarabine (30 mg/m^2/d Days -4 to -2) delivered after instead of concurrent with TMLI and reduced doses of melphalan (100 mg/m^2 Day -2).

TMLI added to strategies to reduce GVHD in patients with haplo-identical donors

Graft versus host disease (GVHD) remains a major cause of morbidity and mortality in patients undergoing allogeneic HCT (46). Strategies to reduce GVHD are especially important in patients without a matched donor such as those with haplo-identical donors. GVHD prophylactic regimens traditionally have used methotrexate, calcineurin or mTOR inhibitors, mycophenolate mofetil and anti-thymocyte globulins. Post-transplant cyclophosphamide (PTCy) is a potent immunosuppressive agent that has been successfully used in combination with a calcineurin or mTOR inhibitors to prevent GVHD in HLA-matched and haploidentical transplants in multiple studies (47–54). PTCy also can be used as a single-agent GVHD prophylaxis after myeloablative HLA-matched related or unrelated bone marrow transplant (47). The mechanisms of action pf PTCy are thought to involve preferential killing or functional impairment of alloreactive T cell and enrichment of the regulatory T cell population which are more resistant to PTCy (47, 55–58).

These strategies while reducing GVHD can reduce the graft versus leukemia (GVL) effects, potentially resulting in higher relapse rates, as demonstrated in patients with AML undergoing haplo-identical donor HCT with RIC conditioning regimens and PTCy (59). Al Malki et al. evaluated the addition of dose escalated TMLI to an established PTCy conditioning regimen (39) to further reduce relapse rates without contributing to NRM or GVHD. The target structures were bone and bone marrow, major lymph node regions and spleen. Liver and brain were treated to 12 Gy. In a phase I trial (NCT02446964) 31 patients [median age 37 (21–58)] with high-risk or R/R acute leukemias or myelodysplastic syndrome underwent haplo-identical HCT conditioning with TMLI, concurrent fludarabine (25 mg/m^2/day on day -7 to day -3) and Cy (14 mg.kg/day on days -7 and -6). TMLI dose was escalated from 12 to 20 Gy. GVHD prophylaxis was PTCy (50 mg/kg/d on days +3 and +4) with tacrolimus/mycophenolate mofetil. All patients engrafted. With a follow-up

of 23.9 months for the whole cohort, 2-year NRM was 13%; cumulative incidence of day 100 grade 2-4 and 3-4 acute GvHD were 52%, 6%, respectively and chronic GVHD at 2 years was 35%. For patients at the recommended phase 2 dose (RP2D) of 20 Gy (n=12) the 1-year relapse rate, PFS and OS were 17%, 74% and 83%; respectively. HaploHCT with TMLI with PTCy was safe and feasible, with promising low relapse rates achieved with acceptable GVHD or NRM.

A phase II trial in patients < age 60 with R/R acute leukemia is ongoing (NCT04262843). For patients age 60 or older with R/R acute leukemia a phase I haploidentical HCT trial (NCT 03490569) of TMLI 12-20 Gy (1.5-2.0 Gy twice a day, days -9 to -5), fludarabine (30 mg/m^2/d Days -4 to -2), melphalan (100 mg/m^2 Day -2) and PTCy (50 mg/m2 days +3 and +4) is ongoing.

TMLI in patients with AML in complete remission undergoing allogeneic HCT

Allogeneic HCT is the preferred curative approach for patients with high risk AML in complete remission. Myeloablative TBI containing conditioning regimens are often utilized. Given the encouraging results in R/R disease, we extended the evaluation of TMLI to AML in CR1/CR2. Stein et al. evaluated in a pilot trial (NCT03467386) a novel conditioning regimen of TMLI 20 Gy without pretransplant chemotherapy, together with PTCy to reduce the risk of GVHD, in patients with AML in CR1/CR2 undergoing matched donor allogeneic HCT. The target structures were bone and bone marrow, major lymph node regions and spleen treated to 20 Gy and liver and brain treated to 12 Gy. Dose escalated TMLI was intended to reduce relapses and to offset the possible reduction in GVL from PTCy. In 18 patients [(median age 40 (19–56)] no grade 3-4 Bearman toxicities or toxicity-related deaths were observed. All patients engrafted without delays. The cumulative incidence of moderate-to-severe cGVHD was 11·9%. Disease relapse at 2 years was 16·7%. At a median follow up of 24.5 months, 2-year estimates of NRM, OS, relapse free survival, and GVHD-/relapse-free survival (GRFS) rate were 0%, 86·7%, 83·3%, and 59.3%, respectively (13). These results compare favorably to historical results at this center where GRFS was 39% at 2 years using TBI 13.2 Gy combined with Cy or etoposide and tacrolimus/sirolimus prophylaxis in patients with AML in remission (60). Based on these encouraging results a larger phase 2 trial has been initiated.

Toxicities with TMI and TMLI

TMI and TMLI have the potential to reduce toxicities compared to TBI. Intermediate and long-term toxicity data were reported on 142 patients who received TMI or TMLI from 2005 to 2016 and who were entered on a study which prospectively followed patients up to 8 years after TMI or TMLI (61, 62). In addition to standard follow-up, thyroid panel, ophthalmologic exams, pulmonary function studies, serum creatinine, glomerular filtration rate, and urine analysis were performed at 100 days, 6 months, 1 year and annually up to 8 years. Median TMI dose was 14 Gy with most patients receiving either 12 Gy (n=64) or 16 Gy (n=30). Median follow-up (range) for all patients was 2 years (0–8) and for alive patients (n=50) 5.5 years (0–8). One patient developed reversible radiation pneumonitis (RP). The crude incidence of RP was 1/142 (0.7%). The cumulative incidence of infection and RP (I/RP) was 22.7% at 2 years post TMI. Mean lung dose (MLD) ≤ 8 Gy was associated with a significantly lower rate of I/RP (2-year CI 20.8% vs 31.8%, p=0.012). The incidence of hypothyroidism, cataract formation and radiation induced renal toxicity was 6.0%, 7.0% and 0%, respectively.

Toxicities appear to be less compared to that reported for conventional TBI. Renal toxicity can range between 0% and 46.7% (63, 64). Rates of hypothyroidism requiring medication replacement range from 10.5% to 12.0% (65–67) and cataract formation has been reported to be as high as 89-100% (63, 68). These toxicities have been shown to correlate with total dose and dose per fraction (8). Therefore, the lower rates of toxicity observed with TMI and TMLI are likely due to organ sparing and reduction in organ dose using IMRT compared to conventional opposed fields used to deliver TBI (69). With conventional TBI these organs would usually receive the full total body dose.

Lung doses in this study were lower than that reported with conventional TBI and probably explain the observed low incidence of radiation pneumonitis. This compares favorably to conventional TBI where radiation pneumonitis rates are approximately 28 to 31% even with the use of lung shielding and fractionation (70–72). Keeping MLD ≤ 8 Gy is recommended to limit the risk of pulmonary I/RP and is a dose constraint on all current trials. The lower incidence of intermediate to late toxicities and no cases of non-engraftment to date suggest that the higher dose rates with the current fractionation schedules do not contribute to organ or marrow dysfunction and are consistent with published pre-clinical studies (73, 74).

Organ sparing on recurrence rates after TMLI

TMLI has raised concerns that organ sparing will spare leukemia cells and increase recurrence rates. We reported on extramedullary (EM) recurrences in the first 101 patients undergoing allogeneic HCT with TMLI at this center. With a median follow-up of 12.8 months, 13 patients developed EM relapses at 19 sites. There was no relationship between dose and

EM relapse. Nine EM relapses occurred in full dose regions (≥ 12 Gy), 5 at sites receiving close to the full dose (10.1 to 11.4 Gy) and 5 at sites receiving 3.6 to 9.1 Gy (75). In multivariate analysis EM disease prior to HCT was the only predictor of EM relapse as has been reported by others (76–79). The risk of EM relapse was comparable to that seen with other HCT conditioning regimens (76, 80–82). These data suggest the use of TMLI does not increase the risk of relapse in non-target regions compared to other conditioning regimens. Our current practice is to continue to offer patients with a history of EM disease TMLI conditioning regimens on clinical trials. Sites of active EM disease sites prior to HCT are included in the target regions. EM relapse rates continue to be monitored on all TMLI trials at this center.

Discussion and future directions

TBI remains a critically important component of the conditioning regimen in patients undergoing HCT with randomized trials continuing to demonstrate superior outcomes with TBI regimens compared with non-TBI regimens (83–88). The role of TBI is the elimination of malignant cells and to provide immunosuppression to prevent rejection of donor hematopoietic stem cells. Fractionation and organ shielding improve the therapeutic ratio of conventional TBI with reduced toxicities and improved outcomes (89–94). Increased toxicities associated with higher dose-rates diminishes above 5 cGy/minute and is further reduced if TBI is fractionated (73, 95–98).

There are limitations with conventional TBI. Dose escalation is not feasible due to increased toxicities and regimen related mortality. TBI is also not tolerated in older patients. TMI and TMLI were developed by our group to address these limitations and an unmet need, specifically patients with advanced, refractory or relapsed hematologic malignancies who have poor outcomes or cannot tolerate standard myeloablative conditioning regimens, and where attempts to improve outcomes by adding or dose escalating conventional total body irradiation (TBI) was not possible due to associated toxicities. The emphasis was on redefining and expanding the use of radiation containing conditioning regimens to a new group of patients.

Most patients treated on TMLI trials at this center are patients with R/R acute leukemia who have no standard-of-care HCT options. The results in this population are very encouraging when compared to historical results and demonstrate that: 1) TMLI results in lower incidences of toxicities compared to TBI (61); 2) all patients have successfully engrafted; 3) extramedullary relapses are infrequent and comparable to other conditioning regimens (75); 4) TMLI doses to 20 Gy, with etoposide and cyclophosphamide in younger patients (< 60 years old) is safe with a 1-year NRM rate of 6% and 2-year OS and PFS of 48% and 33%, respectively (12, 33); and 5) in older patients (≥ 60 years old), adding 12 Gy TMLI to fludarabine and melphalan is feasible with an NRM rate similar to fludarabine-melphalan alone, and with encouraging 5-year OS and EFS of 42% and 41%, respectively (15). The results of these studies warrant larger scale multi-center trials to confirm that these single center results can be reproduced.

More recently TMLI strategies at this center have been extended to other patient populations. Dose escalated TMLI has been added to a PTCy GVHD reduction regimen in R/R acute leukemia patients undergoing HCT with a haplo-identical donor with promising low relapse rates achieved without an increase in GVHD or NRM (39). This approach warrants further investigation given the initial promising results and rapid expansion of haplo-identical HCT.

Given the encouraging results in R/R disease, TMLI is now being evaluated in patients with AML in CR1 and CR2 undergoing matched donor allogenic HCT with results that compare favorably to similar patients treated with traditional TBI and conventional GVHD preventative regimens at this center. This approach is now being evaluated in a larger phase II trial which may eventually lead to a randomized trial evaluating this regimen as a possible alternative to current TBI or non-TBI containing conditioning regimens.

Since initiation of TMI trials at this center, other centers have reported their experience, although most of the experience remains limited to date. Detailed reviews of the TMI clinical experience have recently been published (38, 99–101). Most trials have evaluated myeloablative doses of TMI as part of the conditioning regimen prior to allogeneic HCT. A Phase I trial of TMI (3–12 Gy 1.5 Gy twice daily) with fludarabine (40 mg/m^2/day × 4) and busulfan (4,800 μM∗min) reported a MTD of 9 Gy in patients 18-65 years of age with high risk disease. NRM was 29%, RFS was 43% and OS was 50% (102). A phase II trial of this regimen is ongoing. A Phase I trial combining dose-escalated TMI from 12 to 18 Gy (3 Gy/day) with fludarabine (25mg/m^2 on days−9 to−7) and cyclophosphamide (60 mg/m^2 on days −8 and −7), established an MTD of 15 Gy (103). Other groups are evaluating larger fraction sizes of up to 5 Gy (104). A phase I trial in patients with relapsed hematologic disease undergoing second or greater allogeneic HCT were treated with TMI doses of 6 to 12 Gy. The 2-year NRM, PFS and OS was 17%, 48% and 50%, respectively. The recommend TMI dose was 12 Gy in younger patients and 9 Gy in older patients (105). Initial results of an ongoing prospective pilot trial evaluating TMI and Cy in patients with high risk AML, ALL, or MDS who were older than 50 years old or with comorbidities unable to undergo TBI based regimens were reported (106). With a median follow-up of 14 months, relapse rate was 0% and median OS was 313 days (20–784).

In AML patients undergoing allogeneic HCT with a haplo-identical donor, a pilot trial reported results combining Treg/Tcon adoptive immunotherapy to reduce GVHD with

myeloablative TBI or TMLI and low dose chemotherapy (107–109). The conditioning regimen included TBI for patients up to age 50 years and total marrow/lymphoid irradiation for patients age 51 to 65 years. TMLI was delivered in 2 daily fractions of 1.5 Gy (TMI) and 1.3 Gy (TLI) (total doses 13.5 Gy and 11.7 Gy respectively), followed by thiotepa, fludarabine, and cyclophosphamide. The probability of moderate/severe cGVHD/relapse-free survival was 75% (109).

Trials are in progress evaluating TMI instead of TBI in patients with acute leukemia in remission. At Beijing 307 Hospital a conditioning regimen of TMI 12 Gy in 4 Gy daily fractions combined with pre-transplant Cy (60 mg/kg/d x 2) and at the University Hospitals of Geneva TMI 12 Gy at 4 Gy per day with a simultaneous boost to active marrow to 13.5 Gy in older patients (40-80 years of age) are being evaluated. Other centers have combined TBI with TMI to select targets areas as a form of localized boost (110, 111).

TMI trials have also been reported in patients with multiple myeloma. A phase II trial reported results of 50 patients who underwent a tandem autologous HCT using TMI 12 Gy (4 Gy daily) conditioning followed by a second autologous HCT using melphalan 200 mg/m^2. Additional boost to 24 Gy was delivered to active FDG-PET lesions. The 5-year OS and PFS were 74% and 55%, respectively (112). Other groups have administered TMI concomitantly with melphalan prior to autologous HCT. A phase I trial combined TMI with melphalan (200 mg/m^2) in patients with relapsed or refractory disease (113). An MTD was not reached and the authors concluded that 9 Gy TMI could be combined safely with melphalan. A French multicenter Phase I TMI dose escalation trial evaluating TMI with melphalan (140 mg/m^2) in first relapse patients has been completed (114). TMI as a single modality (14, 16 and 20 Gy at 2 Gy twice daily) in 9 patients with relapsed multiple myeloma prior to autologous HCT has been reported (115). No dose limiting toxicities were observed. A phase I trial at this center is evaluating the combination of 9 Gy TMI with the RIC regimen of fludarabine and melphalan in advanced patients undergoing allogeneic HCT (116).

The implementation of TMI and TMLI has led to using IMRT to deliver TBI (IM-TBI) at this center (NCT04281199) and other centers primarily in patients with acute leukemia in complete remission undergoing allogeneic HCT (117, 118). At this center IM-TBI is performed on prospective clinical trials with uniformly applied dose constraints to reduce bias and to have a IM-TBI clinical guideline foundation upon which to build on in future clinical trials. Our main reasons for implementing IM-TBI are to reduce lung dose and to accurately track radiation dose in TBI patients. Conventional 2D TBI dosimetry only provides an estimate of organ and total body dose as it does not use 3D CT based dosimetry. Both helical tomographic and VMAT IMRT can be used to deliver IM-TBI (119–123). Advantages include improved dose uniformity and improved sparing of critical organs compared to conventional TBI delivery methods (119). This has the potential to reduce toxicities, as predicted from studies of patients undergoing TBI (124) or TMI (61) which demonstrate that a mean lung dose of ≤ 8 Gy results in an increase in OS or a decrease in pulmonary toxicity, respectively. It is important to note that IM-TBI and TMI/TMLI are non-competing approaches being evaluated in different patient groups. Also, unlike TMI or TMLI, myeloablative doses of IM-TBI in older patients and dose escalation is not feasible due to increased toxicities. This will only be possible with dose distributions that spare more normal organs and approach that of TMI and TMLI. As a result, IM-TBI is limited to the same HCT populations that undergo conventional TBI and will have to demonstrate reduced toxicities and superior outcomes if it is to replace conventional TBI.

Combining different forms of targeted systemic radiotherapy such as TMLI and targeted radiopharmaceutical therapy should be evaluated. TMI/TMLI can be viewed as a form of targeted "systemic" radiotherapy that utilizes CT imaging to target anatomic regions likely to harbor disease. Another form of targeted systemic radiotherapy is radioimmunotherapy (RIT) which utilizes radiolabeled monoclonal antibodies to target cancer cells that express a specific antigen. Antibodies directed against CD45, CD33, CD66, CD22, CD25, and CD20 radiolabeled with ^{131}I, β-emitters, or α-emitters have been evaluated in clinical trials as single agents, in combination with other therapies, incorporated in HCT conditioning regimens as an alternative to TBI (125–137), or combined with myeloablative doses of TBI (138–141) in patients with hematologic malignancies. A phase I trial at this center is currently evaluating the combination of RIT added to 12 Gy TMLI, fludarabine and melphalan in R/R acute leukemia undergoing matched donor allogenic HCT (NCT05204147). TMLI and RIT are potentially complementary and can address the limitations of each modality. The addition of RIT to TMLI can add additional dose to cancer cells, including cancer cells in circulation and in organs not targeted by TMLI. With RIT there is unintended normal organ uptake, making TMLI better positioned to be combined with RIT than standard TBI. Finally, radiolabeled antibodies and other radiopharmaceuticals are being evaluated as molecular imaging agents at this center to refine targeting of TMLI in the future (142, 143).

Conclusion

TMI and TMLI continue to be actively investigated at this center and at an increasing number of centers worldwide which has been recently reviewed (144, 145). Figure 3 summarizes the clinical trial strategies currently ongoing at this center. Clinical results show significant promise and demonstrate the ability to offer TMI and TMLI to older patients or those with co-morbidities, regimen related toxicity and mortality rates that are in general lower compared to standard myeloablative conditioning regimens, the ability to dose escalate, and

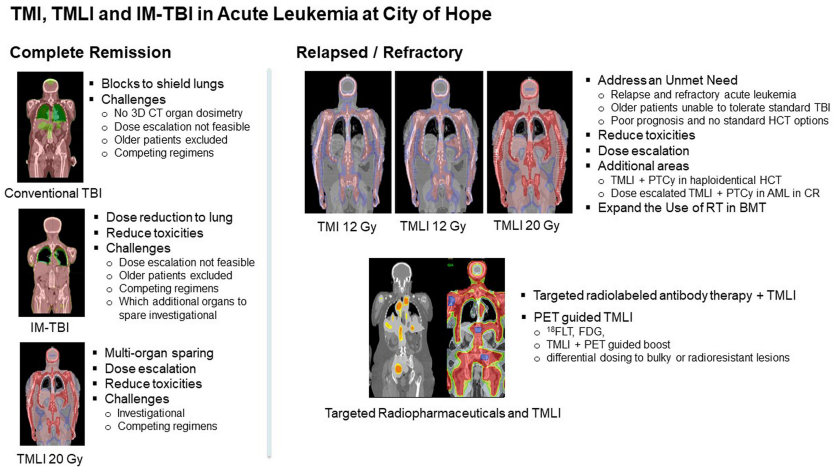

FIGURE 3
Overview of TMI, TMLI and IM-TBI clinical applications in patients with acute leukemia undergoing allogeneic hematopoietic cell transplantation at this center.

encouraging response and survival rates in R/R disease. The initial concerns of increased toxicities, engraftment failure and relapses due to higher dose-rates and organ sparing have not been observed and prospective trials continue to monitor this. These results support the use of helical tomographic or volumetric arc based IMRT for the delivery of TMI and TMLI in future clinical trials.

This rapidly developing field should move towards developing uniform planning and treatment guidelines and standardized reporting of organ doses and dose-rates. Multicenter trials are needed to confirm results reported by single institutions and to answer important questions that remain. The optimum fractionation schedules, fraction sizes, chemotherapy agents, and chemotherapy/TMI/TMLI sequencing need to be defined. Future clinical trials will investigate radiation dose distributions which will span a continuous spectrum ranging from IM-TBI with lung sparing, to IM-TBI with multi-organ sparing, to TMI/TMLI without dose escalation, and to TMI/TMLI with dose escalation. The appropriate dose distributions, target regions, target doses, and organs to spare for each clinical scenario need to be determined. Ultimately clinical trials need to demonstrate that TMI based conditioning regimens offer advantages over current approaches.

In conclusion, the development and implementation of TMI and TMLI requires a collaborative effort between radiation oncology and hematology to apply technology advances in radiation oncology to address an unmet need in HCT and to shift the paradigm towards more effective and safer strategies to integrate radiation therapy into HCT conditioning beyond what is possible with TBI. TMI and TMLI hold significant promise in redefining and expanding the role of radiotherapy in hematopoietic cell transplantation.

Author contributions

JW performed the summary of clinical results and manuscript preparation. AL contributed to the methodology summary and images used in all figures. CH contributed to the methodology summary and reporting of organ dose estimates. All authors (JW, AL, CH, SD, TS, JP, DY, GS, ASa, SH, MA, JR and ASt) provided input and critical review of the manuscript and were actively involved as investigators of the clinical trials and studies reviewed in this manuscript. ASt, JR, MA, GS, SD, SH and JW were principal investigators of the prospective trials and prospective studies summarized in this review. All authors contributed to the article and approved the submitted version.

Conflict of interest

The authors declare that the research was conducted in the absence of any commercial or financial relationships that could be construed as a potential conflict of interest.

Publisher's note

References

1. Schultheiss T, Liu A, Wong J, Olivera G, Kapatoes J. Total marrow and total lymphatic irradiation with helical tomotherapy. *Med Physics* (2004) 31(6):1845.

2. Schultheiss TE, Wong J, Olivera G, Kapatoes J. Normal tissue sparing in total marrow and total lymphatic irradiation with helical tomotherapy. *Int J Radiat Oncol Biol Phys* (2004) 60(1):S544.

3. Wong JYC. *Targeted TBI using helical tomotherapy. tandem bone marrow transplant meeting, keystone, CO*. (Elsevier) (2005).

4. Wong JYC, Liu A, Schultheiss T, Popplewell L, Stein A, Rosenthal J, et al. Targeted total marrow irradiation using three-dimensional image-guided tomographic intensity-modulated radiation therapy: An alternative to standard total body irradiation. *Biol Blood Marrow Transplant* (2006) 12(3):306–15. doi: 10.1016/j.bbmt.2005.10.026

5. Schultheiss TE, Wong J, Liu A, Olivera G, Somlo G. Image-guided total marrow and total lymphatic irradiation using helical tomotherapy. *Int J Radiat Oncol Biol Phys* (2007) 67(4):1259–67. doi: 10.1016/j.ijrobp.2006.10.047

6. Petropoulos D, Worth LL, Mullen CA, Madden R, Mahajan A, Choroszy M, et al. Total body irradiation, fludarabine, melphalan, and allogeneic hematopoietic stem cell transplantation for advanced pediatric hematologic malignancies. *Bone Marrow Transplant* (2006) 37:463–7. doi: 10.1038/sj.bmt.1705278

7. Clift RA, Buckner CD, Appelbaum FR, Sullivan KM, Storb R, Thomas ED. Long-term follow-up of a randomized trial of two irradiation regimens for patients receiving allogeneic marrow transplants during first remission of acute myeloid leukemia. *Blood.* (1998) 92(4):1455–6. doi: 10.1182/blood.V92.4.1455

8. Sampath S, Schultheiss TE, Wong J. Dose response and factors related to interstitial pneumonitis following bone marrow transplant. *Int J Radiat Oncol Biol Physics.* (2005) 63(3):876–84. doi: 10.1016/j.ijrobp.2005.02.032

9. Somlo G, Spielberger R, Frankel P, Karanes C, Krishnan A, Parker P, et al. Total marrow irradiation: A new ablative regimen as part of tandem autologous stem cell transplantation for patients with multiple myeloma. *Clin Cancer Res* (2011) 17(1):174–82. doi: 10.1158/1078-0432.CCR-10-1912

10. Ladbury C, Somlo G, Dagis A, Yang D, Armenian S, Song JY, et al. Long-term follow-up of multiple myeloma patients treated with tandem autologous transplantation following melphalan and upon recovery, total marrow irradiation. *Transplant Cell Ther* (2022) 28(7):367–. doi: 10.1016/j.jtct.2022.04.022

11. Rosenthal J, Wong J, Stein A, Qian D, Hitt D, Naeem H, et al. Phase 1/2 trial of total marrow and lymph node irradiation to augment reduced-intensity transplantation for advanced hematologic malignancies. *Blood.* (2011) 117 (1):309–15. doi: 10.1182/blood-2010-06-288357

12. Stein A, Tsai N-C, Palmer J, Al-Malki M, Aldoss I, Ali H, et al. Total marrow and lymphoid irradiation (TMLI) in combination with cyclophosphamide and etoposide improves the outcome of patients with poor-risk acute leukemia. In: *Presented at the 46th annual meeting of the European society for blood and marrow transplantation*, vol. 2020. (Madrid, Spain: Nature) (2020).

13. Stein AS, Al Malki MM, Yang D, Palmer JM, Tsai NC, Aldoss I, et al. Total marrow and lymphoid irradiation with post-transplantation cyclophosphamide for patients with AML in remission. *Transplant Cell Ther* (2022) 22):10. doi: 10.1016/j.jtct.2022.03.025

14. Somlo G, Forman S, Popplewell L, Krishnan A, Sahebi F, Liu A, et al. Total marrow irradiation (TMI) with helical tomotherapy and PBPC following high-dose melphalan and PBPC as tandem therapy for patients with multiple myeloma. In: *Presented at American society of hematology meeting* (American Society of Hematology) (2005).

15. Jensen LJ, Stiller T, Wong JYC, Palmer J, Stein A, Rosenthal J. Total marrow lymphoid irradiation/Fludarabine/Melphalan conditioning for allogeneic hematopoietic cell transplantation. *Biol Blood Marrow Transplant* (2018) 24:301–7. doi: 10.1016/j.bbmt.2017.09.019

16. Stein A, Palmer J, Tsai N-C, Al Malki MM, Aldoss I, Ali H, et al. Phase I trial of total marrow and lymphoid irradiation transplantation conditioning in patients with relapsed/refractory acute leukemia. *Biol Blood Marrow Transplantation* (2017) 23(4):618–24. doi: 10.1016/j.bbmt.2017.01.067

17. Han C, Schultheiss T, Wong JY. Dosimetric study of volumetric modulated arc therapy fields for total marrow irradiation. *Radiother Oncol* (2012) 102(2):315–20. doi: 10.1016/j.radonc.2011.06.005

18. Han C, Liu A, Wong J. Target coverage and normal organ sparing in dose-escalated total marrow and lymphatic irradiation: a single institution experience. *Front Oncol* (2022) 12. doi: 10.3389/fonc.2022.946725

19. Liu A, Han C, Neylon J. Implementation of targeted total body irradiation as a bone marrow transplant conditioning regimen: A review. In: Wong J, Hui SK, editors. *Total marrow irradiation*, *1st*, vol. p . Switzerland: Springer Nature (2020). p. 29–46.

20. Hahn T, Wingard JR, Anderson KC, Bensinger WI, Berenson JR, Brozeit G, et al. The role of cytotoxic therapy with hematopoietic stem cell transplantation in the therapy of multiple myeloma: an evidence-based review. *Biol Blood Marrow Transplant* (2003) 9(1):4–37. doi: 10.1053/bbmt.2003.50002

21. Barlogie B, Jagannath S, Desikan KR, Mattox S, Vesole D, Siegel D, et al. Total therapy with tandem transplants for newly diagnosed multiple myeloma. *Blood* (1999) 93(1):55–65. doi: 10.1182/blood.V93.1.55

22. Moreau P, Facon T, Attal M, Hulin C, Michallet M, Maloisel F, et al. Comparison of 200 mg/m^2 melphalan and 8 gy total body irradiation plus 140 mg/m^2 melphalan as conditioning regimens for peripheral blood stem cell transplantation in patients with newly diagnosed multiple myeloma: final analysis of the intergroupe francophone du myelome 9502 randomized trial. *Blood* (2002) 99(3):731–5. doi: 10.1182/blood.V99.3.731

23. Chak LY, Sapozink MD, Cox RS. Extramedullary lesions in non-lymphocytic leukemia: Results of radiation therapy. *Int J Radiat Oncol Biol Phys* (1983) 9(8):1173–6. doi: 10.1016/0360-3016(83)90176-1

24. Scarpati D, Frassoni F, Vitale V, Corvo R, Franzone P, Barra S, et al. Total body irradiation in acute myeloid leukemia and chronic myelogenous leukemia: Influence of dose and dose-rate on leukemia relapse. *Int J Radiat Oncol Biol Phys* (1989) 17(3):547–52. doi: 10.1016/0360-3016(89)90105-3

25. Marks DI, Forman SJ, Blume KG, Perez WS, Weisdorf DJ, Keating A, et al. A comparison of cyclophosphamide and total body irradiation with etoposide and total body irradiation as conditioning regimens for patients undergoing sibling allografting for acute lymphoblastic leukemia in first or second complete remission. *Biol Blood Marrow Transplantation* (2006) 12:438–53. doi: 10.1016/j.bbmt.2005.12.029

26. Kal HB, Kempen-Har V. Biologically effective dose in total body irradiation and hematopoietic stem cell transplantation. *Strahlenther Onkol* (2006) 182 (11):672–9. doi: 10.1007/s00066-006-1528-6

27. Clift RA, Buckner CD, Appelbaum FR, Bryant E, Bearman SI, Peterson FB, et al. Allogeneic marrow transplantation in patients with chronic myeloid leukemia in the chronic phase: A randomized trial of two irradiation regimens. *Blood.* (1991) 77(8):1660–5. doi: 10.1182/blood.V77.8.1660.1660

28. Bearman S, Appelbaum FR, Buckner CD, Petersen FB, Fisher LD, Clift RA, et al. Regimen-related toxicity in patients undergoing bone marrow transplantation. *J Clin Oncol* (1988) 6(10):1562–8. doi: 10.1200/JCO.1988.6.10.1562

29. Appelbaum FR, Badger CC, Bernstein ID, Buckner CD, Deeg HJ, Eary JF, et al. Is there a better way to deliver total body irradiation? *Bone Marrow Transplant* (1992) 10 Suppl 1:77–81.

30. Brown RA, Wolff SN, Fay JW, Pineiro L, Collins RHJr., Lynch JP, et al. High-dose etoposide, cyclophosphamide and total body irradiation with allogeneic bone marrow transplantation for resistant acute myeloid leukemia: a study by the north American marrow transplant group. *Leuk Lymphoma* (1996) 22(3-4):271–7. doi: 10.3109/10428199609051758

31. Duval M, Klein JP, He W, Cahn J-Y, Cairo MS, Camitta BM, et al. Hematopoietic stem-cell transplantation for acute leukemia in relapse or primary induction failure. *J Clin Oncol* (2010) 28(23):3730–8. doi: 10.1200/JCO.2010.28.8852

32. Wong JY, Forman S, Somlo G, Rosenthal J, Liu A, Schultheiss T, et al. Dose escalation of total marrow irradiation with concurrent chemotherapy in patients with advanced acute leukemia undergoing allogeneic hematopoietic cell transplantation. *Int J Radiat Oncol Biol Phys* (2013) 85(1):148–56. doi: 10.1016/j.ijrobp.2012.03.033

33. Wong JYC, Tsai N-C, Han C, Palmer J, Liu A, Al Malki M, et al. Phase II study of dose escalated total marrow and lymphoid irradiation (TMLI) in combination with cyclophosphamide and etoposide in patients with poor-risk acute leukemia. Chicgao, IL: Presented at the 62nd ASTRO Annual Meeting (Elsevier) (2020).

34. Forman SJ, Rowe JM. The myth of the second remission of acute leukemia in the adult. *Blood* (2013) 121(7):1077–82. doi: 10.1182/blood-2012-08-234492

35. Gress RE, Miller JS, Battiwalla M, Bishop MR, Giralt SA, Hardy NM, et al. Proceedings from the national cancer institute's second international workshop on the biology, prevention, and treatment of relapse after hematopoietic stem cell transplantation: Part I. *Biol Relapse after Transplantation. Biol Blood Marrow Transplantation* (2013) 19(11):1537–45. doi: 10.1016/j.bbmt.2013.08.010

36. Deeg HJ, Sandmaier BM. Who is fit for allogeneic transplantation? *Blood* (2010) 116(23):4762–70. doi: 10.1182/blood-2010-07-259358

37. Scott BL, Pasquini MC, Logan BR, Wu J, Devine SM, Porter DL, et al. Myeloablative versus reduced-intensity hematopoietic cell transplantation for acute myeloid leukemia and myelodysplastic syndromes. *J Clin Oncol* (2017) 35 (11):1154–61. doi: 10.1200/JCO.2016.70.7091

38. Wong J, Hui SK. *Total marrow irradiation. 1st ed*. New York, NY`: Springer Nature (2020).

39. Al Malki MM, Palmer J, Tsai NC, Mokhtari S, Hui S, Tsai W, et al. Total marrow and lymphoid irradiation as conditioning in haploidentical transplant with posttransplant cyclophosphamide. *Blood Adv* (2022) 6(14):4098–106. doi: 10.1182/bloodadvances.2022007264

40. Aldoss I, Forman SJ, Pullarkat V. Acute lymphoblastic leukemia in the older adult. *J Oncol Pract* (2019) 15(2):67–75. doi: 10.1200/JOP.18.00271

41. Mrozek K, Marcucci G, Nicolet D, Maharry KS, Becker H, Whitman SP, et al. Prognostic significance of the European LeukemiaNet standardized system for reporting cytogenetic and molecular alterations in adults with acute myeloid leukemia. *J Clin Oncol* (2012) 30(36):4515–23. doi: 10.1200/JCO.2012.43.4738

42. Giralt S, Thall PF, Khouri I, Wang X, Braunschweig I, Ippoliti C, et al. Melphalan and purine analog-containing preprative regimens: reduced-intensity conditioning for patients with hematologic malignancies undergoing allogeneic progenitor cell transplantation. *Blood* (2001) 97(3):631–7. doi: 10.1182/blood.V97.3.631

43. Giralt S, Aleman A, Anagnostopoulos A. Fludarabine/melphalan conditioning for allogeneic transplantation in patients with multiple myeloma. *Bone Marrow Transplant* (2002) 30(6):367–73. doi: 10.1038/sj.bmt.1703652

44. Ritchie DS, Morton J, Szer J, Roberts AW, Durrant S, Shuttleworth P, et al. Graft-versus-host disease, donor chimerism, and organ toxicity in stem cell transplantation after conditioning with fludarabine and melphalan. *Biol Blood Marrow Transplantation* (2003) 9:435–42. doi: 10.1016/S1083-8791(03)00128-9

45. de Lima M, Couriel D, Thall PF, Wang X, Madden T, Jones R, et al. Once-daily intravenous busulfan and fludarabine: clinical and pharmacokinetic results of a myeloablative, reduced-toxicity conditioning regimen for allogeneic stem cell transplantation in AML and MDS. *Blood.* (2004) 104(3):857–64. doi: 10.1182/blood-2004-02-0414

46. Arai S, Arora M, Wang T, Spellman SR, He W, Couriel DR, et al. Increasing incidence of chronic graft-versus-host disease in allogeneic transplantation: a report from the center for international blood and marrow transplant research. *Biol Blood Marrow Transplant* (2015) 21(2):266–74. doi: 10.1016/j.bbmt.2014.10.021

47. Luznik L, Fuchs EJ. High-dose, post-transplantation cyclophosphamide to promote graft-host tolerance after allogeneic hematopoietic stem cell transplantation. *Immunol Res* (2010) 47(1-3):65–77. doi: 10.1007/s12026-009-8139-0

48. Luznik L, BolaÃ ± os-Meade J, Zahurak M, Chen AR, Smith BD, Brodsky R, et al. High-dose cyclophosphamide as single-agent, short-course prophylaxis of graft-versus-host disease. *Blood* (2010) 115(16):3224–30. doi: 10.1182/blood-2009-11-251595

49. Luznik L, Jones RJ, Fuchs EJ. High-dose cyclophosphamide for graft-versus-host disease prevention. *Curr Opin Hematol* (2010) 17(6):493–9. doi: 10.1097/MOH.0b013e32833eaf1b

50. Luznik L, O'Donnell PV, Symons HJ, Chen AR, Leffell MS, Zahurak M, et al. HLA-haploidentical bone marrow transplantation for hematologic malignancies using nonmyeloablative conditioning and high-dose, posttransplantion cyclophosphamide. *Biol Blood Marrow Transplantation* (2008) 14:641–50. doi: 10.1016/j.bbmt.2008.03.005

51. Brunstein CG, Fuchs EJ, Carter SL, Karanes C, Costa LJ, Wu J, et al. Alternative donor transplantation after reduced intensity conditioning: results of parallel phase 2 trials using partially HLA-mismatched related bone marrow or unrelated double umbilical cord blood grafts. *Blood* (2011) 118(2):282–8. doi: 10.1182/blood-2011-03-344853

52. BolaÃ ± os-Meade J, Fuchs EJ, Luznik L, Lanzkron SM, Gamper CJ, Jones RJ, et al. HLA-haploidentical bone marrow transplantation with posttransplant cyclophosphamide expands the donor pool for patients with sickle cell disease. *Blood.* (2012) 120(22):4285–91. doi: 10.1182/blood-2012-07-438408

53. Bashey A, Zhang MJ, McCurdy SR, St MA, Argall T, Anasetti C, et al. Mobilized peripheral blood stem cells versus unstimulated bone marrow as a graft source for T-Cell-Replete haploidentical donor transplantation using post-transplant cyclophosphamide. *J Clin Oncol* (2017) 35(26):3002–9. doi: 10.1200/JCO.2017.72.8428

54. Bejanyan N, Pidala JA, Wang X, Thapa R, Nishihori T, Elmariah H, et al. A phase 2 trial of GVHD prophylaxis with PTCy, sirolimus, and MMF after peripheral blood haploidentical transplantation. *Blood Adv* (2021) 5(5):1154–63. doi: 10.1182/bloodadvances.2020003779

55. Kanakry CG, Ganguly S, Zahurak M, BolaÃ ± os-Meade J, Thoburn C, Perkins B, et al. Aldehyde dehydrogenase expression drives human regulatory T cell resistance to posttransplantation cyclophosphamide. *Sci Transl Med* (2013) 5(211):211ra157. doi: 10.1126/scitranslmed.3006960

56. Nunes NS, Kanakry CG. Mechanisms of graft-versus-Host disease prevention by post-transplantation cyclophosphamide: An evolving understanding. *Front Immunol* (2019) 10:2668. doi: 10.3389/fimmu.2019.02668

57. Ganguly S, Ross DB, Panoskaltsis-Mortari A, Kanakry CG, Blazar BR, Levy RB, et al. Donor CD4+ Foxp3+ regulatory T cells are necessary for posttransplantation cyclophosphamide-mediated protection against GVHD in mice. *Blood* (2014) 124(13):2131–41. doi: 10.1182/blood-2013-10-525873

58. Wachsmuth LP, Patterson MT, Eckhaus MA, Venzon DJ, Gress RE, Kanakry CG. Post-transplantation cyclophosphamide prevents graft-versus-host disease by inducing alloreactive T cell dysfunction and suppression. *J Clin Invest* (2019) 129(6):2357–73. doi: 10.1172/JCI124218

59. Ciurea SO, Zhang MJ, Bacigalupo AA, Bashey A, Appelbaum FR, Aljitawi OS, et al. Haploidentical transplant with posttransplant cyclophosphamide vs matched unrelated donor transplant for acute myeloid leukemia. *Blood* (2015) 126(8):1033–40. doi: 10.1182/blood-2015-04-639831

60. Salhotra A, Hui S, Yang D, Mokhtari S, Mei M, Al Malki M, et al. Long-term outcomes of patients with acute myelogenous leukemia treated with myeloablative fractionated total body irradiation TBI-based conditioning with a tacrolimus- and sirolimus-based graft-versus-host disease prophylaxis regimen: 6-year follow-up from a single center. *Biol Blood Marrow Transplant* (2020) 26:292–9. doi: 10.1016/j.bbmt.2019.09.017

61. Shinde A, Yang D, Frankel P, Liu A, Han C, Del Vecchio B, et al. Radiation related toxicities using organ sparing total marrow irradiation transplant conditioning regimens. *Int J Radiat Oncol Biol Phys* (2019) 105(5):1025–33. doi: 10.1016/j.ijrobp.2019.08.010

62. Shinde A, Wong J. Acute and late toxicities with total marrow irradiation. In: Wong J, Hui SK, editors. *Total marrow irradiation*, *1st*. New York, NY: Springer Nature (2020). p. 187–96.

63. Kal HB, Kempen-Harteveld ML. Induction of severe cataract and late renal dysfunction following total body irradiation: Dose-effect relationships. *Anticancer Res* (2009) 29:3305–10.

64. Kersting S, Verdonck LF. Chronic kidney disease after nonmyeloablative stem cell transplantation in adults. *Biol Blood Marrow Transplant.* (2008) 14:403–8. doi: 10.1016/j.bbmt.2007.12.495

65. Berger C, Le-gallo B, Donadieu J, Richard O, Devergie A, Galambrun C, et al. Late thyroid toxicity in 153 long-term survivors of allogeneic bone marrow transplantation for acute lymphoblastic leukaemia. *Bone Marrow Transplant* (2005) 35:991–5. doi: 10.1038/sj.bmt.1704945

66. Farhadfar N, Stan MN, Shah P, Sonawane V, Hefazi MT, Murthy HS, et al. Thyroid dysfunction in adult hematopoietic cell transplant survivors: risks and outcomes. *Bone Marrow Transplant* (2018) 53:977–82. doi: 10.1038/s41409-018-0109-5

67. Medinger M, Zeiter D, Heim D, Halter J, Gerull S, Tichelli A, et al. Hypothyroidism following allogeneic hematopoietic stem cell transplantation for acute myeloid leukemia. *Leukemia Res* (2017) 58:43–7. doi: 10.1016/j.leukres.2017.04.003

68. van Kempen-Harteveld ML, Struikmans H, Kal HB, van der Tweel I, Mourits MP, Verdonck LF, et al. Cataract-free interval and severity of cataract after total body irradiation and bone marrow transplantation: influence of treatment parameters. *Int J Radiat Oncology Biology Physics.* (2000) 48(3):807–15. doi: 10.1016/S0360-3016(00)00669-6

69. Wong JYC, Filippi AR, Dabaja BS, Yahalom J, Specht L. Total body irradiation: Guidelines from the international lymphoma radiation oncology group (ILROG). *Int J Radiat Oncol Biol Phys* (2018) 101(3):521–9. doi: 10.1016/j.ijrobp.2018.04.071

70. Carruthers S, Wallington M. Total body irradiation and pneumonitis risk: a review of outcomes. *Br J Cancer* (2004) 90:2080–4. doi: 10.1038/sj.bjc.6601751

71. Chen C, Abraham R, Tsang R, Crump M, Keating A, Stewart A. Radiation-associated pneumonitis following autologous stem cell transplantation: predictive factors, disease characteristics and treatment outcomes. *Bone Marrow Transplant* (2001) 27:177–82. doi: 10.1038/sj.bmt.1702771

72. Bolling T, Kreuziger DC, Ernst I, Elsayed H, Willich N. Retrospective, monocentric analysis of late effects after total body irradiation (TBI) in adults. *Strahlenther Onkol.* (2011) 187:311–5. doi: 10.1007/s00066-011-2190-1

73. Tarbell NJ, Amato DA, Down JD, Mauch P, Hellman S. Fractionation and dose rate effects in mice: a model for bone marrow transplantation in man. *Int J Radiat Oncol Biol Phys* (1987) 13(7):1065–9. doi: 10.1016/0360-3016(87)90046-0

74. Glass TJ, Hui SK, Blazar BR, Lund TC. Effect of radiation dose-rate on hematopoietic cell engraftment in adult zebrafish. *PLoS One* (2013) 8(9):1–10. doi: 10.1371/journal.pone.0073745

75. Kim JH, Stein A, Tsai N, Schultheiss TE, Palmer J, Liu A, et al. Extramedullary relapse following total marrow and lymphoid irradiation in patinets undergoing allogenejic hematopoietic cell transplantation. *Int J Radiat Oncol Biol Phys* (2014) 89(1):75–81. doi: 10.1016/j.ijrobp.2014.01.036

76. Chong G, Byrnes G, Szer J, Grigg A. Extramedullary relapse after allogeneic bone marrow transplantation for haematological malignancy. *Bone Marrow Transplant* (2000) 26(9):1011–5. doi: 10.1038/sj.bmt.1702659

77. Harris AC, Kitko CL, Couriel DR, Braun TM, Choi SW, Magenau J, et al. Extramedullary relapse of acute myeloid leukemia following allogeneic hematopoietic stem cell transplantation: incidence, risk factors and outcomes. *Haematologica* (2013) 98(2):179–84. doi: 10.3324/haematol.2012.073189

78. Michel G, Boulad F, Small TN, Black P, Heller G, Castro-Malaspina H, et al. Risk of extramedullary relapse following allogeneic bone marrow transplantation for acute myelogenous leukemia with leukemia cutis. *Bone Marrow Transplant* (1997) 20(2):107–12. doi: 10.1038/sj.bmt.1700857

79. Gunes G, Goker H, Demiroglu H, Malkan UY, Buyukasik Y. Extramedullary relapses of acute leukemias after allogeneic hematopoietic stem cell transplantation: clinical features, cumulative incidence, and risk factors. *Bone Marrow Transplant* (2019) 54(4):595–600. doi: 10.1038/s41409-018-0303-5

80. Lee KH, Lee JH, Choi SJ, Lee JH, Kim S, Seol M, et al. Bone marrow vs extramedullary relapse of acute leukemia after allogeneic hematopoietic cell transplantation: risk factors and clinical course. *Bone Marrow Transplant* (2003) 32(8):835–42. doi: 10.1038/sj.bmt.1704223

81. Solh M, DeFor TE, Weisdorf DJ, Kaufman DS. Extramedullary relapse of acute myelogenous leukemia after allogeneic hematopoietic stem cell transplantation: better prognosis than systemic relapse. *Biol Blood Marrow Transplant* (2012) 18(1):106–12. doi: 10.1016/j.bbmt.2011.05.023

82. Mortimer J, Blinder MA, Schulman S, Appelbaum FR, Buckner CD, Clift RA, et al. Relapse of acute leukemia after marrow transplantation: natural history and results of subsequent therapy. *J Clin Oncol* (1989) 7(1):50–7. doi: 10.1200/JCO.1989.7.1.50

83. Blaise D, Maraninchi D, Michallet M, Reiffers J, Jouet JP, Millpied N, et al. Long-term follow-up of a randomized trial comparing the combination of cyclophosphamide with total body irradiation or busulfan as conditioning regimen for patients receiving HLA-identical marrow grafts for acute myeloblastic leukemia in first complete remission. *Blood* (2001) 97(11):3669–71. doi: 10.1182/blood.V97.11.3669

84. Dusenbery KE, Daniels KA, McClure JS, McGlave PB, Ramsay NKC, Blazar BR, et al. Randomized comparison of cyclophosphamide-total body irradiation versus busulfan-cyclophosphamide conditioning in autologous bone marrow transplantation for acute myeloid leukemia. *Int J Radiat Oncol Biol Phys* (1995) 31(1):119–28. doi: 10.1016/0360-3016(94)00335-I

85. Ringden O, Ruutu T, Remberger M, Nikoskelainen J, Volin L, Vindelov L, et al. A randomized trial comparing busulfan with total body irradiation as conditioning in allogeneic marrow transplant recipients with leukemia: A report from the Nordic bone marrow transplantation group. *Blood* (1994) 83(9):2723–30. doi: 10.1182/blood.V83.9.2723.2723

86. Bunin N, Aplenc R, Kamani N, Shaw K, Cnaan A, Simms S. Randomized trial of busulfan vs total body irradiation containing conditioning regimens for children with acute lymphoblastic leukemia: A pediatric blood and marrow transplant consortium study. *Bone Marrow Transplant.* (2003) 32:543–8. doi: 10.1038/sj.bmt.1704198

87. Davies SM, Ramsay NKC, Klein JP, Weisdorf DJ, Bolwell BJ, Cahn JY, et al. Comparison of preparative regimens in transplants for children with acute lymphoblastic leukemia. *J Clin Oncol* (2000) 18(2):340–7. doi: 10.1200/JCO.2000.18.2.340

88. Peters C, Dalle JH, Locatelli F, Poetschger U, Sedlacek P, Buechner J, et al. Total body irradiation or chemotherapy conditioning in childhood ALL: A multinational, randomized, noninferiority phase III study. *J Clin Oncol* (2020) 39 (4):295–307. doi: 10.1200/JCO.20.02529

89. Deeg HJ, Sullivan KM, Buckner CD, Storb R, Applebaum FR, Clift R, et al. Marrow transplantation for acute nonlymphoblastic leukemia in first remission: toxicity and long-term follow-up of patients conditioned with single dose or fractionated total body irradiation. *Bone Marrow Transplant* (1986) 1(2):151–7.

90. Girinsky T, Benhamou E, Bourhis JH, Dhermain F, Guillot-Valls D, Ganansia V, et al. Prospective randomized comparison of single-dose versus hyperfractionated total-body irradiation in patients with hematologic malignancies. *J Clin Oncol* (2000) 18(5):981–6. doi: 10.1200/JCO.2000.18.5.981

91. Labar B, Bogdanic V, Nemet D, Mrsic M, Vrtar M, Grgic-Markulin L, et al. Total body irradiation with or without lung shielding for allogeneic bone marrow transplantation. *Bone Marrow Transplantation* (1992) 9:343–7.

92. Shank B, O'Reilly RJ, Cunningham I, Kernan N, Yaholom J, Brochstein J, et al. Total body irradiation for bone marrow transplantation: the memorial Sloan-Kettering cancer center experience. *Radiother Oncol* (1990) 18 Suppl 1:68–81. doi: 10.1016/0167-8140(90)90180-5

93. Rhoades JL, Lawton CA, Cohen E, Murray KJ, Horowitz MM, Drobyski WM, et al. Incidence of bone marrow transplant nephropathy (BMT-Np) after twice-daily hyperfractionated total body irradiation. *Cancer J Sci Am* (1997) 3:116.

94. Einsele H, Bamberg M, Budach W, Schmidberger H, Hess CF, Wormann B, et al. A new conditioning regimen involving total marrow irradiation, busulfan and cyclophosphamide followed by autologous PBSCT in patients with advanced multiple myeloma. *Bone Marrow Transplant* (2003) 32:593–9. doi: 10.1038/sj.bmt.1704192

95. Travis EL, Peters LJ, McNeil J, Thames HD, Karolis C. Effect of dose-rate on total body irradiation: Lethality and pathologic findings. *Radiotherapy Oncol* (1985) 4:341–51. doi: 10.1016/S0167-8140(85)80122-5

96. Sampath S, Schultheiss TE, Wong J, Sampath S, Schultheiss TE, Wong J. Dose response and factors related to interstitial pneumonitis after bone marrow transplant. *Int J Radiat Oncology Biology Physics* (2005) 63(3):876–84. doi: 10.1016/j.ijrobp.2005.02.032

97. Weiner R, Bortin M, Gale RP, Gluckman E, Kay HEM, Kolb HJ, et al. Interstitial pneumonitis after bone marrow transplantation. *Ann Intern Med* (1986) 104:168–75. doi: 10.7326/0003-4819-104-2-168

98. Ozsahin M, Pene F, Touboul E, Gindrey-Vie B, Dominique C, Lefkopoulos D, et al. Total-body irradiation before bone marrow transplantation. *Results two randomized instantaneous dose rates 157 patients. Cancer.* (1992) 69(11):2853–65.

99. Wong J. Total marrow irradiation: Redefining the role of radiotherapy in bone marrow transplantation. In: Wong J, Hui SK, editors. *Total marrow irradiation*, *1st*. New York, NY: Springer Nature (2020). p. 1–28.

100. Wong JYC, Hui S, Dandapani SV, Liu A. Biologic and image guided systemic radiotherapy. In: Wong JYC, Schultheiss TE, Radany EH, editors. *Advances in radiation oncology. cancer treatment and research*. Heildelberg: Springer International Publishing (2017). p. 155–89.

101. Hoeben BAW, Wong JYC, Fog LS, Losert C, Filippi AR, Bentzen SM, et al. Total body irradiation in haematopoietic stem cell transplantation for paediatric acute lymphoblastic leukaemia: Review of the literature and future directions. *Front Pediatr* (2021) 9:774348. doi: 10.3389/fped.2021.774348

102. Patel P, Aydogan B, Koshy M, Mahmud D, Oh A, Saraf AL, et al. Combination of linear accelerator-based intensity-modulated total marrow irradiation and myeloablative Fludarabine/Busulfan: A phase I study. *Biol Blood Marrow Transplant* (2014) 20(12):2034–41. doi: 10.1016/j.bbmt.2014.09.005

103. Hui S, Brunstein C, Takahashi Y, DeFor T, Holtan SG, Bachanova V, et al. Dose escalation of total marrow irradiation in high-risk patients undergoing allogeneic hematopoietic stem cell transplantation. *Biol Blood Marrow Transplantation* (2017) 23(7):1110–6. doi: 10.1016/j.bbmt.2017.04.002

104. Bao Z, Zhao H, Wang D, Gong J, Zhong Y, Xiong Y, et al. Feasibillity of a novel dose fractionation strategy in TMI/TMLI. *Radiat Oncol* (2018) 13(248):1–10. doi: 10.1186/s13014-018-1201-0

105. Tran MC, Hasan Y, Wang AY, Yenice KM, Partouche J, Stock W, et al. *A phase 1 trial utilizing TMI with fludarabine-melphalan in patients with hematologic malignancies undergoing second allo-SCT*. (American Society of Hematology) (2022). doi: 10.1186/s13014-018-1201-0.

106. Welliver MX, Vasu S, Weldon TE, Zoller W, Addington M, Eiler D, et al. Utilizing organ-sparing marrow-targeted irradiation (OSMI) to condition patients with high-risk hematologic malignancies prior to allogeneic hematopoietic stem cell transplantation: Results from a prospective pilot study. *Int J Radiat Oncol Biol Phys* (2018) 102(3S):E370. doi: 10.1016/j.ijrobp.2018.07.1108

107. Aristei C, Saldi S, Pierini A, Ruggeri L, Piccine S, Ingrosso G, et al. Total marrow/lymphoid irradiation in the conditioning regimen for haploidentical T-cell depleted hematopoietic stem cell transplantation for acute myeloid leukemia. the perugia experience. In: Wong J, Hui SK, editors. *Total marrow irradiation*, *1st ed*. New York, NY: Springer Nature (2020). p. 111–22.

108. Aristei C, Lancellotta V, Carotti A, Zucchetti C, Pierini A, Saldi S, et al. Total marrow/total lymphoid irradiation as conditioning for haploidentical hematopoietic stem cell transplantation in acute myeloid leukemia patients. *Int J Radiat Oncol Biol Phys* (2018) 102(3S):E204–E. doi: 10.1016/j.ijrobp.2018.07.718

109. Pierini A, Ruggeri L, Carotti A, Falzetti F, Saldi S, Terenzi A, et al. Haploidentical age-adapted myeloablative transplant and regulatory and effector T cells for acute myeloid leukemia. *Blood Advances* (2021) 5(5):1199–208. doi: 10.1182/bloodadvances.2020003739

110. Corvo R, Zeverino M, Vagge S, Agostinelli S, Barra S, Taccini G, et al. Helical tomotherapy targeting total bone marrow after total body irradiation for patients with relapsed acute leukemia undergoing an allogeneic stem cell transplant. *Radiotherapy Oncol* (2011) 98(3):382–6. doi: 10.1016/j.radonc.2011.01.016

111. Jiang Z, Jia J, Yue C, Pang Y, Liu Z, Ouyang L, et al. Haploidentical hematopoietic SCT using helical tomortherapy for total-body irradiation and targeted dose boost in patients with high-risk/refractory acute lymphoblastic leukemia. *Bone Marrow Transplant* (2018) 53(4):438–48. doi: 10.1038/s41409-017-0049-5

112. Giebel S, Sobczyk-Kruszelnicka M, Blamek S, SaduÅ›-Wojciechowska M, Najda J, Czerw T, et al. Tandem autologous hematopoietic cell transplantation with sequential use of total marrow irradiation and high-dose melphalan in multiple myeloma. *Bone Marrow Transplant* (2021) 56(6):1297–304. doi: 10.1038/s41409-020-01181-x

113. Patel P, Oh AL, Koshy M, Sweiss K, Saraf SL, Quigley JG, et al. A phase 1 trial of autologous stem cell transplantation conditioned with melphalan 200 mg/m2 and total marrow irradiation (TMI) in patients with relapsed/refractory

multiple myeloma. *Leukemia Lymphoma* (2018) 59(7):1666–71. doi: 10.1080/10428194.2017.1390231

114. Mahe M, Liagostera C, Moreau P, Meyer AD, Lioure B, Batard S, et al. Total marrow irradiation in multiple myeloma - the French myeloma group experience. In: Wong J, Hui SK, editors. *Total marrow irradiation, 1st*. New York, NY: Springer Nature (2020). p. 135–44.

115. Samant R, Tay J, Nyiri B, Carty K, Gerig L, Andrusyk S, et al. Dose-escalated total-marrow irradiation (TMI) for relapsed multiple myeloma. *Int J Radiat Oncol Biol Phys* (2015) 93(3S):S65–S6. doi: 10.1016/j.ijrobp.2015.07.156

116. Sahebi F. Total marrow irradiation in multiple myeloma - the city of hope experience. In: Wong J, Hui SK, editors. *Total marrow irradiation, 1st*. New York, NY: Springer Nature (2020). p. 145–54.

117. Dandapani S, Wong J. Modern total body irradiation (TBI): Intensity modulated radiation treatment (IMRT). In: Wong J, Hui SK, editors. *Total marrow irradiation, 1st*. New York, NY: Springer Nature (2020). p. 177–86.

118. Wong JYC, Filippi AR, Scorsetti M, Hui S, Muren LP, Mancosu P. Supplementary appendix: Total marrow and total lymphoid irradiation in bone marrow transplantation for acute leukaemia. *Lancet Oncol* (2020) 21:e477–e87. doi: 10.1016/S1470-2045(20)30342-9

119. Zhuang AH, Liu A, Schultheiss TE, Wong JYC. Dosimetric study and verification of total body irradiation using helical tomotherapy and its comparison to extended SSD technique. *Med Dosimetry* (2010) 35(4):243–9. doi: 10.1016/j.meddos.2009.07.001

120. Penagaricano JA, Chao M, van Rhee F, Moros EG, Corry PM, Ratanatharathorn V. Clinical feasibility of TBI with helical tomotherapy. *Bone Marrow Transplantation* (2011) 46(7):929–35. doi: 10.1038/bmt.2010.237

121. Springer A, Hammer JA, Winkler E, Track C, Huppert R, Bohm A, et al. Total body irradiation with volumetric modulated arc therapy: Dosimetric data and first clinical experience. *Radiat Oncol* (2016) 11(46). doi: 10.1186/s13014-016-0625-7

122. Sarradin V, Simon L, Huynh A, Gilhodes J, Filleron T, Izar F. Total body irradiation using helical tomotherapy: Treatment technique, dosimetric results and initial clinical experience. *Cancer/Radiotherapie* (2018) 22(1):17–24. doi: 10.1016/j.canrad.2017.06.014

123. Sun R, Cuenca X, Itti R, Nguyen-Quoc S, Vernant JP, Mazeron J-J, et al. First French experiences of total body irradiations using helical TomoTherapy. *Cancer/Radiother* (2017) 21(5):365–72. doi: 10.1016/j.canrad.2017.01.014

124. Esiashvili N, Lu X, Ulin K, Laurie F, Kessel S, Kalapurakal JA, et al. Higher reported lung dose received during total body irradiation for allogeneic hematopoietic stem cell transplantation in children with acute lymphoblastic leukemia is associated wtih inferior survival: A report from the children's oncology group. *Int J Radiat Oncol Biol Phys* (2019) 104(3):513–21. doi: 10.1016/j.ijrobp.2019.02.034

125. Burke JM, Caron PC, Papadopoulos EB, Divgi CR, Sgouros G, Panageas KS, et al. Cytoreduction with iodine-131-anti-CD33 antibodies before bone marrow transplantation for advanced myeloid leukemias. *Bone Marrow Transplant* (2003) 32:549–56. doi: 10.1038/sj.bmt.1704201

126. Rosenblat TL, McDevitt MR, Mulford D, Pandit-Taskar NF, Divgi CR, Panageas KS, et al. Sequential cytarabine and alpha-particle immunotherapy with bismuth-213-lintuzumab (HuM195) for acute myeloid leukemia. *Clin Cancer Res* (2010) 16(21):5303–11. doi: 10.1158/1078-0432.CCR-10-0382

127. Jurcic JG, Ravandi F, Pagel JM, Park JH, Smith BD, Levy MY, et al. Phase I trial of targeted alpha-particle immunotherapy with actinium-225 (225 ac)-lintuzumab (Anti-CD33) and low-dose cytarabine (LDAC) in older patients with untreated acute myeloid leukemia (AML). *Blood* (2015) 126:3794. doi: 10.1182/blood.V126.23.3794.3794

128. Waldmann TA, White JD, Carrasquillo JA, Reynolds JC, Paik CH, Gansow OA, et al. Radioimmunotherapy of interleukin-2R alpha-expressing adult T-cell leukemia with yttrium-90-labeled anti-tac. *Blood* (1995) 86(11):4063–75. doi: 10.1182/blood.V86.11.4063.bloodjournal86114063

129. Pagel JM, Appelbaum FR, Eary JF, Rajendran J, Fisher DR, Gooley T. 131I-anti-CD45 antibody plus busulfan and cyclophosphamide before allogeneic hematopoietic cell transplantation for treatment of acute myeloid leukemia in first remission. *Blood* (2006) 107(5):2184–91. doi: 10.1182/blood-2005-06-2317

130. Mawad R, Gooley TA, Rajendran JG, Fisher DR, Gopal AK, Shields AT, et al. Radiolabeled anti-CD45 antibody with reduced-intensity conditioning and allogeneic transplantation for younger patients with advanced acute myeloid leukemia or myelodysplastic syndrome. *Biol Blood Marrow Transplant* (2014) 20(9):1363–8. doi: 10.1016/j.bbmt.2014.05.014

131. Koenecke C, Hofmann M, Bolte O, Gielow P, Dammann E, Stadler M, et al. Radioimmunotherapy with [188Re]-labelled anti-CD66 antibody int he conditioning for allogeneic stem cell transplantation for high-risk acute myeloid leukemia. *Int J Hematol* (2008) 87:414–21. doi: 10.1007/s12185-008-0043-1

132. Ringhoffer M, Blumstein N, Neumaier B, Glatting G, von Harsdorf S, Buchmann I, et al. 188Re or 90Y-labelled anti-CD66 antibody as part of a dose-reduced conditioning regimen for patients with acute leukaemia or myelodysplastic syndrome over the age of 55: results of a phase I-II study. *Br J Haematol* (2005) 130(4):604–13. doi: 10.1111/j.1365-2141.2005.05663.x

133. Lauter A, Strumpf A, Platzbecker U, Schetelig J, Wermke M, Radke J, et al. 188Re anti-CD66 radioimmunotherapy combined with reduced-intensity conditioning and *in-vivo* T cell depletion in elderly patients undergoing allogeneic haematopoietic cell transplantation. *Br J Haematology* (2009) 148:910–7. doi: 10.1111/j.1365-2141.2009.08025.x

134. Krishnan A, Nademanee A, Fung H, Raubitscheck A, Molina A, Yamauchi D, et al. Phase II trial of a transplantation regimen of yttrium-90 ibritumomab tiuxetan and high-dose chemotherapy in patients wtih non-hodgkin's lymphoma. *J Clin Oncol* (2008) 26(1):90–5. doi: 10.1200/JCO.2007.11.9248

135. Herrera AF, Palmer PhD JM, Adhikarla V, Yamauchi DM, Poku EK, Bading J, et al. Anti-CD25 radioimmunotherapy with BEAM autologous hematopoietic cell transplantation conditioning in Hodgkin lymphoma. *Blood Adv* (2021) 5:5300–11. doi: 10.1182/bloodadvances.2021004981

136. Gyurkocza B, Nath R, Choe H, Seropian S, Stiff PJ, Abhyankar S, et al. High doses of targeted radiation with anti-CD45 iodine (131I) apamistamab [Iomab-b] do not correlate with incidence of mucositis, febrile neutropenia or sepsis in the prospective, randomized phase 3 Sierra trial for patients with relapsed or refractory acute myeloid leukemia. *Blood* (2021) 136:30–1. doi: 10.1182/blood-2020-134624

137. Jurcic JG, Wong JYC, Knox SJ, Wahl DR, Rosenblat TL, Meredith RF. Targeted radionuclide therapy. In: Gunderson LL, Tepper JE, editors. *Clinical radiation oncology, 4th ed*. Philadelphia: Elsevier (2016). p. 399–418.

138. Appelbaum FR, Matthews DC, Eary JF, Badger CC, Kellogg M, Press OW, et al. The use of radiolabeled anti-CD33 antibody to augment marrow irradiation prior to marrow transplantation for acute myelogenous leukemia. *Transplantation.* (1992) 54:829–33. doi: 10.1097/00007890-199211000-00012

139. Matthews DC, Appelbaum FR, Eary JF, Fisher DR, Durack LD, Hui ET, et al. Phase I study of 131I-Anti-CD45 antibody plus cyclophosphamide and total body irradiation for advanced acute leukemia and myelodysplastic syndrome. *Blood* (1999) 94(4):1237–47. doi: 10.1182/blood.V94.4.1237

140. Bunjes D. 188Re-labeled anti-CD66 monoclonal antibody in stem cell transplantation for patients with high-risk acute myeloid leukemia. *Leukemia Lymphoma* (2002) 43(11):2125–31. doi: 10.1080/1042819021000033015

141. Zenz T, Glatting G, Schlenk RF, Buchmann I, Dohner H, Reske SN, et al. Targeted marrow irradiation with radioactively labeled anti-CD66 monoclonal antibody prior to allogeneic stem cell transplantation for patients with leukemia: Results of a phase I-II study. *Haematologica* (2006) 91(2):285–6.

142. Magome T, Froelich J, Holtan SG, Takahashi Y, Verneris MR, Brown K, et al. Whole-body distribution of leukemia and functional total marrow irradiation based on FLT-PET and dual-energy CT. *Mol Imaging* (2017) 16:1536012117732203. doi: 10.1177/1536012117732203

143. Magome T, Froelich J, Takahashi Y, Arentsen L, Holtan S, Verneris MR, et al. Evaluation of functional marrow irradiation based on skeletal marrow composition obtained using dual-energy computed tomography. *Int J Radiat Oncol Biol Phys* (2016) 96(3):679–87. doi: 10.1016/j.ijrobp.2016.06.2459

144. Wong JYC, Filippi AR, Scorsetti M, Hui S, Muren LP, Mancosu P. Total marrow and total lymphoid irradiation in bone marrow transplantation for acute leukaemia. *Lancet Oncol* (2020) 21:e477–e87. doi: 10.1016/S1470-2045(20)30342-9

145. Salhotra A, Stein AS. Role of radiation based conditioning regimens in patients with high-risk AML undergoing allogenic transplantation in remission or active disease and mechanisms of post-transplant relapse. *Front Oncol* (2022) 12:802648. doi: 10.3389/fonc.2022.802648

frontiers | Frontiers in Oncology

TYPE Original Research
PUBLISHED 18 October 2022
DOI 10.3389/fonc.2022.924961

OPEN ACCESS

EDITED BY
Wei Zhao,
Beihang University, China

REVIEWED BY
Alistair Templeton,
Auckland District Health Board, New Zealand
Emily Heath,
Carleton University, Canada

*CORRESPONDENCE
Bulent Aydogan
baydogan@uchicago.edu;
baydogan@radonc.uchicago.edu

SPECIALTY SECTION
This article was submitted to Radiation Oncology, a section of the journal Frontiers in Oncology

RECEIVED 21 April 2022
ACCEPTED 16 September 2022
PUBLISHED 18 October 2022

CITATION
Kavak AG, Surucu M, Ahn K-H, Pearson E and Aydogan B (2022) Impact of respiratory motion on lung dose during total marrow irradiation. *Front. Oncol.* 12:924961. doi: 10.3389/fonc.2022.924961

Impact of respiratory motion on lung dose during total marrow irradiation

Ayse Gulbin Kavak[1], Murat Surucu[2], Kang-Hyun Ahn[3,4], Erik Pearson[3] and Bulent Aydogan[3,4]*

[1]Department of Radiation Oncology, Faculty of Medicine, Gaziantep University, Gaziantep, Turkey, [2]Department of Radiation Oncology, Stanford University School of Medicine, Stanford, CA, United States, [3]Department of Radiation and Cellular Oncology, University of Chicago Pritzker School of Medicine, Chicago, IL, United States, [4]Department of Radiation Oncology, University of Illinois at Chicago Medical Center, Chicago, IL, United States

We evaluated the impact of respiratory motion on the lung dose during linac-based intensity-modulated total marrow irradiation (IMTMI) using two different approaches: (1) measurement of doses within the lungs of an anthropomorphic phantom using thermoluminescent detectors (TLDs) and (2) treatment delivery measurements using ArcCHECK where gamma passing rates (GPRs) and the mean lung doses were calculated and compared with and without motion. In the first approach, respiratory motions were simulated using a programmable motion platform by using typical published peak-to-peak motion amplitudes of 5, 8, and 12 mm in the craniocaudal (CC) direction, denoted here as M1, M2, and M3, respectively, with 2 mm in both anteroposterior (AP) and lateral (LAT) directions. TLDs were placed in five selected locations in the lungs of a RANDO phantom. Average TLD measurements obtained with motion were normalized to those obtained with static phantom delivery. The mean dose ratios were 1.01 (0.98–1.03), 1.04 (1.01–1.09), and 1.08 (1.04–1.12) for respiratory motions M1, M2, and M3, respectively. To determine the impact of directional respiratory motion, we repeated the experiment with 5-, 8-, and 12-mm motion in the CC direction only. The differences in average TLD doses were less than 1% when compared with the M1, M2, and M3 motions indicating a minimal impact from CC motion on lung dose during IMTMI. In the second experimental approach, we evaluated extreme respiratory motion 15 mm excursion in only the CC direction. We placed an ArcCHECK device on a commercial motion platform and delivered the clinical IMTMI plans of five patients. We compared, with and without motion, the dose volume histograms (DVHs) and mean lung dose calculated with the ArcCHECK-3DVH tool as well as GPR with 3%, 5%, and 10% dose agreements and a 3-mm constant distance to agreement (DTA). GPR differed by 11.1 $\pm$ 2.1%, 3.8 $\pm$ 1.5%, and 0.1 $\pm$ 0.2% with dose agreement criteria of 3%, 5%, and 10%, respectively. This indicates that respiratory motion impacts dose distribution in small and isolated parts of the lungs. More importantly, the impact of respiratory motion on the mean lung dose, a critical indicator for toxicity in IMTMI, was not statistically significant ($p > 0.05$) based on the Student's *t*-test. We conclude that most patients treated with IMTMI will have negligible dose uncertainty due to respiratory motion. This is particularly

reassuring as lung toxicity is the main concern for future IMTMI dose escalation studies.

KEYWORDS

organ motion, dose delivery, breathing motion, TMI, total marrow irradiation

Introduction

Changes in the patient anatomy are one of the largest contributors to uncertainties in dose delivery for radiation therapy. Within a single treatment delivery, i.e., intra-fraction, these changes are typically from organ motion related to physiological processes, such as digestion, cardiac motion, and respiration, with the latter typically being the most significant for treatments in the thorax. In the case of total marrow irradiation (TMI), the dose to the lung, as a critical organ at risk (OAR), is often a limiting factor. However, the impact of respiratory motion on the dose uncertainty in the lung has not been previously reported for TMI.

Total body irradiation (TBI) is an integral component of conditioning regimens prior to hematopoietic stem cell transplants. It performs two critical functions, eradicating the malignant cells escaping chemotherapy and immuno suppression to prevent the rejection of donor marrow or hematopoietic cells. Over the last two decades, the use of TBI has been steadily declining due mainly to concerns about toxicities, while alternative drug-based approaches are fast becoming the standard of care for the treatment of hematological malignancies (1–5). Various acute and chronic radiation toxicities reduce the quality of life for patients treated with TBI. Acute effects include temporary hair loss, nausea, vomiting, diarrhea, decreased blood cell count, mouth sores, and skin irritation. Among the chronic effects of TBI are cataracts, infertility, secondary malignancies, and decreased and delayed growth and development in children (2, 3). Toxicities induced by TBI inclusive conditioning regimens, such as pneumonitis, can be life-threatening (6–9). Several studies reported interstitial pneumonitis rates ranging from 6% to 30% with TBI (10–12). Della Volpe et al. (13) reported, in a retrospective study, an increase in lethal lung complications from 3.8% to 19.2% when the lung dose exceeded a threshold of 9.4 Gy. Furthermore, TBI dose escalation studies have failed due to increased fatal complications (8, 9) and are deemed impossible with current treatment techniques.

TMI has been introduced to replace TBI with the aim of reducing toxicity and enhancing the therapeutic ratio (14–16). The main advantage of TMI is the ability to focus radiation on targets and reduce radiation dose to organs at risk (OARs), particularly to the lungs, the dose-limiting organ (6, 17). TMI targets the entirety of the skeletal structure; consequently, most OARs are in close proximity to one or more target structures (18, 19). The lung can be particularly challenging to spare as it is tightly wrapped within the rib cage, a treatment target itself. It has been shown that linac-based intensity-modulated total marrow irradiation (IMTMI) and volumetric arc radiotherapy (VMAT-TMI) can reduce OAR dose by 29%–65% when compared with TBI (17, 20, 21). Similar results were also reported using the helical TMI technique (16).

Several clinical studies have established the clinical feasibility and tolerability of TMI in patients with advanced diseases as part of a conditioning regimen prior to allogeneic stem cell transplantation (22–24). TMI provides a potentially practice-changing RT technique that may allow dose escalation, better dose homogeneity, and lower toxicity. This may be expected to improve upon the current standard of care in the treatment of hematological malignancies and improve outcomes (19). Further studies to investigate technical and dosimetric challenges such as organ motion are imperative to limit toxicity and allow safe dose escalation, which is of great interest especially in the treatment of patients with advanced diseases.

It was suggested that the dose heterogeneity in both the PTV and surrounding healthy tissue increases with increasing respiratory motion amplitude (25). Most of our knowledge regarding lung motion comes from the studies that evaluated either a single point in tumor or internal markers using imaging or external surrogates with devices such as Real-Time Position Management System (RPM, Varian Medical Systems, Palo Alto, CA) (26). A point in the lung may exhibit large displacements due to respiratory motion, which results in significant geometric and dosimetric uncertainties (25–28). Knybel et al. (29) reported average motion amplitude changes to be 6.0 ± 2.2 mm and Liu et al. (30) reported that only 10.8% of the patients experienced tumor motion more than 10 mm. Seppenwoolde et al. (31) reported that the largest tumor motion was 12 ± 2 mm in the CC direction and 2 ± 1 mm in both the anteriorposterior (AP) and lateral (LAT) directions.

The steep dose gradients possible with IMRT enable better target conformity and healthy tissue sparing, especially for irregularly shaped concave target volumes. However, the sharp dose gradient can potentially lead to dose uncertainty due to

imperfections in patient positioning, immobilization, and organ motion (32–34). The goal of this study is to evaluate the impact of respiratory motion on the lung dose during IMTMI.

Materials and methods

Treatment planning

We used the anthropomorphic RANDO phantom (The Phantom Laboratory, Salem, NY) for treatment planning and dose measurement. The RANDO phantom was scanned with a 3-mm slice thickness using a Picker PQ 5000 CT scanner (Philips Medical Systems, Cleveland, OH). The entire skeletal structure was contoured and expanded using a 3-mm isotropic margin to construct the PTV. IMTMI planning followed the technique described previously (4, 14, 15) using the Eclipse treatment planning system (Varian™ Medical Systems, Palo Alto, CA).

The contoured OARs included the following: lenses of the eyes, brain, oral cavity, lungs, liver, kidneys, heart, and small intestine. Each TMI plan had three sub-plans: one for the head and neck, one for the chest, and one for the pelvic region. PTVs in the head and neck sub-plan included the cranium, mandible, and cervical vertebral bodies (C1 to C7). The chest sub-plan included the sternum, ribs, and thoracic vertebral bodies (T1 to T12) and the pelvis sub-plan included the os coxae, femoral head, lumbar vertebral bodies (L1 to L5), and the upper half of the femur. The total prescribed IMTMI dose was 12 Gy. Nine equally spaced 6-MV IMRT beams were created for each sub-plan and optimized to deliver the prescription dose to provide 95% PTV coverage. In order to improve the homogeneity in the junction areas, the chest sub-plan was optimized first and then used as the base plan for both the pelvis and head and neck sub-plans. Although we used only the chest sub-plan in this study, a full IMTMI plan was generated to account for dose from abutting fields and to simulate the IMTMI treatment and actual dose a patient would receive in the clinic. Retrospective patient data in this study were obtained from an IRB-approved clinical trial.

TLD sensitivities

We used thermoluminescent detectors (TLD-100) with a cross-section of 3 mm × 3 mm and a thickness of 0.9 mm. All TLDs were annealed before each exposure in a high-temperature Fisher Scientific Isotemp Oven (Fisher Scientific, Pittsburgh, PA) for 1 h at 400°C and 18 h at 80°C to decrease residual signals. After each exposure, the TLDs were stored at room temperature for 16 h prior to read out. A Harshaw 3500 TLD reader (Thermo Electron Corp., Santa Fe, NM) was used for TLD reading. TLD sensitivities were obtained using three independent exposures to a uniform dose of 0.85 Gy from a 6-MV beam under full scatter conditions, with a field size of 10 × 10 cm^2, a source-to-axis distance of 100 cm, and at a depth of 10 cm in solid water. TLDs were examined according to the protocol defined by Reft et al. (35). The standard deviations of the calibration factors defined uncertainties in individual TLD sensitivities.

Radiation measurement

We modified the plugs that were provided with the RANDO phantom to make enough room for three TLDs while keeping them securely in place to eliminate positioning uncertainty. We selected five points for measurement using the calculated dose distributions to be representative of doses ranging from low to high within the lungs. All points were at least 2 cm deep in the body and 5 cm away from the edge of the phantom to avoid any potential dosimetric error. Three TLD-100 chips were placed in each of the five predetermined locations in the lungs of the RANDO phantom. Each experiment was repeated three times to reduce measurement uncertainty for each simulated respiratory motion.

An expanding foam structure was created to support the phantom and provide repeatable positioning. The motion profiles were generated with an in-house programmable motion platform as shown in Figure 1. Only the chest sub-plan was used in this study as the aim of this study is to evaluate the impact of respiratory motion on the lung dose. The RANDO phantom was first set up to the predetermined isocenter location using surface marks and lasers and then the chest sub-plan treatment was delivered using a Varian Trilogy linear accelerator (Varian Medical Systems Inc., Palo Alto, CA). Dose measurement was first carried out in a static (no motion) phantom as a reference and was repeated with the phantom in motion. We used typical published peak-to-peak motion amplitudes: 5, 8, and 12 mm in craniocaudal (CC) direction for M1, M2, and M3, respectively, and 2 mm for both AP and LAT directions (26, 30, 31). Figure 2 displays the respiratory motion for M3. The motion platform was set in motion and the treatment dose delivery was started after a random delay, as would happen for a patient in the clinic. Additional measurements were carried out with 5-, 8-, and 12-mm peak-to-peak amplitudes in the CC direction only to evaluate the impact of directional respiratory motion during IMTMI.

Statistical analysis

Two-sided, paired Student's *t*-test evaluated statistical significance with p-values < 0.05 using GraphPad Instat version 3.05 (GraphPad Software, San Diego, CA, USA).

FIGURE 1
Experimental setup showing the RANDO phantom immobilized with alpha-cradle on a motion platform.

Patient QA measurement with ArcCHECK

Patient-specific QA for routine IMRT and VMAT in our clinic is done with ArcCHECK (Sun Nuclear, Melbourne, FL), a 3D cylindrical phantom with a diameter of 21 cm and a helical detector grid consisting of 1,386 diode detectors (0.8×0.8 mm^2) placed at intervals of 10 mm. We placed the ArcCHECK on a commercial motion platform as shown in Figure 3 and repeated the treatment delivery and measurement for plans from 5 patients who were treated in our clinic with 9 Gy (150 cGy BID) IMTMI while simulating an extreme case of respiratory motion with a 15 mm excursion in only the CC direction. Gamma index analysis was performed and compared with and without motion using 3%, 5%, and 10% dose agreement with a 3-mm constant distance to agreement (DTA).

3DVH dose reconstruction

The ArcCHECK-3DVH system (Sun Nuclear Corporation, Melbourne, FL, USA) is a commercial DVH-based QA tool. The 3D patient dose is constructed from the measurement data with the provided internal calculation engine, called ArcCHECK planned dose perturbation (ACPDP). The ACPDP algorithm involves the following calculation steps: (a) synchronizing the planned data with the ArcCHECK virtual inclinometer recorded

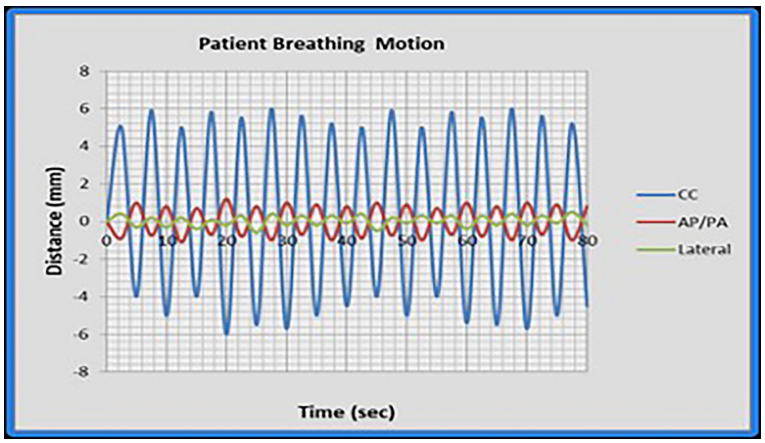

FIGURE 2
The respiratory motion M3 as simulated in this study. Cranio-caudal (CC); anteroposterior (AP); and lateral (LAT) directions.

FIGURE 3
ArcCHECK detector placed array on the motion platform before dose measurement.

data; (b) generating a relative 3D dose grid to a homogeneous cylindrical phantom for each sub-beam; (c) morphing the relative dose based on the ArcCHECK-measured data to produce the 3D absolute dose in the cylindrical phantom; (d) taking the ratio of the reconstructed dose to the TPS-calculated dose for each voxel in the phantom; and (e) perturbing the TPS-calculated dose of the patient by the above ratios (36). The final grid size of the reconstructed dose was kept the same as that of the TPS dose calculation. To perform 3DVH reconstruction, the following data set was gathered: (1) reference DICOM RT plan, (2) DICOM RT dose (TPS-calculated dose for the patient and ArcCHECK geometries, respectively), and (3) ArcCHECK measurement data (.acml).

Results

Point dose measurements with TLD

IMTMI dose distribution of the chest plan shown in Figure 4 demonstrates the planned IMTMI dose coverage for the PTV in the chest and sparing of the lungs in the RANDO phantom. Dose ranged from 4 Gy (blue) to 12 Gy (red). A sharp reduction beyond the target was achieved, which provided a lower dose to surrounding healthy tissue. Dose in the coronal view shown in the left pane also displays the index for three axial planes where the TLD measurements were done. On the right, the three axial planes displayed dose distribution and the location of five measurement points.

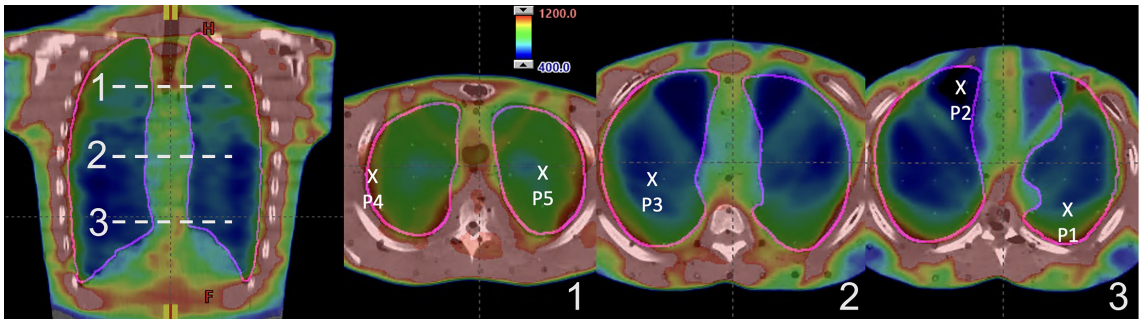

FIGURE 4
IMTMI dose distribution in the RANDO phantom. A coronal slice on the left with the indexing (1–3) for the axial slices where the TLDs were placed. On the right are the three axial slices showing the five measurement points within the lung. Dose range is shown from 400 cGy (blue) to 1,200 cGy (red).

TLD measured doses and associated standard deviations (error bars) in five points within the lungs are shown in Figure 5 for the motions M1, M2, and M3. TLD measurements were normalized to the static reference dose obtained irradiation with no motion. The mean normalized TLD readings (range) were 1.01 (0.98–1.03), 1.04 (1.01–1.09), and 1.08 (1.04–1.12) for M1, M2, and M3, respectively. A statistically significant change in delivered dose was observed for M2 and M3 ($p < 0.05$). Additional measurements performed with 5-, 8-, and 12-mm motion in CC direction only agreed within 1% with the respiratory motions M1, M2, and M3, indicating that the impact of respiratory motion in LAT and AP directions may negligible during IMTMI.

Treatment delivery verification with ArcCHECK

Treatment delivery dose map comparison obtained with and without motion using ArcCHECK for a representative patient is shown in Figure 6. The IMTMI. chest sub-plan had a 96.8% GPR with no motion and 87.1% with motion with 3%/3 mm criteria. This indicates that respiratory motion caused an additional 10.3% of the detectors to measure a dose difference greater than 3%. When the dose difference criterion was increased to 5% with a constant 3-mm DTA, the GPR differed by 2.8% (97% vs. 99.8%). Figure 7 compares the measured dose differences for the three-dose agreement levels used in this study: 3%, 5%, and 10%. Both the blue (+) and red (−) dots identify the detectors or location within the lungs with a measured difference of more than the specified level with motion. As the dose difference criteria increased from 3% to 10%, the number of detectors detecting such a dose difference decreased from 134 to only 1 in 1,386 detectors, respectively. This indicates that the motion would change the dose by more than 10% only in one small, isolated location within the lung of the same patient during IMTMI. For the cohort of 5 patients, the average percent differences in GPR due to respiratory motion was 11.1 ± 2.1% with 3%/3 mm. Nonetheless, it was only 3.8 ± 1.5%, and 0.1 ± 0.2% when a dose agreement criterion of 5% and 10% was used, respectively. Figure 8 shows the comparison of 3DVH for the same patient with and without motion. The percent difference in mean lung dose was less than 3% with motion. For the cohort of five patients evaluated in this study, the effect of respiratory motion on the mean lung dose (5.7 ± 0.3 Gy vs. 5.5 ± 0.2 Gy) was not statistically significant based on the Student's *t*-test ($p > 0.05$).

Discussion

Organ motion is by far the largest contributor to uncertainties in RT. Respiratory motion affects all tumor sites in the thorax and abdomen and is the most profound and relevant for radiotherapy. Organ motion, dose uncertainty, motion mitigation, and management strategies in lung cancer have been studied extensively. Previous IMRT studies have indicated increasing dose discrepancies ranging from 3% to 12% between planned and delivered doses (37–40) due to respiratory motion. Treatment delivery with higher dose rates and smaller monitor-unit (MU) per segment has been associated with larger dosimetric errors (41, 42). Seco et al. (43) argued that interplay between organ (breathing) motion and leaf motion is only significant when considering the case of treatment beams made up of many few-monitor-unit segments, where the segment delivery time (1–2 s) is of the order of the respiratory period (3–5 s). During IMRT with small numbers of MUs per segment, the difference between the motion-averaged and static dose for 30 fractions could range from 6% to 12% for simple to complex respiratory motion functions, respectively (44).

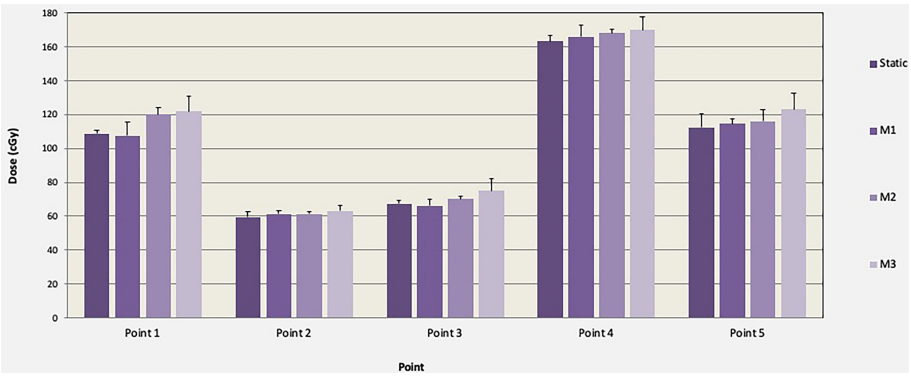

FIGURE 5
Comparison of TLD dose and associated standard deviations (error bars) in cGy with and without motion (M1, M2, and M3) for one TMI fraction of chest plan (150 cGy).

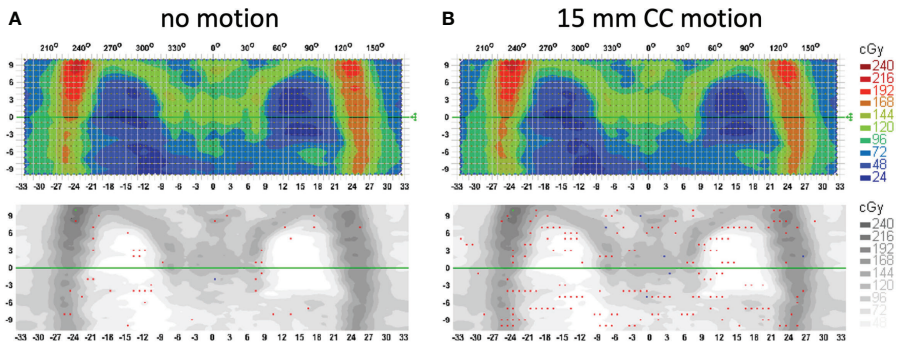

FIGURE 6
Treatment delivery QA comparison for a patient with **(A)** no motion and **(B)** 15 mm CC motion. Measurements were done with an ArcCHECK detector array and analysis is performed with the gamma index criteria of 3%/3 mm. Red and blue dots show the locations (detectors) that fail the 3%/3 mm gamma index passing criteria.

TMI being a complex treatment technique delivering small numbers of MUs per leaf segment is prone to large delivery uncertainties especially when treating bones in the chest and maximally sparing lungs at the same time. Several studies investigated the dosimetric accuracy of both helical and linac-based TMI delivery techniques in human-like phantoms and confirmed that TMI is, regardless of the delivery technique, dosimetrically accurate and safe (5, 17, 44). These studies, nonetheless, were conducted in the "ideal" situation without intrafraction motion. In this study, we performed a comprehensive investigation of dose uncertainty in lungs due to respiratory motion during linac-based IMTMI delivery. To achieve this, an end-to-end test was carried out through immobilization, simulation, planning, treatment delivery, and dose measurement with and without motion using an anthropomorphic phantom and an ArcCHECK placed on a motion platform. When an extreme case of respiratory motion was simulated with a 15-mm peak-to-peak displacement only

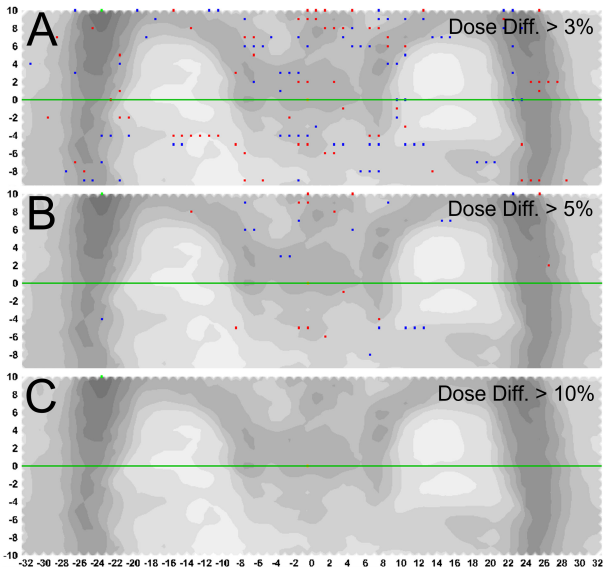

FIGURE 7
Percent difference in measured dose with and without motion. Blue (+) and red (-) dots represent the detectors or location within the lungs with a measured difference greater than **(A)** 3%, **(B)** 5%, and **(C)** 10%, with 3mm distance to agreement criteria.

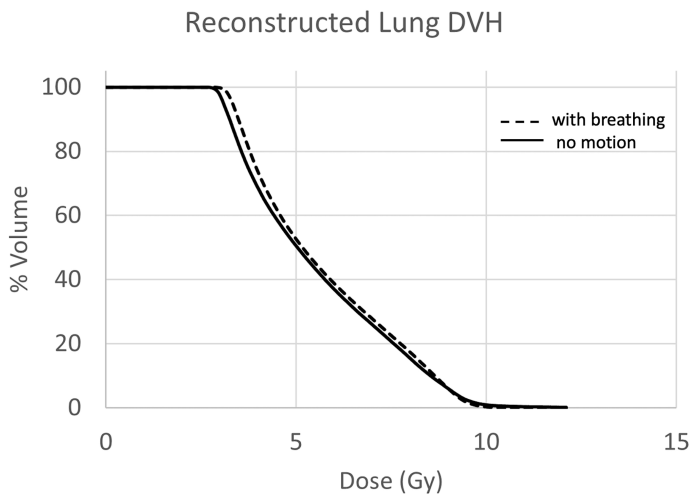

FIGURE 8
Lung DVH comparison with (solid) and without (dashed) motion. The mean dose difference was less than 3%.

the CC direction during IMTMI, none of the patients had more than 6 out of 1386 (0.4%) detectors reporting more than a 10% dose difference. Similarly, we observed a dose difference of more than 5% in only 53 ± 21 (3.8 ± 1.5%) detectors. These results indicate that respiratory motions increase the dose only in small and isolated parts within the lungs. Moreover, the mean lung dose, which is the most relevant measure for toxicity, was not impacted by respiratory motion. One possible explanation for this observation is that the longer treatment times during TMI could have a dose averaging effect. Considering the average lung motion amplitude is 6.0 ± 2.2 in approximately 90% of the patients with a maximum of 12 ± 2 mm (29, 30), it may be safe to assume that an overwhelming majority of patients treated with TMI will have a negligible dose uncertainty due to respiratory motion.

One of the potential limitations of this study is that the respiratory motion was applied to the whole phantom. Nonetheless, our approach is adequate to study the impact of respiratory motion on the lung dose and ignores the dose uncertainty in the target (bony anatomy). Bones in our body are not affected by respiratory motion except for the ribcage, which constitutes only a small portion of the target in TMI. However, further analysis could include more realistic motions to be simulated separately for targets and lungs.

Initial clinical trials have demonstrated that the TMI-inclusive transplant regimens are safe and feasible (22–24, 45). Several Phase 2 studies are ongoing to establish the outcome benefit of adding TMI to the current standard of care (46–48). Furthermore, there is an increased interest in dose escalation studies based on the reports that a TBI dose of 15.6 Gy (30% more than the standard dose of 12 Gy) halved the relapse rate (8). However, treatment outcomes did not improve due to radiation toxicity (9). Respiratory motion is a concern in the management of radiation toxicity as it has the potential to increase the mean lung dose. Our study suggests that the impact of respiratory motion on the lung dose may be negligible. This is particularly assuring as there may be a therapeutic benefit of higher TMI doses, especially for patients with advanced hematological malignancies with poor prognoses.

Data availability statement

The datasets presented in this article are not readily available. Requests to access the datasets should be directed to baydogan@uchicago.edu.

Author contributions

BA and AGK responsible for the conception and design. BA provided oversight as the senior author. AGK, MS, KHA, and BA conducted the experiments. AGK performed statistical analyses. AGK, MS, KHA, EP and BA interpreted the experimental results. EP provided scientific review and improvements. AGK drafted the manuscript. All authors revised and approved the manuscript for submission.

Acknowledgments

The authors thank Dr. Rodney Wiersma for providing his in-house 3D motion platform to perform the TLD measurements in this study. A portion of the study was presented at the AAPM annual meeting in 2011.

Conflict of interest

BA received grant support from Varian Medical Systems Inc, Palo Alto CA.

The remaining authors declare that the research was conducted in the absence of any commercial or financial relationships that could be construed as a potential conflict of interest.

Publisher's note

References

1. Sanders JE. Late effects in children receiving total body irradiation for bone marrow transplantation. *Radiother Oncol* (1990) 18 Suppl 1:82–7. doi: 10.1016/0167-8140(90)90181-U

2. Brochstein JA, Kernan NA, Groshen S, Cirrincione C, Shank B, Emanuel D, et al. Allogeneic bone marrow transplantation after hyperfractionated total-body irradiation and cyclophosphamide in children with acute leukemia. *N Engl J Med* (1987) 317(26):1618–24. doi: 10.1056/NEJM198712243172602

3. Wong JY, Filippi AR, Dabaja BS, Yahalom J, Specht L. Total body irradiation: Guidelines from the international lymphoma radiation oncology group (ILROG). *Int J Radiat Oncol Biol Phys* (2018) 101(3):521–9. doi: 10.1016/j.ijrobp.2018.04.071

4. Wong JY, Filippi AR, Scorsetti M, Hui S, Muren LP, Mancosu P. Total marrow and total lymphoid irradiation in bone marrow transplantation for acute leukemia. *Lancet Oncol* (2020) 21(10):e477–87. doi: 10.1016/S1470-2045(20)30342-9

5. Hui SK, Das RK, Thomadsen B, Henderson D. CT-based analysis of dose homogeneity in total body irradiation using lateral beam. *J Appl Clin Med Phys* (2004) 5:71–9. doi: 10.1120/jacmp.v5i4.1980

6. Hui SK, Verneris MR, Froelich J, Dusenbery K, Welsh JS. Multimodality image guided total marrow irradiation and verification of the dose delivered to the lung, PTV, and thoracic bone in a patient: a case study. *Technol Cancer Res Treat* (2009) 8(1):23–8. doi: 10.1177/153303460900800104

7. Carruthers SA, Wallington MM. Total body irradiation and pneumonitis risk: a review of outcomes. *Br J Cancer* (2004) 90(11):2080–4. doi: 10.1038/sj.bjc.6601751

8. Clift RA, Buckner CD, Appelbaum FR, Bearman SI, Petersen FB, Fisher LD, et al. Allogeneic marrow transplantation in patients with acute myeloid leukemia in first remission: a randomized trial of two irradiation regimens. *Blood* (1990) 76(9):1867–71. doi: 10.1182/blood.V76.9.1867.1867

9. Clift RA, Buckner CD, Appelbaum FR, Bryant E, Bearman SI, Petersen FB, et al. Allogeneic marrow transplantation in patients with chronic myeloid leukemia in the chronic phase: a randomized trial of two irradiation regimens. *Blood* (1991) 77(8):1660–5. doi: 10.1182/blood.V77.8.1660.1660

10. Ozsahin M, Pène F, Touboul E, Gindrey-Vie B, Dominique C, Lefkopoulos D, et al. Total-body irradiation before bone marrow transplantation. results of two randomized instantaneous dose rates in 157 patients. *Cancer* (1992) 69(11):2853–65. doi: 10.1002/1097-0142(19920601)69:11<2853::aid-cncr2820691135>3.0.co;2-2

11. Dusenbery KE, Daniels KA, McClure JS, McGlave PB, Ramsay NK, Blazar BR, et al. Randomized comparison of cyclophosphamide-total body irradiation versus busulfan-cyclophosphamide conditioning in autologous bone marrow transplantation for acute myeloid leukemia. *Int J Radiat Oncol Biol Phys* (1995) 31(1):119–28. doi: 10.1016/0360-3016(94)00335-I

12. Devergie A, Blaise D, Attal M, Tigaud JD, Jouet JP, Vernant JP, et al. Allogeneic bone marrow transplantation for chronic myeloid leukemia in first chronic phase: a randomized trial of busulfan-cytoxan versus cytoxan-total body irradiation as preparative regimen: a report from the French society of bone marrow graft (SFGM). *Blood* (1995) 85(8):2263–8. doi: 10.1182/blood.V85.8.2263.bloodjournal8582263

13. Della Volpe A, Ferreri AJ, Annaloro C, Mangili P, Rosso A, Calandrino R, et al. Lethal pulmonary complications significantly correlate with individually assessed mean lung dose in patients with hematologic malignancies treated with total body irradiation. *Int J Radiat Oncol Biol Phys* (2002) 52(2):483–8. doi: 10.1016/S0360-3016(01)02589-5PMID:11872296

14. Hui SK, Kapatoes J, Fowler J, Henderson D, Olivera G, Manon RR, et al. Feasibility study of helical tomotherapy for total body or total marrow irradiation. *Med Phys* (2005) 32(10):3214–24. doi: 10.1118/1.2044428

15. Aydogan B, Mundt AJ, Roeske JC. Linac-based intensity modulated total marrow irradiation (IM-TMI). *Technol Cancer Res Treat* (2006) 5(5):513–9. doi: 10.1177/153303460600500508

16. Wong JY, Liu A, Schultheiss T, Popplewell L, Stein A, Rosenthal J, et al. Targeted total marrow irradiation using three-dimensional image-guided tomographic intensity-modulated radiation therapy: an alternative to standard total body irradiation. *Biol Blood Marrow Transplant* (2006) 12(3):306–15. doi: 10.1016/j.bbmt.2005.10.026

17. Wilkie JR, Tiryaki H, Smith BD, Roeske JC, Radosevich JA, Aydogan B. Feasibility study for linac-based intensity modulated total marrow irradiation. *Med Phys* (2008) 35(12):5609–18. doi: 10.1118/1.2990779

18. Yeginer M, Roeske JC, Radosevich JA, Aydogan B. Linear accelerator-based intensity-modulated total marrow irradiation technique for treatment of hematologic malignancies: a dosimetric feasibility study. *Int J Radiat Oncol Biol Phys* (2011) 79(4):1256–65. doi: 10.1016/j.ijrobp.2010.06.029

19. Mancosu P, Cozzi L, Muren LP. Total marrow irradiation for hematopoietic malignancies using volumetric modulated arc therapy: A review of treatment planning studies. *Phys Imaging Radiat Oncol* (2019) 11:47–53. doi: 10.1016/j.phro.2019.08.001

20. Aydogan B, Yeginer M, Kavak GO, Fan J, Radosevich JA, Gwe-Ya K. Total marrow irradiation with RapidArc volumetric arc therapy. *Int J Radiat Oncol Biol Phys* (2011) 81(2):592–9. doi: 10.1016/j.ijrobp.2010.11.035

21. Fogliata A, Cozzi L, Clivio A, Ibatici A, Mancosu P, Navarria P, et al. Preclinical assessment of volumetric modulated arc therapy for total marrow irradiation. *Int J Radiat Oncol Biol Phys* (2011) 80(2):628–36. doi: 10.1016/j.ijrobp.2010.11.028

22. Wong JY, Forman S, Somlo G, Rosenthal J, Liu A, Schultheiss T, et al. Dose escalation of total marrow irradiation with concurrent chemotherapy in patients with advanced acute leukemia undergoing allogeneic hematopoietic cell transplantation. *Int J Radiat Oncol Biol Phys* (2013) 85(1):148–56. doi: 10.1016/j.ijrobp.2012.03.033

23. Patel P, Aydogan B, Koshy M, Mahmud D, Oh A, Saraf SL, et al. Combination of linear accelerator-based intensity-modulated total marrow irradiation and myeloablative fludarabine/busulfan: a phase I study. *Biol Blood Marrow Transplant* (2014) 20(12):2034–4. doi: 10.1016/j.bbmt.2014.09.005

24. Patel P, Oh AL, Koshy M, Sweiss K, Saraf SL, Quigley JG, et al. A phase 1 trial of autologous stem cell transplantation conditioned with melphalan 200 mg/m^2 and total marrow irradiation (TMI) in patients with relapsed/refractory multiple myeloma. *Leuk Lymphoma* (2018) 59(7):1666–71. doi: 10.1080/10428194.2017.1390231

25. George R, Keall PJ, Kini VR, Vedam SS, Siebers JV, Wu Q, et al. Quantifying the effect of intrafraction motion during breast IMRT planning and dose delivery. *Med Phys* (2003) 30(4):552–62. doi: 10.1118/1.1543151

26. Quirk S, Becker N, Smith WL. External respiratory motion analysis and statistics for patients and volunteers. *J Appl Clin Med Phys* (2013) 14(2):4051. doi: 10.1120/jacmp.v14i2.4051

27. Plathow C, Fink C, Ley S, Puderbach M, Eichinger M, Zuna I, et al. Measurement of tumor diameter-dependent mobility of lung tumors by dynamic MRI. *Radiother Oncol* (2004) 73(3):349–54. doi: 10.1016/j.radonc.2004.07.017

28. Keall PJ, Mageras GS, Balter JM, Emery RS, Forster KM, Jiang SB, et al. The management of respiratory motion in radiation oncology report of AAPM task group 76. *Med Phys* (2006) 33(10):3874–900. doi: 10.1118/1.2349696

29. Knybel L, Cvek J, Molenda L, Stieberova N, Feltl D. Analysis of lung tumor motion in a Large sample: Patterns and factors influencing precise delineation of internal target volume. *Int J Radiat Oncol Biol Phys* (2016) 96(4):751–8. doi: 10.1016/j.ijrobp.2016.08.008

30. Liu HH, Balter P, Tutt T, Choi B, Zhang J, Wang C, et al. Assessing respiration-induced tumor motion and internal target volume using four-dimensional computed tomography for radiotherapy of lung cancer. *Int J Radiat Oncol Biol Phys* (2007) 68(2):531–40. doi: 10.1016/j.ijrobp.2006.12.066

31. Seppenwoolde Y, Shirato H, Kitamura K, Shimizu S, van Herk M, Lebesque JV, et al. Precise and real-time measurement of 3D tumor motion in lung due to respiratory and heartbeat, measured during radiotherapy. *Int J Radiat Oncol Biol Phys* (2002) 53(4):822–34. doi: 10.1016/S0360-3016(02)02803-1

32. Zelefsky MJ, Fuks Z, Happersett L, Lee HJ, Ling CC, Burman CM, et al. Clinical experience with intensity modulated radiation therapy (IMRT) in prostate cancer. *Radiother Oncol* (2000) 55(3):241–9. doi: 10.1016/S0167-8140(99)00100-0

33. Xing L, Lin Z, Donaldson SS, Le QT, Tate D, Goffinet DR, et al. Dosimetric effects of patient displacement and collimator and gantry angle misalignment on intensity modulated radiation therapy. *Radiother Oncol* (2000) 56(1):97–108. doi: 10.1016/S0167-8140(00)00192-4

34. Manning MA, Wu Q, Cardinale RM, Mohan R, Lauve AD, Kavanagh BD, et al. The effect of setup uncertainty on normal tissue sparing with IMRT for head-and-neck cancer. *Int J Radiat Oncol Biol Phys* (2001) 51(5):1400–9. doi: 10.1016/S0360-3016(01)01740-0

35. Reft CS, Runkel-Muller R, Myrianthopoulos L. *In vivo* and phantom measurements of the secondary photon and neutron doses for prostate patients undergoing 18 MV IMRT. *Med Phys* (2006) 33(10):3734–42. doi: 10.1118/1.2349699

36. SaitoM,KadoyaN,SatoK,ItoK,DobashiS,TakedaK,etal.ComparisonofDVH-based plan verification methods for VMAT: ArcCHECK-3DVH system and dynalog-based dose reconstruction. *J Appl Clin Med Phys* (2017) 18(4):206–14. doi: 10.1002/acm2.12123

37. Jiang SB, Pope C, Al Jarrah KM, Kung JH, Bortfeld T, Chen GT. An experimental investigation on intra-fractional organ motion effects in lung IMRT treatments. *Phys Med Biol* (2003) 48(12):1773–84. doi: 10.1088/0031-9155/48/12/307

38. Yu CX, Jaffray DA, Wong JW. The effects of intra-fraction organ motion on the delivery of dynamic intensity modulation. *Phys Med Biol* (1998) 43(1):91–104. doi: 10.1088/0031-9155/43/1/006

39. Zhao B, Yang Y, Li T, Li X, Heron DE, Huq MS. Statistical analysis of target motion in gated lung stereotactic body radiation therapy. *Phys Med Biol* (2011) 56 (5):1385–95. doi: 10.1088/0031-9155/56/5/011

40. Zhao B, Yang Y, Li T, Li X, Heron DE, Huq MS. Dosimetric effect of intrafraction tumor motion in phase gated lung stereotactic body radiotherapy. *Med Phys* (2012) 39(11):6629–37. doi: 10.1118/1.4757916

41. Li H, Park P, Liu W, Matney J, Liao Z, Balter P, et al. Patient-specific quantification of respiratory motion-induced dose uncertainty for step-and-shoot IMRT of lung cancer. *Med Phys* (2013) 40(12):121712. doi: 10.1118/1.4829522

42. Berbeco RI, Pope CJ, Jiang SB. Measurement of the interplay effect in lung IMRT treatment using EDR2 films. *J Appl Clin Med Phys* (2006) 7(4):33–42. doi: 10.1120/jacmp.v7i4.2222

43. Seco J, Sharp GC, Turcotte J, Gierga D, Bortfeld T, Paganetti H. Effects of organ motion on IMRT treatments with segments of few monitor units. *Med Phys* (2007) 34(3):923–34. doi: 10.1118/1.2436972

44. Surucu M, Yeginer M, Kavak GO, Fan J, Radosevich JA, Aydogan B. Verification of dose distribution for volumetric modulated arc therapy total marrow irradiation in a humanlike phantom. *Med Phys* (2012) 39(1):281–8. doi: 10.1118/1.3668055

45. Tran MC, Hasan Y, Wang AY, et al. A phase 1 trial utilizing TMI with fludarabine-melphalan in patients with hematologic malignancies undergoing second allo-SCT. *Blood Adv* (2022) bloodadvances.2022007530. doi: 10.1182/bloodadvances.2022007530

46. Wong JY, Tsai NC, Han C, Palmer J, Liu A, Al Malki M, et al. Phase II study of dose escalated total marrow and lymphoid irradiation (TMLI) in combination with cyclophosphamide and etoposide in patients with poor-risk acute leukemia. *Int J Radiat Oncol Biol Phys* (2020) 108(3):S155. doi: 10.1016/j.ijrobp.2020.07.912

47. Available at: https://www.clinicaltrials.gov/ct2/show/NCT03121014.

48. Available at: https://clinicaltrials.gov/ct2/show/NCT04187105.

frontiers | Frontiers in Oncology

TYPE Original Research
PUBLISHED 31 October 2022
DOI 10.3389/fonc.2022.1017355

OPEN ACCESS

EDITED BY
Jean El Cheikh,
American University of Beirut Medical Center, Lebanon

REVIEWED BY
Jian Zhou,
Henan Provincial Cancer Hospital, China
Sheng-Li Xue,
The First Affiliated Hospital of Soochow University, China

*CORRESPONDENCE
Savita Dandapani
sdandapani@coh.org

SPECIALTY SECTION
This article was submitted to Radiation Oncology, a section of the journal Frontiers in Oncology

RECEIVED 11 August 2022
ACCEPTED 04 October 2022
PUBLISHED 31 October 2022

CITATION
Ladbury C, Semwal H, Hong D, Yang D, Hao C, Han C, Liu A, Marcucci G, Rosenthal J, Hui S, Salhotra A, Ali H, Nakamura R, Stein A, Al Malki M, Wong JYC and Dandapani S (2022) Role of radiotherapy in treatment of extramedullary relapse following total marrow and lymphoid irradiation in high-risk and/or relapsed/refractory acute leukemia.
Front. Oncol. 12:1017355.
doi: 10.3389/fonc.2022.1017355

Role of radiotherapy in treatment of extramedullary relapse following total marrow and lymphoid irradiation in high-risk and/or relapsed/refractory acute leukemia

Colton Ladbury[1], Hemal Semwal[2,3], Daniel Hong[4], Dongyun Yang[5], Claire Hao[6], Chunhui Han[1], An Liu[1], Guido Marcucci[5], Joseph Rosenthal[6], Susanta Hui[1], Amandeep Salhotra[6], Haris Ali[6], Ryotaro Nakamura[6], Anthony Stein[6], Monzr Al Malki[6], Jeffrey Y. C. Wong[1] and Savita Dandapani[1]*

[1]Department of Radiation Oncology, City of Hope National Medical Center, Duarte, CA, United States, [2]Department of Integrative Biology and Physiology, University of California Los Angeles, Los Angeles, CA, United States, [3]Department of Bioengineering, University of California, Los Angeles, Los Angeles, CA, United States, [4]Department of Physics, Emory University, Atlanta, GA, United States, [5]Division of Biostatistics, City of Hope National Medical Center, Duarte, CA, United States, [6]Department of Hematology and Hematopoietic Cell Transplantation, City of Hope National Medical Center, Duarte, CA, United States

Background: Total Marrow and Lymphoid Irradiation (TMLI) is a promising component of the preparative regimen for hematopoietic cell transplantation in patients with high-risk acute myeloid leukemia (AML) and acute lymphoid leukemia (ALL). Extramedullary (EM) relapse after TMLI is comparable to TBI and non-TBI conditioning regimens. This study evaluates outcomes of patients treated with radiotherapy (RT) with EM relapse previously treated with TMLI.

Methods: A retrospective analysis of five prospective TMLI trials was performed. TMLI targeted bones and major lymphoid tissues using image-guided tomotherapy, with total dose ranging from 12 to 20 Gy. EM recurrences were treated at the discretion of the hematologist and radiation oncologist using RT ± chemotherapy. Descriptive statistics and survival analysis were then performed on this cohort.

Results: In total, 254 patients with refractory or relapsed AML or ALL were treated with TMLI at our institution. Twenty-one patients were identified as receiving at least one subsequent course of radiation. A total of 67 relapse sites (median=2 sites/patient, range=1-16) were treated. Eleven relapsed patients were initially treated with curative intent. Following the initial course of subsequent RT, 1-year, 3-year and 5-year estimates of OS were 47.6%, 32.7% and 16.3%, respectively. OS was significantly better in patients treated with

curative intent, with median OS of 50.7 months vs 1.6 months (p<0.001). 1-year, 3-year and 5-year estimates of PFS were 23.8%, 14.3% and 14.3%, respectively. PFS was significantly better in patients treated with curative intent, with median PFS of 6.6 months vs 1.3 months (p<0.001). Following RT, 86.6% of the sites had durable local control.

Conclusions: RT is an effective modality to treat EM relapse in patients with acute leukemia who relapse after HCT achieving high levels of local control. In patients with limited relapse amenable to curative intent, radiation confers favorable long-term survival. Radiation as salvage treatment for EM relapse after HCT warrants further evaluation.

KEYWORDS

TMLI, ALL, AML, leukemia, radiation, relapse, salvage, HCT role of radiation following TMLI

Introduction

Hematopoietic cell transplantation (HCT) is a form of consolidative therapy that is an essential component of potentially curative treatment regimens for patients with acute myeloid leukemia (AML) and acute lymphocytic leukemia (ALL). Much of the efficacy of HCT is attributed to conditioning with high-dose chemotherapy and, when possible, radiation therapy in the form of total body irradiation (TBI).

Given that the toxicity related to TBI is related to radiation dose to normal tissues, a more targeted form of TBI has been pioneered, called total marrow and lymphoid irradiation (TMLI), which aims to deliver radiation primarily to areas most at risk for leukemic involvement while being able to spare other normal tissues, thereby reducing toxicity (1). This has facilitated treatment of high-risk relapsed/refractory patients with active disease who otherwise would not have been candidates for transplant (2). Previous studies have shown that TMLI can permit target dose escalation while simultaneously limiting dose to critical structures, ultimately leading to more intense conditioning with less toxicity relative to TBI (3, 4). Organ sparing with TMLI has raised concerns of sparing of cancer cells and increased recurrence rates. We reported earlier on extramedullary recurrences in the first 101 patients with advanced refractory or relapsed acute leukemia undergoing allogeneic HCT with TMLI as part of the conditioning regimen at this center. This is a population of patients with more aggressive disease and higher tumor burden than patients undergoing traditional TBI. However, the risk of EM relapse using a TMLI-based conditioning regimen is comparable to that of standard TBI-based HCT conditioning regimens (5–9). Further, EM relapse does not appear to be dose-dependent. With a median follow-up of 12.8 months, 13 patients developed extramedullary relapses at 19 sites. Nine relapses occurred in the target region (≥ 12 Gy), 5 relapses in regions receiving 10.1 to 11.4 Gy and 5 relapses in regions receiving 3.6 to 9.1 Gy (9). Only EM disease prior to HCT predicted for EM relapse on multivariable analysis. Prior EM disease has also been found to be an independent risk factor in the setting of HCT with a TBI conditioning regimen, and therefore should not preclude these patients from undergoing TMLI regimen (6, 10–12). These data suggest the use of TMLI does not increase the risk of relapse in non-target regions.

Due to limited EM relapses in patients who have undergone TMLI-based conditioning, there is an additional question of how to treat relapses following conditioning with TMLI; though systemic therapy is a standard option (13, 14), select recurrences might achieve local control with additional radiation due to high response rates, which can prove to be either an effective salvage or palliative strategy (15, 16). In order to characterize the role of radiation in the treatment of extramedullary relapse, we performed a single-institution retrospective study of patients who underwent TMLI-based conditioning who subsequently developed EM relapse that was treated with radiation, and evaluated oncologic outcomes.

Materials and methods

Patient characteristics

Between 2006 and 2018, 254 patients with AML or ALL undergoing HCT with a TMLI-based conditioning regimen were enrolled in one of five prospective clinical trials. Following IRB approval, patients with a diagnosis of AML and ALL were

included in this analysis. Of those patients, included patients were identified as having received a subsequent course of radiation treatment to extramedullary relapse. Patients without evidence of EM relapse or who did not receive RT treatment for EM relapse were excluded.

Treatment

All patients underwent pre-transplant conditioning with high-dose chemotherapy and TMLI. Patients received one of four chemotherapy regimens on a per protocol basis, with regimens including busulfan/etoposide (VP-16), fludarabine/cyclophosphamide (CTX), fludarabine/melphalan, or VP-16/CTX (3, 4, 17–20). For all five trials, tacrolimus and sirolimus were administered for graft-versus-host disease (GVHD) prophylaxis. The institutional supportive care regimen was used to manage nausea, vomiting, mucositis, and infection risks. Patients were followed weekly with complete differential blood counts and comprehensive metabolic panel tests for the first 100 days after discharge. On days 30 and 100 after HCT, BM biopsy samples were obtained. Patients were then followed with annual BM biopsies at least two years post-transplant. EM relapses were found either on routine workup imaging or because of imaging confirmation of symptomatic lesions. EM relapses were confirmed based on either imaging and/or biopsy. EM recurrences were treated at the discretion of the hematologist and radiation oncologist using RT ± chemotherapy. Generally, radiatyion treatment volumes encompassed gross disease only. However, patients with CNS involvement received whole brain radiation, with or without craniospinal irradiation based on systemic therapy plan and cerebrospinal fluid cytology. Curative versus palliative intent was defined by the treating physicians.

TMLI radiation therapy technique

Details of the TMLI radiation therapy technique have been published in previous studies (3, 21–23). All patients underwent scanning with a large-bore computed tomography simulator with 60-cm field of view (Phillips Medical System, Eindhoven, The Netherlands) for treatment planning purposes. Scans were obtained during shallow breathing, inspiration, and expiration to account for organ motion due to respiration. Patients were immobilized using a full-body Vac-lok bag (Civco Medical Systems, Kalona, IA) and a thermoplastic mask on the head and neck region. All patients were treated with a helical TomoTherapy unit (Accuray, Inc, Sunnyvale, CA), and the lower extremities were treated with a conventional linear accelerator through standard anteroposterior posteroanterior fields. The color-coded Tomotherapy TMLI dose distribution of a patient treated to 12 Gy is shown in Figure 1.

The patients were treated to a total dose of 12 Gy to 20 Gy using TMLI delivered twice daily in 1.25 Gy to 2 Gy fractions. The target structures were defined and included bone, major

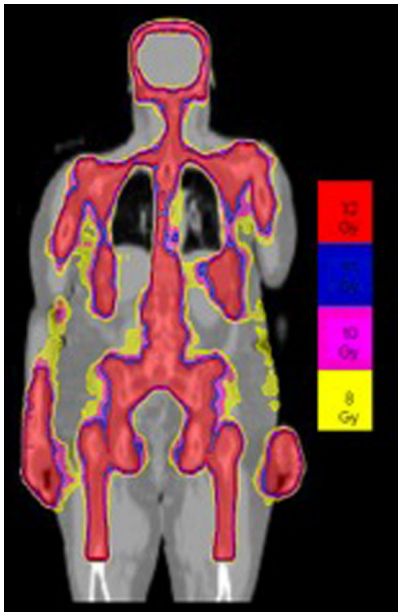

FIGURE 1
Color-coded TMLI plan shows dose to the targeted areas, with relative sparing of dose to critical organs.

lymph node chains, testes, spleen, splenic-hilar lymph nodes, liver, portahepatic lymph nodes, and brain. In the dose escalation trials, only the bone, major lymph node chains, and testes (in some trials) were escalated for each dose level. All other targets remained at 12 Gy. Dose to organs at risk were optimally minimized and included orbit, lens, thyroid, oral cavity, mandible, parotids, larynx, hypopharynx, esophagus, lung, heart, breast, kidney, stomach, small and large intestines, rectum, and bladder. Target coverage was also optimized such that a minimum of 85% of target structure received the prescribed dose.

Study definitions and statistical methods

Descriptive statistics were performed on the identified cohort of patients and the identified EM relapses. Patients and relapses were stratified by treatment intent (curative [radiation treating all known EM disease with or without systemic therapy] vs palliative [radiation limited to symptomatic lesions with or without systemic therapy]). Comparisons between continuous and categorical variables were made with Student's t-test and chi-squared tests, respectively. Overall survival (OS) and progression-free survival (PFS) was estimated using the Kaplan-Meier method, as was local control (LC) of the treated relapses. These were defined from the date of the first fraction of radiation used for treatment of relapse following TMLI. Events for OS included death from any cause. Events for PFS included death or disease progression, whichever came first. Patients who did not experience an event at last follow-up were censored. For purposes of survival analyses, patients were stratified by treatment intent. All analyses were performed using open-source libraries in Python 3.8 (PSF, Wilmington, DE). Statistical significance was set at a p value of <0.05. Data were locked for analysis on January 31, 2021 (analytic date).

Results

Patient characteristics are presented in Table 1. A total of 21 patients were identified who were subsequently treated with radiotherapy for EM relapse, with or without BM relapse, with patients having a median of 2 relapses treated (range: 1-16). At time of transplant, median age was 31 years (21-61 years). The

TABLE 1 Patient characteristics.

Characteristic	All patients (N = 21)	Palliative (N = 10)	Curative (N = 11)	p
Age at transplantation (y) (median [range])	31.0 (21-61)	32.0 (25-61)	29.0 (21-57)	0.433
Follow-Up (m) (median [range])	38.8 (3.9-168.5)	20.9 (3.9-38.8)	61.0 (26.7-168.5)	<0.001
Time to Initial Relapse (m) (median [range])	16.8 (0.9-51.5)	7.2 (0.9-33.1)	18.1 (3.3-51.5)	0.099
Subsequent Courses of Radiation (median [range])	2.0 (1-16)	2.0 (1-16)	2.0 (1-10)	0.555
Race				0.483
Asian	1 (4.8%)	1 (10.0%)	0 (0.0%)	
Hispanic White	8 (38.1%)	3 (30.0%)	5 (45.5%)	
Non-Hispanic White	12 (57.1%)	6 (60.0%)	6 (54.5%)	
KPS				0.159
100	2 (9.5%)	0 (0.0%)	2 (18.2%)	
90	7 (33.3%)	2 (20.0%)	5 (45.5%)	
80	8 (38.1%)	6 (60.0%)	2 (18.2%)	
70	3 (14.3%)	1 (10.0%)	2 (18.2%)	
Unknown	1 (4.8%)	1 (10.0%)	0 (0.0%)	
HCTCI				0.418
0	13 (61.9%)	6 (60.0%)	7 (63.6%)	
1	1 (4.8%)	1 (10.0%)	0 (0.0%)	
2	2 (9.5%)	1 (10.0%)	1 (9.1%)	
3	1 (4.8%)	1 (10.0%)	0 (0.0%)	
4	2 (9.5%)	0 (0.0%)	2 (18.2%)	
5	1 (4.8%)	0 (0.0%)	1 (9.1%)	
Unknown	1 (4.8%)	1 (10.0%)	0 (0.0%)	
Diagnosis				0.038
ALL	8 (38.1%)	1 (10.0%)	7 (63.6%)	
AML	13 (61.9%)	9 (90.0%)	4 (36.4%)	

(Continued)

TABLE 1 Continued

Characteristic	All patients (N = 21)	Palliative (N = 10)	Curative (N = 11)	p
Disease Status at HSCT				0.472
1st CR	2 (9.5%)	1 (10.0%)	1 (9.1%)	
1st Relapse	5 (23.8%)	3 (30.0%)	2 (18.2%)	
2nd Relapse	1 (4.8%)	0 (0.0%)	1 (9.1%)	
3rd Relapse	1 (4.8%)	0 (0.0%)	1 (9.1%)	
>=3rd CR	2 (9.5%)	0 (0.0%)	2 (18.2%)	
Induction Failure	10 (47.6%)	6 (60.0%)	4 (36.4%)	
Prior EM Disease				0.73
No	15 (71.4%)	8 (80.0%)	7 (63.6%)	
Yes	6 (28.6%)	2 (20.0%)	4 (36.4%)	
Pretransplant Conditioning				0.338
Busulfan/VP-16	3 (14.3%)	2 (20.0%)	1 (9.1%)	
Fludarabine/CTX	3 (14.3%)	0 (0.0%)	3 (27.3%)	
Fludarabine/Melphalan	2 (9.5%)	1 (10.0%)	1 (9.1%)	
VP-16/CTX	13 (61.9%)	7 (70.0%)	6 (54.5%)	
TMLI Dose (cGy)				0.834
1200	8 (38.1%)	3 (30.0%)	5 (45.5%)	
1500	2 (9.5%)	1 (10.0%)	1 (9.1%)	
1600	2 (9.5%)	1 (10.0%)	1 (9.1%)	
1700	1 (4.8%)	1 (10.0%)	0 (0.0%)	
2000	8 (38.1%)	4 (40.0%)	4 (36.4%)	
First Relapse Site				0.213
BM	5 (23.8%)	4 (40.0%)	1 (9.1%)	
EM	12 (57.1%)	4 (40.0%)	8 (72.7%)	
EM & BM	4 (19.0%)	2 (20.0%)	2 (18.2%)	
Status				0.023
Deceased	15 (71.4%)	10 (100.0%)	5 (45.5%)	
Living	6 (28.6%)	0 (0.0%)	6 (54.5%)	

RT; radiotherapy, KPS; Karnofsky Performance Score, HCTCI; Hematopoietic Cell Transplantation-specific Comorbidity Index, ALL; acute lymphocytic leukemia, AML; acute myeloid leukemia, HSCT; hematopoietic stem cell transplant, CR; complete response, EM; extramedullary, VP-16; etoposide, CTX; cyclophosphamide, TMLI; total marrow and lymphoid irradiation, BM; bone marrow.

median follow-up from date of transplant of these patients was 32.2 mo (3.9-154.1 mo). 13 (61.9%) of these patients were diagnosed with AML, accounting for 48 (71.6%) of the relapses, and 8 (38.1%) were diagnosed with ALL, accounting for 19 (28.4%) of the relapses. 6 patients had EM disease that had been treated prior to their transplant. 10 patients had received TMLI-based conditioning after induction failure, while 7 were treated after relapse and 4 were treated following complete response. Median time to initial relapse was 16.8 mo (0.9-51.5 mo). Twelve (57.1%) of patients did not have evidence of BM relapse prior to or at the time of initial EM relapse. Of the patients without evidence of BM disease at the time of initial relapse, only two subsequently developed BM relapse, although all but 4 received further systemic therapy after radiation and all but three had disease progression of extramedullary disease following radiation. Five (23.8%) patients had BM relapse prior to initial EM relapse while 4 (19.0%) presented with synchronous BM and EM relapse. Median time from transplant to relapse was 16.8 months.

Descriptive statistics of the EM relapses are presented in Table 2. Radiation treatment intent for the first course of RT to EM relapses was curative in 11 (52.4%) patients and palliative in 10 (47.6%) patients. 67 relapse sites (median=2 sites/patient, range=1-16) were treated, with 16 (23.9%) treated with curative intent and 51 (76.1%) treated for palliation. The majority of EM relapses occurred in soft tissue (34), while there were 23 bone relapses, 6 nodal relapses, and 4 CNS relapses. 12 recurrences were treated with systemic therapy prior to RT. Furthermore, lesions treated with curative intent were more likely to have received initial treatment with systemic therapy (50% vs 17.6%, p=0.023).

At the time of analysis, 6 patients were living, whereas 15 were deceased. One patient with CNS disease remains alive without evidence of disease at last follow-up. Among evaluable

TABLE 2 EM Relapse Characteristics.

Characteristic	All Sites (N = 67)	Palliative (N = 51)	Curative (N = 16)	p
RT Dose (cGy) (median [range])	24.0 (6.0-30.0)	22.0 (6.0-30.0)	24.0 (18.0-30.0)	0.006
Relapse Site				0.213
Bone	23 (34.3%)	19 (37.3%)	4 (25.0%)	
CNS	4 (6.0%)	2 (3.9%)	2 (12.5%)	
Lymph node	6 (9.0%)	6 (11.8%)	0 (0.0%)	
Soft tissue	34 (50.7%)	24 (47.1%)	10 (62.5%)	
Initial Treatment				0.023
Chemo to RT	17 (25.4%)	9 (17.6%)	8 (50.0%)	
RT	50 (74.6%)	42 (82.4%)	8 (50.0%)	
Durable Local Control				0.768
Yes	58 (86.6%)	45 (88.2%)	13 (81.2%)	
No	9 (13.4%)	6 (11.8%)	3 (18.8%)	

RT; radiotherapy, TMLI; total marrow and lymphoid irradiation;,BM; bone marrow, CNS; central nervous system, chemo; chemotherapy.

patients alive at the time of analysis, median follow-up was 38.8 months from the time of initiation of RT. Of the patients who were alive, 4 had initial EM relapse, 1 had concomitant EM and BM relapse, and 1 had BM relapse. 5 patients have no evidence of disease at last follow-up, of which 4 initially had EM relapse only (one went on to develop BM relapse salvaged by repeat transplant and chemotherapy) and 1 had BM relapse. Cause of death attributed to disease progression in all 15 patients.

Full survival curves for OS, PFS, and LC following RT treatment are visualized in Figures 2A–E. Following the initial course of subsequent RT, 1-year, 3-year and 5-year estimates of OS were 47.6%, 32.7% and 16.3%, respectively. Median OS was 10.0 months. OS was significantly better in patients treated with curative intent, with median OS of 50.7 months vs 1.6 months ($p<0.001$) and 5-year OS of 31.2% vs 0%. 1-year, 3-year and 5-year estimates of PFS were 23.8%, 14.3% and 14.3%, respectively. Median PFS was 4.1 months. PFS was significantly better in patients treated with curative intent, with median PFS of 6.6 months vs 1.3 months ($p<0.001$) and 5-year PFS of 27.3% vs 0%. Following RT, 86.6% of the sites had durable local control for the duration of follow-up. 1-year and 5-year estimates of LC were 81.2% and 63.2%, respectively. Of the 9 treated sites that progressed, 5 were initially treated with curative intent and four received a prescription dose of less than 20 Gy (range: 8-25 Gy). No secondary malignancies or significant radiation-induced toxicity were observed.

Discussion

The incidence of EM relapse following TBI based conditioning regimens for HCT is estimated to be between 5% to 20% (5–8). An earlier study of patients treated with TMLI based conditioning regimens suggest similar outcomes, with the primary study evaluating patterns of failure demonstrating an EM relapse rate of 12.9% (9). Treatment of EM relapse in general is complicated, including the role of radiation (15, 16, 24). This question is relevant to patients treated with TMLI conditioning as well, based the difference in prior radiation distribution compared to TBI-based techniques leading to possible variations in the patterns and biology of EM relapse. This study demonstrated that not only is radiation an effective means of achieving local control in EM relapse following TMLI, select patients with more limited disease can achieve favorable long-term outcomes despite being high-risk even before their transplant and subsequent EM relapse.

In the present study, median time to relapse was 16.8 months, which is consistent with the prior study in TMLI (9). Common EM recurrence sites following TBI are the breasts, testes, and bone in ALL, and skin, the head and neck area, breast, bone and testes in AML (25). Of those sites, the testes, bone, and head and neck lymph nodes are included in the TMLI treatment volumes. Although bones represented a significant relapse site in the present study, there were few relapses in the other sites that are otherwise associated with relapse following TBI (3 breast recurrences [all AML], 1 scrotal recurrence [AML], and two head and neck nodal recurrences [both AML]).

When these EM recurrences did occur, RT was shown to be effective way of managing them, with 75% of relapses being treated with radiation first. This provided local tumor control for the duration of follow-up in 86.6% of sites, which is comparable to previously published series (26). Furthermore, in select cases RT proved to be an effective form of consolidative/salvage treatment, with 32.7% and 16.3% 3-year and 5-year OS following RT to first EM relapse, which is overall favorable given these were high-risk patients in the first place who had already relapsed following HCT. This appears to be largely driven by patients with limited relapse still amenable to salvage therapy, evidenced by significantly improved outcomes treated with curative intent due to have EM disease that could be

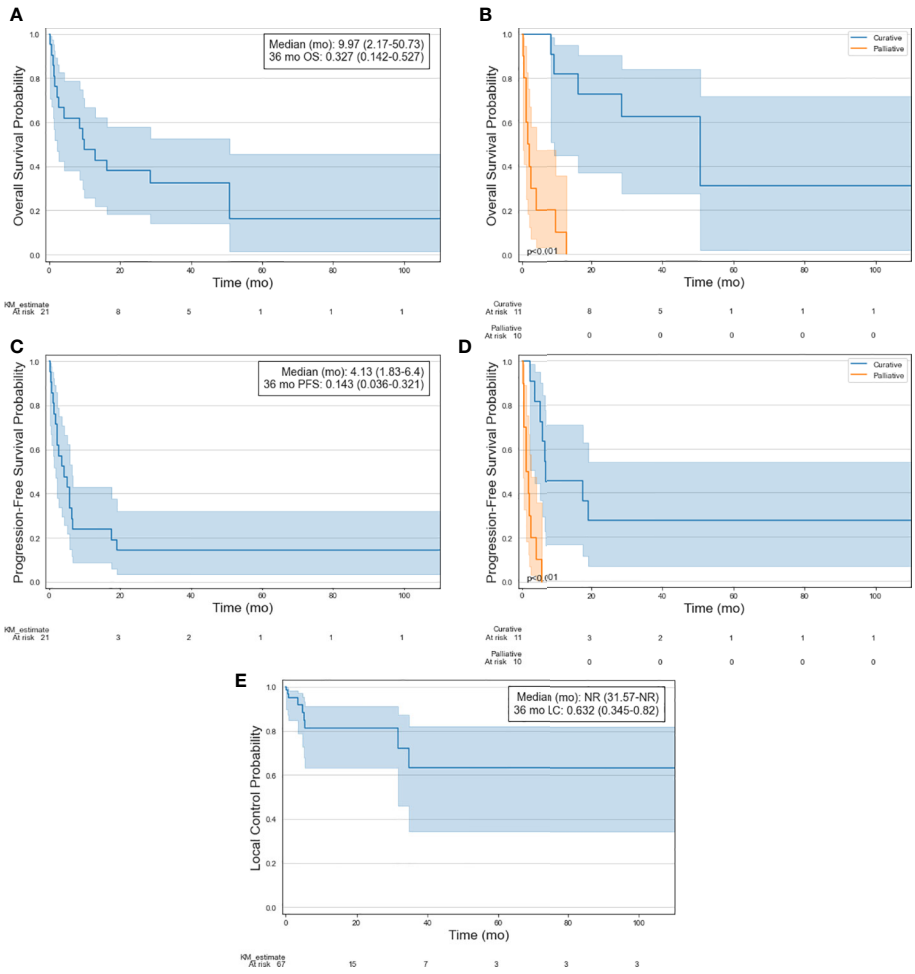

FIGURE 2
Kaplan-Meier curves of selected patient cohort illustrating **(A)** OS, **(B)** OS stratified by treatment intent, **(C)** PFS, **(D)** PFS stratified by treatment intent, and **(E)** LC of treated lesions.

contained in a radiation field. This is further evidenced by 80% of the long-term survivors initially presenting with a single EM relapse without BM involvement. These data are suggestive that in certain scenarios, radiation can be part of a curative regimen for patients with isolated EM relapse after TMLI and HCT. Beyond the efficacy of RT in treating EM relapse, the patients in this cohort did have overall favorable survival outcomes compared to historical controls.

It is important to note that the majority of the patients treated on the included trials were higher risk with worse prognosis compared to most patients undergoing traditional TBI. This is evidenced in this study's cohort, where only 4 patients (19.0%) were in complete remission prior to transplantation. In a study of patients not in CR treated with HCT after relapse or induction failure, Duval et al. reported 3-year overall survival rates of 19% for AML and 16% in younger patients (27). On subset analysis, 3-year OS was 42% and 46% in AML and ALL, respectively, for patients even with the best prognostic factors. In another study, Ganzel et al. reported median OS of 6 months and 5 year OS of 10% following AML relapse (28). In a retrospective study of patients with relapsed/refractory AML, Brandwein et al. sought to examine outcomes following intensive therapy (23% of patients), non-intensive therapy (33%), and best supportive care (44%) (29). Intensive therapy was defined as re-induction with a different intensive induction regimen following induction failure with 2 other regimens. Non-intensive therapy was defined as a hypomethylating agent (HMA) or low-dose cytarabine, with or without another chemotherapy agent. Patients who could not receive either intensive therapy or non-intensive therapy would receive best supportive care. The 5-year OS rates of the entire cohort was 12.6% and was 36.7%, 7.0% and 4.0% for the

intensive therapy, non-intensive therapy, and best supportive care groups, respectively. Our relapsed TMLI cohort presented here is comparable to the intensive therapy described by Brandwein et al, particularly in patients amenable to curative intent treatment (29). The median OS outcomes were 13.6, 9.4, and 2.0 months for the intensive therapy, non-intensive therapy, and best supportive care groups, respectively, compared to 10.0 months in our overall cohort and 51 months in our curative intent cohort.

These outcomes suggest that there might be a role for radiation in managing EM relapse following TMLI, given they may be chemo-resistant after extensive pretreatment with systemic therapies. Indeed, in one retrospective study of relapsed leukemia treated with high-dose chemotherapy followed by donor leukocyte infusion, Choi et al. reported that all patients who relapsed following initial complete response relapsed at extramedullary sites (24). In another study, Ginsberg et al. report on treatment of isolated extramedullary relapse in children of AML (15). Of the 6 patients still alive at last follow up, all received local radiation to the EM relapse plus or minus TBI and subsequent transplant. Overall, these studies and our study support current guidelines from the International Lymphoma Radiation Oncology Group (ILROG), where radiation is recommended for patients with isolated chloroma and inadequate response to chemotherapy, with isolated recurrence after HCT (16). Nevertheless, despite excellent local effect, there is no doubt that EM disease often occurs alongside BM disease or is a harbinger of subsequent BM disease (30, 31). However, it is possible that this pattern could be mitigated by the dose escalation to the bone marrow accomplished by TMLI, evidenced by the fact that only 2 of the 12 patients presenting with isolated EM relapse included in our cohort went on to develop BM relapse. This lends further support to aggressive local treatment of limited EM relapse following TMLI. Our data are also consistent with ILROG guidelines for more advanced disease, with goal being palliation of symptomatic lesions, due to high rates of local control.

This study has several limitations. This is a heterogeneous cohort, including a wide range in dosimetry, GVHD prophylaxis, chemotherapy, and donors, that is not intended to fully represent the patterns of failure of TMLI. For example, it is possible that different systemic therapy regimens may have differential effects on the occurrence of EM relapse, underlying biology, and treatment response. Our cohort is certainly not inclusive of all EM relapses and therefore cannot estimate incidence of relapse beyond a rough estimate, which further applies to the dosimetry and outcomes of relapse following TMLI. Specifically, with regards to outcomes, it is possible this cohort represents a more favorable cohort of patients, given that 57.1% presented with initial EM relapse, as compared to approximately 24.3% in the largest published TMLI cohort (9). Initial EM relapse has been shown to have better prognosis that initial BM ± EM relapse (32). This imbalance is potentially related to patients with more limited systemic disease being selected for subsequent RT but suggests additional roles for RT in limited leukemic disease. Additionally, though our study shows favorable outcomes for EM relapse following TMLI treated with RT, our cohort does not include chemotherapy alone as a standard comparator arm. Therefore, it is not possible to compare outcomes to patients who did not receive any radiation, although half the patients in the curative cohort did receive chemotherapy before radiation with insufficient response, which does lend credence to radiation being a valuable option for resistant disease per ILROG guidelines (16). These limitations will best be addressed by future retrospective studies specifically evaluating patterns of failure in patients treated with TMLI, as well as further planned prospective studies on the role of TMLI in high-risk leukemia. Despite these limitations, all patterns of relapse, outcomes, and dosimetry are from this study are comparable to the largest published series investigating EM relapse following TMLI (9), and therefore support continued investigation of TMLI and the role of RT as a subsequent salvage therapy.

Conclusions

To our knowledge, this is the first analysis to date of salvage/palliative radiation treatment for patients treated with TMLI and HCT who developed EM relapses. RT is an effective modality to treat EM relapse in patients with acute leukemia who were previously treated with TMLI, offering a high probability of durable local control. Furthermore, these patients did not have significantly different OS compared to historical controls, with patients treated with curative intent demonstrating favorable outcomes. These data suggest a subset of patients with limited disease at relapse can potentially be salvaged with the help of radiation. Further investigation of the treatment of EM relapse following TMLI (or HCT in general), in addition to overall patterns of failure, outcomes, and toxicity is warranted.

Data availability statement

The raw data supporting the conclusions of this article will be made available by the authors without undue reservation.

Ethics statement

The studies involving human participants were reviewed and approved by City of Hope National Medical Center Institutional Review Board. Written informed consent for participation was not required for this study in accordance with the national legislation and the institutional requirements.

Author contributions

The authors confirm contribution to the paper as follows: Study conception and design: CL, SD. Data collection: CL. DY. Analysis and interpretation of results: CL, DY. Draft manuscript preparation: CL, SD. All authors contributed to the article and approved the submitted version.

Conflict of interest

SD has received grant funding from Bayer.

The remaining authors declare that the research was conducted in the absence of any commercial or financial relationships that could be construed as a potential conflict of interest.

Publisher's note

References

1. Shinde A, Yang D, Frankel P, Liu A, Han C, Del Vecchio B, et al. Radiation-related toxicities using organ sparing total marrow irradiation transplant conditioning regimens. *Int J Radiat OncologyBiologyPhysics* (2019) 105(5):1025–33. doi: 10.1016/j.ijrobp.2019.08.010

2. Wong JYC, Filippi AR, Scorsetti M, Hui S, Muren LP, Mancosu P. Total marrow and total lymphoid irradiation in bone marrow transplantation for acute leukaemia. *Lancet Oncol* (2020) 21(10):e477–e87. doi: 10.1016/S1470-2045(20)30342-9

3. Wong JYC, Forman S, Somlo G, Rosenthal J, Liu A, Schultheiss T, et al. Dose escalation of total marrow irradiation with concurrent chemotherapy in patients with advanced acute leukemia undergoing allogeneic hematopoietic cell transplantation. *Int J Radiat Oncol Biol Phys* (2013) 85(1):148–56. Elsevier. doi: 10.1016/j.ijrobp.2012.03.033

4. Rosenthal J, Wong J, Stein A, Qian D, Hitt D, Naeem H, et al. Phase 1/2 trial of total marrow and lymph node irradiation to augment reduced-intensity transplantation for advanced hematologic malignancies. *Blood: Content Repository Only!;* (2011) 117(1): 309–15. doi: 10.1182/blood-2010-06-288357

5. Lee KH, Lee JH, Choi SJ, Lee JH, Kim S, Seol M, et al. Bone marrow vs extramedullary relapse of acute leukemia after allogeneic hematopoietic cell transplantation: Risk factors and clinical course. *Bone Marrow Transplant* (2003) 32(8):835–42. Nature Publishing Group. doi: 10.1038/sj.bmt.1704223

6. Chong G, Byrnes G, Szer J, Grigg A. Extramedullary relapse after allogeneic bone marrow transplantation for haematological malignancy. *Bone Marrow Transplant* (2000) 26(9):1011–5. Nature Publishing Group. doi: 10.1038/sj.bmt.1702659

7. Solh M, DeFor TE, Weisdorf DJ, Kaufman DS. Extramedullary relapse of acute myelogenous leukemia after allogeneic hematopoietic stem cell transplantation: Better prognosis than systemic relapse. *Biol Blood Marrow Transplant* (2012) 18(1):106–12. Elsevier. doi: 10.1016/j.bbmt.2011.05.023

8. Mortimer J, Blinder MA, Schulman S, Appelbaum FR, Buckner CD, Clift RA, et al. Relapse of acute leukemia after marrow transplantation: Natural history and results of subsequent therapy. *J Clin Oncol* (1989) 7(1):50–7. doi: 10.1200/JCO.1989.7.1.50

9. Kim JH, Stein A, Tsai N, Schultheiss TE, Palmer J, Liu A, et al. Extramedullary relapse following total marrow and lymphoid irradiation in patients undergoing allogeneic hematopoietic cell transplantation. *Int J Radiat Oncol Biol Phys* (2014) 89(1):75–81. Elsevier Inc. doi: 10.1016/j.ijrobp.2014.01.036

10. Harris AC, Kitko CL, Couriel DR, Braun TM, Choi SW, Magenau J, et al. Extramedullary relapse of acute myeloid leukemia following allogeneic hematopoietic stem cell transplantation: incidence, risk factors and outcomes. *Haematologica* (2013) 98(2):179. doi: 10.3324/haematol.2012.073189

11. Michel G, Boulad F, Small T, Black P, Heller G, Castro-Malaspina H, et al. Risk of extramedullary relapse following allogeneic bone marrow transplantation for acute myelogenous leukemia with leukemia cutis. *Bone marrow transplantation* (1997) 20(2):107–12. doi: 10.1038/sj.bmt.1700857

12. Gunes G, Goker H, Demiroglu H, Malkan UY, Buyukasik Y. Extramedullary relapses of acute leukemias after allogeneic hematopoietic stem cell transplantation: clinical features, cumulative incidence, and risk factors. *Bone Marrow Transplantation* (2019) 54(4):595–600. doi: 10.1038/s41409-018-0303-5

13. Pollyea DA, Bixby D, Perl A, Bhatt VR, Altman JK, Appelbaum FR, et al. NCCN guidelines insights: Acute myeloid leukemia, version 2.2021. *J Natl Compr Cancer Network* (2021) 19(1):16–27. doi: 10.6004/jnccn.2021.0002

14. Brown PA, Shah B, Advani A, Aoun P, Boyer MW, Burke PW, et al. Acute lymphoblastic leukemia, version 2.2021, NCCN clinical practice guidelines in oncology. *J Natl Compr Cancer Network* (2021) 19(9):1079–109. doi: 10.6004/jnccn.2021.0042

15. Ginsberg JP, Orudjev E, Bunin N, Felix CA, Lange BJ. Isolated extramedullary relapse in acute myeloid leukemia: A retrospective analysis. *Med Pediatr Oncol* (2002) 38(6):387–90. doi: 10.1002/mpo.10069

16. Bakst RL, Dabaja BS, Specht LK, Yahalom J. Use of radiation in extramedullary Leukemia/Chloroma: Guidelines from the international lymphoma radiation oncology group. *Int J Radiat OncologyBiologyPhysics* (2018) 102(2):314–9. doi: 10.1016/j.ijrobp.2018.05.045

17. Stein A, Palmer J, Tsai NC, Al Malki MM, Aldoss I, Ali H, et al. Phase I trial of total marrow and lymphoid irradiation transplantation conditioning in patients with Relapsed/Refractory acute leukemia. *Biol Blood Marrow Transplant* (2017) 23(4):618–24. doi: 10.1016/j.bbmt.2017.01.067

18. Jensen LG, Stiller T, Wong JYC, Palmer J, Stein A, Rosenthal J. Total marrow lymphoid Irradiation/Fludarabine/ melphalan conditioning for allogeneic hematopoietic cell transplantation. *Biol Blood Marrow Transplant* (2018) 24(2):301–7. doi: 10.1016/j.bbmt.2017.09.019

19. Al Malki MM, Palmer J, Tsai N-C, Mokhtari S, Hui S, Tsai W, et al. Total marrow and lymphoid irradiation as conditioning in haploidentical transplant with posttransplant cyclophosphamide. *Blood Advances* (2022) 6(14):4098–106. doi: 10.1182/bloodadvances.2022007264

20. Stein AS, Tsai N-C, Palmer JM, Al Malki MM, Aldoss I, Ali H, et al. A phase II study of total marrow and lymphoid irradiation (TMLI) in combination with cyclophosphamide and etoposide in patients with Relapsed/Refractory acute leukemia undergoing allogeneic hematopoietic cell transplantation. *Blood* (2017) 130:4607. doi: 10.1182/blood.V130.Suppl_1.4607.4607

21. Wong JYC, Liu A, Schultheiss T, Popplewell L, Stein A, Rosenthal J, et al. Targeted total marrow irradiation using three-dimensional image-guided tomographic intensity-modulated radiation therapy: An alternative to standard total body irradiation. *Biol Blood Marrow Transplantation* (2006) 12(3):306–15. doi: 10.1016/j.bbmt.2005.10.026

22. Schultheiss TE, Wong J, Liu A, Olivera G, Somlo G. Image-guided total marrow and total lymphatic irradiation using helical tomotherapy. *Int J Radiat OncologyBiologyPhysics* (2007) 67(4):1259–67. doi: 10.1016/j.ijrobp.2006.10.047

23. Hui SK, Verneris MR, Higgins P, Gerbi B, Weigel B, Baker SK. Helical tomotherapy targeting total bone marrow - first clinical experience at the university of Minnesota. *Acta Oncol* (2007) 46(2):250–5. doi: 10.1080/02841860601042449

24. Choi S-J, Lee J-H, Lee J-H, Kim S, Seol M, Lee Y-S, et al. Treatment of relapsed acute myeloid leukemia after allogeneic bone marrow transplantation with chemotherapy followed by G-CSF-primed donor leukocyte infusion: a high incidence of isolated extramedullary relapse. *Leukemia* (2004) 18(11):1789–97. doi: 10.1038/sj.leu.2403523

25. Cunningham I. Extramedullary sites of leukemia relapse after transplant. *Leukemia Lymphoma* (2006) 47(9):1754–67. Taylor & Francis. doi: 10.1080/10428190600632857

26. Song JH, Son SH, Lee JH, Chung SM, Jang HS, Choi BO. Defining the optimal dose of radiation in leukemic patients with extramedullary lesions. *BMC Cancer* (2011) 11:428. BioMed Central. doi: 10.1186/1471-2407-11-428

27. Duval M, Klein JP, He W, Cahn JY, Cairo M, Camitta BM, et al. Hematopoietic stem-cell transplantation for acute leukemia in relapse or primary induction failure. *J Clin Oncology: J Clin Oncol;* (2010) 28(23):3730–8. doi: 10.1200/JCO.2010.28.8852

28. Ganzel C, Sun Z, Cripe LD, Fernandez HF, Douer D, Rowe JM, et al. Very poor long-term survival in past and more recent studies for relapsed AML patients: The ECOG-ACRIN experience. *Am J Hematol* (2018) 93(8):1074–81. Wiley-Liss Inc. doi: 10.1002/ajh.25162

29. Brandwein JM, Saini L, Geddes MN, Liu FF, Yusuf D, Schwann K, et al. Outcomes of patients with relapsed or refractory acute myeloid leukemia: a population-based real-world study. *Am J Blood Res* (2020) 10(4):124–33. Ovid Technologies (Wolters Kluwer Health). https://www.ncbi.nlm.nih.gov/pmc/articles/PMC7486485/

30. Tallman MS, Hakimian D, Shaw JM, Lissner GS, Russell EJ, Variakojis D. Granulocytic sarcoma is associated with the 8;21 translocation in acute myeloid leukemia. *J Clin Oncol* (1993) 11(4):690–7. doi: 10.1200/JCO.1993.11.4.690

31. Byrd JC, Edenfield WJ, Shields DJ, Dawson NA. Extramedullary myeloid cell tumors in acute nonlymphocytic leukemia: a clinical review. *J Clin Oncol* (1995) 13(7):1800–16. doi: 10.1200/JCO.1995.13.7.1800

32. Malempati S, Gaynon PS, Sather H, La MK, Stork LC. Outcome after relapse among children with standard risk all treated on the children's cancer group-1952 study. *J Invest Medicine: BMJ;* (2005) 25(36):S104.5–S. doi: 10.2310/6650.2005.00005.153

frontiers | Frontiers in Oncology

TYPE Original Research
PUBLISHED 10 November 2022
DOI 10.3389/fonc.2022.1045016

OPEN ACCESS

EDITED BY
Sherif Farag,
Indiana University School Of Medicine - Indianapolis, United States

REVIEWED BY
Naoyuki G. Saito,
Indiana University School Of Medicine, United States
Shinsuke Takagi,
Toranomon Hospital, Japan

*CORRESPONDENCE
Susanta K. Hui
shui@coh.org

†These authors have contributed equally to this work

SPECIALTY SECTION
This article was submitted to Radiation Oncology, a section of the journal Frontiers in Oncology

RECEIVED 15 September 2022
ACCEPTED 17 October 2022
PUBLISHED 10 November 2022

CITATION
Lim JE, Sargur Madabushi S, Vishwasrao P, Song JY, Abdelhamid AMH, Ghimire H, Vanishree VL, Lamba JK, Dandapani S, Salhotra A, Lemecha M, Pierini A, Zhao D, Storme G, Holtan S, Aristei C, Schaue D, Al Malki M and Hui SK (2022) Total marrow irradiation reduces organ damage and enhances tissue repair with the potential to increase the targeted dose of bone marrow in both young and old mice. *Front. Oncol.* 12:1045016. doi: 10.3389/fonc.2022.1045016

Total marrow irradiation reduces organ damage and enhances tissue repair with the potential to increase the targeted dose of bone marrow in both young and old mice

Ji Eun Lim[1†], Srideshikan Sargur Madabushi[1†], Paresh Vishwasrao[1], Joo Y. Song[2], Amr M. H. Abdelhamid[1,3,4], Hemendra Ghimire[1], V. L. Vanishree[1], Jatinder K. Lamba[5], Savita Dandapani[1], Amandeep Salhotra[6], Mengistu Lemecha[7], Antonio Pierini[8], Daohong Zhao[9], Guy Storme[10], Shernan Holtan[11], Cynthia Aristei[3], Dorthe Schaue[12], Monzr Al Malki[6†] and Susanta K. Hui[1*†]

[1]Department of Radiation Oncology, City of Hope National Medical Center, Duarte, CA, United States, [2]Department of Pathology, City of Hope Comprehensive Cancer Center, Duarte, CA, United States, [3]Radiation Oncology Section, Department of Medicine and Surgery, Perugia University and General Hospital, Perugia, Italy, [4]Department of Oncology and Nuclear Medicine, Faculty of Medicine, Ain Shams University, Cairo, Egypt, [5]Department of Pharmacotherapy and Translational Research, College of Pharmacy, University of Florida, Gianesville, FL, United States, [6]Department of Hematology and Hematopoietic Cell Transplantation, City of Hope National Medical Center, Duarte, CA, United States, [7]Department of Molecular and Cellular Biology, Beckman Research Institute, Duarte, CA, United States, [8]Division of Hematology and Bone Marrow Transplantation, Perugia General Hospital, Perugia, Italy, [9]Department of Biochemistry and Structural Biology, Univeristy of Texas (UT) Health San Antonio, San Antonio, TX, United States, [10]Department of Radiotherapy Universitair Ziekenhuis (UZ) Brussels, Brussels, Belgium, [11]Blood and Marrow Transplant Program, Department of Medicine, University of Minnesota, Minneapolis, MN, United States, [12]Department of Radiation Oncology, University of California, Los Angeles (UCLA), Los Angeles, CA, United States

Total body irradiation (TBI) is a commonly used conditioning regimen for hematopoietic stem cell transplant (HCT), but dose heterogeneity and long-term organ toxicity pose significant challenges. Total marrow irradiation (TMI), an evolving radiation conditioning regimen for HCT can overcome the limitations of TBI by delivering the prescribed dose targeted to the bone marrow (BM) while sparing organs at risk. Recently, our group demonstrated that TMI up to 20 Gy in relapsed/refractory AML patients was feasible and efficacious, significantly improving 2-year overall survival compared to the standard treatment. Whether such dose escalation is feasible in elderly patients, and how the organ toxicity profile changes when switching to TMI in patients of all ages are critical questions that need to be addressed. We used our recently developed 3D image-guided preclinical TMI model and evaluated the radiation damage and its repair in key dose-limiting organs in young (~8 weeks) and old

(~90 weeks) mice undergoing congenic bone marrow transplant (BMT). Engraftment was similar in both TMI and TBI-treated young and old mice. Dose escalation using TMI (12 to 16 Gy in two fractions) was well tolerated in mice of both age groups (90% survival ~12 Weeks post-BMT). In contrast, TBI at the higher dose of 16 Gy was particularly lethal in younger mice (0% survival ~2 weeks post-BMT) while old mice showed much more tolerance (75% survival ~13 weeks post-BMT) suggesting higher radio-resistance in aged organs. Histopathology confirmed worse acute and chronic organ damage in mice treated with TBI than TMI. As the damage was alleviated, the repair processes were augmented in the TMI-treated mice over TBI as measured by average villus height and a reduced ratio of relative mRNA levels of amphiregulin/epidermal growth factor (*areg*/*egf*). These findings suggest that organ sparing using TMI does not limit donor engraftment but significantly reduces normal tissue damage and preserves repair capacity with the potential for dose escalation in elderly patients.

KEYWORDS

total marrow irradiation, bone marrow transplantation, aging, tissue damage, tissue repair, DNA damage

Introduction

Total body irradiation (TBI) has been a standard component of the conditioning regimen for hematopoietic stem cell transplantation (HSCT) for hematological malignancies (1–3). The success of HSCT is often determined by a balance of providing adequate conditioning for engraftment and eradicating residual cancerous cells versus organ toxicity from conditioning and the subsequent risk of graft-versus-host disease. Previous research has shown that increasing the TBI dose (12 Gy to 15.75 Gy) in patients with high risk of relapse reduced leukemia relapse, although there was no survival benefit because of treatment-related mortality due to radiation toxicity to organs (4). To reduce the irradiation toxicity in the vital organs and to increase targeting of residual cancer cells, computed tomography (CT) image-guided total marrow irradiation (TMI) was developed and translated for clinical studies (5–7). Several research groups have used the TMI conditioning regimen to improve the outcome of patients with leukemia in HSCT (8–10). Our recent success with clinical TMI suggests that targeted marrow radiation is feasible and improves survival by decreasing both toxicity and relapse (11, 12). Furthermore, we recently initiated a dose escalation study in the older patient population (>55 years) to expand the HCT for patients with relapsed/refractory AML (CTN # NCT03494569). Determination of how the toxicity profile will change between TBI to TMI and whether dose escalation will be feasible in older patients is an unmet need.

TBI with or without chemotherapy prior to HCT has short-term and long-term treatment-related toxicities including acute and chronic GVHD, pneumonitis, mucositis, diarrhea, cardiac dysfunction, hypothyroidism and chronic kidney disease (13–18). Efforts to reduce TBI toxicities include hypo/hyper fractionation, dose rate, shielding organs at risk (OAR) and conformal Intensity modulated techniques to give higher doses to the target volume while sparing doses to surrounding tissues (19–26). Although these efforts provide some protection to OAR and improve treatment related toxicities, long-term toxicities are still a major concern. TMI is a compelling alternative as it provides an opportunity for dose escalation towards enhanced leukemia cell killing without severe tissue/organ adverse effects observed with TBI. This is particularly crucial for older patients who cannot receive myeloablative conditioning, resulting in increased relapse and graft failure risks. Therefore, dose escalation using TMI in the elderly offers a real chance to enhance the therapeutic ratio and addresses an urgent clinical need. However, a comparative evaluation of organ toxicity, particularly for dose escalation, between TMI and TBI cannot be achieved in the clinic because of increased treatment-related mortality reported earlier (4).

Previous research has indicated several mechanisms by which TMI may prove more beneficial than TBI as a conditioning platform (27). We previously evaluated dosimetric and biological differences of TMI versus TBI in rodents early point after irradiation (28). Our first-generation film-based preclinical 2D TMI model provided limited

dosimetric information for vital organs, thereby limiting mechanistic understanding of tissue damage from TMI or TBI. To overcome this limitation, we recently developed a three-dimensional multimodal image-guided TMI model for preclinical mouse study, which provided organ-specific quantitative dosimetry (dose volume histogram) and successfully used this TMI technique in BMT model (29).

The next critical step is an assessment of how TBI versus TMI causes changes in vital organ tissue damage and repair mechanisms. Previous studies suggest amphiregulin (AREG), the epidermal growth factor (EGF) receptor ligand has a critical role in organ development and promotes tissue repair under inflammatory conditions (30–32). Additionally, circulating AREG is elevated at the onset of acute and life-threatening GVHD (33) a major treatment related toxicity after radiation conditioning, and it portends poor prognosis. It is found during states of unresolved tissue damage, particularly if markedly elevated *relative* to EGF (34). In addition, AREG is activated in type 2 immune response and inflammatory lesions (34–36). Here we demonstrate that AREG/EGF levels correlate with damage/repair processes in organs post radiation and BMT in mice, furthering our ability to distinguish between TBI versus TMI in the context of gastrointestinal resistance and the effects of aging.

Materials and method

Animals

Animal studies were approved by the Institutional Animal Care and Use Committee at the City of Hope, National Medical Center, Duarte, CA. The C57BL/6J mice (JAX 000664) and B6.SJL-Ptprc^{a} Pepc^{b}/BoyJ (JAX 002014) were purchased from Jackson laboratory, Maine, USA, and housed at the COH animal facility.

TMI treatment plan

The image guide-TMI treatment strategy was developed as described (29). Both young and old mice were irradiated with TMI/TBI (2 fractions 24h apart) at -2 and -1 day before BMT. The radiation treatment used in this study: TMI (12:4), TBI (12:12), TMI (16:4), and TBI (16:16), with the first value indicating the dose delivered to the bone marrow and spleen and the second value indicating the dose to all other organs. Radiation beam layout of TBI and TMI by regions (beam size, isocenter location, normalization point) is provided in supplementary figure S1 and supplement table 1 [modified Supplementary Table 1 of (29)]. For TBI planning, mouse CBCT scans were divided into 3 regions for treatment optimization, and parallel opposed beams with a beam size of 40 mm square collimators were used to create a homogenized dose within the center of the beams in each region. For TMI planning, mouse CT scans were divided into 7 regions for treatment optimization. Beam sizes varied (40 x 40mm to 5mm square or circle) for different regions using different collimator settings. Supplementary Figure S1C, shows a parallel opposed radiation beam width (green) covering the spine. In addition, the prescribed dose to the head including skull and oral cavity was maintained at 12 Gy for all TMI treatment plans, to prevent increased toxicities like mucositis in dose escalated treatments.

Congenic bone marrow transplantation and engraftment

A congenic BMT was carried out by transplanting donor (CD45.1) BM cells into irradiated recipient (CD45.2) mice. The recipient mice were irradiated with TMI/TBI (2 fractions, 24 h apart) and transplanted with donor BM cells 24 h post radiation. Donor Bone marrow (BM) were harvested from femur and tibiae of young donor mice (8 weeks old, B6.SJL-Ptprc^{a} Pepc^{b}/BoyJ and a total of 25 million whole BM cells were injected into irradiated recipient mice (8 weeks young or 90 weeks old mice, CD45.2, C57BL/6j, JAX 000664) for BMT. To check donor engraftment, peripheral blood was collected from the tail vein and cells were stained with Percp-Cy5.5 anti-CD45.1 antibody (#110728, Biolegend) and APC anti-CD45.2 antibody (#109814, Biolegend) after RBC lysis with ACK (#A1049201, Thermo scientific). Donor chimerism was analyzed by flow cytometry using a BD LSR Fortessa (BD Biosciences, San Jose, CA) with data analysis using FlowJo V10.1 software.

H&E and trichrome staining

Tissue damage was estimated at 12 weeks after Rx/BMT by H&E staining including aged-matched unirradiated controls. Liver, gut, and lung tissues were collected and fixed with 10% Neutral Buffered Formalin for 2 days. Specifically, for gut harvest, 1 cm of jejunum (~14 cm apart from the stomach) were collected. Formalin-fixed, paraffin embedded tissues (FFPET) were cut at 3-4-micron sections and stained with hematoxylin and eosin (H&E) for morphologic evaluation. Villus height was quantified using Image J (NIH).

FFPET sections were also stained with a Trichrome kit to determine the extent of fibrosis in the lung, liver and gut according to the manufacturer's recommended protocol (StatLab, Cat# KTMTR2LT).

Immunofluorescence staining

Tissues were fixed in 10% neutral buffered formalin (NBF) for 1-2 days and incubated in 30% sucrose in PBS for 2 days at 4°C and then embedded in OCT compound. Frozen sections were used for immunofluorescence staining. To detect γ-H2AX Phospho-Histone H2AX (Ser139) (#2577, Cell signaling, USA), and FITC conjugated anti-Rabbit secondary antibody were used. Phalloidin-Fluor 594 (ab176757, Abcam, USA) was used for F-actin staining. Cells were mounted with Vectashield mounting medium containing DAPI (Vector Laboratories, USA) and scanned under a Zeiss LSM 900 confocal microscope (Carl Zeiss). Cell counts of $\gamma H2AX^+$ and total cells were measured by ImageJ.

qPCR analysis

Tissue mRNA was extracted using the RNeasy mini kit (Qiagen, #74106, USA). For cDNA synthesis, 1 µg mRNA was reverse transcribed using the high capacity cDNA reverse transcription kits (Life technologies #4369913, USA). Real time PCR was proceeded with Taqman Fast Advanced Master Mix (Thermo Scientific #4444965) according to the manufacturer's instructions. The following Taqman probes were used for qRT-PCR: Taqman probes Mouse Amphiregulin (Mm00437583_m1), Taqman probes Mouse EGF (Mm00438696_m1), and Taqman probes Mouse GAPDH (Mm99999915_g1). All reactions were run in duplicate with 45 cycles, on a Quant Studio 3 (Applied Biosystems, by Thermo Scientific, USA). qPCR cycle: Initial denaturation 95°C, 20 s; 45 cycles 95°C, 1 s; 60°C. 20s. ΔCt method was used for the calculation of target gene expression by normalizing to the housekeeping gene, GAPDH.

Statistics

All data are presented as Means ± SEM values. Statistical analyses were conducted using Prism (GraphPad) software. The unpaired Student's t-test, Log-rank (Mantel-Cox) test, and Two-way ANOVA test were applied for testing at a 5% level of significance (*P-value < 0.05).

Result

TMI treatment plan maintains prescription dose to bone marrow while reducing doses to vital organs

One of the most important advantages of our image guided TMI set-up is the ability to control the radiation dose to all organs, allowing us to precisely deliver BM treatment at a reduced dose to vital organs such as liver, lung, gut, and kidney, i.e. limiting normal tissue damage. Using this system, we have previously shown that TMI (12:4) is myeloablative in young mice (29) with further dose escalation feasible to 16 Gy BM dose, a 33% increase in dose, without changing the dose to the rest of the body which was maintained at 4 Gy, i.e. 16:4. Dose painting clearly indicates that the radiation dose in TMI is reduced in comparison to TBI which receives 100% of prescribed doses (Figure 1A). The mean organ dose to 50% volume (D50) is significantly reduced in all vital organs following TMI, be it in the (12:4) setting or at (16:4). For instance, there is 55-60% less dose to lung, 36-40% less to kidney, 55-60% less to liver, and the GI dose dropped by 55-60%, compared to TBI (~100% dose to all organs) (Figures 1B–D). The D10 (dose cover 10% volume) for liver, lung and kidney was ~80-90% of the prescribed dose, whereas D10 for GI was about 50% of the prescription dose suggesting that ~10% volume of lung, kidney and liver must have been near the planning target volume (PTV) i.e bone marrow. Importantly, the radiation dose to the BM was similar between TMI and TBI. The DVH of different organs is shown (Table 1). Overall, this supports the notion that compared to TBI, TMI treatment planning significantly reduces normal tissue exposure.

TMI based dose escalation is well tolerated in both young and old mice

We evaluated whether dose escalation was feasible in both young and old mice. The study design is shown (Figure 2A). In both age groups, TMI (12:4) and TMI (16:4) were well tolerated and ~over 70% of mice survived 3 months post BMT (Figures 2B, C). Although TBI 16 Gy was well tolerated in old mice (Figure 2B), it was lethal in young mice (Figure 2C). Old mice treated with TMI (12:4) or TBI (12:12) had increased 12-week survival post BMT compared to aged-matched controls (Figure 2B). Despite TMI (16:4) and TBI (16:16) having similar overall 3 months survival, although not significant, the onset of mortality was much earlier when 16 Gy was given in the TBI setting (within 2-3 weeks of exposure), reminiscent of hematopoietic acute radiation syndrome (Figure 2B, p=0.09). This also suggests that the cause of death in 16 Gy TMI mice was likely different.

As part of toxicity analysis, body weight was measured before Rx/BMT treatment and then every week post BMT to determine % weight loss post BMT. The body weight of untreated young control mice started at a baseline average of 20g ± 2g and increased over time unlike untreated old control mice that decreased from their baseline value of 40g±5g) (Figures 2D, E). As expected, all irradiated mice (young and old) showed significant weight reduction compared to untreated

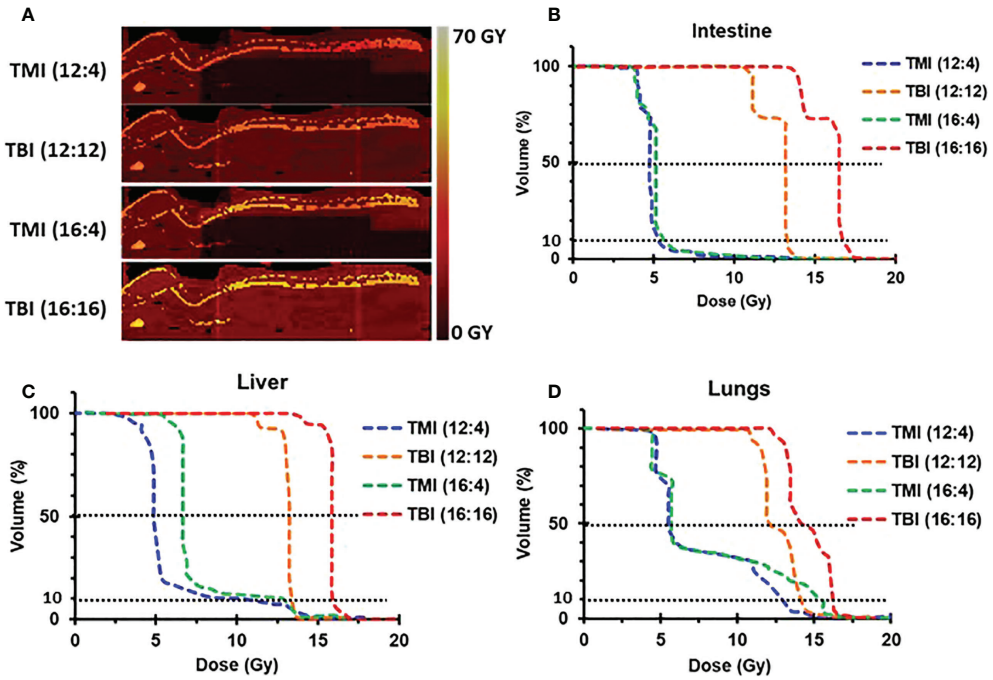

FIGURE 1
TMI vs. TBI strategy. Dose distribution for different radiation treatment regimens. **(A)** Radiation dose distribution of imaged-guided TMI or TBI strategy. Color painting of radiation dose 0-60 Gy. TMI showed 40-75% less radiation dose in liver, lung, and gut than TBI. **(B)** Dose volume histogram (DVH) of intestine. **(C)** DVH of liver. **(D)** DVH of lungs.

aged-matched controls at 1-2 week after exposure (p-value in Supplementary Figures S2–S4) with little or no difference between TMI (12:4) or TBI (12:12) amongst young and old mice, respectively (Figure 2E $p<0.05$, Figure 2D). Old mice treated with TBI (16:16) showed accelerated weight loss at 2 weeks after TBI which was not observed in TMI (16:4) treated mice (Figure 2D). Young mice, starting at a much lower baseline weight than old mice (20g vs 40g), were unable to tolerate treatment with TBI (16:16) and died within a week suggesting acute GI-death (Figure 2E). In addition, because there is the difference of body weight between young control and old control mice, we checked the food intake in old vs. young mice. The food intake and caloric intake per day was not different between young and old mice (Supplementary Figure S5). This is in line with what we know about the importance of age and weight as it relates to *in vivo* radiation toxicity in mice. Further, examining donor engraftment in peripheral blood of Rx/BMT old recipient mice we observed more than 90% donor chimerism at 4 and 8 weeks irrespective of age (young or old), of treatment type (TMI or TBI at 12 Gy), or radiation dose when given as TMI (12 or 16 Gy) (Figures 2F–I). In essence, TMI and TBI at the 12 Gy BM dose are isoeffective with respect to donor chimerism.

TABLE 1 Dose Distribution for different radiation treatment.

Regimens	TMI (12:4)		TBI (12:12)		TMI (16:4)		TBI (16:16)	
Dase stat	D50 (Gy)	D10 (Gy)	D50 (Gy)	D10 (Gy)	D50 (Gy)	D10 (Gy)	D50 (Gy)	D10 (Gy)
Intestine	4.8	5	11.9	12.6	5.2	5.4	15.5	16.4
Lungs	6.7	11.3	11.4	12.6	8.1	14.9	14.9	16.4
Liver	5.5	9.3	12.3	12.6	6.2	12	16	16.4
Kidneys	7.75	10.2	12.4	12.75	9.55	13.2	16.15	16.65
Spleen	12.9	17.8	12.7	12.9	17.2	Z4.6	16.5	16.8
PTV (Bones)	31.6	35.8	32	36.8	42.2	47.9	42.5	48.7

Dosimetry of PTV (Bones) and vital organs (Liver, Lung, Kidney, Intestine, spleen) of TMI (12:4), (16:4) and TBI (12:12), (16:16). D50 = mean radiation dose covering 50% of tissue volume, D10 = highest radiation dose covering 50% of tissue volume. D10 = highest radiation dose covering 10% of tissue volume.

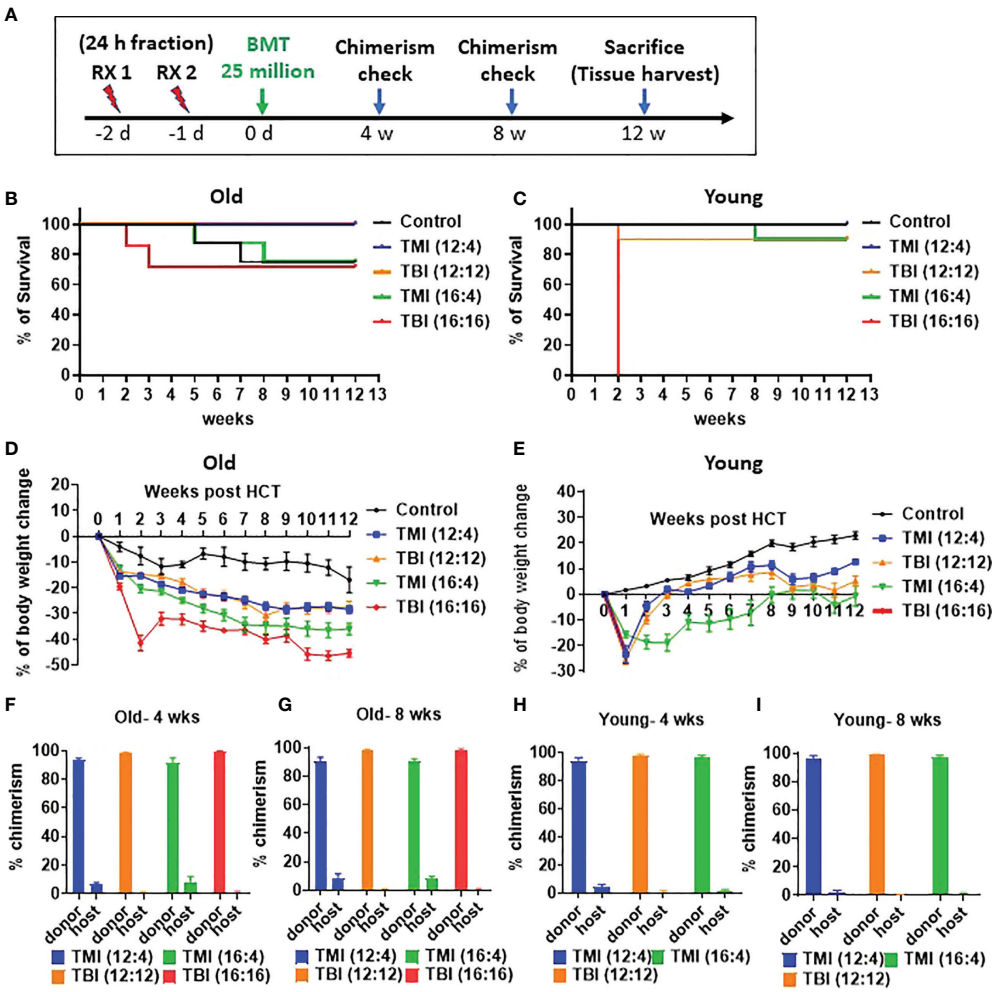

FIGURE 2
Comparison of TMI vs. TBI in survival, and donor engraftment in old and young mice. **(A)** Experiment schema. A total of 25 million of whole bone marrow cells were injected at 1 day intravenously after 2 times irradiation. **(B)** Survival rate of old mice for 12 weeks after BMT (Old control, n=8; TMI (12:4), n=10; TBI (12:12), n=10; TMI (16:4), n=8; TBI (16:16), n=7). **(C)** Survival rate of young mice for 12 weeks after BMT (Young control, n=8; TMI (12:4), n=10; TBI (12:12), n=10; TMI (16:4), n=10; TBI (16:16), n=10). **(D)** Body weight changes of old mice for 12 weeks after Rx/BMT. Mean ± SEM value. P-value are shown in Supplementary Figure S2 and body weight changes of individual mice were shown in Supplementary Figure 4A. **(E)** Body weight changes of young mice for 12 weeks after Rx/BMT. Mean ± SEM value. P-value are shown in Supplementary Figure S3 and body weight changes of individual mice were shown in Supplementary Figure 4B. **(F, G)** Donor engraftment of peripheral blood in old mice at 4 weeks and 8 weeks after Rx/BMT. Donor: CD45.1, Host: CD45.2. **(H, I)** Donor engraftment of peripheral blood in young mice at 4 weeks and 8 weeks after Rx/BMT. Donor: CD45.1, Host: CD45.2. Data represent the mean ± SEM, unpaired t test, Two-way ANOVA test, Log-rank Mantel-Cox test).

TMI causes less acute DNA damage in the gut

We compared the extent of damage by measuring DNA double strand break (DSB) following TMI or TBI treatment using histone H2AX phosphorylation at Ser-139, i.e. γH2AX (17). At 5 hours after irradiation, the jejunum from TBI (12:12) treated mice showed a substantial γH2AX signal, in comparison to TMI treated gut (Figures 3A, B and Supplementary Figure 6). This suggests that at equal BM dose, TBI caused more severe DNA damage in the gut than TMI.

TMI reduces organ damage to liver and gut compared to TBI

We hypothesized that TMI treatment elicits less damage to normal tissues compared to TBI. There were some changes in other organs in old mice and after TMI and TBI (Figure 4A),

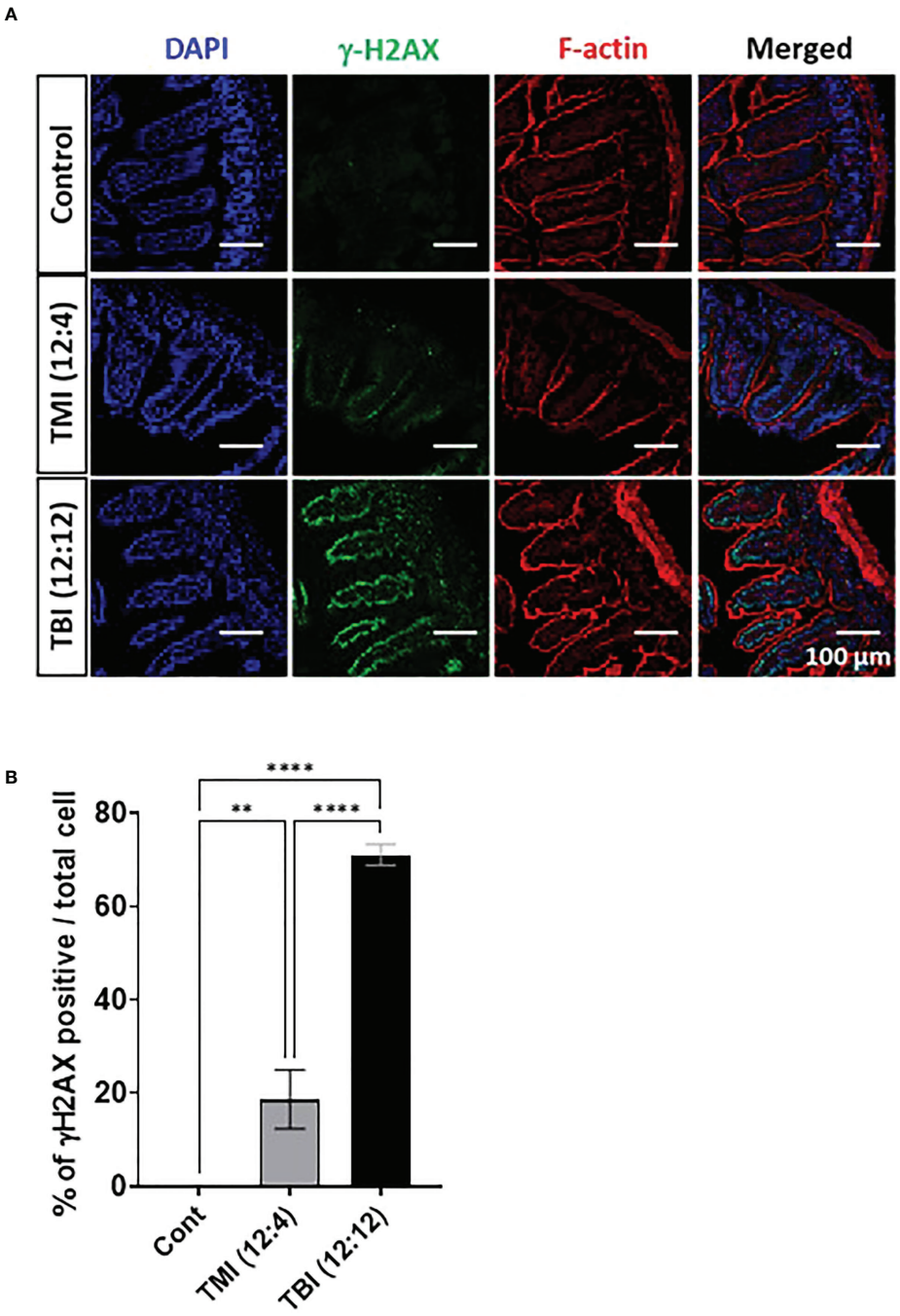

FIGURE 3
TMI reduces acute DNA damage than TBI. The mice were treated with TMI and TBI and 5 h post Rx DNA DSB was assessed by staining for γH2AX by immunofluorescence. **(A)** Immunofluorescence staining of γH2AX at 5h after irradiation. (Green = γH2AX, Red = F-actin, Blue = DAPI). (Young control, n=4; TMI (12:4), n=4; TBI (12:12), n=4) **(B)** Percentage of γH2AX positive cells/total cells. Three fields in each section and 2 different tissue sections from 4 mice in each group were used for calculations. Enlarged images are shown in Supplementary Figure S6. (**< 0.01, ****<0.0001, unpaired t test). Scale bar = 100 μm **(A)**.

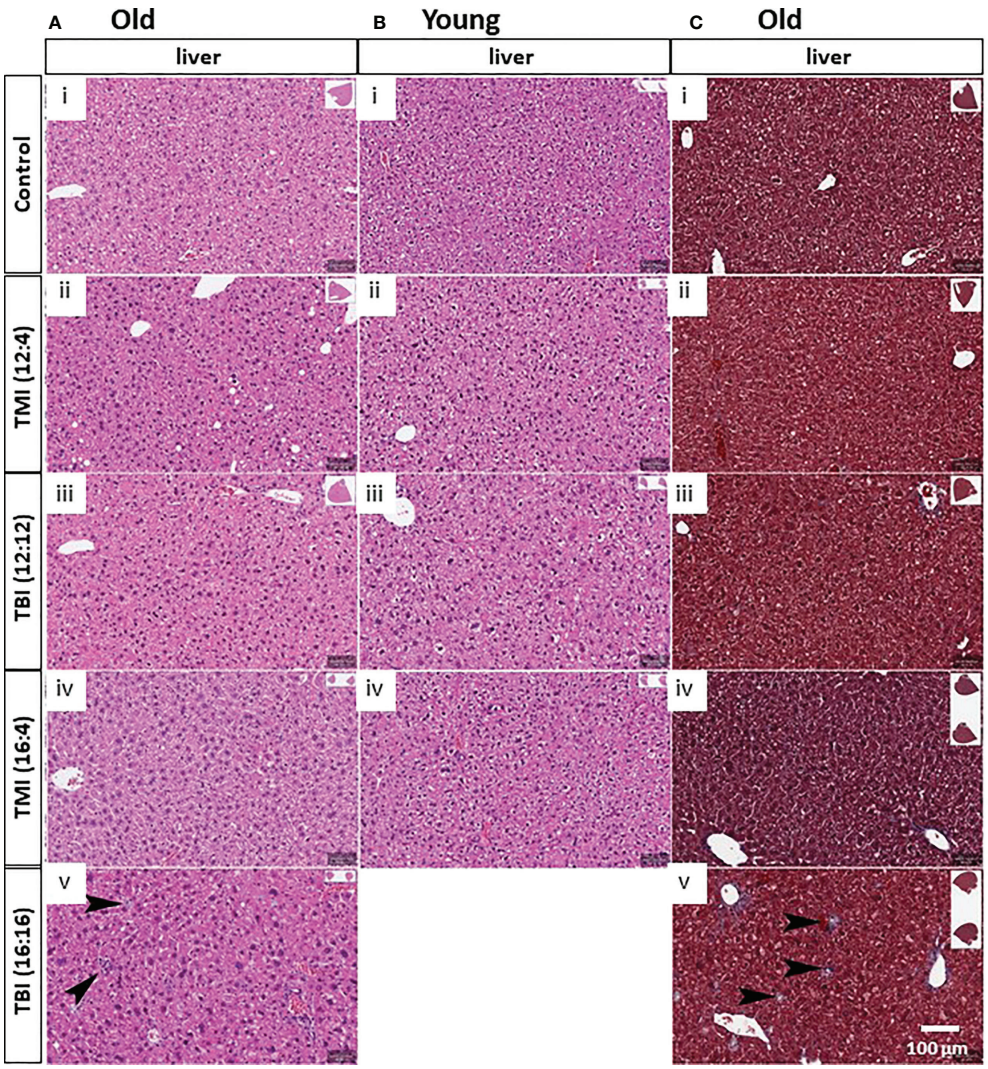

FIGURE 4
Damage of liver in TMI, TBI and untreated control in young and old mice at 12 weeks after BMT. **(A)** Liver histopathology in old mice. With TBI (16:16), there was increased portal inflammation and hepatocytes (arrows) present consistent with hepatocyte damage and turnover. Nuclear pleomorphism in the hepatocytes can be seen with increased radiation dosage. (i) Old control, (ii) TMI (12:4), (iii) TBI (12:12), (iv), TMI (16:4) and (v) TBI (16:16). **(B)** Liver histopathology in young mice. Increased nuclear pleomorphism in the hepatocytes can be seen with increased radiation dosage. (i) Young control, (ii) TMI (12:4), (iii) TBI (12:12), (iv), and TMI (16:4). **(C)** Trichrome staining in liver of old mice group. Increased fibrosis can be seen associated with the histocytes and portal inflammation. (i) Old control, (ii) TMI (12:4), (iii) TBI (12:12), (iv), TMI (16:4) and (v) TBI (16:16). Scale bar = 100 µm **(A–C)**.

such as increased portal inflammation as well as increased number of histiocytes indicative of liver damage and hepatocyte turnover (Figure 4A, arrows). Although, no such liver damage was observed in young mice (Figure 4B), but TBI (16:16) was lethal to young mice. Further, Trichrome stains of the liver also showed increased fibrosis associated with the inflammatory cells and histiocytes (Figure 4C, arrows). Of note, with increased radiation dose, one can appreciate the nuclear pleomorphism of the hepatocytes with increased nuclear size as well as occasional binucleated hepatocytes, indicating cellular damage (Figure 4A).

Intestine is one of the most radiosensitive organs as intestinal cells are highly proliferative. Therefore, we evaluated whether reduced organ dose in TMI protected the organ in comparison to TBI and what effect dose escalation would have on intestinal damage/repair. Histological assessment at the 3 months follow-up time point showed that TBI (12:12) and (16:16) treated old mice and TBI (12:12) treated young mice had pronounced intestinal damage in comparison to TMI (both dose levels and all age groups) (Figures 5A, B and Supplementary Figure S7). The H&E of TBI (12:4) and TBI (16:4) showed the blunt villi morphology

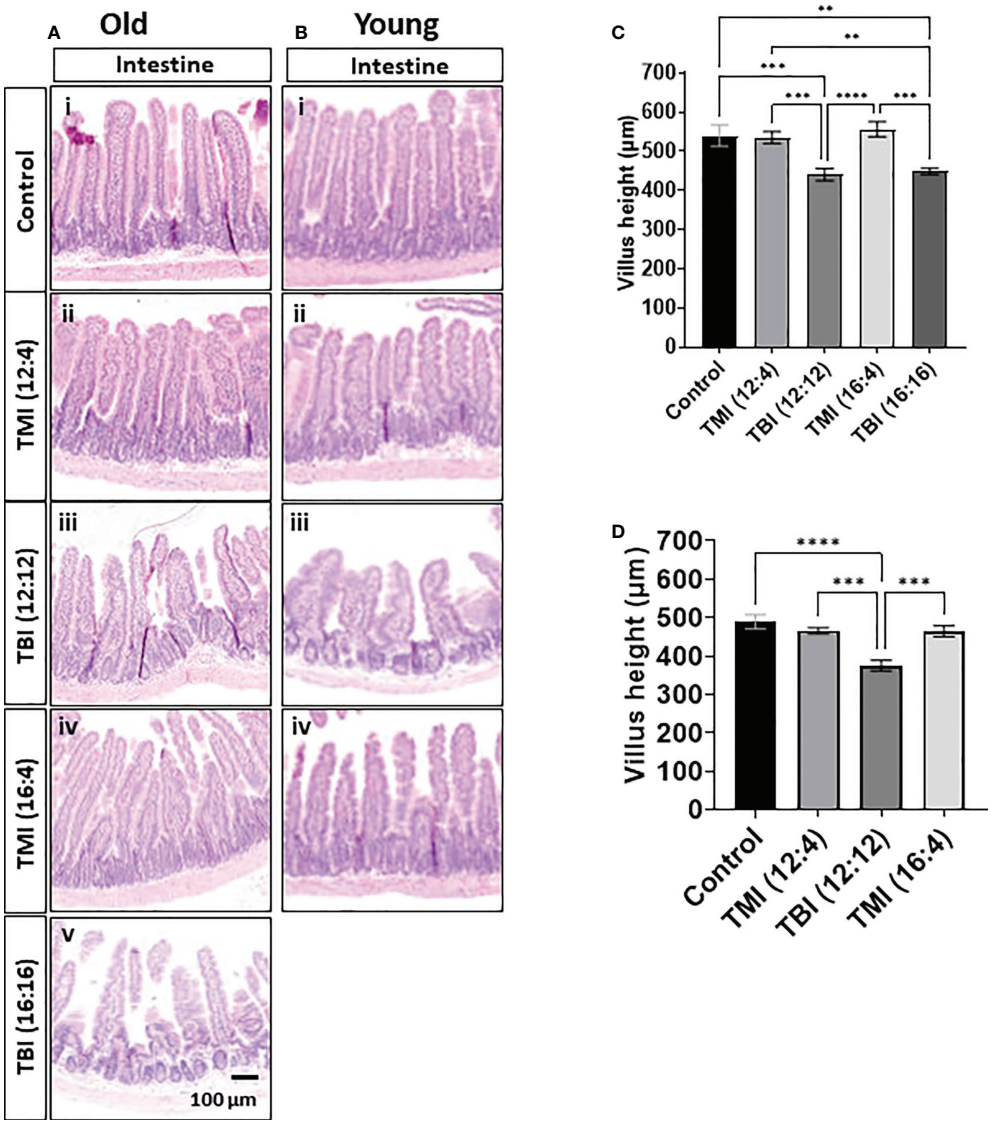

FIGURE 5
Damage of intestine in TMI, TBI, and untreated control at 12 weeks after BMT. The jejunum (~14 cm apart from the stomach) was collected and fixed for paraffin cross-section. Paraffin sections were stained with hematoxylin and eosin. **(A)** Intestinal anatomical changes in old mice. The H&E of TBI (12:4) and TBI (16:4) showed the blunt villi morphology and crypts hyperplasia compared to TMI (12:4) and TMI (16:4). (i) Old control, (ii) TMI (12:4), (iii) TBI (12:12), (iv), TMI (16:4) and (v) TBI (16:16). **(B)** Intestinal anatomical changes in young mice. (i) Young control, (ii) TMI (12:4), (iii) TBI (12:12), (iv), and TMI (16:4). The H&E of TBI (12:4) showed the blunt villi morphology and crypts hyperplasia compared to TMI (12:4) and TMI (16:4). **(C)** Measurements of villus height in old mice. (Old control n=5, TMI (12:4), n=6; TBI (12:12), n=7; TMI (16:4), n=6; TBI (16:16), n=5). Enlarged images are shown in Supplementary Figure 7A. **(D)** Measurements of villus height in young mice. (Young control, n=4; TMI (12:4), n=5; TBI (12:12), n=4; TMI (16:4), n=5). Enlarged images are shown in Supplementary Figure 7B. The villi height of 2 different gut section per each mouse was measured by ImageJ. (**< 0.01, ***<0.001, ****<0.0001, unpaired t-test). Scale bar = 100 µm **(A, B)**.

and crypts hyperplasia compared to TMI (12:4) and TMI (16:4). TBI (both dose levels) given to old mice caused a 20% loss in villus height which was similar in young mice (~25% reduction) after TBI (lower dose) treatment. In contrast, TMI treated mice showed more healthy villus length comparable to untreated age and Sex-matched control mice (Figures 5C, D).

In addition, damage assessment to the lung was also carried out at 3 months post BMT. For the old mice there was mild reduction of alveolar spaces and thinning of the space walls with higher doses of radiation compared to the control. According to histopathology there were no noticeable changes in the lung, be it in the alveolar spaces or any signs of lung fibrosis both for

young and old mice treated with TMI and TBI at 3 months post treatment (Supplementary Figures S8A, B). However, because the present treatment TMI plan covers a substantial amount of the lungs (Supplementary Figure S1C), proper pathological assessment of lung damage comparing TBI and TMI is challenging and needs further studies.

TBI causes persistent tissue damage after Rx/BMT

Elevated AREG/EGF ratios can be a sign of unresolved tissue damage highly relevant for BMT and the onset of conditioning induced toxicity like GVHD. The relative abundance of *areg* and *egf* mRNA in the gut (jejunum) was examined by qPCR with 12 Gy as the reference dose. A significant reduction in the *areg/egf* ratio was observed when switching from TBI to TMI in both young and old mice at 12 weeks post Rx/BMT treatment (Figures 6A–F) with *areg* and *egf* both responding, albeit inversely. These trends in AREG and EGF were noticeable even a day or a week after TMI compared to TBI in the absence of BMT, at least in young mice (Figures 6G–I). Although both radiation schemes drive an acute rise in AREG, levels return to normal within one week after TMI, but not after TBI (Figure 6I). These results correlated with chronic GI damage identified by histopathology (see above).

Discussion

This is the first preclinical 3D image guided bone marrow transplant study in both young and old mice for a direct, comparative evaluation of tissue damage and repair in the context of two treatment modalities, TBI and TMI. TMI is a novel, targeted, radiotherapeutic HCT pre-conditioning regimen for many hematological malignancies and disorders that is shifting the current clinical paradigm. It is based on advances in radiation dose delivery that allow us to precisely modulate doses to planned target volumes and OARs, e.g., lung, liver, GI, and kidney - a unique feature that promises to create new opportunities in Radiation Oncology. TMI can safely enhance the dose to the entire bone marrow, including "sanctuary sites" to increase leukemia cell killing, while further reducing exposure of OARs limiting acute and chronic radiation induced toxicities.

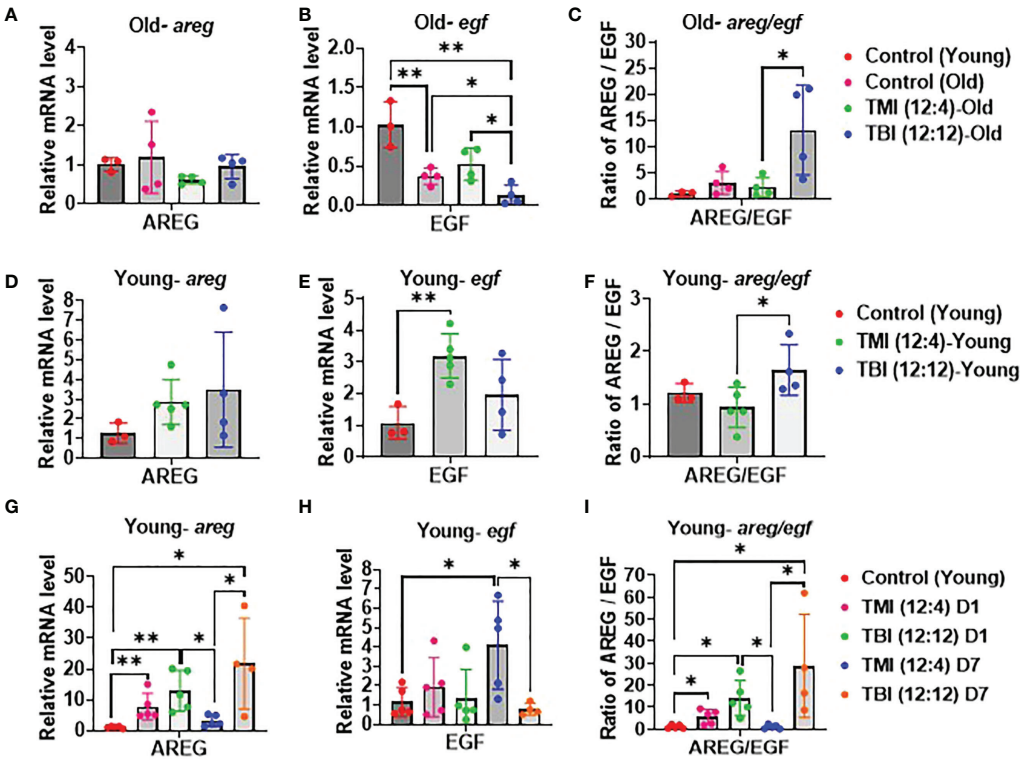

FIGURE 6
Damage and repair in TMI, TBI, and untreated control in young mice. **(A–C)** Relative mRNA level of AREG/EGF ratio, AREG and EGF expression. qPCR analysis in old mice at 12 weeks after Rx/BMT. **(D–F)** Relative mRNA level of AREG/EGF ratio, AREG and EGF expression. qPCR analysis in young mice at 12 weeks after Rx/BMT. **(G–I)** Relative mRNA level of AREG/EGF ratio, AREG and EGF expression in young mice at day 1 and day 7 after irradiation without BMT. (* <0.05, **< 0.01, unpaired t test).

Although a dose reduction to normal tissues during TMI has been reported in the clinical setting, the actual damage and/or repair in organs has yet to be characterized. In addition, the impact of dose escalation on long term toxicities in vulnerable patient populations such as pediatric and older patients have not been studied. Here we evaluated the feasibility of dose escalation in young and old mice and characterized the acute and chronic organ damage post radiation and BMT.

The principal idea of TBI is to deliver a uniform dose of ionizing radiation to the entire body, however radiosensitivity is not uniform across all organs resulting in treatment related toxicities of OAR. Despite this, TBI as conditioning for curative HCT has been used successfully for over half a century. With the advancement of chemotherapeutic agents and radiation delivering techniques, the focus has been to increase the therapeutic ratio. Currently, TMI is one of the major innovations in Radiation Oncology that shows promising results with a meaningful reduction in treatment related toxicities and better disease free and overall survival. By and large, the benefits of organ sparing using TMI in the clinic tend to be deduced from comparisons with historical TBI data (37, 38), but the actual organ damage and tissue repair processes have never been prospectively investigated, especially in the context of aging and dose escalation.

Here, image guided TMI treatment plans reduced the prescription dose to vital organs by 40-75%, while it was ~100% in TBI as shown earlier (Darren et al., 2021). Importantly, donor engraftment was equally high in TMI and TBI treated young and old mice. TBI treated mice showed persistently elevated AREG/EGF ratios, which has been linked to states of unresolved tissue damage (34). Compared to TBI, TMI not only caused less DNA damage in the GI, but AREG/EGF levels were also lower, and tissue regeneration accelerated according to GI pathophysiology. The appeal in reducing tissue damage lies in its potential to further attenuate treatment related complications like GvHD in the allogeneic transplant setting (see abstract Srideshikan et al. ASH 2022). This study suggests that myeloablation is limited by the tolerance dose of major organs, including the BM itself. In fact, the TMI model is a useful platform for future investigation into radiation tolerance limits of BM stroma as it relates to supporting full engraftment and increasing the anti-leukemic effect in older patients who have limited treatment options.

Although dose escalation using TMI was feasible in both young and old mice with no significant difference in chimerism or survival, younger mice were particularly sensitive to dose escalation using TBI. In contrast, reduced turnover and/or increased baseline cellular senescence in aged organs could have driven radio-resistance. This is in line with Hudson et al., who reported that organs of younger mice are more susceptible to radiation-induced DNA damage (39). Differences in individual's radio-sensitivities will also relate back to germline differences in DNA repair genes as well as immune signaling genes that determine how unrepaired damage feeds into inflammatory and immune pathways and drive the chronicity of organ damage.

Organ damage in old animals tends not to be studied much, partly for financial reasons. Our current study is the first focusing on the effects of irradiation and BMT in old mice. It is known that the myeloid to lymphoid cell ratio increases as we age, suggesting a myeloid bias in older mice (40). Interestingly, we show that transplanting younger donor BM cells into a heavily irradiated, aged BM microenvironment resulted in BM cells resembling younger mice. The myeloid to lymphoid cell ratio was reduced after BMT in old mice in comparison to untreated, aged and sex matched control mice (not shown). Similarly, Guderyon et al. reported that mobilization-based transplantation of young donor hematopoietic stem cells without irradiation expands lifespan in aged mice (41). This suggests that an aged BM microenvironment can adequately support younger donor BM progenitor cells at least initially, even after irradiation. Whether or not this can be maintained indefinitely is crucial for long-term survival, and a question that needs to be addressed (42).

There are some limitations of the current study. Some vital organs that are closer to the skeletal system, such as lungs and kidney, are still exposed to high dose of prescribed doses. As our CT scan reveals, substantial lung volume of the lungs, particularly closer to the spine and posterior region receives dose as high as prescription dose. This also limited our ability for pathological evaluation of lungs after TMI. In the future, we will develop 3D sections of an entire lung to identify high dose and low dose region. Also, we recently simulated a novel sparse orthogonal collimator–based intensity modulated preclinical TMI, which will significantly reduce radiation dose to lungs and kidney and enhance dosimetric conformality to the skeletal system (43).

In conclusion, this is a novel 3D TMI preclinical BMT model that demonstrates reduced organ damage and enhanced tissue repair in TMI treated mice over TBI. The dose escalation was tolerated in old mice, suggesting a potential HCT conditioning regimen using TMI for older patients who do not qualify for myeloablative conditioning. Further studies are warranted to understand the effect of dose escalation on BME, donor engraftment, HSCs maintenance and organ damage/repair.

Data availability statement

The original contributions presented in the study are included in the article/Supplementary Material. Further inquiries can be directed to the corresponding author.

Ethics statement

The animal study was reviewed and approved by Institute of Animal Care and Use Committee (IACUC):#16064.

Author contributions

JL, concept and experimental design, data analysis, interpretation of results and manuscript writing and editing. SH, MM and SSM, concept and experimental design, interpretation of results and manuscript writing and editing. PV, data acquisition, interpretation of results and manuscript editing. HG and AA, experimental design and TMI/TBI treatment. VVL, data acquisition, analysis, and manuscript editing. ML, Experimental design, and data analysis for food intake studies. JS, histopathological analysis, and manuscript writing and editing. SD, AP, CA, DS, DZ, GS, JL and SH, interpretation of results and manuscript writing. All authors contributed to the article and approved the submitted version.

Funding

This work has been supported by NIH grants, 2R01CA154491 (SH) and ONCOTEST (Ghent, Belgium) (SH). The content is solely the responsibility of the authors and does not necessarily represent the official views of the National Institutes of Health.

Acknowledgments

We would like to thank Dr Keiichi Itakura, Beckman Research Institute, Professor Emeritus, and Prof Jeffery Wong, Department of Radiation Oncology, City of Hope National medical center for scientific discussion and editing of the manuscript. We would like to thank David Kwon, senior RA, Beckman Research Institute, City of Hope National medical center for the rigorous editing of the manuscript.

Conflict of interest

Susanta K. Hui receives honoraria from and consults for Janssen Research & Development, LLC.

The remaining authors declare that the research was conducted in the absence of any commercial or financial relationships that could be construed as a potential conflict of interest.

Publisher's note

Supplementary material

The Supplementary Material for this article can be found online at: https://www.frontiersin.org/articles/10.3389/fonc.2022.1045016/full#supplementary-material

References

1. Gilson D, Taylor R. Total body irradiation. report on a meeting organized by the BIR oncology committee, held at the royal institute of British architects, London, 28 November 1996. *Br J Radiol* (1997) 70(840):1201–3. doi: 10.1259/bjr.70.840.9505836

2. Wong JY, Filippi AR, Scorsetti M, Hui S, Muren LP, Mancosu P. Total marrow and total lymphoid irradiation in bone marrow transplantation for acute leukaemia. *Lancet Oncol* (2020) 21(10):e477–87. doi: 10.1016/S1470-2045(20)30342-9

3. Copelan EA. Hematopoietic stem-cell transplantation. *N Engl J Med* (2006) 354(17):1813–26. doi: 10.1056/NEJMra052638

4. Clift RA, Buckner CD, Appelbaum FR, Bearman SI, Petersen FB, Fisher LD, et al. Allogeneic marrow transplantation in patients with acute myeloid leukemia in first remission: a randomized trial of two irradiation regimens. *Blood* (1990) 76(9):1867–71. doi: 10.1182/blood.V76.9.1867.1867

5. Hui SK, Kapatoes J, Fowler J, Henderson D, Olivera G, Manon RR, et al. Feasibility study of helical tomotherapy for total body or total marrow irradiation a. *Med Phys* (2005) 32(10):3214–24. doi: 10.1118/1.2044428

6. Wong JY, Liu A, Schultheiss T, Popplewell L, Stein A, Rosenthal J, et al. Targeted total marrow irradiation using three-dimensional image-guided tomographic intensity-modulated radiation therapy: an alternative to standard total body irradiation. *Biol Blood Marrow Transplant* (2006) 12(3):306–15. doi: 10.1016/j.bbmt.2005.10.026

7. Hui SK, Verneris MR, Higgins P, Gerbi B, Weigel B, Baker SK, et al. Helical tomotherapy targeting total bone marrow–first clinical experience at the university of Minnesota. *Acta Oncol* (2007) 250–5. doi: 10.1080/02841860601042449

8. Wong JY, Rosenthal J, Liu A, Schultheiss T, Forman S, Somlo G. Image-guided total-marrow irradiation using helical tomotherapy in patients with multiple myeloma and acute leukemia undergoing hematopoietic cell transplantation. *Int J Radiat Oncol Biol Phys* (2009) 73(1):273–9. doi: 10.1016/j.ijrobp.2008.04.071

9. Mancosu P, Cozzi L, Muren LP. Total marrow irradiation for hematopoietic malignancies using volumetric modulated arc therapy: A review of treatment planning studies. *Phys Imaging Radiat Oncol* (2019) 11:47–53. doi: 10.1016/j.phro.2019.08.001

10. Shen J, Wang X, Deng D, Gong J, Tan K, Zhao H, et al. Evaluation and improvement the safety of total marrow irradiation with helical tomotherapy using repeat failure mode and effects analysis. *Radiat Oncol* (2019) 14(1):1–7. doi: 10.1186/s13014-019-1433-7

11. Al Malki MM, Palmer J, Tsai NC, Mokhtari S, Hui S, Tsai W, et al. Total marrow and lymphoid irradiation as conditioning in haploidentical transplant with posttransplant cyclophosphamide. *Blood Adv* (2022) 6(14):4098–106. doi: 10.1182/bloodadvances.2022007264

12. Stein A. Dose escalation of total marrow and lymphoid irradiation in advanced acute leukemia. In: *Total marrow irradiation*. Springer Nature Switzerland (2020). p. 69–75.

13. Sabloff M, Tisseverasinghe S, Babadagli ME, Samant R. Total body irradiation for hematopoietic stem cell transplantation: What can we agree on? *Curr Oncol* (2021) 28(1):903–17. doi: 10.3390/curroncol28010089

14. Malicki J, Kosicka G, Stryczyńska G, Wachowiak J. Cobalt 60 versus 15 MeV photons during total body irradiation: doses in the critical organs and complexicity of the procedure. *Ann Transplant* (2001) 6(1):18–22.

15. Chiang Y, Tsai CH, Kuo SH, Liu CY, Yao M, Li CC, et al. Reduced incidence of interstitial pneumonitis after allogeneic hematopoietic stem cell transplantation using a modified technique of total body irradiation. *Sci Rep* (2016) 6:36730. doi: 10.1038/srep36730

16. Ujaimi RK, Isfahanian N, Russa DJL, Samant R, Bredeson C, Genest P. Pulmonary toxicity following total body irradiation for acute lymphoblastic leukaemia: The Ottawa hospital cancer centre (TOHCC) experience. *J Radiother Pract* (2015) 15(1):54–60. doi: 10.1017/S1460396915000497

17. Hill-Kayser CE, Plastaras JP, Tochner Z, Glatstein E. TBI during BM and SCT: review of the past, discussion of the present and consideration of future directions. *Bone Marrow Transplant* (2011) 46(4):475–84. doi: 10.1038/bmt.2010.280

18. Felice DEF, Grapulin L, Musio D, Pomponi J, Cinzia DIF, Iori AP, et al. Treatment complications and long-term outcomes of total body irradiation in patients with acute lymphoblastic leukemia: A single institute experience. *Anticancer Res* (2016) 36(9):4859–64. doi: 10.21873/anticanres.11049

19. Thomas ED, Clift RA, Hersman J, Sanders JE, Stewart P, Buckner CD, et al. Marrow transplantation for acute nonlymphoblastic leukemic in first remission using fractionated or single-dose irradiation. *Int J Radiat Oncol Biol Phys* (1982) 8 (5):817–21. doi: 10.1016/0360-3016(82)90083-9

20. Shank B, Chu FC, Dinsmore R, Kapoor N, Kirkpatrick D, Teitelbaum H, et al. Hyperfractionated total body irradiation for bone marrow transplantation. results in seventy leukemia patients with allogeneic transplants. *Int J Radiat Oncol Biol Phys* (1983) 9(11):1607–11. doi: 10.1016/0360-3016(83)90412-1

21. Deeg HJ, Sullivan KM, Buckner CD, Storb R, Appelbaum FR, Clift RA, et al. Marrow transplantation for acute nonlymphoblastic leukemia in first remission: toxicity and long-term follow-up of patients conditioned with single dose or fractionated total body irradiation. *Bone Marrow Transplant* (1986) 1(2):151–7.

22. Gopal R, Ha CS, Tucker SL, Khouri IF, Giralt SA, Gajewski JL, et al. Comparison of two total body irradiation fractionation regimens with respect to acute and late pulmonary toxicity. *Cancer* (2001) 92(7):1949–58. doi: 10.1002/1097-0142(20011001)92:7<1949::AID-CNCR1714>3.0.CO;2-1

23. Giebel S, Miszczyk L, Slosarek K, Moukhtari L, Ciceri F, Esteve J, et al. Extreme heterogeneity of myeloablative total body irradiation techniques in clinical practice: a survey of the acute leukemia working party of the European group for blood and marrow transplantation. *Cancer* (2014) 120(17):2760–5. doi: 10.1002/cncr.28768

24. Cheng JC, Schultheiss TE, Wong JY. Impact of drug therapy, radiation dose, and dose rate on renal toxicity following bone marrow transplantation. *Int J Radiat Oncol Biol Phys* (2008) 71(5):1436–43. doi: 10.1016/j.ijrobp.2007.12.009

25. Altschuler C, Resbeut M, Blaise D, Maraninchi D, Stoppa AM, Lagrange JL, et al. Fractionated total body irradiation and bone marrow transplantation in acute lymphoblastic leukemia. *Int J Radiat Oncol Biol Phys* (1990) 19(5):1151–4. doi: 10.1016/0360-3016(90)90220-E

26. Schneider RA, Schultze J, Jensen JM, Hebbinghaus D, Galalae RM. Long-term outcome after static intensity-modulated total body radiotherapy using compensators stratified by pediatric and adult cohorts. *Int J Radiat Oncol Biol Phys* (2008) 70(1):194–202. doi: 10.1016/j.ijrobp.2007.05.035

27. Wong JYC, Filippi AR, Dabaja BS, Yahalom J, Specht L. Total body irradiation: Guidelines from the international lymphoma radiation oncology group (ILROG). *Int J Radiat Oncol Biol Phys* (2018) 101(3):521–9. doi: 10.1016/j.ijrobp.2018.04.071

28. Hui S, Takahashi Y, Holtan SG, Azimi R, Seelig D, Yagi M, et al. Early assessment of dosimetric and biological differences of total marrow irradiation versus total body irradiation in rodents. *Radiother Oncol* (2017) 124(3):468–74. doi: 10.1016/j.radonc.2017.07.018

29. Zuro D, Madabushi SS, Brooks J, Chen BT, Goud J, Salhotra A, et al. First multimodal, three-dimensional, image-guided total marrow irradiation model for preclinical bone marrow transplantation studies. *Int J Radiat Oncol Biol Phys* (2021) 111(3):671–83. doi: 10.1016/j.ijrobp.2021.06.001

30. Qi Y, Operario DJ, Georas SN, Mosmann TR. The acute environment, rather than T cell subset pre-commitment, regulates expression of the human T cell cytokine amphiregulin. *PloS One* (2012) 7(6):e39072. doi: 10.1371/journal.pone.0039072

31. Berasain C, Avila MA. Amphiregulin. *Semin Cell Dev Biol* (2014) 28:31–41. doi: 10.1016/j.semcdb.2014.01.005

32. Zaiss DMW, Gause WC, Osborne LC, Artis D. Emerging functions of amphiregulin in orchestrating immunity, inflammation, and tissue repair. *Immunity* (2015) 42(2):216–26. doi: 10.1016/j.immuni.2015.01.020

33. Holtan SG, Shabaneh A, Betts BC, Rashidi A, MacMillan ML, Ustun C, et al. Stress responses, M2 macrophages, and a distinct microbial signature in fatal intestinal acute graft-versus-host disease. *JCI Insight* (2019) 5(17):e129762. doi: 10.1172/jci.insight.129762

34. Atkins SLP, DeFor TE, MacMillan ML, Turcotte L, Rashidi A, Weisdorf DJ, et al. Elevated AREG/EGF ratio prior to transplantation is associated with pre-transplant clostridium difficile infection, unresolved tissue damage, and poorer overall survival. *Blood* (2018) 132:3353. doi: 10.1182/blood-2018-99-115686

35. Ceafalan LC, Manole E, Tanase CP, Codrici E, Mihai S, Gonzalez A, et al. Interstitial outburst of angiogenic factors during skeletal muscle regeneration after acute mechanical trauma. *Anatomical Rec* (2015) 298(11):1864–79. doi: 10.1002/ar.23254

36. Holtan SG, Khera N, Levine JE, Chai X, Storer B, Liu HD, et al. Late acute graft-versus-host disease: a prospective analysis of clinical outcomes and circulating angiogenic factors. *Blood J Am Soc Hematol* (2016) 128(19):2350–8. doi: 10.1182/blood-2015-09-669846

37. Haraldsson A, Wichert S, Engström PE, Lenhoff S, Turkiewicz D, Warsi S, et al. Organ sparing total marrow irradiation compared to total body irradiation prior to allogeneic stem cell transplantation. *Eur J Haematol* (2021) 107(4):393–407. doi: 10.1111/ejh.13675

38. Shinde A, Yang D, Frankel P, Liu A, Han C, Del Vecchio B, et al. Radiation-related toxicities using organ sparing total marrow irradiation transplant conditioning regimens. *Int J Radiat Oncol Biol Phys* (2019) 105(5):1025–33. doi: 10.1016/j.ijrobp.2019.08.010

39. Hudson D, Kovalchuk I, Koturbash I, Kolb B, Martin OA, Kovalchuk O. Induction and persistence of radiation-induced DNA damage is more pronounced in young animals than in old animals. *Aging (Albany NY)* (2011) 3(6):609. doi: 10.18632/aging.100340

40. Morrison SJ, Wandycz AM, Akashi K, Globerson A, Weissman IL. The aging of hematopoietic stem cells. *Nat Med* (1996) 2(9):1011–6. doi: 10.1038/nm0996-1011

41. Guderyon MJ, Chen C, Bhattacharjee A, Ge G, Fernandez RA, Gelfond JA, et al. Mobilization-based transplantation of young-donor hematopoietic stem cells extends lifespan in mice. *Aging Cell* (2020) 19(3):e13110. doi: 10.1111/acel.13110

42. Dorshkind K, Höfer T, Montecino-Rodriguez E, Pioli PD, Rodewald HR. Do haematopoietic stem cells age? *Nat Rev Immunol* (2020) 20(3):196–202. doi: 10.1038/s41577-019-0236-2

43. Abdelhamid AMH, Jiang L, Zuro D, Liu A, Madabushi SS, Ghimire H, et al. Feasibility of a novel sparse orthogonal collimator-based preclinical total marrow irradiation for enhanced dosimetric conformality. *Front Oncol* (2022) 12:941814. doi: 10.3389/fonc.2022.941814

frontiers | Frontiers in Oncology

TYPE Original Research
PUBLISHED 08 December 2022
DOI 10.3389/fonc.2022.1035375

OPEN ACCESS

EDITED BY
Kevin X. Liu,
Massachusetts General Hospital and Harvard Medical School, United States

REVIEWED BY
Bianca Hoeben,
University Medical Center Utrecht, Netherlands
Luca Castagna,
Azienda Ospedaliera Ospedali Riuniti Villa Sofia Cervello, Italy
Gerhard C. Hildebrandt,
University of Missouri, United States

*CORRESPONDENCE
Cynthia Aristei
cynthia.aristei@unipg.it

SPECIALTY SECTION
This article was submitted to Radiation Oncology, a section of the journal Frontiers in Oncology

RECEIVED 02 September 2022
ACCEPTED 10 November 2022
PUBLISHED 08 December 2022

CITATION
Saldi S, Fulcheri CPL, Zucchetti C, Abdelhamid AMH, Carotti A, Pierini A, Ruggeri L, Tricarico S, Chiodi M, Ingrosso G, Bini V, Velardi A, Martelli MF, Hui SK and Aristei C (2022) Impact of total marrow/lymphoid irradiation dose to the intestine on graft-versus-host disease in allogeneic hematopoietic stem cell transplantation for hematologic malignancies.
Front. Oncol. 12:1035375.
doi: 10.3389/fonc.2022.1035375

Impact of total marrow/lymphoid irradiation dose to the intestine on graft-versus-host disease in allogeneic hematopoietic stem cell transplantation for hematologic malignancies

Simonetta Saldi[1], Christian Paolo Luca Fulcheri[2], Claudio Zucchetti[2], Amr Mohamed Hamed Abdelhamid[3,4], Alessandra Carotti[5], Antonio Pierini[5], Loredana Ruggeri[5], Sara Tricarico[5], Marino Chiodi[6], Gianluca Ingrosso[3], Vittorio Bini[7], Andrea Velardi[5], Massimo Fabrizio Martelli[5], Susanta Kumar Hui[8] and Cynthia Aristei[3]*

[1]Section of Radiation Oncology, Hospital of Santa Maria della Misericordia, Perugia, Italy, [2]Medical Physics, Hospital of Santa Maria della Misericordia, Perugia, Italy, [3]Radiation Oncology Section, Department of Medicine and Surgery, University of Perugia and Perugia General Hospital, Perugia, Italy, [4]Department of Oncology and Nuclear Medicine, Faculty of Medicine, Ain Shams University, Cairo, Egypt, [5]Division of Hematology and Clinical Immunology, Department of Medicine, University of Perugia, Perugia, Italy, [6]Radiology Unit, S. Maria Della Misericordia Hospital, Perugia, Italy, [7]Internal Medicine, Endocrine and Metabolic Science Section, University of Perugia, Perugia, Italy, [8]Department of Radiation Oncology, City of Hope National Medical Center, CA, United States

Background and purpose: Graft-versus-host disease (GvHD) is a leading cause of non-relapse mortality in patients undergoing allogeneic hematopoietic stem cell transplantation. The Perugia Bone Marrow Transplantation Unit designed a new conditioning regimen with total marrow/lymphoid irradiation (TMLI) and adaptive immunotherapy. The present study investigated the impact of radiotherapy (RT) doses on the intestine on the incidence of acute GvHD (aGvHD) in transplant recipients, analyzing the main dosimetric parameters.

Materials and methods: Between August 2015 and April 2021, 50 patients with hematologic malignancies were enrolled. All patients underwent conditioning with TMLI. Dosimetric parameters (for the whole intestine and its segments) were assessed as risk factors for aGvHD. The RT dose that was received by each intestinal area with aGvHD was extrapolated from the treatment plan for each patient. Doses were compared with those of the whole intestine minus the affected area.

Results: Eighteen patients (36%) developed grade ≥2 aGvHD (G2 in 5, G3 in 11, and G4 in 2). Median time to onset was 41 days (range 23–69 days). The skin

was involved in 11 patients, the intestine in 16, and the liver in 5. In all 50 TMLI patients, the mean dose to the whole intestine was 7.1 Gy (range 5.07–10.92 Gy). No patient developed chronic GvHD (cGvHD). No dosimetric variable emerged as a significant risk factor for aGvHD. No dosimetric parameter of the intestinal areas with aGvHD was associated with the disease.

Conclusion: In our clinical setting and data sample, we have found no clear evidence that current TMLI dosages to the intestine were linked to the development of aGvHD. However, due to some study limitations, this investigation should be considered as a preliminary assessment. Findings need to be confirmed in a larger cohort and in preclinical models.

KEYWORDS

TMLI, graft-versus-host disease, tomotherapy, intestine dose radiotherapy, HSCT = hematopoietic stem cell transplant, intestinal acute graft-versus-host disease

Introduction

Hematopoietic stem cell transplantation (HSCT), the most effective post-remission treatment for acute leukemia (AL), is indicated for patients in ≥ second complete remission (CR) or in first CR with unfavorable cytogenetics and molecular markers (intermediate–high-risk AL) (1). HSCT achieves its effect through the conditioning regimen's myeloablation and the graft's elimination of residual leukemic cells [graft *vs*. leukemia (GvL) effect]—thanks to its donor T-lymphocyte content (2). On the other hand, this can cause graft-versus-host disease (GvHD), a leading cause of non-relapse mortality (3).

GvHD is usually distinguished as acute or chronic, each with a different underlying mechanism. Acute GvHD (aGvHD) includes a combination of symptoms and signs that usually occur in the first 100 days posttransplant but may have a later onset. Chronic GvHD (cGvHD), the most frequent cause of late non-relapse morbidity and mortality, might affect several organs, determining functional impairment (4, 5). Approximately 30%–50% of HSCT recipients develop aGvHD typically affecting the skin, gastrointestinal (GI) tract, and liver, and 10%–70% are affected by cGvHD (6, 7) that manifests like autoimmune diseases such as eosinophilic fasciitis or scleroderma-like skin disease (8).

Risk factors for aGvHD include unrelated or alternative donors, donor parity, donor–recipient sex mismatch, elderly recipient, advanced-stage disease, low regulatory T-cell content in the graft (9). Furthermore, conditioning regimens that included total body irradiation (TBI) were associated with a higher incidence of aGvHD than chemotherapy alone (10–12). On the other hand, the large Forum Randomized Controlled Trial did not show significant differences in aGvHD in children after chemotherapy or 6 × 2 Gy TBI conditioning (13). The robust GI structure and function in young patients might have enabled them to tolerate higher GI doses with TBI.

Radiation dose correlated with aGvHD severity. In a mouse model, Hill et al. (14) showed that a higher TBI dosage (13 Gy *vs*. 9 Gy) led to greater intestinal damage and more severe GvHD. High-dose TBI (15.75 Gy *vs*. 12 Gy) was also associated with more aGvHD in a clinical study by Clift et al. (15). In a large series of patients who had received matched or mismatched stem cell transplantation, TBI >12 Gy emerged as a risk factor for GvHD (44% with doses >12 Gy *vs*. 28% with 0–12 Gy, p = 0.001) (16).

Radiation-related damage to the GI tract plays a major role in aGvHD development and its systemic involvement by triggering and propagating the cytokine storm (17). Critically, the TBI dose can injure the intestinal mucosa, inducing inflammation and promoting translocation of inflammatory stimuli, thus further damaging the GI tract. Furthermore, the conditioning regimen injures tissues and activates inflammatory cytokines tumor necrosis factor (TNF)-α and interleukin (IL)-1. Tissue damage is amplified by donor T-cell activation leading to IL-2 and interferon (IFN)-γ secretion. Intestinal mucosal damage increases the release of lipopolysaccharides and stimulates cytokine production by lymphocytes and macrophages in the GI tract and by keratinocytes, dermal fibroblasts, and macrophages in the skin (18).

In order to reduce the radiotherapy (RT) dose to the GI tract and to other organs at risk (OARs) of toxicity, such as the lungs, heart, and kidneys (19), total marrow irradiation (TMI) and total marrow/lymphoid irradiation (TMLI) were introduced into the conditioning regimens (20–23). Unlike TBI, the radiation target volumes for TMI is only the skeleton, while total lymphoid irradiation (TLI) is targeted at major lymph node chains and non-lymphoid organs, such as the spleen and liver. Preclinical

data in a murine model confirmed that, compared with TBI, TMI reduced the dose to the GI tract and thus the risk of aGvHD-mediated tissue damage (24). In a retrospective cohort analysis, Haraldsson et al. (25) reported less aGvHD after TMI with tomotherapy than two-dimensional (2D) TBI.

The present study assessed whether clinical parameters and the dose delivered to the intestine were risk factors for aGvHD in patients undergoing TMLI in the conditioning regimen for HSCT.

Patients and methods

Between August 2015 and April 2021, this prospective observational study recruited 50 patients [median age 56 years, range 23–70 years; 33 men; 17 women; 44 with acute myeloid leukemia (AML), 3 with acute lymphoid leukemia (ALL), and 3 with myelodysplastic syndrome]. The study was conducted in accordance with the 1975 Helsinki Declaration, as revised in 2000, and all patients provided written informed consent. The indication for TMLI was age >50 years old. Six unfit patients (i.e., with comorbidities that precluded TBI) who were <50 years old also received TMLI. Before conditioning, no patient was affected by GI disturbances. Table 1 reports details of these 50 patients.

Radiotherapy

TMLI was administered to all patients by helical tomotherapy in nine fractions delivered twice daily for 4.5 consecutive days. Using a Simultaneous Integrated Boost (SIB) procedure, target volumes were skeletal bones for TMI (total dose 13.5 Gy) and major lymph node chains and spleen for TLI (total dose 11.5 Gy). Patients with ALL received 13.5 Gy to the brain. All patients were reproducibly immobilized using a vacuum cushion and a 5-point open-face thermoplastic mask for the head, neck, and shoulders. Since the tomotherapy unit treats up to 135 cm in length, treatment was split into two plans: the upper, comprising approximately from the vertex to the knees, and the lower, from approximately the toes to the hip bone. All patients underwent two computed tomography (CT) scans, using 10-mm slice thickness, in opposite directions, with the patient rotated through 180 degrees. To reach an acceptable dose homogeneity in the junction region of the plans, a controlled dose gradient was created using five regions inside the overlap volume.

On the CT images, one expert radiation oncologist (SS) contoured OARs (Table 1) and target structures using the Pinnacle TPS v.16 (Philips) contouring tool. Before transferring images and RT structures to the Accuray® Planning Station 5.1.1 for plan optimization, expert medical physicists (CZ, CF) reviewed the volumes and created planning regions of interest (ROIs) (e.g., remaining volume at risk, healthy lungs, junctions) using a fully automated Pinnacle script.

Plan setup and optimization were done using a dedicated protocol with the following parameters: "fine" dose calculation grid, 5.02-cm field width; fixed jaw mode. For the upper and lower plans, planning modulation factors were in the range of 3.0–3.7 and 2.0–2.5, respectively; the pitch was in the range of 0.32–0.43 for the upper plan and was set at 0.287 for the lower. The pitch value of the upper plan was selected to minimize the thread effect, especially for off-axis targets such as the arms, and to reach a compromise between dose homogeneity and gantry period.

Treatment planning system planning optimization goals were set so that 100% of the prescribed dose covered 60% of the planning target volume (PTV) and at least 95% of the prescribed dose covered 90% of the PTV.

The optimization procedure focused on dose reduction to the main OARs, i.e., the heart, bowel, liver, lungs, and kidneys, and was iterated at least 500 times. Treatment plans were assessed and approved according to the following criteria: individual patient factors and needs, dose distribution conformity and homogeneity (as visually assessed), hot spots within the target, adequate treatment time for patient compliance, achievement of target coverage objectives, and average doses to the OARs in accordance with our center's reference values (Table 2). Treatment plans were satisfactory when doses fell within the ranges shown in Table 2. By respecting these constraints, no plan has to date fallen outside of our median range. If it were to happen, the plan would be redone.

TABLE 1 Details of 50 patients who underwent a TLMI-based conditioning regimen to hematopoietic stem cell transplantation (HSCT).

Sex	
Male	33
Female	17
Age (years)	
Median	56
Range	23–70
Hematologic malignancies	
Acute myeloid leukemia	44
Acute lymphoid leukemia	3
Myelodysplastic syndrome	3
Genetic risk stratification at diagnosis	
Favorable	4
Intermediate	21
Adverse	22
Missing information	3
Disease status at HSCT	
First complete remission (CR)	24
≥ Second CR	21
Advanced	5
Minimal residual disease (MRD)	
MRD positive	33
No MRD	17

10.3389/fonc.2022.1035375

TABLE 2 Organs at risk (OARs) average and range of median doses.

Organ	Median dose in Gy Average (Range)*
Anus	7.2 (3.14 – 14.81)
Bladder	8.98 (6.44 – 13.37)
Brain	8.87 (7.74 – 13.57)
Esophagus	11.4 (8.47 – 13.9)
Heart	6.35 (5.30 – 9.04)
Kidney (left)	6.27 (5.08 – 9.3)
Kidney (right)	5.69 (4.42 – 8.85)
Large bowel	7.93 (6.34 – 11.73)
Lens (left)	3.2 (1.85 – 5.19)
Lens (right)	3.3 (1.92 – 4.91)
Liver	7.72 (5.7– 10.21)
Lung (left)	8.97 (6.35 – 10.98)
Lung (right)	8.7 (6.31 – 10.65)
Oral cavity	8.83 (5.59 – 12.45)
Rectum	7.75 (5.55 – 11.66)
Small bowel	6.43 (5.61 – 10.59)
Stomach	8.39 (5.5 – 12.81)
Thyroid	10.95 (7.31 – 13.94)

*Average and range (minimum and maximum median dose) of median doses in 75 patients with diverse hematologic malignancies. Values derive from a retrospective analysis of our entire series of 75 TMLI patients, starting in 2015. They were gradually reduced over time to account for updates in skills and for values reported elsewhere.

Transplantation procedure

Figure 1 illustrates the conditioning regimen and graft composition, showing TMLI was followed by thiotepa (5–7.5 mg/kg), fludarabine (150 mg/m^2), and cyclophosphamide (20 mg/kg per day in Human leukocyte antigens (HLA)-matched HSCT; 30 mg/kg per day in HLA-haploidentical HSCT). Donors were HLA-matched related for 11 patients and HLA-haploidentical mismatched family members for 39. Apheresis procedures were described in full elsewhere (23). All patients received an infusion of 2×10^6/kg donor regulatory T cells (Tregs) on day -4 followed by 1×10^6/kg conventional T cells (Tcons) on day -1. A megadose of $>6 \times 10^6$/kg positively selected CD34$^+$ hematopoietic progenitor cells was infused on day 0.

Prophylaxis for Acute graft-versus-host disease (aGvHD) and infections

aGvHD prophylaxis consisted of *ex vivo* T-lymphocyte depletion by positive immunoselection of CD34$^+$ peripheral hematopoietic progenitor cells and donor Tregs. No pharmaceutical immunosuppressive therapy was given posttransplant. All patients received antibacterial, antifungal, antiviral, and anti-*Pneumocystis carinii* prophylaxis. GI status and all symptoms were registered in each patient's chart before, during, and after TMLI and after transplantation.

aGvHD assessment

Engrafted patients who survived more than 30 days were evaluable for aGvHD, which was assessed according to the Glucksberg score (26). The grade was determined by the worst disease stage in any organ. Diagnosis of intestinal aGvHD was confirmed by means of a CT scan in the acute phase of intestinal inflammation. aGvHD areas were defined by indicative radiological signs (i.e., luminal dilation with small bowel wall thickening ("ribbon sign") and air/fluid levels suggesting an ileus) (27).

Dosimetric analysis

For the whole intestine and separately for the small intestine, large intestine, duodenum, sigmoid, and rectum, the following dosimetric parameters were analyzed: dose received by 5 cc (D5cc), 10 cc (D10cc), 30 cc (D30cc), 50 cc (D50cc), 80 cc (D80cc); mean dose (Dmean); maximum dose (Dmax); volumes that received 5 Gy (V5Gy), 7 Gy (V7Gy), 9 Gy (V9Gy), 11 Gy (V11Gy), 13 Gy (V13Gy), or more. For the purposes of this study, an expert radiologist (MC) contoured on the planning CT images the areas that had radiological signs indicative of aGvHD on diagnostic CT scans, an example is provided in Figure 2. The RT dose that was received by each intestinal area with aGvHD (V5Gy, V7Gy, V9Gy, V11Gy, V13Gy, Dmin, Dmean, Dmax) was extrapolated from the treatment plan for each patient. Doses to each intestinal area with aGvHD were compared with those of the whole intestine minus the affected area.

Statistical analyses

Dosimetric parameters as above and clinical variables {age, body mass index (BMI), residual disease at transplant [minimal residual disease (MRD) >0.1% blasts at cytofluorimetric analysis of bone marrow]} were assessed as risk factors for aGvHD. The Shapiro–Wilk test checked if variables were normally distributed. As they were non-normally distributed, data were expressed as median (min–max). The Mann–Whitney and Wilcoxon tests were used for continuous/discrete variables, i.e., independent and paired data, respectively. The chi-square test with Yates' correction or Fisher's exact test was used to compare categorical variables. Univariate estimates of time-related outcome measures for survival curves were determined using the Kaplan–Meier product-limit method. All statistical analyses were performed using IBM-SPSS® version 26.0 (IBM Corp., Armonk, NY, USA, 2019). In all analyses, a two-sided p-value ≤0.05 was considered significant.

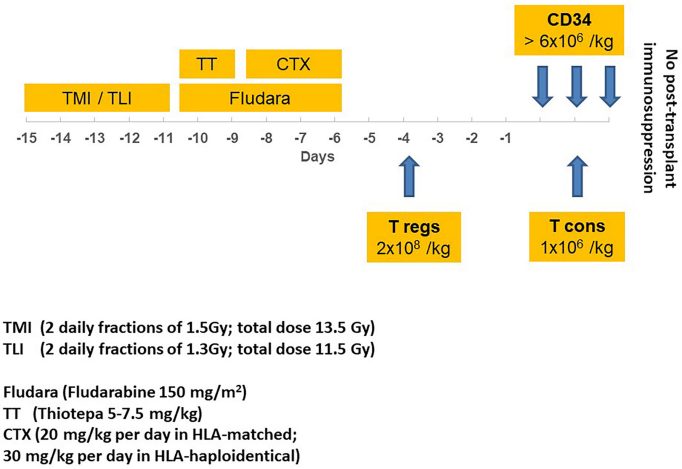

FIGURE 1
Transplantation schema, illustrating TMI/TLI* irradiation, drugs, timing, and immunotherapy before hematopoietic stem cell transplantation with CD34$^+$ cells. *A SIB procedure was used to deliver different TMI and TLI total doses (respectively, 13.5 Gy and 11.5 Gy); TMI, total marrow irradiation; TLI, total lymphoid irradiation; CTX, cyclophosphamide; Fludara, fludarabine; T regs, regulatory T cells; T cons, conventional T cells.

Results

All 50 patients achieved primary sustained engraftment with full donor-type chimerism. Table 3 summarizes outcomes.

In the first 3 months posttransplant 30/50 (60%) transplant recipients developed an infectious complication that was defined as organ damage coupled with fever (26 pulmonary, 21 GI, 9 genitourinary). Infections were due to bacteria, fungi, and viruses, but infectious agents were not always identified.

All patients were evaluable for aGvHD. Eighteen patients (36%) developed grade ≥2 aGvHD (G2 in 5, G3 in 11, and G4 in 2). Infections and other sources of inflammation were ruled out as underlying causes. The median time to onset was 41 days (range 23–69 days). The skin was affected in 11 patients and the

FIGURE 2
CT scan of one representative patient. **(A)** shows intestinal areas with aGvHD as outlined in pale yellow. **(B)** shows aGvHD as contoured on this patient's original treatment plan and dose distribution.

10.3389/fonc.2022.1035375

TABLE 3 Outcomes of TMLI and hematopoietic stem cell transplantation in 50 patients with hematologic malignancies.

Engraftment	50 patients
Infections in 30 patients	
Pulmonary	26
Gastrointestinal	21
Genitourinary	9
Acute GvHD in 18 patients	
Intestinal	16
Liver	5
Skin	11
Chronic GvHD	0
Follow-up in months	34 (1–80)
Transplant-related mortality (TRM)	16% (median time to death: 5.2 months)
Leukemia-free survival*	74.4%

* at 60 months.

liver in 5. At diagnosis of aGvHD, the CT scan was positive for intestinal involvement in 16/18 patients. All 18 patients received steroids as first-line therapy. Second-line treatment was administered to 13 patients either for early steroid withdrawal or to achieve a better aGvHD response. Agents included cyclosporine, anti-thymocyte globulin, extracorporeal photopheresis, and ruxolitinib. aGvHD resolved in 16/18 patients who fully withdrew from immunosuppressive treatments. At a median follow-up of 34 months (range 1–80 months), no patient has developed cGvHD.

In the 18 patients with aGvHD, neither age ($p = 0.666$), BMI ($p = 0.495$), nor residual disease ($p = 0.653$) at transplant was found to be a risk factor.

In the entire cohort of 50 patients, the mean TMLI dose to the whole intestine was 7.1 Gy (range 5.07–10.92 Gy). No dosimetric variable emerged as a significant risk factor for aGvHD (Table 4). No dosimetric parameter of the intestinal areas with aGvHD was associated with the disease (Table 5).

When 13 patients with G3 and G4 aGvHD were compared with 32 patients who were aGVHD-free, no dosimetric parameter emerged as significant.

Discussion

TMLI was recently introduced into the Perugia Unit's conditioning regimen as an alternative to TBI in association with a graft containing Tregs and Tcons (28). The inoculum content of a megadose of T cell-depleted $CD34^+$ cells and donor Tregs constituted the only prophylaxis for aGvHD that otherwise would have been triggered by the Tcon content. Indeed, evidence from murine haploidentical transplant models showed that confusion of Tregs with Tcons prevented lethal aGvHD by suppressing alloreactive T-cell proliferation in the lymph nodes and non-lymphoid tissues, i.e., the skin, liver, gut, and lung. Since the expansion of non-alloreactive T cells was not inhibited, immunological reconstitution proceeded unhindered (29–32).

The choice of TMLI or TBI was dictated by the patient's age and condition. The present study protocol was designed to offer HSCT to patients with hematologic malignancies who were ineligible for TBI, i.e., 44 patients because of age, which was >50 years, and 6 younger patients who had comorbidities that were counterindications to TBI. The study's inclusion criteria precluded a TBI control group.

In a previous series of high-risk AML patients, RT tailoring in the conditioning regimens to suit individual needs was associated with an exceptional 75% of cGvHD/relapse-free survival, despite T-cell depletion strategies. Grade ≥2 aGvHD occurred in 15 patients, i.e., in 3/19 (16%) who underwent TBI and surprisingly in 12/31 (39%) who underwent TMLI (33). Although older age was hypothesized to have been a factor in the development of aGvHD (33), it did not emerge as a risk factor in the present series, with ages ranging from 23 to 70 years old. The discrepancy may be resolved in the future by conducting a prospective study with the same eligibility criteria.

The present study focused on radiation-related damage to the intestine, as it was reported to play a major role in the development of aGvHD and its systemic involvement by propagating the cytokine storm (17). We found no evidence that TMLI dosages to the intestine were linked to the development of aGvHD in HSCT recipients for the current level of dose exposure (mean dose 7.1 Gy; range: 5.07–10.92 Gy). Risk factors other than RT may have triggered aGvHD in our patients. One culprit may have been the Tcon content in the graft as T cell-depleted grafts were associated with a lower aGvHD incidence (9%) in our previous series of HSCT patients who were conditioned with single-dose or hyperfractionated TBI (34).

We further investigated whether RT doses to the entire intestine or its diverse segments were risk factors for aGvHD, taking into account CT evidence of aGvHD and radiosensitivity variations in the different segments. In fact, some intestinal cells, like potential stem cells, are highly radioresistant and are activated at high-dose (9 Gy) irradiation. Like these potential stem cells, cells contributing to the recovery of crypts and highly apoptosis-sensitive cells are also found in different percentages in the large and small intestine, providing different radiosensitivity indices and making the small intestine more radiosensitive than the colon and rectum (35).

The present results did not identify any dosimetric variable that correlated with aGvHD in the whole intestine or its segments. Furthermore, no parameter emerged as linked to aGvHD even when the analysis was restricted to the radiological area where damage was visible on the CT scan.

Several hypotheses were explored to account for the present results. In the first instance, RT dose to the GI, tissue damage, and aGvHD occurrence are possibly nonlinear. Our clinical priority of

10.3389/fonc.2022.1035375

TABLE 4 Impact of dose delivered to the whole intestine and its segments on aGvHD.

Dosimetric variables	aGvHD (yes) (n = 18)		aGvHD (not) (n = 32)		
	Median	Min–max	Median	Min–max	p-value
D5cc duodenum	11.2	8.43 - 13.00	11.2	7.90 - 12.97	0.5783
D10cc duodenum	10.5	7.75 - 12.54	10.7	7.39 - 12.23	0.7387
D30cc duodenum	8.3	4.56 - 11.73	8.6	5.15 - 10.59	0.751
V5Gy duodenum	57.9	24.37 - 640.71	51.4	17.85 - 95.20	0.1693
V7Gy duodenum	39.3	14.37 - 443.80	39.3	15.53 - 85.02	0.3631
V9Gy duodenum	23.7	2.00 - 293.10	23.6	0.22 - 61.44	0.5992
V11Gy duodenum	5.8	0.00 - 125.17	6.8	0.00 - 23.32	0.7311
V13Gy duodenum	0.0	0.00 - 4.98	0.0	0.00 - 4.87	0.9145
D5cc large intestine	13.2	11.78 - 14.11	13.1	11.44 - 14.28	0.233
D10cc large intestine	13.0	11.64 - 13.94	13.0	11.32 - 14.05	0.3575
D30cc large intestine	12.7	11.28 - 13.55	12.5	10.99 - 13.73	0.3903
D50cc large intestine	12.4	10.89 - 13.29	12.1	10.69 - 13.62	0.284
D80cc large intestine	12.0	10.20 - 13.06	11.7	10.26 - 13.51	0.2841
V5Gy large intestine	1,498.3	504.76 – 2,689.28	1,161.4	538.29 – 2,317.66	0.531
V7Gy large intestine	931.0	323.83 – 1,856.46	690.5	352.30 – 1,606.63	0.2331
V9Gy large intestine	540.0	180.38 – 1,234.07	379.6	176.36 – 1,369.81	0.2331
V11Gy large intestine	240.1	46.12 - 761.86	156.2	29.63 - 836.66	0.2751
V13Gy large intestine	11.6	0.00 - 92.88	8.9	0.00 - 217.02	0.2369
D5cc rectum	10.7	5.83 - 13.01	10.4	4.19 - 12.18	0.413
D10cc rectum	9.3	4.92 - 12.50	8.5	3.81 - 11.62	0.3122
V5Gy rectum	45.0	9.05 - 135.08	38.4	2.14 - 162.84	0.4669
V7Gy rectum	18.9	0.83 - 82.28	18.4	0.28 - 57.04	0.6712
V9Gy rectum	10.8	0.00 - 77.11	8.4	0.00 - 43.59	0.3902
V11Gy rectum	4.1	0.00 - 76.63	3.3	0.00 - 19.72	0.2027
V13Gy rectum	0.1	0.00 - 5.12	0.0	0.00 - 1.07	0.0769
D5cc sigmoid	11.8	10.26 - 13.37	12.0	9.33 - 13.33	0.3026
D10cc sigmoid	11.4	7.47 - 13.01	11.6	8.09 - 13.01	0.1725
D30cc sigmoid	9.9	4.37 - 12.13	10.0	6.01 - 11.90	0.908
V5Gy sigmoid	73.7	11.23 - 159.12	65.7	31.00 - 240.90	0.7927
V7Gy sigmoid	52.6	10.47 - 139.73	54.8	18.30 - 147.52	0.8241
V9Gy sigmoid	35.7	7.11 - 102.37	37.2	6.09 - 84.98	0.4793
V11Gy sigmoid	16.3	0.22 - 58.16	17.7	0.37 - 43.34	0.4669
V13Gy sigmoid	0.5	0.00 - 10.26	0.4	0.00 - 10.12	0.7799
D5cc small intestine	12.3	11.55 - 13.75	12.2	11.09 - 13.75	0.7694
D10cc small intestine	12.0	11.40 - 13.55	11.8	10.83 - 13.70	0.5991
D30cc small intestine	11.6	10.77 - 13.11	11.4	10.18 - 13.60	0.6934
D50cc small intestine	11.2	10.36 - 12.78	11.2	9.84 - 13.55	0.6565
D80cc small intestine	10.8	9.92 - 12.42	10.8	9.27 - 13.43	0.642
V5Gy small intestine	1,167.3	595.25 – 3,061.58	1,071.2	522.12 – 3,068.37	0.5715
V7Gy small intestine	589.4	271.24 – 1,069.72	556.7	255.00 – 1,166.77	0.8241
V9Gy small intestine	250.3	143.99 - 574.82	258.0	95.19 - 877.30	0.9035
V11Gy small intestine	68.1	19.69 - 266.15	63.6	6.46 - 572.45	0.6134
V13Gy small intestine	0.3	0.00 - 35.95	0.7	0.00 - 165.66	0.5763
D5cc whole intestine	13.3	11.85 - 14.11	13.2	11.68 - 14.28	0.2932
D10cc whole intestine	13.1	11.74 - 13.96	13.0	11.58 - 14.06	0.3472
D30cc whole intestine	12.8	11.54 - 13.57	12.6	11.30 - 13.76	0.363
D50cc whole intestine	12.5	11.37 - 13.32	12.3	11.08 - 13.69	0.3848

(Continued)

TABLE 4 Continued

Dosimetric variables	aGvHD (yes) (n = 18)		aGvHD (not) (n = 32)		
	Median	Min–max	Median	Min–max	p-value
D80cc whole intestine	12.1	11.14 - 13.09	12.0	10.78 - 13.62	0.3319
V5Gy whole intestine	2,802.6	1,155.91 – 5,925.41	2,380.1	1,102.50 – 5,011.60	0.492
V7Gy whole intestine	1,537.8	636.36 – 3,042.76	1,286.3	647.01 – 2,653.46	0.1822
V9Gy whole intestine	834.8	380.51 – 1,636.88	709.8	313.04 – 2,202.96	0.2577
V11Gy whole intestine	314.7	99.61 - 851.36	247.6	57.91 – 1,430.08	0.1513
V13Gy whole intestine	12.7	0.00 - 99.62	11.6	0.00 - 387.55	0.3472

Statistical analyses were based on Mann–Whitney test; significance was set at $p < 0.05$.

TABLE 5 RT dose to intestinal areas developing aGvHD vs. RT dose to non-affected intestine.

Dosimetric variables	GvHD		Gut without GvHD		
	Median	Min–max	Median	Min–max	p-value
V5Gy	722.8	186.99 – 3,206.06	1,703	391.05 – 3,829.56	0.3635
V7Gy	469.680	93.32 – 2,124.64	848.1	218.46 – 1,865.70	0.3635
V9Gy	219.380	39.68 – 1,196.45	628.5	146.48 – 1,075.89	0.3066
V11Gy	111.81	2.76 - 543.21	253.3	40.85 - 489.29	0.2115
V13Gy	8.340	0.00 - 52.46	8.83	0.00 - 68.16	0.2115
Dmin	3.100	2.13 - 6.33	3.09	2.00 - 4.18	0.1318
Dmean	7.280	5.84 - 10.47	7.52	5.06 - 8.86	0.2012
Dmax	13.800	12.22 - 15.32	13.98	12.62 - 14.78	0.256

Statistical analyses were based on Wilcoxon signed rank test; significance was set at $p < 0.05$.

administering low RT doses to the intestine so as to preserve intestinal function and prevent aGvHD may have been transformed into a drawback, as low doses were administered to the whole intestine and its segments, thus making a significant finding hard to emerge. On the other hand, we have to admit that the large dose variations in the intestine and the small cohort of patients further limit resolving the difference. Secondly, it was difficult to define the exact RT dose for the whole intestine and its segments. Indeed, organ motion and natural variations in volume impact upon dose delivery and intertreatment and intratreatment sessions. Intriguingly, several preclinical studies showed that commensal bacteria influenced the pathophysiology of GvHD (36). When evaluating long-term changes in gut microbiota after TBI in a murine model, Zhao et al. (37) demonstrated quantitative and qualitative changes in microbial diversity. The results of ongoing trials of targeted modulation strategies in HSCT recipients (36, 38) are eagerly awaited.

Finally, contributing to the complexity of untangling the role of RT is a combination of immune modulation as induced by GI radiation and adoptive therapy with Tcons and Tregs. Thus, a preclinical model will be a helpful guide in understanding the role of TMI in aGvHD. Indeed, we have already observed that lowering the radiation dose (~4 Gy) to the GI attenuated tissue damage, with less donor T-cell traffic to the GI system that resulted in reduced aGvHD.

Ultimately, since the present small sample size of 50 patients with 18 cases of aGvHD may account for our lack of significance, this investigation should be considered as a preliminary assessment. Recruitment is continuing, as are studies in preclinical models, in an attempt to explore other potential triggers of aGvHD and provide more definitive findings about its prevention.

Data availability statement

The raw data supporting the conclusions of this article will be made available by the authors, without undue reservation.

Ethics statement

Ethical review and approval was not required for the study on human participants in accordance with the local legislation and institutional requirements. The patients/participants

provided their written informed consent to participate in this study.

Author contributions

SS, CF, CZ, AA, AP, MC, GI, SH and CA contributed to conception and design of the study. SS, CF and CZ organized the database. VB performed the statistical analysis. SS, CA and SH wrote the first draft of the manuscript. CF, AP, CZ, AA wrote sections of the manuscript. All authors contributed to manuscript revision, read, and approved the submitted version.

Conflict of interest

The authors declare that the research was conducted in the absence of any commercial or financial relationships that could be construed as a potential conflict of interest.

Publisher's note

References

1. Papadopoulos EB, Carabasi MH, Castro-Malaspina H, Childs BH, Mackinnon S, Boulad F, et al. T-cell–depleted allogeneic bone marrow transplantation as postremission therapy for acute myelogenous leukemia: Freedom from relapse in the absence of graft-versus-host disease. *Blood* (1998) 91(3):1083–90. doi: 10.1182/blood.v91.3.1083

2. Weiden PL, Flournoy N, Thomas ED, Prentice R, Fefer A, Buckner CD, et al. Antileukemic effect of graft-versus-host disease in human recipients of allogeneic-marrow grafts. *N Engl J Med* (1979) 300(19):1068–73. doi: 10.1056/NEJM197905103001902

3. Ramdial JL, Mehta RS, Saliba RM, Alousi AM, Bashir Q, Hosing C, et al. Acute graft-versus-host disease is the foremost cause of late nonrelapse mortality. *Bone Marrow Transplant* (2021) 56(8):2005–12. doi: 10.1038/s41409-021-01274-1

4. Zeiser R, Blazar BR. Acute graft-versus-host disease-biologic process, prevention, and therapy. *New Engl J Med* (2017) 377:2167–79. doi: 10.1056/NEJMra1609337

5. Filipovich AH, Weisdorf D, Pavletic S, Socie G, Wingard JR, Lee SJ, et al. National institutes of health consensus development project on criteria for clinical trials in chronic graft-versus-host disease: I. diagnosis and staging working group report. *Biol Blood Marrow Transplant* (2005) 11(12):945–56. doi: 10.1016/j.bbmt.2005.09.004

6. Jacobsohn DA, Vogelsang GB. Acute graft versus host disease. *Orphanet J Rare Dis* (2007) :2:35. doi: 10.1186/1750-1172-2-35

7. Arai S, Arora M, Wang T, Spellman SR, He W, Couriel DR, et al. Increasing incidence of chronic graft-versus-host disease in allogeneic transplantation: a report from the center for international blood and marrow transplant research. *Biol Blood Marrow Transpl* (2015) 21(2):266–74. doi: 10.1016/j.bbmt.2014.10.021

8. Hymes SR, Turner ML, Champlin RE, Couriel DR. Cutaneous manifestations of chronic graft-versus-host disease. *Biol Blood Marrow Transplant* (2006) 12 (11):1101–13. doi: 10.1016/j.bbmt.2006.08.043

9. Harris AC, Ferrara JLM, Levine JE. Advances in predicting acute GVHD. *Br J Haematol* (2013) 160(3):288–302. doi: 10.1111/bjh.12142

10. Clift RA, Buckner CD, Thomas ED, Bensinger WI, Bowden R, Bryant E, et al. Marrow transplantation for chronic myeloid leukemia: a randomized study comparing cyclophosphamide and total body irradiation with busulfan and cyclophosphamide. *Blood* (1994) 84(6):2036–43. doi: 10.1182/blood.v84.6.2036.bloodjournal8462036

11. Nakasone H, Fukuda T, Kanda J, Mori T, Yano S, Kobayashi T, et al. Impact of conditioning intensity and TBI on acute GVHD after hematopoietic cell transplantation. *Bone Marrow Transplant* (2015) 50(4):559–65. doi: 10.1038/bmt.2014.293

12. Khimani F, Dutta M, Faramand R, Nishihori T, Perez AP, Dean E, et al. Impact of total body irradiation-based myeloablative conditioning regimens in patients with acute lymphoblastic leukemia undergoing allogeneic hematopoietic stem cell transplantation: Systematic review and meta-analysis. *Transplant Cell Ther* (2021) 27(7):620.e1–9. doi: 10.1016/j.jtct.2021.03.026

13. Peters C, Dalle J-H, Locatelli F, Poetschger U, Sedlacek P, Buechner J, et al. Total body irradiation or chemotherapy conditioning in childhood ALL: A multinational, randomized, noninferiority phase III study. *J Clin Oncol* (2021) 39 (4):295–307. doi: 10.1200/JCO.20.02529

14. Hill GR, Crawford JM, Cooke KR, Brinson YS, Pan L, Ferrara JLM. Total body irradiation and acute graft-versus-host disease: The role of gastrointestinal damage and inflammatory cytokines. *Blood* (1997) 90(8):3204–13. doi: 10.1182/blood.v90.8.3204

15. Clift RA, Buckner CD, Appelbaum FR, Bearman SI, Petersen FB, Fisher LD, et al. Allogeneic marrow transplantation in patients with acute myeloid leukemia in first remission: a randomized trial of two irradiation regimens. *Blood* (1990) 76 (9):1867–71. doi: 10.1182/blood.V76.9.1867.1867

16. Nash RA, Pepe MS, Storb R, Longton G, Pettinger M, Anasetti C, et al. Acute graft-versus-host disease: analysis of risk factors after allogeneic marrow transplantation and prophylaxis with cyclosporine and methotrexate. *Blood* (1992) 80(7):1838–45. doi: 10.1182/blood.V80.7.1838.1838

17. Henden AS, Hill GR. Cytokines in graft-versus-host disease. *J Immunol* (2015) 194(10):4604–12. doi: 10.4049/jimmunol.1500117

18. Ferrara JL, Levine JE, Reddy P, Holler E. Graft-versus-host disease. *Lancet* (2009) 373(9674):1550–61. doi: 10.1016/S0140-6736(09)60237-3

19. Zuro D, Madabushi SS, Brooks J, Chen BT, Goud J, Salhotra A, et al. First multimodal, three-dimensional, image-guided total marrow irradiation model for preclinical bone marrow transplantation studies. *Int J Radiat Oncol Biol Phys* (2021) 111(3):671–83. doi: 10.1016/j.ijrobp.2021.06.001

20. Wong JYC, Liu A, Schultheiss T, Popplewell L, Stein A, Rosenthal J, et al. Targeted total marrow irradiation using three-dimensional image-guided tomographic intensity-modulated radiation therapy: an alternative to standard total body irradiation. *Biol Blood Marrow Transplant* (2006) 12(3):306–15. doi: 10.1016/j.bbmt.2005.10.026

21. Rosenthal J, Wong J, Stein A, Qian D, Hitt D, Naeem H, et al. Phase 1/2 trial of total marrow and lymph node irradiation to augment reduced-intensity transplantation for advanced hematologic malignancies. *Blood* (2011) 117 (1):309–15. doi: 10.1182/blood-2010-06-288357

22. Hui SK, Kapatoes J, Fowler J, Henderson D, Olivera G, Manon RR, et al. Feasibility study of helical tomotherapy for total body or total marrow irradiation: TBI and TMI using helical tomotherapy. *Med Phys* (2005) 32(10):3214–24. doi: 10.1118/1.2044428

23. Hui SK, Verneris MR, Higgins P, Gerbi B, Weigel B, Baker SK, et al. Helical tomotherapy targeting total bone marrow - first clinical experience at the university of Minnesota. *Acta Oncol* (2007) 46(2):250–5. doi: 10.1080/02841860601042449

24. Hui S, Takahashi Y, Holtan SG, Azimi R, Seelig D, Yagi M, et al. Early assessment of dosimetric and biological differences of total marrow irradiation versus total body irradiation in rodents. *Radiother Oncol* (2017) 124(3):468–74. doi: 10.1016/j.radonc.2017.07.018

25. Haraldsson A, Wichert S, Engström PE, Lenhoff S, Turkiewicz D, Warsi S, et al. Organ sparing total marrow irradiation compared to total body irradiation

prior to allogeneic stem cell transplantation. *Eur J Haematol* (2021) 107(4):393–407. doi: 10.1111/ejh.13675

26. Glucksberg H, Storb R, Fefer A. Clinical manifestations of graft-versus-host disease in human recipients of marrow from hl-a-matched sibling donor, s. *Transplantation* (1974) 18:295–304. doi: 10.1097/00007890-197410000-00001

27. Vogelsang GB, Lee L, Bensen-Kennedy DM. Pathogenesis and treatment of graft-versus-host disease after bone marrow transplant. *Annu Rev Med* (2003) 54 (1):29–52. doi: 10.1146/annurev.med.54.101601.152339

28. Wong JY, Hui SK. Total Marrow/Lymphoid irradiation in the conditioning regimen for haploidentical T-Cell-Depleted hematopoietic stem cell transplantation for acute myeloid leukemia: The perugia experience. In: *Total marrow irradiation*. Springer Nature Switzerland AG: Springer International Publishing (2020). p. 111–21.

29. Hoffmann P, Ermann J, Edinger M, Fathman CG, Strober S. Donor-type CD4(+)CD25(+) regulatory T cells suppress lethal acute graft-versus-host disease after allogeneic bone marrow transplantation. *J Exp Med* (2002) 196(3):389–99. doi: 10.1084/jem.20020399

30. Nguyen VH, Shashidhar S, Chang DS. The impact of regulatory T cells on T-cell immu- nity following hematopoietic cell transplantation. *Blood* (2008) 111:945–53. doi: 10.1182/blood-2007-07-103895

31. Di Ianni M, Falzetti F, Carotti A, Terenzi A, Castellino F, Bonifacio E, et al. Tregs prevent GVHD and promote immune reconstitution in HLA-haploidentical transplantation. *Blood* (2011) 117(14):3921–8. doi: 10.1182/blood-2010-10-311894

32. Martelli MF, Ianni D, Ruggeri M. HLA-haploidentical transplantation with regulatory and conventional T cell adoptive immunotherapy prevents acute leukemia relapse. *Blood* (2014) 124:638–44. doi: 10.1182/blood-2014-03-564401

33. Pierini A, Ruggeri L, Carotti A, Falzetti F, Saldi S, Terenzi A, et al. Haploidentical age-adapted myeloablative transplant and regulatory and effector T cells for acute myeloid leukemia. *Blood Adv* (2021) 5(5):1199–208. doi: 10.1182/bloodadvances.2020003739

34. Aristei C, Carotti A, Palazzari E, Amico L, Ruggeri L, Perrucci E, et al. The total body irradiation schedule affects acute leukemia relapse after matched T cell–depleted hematopoietic stem cell transplantation. *Int J Radiat Oncol Biol Phys* (2016) 96(4):832–9. doi: 10.1016/j.ijrobp.2016.07.025

35. Potten CS, Grant HK. The relationship between ionizing radiation-induced apoptosis and stem cells in the small and large intestine. *Br J Cancer* (1998) 78 (8):993–1003. doi: 10.1038/bjc.1998.618

36. Lee KA, Luong MK, Shaw H, Nathan P, Bataille V, Spector TD. The gut microbiome: what the oncologist ought to know. *Br J Cancer* (2021) 125(9):1197–209. doi: 10.1038/s41416-021-01467-x

37. Zhao Y, Zhang J, Han X, Fan S. Total body irradiation induced mouse small intestine senescence as a late effect. *J Radiat Res* (2019) 60(4):442–50. doi: 10.1093/jrr/rrz026

38. Yu J, Sun H, Cao W, Han L, Song Y, Wan D, et al. Applications of gut microbiota in patients with hematopoietic stem-cell transplantation. *Exp Hematol Oncol* (2020) 9(1):35. doi: 10.1186/s40164-020-00194-y

frontiers | Frontiers in Oncology

TYPE Original Research
PUBLISHED 05 January 2023
DOI 10.3389/fonc.2022.1042652

OPEN ACCESS

EDITED BY
Bulent Aydogan,
The University of Chicago,
United States

REVIEWED BY
James Chow,
University of Toronto, Canada
Kang-Hyun Ahn,
University of Chicago Medicine,
United States

*CORRESPONDENCE
Jeffrey Y. C. Wong
jwong@coh.org

†These authors have contributed equally to this work and share first authorship

SPECIALTY SECTION
This article was submitted to Radiation Oncology, a section of the journal Frontiers in Oncology

RECEIVED 17 October 2022
ACCEPTED 15 December 2022
PUBLISHED 05 January 2023

CITATION
Ladbury C, Han C, Liu A and Wong JYC (2023) Volumetric modulated arc therapy based total marrow and lymphoid irradiation: Workflow and clinical experience. *Front. Oncol.* 12:1042652. doi: 10.3389/fonc.2022.1042652

Volumetric modulated arc therapy based total marrow and lymphoid irradiation: Workflow and clinical experience

Colton Ladbury†, Chunhui Han†, An Liu and Jeffrey Y. C. Wong*

Department of Radiation Oncology, City of Hope National Medical Center, Duarte, CA, United States

Background: The aim of this study is to report historical treatment planning experience at our institution for patients receiving total marrow and lymphatic irradiation (TMLI) using volumetric modulated arc therapy (VMAT) as part of the conditioning regimen prior to hematopoietic stem cell transplant.

Methods: We identified a total of fifteen patients with VMAT TMLI, ten with a prescription dose of 20 Gy (targeting the skeletal bones, lymph nodes, spleen, and spinal canal, with 12 Gy to the brain and liver) and five with a prescription dose of 12-16 Gy (targeting the skeletal bones, lymph nodes, spleen, and spinal canal). Representative dosimetric parameters including total treatment time, mean and median dose, D80, and D10 (dose covering 80% and 10% of the structure volume, respectively) for targets and normal organs were extracted and compared to historical patients treated with helical tomotherapy.

Results: The median treatment time for the first and subsequent fractions was 1.5 and 1.1 hours, respectively. All the target volumes had a mean dose greater than the prescribed dose except the ribs, which had an average mean dose of 19.5 Gy. The skeletal bones had an average mean dose of 21.1 Gy. The brain and liver have average mean doses of 14.8 and 14.1 Gy, respectively. The mean lung dose had an average of 7.6 $\pm$ 0.6 Gy for the 20-Gy cohort. Relative to the prescription dose of 20 Gy, the average mean dose for the normal organ volumes ranged from 16.5% to 72.0%, and the average median dose for the normal organs ranged from 16.5% to 71.0%. Dosimetry for patients treated to 12-16 Gy fell within expected ranges based on historical helical tomotherapy plans.

Conclusions: Dosimetric data in the VMAT TMLI plans at our institution are summarized for 20 Gy and 12-16 Gy cohorts. Dose distributions and treatment times are overall similar to plans generated with helical tomotherapy. TMLI may be delivered effectively using a VMAT technique, even at escalated doses.

KEYWORDS

TMLI (total marrow and lymphatic irradiation), IMRT (intensity modulated radiation therapy), VMAT (volumetric modulated arc therapy), radiation, dosimetry, HCT (hematopoietic cell transplant)

1 Introduction

Total body irradiation (TBI) is a critical component of the conditioning regimen for hematopoietic cell transplantation, increasing the probability of a successful transplant by helping eradicate cancerous cells and/or decreasing risk of graft rejection (1, 2). Traditionally, TBI has been administered using two-dimensional treatment planning with an anteroposterior (AP) and posteroanterior (PA) fields (3). When myeloablative doses, typically in the range of 12-13.2 Gy, are administered, this requires shielding of critical organs such as the lungs to reduce the risk of morbidity. Organs that are not shielded receive the full prescription dose. As a result, TBI is associated with a multitude of acute and chronic complications including pneumonitis, renal dysfunction, and hypothyroidism (4). The morbidity associated with TBI treatment has proven prohibitive for achieving dose escalation, which might otherwise be a valuable means of decreasing risk of relapse (5–8).

Advances in radiation technology have offered an alternative to conventional TBI that can help overcome those shortcomings. Intensity modulated radiation therapy (IMRT), which has become widely available in the early 2000s, has the capability to provide focused and conformal dose distributions that can better target regions of interest while limiting dose to organs at risk (OARs) (9). This led to the development of total marrow and lymphatic irradiation (TMLI), which focused radiation on structures critical for reducing relapse rates (bone marrow ± lymph nodes), and sparing other organs such as the brain, lungs, heart, kidneys, and testis (10–13). This approach has been shown to reduce toxicities (14). Further, by limiting dose to OARs, dose escalation has been facilitated without excessive toxicity (15, 16).

Historically, TMLI treatments have been administered using helical tomotherapy (HT) machines due to their ability to treat the length of the body without requiring multiple isocenters and treatment fields, and therefore multiple image acquisitions for image guidance (13). To date, our institution has treated over 400 patients using HT-based TMLI. However, conventional C-arm linear accelerators are more prevalent than HT machines, and therefore a TMLI technique provides access for more patients receiving TMLI treatments. Starting in 2021, our institution began administering clinical TMLI treatments using VMAT fields. We have delivered TMLI treatments using VMAT fields on conventional linear accelerators for 15 patients with prescription dose ranging from 12 Gy to 20 Gy. Herein, we report our treatment planning and delivery experience.

2 Materials and methods

2.1 VMAT TMLI technique

2.1.1 Simulation

Patients are immobilized using a thermoplastic mask from the head to shoulder region and covering the feet, in addition to a full body vacuum bag (VakLok). For patients shorter than 105-135 cm, the CT simulation scan spans the top of the skull to the bottom of the feet, in a feet-first supine position. For taller patients, two separate simulation CTs are acquired: one for the upper body in a head-first supine position and one for the lower body in a head-first supine position, with overlap in the pelvis and proximal thigh regions. Both arms are kept straight and close to the body with hands forming loose fists. Three radiopaque triangulation markers are placed in the abdominal area in the same axial plane to mark the origin of the coordinates used in the CT images. Additionally, two radiopaque markers are placed in an axial plane at the upper thigh level to assist with setup of treatment fields for the upper body and lower extremities. Lastly, a set of three radiopaque triangulation markers are placed at the mid-shin level to mark the origin for the lower-extremity CT simulation.

Computed tomography (CT) simulation is obtained using 7.5 mm slice thickness. Images are acquired with patients breathing using shallow respirations. To fully model respiratory movement, end of expiration and end of inspiration breath hold CT scans are also acquired for the thoracic and abdominal regions. CT simulation scans are then sent to the Eclipse treatment planning system (Varian Medical Systems, Palo Alto, CA). The scans are registered based on bony anatomy to generate a whole-body image set used for a single treatment plan.

To facilitate treatment planning, the upper body and lower extremity CT simulation are concatenated to form a whole-body CT image set. A commercial software application (Velocity, Varian Medical Systems, Inc., Palo Alto, California) is used to concatenate the CT images based on deformable image registration results.

2.1.2 Treatment planning

All contouring and planning were performed using the Eclipse (Varian Medical Systems, Palo Alto, CA) v16.1 treatment planning system. At our institution, all structures are delineated the same way in VMAT and HT cases and the same dosimetric guidelines are used for plan optimization, facilitating comparison of the two techniques (17). Following CT simulation, normal organs and target structures are delineated on the image set according to the specific treatment protocol. Artificial intelligence based auto-segmentation algorithms are used to help contour both targets and normal organs, which are manually adjusted by the treating physician and dosimetrist as needed. Target volumes at minimum include all bones and associated marrow, major lymph node chains, and the spleen. Depending on the protocol, the brain, liver, and testes are sometimes included as target volumes. The planning target volume (PTV) includes a 5-10 mm margin on bone, cropped away from skin, esophagus, and kidney by at least 5 mm. The mandible is excluded to facilitate organ sparing. No anterior margin is used for vertebra and pelvic bones, and no inner

margin us used for ribs and skull to facilitate organ sparing. Avoidance structures include the brain, eyes, lenses, optic nerves, parotid glands, oral cavity, thyroid, lungs, heart, esophagus, breasts (in females), stomach, small intestine, liver, kidneys, bladder, rectum, ovaries and uterus (in females), and testes (in males, unless included in target volume). Using the end-expiration and end-inspiration scans, respiratory motion is accounted for in relevant organs including esophagus, kidneys, spleen, and liver.

Following delineation of treatment and avoidance structures, treatment plans are generated for a Varian TrueBeam linear accelerator with a 120-leaf multi-leaf collimator (MLC), with a leaf width of 5 mm for the central 40 leaf pairs and a leaf width of 1 cm for the peripheral 20 leaf pairs. The maximum field dimension is 40 cm × 40 cm and the maximum MLC travel is 15 cm. For adult patients, four to five isocenters are typically required for the upper body to mid-thigh TMLI treatment plan, with two VMAT arc fields per isocenter (one to two fields are used for the inferior isocenter). Isocenters are placed along the longitudinal axis, with no lateral or antero-posterior shifts. Isocenters are typically separated by no more than 24 cm. The collimator angle is at 90°C so that the MLC leaves move along the longitudinal direction of the patient. Asymmetric jaws are used along the patient's longitudinal direction so that two arc fields at each isocenter are coplanar and cover different lengths of the patient body.

For the lower body, from the mid-thigh to the bottom of the feet, either a VMAT or three-dimensional technique can be used. For the VMAT technique, typically three large aperture, coplanar fields are used. For the three-dimensional technique, three to four static AP/PA photon fields in two to three isocenters are planned in a feet-first supine position. Plans are generated using a six-megavoltage photon beam for all VMAT fields and optimization for all isocenters is carried out simultaneously. The automatic feathering option for the optimizer was enabled in plan optimization, which leads to a smooth dose gradient with each VMAT field in the dose junction regions to minimize dose variation due to setup uncertainties. The upper body VMAT TMLI plan is summed with the lower extremity plans for verification of adequate dose in the junction region at the upper thigh. Visualization of field arrangement is shown in Figure 1A.

Treatments are planned to total doses of 12-20 Gy based on clinical protocol, given in 1.5-2 Gy fractions, respectively. For all plans dose was prescribed to skeletal bones (excluding the ribs and skull), ribs, skull, lymph nodes, spinal canal, and spleen. For the 20 Gy plans, the brain and liver are treated to 12 Gy. Plans are optimized such that a minimum of 85% of the PTV received prescription dose. Planning dose constraints include mean lung dose of less than 8 Gy based on prior toxicity analyses from our institution and association with survival in a Children's Oncology Group study (18). This objective is achieved by prioritizing lung sparing over target coverage in the thoracic region. The maximum dose to normal organs was based off reference tables generated by historical TMLI plan data from our institution. Overall hotspots were limited as possible.

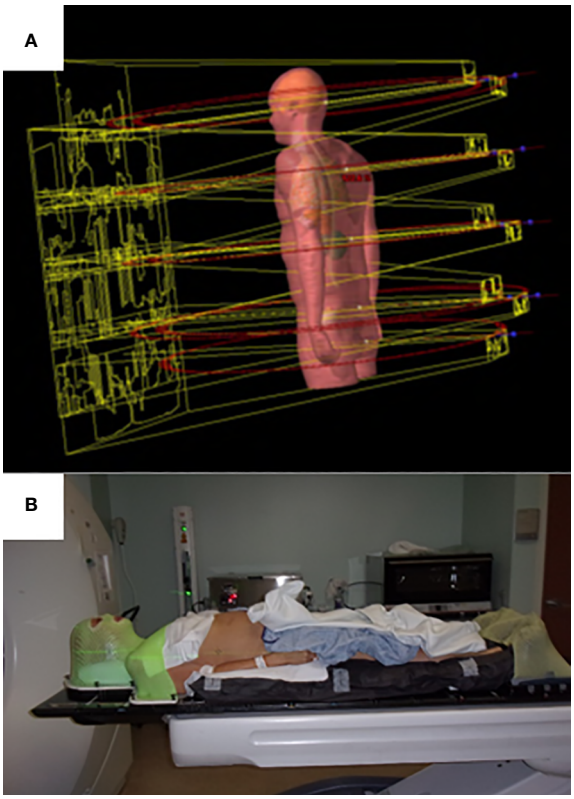

FIGURE 1
Upper body field arrangement **(A)** and setup **(B)** for patient treated with VMAT TMLI.

Plan optimization typically requires at least 2-3 hours. At our institution, we have developed a standalone application to automatically optimize VMAT TMLI plans. This application can be run overnight without user intervention. This application is written in the C# programming language and is built on top of the Eclipse Scripting Application Programming Interface (ESAPI) from Varian Medical Systems. The dosimetrist first delineates the structures and sets up the fields. Then this application is run to optimize the plan. All the VMAT fields at multiple isocenters are optimized in one single plan. The application automatically applies optimization parameters to the targets and normal organs; it also sets up other relevant parameters for the optimizer. The optimization parameters are dosimetric parameters used in construction of the objective function for optimization. These include upper and lower dose-volume objectives for each target, upper dose-volume objectives for normal organs, mean dose objectives for certain organs, and priority values for each objective. Other relevant parameters for the optimizer" refer to those settings that are not dosimetric constraints but are used by the optimizer. Examples

of such settings are whether jaw tracking will be used in optimization and the MU objective in optimization. The optimization parameters are determined from prior dosimetric planning experience. At the end of optimization, the application calculates the plan dose and performs dosimetric evaluation. The application will re-optimize the plan automatically if necessary to improve the dosimetric quality of the treatment plan. The application checks plan quality by evaluating representative dosimetric parameters. If certain dosimetric parameters do not meet planning criteria, the application can adjust relevant optimization parameters and re-optimize the treatment plan. The in-house application currently does not change constraints and priority values based on individual patient anatomy. The application does not use artificial intelligence techniques.

2.1.3 Treatment delivery

Prior to treatment delivery, plans undergo quality assurance with standard IMRT protocols. Currently our institution utilizes machine trajectory files and an independent calculation engine. A commercial software application (MobiusFX version 4.0, Varian Medical Systems, Inc., Palo Alto, California) analyzes trajectory log data after the VMAT TMLI fields are run on the Linac. The software calculates three-dimensional dose distribution based on the trajectory log data and compares the dose with the plan dose. Our institution uses three-dimensional Gamma analysis to check patient-specific QA results from the MobiusFX system. To facilitate more efficient treatment delivery, a separate setup appointment occurs either the Friday before or the day before the start of treatment to obtain imaging to aid with determining optimal patient alignment. Patients are immobilized using a thermoplastic mask in the head and neck and feet regions and a full body vacuum bag (Figure 1B). Treatments are then administered twice a day, with at least six hours between treatments. For image guidance, two cone beam (CB) CTs are obtained for each fraction: one in the head and neck isocenter region and one in abdominopelvic isocenter region. The CBCTs are registered to the simulation CT, with the shifts required for two CBCT scans averaged to correct the couch position. In addition, for each isocenter, orthogonal kilovoltage port films, at 45°C and 315°C in the thoracic region to obtain a clear view of the spine without obstruction from the arms, are taken to confirm accurate positioning. The 120 Gy plans were given in eight equal fractions with two fractions (separated by at least 6 hours) delivered each day. The 20 Gy plans were given in ten equal fractions with two fractions (separated by at least 6 hours) delivered each day.

2.2 Treatment plan analysis

In this study, treatment plans were analyzed for the 20 Gy (10 patients) and 12-16 Gy (five patients) cohorts. An example treatment plan with dose-volume histograms (Figure 2A) and three-dimensional dose distribution (Figure 2B) of a patient treated to 20 Gy is visualized. We extracted the total duration of treatment for each fraction, calculated as the total time the patient was on the treatment table. Due to the first fraction requiring additional time, the first fraction was analyzed separate from remaining fractions. This time does include a brief break between treatment of the upper body and the legs where the patient is allowed to rest when orientation changes. We extracted and analyzed dosimetric parameters including mean and median dose (D50), D80, and D10 for all plans. The TMLI treatment plan for each patient was retrieved and the treatment plan data containing dose and structure contours were exported as DICOM files. In-house software applications were developed to extract and analyze dosimetric parameters for the targets and normal organs from the DICOM data files. To illustrate the spread of values for each dosimetric parameter, we calculated and presented the 1st quartiles and 3rd quartiles, in addition to the average values, for each dosimetric parameter in each cohort, where the 1st quartile is defined as the middle value between the

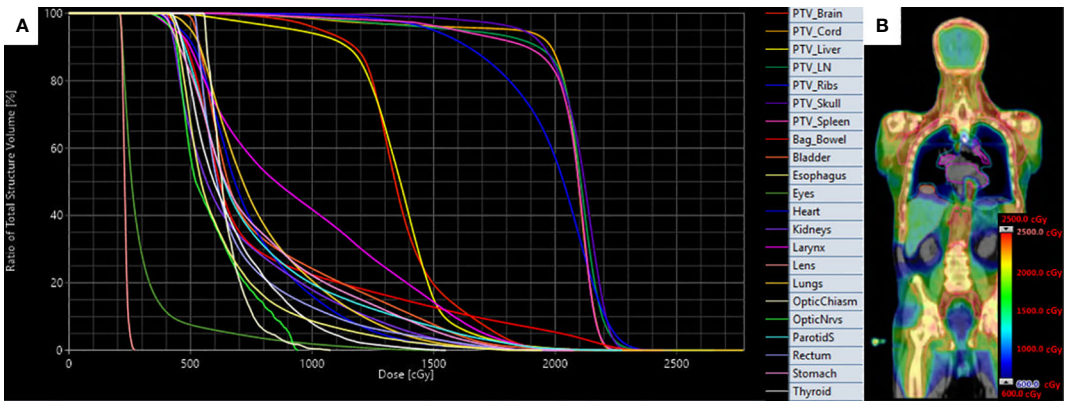

FIGURE 2
Target and organ-at-risk dose volume histograms **(A)** and three-dimensional dose distribution **(B)** of patient treated with VMAT TMLI to 20 Gy.

minimum value and the median value, and the 3rd quartile is defined as the middle value between the maximum value and the median value for a given parameter. Statistical analysis in this study was performed with a data analysis software system (Excel version 2102, Microsoft Corp., Redmond, WA).

3 Results

A total of 15 patients' treatment plans were analyzed. All patients were diagnosed with acute myeloid leukemia (AML). None patients were male. Median age was 53 (range 25-69). Median height was 167.5 cm (range 155-186 cm). Median weight was 70.2 kg (range 46.9-95.5 cm).

Table 1 lists treatment duration statistics for the VMAT TMLI plans. The median treatment time for the first and subsequent fractions was 1.5 (range: 1.2-2.4) and 1.1 (range: 0.6-1.9) hours, respectively. The mean treatment time decreased from 1.3 hours for the first two patients treated in 2017 to 0.9 hours for the final two patients treated in 2022.

Table 2 lists mean dose and median dose statistics (average, standard deviation, and 1st and 3rd quartiles) for each structure with the 20-Gy cohort. Of note, the brain and liver were prescribed 12 Gy while the other target volumes were prescribed 20 Gy. All the target volumes had a mean dose greater than the prescribed dose except the ribs, which had an average mean dose of 19.5 Gy. The skeletal bones had an average mean dose of 21.1 Gy. The brain and liver have average mean doses of 14.8 and 14.1 Gy, respectively. Relative to the prescription dose of 20 Gy, the average mean dose for the normal organ volumes ranged from 16.5% to 72.0%, and the average median dose for the normal organs ranged from 16.5% to 71.0%. Among the normal organ structures, the lenses showed the lowest average mean and median dose values while the female breasts showed the highest average mean and median dose values. The mean lung dose had an average of 7.6 ± 0.6 Gy for the 20-Gy cohort. Table 3 lists statistics of D80 and D10 for targets and normal organs with the 20-Gy cohort.

Figure 3 shows distributions of mean dose for target volumes and major normal organ volumes in the VMAT TMLI plans for the 20-Gy cohort. The minimum, maximum, and first, second, and third quartiles of the mean dose are shown in the box plot for each target and each normal organ. Figure 4 shows the mean dose data to targets and normal organ volumes in the three 12-Gy VMAT TMLI treatment plans overlain over dosimetry from our historic 12-Gy helical tomotherapy cohort. Additional dose statistics for the two patients treated with 14 or 16 Gy are shown in Table 4.

TABLE 1 Statistics of treatment times for patients treated with VMAT TMLI.

	First Fraction (hrs)	Subsequent Fractions (hrs)
Mean	1.6	1.1
Median	1.5	1.1
Range	1.2-2.4	0.6-1.9
Interquartile range (IQR)	1.3-1.9	1.0-1.2

4 Discussion

This study details the treatment technique our institution has used for our initial fifteen VMAT based TMLI patients, as well as a dosimetric summary of the resulting treatment plans. Using this technique, suitable target volume coverage and normal organ sparing is achievable, even with dose escalation to 20 Gy. Our approach could be used by other institutions to implement TMLI using VMAT, particularly when helical tomotherapy is not available.

Han et al. have performed the largest dosimetric analysis to date of patients treated with TMLI, including patients treated to an escalated dose of 20 Gy (17). Their analysis included a total of 120 patients treated to 20 Gy, with almost all patients treated with helical tomotherapy (four patients were treated with VMAT). The dosimetry in our study, with average mean dose to the target volumes ranging from 19.5 Gy (ribs) to 21.1 Gy (skeletal bones) is nearly identical to their cohort, where doses ranged from 19.3 Gy (ribs) to 20.8 Gy (skeletal bones). Dosimetry to the intermediate dose regions of the brain and liver were also similar, at 14.8 and 14.1 Gy, respectively, in our study and 13.6 and 12.9 Gy, respectively, in their study. Normal organ dose ranged from 13.0-76.0% in their study compared to 16.5% to 72.0% in our study, corresponding to lens dose and female breast dose in both studies. The same trends can be applied to the three patients treated to 12 Gy in our study. Although we had insufficient numbers to generate descriptive statistics, the mean doses fell within the same range as our historical helical tomotherapy cohort. In total, these data support the idea that VMAT TMLI can achieve comparable dosimetry to plans generated using helical tomotherapy. The ability to deliver TMLI with VMAT is critical for more widespread availability of TMLI as a treatment option when designing transplant conditioning regimens. Initial trials of TMLI utilized helical tomotherapy due to increased ease of treating lengths of the body without requiring several isocenters (10–13). However, traditional C-arm linear accelerators are more commonly available in radiation oncology departments, so VMAT would facilitate implementation of TMLI in institutions where it otherwise would not be feasible.

The feasibility of VMAT TMI was first established in 2011 (19, 20). VMAT was shown to lead to comparable dosimetry to helical tomotherapy approaches, as well as a reduction in beam

TABLE 2 Statistics of mean dose and median dose (D50) for each structure with the 20-Gy cohort.

	Mean dose (Gy)			Median dose (Gy)		
Structure	Avg ± StdDev	1st quartile	3rd quartile	Avg ± StdDev	1st quartile	3rd quartile
Skeletal Bones	21.1 ± 0.2	20.9	21.2	21.4 ± 0.4	21.2	21.6
Lymph Nodes	20.5 ± 0.5	20.3	20.8	21.3 ± 0.6	21.0	21.7
Spinal Canal	20.5 ± 0.5	20.3	20.6	21 ± 0.7	20.7	21.1
Skull	20.7 ± 0.7	20.1	21.2	21.2 ± 0.7	20.7	21.6
Ribs	19.5 ± 0.7	19.2	19.8	20.5 ± 0.8	20.2	20.8
Bladder	9.3 ± 1.5	8.3	10.2	8.4 ± 1.8	7.0	9.6
Body	13.3 ± 1.5	12.1	14.2	15 ± 1.6	14.1	16.0
Brain	14.8 ± 1.1	13.9	15.1	14.6 ± 1.2	13.7	14.8
Breasts	14.4 ± 0.8	14.0	14.8	14.2 ± 1.2	13.6	14.8
Esophagus	6.8 ± 1.4	6.1	7.0	6.1 ± 1.2	5.5	6.1
Eyes	4.2 ± 1	3.2	5.1	3.7 ± 0.9	3.0	4.3
Heart	7.5 ± 1.1	7.0	7.6	6.6 ± 1.3	6.1	6.8
Kidneys	7.5 ± 0.5	7.0	7.8	6.2 ± 0.5	5.7	6.6
Lens	3.3 ± 1	2.4	4.2	3.3 ± 1	2.4	4.1
Liver	14.1 ± 1.1	13.5	14.4	14.2 ± 1	13.5	14.9
Lower GI	9.6 ± 1.6	8.3	11.1	8.5 ± 2	7.0	10.4
Lungs	7.6 ± 0.6	7.4	7.9	6.7 ± 0.5	6.4	7.1
Oral Cavity	4.8 ± 1	4.0	5.3	3.9 ± 1	3.1	4.5
Ovaries	6.7 ± 3.1	4.9	7.9	6.1 ± 3	4.3	7.1
Parotids	8.2 ± 1	7.6	8.7	7.3 ± 1	6.6	7.7
Rectum	6.7 ± 0.9	6.1	7.2	5.7 ± 0.8	4.9	6.3
Thyroid	7.7 ± 1.2	6.8	8.1	7.1 ± 1.2	6.2	7.9
Upper GI	8.6 ± 1.3	7.8	9.1	7.7 ± 1.4	6.8	8.1

TABLE 3 Statistics of D80 and D10 for each structure with the 20-Gy cohort.

	D80 (Gy)			D10 (Gy)		
Structure	Avg ± StdDev	1st quartile	3rd quartile	Avg ± StdDev	1st quartile	3rd quartile
Skeletal Bones	20.4 ± 0.2	20.3	20.6	22.6 ± 0.6	22.2	22.9
Lymph Nodes	20.1 ± 0.4	19.7	20.3	22.5 ± 0.6	22.0	23.0
Spinal Canal	20.1 ± 0.4	20.0	20.2	21.8 ± 0.8	21.3	22.5
Skull	19.7 ± 0.6	19.5	20.1	22.6 ± 1	22.1	23.0
Ribs	17.3 ± 1.5	16.0	18.1	22.5 ± 0.7	22.1	23.0
Bladder	6.4 ± 1.2	5.7	7.3	14.4 ± 2	13.4	15.3
Body	5.1 ± 3.4	3.2	7.1	21.7 ± 0.5	21.4	22.1

(Continued)

TABLE 3 Continued

	D80 (Gy)			D10 (Gy)		
Structure	Avg ± StdDev	1st quartile	3rd quartile	Avg ± StdDev	1st quartile	3rd quartile
Brain	13.2 ± 0.8	12.5	13.6	17.6 ± 1.5	16.8	17.9
Breasts	11.2 ± 0.5	10.9	11.5	19.3 ± 1	18.8	19.7
Esophagus	5.1 ± 0.9	4.8	5.2	10 ± 2.5	8.6	10.1
Eyes	3 ± 0.8	2.4	3.4	6.4 ± 2.1	4.3	7.3
Heart	5.1 ± 1.1	4.5	5.6	11.7 ± 1.6	11.2	12.3
Kidneys	4.9 ± 0.5	4.6	5.2	12.6 ± 1	12.0	12.8
Lens	2.8 ± 0.8	2.2	3.1	4 ± 1.6	2.5	5.5
Liver	12.8 ± 0.7	12.4	13.4	16.7 ± 1.9	15.5	17.0
Lower GI	6.2 ± 1.5	5.0	7.9	16 ± 2.1	15.4	17.3
Lungs	5.4 ± 0.4	5.1	5.8	11.5 ± 1.3	11.5	12.1
Oral Cavity	3 ± 0.7	2.4	3.4	8.6 ± 2	7.5	9.7
Ovaries	4.7 ± 1.3	4.0	5.2	9.4 ± 5.2	6.5	11.5
Parotids	5.5 ± 0.9	5.2	5.8	12.9 ± 1.6	11.5	13.9
Rectum	5.1 ± 0.7	4.5	5.7	10.3 ± 2.2	9.5	11.1
Thyroid	5.6 ± 0.9	5.0	5.8	11.3 ± 1.7	9.8	12.7
Upper GI	6.2 ± 1.1	5.4	6.4	12.9 ± 2.2	11.3	13.5

on time. However, it is important to note that treatment time is still significant due to additional time required to set up multiple fields and isocenters, as shown in Table 1, though the total treatment time is still comparable to our experience with helical tomotherapy, where the median treatment time for the first and subsequent fractions was 1.6 (range: 1.2-2.6) and 1.4 (range: 0.6-2.3) hours, respectively. Further improvements in workflows therefore may be able to better capitalize on VMAT to speed up

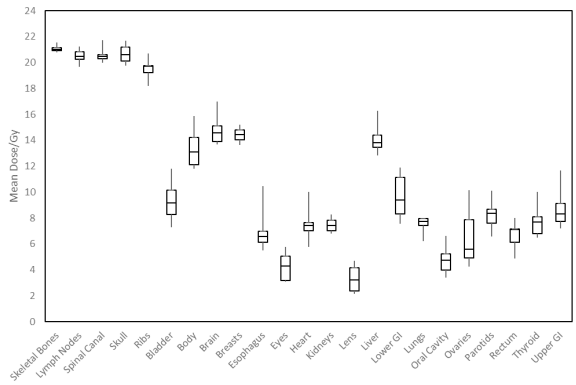

FIGURE 3
Distribution of mean dose (D_{mean}) for target volumes and major normal organs in the 20-Gy cohort. The median value of D_{mean} for each structure is shown at the horizontal bar in the middle of each rectangle. The 1st and 3rd quartiles are shown as the lower and upper horizontal sides of each rectangle. The minimum and maximum range of D_{mean} is shown as the vertical lines extending from each rectangle.

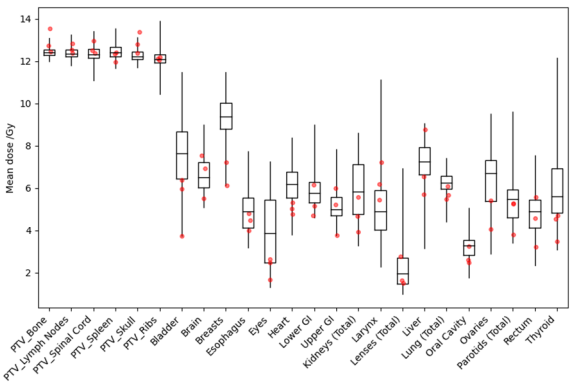

FIGURE 4
Distribution of mean dose (D_{mean}) for target volumes and major normal organs in the historical 12-Gy TMLI treatment plans. The median value of D_{mean} for each structure is shown at the horizontal bar in the middle of each rectangle. The 1st and 3rd quartiles are shown as the lower and upper horizontal sides of each rectangle. The minimum and maximum range of D_{mean} is shown as the vertical lines extending from each rectangle. The red dots are D_{mean} data in the three VMAT TMLI treatment plans in the 12-Gy cohort.

10.3389/fonc.2022.1042652

TABLE 4 Dose statistics for patients treated to 14 and 16 Gy.

	14 Gy				16 Gy			
Structure	Mean dose (Gy)	Median dose (Gy)	D80 (Gy)	D10 (Gy)	Mean dose (Gy)	Median dose (Gy)	D80 (Gy)	D10 (Gy)
Skeletal Bones	14.86	15.04	14.43	15.79	16.65	16.98	16.3	17.81
Lymph Nodes	14.49	15.2	14.43	15.89	16.21	16.96	16.21	17.77
Spinal Canal	14.84	14.77	14.46	15.52	16.25	16.73	15.6	17.26
Skull	14.89	15.27	14.21	16.2	16.3	16.91	16.14	17.82
Ribs	14.13	14.9	13.47	15.84	16.3	16.72	15.63	17.68
Bladder	5.43	4.57	3.98	8.6	7.91	7.97	5.68	10.68
Body	8.07	8.67	0.63	15.06	11.24	12.56	5.67	17.29
Brain	5.73	4.33	2.7	11.99	9.03	8.49	4.38	15.24
Breasts	8.39	7.96	6.19	12.03	N/A	N/A	N/A	N/A
Esophagus	4.43	3.84	3.42	6.31	5.28	4.39	3.88	8.11
Eyes	3.06	2.67	2.37	4.58	2.64	2.55	2.2	3.28
Heart	4.27	3.94	2.86	6.26	6.32	5.47	4.06	10.25
Kidneys	4.33	3.65	3.21	6.65	5.85	5.09	3.99	9.14
Lens	2.39	2.4	2.19	2.68	2.27	2.24	2.11	2.47
Liver	7.56	6.22	5.08	12.83	10.27	9.69	7.73	14.75
Lower GI	5.91	5.1	3.64	9.83	8.27	8	5.16	12.75
Lungs	5.98	5.28	4.16	9.51	6.99	5.9	4.66	11.32
Oral Cavity	3.18	2.49	1.95	6.14	3.41	3.02	2.07	5.62
Ovaries	4.53	4.05	3.68	5.81	N/A	N/A	N/A	N/A
Parotids	4.57	4.06	3.34	6.72	6.02	5.7	4.07	9.01
Rectum	4.72	3.98	3.48	7.75	5.47	4.9	4.36	7.56
Thyroid	4.72	4.34	3.9	6.27	5.76	5.3	4.55	7.94
Upper GI	4.45	3.79	3.33	6.93	6.91	6.48	5.46	9.38

N/A, not applicable.

treatment delivery. Importantly, using flattening filter free beams would not decrease treatment time, as it is maximum gantry speed and not dose rate that is the primary limitation on delivery time.

Compared to helical tomotherapy, VMAT has the potential advantage of allowing dose rate modulation in certain anatomical regions, although the dose rate effect on normal tissue complications needs further investigation. Most modern C-arm linacs allows the user to change the nominal dose rate for each VMAT field. Currently, the maximum nominal dose rate of 600 monitor units (MU)/min was used in all the VMAT TMLI fields at our institution. At this nominal dose rate, effective dose rates between VMAT and helical tomotherapy techniques are comparable: with a fractional dose of 2 Gy, the dose rate to targets and lung are 1.6 Gy/min and 0.8 Gy/min, respectively, with VMAT compared to 1.8 Gy/min and 0.9 Gy/min with helical tomotherapy. If the nominal dose rate for VMAT fields in the lung region is reduced by 100 MU/min, the effective dose rate to the lung can be further reduced at the expense of longer beam-on time in the lung region.

Several subsequent studies have now been performed using VMAT TMLI. An initial report by Han et al. was the first to compare VMAT TMLI plans to helical tomotherapy plans (21). In this analysis, VMAT plans were found to have a more than 10% reduction of average median dose in 16 organs. Further, beam-on time for VMAT plans was about 50% shorter. Larger

studies have evaluated the use of VMAT TMLI to a total dose of 12 Gy (22, 23). In the study by Mancosu et al., plans for 21 patients were evaluated, demonstrating 95% of prescription dose covered greater than 99% of the PTV in junctional regions between isocenters (22). In the study by Loginova et al, 157 patients treated with helical tomotherapy and 52 patients treated with VMAT were evaluated (23). There were no observed differences in acute, subacute, or late toxicities, as well as similar dose distributions. In total, these studies in combination with the present study demonstrate the overall feasibility and desirability of implementation of VMAT TMLI techniques.

This study is limited due to sample size, particularly for treatment doses less than 20 Gy. However, the dosimetry is consistent with prior reports, and to our knowledge this is the largest dosimetric report of dose-escalated VMAT TMLI to date. Due to a lack of dose escalated VMAT TMLI in the literature, this study further supports its implementation, at both standard myeloablative doses and escalated doses. Though implementation of VMAT TMLI is logistically challenging and is still associated with long treatment times due to requiring multiple image acquisitions for patient setup, we are actively seeking to further optimize planning and clinical workflows, which will be crucial for making TMLI more widely available in the radiation oncology community.

5 Conclusions

Treatment delivery with VMAT has the potential to increase availability of TMLI. Based on our initial experience, delivery of TMLI with VMAT is feasible and achieves target volume and normal organ dosimetry comparable to historical helical tomotherapy TMLI plans. Treatment procedures detailed in this study, and resulting dosimetry, can be used to inform implementation of VMAT TMLI at other institutions.

Data availability statement

The raw data supporting the conclusions of this article will be made available by the authors, without undue reservation.

Ethics statement

Ethical review and approval was not required for the study on human participants in accordance with the local legislation and institutional requirements. Written informed consent for participation was not required for this study in accordance with the national legislation and the institutional requirements.

Author contributions

CL performed data collection, data analysis, and manuscript preparation. CH participated in the design of this study and performed data collection and data analysis. AL participated in the design of this study and performed critical review of the manuscript. JW is recipient of funding from Varian Inc. to support the development, treatment planning and implementation of TrueBeam based TBI and TMLI at this center. He participated in the design of this study, creation of methods for this study, and data analysis, and performed critical review of the manuscript. All authors contributed to the article and approved the submitted version.

Funding

This research was partially supported by funding provided by Varian Medical Systems, Inc. The funder Varian Medical Systems, Inc. was not involved in the study design, collection, analysis, interpretation of data, the writing of this article or the decision to submit it for publication.

Conflict of interest

Dr. JW has received grant funding from Varian Inc. to support the development, treatment planning and implementation of TrueBeam based TBI and TMLI at this center.

The remaining authors declare that the research was conducted in the absence of any commercial or financial relationships that could be construed as a potential conflict of interest.

Publisher's note

References

1. Thomas E, Buckner C, Banaji M, Clift R, Fefer A, Flournoy N, et al. One hundred patients with acute leukemia treated by chemotherapy, total body irradiation, and allogeneic marrow transplantation. *Blood* (1977) 49:511–33. doi: 10.1182/blood.V49.4.511.511

2. Paix A, Antoni D, Waissi W, Ledoux M-P, Bilger K, Fornecker L, et al. Total body irradiation in allogeneic bone marrow transplantation conditioning regimens: A review. *Crit Rev Oncology/Hematology* (2018) 123:138–48. doi: 10.1016/j.critrevonc.2018.01.011

3. Wong JYC, Filippi AR, Dabaja BS, Yahalom J, Specht L. Total body irradiation: Guidelines from the international lymphoma radiation oncology group (ILROG). *Int J Radiat OncologyBiologyPhysics* (2018) 101:521–9. doi: 10.1016/j.ijrobp.2018.04.071

4. Chou RH, Wong GB, Kramer JH, Wara DW, Matthay KK, Crittenden MR, et al. Toxicities of total-body irradiation for pediatric bone marrow transplantation. *Int J Radiat OncologyBiologyPhysics* (1996) 34:843–51. doi: 10.1016/0360-3016(95)02178-7

5. Marks DI, Forman SJ, Blume KG, Pérez WS, Weisdorf DJ, Keating A, et al. A comparison of cyclophosphamide and total body irradiation with etoposide and total body irradiation as conditioning regimens for patients undergoing sibling allografting for acute lymphoblastic leukemia in first or second complete remission. *Biol Blood Marrow Transplant* (2006) 12:438–53. doi: 10.1016/j.bbmt.2005.12.029

6. Clift RA, Buckner CD, Appelbaum FR, Bearman SI, Petersen FB, Fisher LD, et al. Allogeneic marrow transplantation in patients with acute myeloid leukemia in first remission: a randomized trial of two irradiation regimens. *Blood* (1990) 76:1867–71. doi: 10.1182/blood.V76.9.1867.1867

7. Clift RA, Buckner CD, Appelbaum FR, Bryant E, Bearman SI, Petersen FB, et al. Allogeneic marrow transplantation in patients with chronic myeloid leukemia in the chronic phase: a randomized trial of two irradiation regimens. *Blood* (1991) 77:1660–5. doi: 10.1182/blood.V77.8.1660.1660

8. Clift RA, Buckner CD, Appelbaum FR, Sullivan KM, Storb R, Thomas ED. Long-term follow-up of a randomized trial of two irradiation regimens for patients receiving allogeneic marrow transplants during first remission of acute myeloid leukemia. *Blood* (1998) 92:1455–6. doi: 10.1182/blood.V92.4.1455

9. Bucci MK, Bevan A, Roach IIIM. Advances in radiation therapy: Conventional to 3D, to IMRT, to 4D, and beyond. *CA: A Cancer J Clin* (2005) 55:117–34. doi: 10.3322/canjclin.55.2.117

10. Wong JYC, Liu A, Schultheiss T, Popplewell L, Stein A, Rosenthal J, et al. Targeted total marrow irradiation using three-dimensional image-guided tomographic intensity-modulated radiation therapy: An alternative to standard total body irradiation. *Biol Blood Marrow Transplant* (2006) 12:306–15. doi: 10.1016/j.bbmt.2005.10.026

11. Rosenthal J, Wong J, Stein A, Qian D, Hitt D, Naeem H, et al. Phase 1/2 trial of total marrow and lymph node irradiation to augment reduced-intensity transplantation for advanced hematologic malignancies. *Blood* (2011) 117:309–15. doi: 10.1182/blood-2010-06-288357

12. Schultheiss TE, Wong J, Liu A, Olivera G, Somlo G. Image-guided total marrow and total lymphatic irradiation using helical tomotherapy. *Int J Radiat OncologyBiologyPhysics* (2007) 67:1259–67. doi: 10.1016/j.ijrobp.2006.10.047

13. Hui SK, Kapatoes J, Fowler J, Henderson D, Olivera G, Manon RR, et al. Feasibility study of helical tomotherapy for total body or total marrow irradiationa). *Med Phys* (2005) 32:3214–24. doi: 10.1118/1.2044428

14. Shinde A, Yang D, Frankel P, Liu A, Han C, Del Vecchio B, et al. Radiation-related toxicities using organ sparing total marrow irradiation transplant conditioning regimens. *Int J Radiat OncologyBiologyPhysics* (2019) 105:1025–33. doi: 10.1016/j.ijrobp.2019.08.010

15. Stein A, Palmer J, Tsai N-C, Al Malki MM, Aldoss I, Ali H, et al. Phase I trial of total marrow and lymphoid irradiation transplant conditioning in patients with relapsed/refractory acute leukemia. *Biol Blood Marrow Transplant* (2017) 23:618–24. doi: 10.1016/j.bbmt.2017.01.067

16. Al Malki MM, Palmer J, Tsai N-C, Mokhtari S, Hui S, Tsai W, et al. Total marrow and lymphoid irradiation as conditioning in haploidentical transplant with posttransplant cyclophosphamide. *Blood Adv* (2022) 6:4098–106. doi: 10.1182/bloodadvances.2022007264

17. Han C, Liu A, Wong JYC. Target coverage and normal organ sparing in dose-escalated total marrow and lymphatic irradiation: A single-institution experience. *Front Oncol* (2022) 12:946725. doi: 10.3389/fonc.2022.946725

18. Esiashvili N, Lu X, Ulin K, Laurie F, Kessel S, Kalapurakal JA, et al. Higher reported lung dose received during total body irradiation for allogeneic hematopoietic stem cell transplantation in children with acute lymphoblastic leukemia is associated with inferior survival: A report from the children's oncology group. *Int J Radiat Oncol Biol Phys* (2019) 104:513–21. doi: 10.1016/j.ijrobp.2019.02.034

19. Fogliata A, Cozzi L, Clivio A, Ibatici A, Mancosu P, Navarria P, et al. Preclinical assessment of volumetric modulated arc therapy for total marrow irradiation. *Int J Radiat OncologyBiologyPhysics* (2011) 80:628–36. doi: 10.1016/j.ijrobp.2010.11.028

20. Aydogan B, Yeginer M, Kavak GO, Fan J, Radosevich JA, Gwe-Ya K. Total marrow irradiation with RapidArc volumetric arc therapy. *Int J Radiat OncologyBiologyPhysics* (2011) 81:592–9. doi: 10.1016/j.ijrobp.2010.11.035

21. Han C, Schultheisss TE, Wong JYC. Dosimetric study of volumetric modulated arc therapy fields for total marrow irradiation. *Radiother Oncol* (2012) 102:315–20. doi: 10.1016/j.radonc.2011.06.005

22. Mancosu P, Navarria P, Castagna L, Reggiori G, Stravato A, Gaudino A, et al. Plan robustness in field junction region from arcs with different patient orientation in total marrow irradiation with VMAT. *Physica Med* (2015) 31:677–82. doi: 10.1016/j.ejmp.2015.05.012

23. Loginova AA, Tovmasian DA, Lisovskaya AO, Kobyzeva DA, Maschan MA, Chernyaev AP, et al. Optimized conformal total body irradiation methods with helical TomoTherapy and elekta VMAT: Implementation, imaging, planning and dose delivery for pediatric patients. *Front Oncol* (2022) 12:785917. doi: 10.3389/fonc.2022.785917

Frontiers in Oncology

Advances knowledge of carcinogenesis and tumor progression for better treatment and management

The third most-cited oncology journal, which highlights research in carcinogenesis and tumor progression, bridging the gap between basic research and applications to imrpove diagnosis, therapeutics and management strategies.

Discover the latest Research Topics

See more →

Frontiers

Avenue du Tribunal-Fédéral 34
1005 Lausanne, Switzerland
frontiersin.org

Contact us

+41 (0)21 510 17 00
frontiersin.org/about/contact